National Research Council Canada
Conseil national de recherches Canada

NRC · CNRC

Canadian Journal of Fisheries and Aquatic Sciences

Journal canadien des sciences halieutiques et aquatiques

ISSN 0706-652X / CJFSDX 53(11) 2397–2657 (1996)

The *Canadian Journal of Fisheries and Aquatic Sciences*, previously published as *Contributions to Canadian Biology* 1901–1925, *Contributions to Canadian Biology and Fisheries* 1926–1934, *Journal of the Biological Board of Canada* 1934–1937, and *Journal of the Fisheries Research Board of Canada* 1938–1979, is issued monthly to form annual volumes of 12 numbers plus supplements.

Editorial policy: The *Journal* publishes original research articles, critical reviews, perspectives (essays of opinion or hypothesis), and comments. Papers may concern cells, organisms, populations, ecosystems, or processes that affect aquatic production systems, and they should lead to identifiable conclusions or synthesis, which variously may amplify, modify, question, or redirect accumulated knowledge embodied in contemporary perceptions of a particular state of fisheries and aquatic sciences. They should demonstrate clearly a contribution to knowledge beyond the confirmation state. Originality should relate to more than the particular (a certain year, place, taxon, or chemical compound) such that existing understanding is reformulated or extended.

Manuscripts for publication should be submitted to **Dr. D.G. Cook**, Canadian Journal of Fisheries and Aquatic Sciences, NRC Research Press, National Research Council of Canada, Ottawa, ON K1A 0R6, Canada (613-993-2209; fax: 613-952-7656; e-mail: journal.cjfas@nrc.ca).

Submissions in either English or French are acceptable. The information must be original, that is, not copyrighted, published, or submitted elsewhere except in abstract form or unless by written consent of the Editor. NRC accepts no responsibility for statements or opinions expressed by a contributor. Acceptance of an advertisement, announcement, or other material does no imply endorsement by either the *Journal*'s Editors or NRC. The use of proprietary names does not imply endorsement of the product or company.

Correspondence concerning accepted manuscripts and corrected proofs should be sent to NRC Research Press, National Research Council of Canada, Ottawa, ON K1A 0R6, Canada.

Instructions to Authors are published once a year in the first issue of each volume; copies can be obtained from the Editorial Office, the Publishing Office, or at http://www.nrc.ca/cisti/journals/.

Microfilm: Issues from 1934 through the current volume can be purchased on 16- or 35-mm microfilm. Photocopies of individual articles or issues can be purchased from University Microfilms International, 330 North Zeeb Road, Ann Arbor, MI 48106, U.S.A.

U.S. periodical postage paid at Champlain, N.Y., and at additional mailing offices. Attention U.S. POSTMASTER: Send address changes to **Canadian Journal of Fisheries and Aquatic Sciences**, c/o USACAN Media Distribution Center, P.O. Box 2888, Plattsburg, NY 12901, U.S.A.

Publié sans interruption depuis 1901, le *Journal canadien des sciences halieutiques et aquatiques* a paru sous plusieurs titres : *Contributions to Canadian Biology* 1901–1925, *Contributions to Canadian Biology and Fisheries* 1926–1934, *Journal of the Biological Board of Canada* 1934–1937, et *Journal of the Fisheries Research Board of Canada* 1938–1979. Le *Journal* paraît tous les mois, formant ainsi un volume de 12 numéros, et offre en plus jusqu'à deux suppléments par année.

Politique de rédaction : Le journal publie des articles fondés sur une recherche originale, des critiques, des essais portant sur une opinion ou une hypothèse (perspectives) et des commentaires. Les textes peuvent avoir trait aux cellules, aux organismes, aux populations, aux écosystèmes ou aux processus qui influent sur les systèmes de production aquatique. Ils doivent aboutir à des conclusions ou synthèses précises qui, de diverse façons, peuvent accroître, modifier, remettre en question ou réorienter le bagage actuel de connaissances et perceptions dans une discipline donnée des sciences aquatiques. Ils doivent clairement démontrer qu'ils contribuent aux connaissances en faisant plus de corroborer des faits. L'originalité doit dépasser le caractère particulier (une année, un endroit, un taxon ou un composé chimique donnée) et tenir à une épuration ou une reformulation des connaissances actuelles.

Les auteurs doivent adresser leurs **manuscrits** à **D.G. Cook**, Journal canadien des sciences halieutiques et aquatiques, Presses scientifiques du CNRC, Conseil national de recherches du Canada, Ottawa, ON K1A 0R6, Canada (613-993-2209); télécopieur : 613-952-7656; courrier électronique : journal.cjfas@nrc.ca).

Les contributions peuvent être en anglais ou en français. Elles doivent être originales, c.-à.-d. qu'elles ne doivent pas avoir fait l'objet d'un copyright, avoir été publiées ou soumises ailleurs, sauf sous forme abrégée ou avec le consentement du rédacteur. Le CNRC ne se tient en aucune façon responsable des opinions exprimées par un collaborateur ou des déclarations qui pourrait faire ce dernier. La publication d'annonces publicitaires, d'avis et autres n'implique pas l'endossement de leur contenu par les directeurs du *Journal* ou du CNRC. L'utilisation des noms de marques de commerce ne signifie aucunement une sanction du produit en question ou de la compagnie qui le fabrique.

La correspondance ayant trait aux manuscrits acceptés et les **épreuves corrigés** doivent être envoyées aux Presses scientifiques du CNRC, Conseil national de recherches du Canada, Ottawa, ON K1A 0R6, Canada.

Recommandations aux auteurs sont publiés une fois par année dans le premier numéro de chaque volume. On peut s'en procurer une copie, sur demande, au Bureau de la rédaction, au Bureau des publications et au http://www.nrc.ca/cisti/journals/.

Microfilms : On peut acheter sur microfilms de 16 ou 35 mm tous les numéros depuis 1934. Des photocopies d'articles ou de numéros individuels sont aussi en vente auprès de University Microfilms International, 330 North Zeeb Road, Ann Arbor, MI 48106, É.-U.

This journal is indexed or abstracted in / Ce journal est signalé ou résumé dans
Aquatic Sciences and Fisheries Abstracts, Biological & Agricultural Index, CAB Abstracts (Centre for Agriculture and Biosciences), Chemical Abstracts, Current Awareness in Biological Sciences, Current Contents, FAO Freshwater and Aquaculture Contents Tables, FAO Marine Science Contents Tables, GEOBASE – Geo Abstracts, Meteorological and Geoastrophysical Abstracts, Oceanic Abstracts, Science Citation Index, Biological Abstracts, Environment Abstracts, Environmental Periodicals Bibliography, GEOREF, Life Sciences Collection, and PASCAL Database

Volume 53, Number 11, November 1996

Canadian Journal of Fisheries and Aquatic Sciences

Published by the National Research Council of Canada

Volume 53, numéro 11, novembre 1996

Journal canadien des sciences halieutiques et aquatiques

Publié par le Conseil national de recherches du Canada

Editor / directeur scientifique D.G. Cook

Assistant to the Editor / adjointe au directeur scientifique **M.M. Milne**

Consulting Editor / rédacteur-conseil **P.E.K. Symons** (Victoria, B.C.)

Consulting Editor / rédactrice-conseil **N. Moir** (Nepean, Ont.)

Editorial Board / conseil des rédaction

S.E. Campana, *DFO/MPO, Dartmouth*
E.M.P. Chadwick, *DFO/MPO, Moncton*
L.M. Dickie, *DFO/MPO, Dartmouth*
G.S. Jamieson, *DFO/MPO, Nanaimo*
J.R.M. Kelso, *DFO/MPO, Sault Ste. Marie*
K.R. Munkittrick, *DoE/MdE, Burlington*
J.D. Neilson, *DFO/MPO, St. Andrews*
L.S. Parsons, *DFO/MPO, Ottawa*
R.M. Peterman, *Simon Fraser University*
R.D. Robarts, *DoE/MdE, Saskatoon*
J.C. Roff, *University of Guelph*
D.M. Rosenberg, *DFO/MPO, Winnipeg*
P. Schwinghamer, *DFO/MPO, St. John's*
(Deputy editor / rédacteur adjoint)
C.J. Walters, *University of British Columbia*
W.G. Warren, *DFO/MPO, St. John's*
N.H.F. Watson, *DFO/MPO, Halifax*

NRC Research Press / Presses scientifiques du CNRC

Editor-in-chief / directeur général **Bruce P. Dancik**

Assistant Editor-in-chief / directeur général adjoint **Iain E.P. Taylor**

Publishing Office / Bureau des publications

(Fax / télécopieur : 613-952-7656; e-mail / courrier électronique : research.journals@nrc.ca;
URL: http://www.nrc.ca/cisti/journals/)

Director / directrice **Aldyth Holmes**

Business Manager / gestionnaire des affaires **Paul McClymont**

Production Manager / gestionnaire de la production **Susan R. Strahlendorf**

Senior Publication Officer / agent principal de publication **Mike Boroczki**

Publication Officers / agentes de publication **Jennifer Douglas (613-993-0368), Jennifer McColl (613-993-4500)**

Publication Officer (French manuscripts) / agente de publication (manuscrits français) **Ginette Fortier (613-993-9117)**

Advertising / annonces publicitaires **Hoda Jabbour (613-993-9085)**

Reprints / tirés à part **Judy Heyman (613-993-0151)**

Subscriptions / abonnements **Helen Goulet (613-993-9084)**

© National Research Council of Canada 1996. All rights reserved.

No part of this publication may be reproduced, stored, or transmitted in any form or by any means, without the written permission of the publisher, except as stated below.

The National Research Council of Canada grants **permission*** to individuals to make single copies of articles for personal use. Any person may reproduce short excerpts from articles in the journal for any purpose that respects the moral rights of authors, provided that the source is fully acknowledged. As a courtesy, the consent of authors of such material should be obtained directly from the author.

Authorization to reproduce items for other than personal use, as stated above, is granted by the National Research Council of Canada provided that the copyright fee of $3.00 per copy is paid directly to the Copyright Clearance Center (CCC) Transactional Reporting Service, 21 Congress Street, Salem, MA 01970, U.S.A. 0706-652x/96 $3.00 + 0.00.

*The above permission does not extend to other kinds of copying, such as copying for general distribution, for advertising, or promotional purposes, for creating new collective works, or for resale. For such copying, arrangements must be made with the publisher, National Research Council of Canada, Ottawa, ON K1A 0R6, Canada.

© Conseil national de recherches du Canada 1996. Tous droits réservés.

Il est interdit de reproduire, de sauvegarder ou de transmettre quelque partie de la présente publication dans quelque format ou de quelque façon sans le consentement écrit de l'éditeur, à l'exception des conditions suivantes.

Le Conseil national de recherches du Canada accorde aux particuliers le droit de faire des copies individuelles pour leur usage personnel. Toute personne peut reproduire de courts extraits des articles de la Revue pour autant que les droits moraux de l'auteur soient respectés et que la mention de provenance soit clairement indiquée. Il est de convenance de demander le consentement de l'auteur avant de faire mention de son travail.

On obtiendra l'autorisation de reproduire des articles à d'autres fins que l'usage personnel (tel qu'on l'a décrit ci-dessus) auprès du Conseil national de recherches du Canada pour autant que des redevances de droits d'auteurs de 3,00 $/copie soient versées au Copyright Clearance Center (CCC) Transactional Reporting Service, 21 Congress Street, Salem, MA 01970, U.S.A. 0706-652x/96 3,00 $ + 0,00.

*La permission ci-dessus ne s'applique pas à la reproduction à grande échelle, telle que la reproduction aux fins de distribution générale, publicitaire ou promotionnelle, de compilation de nouveaux ouvrages collectifs ou de revente. Dans de tels cas, il faudra ratifier une entente particulière avec l'éditeur, le Conseil national de recherches du Canada, Ottawa, ON K1A 0R6, Canada.

Subscription information

The *Canadian Journal of Fisheries and Aquatic Sciences* (ISSN 0706-652X) is published monthly by the National Research Council of Canada. 1997 annual subscription rates (second class postage) for Canada are $461CAN institutional and $157CAN personal, for US & foreign $461US institutional and $167US personal. For air mail add $150US to foreign rate. Canadian customers please include 7% GST (GST no. R121491807). In Quebec please add a further 6.5% QST to the total price including GST (QST no. 1006178088). Subscriptions are entered for the calendar year. Remittances should be made payable to the Receiver General for Canada credit NRC. Price for regular single issues: institutional, $60.00; personal, $25.00. Supplements will be priced separately. Special rates apply to members of Canadian scientific and engineering societies if they subscribe through their respective societies.

There are no refunds on cancelled subscriptions once delivery has begun. Claims for missing issues should be made within four months (N. America) or six months (outside N. America) following the date of publication. The publisher expects to supply missing issues only when losses have occurred in transit and when the reserve stock will permit. For change of address and subscription enquiries: Subscription Office, NRC Research Press, National Research Council Canada, Ottawa, ON K1A 0R6, Canada; tel: 613-993-9084; fax: 613-952-7656; e-mail: research.journals@nrc.ca.

Microform backfiles are available from UMI, P.O. Box 1346, Ann Arbor, MI 48106-1346, U.S.A., and Micromedia Ltd., 20 Victoria St., Toronto, ON M5C 2N8, Canada.

Renseignements sur l'abonnement

Journal canadien des sciences halieutiques et aquatiques (ISSN 0706-652X) est une publication mensuelle du Conseil national de recherches du Canada. Le prix de l'abonnement annuel au Canada (courrier de deuxième classe) est de 461 $CAN pour les organismes et de 157 $CAN pour les particuliers. À l'étranger (y compris les É.-U.), le prix de l'abonnement est de 461 $US pour les organismes et de 167 $US pour les particuliers. L'expédition par avion exige des frais de 150 $US en sus du prix d'abonnement à l'étranger. Les clients du Canada doivent ajouter la TPS de 7% (nº de TPS R121491807). Au Québec, il faut ajouter la TVQ de 6,5% au prix total, TPS comprise (nº de TVQ 1006178088). Les abonnements sont pour l'année civile. Tout paiement doit être adressé au Receveur général du Canada, crédit du CNRC. Le prix par numéro est de 60 $ pour les organismes et de 25 $ pour les particuliers. Le prix des hors-série varie. Les membres des sociétés canadiennes de sciences et de génie bénéficient de taux préférentiels en s'abonnant via leurs sociétés respectives.

Aucun remboursement ne sera accordé ni aucune annulation acceptée une fois que les livraisons auront commencé. Les réclamations de numéros manquants devront être soumises dans les quatre mois (Amérique du Nord) ou dans les six mois (à l'extérieur de l'Amérique du Nord) suivant la date de publication. L'éditeur ne fournira de numéros manquants que si le document a été perdu pendant l'expédition et que si le stock le permet. Adressez tout changement d'adresse ou toute question quant à l'abonnement au : Bureau des abonnements, Presses scientifiques du CNRC, Conseil national de recherches Canada, Ottawa, ON K1A 0R6, Canada; téléphone : 613-993-9084; télécopieur : 613-952-7656; courrier électronique : research.journals@nrc.ca.

On peut obtenir les fichiers rétrospectifs sur **microforme** auprès de UMI, P.O. Box 1346, Ann Arbor, MI 48106-1346, É.-U., et auprès de Micromedia Ltée, 20 rue Victoria, Toronto, ON M5C 2N8, Canada.

Role of food web structure on lipid and bioaccumulation of organic contaminants by lake trout (*Salvelinus namaycush*)

Ellen Bentzen, David R.S. Lean, William D. Taylor, and Don Mackay

Abstract: The interacting roles of food web structure and lipid content on bioaccumulation of PCB and DDT in lake trout (*Salvelinus namaycush*) was evaluated in Ontario inland lakes and Great Lakes. It previously has been reported that longer food chains resulted in greater bioaccumulation of PCBs (Rasmussen et al. 1990. Can. J. Fish. Aquat. Sci. **47**: 2030–2038); however, longer food chains also resulted in increased lipid content, and it is uncertain whether the measured bioaccumulation was attributable to food chain length or lipid content. ANCOVA demonstrated that both factors are significant. PCB and DDT concentrations were each proportional to lipid content in all systems but the magnitude of the concentrations varied, due to either food chain length or differences in contaminant loading. It is suggested that the presence of *Mysis relicta* is especially important with respect to the observed food web effects and as a vector for contaminant transport from contaminated sediments. Significant differences between the Great Lakes and inland lakes were identified which largely result from differences in loadings of contaminants. The observed significant relationship between concentrations of PCBs and DDTs suggests that similar relationships could apply to other contaminants with similar chemical and bioaccumulative properties.

Résumé : Les auteurs ont évalué l'effet des interactions entre la structure du réseau trophique et la teneur en lipides sur la bioaccumulation des BPC et du DDT chez le touladi (*Salvelinus namaycush*) dans des lacs de l'intérieur de l'Ontario et dans les Grands Lacs. On avait déjà signalé que plus la chaîne alimentaire est longue, plus les BPC s'accumulent dans les tissus (Rasmussen et al. 1990. J. can. sci. halient. aquat. **47**: 2030–2038); mais aussi, plus elle est longue, plus les lipides s'accumulent dans les tissus de sorte qu'il n'est pas certain si la bioaccumulation mesurée est attribuable à la longueur de la chaîne alimentaire ou à la teneur en lipides. Les analyses de covariance montrent que ces deux facteurs ont de l'importance. Dans tous les réseaux, les concentrations de BPC et de DDT étaient chacune proportionnelles àla teneur en lipides, mais les valeurs qu'elles prenaient variaient soit à cause de la longueur de la chaîne alimentaire, soit à cause de charges différentes en contaminants. Les auteurs formulent l'hypothèse à l'effet que *Mysis relicta* exerce un rôle majeur sur le plan des effets observés qu'on associe à la chaîne trophique et comme vecteur pour le transport des contaminants à partir de sédiments contaminés. Par ailleurs, ils ont déterminé des écarts marqués, issus avant tout de différences dans la charge en contaminants, entre les Grands Lacs et les lacs de l'intérieur. La relation significative existant entre la concentration des BPC et celle du DDP pointe vers des relations semblables avec d'autres contaminants aux propriétés chimiques et de bioaccumulation semblables.
[Traduit par la Rédaction]

Introduction

Geographically proximate lakes should receive similar atmospheric loadings of hydrophobic organic contaminants (HOCs), and this might be expected to result in similar HOC concentrations in fish. However, Rasmussen et al. (1990) noted that PCBs in lake trout (*Salvelinus namaycush*) of Ontario lakes varied from near detection levels (10 ng/g ww) to well above the 2000 ng/g consumption guideline. They suggested that some of this variation was explained by aquatic food web structure. Lakes were divided into three food web classes according to presence or absence of certain planktivores; lakes with these planktivores tended to have lake trout with higher levels of PCBs. Class 1 lakes were those without planktivores and PCBs were low. Pelagic planktivorous fish, including lake herring (*Coregonus artedii*) or rainbow smelt (*Osmerus mordax*), were present in both Class 2 and 3 lakes, the difference between these being the presence of the invertebrate planktivore *Mysis relicta* in Class 3 lakes. Lake trout become piscivorous when larger than 300 mm in Class 2 and 3 lakes, but remain mostly planktivorous in Class 1 lakes (Martin 1966). Planktivores thus provide additional links in the food chains; longer food chains potentially result in increased bioaccumulation of HOCs (Oliver and Niimi 1988; Evans et al. 1991). Elevated toxaphene in lake trout of a subarctic lake recently was suggested to be attributable to food chain length (Kidd et al. 1995).

Using Ontario Ministry of Environment and Energy (OMOEE) published data, Rasmussen et al. (1990) con-

Received March 23, 1995. Accepted May 1, 1996.
J12835

E. Bentzen and D. Mackay. Environmental and Resource Studies, Trent University, Peterborough, ON K9J 7B8, Canada.
D.R.S. Lean. Environment Canada, National Water Research Institute, P.O. Box 5050, Burlington, ON L7R 4A6, Canada.
W.D. Taylor. Department of Biology, University of Waterloo, Waterloo, ON N2L 3G1, Canada.

© 1996 NRC Canada

structed a multiple regression equation for predicting average trout PCB concentration from three independent variables: the three classes, trout percent lipid, and latitude. Latitude was included because lakes further north tend to be less contaminated. The regression was generated on data from 84 inland lakes and 13 Great Lakes sites (included as Class 3) and had an $r^2 = 0.74$.

There are, however, several problems which require resolution if this is to be a valid tool for predicting PCB content of lake trout. As noted by Rasmussen et al. (1990), there was a positive relationship between lake class and trout lipid. This prevented interpretation of how these two variables independently influence PCB concentration. It raises the question of whether increased PCBs of trout from lakes with longer food chains are due to increased lipid because a larger lipid reservoir can result in a greater capacity to retain hydrophobic contaminants (Mackay 1979, 1982). Therefore, the role of increased food chain length in enhancing PCB concentration may be the effect of differences in trout diets resulting in higher lipid.

Two further problems concern inclusion of the Great Lakes with inland Class 3 lakes. There likely are some major differences between the Great Lakes and inland lakes. PCB concentrations in Great Lakes fish seemed both substantially higher than the inland lakes and highly variable (cf. table 1 in Rasmussen et al. 1990). Relative to inland Class 3 lakes, the mean trout PCBs for Lakes Ontario and Huron were nearly threefold and twofold higher, while Superior was similar in magnitude. Point-source loading of PCBs into some Great Lakes may be an important difference relative to atmospherically driven inland lakes. Lake Ontario, for example, is estimated to receive more than 80–90% of PCBs from direct inputs, especially from the Niagara River, but in Superior, less than 5% of PCBs are point source (Baumann and Whittle 1988; Strachan and Eisenreich 1988, *cited in* in Arimoto 1989). Such high direct inputs of PCBs generally result in higher contamination in biota. Furthermore, the Great Lakes food chain may be longer or planktivory more intense due to planktivores not found in the inland lakes (Jensen et al. 1982), which may result in further bioaccumulation of HOCs. Differences between the Great Lakes and the inland lakes thus require further examination.

A fourth issue is the use of "class" as an independent variate in a regression model. Its use imposes a numerical value on what is actually a category, but, for example, Class 3 lakes do not necessarily have a food web effect three times that of Class 1 lakes, and "class" is not normally distributed. All of these problems are readily addressed by use of analysis of covariance (ANCOVA), which allows comparison of the relationship between the predicted variable and independent variables for different groups. If slopes of the relationships are found to be constant for all groups, contrast tests can be constructed specifically to examine differences between groups. In this case, each Great Lake can be assigned as a separate group, to test if there are significant differences both among the Great Lakes and between the Great Lakes and inland lakes for partitioning of HOCs into lipid. We have done this for both PCBs and DDTs to examine how bioaccumulation of different HOCs is influenced by food web effects and differences in loading of contaminants. This approach also permits examination of the role of food web type independent of the consequence of food web on lipid content of trout. This was pursued using a more extensive Ontario lakes data set than was available to Rasmussen et al. (1990). It included more data on Lakes Ontario, Huron, and Superior, a few more data for inland lakes, and data for DDT.

Our objective was to explore in detail, using ANCOVA, the relationship between concentrations of both PCB and DDT as a function of lipid content and food chain structure for inland and Great Lakes in order to better predict contaminant concentrations in lake trout. We examined whether differences in food web structure significantly influence partitioning of HOCs into lipid in ways other than the effect of food webs on lipid content. The finding by Rasmussen et al. (1990) that aquatic food webs directly or indirectly (through alterations in lipid content) influence PCB concentrations of lake trout for lakes subject to atmospheric loading was an important contribution to our understanding of contaminant fate in remote lakes. However, most other models that estimate food chain bioaccumulation of HOCs have been applied to Great Lakes fish (e.g., Thomann and Connolly 1984; Gobas 1994). Because the Great Lakes food webs are complex, it is not an easy task to quantify how differences in diet influence the degree of bioaccumulation of HOCs by a top predator, although it is frequently considered to be responsible for variations in fish HOC content. The inland lakes provide different food webs that remain distinct from one another. Another goal was to evaluate whether the Great Lakes are different from inland lakes with respect to fate of contaminants. Differences between the inland lakes and Great Lakes as well among the Great Lakes were explored using ANCOVA plus some analysis of variance (ANOVA).

Methods

The data used are from the Ontario Sport Fish Contaminants Monitoring Program of Ontario Ministries of Natural Resources (OMNR) and OMOEE. Skinless, boneless dorsal portions of sport fish collected from a variety of lake and river sites were analyzed for selected HOCs. Further sampling and analytical details are available in OMOEE (1986) and McMurtry et al. (1989). In brief, analyses for PCBs and DDTs were performed by the Water Resources Branch (OMOEE) using a Hewlett-Packard 5700 gas chromatograph with packed glass column and ^{63}Ni electron capture detector (Crawford and Brunato 1978; Rees et al. 1979–1980). Percent lipid, fish length, and mass were recorded. Results of this survey are summarized in the *Guide to Eating Ontario Sport Fish* (OMOEE and OMNR 1993–1994). Data used by Rasmussen et al. (1990) were from a published report of mean total PCBs per lake (Crawford and Brunato 1978; Rees et al. 1979–1980). In our study, HOC data of individual fish from a larger number of inland Ontario lakes and Great Lakes sites were obtained directly from OMOEE. PCBs and the sum of DDT and its metabolites (ΣDDTs) are reported for lake trout. (The data are available from the authors; an ASCII file will be forwarded upon receipt of a PC-formatted diskette.)

For each lake, lake averages for the following variables were calculated: lake trout percent lipid, length, summed DDT (ΣDDT= *pp*DDE + *op*DDT + *pp*DDD + *pp*DDT), total PCBs, and lipid-normalized total PCBs and ΣDDT. The number of fish per lake varied from 2 to 61 individuals, but 5–20 fish were usually analyzed. The term "average" refers to the mean estimated within a given lake; "mean" refers to means estimated for a group of lakes or for several sites within one of the Great Lakes. There were occasional missing data; for example, DDT was not always determined. Averages from 21, 15, and 52 sites in Lakes Ontario, Huron, and Superior were cal-

© 1996 NRC Canada

culated. Some of these were from different years at the same site. A single average value for Lake Michigan used in the analysis by Rasmussen et al. (1990) was not included in these statistical analyses because its value of 10 590 ng/g (ww) PCBs was 3 times greater than any other means. Thus, it had undue influence on the regression analyses and, as a single value, had no variance for ANOVA or ANCOVA.

Classification of lakes as to pelagic community type were obtained from Rasmussen et al. (1990), from OMNR files (fish species), or from Dadswell (1974) (presence/absence of mysids). To examine the roles of either more complex food web structures or of different loading of HOCs into the Great Lakes in these analyses, the Great Lakes (GL) were treated either as separate lake classes or were included with the inland Class 3 lakes.

Statistical analyses

Statistics were done with SYSTAT (Wilkinson 1990) and Quattro Pro (Borland International, Inc., California). Lake averages were log-10 transformed because they demonstrated nonnormal distributions and heterogenous variances for the inland lakes. Geometric means were back-transformed for reporting. Predicted values from ANCOVA were back-transformed following correction for bias from conversion of log-to-ordinary scales (Zar 1968; Sprugel 1983).

ANCOVAs were used to isolate effects of food web type by using lipid content of trout as a covariate. No heterogeneity of slopes between concentration and percent lipid was observed. Common slopes and intercepts then were computed using the predicted values generated by the ANCOVA model. ANCOVAs for PCB versus lipid by class-group were performed using the six groups as well a three-class grouping in which the GL were included as part of the inland Class 3 lakes. Sums-of-squared residuals (SSR) were estimated for each class-group for comparison of combining the GL as part of Class 3 versus treating them as separate groups. SSR were divided by their respective n for comparison of goodness-of-fit between groups. ANCOVAs were also performed for ΣDDT versus lipid, ΣDDT versus PCB, and PCB versus length, all by class-group. Orthogonal contrast tests followed the ANCOVAs to test for differences among the intercepts of the different groups. The orthogonal contrast test for PCB versus lipid and PCB versus length, both by class-group, followed the five tests described below; tests used for the other two ANCOVAs will be described with the results.

A multiple regression was computed for PCB as a function of percent lipid and lake class, where the GL were part of Class 3. SSR were computed for comparison with the SSR from the ANCOVA models.

Residuals and residual diagnostics were generated by SYSTAT for each model to identify significant outliers with undue influence on the model. One lake from each of Class 1 and Class 2 was deleted from the analyses, as well as two points from the Lake Superior data set. These two lakes were anomalous with respect to their percent lipid (11.6% for Redpine and 0.8% for McCarthy, Class 1 and 2, respectively), and the two Superior sites had very low mean PCBs relative to the remaining 50 Superior means (data shown in figures). In addition, Lake Clear (Class 3; 45°26′N, 77°12′W) was not included in analyses for PCBs because high levels of PCBs were the result of transformer oils being used on local roads (MacDonald et al. 1992).

ANOVAs were performed on six groups: the three inland lakes classes and Lakes Ontario, Huron, and Superior each as a separate group. ANOVAs were followed by orthogonal contrast tests, allowing five tests among the six groups. This was done to establish differences for percent lipid, length, and lipid-normalized PCBs and DDTs. With five degrees of freedom, there are several possible orthogonal contrast design matrices, but all must follow specific rules and only one matrix must be chosen (Cochran and Cox 1957). The following five orthogonal tests were done each for percent lipid and length: (1) lack of planktivores (Class 1) versus presence of planktivores (all other groups), (2) among lakes with planktivores, lack of mysids (Class 2) versus presence of mysids (Class 3 and GL), (3) inland lakes with mysids (Class 3) versus GL, (4) Lake Ontario versus Huron and Superior, and (5) Lake Huron versus Superior. Note that once a group is targeted in an orthogonal contrast, it is excluded in subsequent contrasts, which is why it is possible to construct alternative orthogonal design matrices. The number of tests is limited to the degrees of freedom from the overall ANOVA. This circumvents the problem of type I or II errors from multiple unplanned comparisons (Day and Quinn 1989). For ANOVA on lipid-normalized PCBs and DDTs, an alternative contrast matrix to the one described above was used because some of the GL means were lower than the inland lakes and a matrix was chosen to better discriminate differences which likely result due to differences in loadings of these contaminants. The design used will be described with the results.

Fig. 1. Distribution of lake-average PCB in lake trout versus latitude for the three classes of inland lakes and the three Great Lakes used in this analysis.

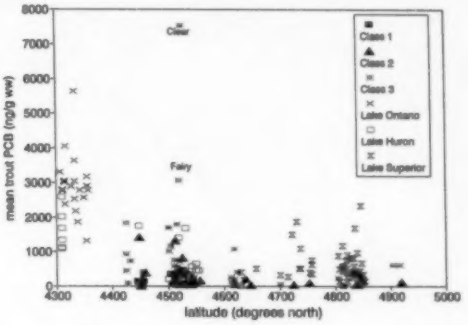

It is likely that lake averages estimated from few fish are a poor representation of the actual population mean. Checks were performed to detect if lake averages based upon less than 9 fish had undue influence or were outliers in the ANCOVA regressions. ANCOVAs were repeated including lake averages estimated from 9+ fish and the results were the same relative to those based upon the entire data set. A comparison was made on the SSR (divided by n) for the observed PCB lake averages versus predicted values estimated from percent lipid within class for each of the averages based upon 9+ or <9 trout. Lake averages estimated from 9+ trout for Class 2 lakes lied closer to the regression line (lower SSR), since a couple of lake averages based upon fewer fish were potential outliers. On the other hand, the SSR for 9+ trout for Class 3 lake averages was somewhat higher than for the <9 trout averages, apparently due to more fish being collected from some lakes of known higher contaminant levels (also larger lakes). Overall, in all three classes, most of the lake averages estimated from either 9+ or <9 trout were evenly distributed along the regression line and it was concluded that there was no reason to exclude averages estimated from fewer fish.

Results

Most inland lakes sampled for lake trout PCBs and DDTs were in central Ontario south of 46°N and between 76 and 80°W; this region included lakes with the highest PCBs and ΣDDTs (Fig.1, shown for PCBs). Lake-average PCB concentrations in trout ranged from detection limits (10 ng/g ww) to >3000 ng/g ww (Figs. 1 and 2); lake-average ΣDDT ranged to 6900 ng/g ww (Fig. 3). With exception of contaminated Lake Clear, Fairy Lake (45°20′N, 79°11′W) trout had the highest average PCBs among the inland lakes. Individual fish in this lake ranged as high as 8900 ng/g ww (70-cm trout),

© 1996 NRC Canada

Fig. 2. Relationship between PCBs and percent lipid (both log-10 transformed) for (A) the actual lake averages and (B) the results of the ANCOVA fit of PCB on percent lipid, scaled for each group. All groups were significantly different with respect to their intercepts, except for Lake Superior and Class 2 inland lakes.

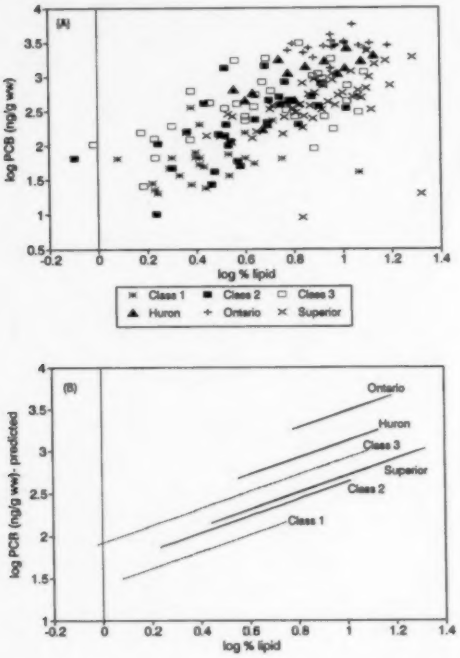

Fig. 3. Relationship between ΣDDTs and percent lipid (both log-10 transformed) for (A) the actual lake averages and (B) the results of the ANCOVA fit of ΣDDT on percent lipid, scaled for each group. When all data are included, all groups were significantly different with respect to their intercepts, except for Lake Ontario and Class 2 inland lakes. Some lakes are indicated where it is possible that DDTs were in their watersheds (see text); when these lakes are excluded in ANCOVA, the intercept for Class 3 lakes was not different from Class 2 and Lake Ontario.

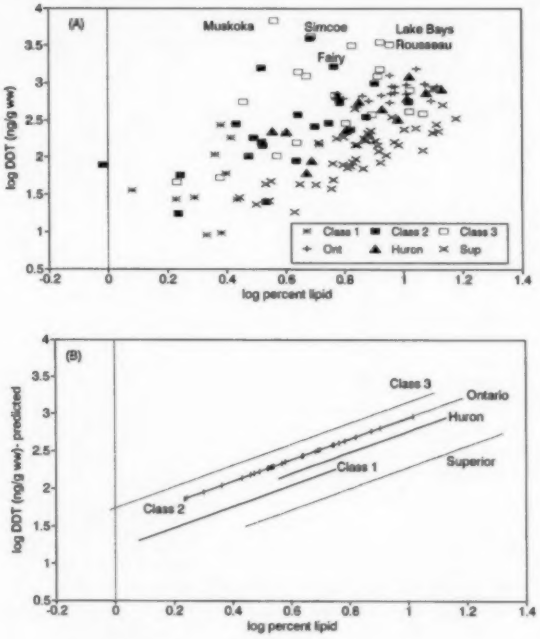

overlapping levels in Lake Ontario trout. High ΣDDT levels were observed in Lake Muskoka (45°00′N, 79°25′W) and other nearby lakes, with individual trout concentrations in excess of 50 000 ng/g ww (90-cm trout). DDT was used in the Muskoka lakes region, and possibly elsewhere, between the 1940s and 1968 (Boelens and Rumsey 1972); some of these lakes are indicated in Fig. 3.

ANCOVA regression results

Using lipid as covariate demonstrated that there was a consistent relationship between PCB and lipid content of trout among the three lake classes and the three GL ($r^2 = 0.73$, $p < 0.00001$; Table 1), but there clearly was an additional effect of food web or contaminant loading on PCB concentration. The relationship between PCB and lipid was the same among all groups (common slope of 1.09 for log PCB on log percent lipid). Differences among groups were demonstrated by the different intercepts obtained among the inland lake classes and Lakes Huron and Ontario ($p < 0.001$), although Superior was similar to Class 2 (Table 1; Fig. 2). ANCOVA among inland lake classes excluding GL produced a lower r^2 (0.52) but the same common slope and intercepts similar to those obtained when the GL were included (Table 1). Inclusion of GL does not improve the relationship between PCBs and percent lipid among the inland lakes even though the overall r^2 was higher. The unexplained variance among the inland lakes is the same whether or not the GL are included in the model, demonstrated by similar SSR obtained in ANCOVAs for the three inland lake classes with and without GL (Table 1). It also shows that the unexplained variance among the inland lakes is fairly high.

Combining GL with Class 3 inland lakes increased unexplained variance (higher SSR) for the large Class 3 group (ANCOVA, $r^2 = 0.61$; Table 1). This would be due to combining significantly higher GL PCBs with the mean for Class 3 inland lakes. The ANCOVA-derived common slope was higher and the intercepts lower than those obtained by the six-group estimate. Similarly, a multiple regression derived using three groups does not perform as well as the six-class ANCOVA model, with inflated SSR. A multiple regression model derived from six groups is not really possible because it is not a simple matter to a priori determine the ranking of "class" for each of the GL.

The relationship between ΣDDT and percent lipid was consistent among the groups, similar to PCBs, with different intercepts ($p < 0.00001$). The common slope of 1.42 was higher relative to PCB/lipid and the pattern of intercepts was different (Table 2; Fig. 3). Intercepts increased among the three inland lakes classes ($p = 0.01$–0.05), but were lower for the GL. The contrast tests demonstrated that Lake Superior had the lowest intercept ($p < 0.0001$) and the intercept for Lake Huron was lower ($p = 0.03$) than Lake Ontario and

© 1996 NRC Canada

Table 1. Intercepts and common slopes for PCB versus percent lipid (log-transformed data) for various ANCOVA models, as indicated.

	n	Intercept	SSR
Six groups: ANCOVA, $r^2 = 0.73$			
Class 1	23	1.37	0.08815
Class 2	28	1.57	0.18135
Class 3	36	1.85	0.13603
Ontario	19	2.38	0.02016
Huron	15	2.04	0.06334
Superior	50	1.69	0.03682
Common slope = 1.09			
Inland lakes only: ANCOVA, $r^2 = 0.52$			
Class 1	23	1.40	0.08372
Class 2	28	1.61	0.19054
Class 3	36	1.90	0.13378
Common slope = 1.03			
GL included as Class 3: ANCOVA $r^2 = 0.61$			
Class 1	23	1.32	0.08975
Class 2	28	1.50	0.17763
Class 3	36	1.80	0.14208
Ontario	19	1.80	0.24718
Huron	15	1.80	0.08269
Superior	50	1.80	0.07951
Common slope = 1.21			
Multiple regression model: $r^2 = 0.61$			
Class 1	23		0.09055
Class 2	28		0.17930
Class 3	36		0.14205
Ontario	19		0.25168
Huron	15		0.08415
Superior	50		0.07748

Note: In each ANCOVA, slopes were found not to be significantly different ($p > 0.05$). Sum-of-squared residuals (SSR) were computed for each group and divided by their respective number (n). For models where the Great Lakes (GL) were part of the inland Class 3 lakes, the SSR were separated for the Class 3 inland lakes and each GL for comparison with the other models. SSR for the multiple regression model where the GL were included with inland Class 3 lakes are also given.

inland Class 2 and 3 lakes. The intercept for inland Class 3 lakes was the highest of all groups ($p = 0.03$). Lake Ontario was similar to Class 2 inland lakes ($p = 0.99$) and these are represented by one line in Fig. 3B.

Although not flagged as significant outliers by residual analyses, there are several inland lakes with substantially higher average ΣDDT which might influence the observed common slope (Fig. 3A). To investigate this possibility, we eliminated seven Class 3 and two Class 2 lakes (identified in Table 2) from the data and repeated the ANCOVA. There was a 10% increase in r^2, and the intercepts for both Classes 2 and 3 were reduced (Table 2). Contrast tests demonstrated that Class 3 no longer had a higher ($p > 0.8$) intercept relative to Class 2 and Lake Ontario. The common slope was still similar to that obtained including all data.

Differences in percent lipid could be due to differences in average length, and length possibly substituted for percent lipid in the PCB or DDT model. Lipid varied with length (ANCOVA, $r^2 = 0.49$, $p = 0.00001$) with a striking difference between intercepts for the inland lake classes and the GL, demonstrating greater lipid per unit length by GL trout (Fig. 4). Because differences in average length varied little among the groups (Table 3), PCB covaried with length ($p = 0.0002$), but $r^2 = 0.63$ was 10% lower than for ANCOVA of PCB on percent lipid (Table 2; Fig. 5). The same slope was obtained among the groups ($p = 0.81$) with different intercepts ($p < 0.00001$; Table 2). Orthogonal contrast tests demonstrated incremental increases in intercept among the inland lake classes ($p < 0.00001$), with Ontario being higher than Huron and Superior ($p < 0.00001$), but with Superior less than Huron ($p = 0.009$; Table 2) and similar to Class 3.

There was a highly significant linear relationship between ΣDDT and PCB ($r^2 = 0.86$, $n = 133$; Fig. 6). ANCOVA (six groups) for ΣDDT versus PCB resulted in differences among

© 1996 NRC Canada

Table 2. Intercepts and common slopes for three six-group ANCOVA models: DDT versus either percent lipid (all lakes and with some lakes deleted) or PCB, and PCB versus length (all data log-10 transformed).

	DDT – % lipid (all data)		DDT – % lipid (lakes deleted)		DDT–PCB		PCB–length	
	n	Intercept	*n*	Intercept	*n*	Intercept	*n*	Intercept
Class 1	12	1.19	12	1.17	13	–0.24	22	–0.58
Class 2	20	1.53	19	1.38	20	–0.083	29	–0.27
Class 3	23	1.74	16	1.45	23	–0.093	36	0.079
Lake Ontario	18	1.53	18	1.48	19	–0.81	21	0.93
Lake Huron	13	1.34	13	1.30	12	–0.59	15	0.48
Lake Superior	45	0.86	45	0.82	46	–0.73	52	0.21
ANCOVA, r^2 (n)	0.62 (131)		0.72 (122)		0.86 (133)		0.63 (175)	
Common slope	1.42		1.48		1.07		1.43	

Note: ANCOVAs shown here were highly significant ($p < 0.00001$); r^2 and the total number of data (n) are shown for each. The lakes deleted from the second ANCOVA for DDT–lipid are Haliburton and Chandos (Class 2), Fairy, Vernon, Muskoka, Lake of Bays, Skeleton, Rosseau, and Simcoe (see text for details).

Fig. 4. ANCOVA of trout percent lipid and length of lake trout for the three Great Lakes and three inland lakes classes.

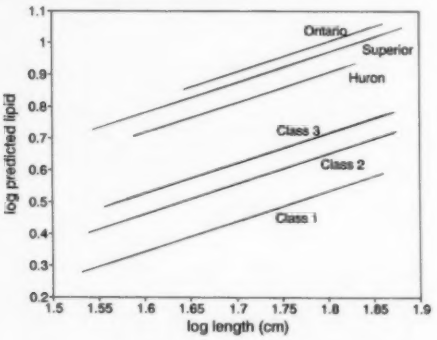

Fig. 5. Relationship between PCBs and length (both log-10 transformed) for the ANCOVA-predicted fit. The intercepts for Lake Superior and Class 2 inland lakes are not significantly different.

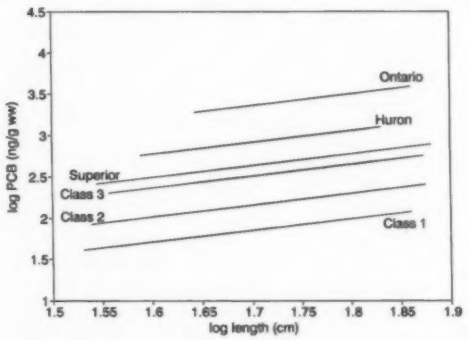

groups for intercepts ($p < 0.00001$) and equal slope ($p = 0.39$). Orthogonal contrast tests on intercepts first compared inland lakes against GL and then tested among inland lake classes (excluding GL) and among the GL (excluding inland lakes). The intercepts for the inland lake classes and GL were different ($p < 0.00001$): those for all GL fell below the intercepts for the inland lakes (Table 2). This indicates a lower ratio of ΣDDT to PCB for the GL, or conversely, higher DDTs in the inland lakes. There was a marginally different intercept between Class 1 and Classes 2 and 3 ($p = 0.06$) and no difference between Classes 2 and 3 ($p = 0.89$). The intercept for Lake Huron was higher than Ontario and Superior ($p = 0.01$), while those for Lakes Ontario and Superior were similar ($p = 0.63$).

ANOVA results on geometric means among groups

The increase in percent lipid was significant from Class 1 through 3 inland lakes and was higher still in all three GL. There was no difference between Lakes Huron and Superior in percent lipid ($p = 0.34$), which was marginally lower than for Ontario ($p = 0.06$). Class 1 lake trout were shorter than those from the other groups ($p < 0.00001$). Lake Ontario trout were slightly longer than trout from Lakes Huron and Superior ($p = 0.03$) and similar to trout from Class 3 inland lakes (Table 3).

Discussion

Our results clarified that the role of food web on bioaccumulation of PCBs and DDTs was additional to the influence of food web on lipid content of trout of inland lakes. Separate from the role of food web, it was demonstrated that there are important differences between lakes which probably reflect differences in loading of PCBs or DDTs. The relationship between PCBs or ΣDDTs and percent lipid was consistent across diverse systems because the slopes of the log-transformed HOC–lipid relationships were the same across all groups. What distinguishes the inland lake classes and the Great Lakes are their intercepts (Figs. 2 and 3), which represent the effects of food web and/or loading of contaminants. Because the relationship between PCBs and DDTs also was

© 1996 NRC Canada

Table 3. Geometric means (reverted to ordinary scale), range, and contrast test results estimated for the three inland lakes classes and Lakes Ontario, Huron, and Superior.

	Inland lakes			Great Lakes		
Parameter	Class 1	Class 2	Class 3	Lake Ontario	Lake Huron	Lake Superior
Percent lipid						
Mean	2.6	4.0	4.8	9.3	6.8	7.8
Range	1.2–5.7	1.7–10.4	1.0–12.3	6.0–15.4	3.6–13.5	2.8–21.0
Contrast prob.	*****	*****	*****	0.06	0.34	
n	23	28	36	19	15	52
Length (cm)						
Mean	47.0	55.1	57.4	57.7	52.7	52.2
Range	34.0–72.5	34.6–75.0	36.0–74.6	44.0–72.5	38.8–67.7	35.0–76.1
Contrast prob.	****	0.96	0.12	*	0.83	
n	23	28	36	21	15	52
PCB/lipid (μg/g)						
Mean	2.4	4.3	8.3	29.8	13.1	5.1
Range	0.4–15.1	0.6–40.6	1.2–47.1	14.7–50.8	3.6–32.0	0.1–18.5
Contrast prob.	**		*****	*****	****	**
n	23	29	36	19	15	52
ΣDDT/lipid (μg/g)						
Mean	1.3	3.4	5.5	3.4	2.2	0.7
Range	0.1–7.9	0.4–42.8	1–110	1.6–5.6	0.7–5.3	0.2–2.9
Contrast prob.	***	0.9	***	0.18		*****
n	14	19	24	20	13	46

Note: Lipid-normalized DDT were calculated as the ratio of ΣDDT to percent lipid raised to the power of 1.4, derived from the slope of the relationship between DDT and percent lipid (log-transformed). Significant differences from orthogonal contrast test results (see text for details) are indicated by asterisks; nonsignificant differences are indicated by the probability (prob.): *****differences significant at $p < 0.000001$; ****differences significant at $p < 0.00001$; ***differences significant at $p < 0.0001$; **differences significant at $p = 0.001$–0.01; *differences significant at $p = 0.01$–0.05. Note for six groups that there are five possible tests: thus, no significance level is indicated for one group in each case.

constant across diverse systems (Fig. 6), these results could be indicative of other contaminants with similar general chemical properties and tendencies to bioaccumulate.

When the log-based regressions are back-transformed, the intercepts become the slopes of the relationships between contaminant and lipid. Hence, the actual untransformed PCB or ΣDDT relationship against lipid varied as a function of food web or variations in loading (Figs. 7 and 8). In the case of PCBs, because the log-based relationship had a slope of 1, the untransformed relationship is linear, but for DDTs with the log-based slope of 1.4, the untransformed relationship is exponential.

Partitioning of PCBs or ΣDDTs into lipid was influenced separately by food webs and variations in loading rates. Class 1 lake trout, on average, did not grow as large or produce as much lipid as trout from either Class 2 or 3 lakes, probably due to a largely planktivorous diet (Martin 1966; Kerr 1971). They also bioaccumulated both PCBs and DDTs to a lower extent. Lake trout in lakes with mysids tended to produce more lipid but also bioaccumulated PCBs and DDTs per unit lipid to a greater extent, evident by higher slopes for Class 3 relative to Class 2 lakes (Figs. 7 and 8). Effect of loading relative to food web type on bioaccumulation was demonstrated by comparison of bioaccumulation of PCBs or DDTs into lipid between Class 3 inland lakes and the three Great Lakes. PCBs in Lake Ontario lake trout bioaccumulated to a much larger extent relative to all other groups, probably reflecting the significant inputs of PCBs from the Niagara River. DDTs, on the other hand, bioaccumulated to an extent comparable with Class 2 inland lakes. In Lake Superior, bioaccumulation of PCBs was similar to inland Class 2 lakes despite higher percent lipid, higher mean PCB, and a Class 3 food web structure (Fig. 7), while bioaccumulation of ΣDDTs was lower than any other group (Fig. 8). Superior is slightly further north than the majority of the sampled inland lakes (Fig. 1) and may receive lower atmospheric deposition of PCB or DDTs. Swackhamer et al. (1988), however, observed higher levels of HOCs both in water and in lake trout from Siskiwit Lake, situated on an island in Lake Superior. These observations suggest that the larger volume of Superior further reduced bioaccumulation of HOCs. Inland Class 3 lakes displayed the greatest bioaccumulation of ΣDDT, reflecting lakes which probably had direct applications of DDT in their watersheds.

These contaminants result from a range of loading rates from atmospherically driven (inland lakes, Lake Superior) to

© 1996 NRC Canada

Fig. 6. Relationship between ΣDDT and PCBs (both log-10 transformed) for the inland lakes and the three Great Lakes. All three Great Lakes fall significantly below the three classes of inland lakes, indicating a lower amount of ΣDDT relative to PCBs in their lake trout.

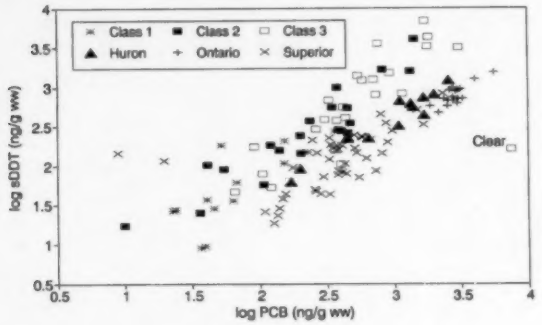

Fig. 7. Predicted PCBs after back-transformation from the log-10-based relationship. The common slope from the log-based ANCOVA regression was 1; hence the slopes shown here are linear.

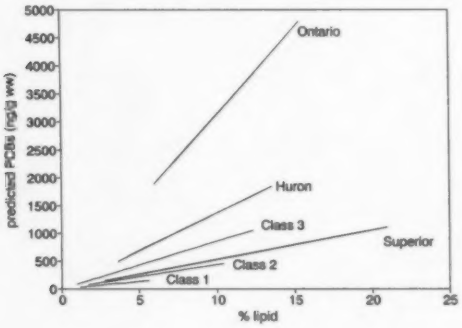

combined atmospheric and point source (Lakes Ontario and Huron; Eisenreich et al. 1981; Hoff et al. 1992). Estimated atmospheric inputs of PCBs and DDTs are, respectively, about 10 and 50% to Lake Ontario, 80 and 90% to Lake Huron, and more than 95% of each to Lake Superior (Strachan and Eisenreich 1988, *cited in* Arimoto 1989). Lake Clear, as the only inland lake trout lake of known significant point-source PCB loading, was extreme in the PCB – percent lipid (Fig. 2) and PCB–ΣDDT (Fig. 6) relationships. With such a range of external and internal influences on rate of partitioning of PCBs and DDTs into lipid, it is likely that the relationships derived here are universal: what will vary is the overall magnitude (i.e., the intercept of the log–log relationship). Data for lake trout from other regions should be comparable with these results with some understanding of sources of PCBs or DDTs into the lakes.

Rasmussen et al. (1990) included latitude as an independent variable in their multiple regression equation, but this was significant because of high values for Lakes Ontario and Michigan at the southern latitude extreme and few values for Lakes Huron and Superior. Without the Great Lakes, latitude was not a significant variable in average PCB concentrations

Fig. 8. Predicted DDTs after back-transformation from the log-10-based relationship. The common slope from the log-based ANCOVA was 1.42; hence the slopes shown here are exponential.

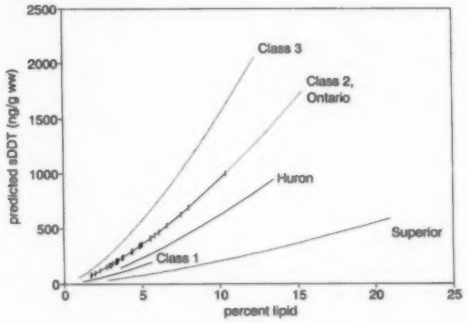

among the inland lakes, probably because most of the sampling effort for lake trout organic contaminants was in south-central Ontario (Fig. 1). Latitude also was not significant with the larger Great Lakes data available for these analyses because of fairly high values for Lakes Huron and Superior. Perusal of the data does suggest that inland lakes further removed from the Great Lakes industrial area are less contaminated, but this includes lakes further east and west as well as further north. Therefore, geographic variability is probably important but cannot be accounted for by these data.

It is a common practice to compare among effects using lipid-normalized HOCs, although there has been debate over its interpretation and utility (Borgmann and Whittle 1992; Hebert and Keenleyside 1995). Lipid-normalized PCBs or DDTs are simply the slopes of untransformed relationships between contaminant and percent lipid for each group which are derived from the intercepts of the log-transformed relationship. Thus, the relationship $\log(\text{PCB}) = B_0 + B_1 \cdot \log(\text{lipid})$, where B_0 is the intercept, and the slope $B_1 = 1$ for PCB, becomes $\text{PCB} = B_0 \cdot (\text{lipid})^1$ and $\text{PCB/lipid} = B_0$ when untransformed. Because the slope for DDT was 1.4, percent lipid is adjusted by the exponent 1.4 prior to normalizing DDT data. Lipid-normalized data are shown in Table 3; note that a factor of 10 difference from the log intercept data in Tables 1 and 2 when back-transformed is due to expression of normalized data as micrograms HOC per gram lipid. Patterns between the groups and the results of ANOVA on lipid-normalized data were the same as the contrast tests on the intercepts from the ANCOVAs (Table 3; Figs. 7 and 8).

Lipid-normalized data (or ANCOVA intercepts) are suitable for comparisons between populations, such as different lakes or within the Great Lakes over time. For the inland lakes, different food webs result in populations that are significantly different in lipid content, but additionally have differing degrees of bioaccumulation of HOCs attributable to food web type. When comparing between populations with similar food web structure (Class 3 inland lakes, Great Lakes, Lake Clear), the lipid-normalized HOCs show where loadings are different. This cannot be done for individual fish because lipid content varies due to differences in individual activities or foraging success (e.g., see Borgmann and Whittle 1992), but which are averaged out over populations.

© 1996 NRC Canada

Lake trout collected from lakes elsewhere may be compared with these data by comparing lake-average lipid-normalized PCBs or DDTs and average percent lipid. For example, if the food web status of a remote lake is not known, but lake trout observed to have both their percent lipid and HOC per unit lipid comparable with the values reported here for Class 3 inland lakes, it would suggest some form of similarly long food chain and an atmospheric source of contaminants. Higher lipid-normalized PCBs but similar percent lipid values could be indicative of a higher loading rate of PCBs into the lake in question, while lower lipid-normalized HOCs would suggest lower loading rates, etc.

The recognition by Rasmussen et al. (1990) that different aquatic food web structures for lake trout influence bioaccumulation of organic contaminants in lakes subject to no known point-source inputs of HOCs remains an exceedingly important contribution to our understanding of these processes. The multiple regression equation they developed was useful in identifying food web influences on PCBs in lake trout, but cannot be used as a quantitative tool, for both mechanistic and statistical reasons. There is no justification for combining Great Lakes with inland lakes because they have significantly different PCBs, ΣDDT, percent lipid, and size relative to the inland lakes and among each other. Means for DDT were actually lower than inland lakes despite higher lipid and larger size. The percent lipid versus length (Fig. 4) was distinctly different in all three Great Lakes relative to the inland lakes, suggesting important differences in the diets of the lake trout. There are fish species such as alewife (*Alosa pseudoharengus*) which are prey for lake trout in the Great Lakes but are absent in most inland lakes (Scott and Crossman 1973; Jensen et al. 1982). Another problem with the multiple regression is that class is used as a discrete variable but has no real numeric value, which is imposed upon it in multiple regression, but not in ANCOVA.

The influence of aquatic food web structure thus is clearly important, but is an initial step in identifying biological mechanisms behind fate of contaminants. The variability among the inland lakes divided into three food web classes was large. Class 2 lakes were identified as lakes with populations of deepwater planktivorous fish. However, not all the same planktivores may be present, and could include lake whitefish (*Coregonus clupeaformis*), brook trout (*Salvelinus fontinalis*), lake herring, and/or rainbow smelt. Not all lakes with mysids (Class 3) resulted in highly contaminated or fatter lake trout. Thus, there may be variable roles of planktivores as diet items and vectors for contaminants into lake trout. Presence or absence of certain planktivores does not describe intensity of predation along the food chain or their importance in the diet of lake trout. Several studies have reported variable diets as responsible for variations in contaminants of Great Lakes salmonids (Delfino 1979; Jensen et al. 1982; Borgmann and Whittle 1991).

Variations in planktivore predation intensity on zooplankton could have important consequences on initial fate of HOCs in the water which could influence their transfer up the food chain. Taylor et al. (1991) demonstrated an inverse relationship between HOC concentration in zooplankton and zooplankton biomass of Ontario lakes. For PCBs, 71% of their variation was explained by this relationship. Concentrations of PCBs and ΣDDTs in the zooplankton ranged from 0.1 to 2.6 ng/g ww and from 3 to 37 ng/g ww, and zooplankton biomass from 100 to 1100 μg/L ww (note biomass units in Taylor et al. 1991 should read g/m^3 dw). Thus, substantial differences in zooplankton biomass and degree of HOC contamination may be observed. Grazing by mysids has been frequently documented to have a major effect on structuring zooplankton biomass and size relative to grazing by planktivorous fish (e.g., Lasenby et al. 1986; Nero and Sprules 1986; Sprules and Bowerman 1988; Langeland et al. 1991; Lasenby 1991). Large, slow-moving cladoceran zooplankton tend to be the most susceptible to intense planktivory (Beattie and Clancey 1991; Richards et al. 1991). There was a trend to reduced zooplankton biomass and mean size in Class 3, and to a lesser extent in Class 2, relative to Class 1 lakes observed in a recent survey of 23 Ontario lakes (Almond et al. 1996), but biomass among the Class 3 lakes was variable. Both Class 2 and 3 lakes may have variations in planktivorous fish abundance and hence predation rates from that source, and *Mysis* may not be equally important predators among Class 3 lakes. This underscores the problem with classification based upon presence/absence of organisms; presence is no indication of impact on the food web.

It is possible that planktivore grazing, by altering biomass and hence zooplankton contaminant concentrations, plays an important role in the transfer of HOC from water to lake trout. Lower zooplankton biomass with higher HOC levels in that biomass of lakes with abundant planktivores could be a cause behind enhanced bioaccumulation of HOCs in predatory fish. The energy costs to the consumer in obtaining food when it is small are greater than when it is large (Kerr 1971). Thus, not only do zooplankton contain higher contaminant levels in high-planktivore lakes, but a larger biomass of zooplankton is required for the same amount of growth relative to a fish diet for the lake trout. It is interesting to note that zooplankton biomass is extremely low in Lake Ontario, with a very small contribution from larger species such as *Daphnia* (Lean et al. 1990; Mazumder et al. 1992), and salmonoid species PCB levels remain high (Borgmann and Whittle 1991, 1992). Fairy Lake also has a very low zooplankton biomass (Almond et al. 1996) and the highest trout PCB concentrations (Fig. 1), yet the ratio of ΣDDT to PCB did not indicate that Fairy was an outlier with point-source PCB loading. It might be possible to describe lakes based upon an index of zooplankton biomass and size structure instead of the three-level lake food web classification. It is not easy to determine if *Mysis* and/or pelagic forage fish are actually important in any given lake, but it is fairly simple to measure zooplankton biomass and size distribution, and hence determine impact by planktivores.

Because lake sediments are ultimately a reservoir for deposited contaminants (Baker and Eisenreich 1989; Mackay 1989), another unique role of mysids may be as a vector for contaminant transport into the water column. *Mysis* feed upon bottom- sediment-associated materials during the day and migrate at night into the pelagic to feed upon plankton (Lasenby et al. 1986; Johannsson 1992). Lester and McIntosh (1994) demonstrated that mysids in contact with contaminated Lake Champlain sediments accumulated more PCBs than those with restricted access to sediments. Mysids also have been implicated as a likely sediment to water vector for transport of lead (Evans and Lasenby 1983), zinc and cad-

© 1996 NRC Canada

mium (Van Duyn-Henderson and Lasenby 1986), and a PCB (Klump et al. 1991). Klump et al. (1991) pointed out that the top 2–4 cm of sediments contain approximately 20–40 yr of deposition of HOCs and thus benthic organisms could be in contact with contaminated sediments for many years to come. Planktivorous juvenile trout up to 3 yr of age may feed extensively on mysids (Trippel and Beamish 1989), and adult trout prey upon mysids (Lasenby et al. 1986; Bowles et al. 1991; Langeland et al. 1991). Delfino (1979) suggested that benthic invertebrates could be responsible for more than 50% of PCB concentration in Lake Michigan lake trout. This link to sediments may help explain the high DDT concentrations observed in some of the Class 3 lakes where DDTs may have been applied to their watersheds 10–15 yr prior to collection of the lake trout.

There are many useful observations from these analyses, but there are also points that remain to be examined to determine factors behind the unexplained variation in HOC bioaccumulation among inland lakes. However, these results demonstrate a consistent relationship between PCBs or DDT and percent lipid (same slope on log–log relationship) that varied as a function of food web type or contaminant loading rates that was additional to the effect of food web on lipid content. Because of unresolved differences influencing concentration and fate of contaminants in the three Great Lakes examined here, they must be treated independently. We have shown that population-based percent lipid and lipid-normalized HOCs are indicative of overall food web and loading effects. We suggest that intensity of planktivore predation may be a driving force behind initial rates of bioaccumulation of HOCs, and that *Mysis relicta* may play several important roles in contaminant fate by reducing zooplankton biomass and as a vector from contaminated sediments into the pelagic, which merits further study.

Acknowledgements

Support came from the Research Advisory Council (OMOEE) to D.L. and E.B., Great Lakes University Research Fund, NSERC research grants to D.L., D.M., and W.D.T., and NSERC/Industrial support to D.M. We thank W. Scheider and K. Somers (OMOEE) for providing access to the data and L. Milford and C. Hauschild for assistance in inputting the data. We also thank U. Borgmann and other reviewers for useful suggestions regarding the statistics.

References

Almond, M.J.R., Bentzen, E., and Taylor, W.D. 1996. Size structure and species composition of plankton communities in deep Ontario lakes with and without *Mysis relicta* and planktivorous fish. Can. J. Fish. Aquat. Sci. **53**: 315–325.

Arimoto, L. 1989. Atmospheric deposition of chemical contaminants to the Great Lakes. J. Great Lakes Res. **15**: 339–356.

Baker, J.E., and Eisenreich, S.J. 1989. PCBs and PAHs as tracers of particle dynamics in large lakes. J. Great Lakes Res. **15**: 84–103.

Baumann, P.C., and Whittle, D.M. 1988. The status of selected organics in the Laurentian Great Lakes: an overview of DDT, PCBs, dioxins, furans, and aromatic hydrocarbons. Aquat. Toxicol. **11**: 241–257.

Beattie, W.D., and Clancey, P.T. 1991. Effects of *Mysis relicta* on the zooplankton community and kokanee population of Flathead Lake, Montana. Am. Fish. Soc. Symp. **9**: 39–48.

Boelens, R.G.V., and Rumsey, C.R. 1972. DDT residues in the Muskoka lakes system. Report 2 on Water Quality Evaluation Program in the Muskoka lakes. Ontario Ministry of the Environment, Rexdale, Ont.

Borgmann, U., and Whittle, D.M. 1991. Contaminant concentration trends in Lake Ontario lake trout (*Salvelinus namaycush*): 1978 to 1988. J. Great Lakes Res. **17**: 368–381.

Borgmann, U., and Whittle, D.M. 1992. Bioenergetics and PCB, DDE, and mercury dynamics in Lake Ontario lake trout (*Salvelinus namaycush*): a model based on surveillance. Can. J. Fish. Aquat. Sci. **49**: 1086–1096.

Bowles, E.C., Rieman, B.E., Mauser, G.R., and Bennett, D.H. 1991. Effects of introduction of *Mysis relicta* on fisheries in Northern Idaho. Am. Fish. Soc. Symp. **9**: 65–71.

Cochran, W.G., and Cox, G.M. 1957. Experimental designs. John Wiley & Sons, New York.

Crawford, G., and Brunato, R. 1978. An inventory of data on PCB and mirex levels in Ontario sports fish. Ont. Minist. Environ. Rep. 7801.

Dadswell, M.J. 1974. Distribution, ecology, and postglacial dispersal in certain crustaceans and fishes in Eastern North America. National Museum of Canada, Ottawa, Ont.

Day, R.W., and Quinn, G.P. 1989. Comparisons of treatments after an analysis of variance in ecology. Ecol. Monogr. **59**: 433–463.

Delfino, J.J. 1979. Toxic substances in the Great Lakes. Environ. Sci. Technol. **13**: 1462–1478.

Eisenreich, S.J., Looney, B.B., and Thornton, J.D. 1981. Airborne organic contaminants in the Great Lakes ecosystem. Environ. Sci. Technol. **15**: 30–38.

Evans, R.D., and Lasenby, D.C. 1983. Relationship between body-lead concentration of *Mysis relicta* and sediment-lead concentration in Kootenay Lake, B.C. Can. J. Fish. Aquat. Sci. **40**: 78–81.

Evans, M.S., Noguchi, G.E., and Rice, C.P. 1991. The biomagnification of polychlorinated biphenyls, toxaphene, and DDT compounds in a Lake Michigan offshore food web. Arch. Environ. Contam. Toxicol. **20**: 87–93.

Gobas, F.A.P.C. 1994. Modelling the accumulation and toxicity of organic chemicals in aquatic food chains. *In* Chemical dynamics in freshwater ecosystems. *Edited by* F.A.P.C. Gobas and J.A. McCorquodale. Lewis Publishers, Inc., Boca Raton, Fla. pp. 129–152.

Hebert, C.E. and Keenleyside, K.A. 1995. To normalize or not to normalize? Fat is the question. Environ. Toxicol. Chem. **14**: 801–807.

Hoff, R.M., Muir, D.C.G., and Grift, N.P. 1992. Annual cycle of polychlorinated biphenyls and organohalogen pesticides in air in southern Ontario. 2. Atmospheric transport and sources. Environ. Sci. Technol. **26**: 276–283.

Jensen, A.L., Spigarelli, S.A., and Thommes, M.M. 1982. PCB uptake by five species of fish in Lake Michigan, Green Bay of Lake Michigan, and Cayuga Lake, New York. Can. J. Fish. Aquat. Sci. **39**: 700–709.

Johannsson, O. 1992. Life history and productivity of *Mysis relicta* in Lake Ontario. J. Great Lakes Res. **18**: 154–168.

Kerr, S.R. 1971. A simulation model of lake trout growth. J. Fish. Res. Board Can. **28**: 815–819.

Kidd, K.A., Schindler, D.W., Muir, D.C.G., Lockhart, W.L., and Hesslein, R.A. 1995. High concentrations of toxaphene in fishes from a subarctic lake. Science (Washington, D.C.), **269**: 240–242.

Klump, J., Kaster, J.L., and Sierszen, M.E. 1991. *Mysis relicta* assimilation of hexachlorobiphenyl from sediments. Can. J. Fish. Aquat. Sci. **48**: 284–289.

Langeland, A., Carl, L.M., Hicks, F.J., and Munroe, B. 1991. The impact of predation by *Mysis relicta* and fish on zooplankton in four oligotrophic, north temperate lakes. Am. Fish. Soc. Symp. **9**: 88–97.

Lasenby, D.C. 1991. Comments on the roles of native and intro-

© 1996 NRC Canada

duced *Mysis relicta* in aquatic ecosystems. Am. Fish. Soc. Symp. **9**: 17–22.

Lasenby, D.C., Northcote, T.G., and Furst, M. 1986. Theory, practice and effects of *Mysis relicta* introduction to North America and Scandinavian lakes. Can. J. Fish. Aquat. Sci. **43**: 1277–1284.

Lean, D.R.S., Neilson, M.A., Stevens, R.J.J., and Mazumder, A. 1990. Response of Lake Ontario to reduced phosphorus loading. Verh. Int. Ver. Limnol. **24**: 420–425.

Lester, D.C., and McIntosh, A. 1994. Accumulation of polychlorinated biphenyl congeners from Lake Champlain sediments by *Mysis relicta*. Environ. Toxicol. Chem. **13**: 1825–1841.

MacDonald, C.R., Metcalfe, C.D., Metcalfe, T., and Balch, G.C. 1992. Temporal trends and distribution of PCB congeners in a small contaminated lake in Ontario, Canada. *In* Chemical dynamics in freshwater ecosystems. *Edited by* F.A.P.C. Gobas and J.A. McCorquodale. Lewis Publishers. Inc., Boca Raton, Fla. pp. 211–236.

Mackay, D. 1979. Finding fugacity feasible. Environ. Sci. Technol. **13**: 1218–1223.

Mackay, D. 1982. Correlation of bioconcentration factors. Environ. Sci. Technol. **16**: 274–278.

Mackay, D. 1989. Modelling the long-term behaviour of an organic contaminant in a large lake: application to PCBs in Lake Ontario. J. Great Lakes Res. **15**: 283–297.

Martin, N.V. 1966. The significance of food habits in the biology, exploitation, and management of Algonquin Park, Ontario, lake trout. Trans. Am. Fish. Soc. **95**: 415–422.

Mazumder, A., Lean, D.R.S., and Taylor, W.D. 1992. Dominance of small filter feeding zooplankton in the Lake Ontario foodweb. J. Great Lakes Res. **18**: 456–466.

McMurtry, M.J., Wales, D.L., Scheider, W., Beggs, G.L., and Dimond, P.E. 1989. Relationship of mercury concentrations in lake trout (*Salvelinus namaycush*) to the physical and chemical characteristics of Ontario lakes. Can. J. Fish. Aquat. Sci. **46**: 426–434.

Nero, R.W., and Sprules, W.G. 1986. Zooplankton species abundance and biomass in relation to occurrence of *Mysis relicta* (Malacostraca: Mysidacea). Can. J. Fish. Aquat. Sci. **43**: 420–434.

Oliver, B.G., and Niimi, A.J. 1988. Trophodynamic analysis of polychlorinated biphenyl congeners and other chlorinated hydrocarbons in Lake Ontario ecosystem. Environ. Sci. Technol. **22**: 388–397.

OMOEE. 1986. Handbook of analytical methodologies for environmental samples. Ontario Ministry of the Environment, Laboratory Services Branch, Rexdale, Ont.

OMOEE and OMNR. 1993–1994. Guide to eating Ontario sport fish. 17th ed. Queen's Printer for Ontario, Toronto, Ont.

Rasmussen, J.B., Rowan, D.J., Lean, D.R.S., and Carey, J.H. 1990. Food chain structure in Ontario lakes determines PCB levels in lake trout (*Salvelinus namaycush*) and other pelagic fish. Can. J. Fish. Aquat. Sci. **47**: 2030–2038.

Rees, G.A.V., Crawford, G., and Brunato, R. 1979–1980. Addendum 1 and 2. Ont. Minist. Environ. Rep. 7901.

Richards, R., Goldman, C., Bryon, E., and Levitan, C. 1991. The mysids and lake trout of Lake Tahoe: a 25-year history of changes in the fertility, plankton, and fishery of an alpine lake. Am. Fish. Soc. Symp. **9**: 30–38.

Scott, W.B., and Crossman, E.J. 1973. Freshwater fishes of Canada. Bull. Fish. Res. Board Can. No. 184.

Sprugel, D.G. 1983. Corrections for bias in log-transformed allometric equations. Ecology, **64**: 209–210.

Sprules, W.G., and Bowerman, J.E. 1988. Omnivory and food chain length in zooplankton food webs. Ecology, **69**: 418–426.

Swackhamer, D.L., McVeety, B.D., and Hites, R.A. 1988. Deposition and evaporation of polychlorobiphenyl congeners to and from Siskiwit Lake, Isle Royale, Lake Superior. Environ. Sci. Technol. **22**: 664–672.

Taylor, W.D., Carey, J.H., Lean, D.R.S., and McQueen D.J., 1991. Organochlorine concentrations in the plankton of lakes in southern Ontario and their relationship to plankton biomass. Can. J. Fish. Aquat. Sci. **48**: 1960–1966.

Thomann, R.V., and Connolly, J.P. 1984. Model of PCB in the Lake Michigan lake trout food chain. Environ. Sci. Technol. **18**: 65–72.

Trippel, E.A., and Beamish, F.W.H. 1989. Lake trout (*Salvelinus namaycush*) growth potential predicted from cisco (*Coregonus artedii*) population structure and conductivity. Can. J. Fish. Aquat. Sci. **46**: 1531–1538.

Van Duyn-Henderson, J.A., and Lasenby, D.C. 1986. Zinc and cadmium transport by the vertically migrating opossum shrimp, *Mysis relicta*. Can. J. Fish. Aquat. Sci. **43**: 1726–1732.

Wilkinson, L. 1990. SYSTAT: the system for statistics. Systat Inc., Evanston, Ill.

Zar, J.H. 1968. Calculation and miscalculation of the allometric equation as a model in biological data. BioScience, **18**: 1118–1120.

© 1996 NRC Canada

Feeding, growth, and habitat associations of young-of-year walleye (*Stizostedion vitreum*) in a river affected by a mine tailings spill

Amy L. Leis and Michael G. Fox

Abstract: We investigated the early life ecology of walleye (*Stizostedion vitreum*) inhabiting a northern Ontario river affected by a 300 000-tonne gold mine tailings spill and compared feeding, growth, and habitat selection of young-of-year (YOY) in a 5- km tailings-affected reach with those of an unaffected downstream reach. The study took place from June to August 1992, 1.5 yr after the spill occurred. Growth rates of YOY were not significantly different between reaches until late July, when YOY in the tailings reach were significantly smaller than those of the reference reach. Smaller body size in the tailings reach was accompanied by lower stomach fullness, a higher proportion of empty stomachs, and a progressive decline in catches of walleye, indicating poor feeding conditions, high mortality, and (or) emigration. YOY >25 mm total length captured in both reaches were almost entirely piscivorous and fed mainly upon YOY yellow perch (*Perca flavescens*) and white sucker (*Catostomus commersoni*). Walleye catch-per-unit-effort was positively correlated with the catch of YOY yellow perch and white sucker, but was not associated with any microhabitat variable except temperature. The data suggest that juvenile walleye in this system are habitat generalists and that they may be selecting areas on the basis of piscine prey abundance.

Résumé : Nous avons étudié l'écologie de dorés (*Stizostedion vitreum*) tôt au début du cycle vital vivant dans un cours d'eau du nord de l'Ontario qui avait été contaminé par le déversement de 300 000 tonnes de résidus d'une mine d'or. Nous avons comparé l'alimentation, la croissance et la sélection d'habitats chez des jeunes de l'année dans un tronçon de 5 km touché par les résidus à celles de jeunes situés dans un tronçon non atteint et situé plus en aval. L'étude s'est déroulée de juin à août 1992, soit 1,5 ans après le déversement. Le taux de croissance ne différait pas beaucoup entre les deux groupes avant la fin-juillet, date à laquelle les jeunes de l'année situés dans le tronçon atteint sont devenus significativement plus petits que ceux du tronçon de référence. Chez les premiers, leur plus petite taille s'accompagnait du fait que leur estomac était moins rempli, qu'on trouvait davantage d'estomacs vides et qu'on en capturait de moins en moins, ce qui est indicatif d'une mauvaise alimentation, d'une mortalité élevée et (ou) d'une émigration. Les jeunes de l'année de plus de 25 mm longueur totale capturés dans les deux tronçons étaient presque exclusivement piscivores; ils se nourrissaient principalement de perchaudes (*Perca flavescens*) et de meuniers noirs (*Catostomus commersoni*) de l'année. Il existe une corrélation positive entre les prises par effort de pêche du doré et celles de la perchaude et du meunier, mais sans qu'elle soit associée à aucune variable des microhabitats sauf la température. Ces résultats paraissent indiquer que, dans ce système, le doré juvénile est un généraliste sur le plan de l'habitat et qu'il choisit peut-être ses secteurs en fonction de l'abondance du poisson lui servant de proie.
[Traduit par la Rédaction]

Introduction

The habitat requirements of a fish species may vary significantly with life stage as a result of changes in size, the ability to utilize food sources, and changes in locomotory capability. Little is known about the early life ecology of many larval and juvenile fish, or about the influence of pollution events on the early life stages under natural conditions. Young fish are often difficult to collect and identify, and specific habitat requirements of the young of many species are poorly understood (Scott and Nielsen 1989). Larval and juvenile fish are also often more sensitive to environmental quality and variability when compared with adult fish. In developing management strategies for fish species and in mitigating environmental degradation, the needs of these early life stages must be considered.

One type of environmental disturbance which may adversely affect riverine fish populations is the discharge of mine wastes into river systems either as the result of mine drainage or structural failure. Abandoned mine sites are of particular concern because there are some 6000 of these in Canada (Campbell and Marshall 1991), and few of these are being monitored. Metal contamination, acid generation from tailings rock, and sediment deposition from tailings spills are all potential threats posed by operating and abandoned mine sites. This type of industrial pollution threatens water and sediment quality as well as habitat areas that may be critical to the survival of young fish. Suspended fine-grained tailings released into a river system tend to settle out in low-flow areas. These low-flow, backwater habitats in river systems

Received August 10, 1995. Accepted May 1, 1996.
J13035

A.L. Leis[1] **and M.G. Fox.**[2] Watershed Ecosystems Graduate Program and Environmental and Resource Studies Program, Trent University, Peterborough, ON K9J 7B8, Canada.

[1] Present address: Golder Associates Ltd., 202–2174 Airport Drive, Saskatoon, SK S7L 6M6, Canada.
[2] Author to whom correspondence should be addressed.

© 1996 NRC Canada

Fig. 1. Location of the Montreal River and the reference and mine tailings-affected reaches used in this study. Included in the reference reach are sites in Sydney Creek between Highway 65 and the river.

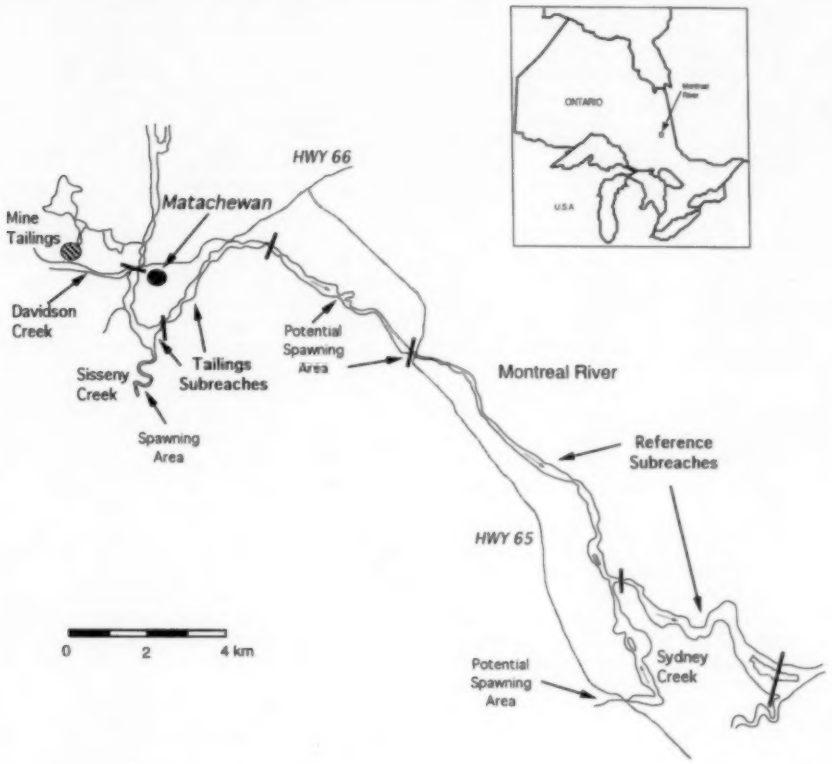

are considered to be important nursery areas for young fish (Holland 1986; Sheaffer and Nickum 1986). Whereas much of the research on the effects of mine tailings on rivers has been focussed on metal contamination (e.g., Czarnezki 1985; Davies 1987; Dwyer et al. 1988), effects on fish habitat and feeding ecology remain largely unexplored.

In this study, we examine the early life ecology of walleye (*Stizostedion vitreum*) in a northern Ontario river subjected to a mine tailings spill in 1990. Our first objective was to determine whether there were differences in abundance, food consumption, and growth of young-of-year (YOY) inhabiting the area affected by the mine tailings spill, relative to an unaffected area of the river. Although much is known about the ecology of YOY walleye in lakes and artificial rearing ponds, there are few data on YOY of riverine populations, particularly in relation to habitat requirements (see Colby et al. 1979; Pitlo 1992). For example, studies undertaken by Holland (1986) and Sheaffer and Nickum (1986) to identify significant nursery habitats for a variety of species in the Mississippi River system were unable to determine specific walleye rearing habitat requirements because of the low abundance of young walleye in the samples collected. Because of the paucity of data on the early life history and ecology of this important game species, our second objective was to investigate the habitat associations and life history of YOY from the study river.

Methods

Study area

The study was conducted on the Montreal River, a large Canadian Shield river approximately 200 km long and ranging from 50 to 200 m wide (Fig. 1). This river was affected by a 300 000-tonne (t) spill near the town of Matachewan in October 1990, the result of the collapse of a tailings dyke from an abandoned gold mine. The fine-grained tailings entered the Montreal River from Davidson Creek and settled to cover much of the bottom over a 5-km stretch of river. The tailings contain high concentrations of several trace heavy metals (Pb, Zn, Cd, Cu, Mn, and Ni). A laboratory bioassay showed that these tailings are lethal to mayfly nymphs and have negative growth effects on chironomid larvae (Bedard and Petro 1991). Walleye and other fish species inhabiting this river were thought to be spawning in areas of the river affected by this spill.

The study area is located between 47°58′ latitude, 80°40′ longitude and 47°50′ latitude, 80°25′ longitude. Fish sampling and habitat assessment were conducted from June 8 to August 2, 1992, in two river reaches: the 5-km area where most of the tailings settled and a reference area approximately 10 km downstream (Fig. 1). Spawning walleye were observed in Sisseny Creek, which flows into the tailings-affected reach approximately 1.5 km downstream of the origin of the spill. A downstream reference area was chosen for the study because river surveys and a telemetry study of adult walleye suggested that there were no walleye spawning in the main stem of the river upstream of, or in the vicinity of, the tailings spill (E. Paleczny, Ontario Ministry of Natural Resources, Swastika,

© 1996 NRC Canada

Ont., personal communication). This was later confirmed by the absence of larval walleye in tow net collections from the river above Sisseny Creek and above the spill. The lower section of Sydney Creek was included as part of the reference area, as walleye were historically known to spawn in areas of this creek and because the lower section was comparable in width and depth with the river main stem. Deposits of tailings had been identified and mapped in the study area the previous year by the Ontario Ministry of Natural Resources (OMNR), Kirkland Lake District. The survey showed that there was no detectable settlement of tailings in the reference reach (E. Paleczny, personal communication), and we did not encounter any mine tailings in the substrate of reference sites during our habitat assessments.

Fish collection and handling

YOY walleye were collected during the first month of the study by tow net sampling, and subsequently by seining. Tow net sampling was conducted from June 7 to July 7, 1992. A total of 26 sites were used: five embayment, five main channel, and three pool sites per reach. Each of these sites was sampled three or four times over the duration of the investigation. All tow sampling sites were less than 5 km downstream of known or suspected walleye spawning areas, and those selected within the tailings-affected reach were known to contain mine tailings deposits on the substrate. Pool sites ranged in depth from 5 to 14 m. All embayment sites had water velocities less than 0.03 $m \cdot s^{-1}$.

Tow net sampling was conducted with a circular meter net (1-mm Nitex mesh), towed alongside a small boat. A flowmeter mounted inside the opening of the net during towing was used to calculate water volume flowing through the net. The tow net was effective in capturing walleye larvae and juveniles up to 30 mm in total length (TL). Sampling times were between dusk (approximately 21:00) and 03:00. This sampling period was selected because the catch of many larval fish species, including walleye, has been found to be greater during nocturnal sampling (Priegel 1970; Gale and Mohr 1978). In addition, Mathias and Li (1982) found walleye fry to have a feeding peak before dusk, so that fish captured for several hours after dark should have food present in the gut.

Each week, a minimum of three sites of each classification (embayment, main channel, and pool) were sampled in both tailings and reference reaches. Three replicate tows per site were conducted; each tow was approximately 3 min in length and filtered an average of 100 m^3 of water. Fish captured in the tows were removed from the samples, placed in 5% formalin, and later identified to species using criteria outlined in Auer (1982).

Juvenile walleye were collected between July 7 and August 2 by seining in shallow (≤2 m) sites along the shoreline with a 25 × 2 m bag seine (6.4-mm mesh). Sites were sampled from late afternoon until dusk, approximately 17:00–21:00. Captured fish were counted by species at the sampling site. YOY walleye were killed by ice water shock and later preserved in 10% formalin. A total of 22 tailings and 25 reference sites were seined in the study. Most sites were sampled between two and four times during this investigation.

Walleye were measured to the nearest 0.1 mm TL (larvae) or the nearest 1 mm (juveniles) in the laboratory and wet-weighed to the nearest 0.001 g (larvae) or 0.01 g (juveniles). Gut content (walleye ≤15 mm) or stomach content (walleye >15 mm) was analyzed on non-yolk-sac fry. Stomach (gut) content biomass was estimated for walleye by converting prey lengths into dry mass. Length–mass regressions for zooplankton (Culver et al. 1985) and for macroinvertebrates (Smock 1980; Fox and Flowers 1990) were used for prey mass calculations.

Habitat assessment

Temperature and water velocity were determined at all tow and seine netting sites with a hand-held thermometer and a standard Teledyne Gurley current meter. Water depth was initially determined from OMNR bathymetric maps of the Montreal River, and later verified at each site.

Substrate composition was also determined initially from OMNR habitat maps of the area. The substrate at all netting sites was later confirmed in the field by Eckman or hand grabs of substrate material from at least three randomly chosen points within the sampling area. The percent composition of coarse (boulder, rubble, gravel), fine (sand, silt and tailings), and organic sediment was estimated from these samples. For the calculation of correlation coefficients, substrate was classified as coarse, fine, or organic.

Vegetation was not present or was sparse throughout the river during the period of tow net sampling. Vegetative cover and macrophyte species present were evaluated twice during seine sampling: once in early July and once in late July. Most sites were seined only once between the two vegetation estimates. There was little vegetation in any of the sites in early July, and what was present consisted of short, newly emerging shoots. Beginning on July 22, each seine site was again evaluated for vegetative cover and composition. Percent cover was determined following each seine haul by visually estimating the amount of the seined area with vegetation present. The species of vegetation present were then identified, and the percentage of each species present was estimated by counting the number of plant stems by species in 50-cm^2 quadrants. For data analysis, plant species were categorized as either emergent, submergent, or floating.

Data analysis

Analysis of covariance (ANCOVA) was used for comparing the growth rates of walleye captured in reference and tailings reaches. For this analysis, each study reach was divided into two subreaches, the dividing line in each case being the mouth of the major creek flowing into the river (see Fig. 1). Although these subreaches are not true replicates because of their spatial continuity, the analysis does take into account within-reach variation. It also allowed us to examine the possibility that tailings effects on walleye growth were diminished downstream of the spill. Because of the change in growth pattern during the final week of sampling, analysis of variance (ANOVA) was used to detect differences in walleye length at this time between reference and tailings reaches.

Body condition was calculated using Fulton's condition factor (Bagenal and Tesch 1978). Differences in body condition between walleye from the two reference and two tailings subreaches were examined with ANCOVA, using $(\text{length})^3$ as the covariate. Because few large walleye were captured in the tailings reach, the analysis of body condition included only comparably sized fish.

Differences in feeding and stomach content were investigated by separating the walleye into three length categories: 9–25, 25–45, and 45–80 mm. These size ranges were selected to reflect changes in the feeding ecology of young walleye reported in the literature. Based on these accounts, we expected walleye in the 9–25 mm category to be feeding almost exclusively on planktonic crustaceans. At larger sizes, they typically switch to larger prey, finally becoming piscivorous at a body length of 50 mm or greater (Smith and Pycha 1960; Johnson 1969; Priegel 1969; Mathias and Li 1982).

Stomach contents on a given day may not be totally independent of site of capture because the emptying of walleye stomachs requires less than 8 h in juveniles of the size captured in this study (see Fox 1991). For this reason, we employed a nested design ANOVA for comparing stomach fullness (K_f, milligrams dry prey mass per milligram fish mass) between fish from reference and tailings reaches, with individual sites nested within reach. Because stomach content (as opposed to gut content) was evaluated for fish larger than 15 mm, 9–15 and 16–25 mm subgroups were examined separately. Sites where less than five fish were captured were not included in any of the stomach content analyses, as such small samples would probably not give a reliable estimate of stomach fullness at an individual site. Assumptions of each statistical test were evaluated by inspection of

© 1996 NRC Canada

Fig. 2. Total length of YOY walleye captured in the reference and tailings reaches in the Montreal River, June–August 1992. Lines shown are the least-squares regressions for length over time in the two river reaches.

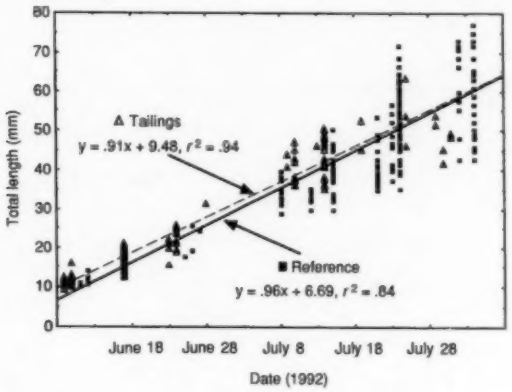

Fig. 3. Body condition of YOY walleye captured in the reference and tailings reaches in the Montreal River, expressed in terms of Fulton's condition factor ($K = 10^5$ (mass, g)· (length, mm)$^{-3}$). Lines shown are the least-squares length–mass regressions in the two river reaches.

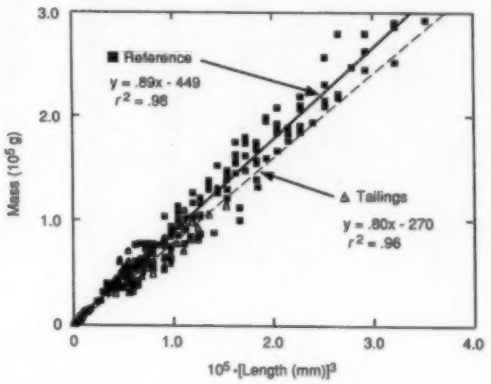

residual plots and the data were $\log_e(1 + x)$-transformed when necessary to meet these assumptions.

The proportion of stomach content by prey type was calculated on each individual on a dry mass basis and expressed as an average for the various size and reach categories. Walleye with empty stomachs were not included in prey type calculations, but proportions of walleye with empty stomachs were calculated and tested for significant differences between reference and tailings reaches with chi-square analysis.

Habitat and interspecific associations were analyzed in several ways. Capture data on walleye and other species, expressed per volume of water filtered through tow nets, or per area seined, were used as measures of relative abundance. Catch-per-unit-effort (CUE) data were analyzed with nonparametric statistics, due to the many null catches of some species, and the nonnormal distribution of aggregate catch data. To determine whether YOY walleye abundance in the first few weeks of life was influenced by microhabitat, we compared walleye CUE in three site types (embayment, main channel, or pool) with a Kruskal–Wallis ANOVA. For fish captured by seining, CUE of walleye and the mean total CUE of all fish combined were compared between reference and tailings subreaches with a Mann–Whitney U test. Finally, Spearman correlations were used to determine the degree of association between individual habitat parameters and walleye CUE, and between walleye CUE and that of other fish species.

Results

Growth and body condition

A total of 418 YOY walleye were captured: 188 by tow sampling and 230 by seine sampling. Seventy-four percent of the walleye captured by tow sampling were captured in the tailings-affected reach whereas only 30% of the walleye captured by seine sampling were captured in this reach. Change in length over the first 8 wk of life was nearly linear, the rate being about 0.9 mm·d^{-1} (Fig. 2). Growth trajectories were not different between reaches when within-reach data were pooled (ANCOVA, slopes, $P = 0.20$). However, the slopes of the growth trajectories in both reference subreaches were superior to those of both tailings subreaches, the differences being significant between the lower tailings subreach and both reference subreaches (ANCOVA, slopes, $P < 0.001$ in both comparisons). There were no differences between growth trajectories of subreaches within their respective reaches (ANCOVA, slopes, $P = 0.77$ reference reach, $P = 0.46$ tailings reach).

Walleye from the tailings reach were larger, during most of the study period, than those from the reference area (ANCOVA, intercepts, $P = 0.013$). However, a comparison of the size of juveniles collected during the last two sample periods showed little or no body length increase in walleye collected from the tailings reach over this period (Fig. 2). Although captures during the last week of the study were too few to effect meaningful comparisons at the subreach level, juveniles captured in the reference reach during this period were larger than those captured in the tailings reach (ANOVA, $F_{1,42} = 10.7$, $P = 0.003$).

Body condition, expressed as Fulton's condition factor, increased from an average of 0.41 in walleye fry around the time of first feeding to 0.90 in juveniles 40–80 mm TL collected approximately 7 wk later. Although average walleye body condition over the course of the study could not be statistically compared between reaches, YOY captured in the reference reach had a higher mean condition factor than those from the tailings reach, and also a significantly greater increase in mass with length (Fig. 3; ANCOVA, slopes, $P < 0.001$). This was the case even when the larger walleye captured from the reference reach (>65 mm TL) were excluded from the comparison. When comparisons were made among subreaches, the two reference subreaches had greater length–mass trajectories than both tailings subreaches, but the trajectory for walleye in the upper tailings subreach was significantly lower than those of the lower tailings and both reference subreaches (ANCOVA, slopes, $P < 0.025$ in all three comparisons).

Prey type and quantity of food consumed

The diet of 9–25 mm walleye was composed primarily of cladocerans, copepods, and chironomid larvae and pupae (Fig. 4). Approximately 70% (by mass) of the stomach contents of

© 1996 NRC Canada

Fig. 4. Composition of stomach contents of YOY walleye captured in the reference and tailings reaches, represented as a percentage of total stomach content biomass. Data are pooled for walleye captured within each reach.

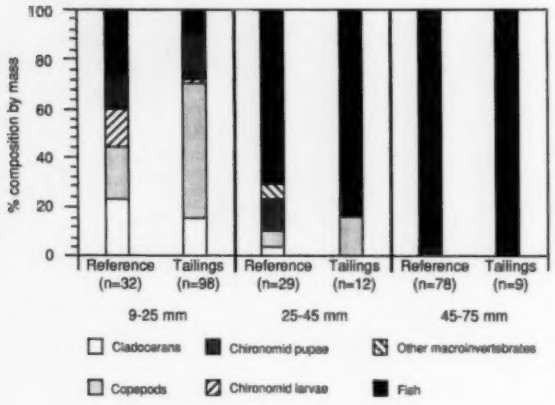

Fig. 5. Comparison of stomach fullness (K_f) of YOY walleye captured in the reference and tailings reaches. Means and standard errors shown in the figure were calculated by pooling data for walleye captured within each reach. Sample size is shown above the error bars.

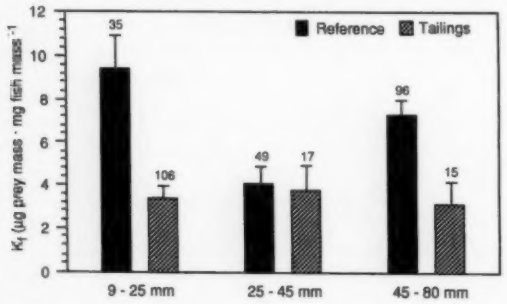

walleye this size from the tailings reach consisted of zooplankton whereas zooplankton constituted less than half of the stomach contents of those captured in the reference reach. Nine and 26% of the stomach contents of these small walleye consisted of larval fish 3–5 mm in length in tailings and reference sites, respectively.

Once the walleye were between 25 and 45 mm in length, larval and juvenile fish comprised over 70% of the stomach contents in both reaches. Walleye >45 mm were almost exclusively piscivorous. The actual species of fish eaten were difficult to quantify; however, the most frequently observed prey species in the stomachs of the larger walleye were yellow perch (*Perca flavescens*) and white sucker (*Catostomus commersoni*).

Stomach fullness was higher in 9–15 mm walleye from reference sites (Fig. 5; $F_{1,121} = 17.6$, $P < 0.0001$). However, within-reach variability was high, as indicated by a significant site within reach term ($F_{1,121} = 17.6$, $P < 0.01$). K_f could not be statistically compared in 25–45 or 45–80 mm walleye

Table 1. Proportion (%) of juvenile walleye containing empty stomachs in the reference and tailings reaches, Montreal River, summer 1992.

	9–25 mm	25–45 mm	45–80 mm
Control	8.6	42.9	15.6
Tailings	8.2	35.3	40.0

Fig. 6. CUE of larval and juvenile walleye captured by tow netting in three macrohabitat types in the Montreal River, June 8–30, 1992.

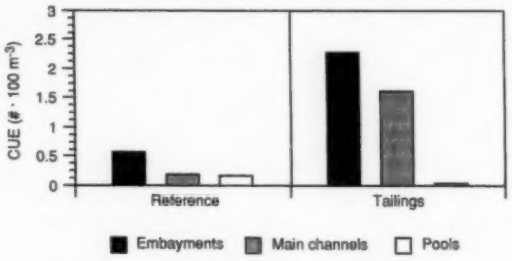

from the two reaches because there were few sites where more than five walleye were captured. However, Fig. 5 suggests that there may have been a difference between reaches in stomach fullness of 45–80 mm walleye. This was due in part to the high proportion of empty stomachs in walleye of this size category captured in tailings sites (Table 1). These walleye had a higher proportion of empty stomachs than those captured in reference sites ($\chi^2 = 5.0$, $P = 0.025$).

Habitat and species associations

Mean catches of walleye by tow netting were higher at embayment sites than main channels and pools in both reference and tailings reaches (Fig. 6); however, the differences were not significant in either reach or with all sites combined (Mann–Whitney U test, $P > 0.15$ in all cases). CUE of walleye captured by tow netting was higher overall in the tailings reach (Fig. 6). This difference was not significant between reaches (Mann–Whitney U test, $P = 0.11$), but CUE in the lower tailings subreach was significantly higher than that of the upper control subreach ($P = 0.02$). Although the mean CUE of walleye was lower at reference sites, CUE by tow netting of all fish species combined was significantly higher in the reference reach (mean CUE, reference: 390 fish·100 m^{-3}; tailings: 107 fish·100 m^{-3}; Mann–Whitney U test, $P = 0.003$). However, this difference was entirely attributable to the high abundance of fish in the upper reference subreach relative to the other three subreaches.

Depth, water velocity, and dominant substrate material at tow sampling sites are summarized in Table 2. These data suggest that there were some differences between reaches in the depth and velocity of tow netting sites that could have influenced the relative abundance of walleye. However, the weak negative correlation between water depth and walleye CUE would have favoured the reference sites whereas walleye CUE in tow nets was higher in the tailings sites (Table 3).

© 1996 NRC Canada

Table 2. Summary of habitat characteristics at two net sampling sites (values in parentheses represent ±1 SE).

Site type	Mean depth (m)	Mean velocity ($m \cdot s^{-1}$)	Dominant substrate material
Reference sites			
Embayments	3.5 (0.3)	0.01 (0.004)	Organic/sand
Main channels	3.8 (0.8)	0.04 (0.004)	Organic/sand
Pools	6.0 (0.8)	0.04 (0.02)	Organic
Tailings sites			
Embayments	1.7 (0.1)	0.01 (0.004)	Sand with tailings
Main channels	1.9 (0.01)	0.1 (0.06)	Sand/organic with tailings
Pools	7.5 (3.4)	0.1 (0.01)	Sand/organic with tailings

Table 3. Spearman correlation coefficients (r_s) between CUE of walleye captured by two nets and habitat parameters and CUE of other fish species captured at sites in the reference and tailings reaches of the Montreal River.

	Reference sites	Tailings sites	All sites combined
Habitat parameter			
Temperature (°C)	0.08	–0.03	–0.10
Velocity ($m \cdot s^{-1}$)	–0.09	–0.17	–0.09
Depth (m)	–0.34	–0.28	–0.34*
Substrate (% coarse)	0.21	–0.08	0.08
Substrate (% fine)	0.03	0.03	0.18
Substrate (% organic)	–0.03	0.16	–0.13
CUE			
YOY yellow perch	0.16	0.64***	0.42**
YOY white sucker	–0.14	0.39*	0.11
YOY other species	0.12	0.29	0.24

Note: Starred probabilities are Bonferroni-adjusted for family-wise levels of significance: *$P < 0.05$, **$P < 0.01$, ***$P < 0.001$.

No significant correlations were detected between walleye CUE in tow nets and any of the other abiotic variables. However, walleye CUE was significantly correlated with CUE of YOY yellow perch in reference and tailings sites, and with CUE of YOY white sucker in tailings sites.

CUE of walleye captured by seine was higher in the reference reach (mean: 2.9 fish·100 m^{-2}) than in the tailings reach (mean: 0.85 fish·100 m^{-2}; Mann–Whitney U test, $P < 0.001$). This difference was evident at the subreach level, as CUE's of walleye captured by seine in the reference subreaches were higher than those of both tailings subreaches (Mann–Whitney U test, $P < 0.047$ in all comparisons). The temporal pattern of walleye abundance differed in the two reaches, as CUE was relatively constant through July in the reference reach, but declined sharply in the tailings reach during this time period (Fig. 7).

Mean CUE by seining of all fish species combined was also higher in the reference reach (reference: 460 fish·100 m^{-2}; tailings: 155 fish·100 m^{-2}; Mann–Whitney U test, $P < 0.001$). This difference was also evident at the subreach level with CUE's of all fish combined being greater in the two reference subreaches than in both tailings subreaches (Mann–Whitney U test, $P < 0.001$ in all comparisons). During seine sampling, walleye CUE was significantly correlated with CUE of YOY yellow perch and YOY white sucker in reference sites, and with CUE of cyprinids and YOY white sucker at tailings sites (Table 4). When reaches were pooled, walleye CUE was significantly correlated with CUE of YOY yellow perch, YOY white sucker, and cyprinid species.

Water temperature was the only environmental variable significantly correlated with CUE of seine-netted walleye. Water temperature in sites where walleye were captured by seine was, on average, 0.6°C (reference reach) and 1.5°C (tailings reach) warmer than sites where no walleye were captured (Table 5).

Discussion

Comparison of reference and tailings reaches

Growth, body condition, and feeding

YOY walleye from the tailings reach were initially larger

© 1996 NRC Canada

Fig. 7. Weekly change in CUE of juvenile walleye captured by seine in the littoral zone of the reference and tailings reaches in the Montreal River, July–August 1992. Vertical bars represent 1 SE.

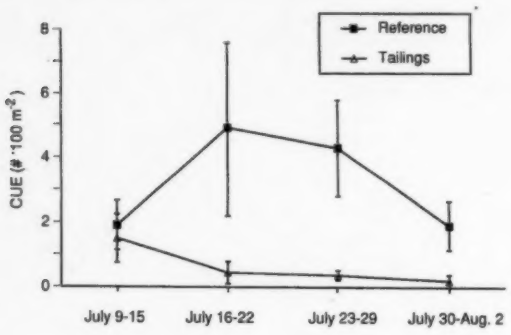

than those from the reference reach. Growth trajectories of the walleye from these reaches were comparable until they reached about 50 mm in length, but YOY above this size were not found in the tailings reach by the end of July (Fig. 2). The size variation we observed early in the study may have been the result of earlier hatching of walleye eggs in the tailings reach. During an egg incubation experiment on the Montreal River in 1992, warmer water temperatures in Sisseny Creek allowed artificially incubated walleye eggs to begin hatching several days earlier than eggs placed at river sites downstream (Leis and Fox 1994). Spawning walleye were captured in May of 1992 and 1993 in Sisseny Creek, and the YOY captured in the tailings reach probably originated from this spawning area. Although spawning sites on the Montreal River downstream of Sisseny Creek could not be confirmed, there were several areas along the river where walleye could have spawned. YOY walleye captured in the reference reach may have originated from cooler spawning sites in the river, resulting in a later hatch and therefore smaller size.

The reversal of size differences at the end of July, resulting in significantly larger juvenile walleye in the reference reach, may have been the result of poor growth, high mortality, and (or) the emigration of larger juveniles into other areas of the river. Differences between reaches in body condition and the proportion of empty stomachs in the larger juveniles suggest that conditions for growth were relatively poor in tailings sites. The relatively low number of walleye captured in tailings sites near the end of the study (13 versus 129 captured in reference sites between July 18 and August 2) is suggestive of either high localized mortality or emigration, but the sampling regime was not intensive enough to provide an explanation for the observed trends.

Stomach content data from our study suggest that food availability was low in the tailings reach of the river. It is likely that the mine tailings had an impact on food availability, but in the absence of preimpact data, one cannot rule out the possibility that the feeding and body size differences observed may have been influenced by differences in upstream and downstream habitat, independent of the mine tailings. However, there is evidence from other studies on the Montreal River that the tailings have had a negative impact on benthic prey organisms and the early life stages of fish. Bedard and Petro (1991) found that Cu concentration in sediment from the tailings reach was high enough to be above the Severe Effect Level (Persaud et al. 1991), and Cd, Cr, Pd, and Zn concentrations were above the Lowest Effect Level, based on the occurrence of benthic invertebrate species. Walleye egg incubation experiments conducted in the Montreal River in 1992 and 1993 showed that egg survival was significantly lower in the tailings reach of the river than in upstream or downstream reference sites, the effect being due to either metal toxicity or hypoxia from settlement of the fine tailings (Leis and Fox 1994). Finally, yearling yellow perch sampled from the tailings area at the time of our study had significantly lower stomach fullness than those collected from both upstream and downstream reference areas (J. Draves, Trent University, Peterborough, Ont., unpublished data).

Previously published accounts of lake populations of walleye indicate that zooplankton are preferentially chosen as food by YOY smaller than 50 mm, and piscivory is generally initiated when walleye are between 30 and 60 mm in length (Smith and Pycha 1960; Johnson 1969; Priegel 1969; Bulkley et al. 1976; Jackson et al. 1992). Piscivory has been observed in walleye as small as 10 mm in other populations (Priegel 1969; Bulkley et al. 1976), but it is not considered commonplace and has been hypothesized to relate to the abundance of prey in appropriate size ranges for the young walleye (Mathias and Li 1982).

Although few studies are available on prey consumption of YOY walleye in riverine environments, the switch to early piscivory by juvenile walleye in the Montreal River contrasts with the typical feeding habits reported in lake walleye populations. Early piscivory in the river may be related to limited availability of zooplankton in their environment. For the 25–45 mm size range of walleye, the high number of empty stomachs, low K_f values, and the types of prey selected support this hypothesis. Juvenile walleye from the Shawanaga River in Ontario also switched to almost complete piscivory by the time they reached a length of 30 mm, and the density of zooplankton was very low in this river (Fox 1990). Johnston and Mathias (1994), in experimental feeding trials with young walleye between 9 and 15 mm, found that when prey density was low the walleye tended to select larger prey items. This may be the response we detected in the young walleye from the Montreal River, where larvae as small as 10 mm were consuming fish larvae 3–4 mm in length.

Habitat selection

The initial differences seen in CUE between reference and tailings sites were most likely due to the location of spawning sites and the downstream drift of larval walleye. The higher CUE in the tailings reach early in the study suggests that most of the young walleye were produced in or upstream of this reach, likely at the spawning site on Sisseny Creek. In the latter half of the study the fish appear to have moved out of the tailings reach, as evidenced by the higher CUE in the reference reach. This may indicate that the walleye were moving in search of food or habitat, or simply in response to the flow of the river. However, during the seine sampling, young walleye were captured progressively further upstream of the mouth of Sisseny Creek in the tailings reach, suggesting that

© 1996 NRC Canada

Table 4. Spearman correlation coefficients (r_s) between CUE of walleye captured by beach seining and habitat parameters and CUE of other fish species captured at sites in the reference and tailings reaches of the Montreal River.

	Reference sites	Tailings sites	All sites combined
Habitat parameter			
Temperature (°C)	0.32	0.42**	0.43***
Velocity ($m \cdot s^{-1}$)	–0.34	–0.22	–0.23
Substrate (% coarse)	–0.17	–0.08	–0.11
Substrate (% fine)	–0.06	–0.21	–0.16
Substrate (% organic)	0.32	0.31	0.32
Cover (% emergent)	0.17	–0.06	0.08
Cover (% submergent)	0.29	–0.31	–0.11
Emergent density	0.15	–0.07	0.08
Submergent density	0.22	–0.30	–0.14
CUE			
YOY yellow perch	0.59***	0.32	0.54***
YOY white sucker	0.51**	0.36*	0.53***
YOY other species	0.15	0.24	0.21
Cyprinids	0.22	0.46**	0.43***

Note: Starred probabilities are Bonferroni-adjusted for family-wise levels of significance: $*P < 0.05$, $**P < 0.01$, $***P < 0.001$.

Table 5. Comparison of water velocity and temperature characteristics of sites where walleye were captured by seine versus sites where no walleye were captured (values in parentheses represent ±1 SE).

	Reference sites		Tailings sites	
	Walleye captured (n = 25)	Not captured (n = 23)	Walleye captured (n = 15)	Not captured (n = 56)
Mean velocity ($m \cdot s^{-1}$)	0.01 (0.01)	0.05 (0.02)	0.02 (0.02)	0.02 (0.01)
Mean temperature (°C)	20.5 (0.21)	19.9 (0.15)	20.7 (0.39)	19.2 (0.17)***

Note: Starred probability was Bonferroni-adjusted for family-wise level of significance: $***P < 0.001$.

by this stage of development the walleye were not limited to downstream movement.

Habitat associations of walleye captured by tow net sampling showed similar trends in the two study reaches. CUE of these larvae and young juveniles was higher, on average, at embayment sites than in main channel or pool sites. Embayment sites were generally shallower and had lower flow rates than the other two macrohabitats (Table 2); however, neither of these habitat parameters was significantly correlated with CUE of tow net sampled walleye. A more likely explanation is that eddy flow in embayments may have initially drawn young walleye into them prior to their development of full locomotory ability. The high relative abundance of food in embayments, including the YOY of other fish species, may have also attracted the young walleye once their swimming ability was more fully developed.

The larger, seine-captured walleye showed no significant habitat correlations, except for a positive correlation with water temperature. Walleye were associated primarily with the presence of prey species in both reaches. This suggests that the primary criterion for habitat selection by young walleye in the Montreal River was the availability of food. CUE of all species combined in the reference reach was consistently higher than in the tailings reach, and the difference increased through the sample period. CUE of juvenile walleye seined in the tailings reach decreased through the sampling period, but this trend did not occur in the reference reach until the last sample period (Fig. 7). These data suggest either that YOY mortality was relatively high in the tailings reach or that the walleye and other species were moving out of the tailings reach in search of more abundant prey.

Habitat association trends of walleye in the Montreal River do correspond to the few published accounts of walleye habitat associations in riverine environments. Previous studies that have investigated nursery habitat in rivers have also found low-flow, embayment, or backwater habitats to be important as rearing habitats for young walleye and many other species of fish. Holland (1986) and Sheaffer and Nickum (1986) found concentrations of larval fish, including walleye, to be highest in backwater areas of the Upper Mississippi River. These backwater areas were characterized by low velocity, shallow depth, high temperature, and silty substrate. The abundance of young fish in these backwater areas was hypothesized to relate

© 1996 NRC Canada

to higher biological productivity, and therefore a greater abundance of prey, as well as the capacity of these areas to provide a refugee from high current velocities.

Montreal River walleye were generally found in areas of the river characterized by higher than average water temperatures (Table 5). Juvenile walleye were also found in areas with a relatively high abundance of small fish. However, the juvenile walleye in this river were not habitat specialists, and there was no evidence that they were favouring a particular substrate, vegetation type, or areas with or without abundant cover. The reasons for their association with warmer areas in the river may be related to their own thermal preference or that of potential prey. Preference for warmer sites is consistent with studies that show that the optimum temperature for growth and consumption is 22°C for large juveniles (Koenst and Smith 1976) and 25°C for small juveniles (Smith and Koenst 1975, *cited in* Hokanson 1977). Water temperatures in the river during the period of study were generally below these optima, even in shallow areas.

In summary, data from our study show that larval and juvenile walleye inhabiting a reach of the Montreal River where a gold mine tailings spill occurred in 1990 exhibited slower growth, poorer body condition, and a greater decline in abundance than individuals inhabiting a reach that was unaffected by the spill. Comparison of changes in feeding, growth, body condition, and abundance over time suggests that early life stages of walleye were adversely affected by the tailings spill, and either experienced high mortality or emigrated from the affected reach of the river. Walleye in the river were not specialized in their habitat requirements, but their abundance was positively correlated with water temperature and the abundance of piscine prey. Although our results suggest that riverine walleye become piscivorous early in life relative to lake populations, further research is required on other riverine populations to determine whether the patterns exhibited by juveniles in the Montreal River are generally applicable to other lotic systems.

Acknowledgements

This project was funded by a research grant from OMNR, Kirkland Lake District. Ed Paleczny was the study liaison for OMNR and provided habitat and tailings maps of the Montreal River, as well as information on the walleye population. James Draves and Nancy Orr assisted in the collection of field data. Drs. John Casselman, Nick Collins, Erica Nol, and Perce Powles provided helpful comments on an earlier draft of this manuscript.

References

Auer, N.A. (*Editor*). 1982. Identification of larval fishes of the Great Lakes Basin with emphasis on the Lake Michigan drainage. Spec. Publ. 82–3. Great Lakes Fishery Commission, Ann Arbor, Mich.

Bagenal, T.B., and Tesch, F.W. 1978. Age and growth. *In* Methods for the assessment of fish production in fresh waters. *Edited by* T.B. Bagenal. IBP Handbook No. 3. Blackwell Scientific Publications, Oxford, U.K. pp. 101–136.

Bedard, D., and Petro, S. 1991. Montreal River study laboratory sediment bioassay report. Available from Water Resources Branch, Ontario Ministry of the Environment, Rexdale, Ont.

Bulkley, R.V., Spykermann, V.L., and Inmon, L.E. 1976. Food of the pelagic young of walleye and five cohabiting fish species in Clear Lake, Iowa. Trans. Am. Fish. Soc. **105**: 77–83.

Campbell, D., and Marshall, I. 1991. Mining. *In* The state of Canada's environment. *Edited by* D. Campbell and I. Marshall. Government of Canada, Ottawa, Ont. pp. 11.1–11.25.

Colby, P.J., McNichol, R.E., and Ryder, R.A. 1979. Synopsis of biological data on the walleye *Stizostedion v. vitreum* (Mitchell 1818). FAO Fish. Synop. No. 119.

Culver, D.A., Boucherle, M.M., Bean, D.J., and Fletcher, J.W. 1985. Biomass of freshwater crustacean zooplankton from length weight regressions. Can. J. Fish. Aquat. Sci. **42**: 1380–1390.

Czarnezki, J.M. 1985. Accumulation of lead in fish from Missouri streams impacted by lead mining. Bull. Environ. Contam. Toxicol. **34**: 736–745.

Davies, B.E. 1987. Consequences of environmental contamination by lead mining in Wales. Hydrobiologia, **149**: 213–220.

Dwyer, F.J., Schmitt, C.J., Finger, S.E., and Mehrle, P.M. 1988. Biochemical changes in longear sunfish, *Lepomis megalotis*, associated with lead, cadmium and zinc from mine tailings. J. Fish Biol. **33**: 307–317.

Fox, M.G. 1990. Shawanaga River walleye early life history study. Part 2: larvae and juveniles. Report prepared for the Ontario Ministry of Natural Resources, Parry Sound District.

Fox, M.G. 1991. Food consumption and bioenergetics of young-of-the-year walleye: model predictions and population density effects. Can. J. Fish. Aquat. Sci. **48**: 434–441.

Fox, M.G., and Flowers, D.D. 1990. Effect of fish density on growth, survival, and food consumption by juvenile walleye in rearing ponds. Trans. Am. Fish. Soc. **119**: 112–121.

Gale, W.F., and Mohr, H.W.J. 1978. Larval fish drift in a large river with a comparison of sampling methods. Trans. Am. Fish. Soc. **107**: 46–55.

Hokanson, K.E.F. 1977. Temperature requirements of some percids and adaptations to the seasonal temperature cycle. J. Fish. Res. Board Can. **34**: 1524–1550.

Holland, L.E. 1986. Distribution of early life history stages of fishes in selected pools of the Upper Mississippi River. Hydrobiologia, **136**: 121–130.

Jackson, J.J., Willis, D.W., and Fielder, D.G. 1992. Food habits of young-of-year walleyes in Okobojo Bay of Lake Oahe, South Dakota. J. Freshwater Ecol. **7**: 329–341.

Johnson, F.H. 1969. Environmental and species associations of the walleye in Lake Winnibigoshish and connecting waters, including observations on food habits and predator prey relationships. Minn. Fish. Invest. **5**: 5–36.

Johnston, T.A., and Mathias, J.A. 1994. Feeding ecology of walleye, *Stizostedion vitreum*, larvae: effects of body size, zooplankton abundance, and zooplankton community composition. Can. J. Fish. Aquat. Sci. **51**: 2077–2089.

Koenst, W.M., and Smith, L.L. Jr. 1976. Thermal requirements of the early life history stages of walleye, *Stizostedion vitreum vitreum*, and sauger, *Stizostedion canadense*. J. Fish. Res. Board Can. **33**: 1130–1138.

Leis, A.L., and Fox, M.G. 1994. Effect of mine tailings on the in situ survival of walleye (*Stizostedion vitreum*) eggs in a northern Ontario River. Écoscience, **1**: 215–222.

Mathias, J.A., and Li, S. 1982. Feeding habits of walleye larvae and juveniles: comparative laboratory and field studies. Trans. Am. Fish. Soc. **111**: 722–735.

Persaud, D., Jaagumagi, R., and Hayton, A. 1991. Provincial sediment quality guidelines. Ontario Ministry of the Environment, Toronto, Ont.

Pitlo, J.J. 1992. Walleye and sauger (*Stizostedion* spp.) in the Upper Mississippi River: early life history. Fish Technical Section Upper Mississippi River Conservation Committee, Rock Island, Ill.

Priegel, G.R. 1969. Food and growth of young walleye in Lake Winnebago, Wisconsin. Trans. Am. Fish. Soc. **98**: 121–124.

© 1996 NRC Canada

Priegel, G.R. 1970. Reproduction and early life history of the walleye in the Lake Winnebago region. Wis. Dep. Nat. Resour. Tech. Bull.

Scott, M.T., and Nielsen, L.A. 1989. Young fish distribution in the backwaters and main channel borders of the Kanawha River, West Virginia. J. Fish Biol. **35**(Suppl. A): 21–27.

Sheaffer, W.A., and Nickum, J.G. 1986. Backwater areas as nursery habitats for fishes in Pool 13 of the Upper Mississippi River. Hydrobiologia, **136**: 131–140.

Smith, L.L., and Pycha, R.L. 1960. First-year growth of the walleye, *Stizostedion vitreum vitreum* (Mitchill), and associated factors in the red lakes, Minnesota. Limnol. Oceanogr. **5**: 281–300.

Smock, L.A. 1980. Relationships between body size and biomass of aquatic insects. Freshwater Biol. **10**: 375–383.

© 1996 NRC Canada

Sequence variation in ribosomal DNA of Pacific (*Clupea pallasi*) and Atlantic herring (*Clupea harengus*)

Michael J. Domanico, Ruth B. Phillips, and Jake F. Schweigert

Abstract: Nucleotide sequence variation in the ribosomal DNA (rDNA) of Pacific (*Clupea pallasi*) and Atlantic herring (*Clupea harengus*) was examined using restriction enzyme analysis and DNA sequencing. Restriction maps of the rDNA repeat were similar in these two species, with a difference at only one site in the intragenic spacer region. This restriction site was also polymorphic within Pacific herring populations, but did not reveal any stock-specific patterns. The degree of sequence divergence of the ITS 1 averaged 1.3% between the Atlantic and the Pacific herring and 0.34% between the Pacific herring from different coastal regions of British Columbia. This result suggests a divergence time of 3.1 million yr between Atlantic and Pacific herring which is consistent with dispersal of herring into the Pacific Ocean in the mid-Pliocene.

Résumé : Nous avons déterminé au moyen d'une analyse par des enzymes de restriction et par séquençage de l'ADN, la variation observée au niveau des séquences nucléotidiques de l'ADN ribosomique (ADNr) entre le hareng du Pacifique (*Clupea pallasi*) et le hareng de l'Atlantique (*Clupea harengus*). Les cartes de restriction des segments répétés de l'ADNr sont semblables chez les deux espèces, à l'exception d'un seul site dans la séquence d'espacement intragénique. Ce site de restriction est également polymorphique àl'échelle des populations de hareng du Pacifique, mais ne révèle aucune caractéristique associée à des stocks. Le degré de divergence des séquences au site de l'ITS 1 est de 1,3 % en moyenne entre le hareng du Pacifique et le hareng de l'Atlantique et de 0,34 % entre le hareng du Pacifique provenant de différentes régions le long de la côte de la Colombie-Britannique. Ces résultats paraissent indiquer que le hareng de l'Atlantique et la hareng du Pacifique se sont séparés il y a 3,1 millions d'années. Cette conclusion est conforme à la date de dispersion du hareng dans le Pacifique au milieu du pliocène. [Traduit par la Rédaction]

Introduction

Pacific (*Clupea pallasi*) and Atlantic herring (*Clupea harengus*) are currently recognized as distinct species (Robins et al. 1991). Although these fish are similar in morphology, Atlantic herring generally have a greater number of vertebrae, longer heads, and smaller eyes than Pacific herring (Grant 1986). The morphological similarity between Atlantic and Pacific herring implies a recent separation, probably during the late Pliocene or early Pleistocene periods (Grant 1986).

The degree of genetic differentiation between Atlantic and Pacific herring has been analyzed in studies using allozyme variation and mitochondrial DNA (mtDNA) restriction data. A high degree of variation in allozyme allele frequencies between species was found with an average genetic distance of 0.27, typical of a species level of divergence in fish (Grant 1986). Based on genetic distance, the estimated divergence time between Atlantic and Pacific herring was 3.6–6.6 million yr ago, suggesting that ancestral herring dispersed into the Pacific Ocean soon after the Bering Sea opened in the mid-Pliocene, 3.0–3.5 million yr ago (Grant 1986). However, an estimate of only 2.6% sequence divergence between the two taxa was obtained from the analysis of mtDNA restriction site data (Kornfield and Bogdanowicz 1985). This would correspond to a divergence time of 1 million yr based on the evolutionary rate of primate mtDNA (Thomas et al. 1986), and would be substantially less than that predicted on the basis of allozyme variation, if the evolutionary rate of fish is similar to mammals. However, recent evidence suggests that mtDNA evolves slower in fishes (Thomas and Beckenbach 1989), so that 2.6% sequence divergence may correspond to 3–6 million yr ago.

Genetic variation has also been examined within populations of Pacific and Atlantic herring. Allozyme studies showed that there was little genetic differentiation in Atlantic herring on either side of the Atlantic Ocean (Grant 1987). Similar studies on Pacific herring provided evidence for two genetic races in the North Pacific, an Asian – Bering Sea race and an eastern North Pacific race (Grant and Utter 1984). A study of different spawning populations off British Columbia's coast showed little differentiation within this smaller geographic region (Schweigert and Withler 1990). Similar results were found when restriction enzyme analysis of mtDNA was done on these same populations, suggesting that there may be sufficient migration over hundreds of kilometres between the large spawning populations to prevent the formation of discrete genetic stocks.

Received July 6, 1993. Resubmitted July 31, 1995.
Accepted May 1, 1996.
J11749

M.J. Domanico and R.B. Phillips.[1] Department of Biological Sciences, University of Wisconsin-Milwaukee, Milwaukee, WI 53201, U.S.A.
J.F. Schweigert. Department of Fisheries and Oceans, Pacific Biological Station, Nanaimo, BC V9R 5K6, Canada.

[1] Author to whom correspondence may be addressed.

© 1996 NRC Canada

Fig. 1. Map of the coast of British Columbia showing six sampling locations for Pacific herring.

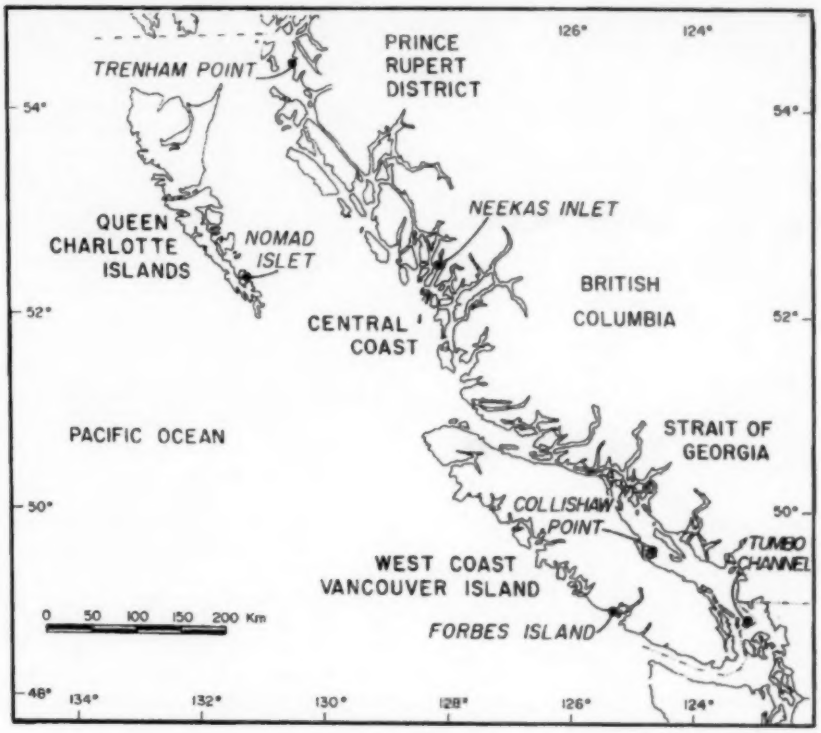

Analysis of ribosomal DNA (rDNA) is an alternative method for determining genetic differentiation between populations. The repeating unit of rDNA contains coding and noncoding regions which evolve at different rates and can be used to compare both distantly and closely related populations (Gerbi 1985).

Restriction site mapping of the whole rDNA repeating unit has been used successfully for stock identification of Arctic char (*Salvelinus alpinus*) and Dolly Varden (*Salvelinus malma*) (Phillips and Pleyte 1991). Fixed restriction site differences were found in allopatric populations of Arctic char from different geographic regions, but not in sympatric populations from the same region (Phillips and Pleyte 1991). Sequencing of the ITS 1 and a variable portion of the 28S RNA was useful for comparing relationships among the great apes and humans (Gonzalez et al. 1990) and for phylogeny of fishes in the genus *Salvelinus* (Pleyte et al. 1992) and genus *Oncorhynchus* (Domanico 1994).

In this study, a restriction fragment length polymorphism (RFLP) of rDNA was examined in five Pacific herring populations from British Columbia and one Atlantic herring population from New Brunswick. Restriction site data were analyzed to determine if any variable sites existed which could be used for identification of spawning populations in the coastal waters of British Columbia. DNA sequence variation of the ITS 1 was also analyzed for two individuals from three Pacific populations and one Atlantic population. By including Atlantic herring, we were able to obtain a more accurate estimate of the amount of genetic divergence between Atlantic and Pacific herring.

Materials and methods

Materials and extractions

Pacific herring were sampled from six spawning locations in the coastal waters of British Columbia: Forbes Island (West Coast of Vancouver Island), Collishaw Point (Strait of Georgia), Tumbo Channel (Straight of Georgia), Trenham Point (Prince Rupert District), Nomad Islet (Queen Charlotte Islands), and Neekas Inlet (central coast of British Columbia) (Fig. 1). Each sampling area represents a different geographical region of British Columbia's coast. Atlantic herring were sampled from the coastal waters of New Brunswick. Fish from each area were treated as separate populations. The Collishaw Point fish were obtained in 1989, while the other populations were obtained in 1990.

DNA was extracted from at least 10 fish from each sampling area. Genomic DNA was extracted from fish livers by phenol extraction (Popodi et al. 1985) for most of the samples, and using the Stratagene DNA extraction kit for some of the later samples.

Restriction mapping of rDNA and RFLP analysis

Restriction mapping of the rDNA of Atlantic and Pacific herring was done using methods described previously (Phillips et al. 1992). We used 12 restriction enzymes: *Bam* HI, *Bgl* II, *Bcl* I, *Dra* I, *Eco* RI, *Hind* III, *Kpn* I, *Nhe* I, *Pst* I, *Pvu* II, *Ssp* I, and *Xba* I. DNA fragment patterns from single and double digestions were analyzed to infer the restriction site maps.

The multiple banding patterns in the Pacific samples were com-

© 1996 NRC Canada

Fig. 2. Restriction map of the rDNA repeating unit from (*a*) Pacific herring and (*b*) Atlantic herring. Ba = *Bam* HI, Bc = *Bcl* I, B = *Bgl* II, D = *Dra* I, E = *Eco* RI, H = *Hind* III, K = *Kpn* I, N = *Nhe* I, P = *Pst* I, Pv = *Pvu* II, S = *Ssp* I, X = *Xba* I. Asterisks designate polymorphic sites.

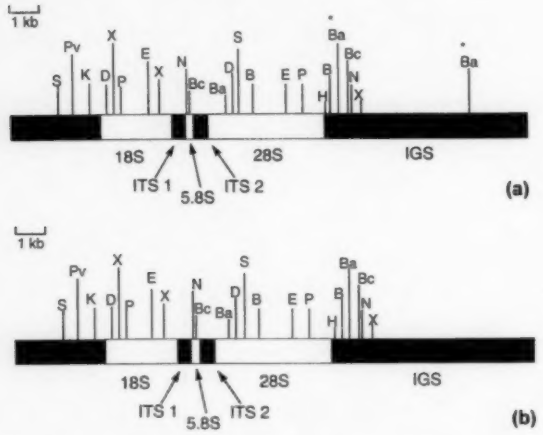

pared by calculating the percent difference (*D*) between fragment patterns (Wayne et al. 1991). This technique has been used for comparison of multiple bands obtained in DNA fingerprinting studies. Six individuals from each population were compared. The percent difference between restriction fragments of two individuals was calculated by dividing the number of fragments that differed by the total number of fragments times 100. The average percent difference is the average of all *D* values for each population, and gives an estimate of how many bands differ among samples.

Amplification and sequencing of the ITS 1 of the rDNA

The ITS 1 region of the rDNA was amplified from genomic DNA using the polymerase chain reaction (Saiki et al. 1988) for two individuals from three of the Pacific populations (Strait of Georgia, central coast, and Prince Rupert District) and the Atlantic population. The known 18S rDNA sequence from *Xenopus laevis* (Salim and Maden 1981) was used to design the forward primer "18S" (5′TTGTACACACCGCCCGTCGC3′), and the known 5.8S sequence from rainbow trout (*Oncorhynchus mykiss*) (Nazar and Roy 1978) was used to design the reverse primer "5.8S" (AGCTTGCTGCGTTCTTCATCGA3′).

PCR reactions of 100-μL volume consisted of 1 μg of genomic DNA, 10 μL of 10× buffer (0.5 M KCl, 0.01 M Tris–Cl, pH 8.0, 0.1% gelatin, 0.015 M $MgCl_2$), 200 μmol of each deoxynucleotide triphosphate (dATP, dCTP, dGTP, dTTP), 90 pmol of each primer, and 2.5 units of *Taq* polymerase. Amplifications were carried out with 35 repetitions of a three-step cycle: (1) denaturation at 94°C for 1.5 min, (2) annealing at 55°C for 2 min, and (3) extension at 72°C for 3 min, and ending in a final extension at 72°C for 7 min.

For TP2 and H2A, the PCR products were purified with miniprep spun columns (Pharmacia) and then were treated with T4 DNA polymerase (Promega) to produce blunt-ended fragments which were ligated into M13 phagescript (Stratagene) vector. Ligated vector was transformed into *E. coli* strain (DH5αF′) and plated on YT plates. The cloned single-stranded phage DNA was sequenced using the dideoxy sequencing method (Sanger et al. 1977).

Direct sequencing of PCR products was performed on the remaining six individuals. A biotinylated 28S primer was used in the PCR amplification, and dynabeads M-280 streptavidin (Dynal) were used to separate the strands for sequencing, according to the manufacturer's instructions. The forward primer (5′CTTGACTATCTAGAGGAAGT3′) was designed from the 18S gene from *X. laevis* (Salim and Maden 1981), and the reverse biotinylated primer (5′ATATGCTTAAATTCAGCGGG3′) was designed from the 28S sequence of *X. laevis* (Ware et al. 1983). The forward sequencing primer (5′CCGTAGGTGAACCTGCG3′) was also designed from the *X. laevis* 18S gene.

Sequences were aligned visually to yield a minimal number of evolutionary steps with gaps inserted to maintain alignment. Alignment gaps in runs of three or more identical bases were eliminated from the analysis. Percent sequence divergences were estimated by dividing the number of variable sites by the total number of sites.

Genetic distances were estimated by the Jukes–Cantor method with the molecular evolutionary genetics analysis (MEGA) program (Kumar et al. 1993). A tree was constructed from the genetic distances with the neighbor-joining (Saitou and Nei 1987) option of MEGA.

Results

Restriction enzyme analysis of rDNA

The restriction site maps generated with 12 restriction enzymes were the same for all the Pacific herring populations, except for a polymorphism involving two variable restriction sites with the *Bam* HI enzyme (Fig. 2*a*). The Atlantic herring map was the same except that one of these sites was fixed and the other missing in Atlantic herring (Fig. 2*b*).

Restriction patterns obtained by digesting DNA with *Bam* HI and hybridization with the 28S probe showed considerable variation among the populations. A common 3.5-kb band was found in all of the Pacific and Atlantic populations. The band was wider and less intense in the Pacific herring samples than in the Atlantic sample, suggesting that some of the rDNA units of Pacific herring were lacking one of the restriction sites. When the Pacific samples were digested with *Bam* HI and probed with the 18S probe (PEB-4), one large band (~14 kb) appeared, but the 3.5-kb band was not observed, indicating that the 3.5-kb band resulted from a restriction site 3′ to the *Bam* HI site in the 28S RNA gene. Digestion of DNA with *Bam* HI and hybridization with the 28S probe produced a pattern of multiple bands in the Pacific fish as a result of length variability in the IGS in different rDNA units. The average number of bands was greatest in fish from the central coast sample (Neekas Inlet) (Table 1). The banding patterns were compared between individuals from the different locations. The percent differences (*D* values) between individuals were 75% for Forbes Island, 60% for Neekas Inlet, 81% for Tumbo Channel, 77% for Nomad Islet, and 84% for Trenham Point. The average *D* for all groups was 75%. Comparisons were made using six samples from each group. A comparison was also made between the Neekas Inlet population and Trenham Point population to evaluate the difference between two populations. The percent difference between these groups was found to be 76%, indicating that the amount of variation between two groups is approximately the same as within each group. This region of the rDNA shows high intraindividual variation in fish from all regions and is too variable for distinguishing among spawning populations.

DNA sequence analysis of the ITS 1

The ITS 1 was sequenced for two individuals from each of three Pacific spawning populations, Strait of Georgia, central coast, and Prince Rupert District, and the Atlantic population (Fig. 3). The lengths of the ITS 1 were 378 and 380 bp in the

© 1996 NRC Canada

Table 1. Summary of the multiple banding pattern found when Pacific herring DNA is cut with *Bam* HI and hybridized with the 28S rDNA probe (I-19).

Region	Sampling site	Sampling size	Average no. of bands	Range	*D*
Strait of Georgia	Collishaw Point	6	2.5	3–6	0.3
	Tumbo Channel	6	3.1	2–6	
West coast of Vancouver Island	Forbes Island	9	3.2	–4	0.75
Central coast	Neekas Inlet	6	6	–3	0.6
Queen Charlotte Islands	Nomad Islet	6	2.5	–4	0.77
Prince Rupert District	Trenham Point	9	3.2	–4	0.84

Note: The percent difference (*D*) (Wayne et al. 1991) between restriction fragments between individuals was calculated by dividing the number of fragments that differed by the total number of fragments times 100.

Strait of Georgia sample (Collishaw Point), 379 and 380 bp in the central coast sample (mouth of Neekas Inlet), 378 and 381 bp in the Prince Rupert District sample (Trenham Point), and 373 and 377 bp in the Atlantic population. The percent sequence divergence between samples ranged from 0.0% between the two Atlantic herring to 1.6% between the Atlantic herring and the Trenham Point sample, TP2 (Table 2). The neighbor-joining tree placed both Atlantic herring together, but no two Pacific fish from the same spawning location were grouped together (Fig. 4).

Discussion

Restriction analysis of herring rDNA

Because rDNA is composed of repeating units, and often found at different locations of the genome, it is possible that some units may contain a particular restriction site which others lack. Band intensity differences are visualized on the autoradiographs when this occurs. Such differences are found in Pacific herring when genomic DNA is digested with *Bam* HI and probed with the 28S probe (I-19). The common 3.5-kb fragment appears to be produced by a fixed restriction site in the 28S gene and a variable *Bam* HI site in the IGS region which is found in some but not all units in every individual. In the other rDNA units the second site is farther out in the IGS so that larger fragments are obtained. The multiple banding pattern found in Pacific herring is the result of intraindividual variation in the position of this second restriction site in different rDNA units. The IGS often contains multiple copies of short repeats, and variation in the number of these between the two *Bam* HI sites could produce a multiple banding pattern. Variation in methylation of the sites or base changes in the different units could also produce this type of pattern. In lake trout (*Salvelinus namaycush*), analysis of cloned rDNA showed that this region has a variable number of 89 bp repeats in different rDNA units (Zhuo et al. 1995).

The herring populations in the present study showed no fixed restriction site differences in the rDNA, but minor sites and multiple banding patterns were observed. The most visible differences between the populations occurred among the multiple banding patterns obtained with *Bam* HI digestions and the 28S probe (I-19). Restriction digestion of rDNA with *Bam* HI did not produce multiple bands in Atlantic herring when probed with the 28S probe (I-19), so this method could be used to distinguish Atlantic from Pacific herring. The intrapopulation variation in banding patterns was similar to interpopulation variation. These results are in agreement with previous allozyme studies which found no evidence for discrete stocks of Pacific herring in British Columbia.

Sequence analysis of the ITS 1

The ITS 1 (internal transcribed spacer) has an intermediate rate of evolution and appears to evolve linearly with time, at least in the separation of primate and rodent lineages (Gonzalez et al. 1990). The size of the ITS 1 varies considerably in different species. It is 550–595 bp in salmonid fishes (Pleyte et al. 1992; Domanico 1994), 567 bp in *X. laevis*, 1000 bp in mouse, and 1095 bp in humans (Gonzalez et al. 1990). The herring ITS 1 proved to be somewhat smaller, ranging from 378 to 383 bp in the Pacific populations and from 373 to 376 bp in the Atlantic population.

The ITS 1 DNA sequences from two individuals from each of three Pacific herring populations and two individuals from an Atlantic population were compared to see if there was enough sequence divergence in this less conserved region for rDNA analysis to be useful for population comparisons. Although there were differences in sequence between different individuals, there was no stock-specific variation.

In previous work (Pleyte et al. 1992; Domanico 1994; Phillips et al. 1994), we have found that intraindividual variation occurs in the number of bases in runs of a single base, e.g., CCC versus CCCC. Excluding variations in such runs, there were only four variable sites among all samples sequenced, and three of these were phylogenetically informative (Fig. 3). At two of these sites the two Atlantic herring were different from all other samples, and at the third site the two Atlantic herring and TP1 were different from the other samples. Percent sequence divergence averaged 1.3% between the Atlantic and Pacific herring, and 0.34% between the different Pacific herring.

© 1996 NRC Canada

Fig. 3. Aligned DNA sequences from six Pacific herring from three locations and two Atlantic herring from one location. Sites in common with the first are shown as dots. CP = Collishaw Point, MNI = mouth of Neekas Inlet, TP = Trenham Point, and AT = Atlantic herring. Alignment gaps in runs of like bases are shown by plus signs. If alignment gaps are omitted, there are four variable sites which are designated by asterisks. All of these except site 201 are phylogenetically informative.

```
                                                                    ++
CP1 5'  ACGGCACGCG CACGATGCAG GCGTCTCAGC TCGGGCTGCT ACCCC--TTC
CP3 5'  .......... .......... .......... .......... .....C-...
MNI25'  .......... .......... .......... .......... .....--...
MNI35'  .......... .......... .......... .......... .....C-...
TP1 5'  .......... .......... .......... .......... .....--...
TP2 5'  .......... .......... .......... .......... .....CC...
AT2 5'  .......... .......... .......... .......... .....C-...
AT5 5'  .......... .......... .......... .......... .....C-...

                              *  *
CP1     CAAGCCGAGG CGGCGTAGGT GGGGCGAAGG GATCGAAGGG ACCTCGGTCC
CP3     .......... .......... .A........ .......... ..........
MNI2    .......... .......... .A........ .......... ..........
MNI3    .......... .......... .A........ .......... ..........
TP1     .......... .......... .A........ .......... ..........
TP2     .......... .......... .A........ .......... ..........
AT2     .......... .........C .-........ .......... ..........
AT5     .......... .........C .-........ .......... ..........

CP1     CGGTCCCCAG CCTTGCCGAA ACCCCCCTCT GTGCTTTGTT TTTTTCTCCT
CP3     .......... .......... .......... .......... ..........
MNI2    .......... .......... .......... .......... ..........
MNI3    .......... .......... .......... .......... ..........
TP1     .......... .......... .......... .......... ..........
TP2     .......... .......... .......... .......... ..........
AT2     .......... .......... .......... .......... ..........
AT5     .......... .......... .......... .......... ..........

                                        +
CP1     TCGGGAGAAA TCAACTACCC CCGGGAAA-C ACTCAAGGCC TCCCTGTCCC
CP3     .......... .......... .........A. .......... ..........
MNI2    .......... .......... .........A. .......... ..........
MNI3    .......... .......... .........A. .......... ..........
TP1     .......... .......... .........-. .......... ..........
TP2     .......... .......... .........-. .......... ..........
AT2     .......... .......... .........-. .......... ..........
AT5     .......... .......... .........-. .......... ..........

        *          ++
CP1     CGGTTCACGC CGGG-CTGGG TTGCCAGACC GAGTACCAAC TCCGTCGCTG
CP3     .......... ....-..... .......... .......... ..........
MNI2    .......... ....-..... .......... .......... ..........
MNI3    .......... ....-..... .......... .......... ..........
TP1     .......... ....-..... .......... .......... ..........
TP2     T......... ....G..... .......... .......... ..........
AT2     .......... ...--..... .......... .......... ..........
AT5     .......... ....G..... .......... .......... ..........

CP1     TTCGGGTTCG CTCGTTCAGC GGCGGGCGGC TTAAAGTTCC CCGGGCTCAC
CP3     .......... .......... .......... .......... ..........
MNI2    .......... .......... .......... .......... ..........
MNI3    .......... .......... .......... .......... ..........
TP1     .......... .......... .......... .......... ..........
TP2     .......... .......... .......... .......... ..........
AT2     .......... .......... .......... .......... ..........
AT5     .......... .......... .......... .......... ..........

              +                                 *   + + +
CP1     ACCCGGGGCG CTCGGTCACT TAACCCCACA AAAAAAAAC- TTTTCTTCCG
CP3     .......... .......... .......... ...A...... ..........
MNI2    .......... .......... .......... ...A.....- ..........
MNI3    .......... .......... .......... ...A.....- ..........
TP1     .......... .......... .......... ...C.....- ..........
TP2     .......... .......... .......... ...A...-.T ..........
AT2     .......-.. .......... .......... ...C...-.- -.........
AT5     .......... .......... .......... ...C.....- -.........

                        +
CP1     GTTCTGGGCC AAAACAA-CA ATCAAAAAGA GTA 3' 377bp
CP3     .......... .......... .......... ... 3' 379bp
MNI2    .......... .......... .......... ... 3' 378bp
MNI3    .......... .......... .......... ... 3' 379bp
TP1     .......... .......... .......... ... 3' 377bp
TP2     .......... .......A.. .......... ... 3' 380bp
AT2     .......... .......A.. .......... ... 3' 372bp
AT5     .......... .......A.. .......... ... 3' 376bp
```

Previous work on ITS 1 in the genus *Oncorhynchus* found 2.33% divergence among the closely related *O. keta* and *O. gorbuscha* which are thought to have diverged 5.5 million yr ago (Smith et al. 1982). From these results, a rate of sequence divergence of 0.42% per million years can be calculated which is similar to that obtained for primates for the ITS 1 (Gonzalez et al. 1990). Using this rate the sequence divergence of 1.3% would correspond to a divergence of 3.1 million yr between Pacific and Atlantic herring. This is similar to previous estimates of 3–6 million yr from allozyme data and suggests dispersal of herring into the Pacific Ocean in the mid-Pliocene.

Fig. 4. Tree generated from Jukes–Cantor distances of the herring ITS 1 DNA sequences using the neighbor-joining option of the MEGA program (Kumar et al. 1993). CP = Collishaw Point, MNI = mouth of Neekas Inlet, TP = Trenham Point, and AT = Atlantic herring. The numbers following letters identifying sampling sites distinguish between the two individuals from the same site.

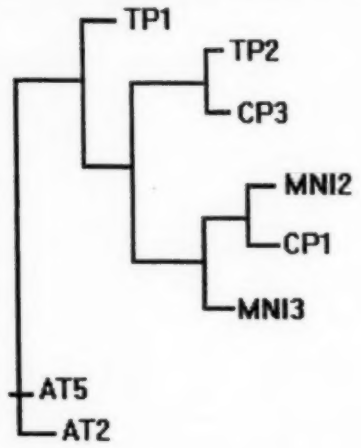

Table 2. Pairwise percent sequence divergences between six Pacific herring sampled from three locations and two Atlantic herring from one location.

	CP1	CP2	MNI1	MNI2	TP1	TP2	AT1	AT2
CP1	—	0.26	0.26	0.26	0.50	0.80	1.3	1.3
CP2		—	0.0	0.0	0.26	0.50	1.3	1.3
MNI1			—	0.0	0.26	0.50	1.3	1.3
MNI2				—	0.26	0.50	1.3	1.3
TP1					—	0.80	1.1	1.6
TP2						—	1.6	1.6
AT1							—	0.0
AT2								—

Note: Pacific herring: CP, Collishaw Point – Strait of Georgia, B.C.; MNI, mouth of Neekas Inlet – central coast of B.C.; TP, Trenham Point – Prince Rupert District, B.C. Atlantic herring: AT, New Brunswick.

Acknowledgments

We would like to thank Bob Armstrong, Fisheries Branch, Department of Fisheries and Oceans, Nanaimo, B.C., for assistance in sample collection. Funding for research was provided by the Department of Fisheries and Oceans, Pacific Biological Station, Nanaimo, B.C.

© 1996 NRC Canada

References

Domanico, M.J. 1994. Phylogenetic analysis of Pacific salmon using nuclear and mitochondrial DNA sequences. Ph.D. dissertation, University of Wisconsin-Milwaukee, Milwaukee, Wis.

Gerbi, S.A. 1985. Evolution of ribosomal DNA. *In* Molecular evolutionary genetics. *Edited by* R.J. MacIntyre. Plenum Press, New York, N.Y. pp. 419–517.

Gonzalez, I.L., Sylvester, J.E., Smith, T.F., Stambolian, D., and Schmickel, R.D. 1990. Ribosomal RNA gene sequence and hominoid phylogeny. Mol. Biol. Evol. **7:** 203–219.

Grant, W.S. 1986. Biochemical genetic divergence between Atlantic, *Clupea harengus*, and Pacific, *C. pallasi*, herring. Copeia, **1986**(3): 714–719.

Grant, W.S. 1987. Genetic divergence between congeneric Atlantic and Pacific ocean fishes. *In* Population genetics and fishery management. *Edited by* N. Ryman and F. Utter. University of Washington Press, Seattle, Wash. pp. 225–246.

Grant, W.S., and Utter, F.M. 1984. Biochemical population genetics of Pacific herring (*Clupea pallasi*). Can. J. Fish. Aquat. Sci. **46:** 856–864.

Kornfield, I., and Bogdanowicz, S.M. 1985. Differentiation of mitochondrial DNA in Atlantic herring, *Clupea harengus*. Proceedings of the Stock Identification Workshop, Panama City Beach, Fla. pp. 187–188.

Kumar, S., Tamura, K., and Nei, M. 1993. MEGA: molecular evolutionary genetics analysis, version 1.0. The Pennsylvania State University, University Park, Pa.

Nazar, R.N., and Roy, K.L. 1978. Nucleotide sequence of rainbow trout (*Salmo gairdneri*) ribosomal 5.8S ribonucleic acid. J. Biol. Chem. **253:** 395–399.

Phillips, R.B., and Pleyte, K.A. 1991. Nuclear DNA and salmonid phylogenetics. J. Fish Biol. **39**(Suppl. A): 259–275.

Phillips, R.B., Pleyte, K.A., and Brown, M.R. 1992. Salmonid phylogeny inferred from ribosomal DNA restriction maps. Can. J. Fish. Aquat. Sci. **49:** 2345–2353.

Phillips, R.B., Manley, S.A., and Daniels, T.J. 1994. Systematics of the salmonid genus *Salvelinus* inferred from ribosomal DNA sequences. Can. J. Fish. Aquat. Sci. **51**(Suppl. 1): 198–204.

Pleyte, K.A., Duncan, S., and Phillips, R.B. 1992. Phylogenetic analysis of the genus *Salvelinus* from the ITS-1 of ribosomal DNA. Mol. Phylogenet. Evol. **1:** 223–230.

Popodi, E.M., Greve, D., Phillips, R.B., and Wejksnora, P.J. 1985. The ribosomal RNA genes of three salmonid species. Biochem. Genet. **23:** 997–1010.

Robins, C.R. , Bailey, R.M., Bond, C.E., Brooker, J.R., and Lachner, E.A. 1991. A list of common and scientific names of fishes from the United States and Canada. 5th ed. Am. Fish. Soc. Spec. Publ. No. 20. American Fisheries Society, Bethesda, Md.

Saiki, R., Gelfund, D., Stoffel, S., Scharf, S., Higuchi, R., Horn, G., Mullis, K., and Erlich, H. 1988. Primer directed enzymatic amplification of DNA with a thermostable DNA polymerase. Science (Washington, D.C.), **239:** 487–491.

Saitou, N., and Nei, M. 1987. The neighbor joining method: a new method for reconstructing phylogenetic trees. Mol. Biol. Evol. **4:** 406–425.

Salim, M., and Maden, B.E. 1981. Nucleotide sequence of *Xenopus leavis* 18S ribosomal RNA inferred from gene sequence. Nature (Lond.), **291:** 205–208.

Sanger, F., Nicklen, S., and Coulson, A.R. 1977. DNA sequencing with chain-terminating inhibitors. Proc. Natl. Acad. Sci. U.S.A., **74:** 5463–5467.

Schweigert, J.F., and Withler, R.E. 1990. Genetic differentiation of Pacific herring based on enzyme electrophoresis and mitochondrial DNA analysis. Am. Fish. Soc. Symp. **7:** 459–469.

Smith, G.R., Swirydczuk, K., Kimmel, P.G., and Wilkinson, B.H. 1982. Fish biostratiography of late Miocene to Pleistocene sediments of the western Snake River plain, Idaho. Idaho Bur. Mines Geol. Bull. **26:** 519–541.

Thomas, W.K., and Beckenbach, A.T. 1989. Variation in salmonid mitochondrial DNA: evolutionary constraints and mechanisms of substitution. J. Mol. Evol. **29:** 233–245.

Thomas, W.K., Withler, R.E., and Beckenbach, A.T. 1986. Mitochondrial DNA analysis of Pacific salmonid evolution. Can. J. Zool. **64:** 1058–1064.

Ware, V.C., Tague, B.W., Clark, C.G., Gourse, R.L., Brand, R.C., and Gerbi, S.A. 1983. Sequence analysis of 28S ribosomal DNA from the amphibian *Xenopus laevis*. Nucleic Acids Res. **11:** 7795–7817.

Wayne, R.K., Lehman, N., Gersion, D., et al. 1991. Conservation genetics of the endangered Isle Royale grey wolf. Conserv. Biol. **5:** 41–52.

Zhuo, L., Reed, K.M., and Phillips, R.B. 1995. Hypervariability of ribosomal DNA at multiple chromosomal sites in lake trout (*Salvelinus namaycush*). Genome, **38:** 487–496.

© 1996 NRC Canada

Effects of didecyldimethylammonium chloride (DDAC) on the swimming performance, gill morphology, disease resistance, and biochemistry of rainbow trout (*Oncorhynchus mykiss*)

Antony W. Wood, Blair D. Johnston, Anthony P. Farrell, and Christopher J. Kennedy

Abstract: The acute lethal and sublethal toxicity of didecyldimethylammonium chloride (DDAC) to juvenile rainbow trout (*Oncorhynchus mykiss*) was investigated. The nominal 96-h LC_{50} value in a flow-through exposure system was 0.409 mg·L^{-1}. Investigation of the effects of acute sublethal exposures on blood chemistry, swimming performance, disease resistance, and gill morphology revealed no adverse effects after a 24-h exposure to 0.1 mg DDAC·L^{-1}. Primary and secondary biochemical indicators of stress, i.e., plasma cortisol, glucose, and lactate levels, were only significantly elevated after a 24-h exposure to DDAC at 0.4 mg·L^{-1}. However, swimming performance decreased significantly after 12- and 24-h exposures to both 0.2 and 0.4 mg·L^{-1}. Scanning electron microscopic analysis revealed no gross disruptions to gill epithelial surfaces as a result of toxicant exposure. A disease challenge test revealed that exposure to sublethal concentrations of DDAC for 24 h had no significant effects on the susceptibility of rainbow trout to lethal infection from *Vibrio anguilarum* after 14 d. The results suggest that DDAC has a very steep dose–response relationship during acute exposures. Those responsible for regulating the outflow of DDAC into fish-bearing waters should take this into account.

Résumé : Les auteurs ont étudié la toxicité aiguë létale et sublétale du chlorure de didécyldiméthylammonium (CDDA) chez des juvéniles de la truite arc-en-ciel (*Oncorhynchus mykiss*). Ils ont établi à 0,409 mg·L^{-1} la CL_{50} 96 h nominal dans un circuit où l'eau en circulation est renouvelée. À l'examen, ils ont constaté qu'une exposition sublétale aiguë (0,1 mg CDDA·L^{-1}) pendant 24 h n'avait aucun effet nocif sur la chimie du sang, l'efficacité de la nage, la résistance à la maladie et la morphologie des branchies. Des indicateurs biochimiques primaires et secondaires du stress, c.-à-d. la concentration du cortisol, du glucose et du lactate plasmatiques, était significativement supérieure seulement au bout de 24 h d'exposition au CDDA à la concentration de 0,4 mg·L^{-1}. Toutefois, l'efficacité de la nage avait diminué de manière significative après des expositions de 12 et de 24 h aux deux concentrations de 0,2 et de 0,4 mg·L^{-1}. L'analyse par microscopie électronique à balayage n'a pas mis en évidence de lésions graves de l'épithélium branchial consécutives à l'exposition à ce toxique. Un test de provocation de maladies a montré que l'exposition au CDDA en concentration sublétale pendant 24 h n'avait pas d'effet significatif sur la vulnérabilité de la truite arc-en-ciel à une infection létale par *Vibrio anguilarum* au bout de 14 jours. Les résultats indiquent que la courbe dose-réponse aux expositions aiguës du CDDA a une pente très forte. Les organismes responsables de réglementer son rejet dans des eaux habitées par le poisson doivent tenir compte de ceci.
[Traduit par la Rédaction]

Introduction

A large sector of the forest products industry in British Columbia involves the export of green, fresh-milled softwood lumber to varied destinations throughout the world. Due to its high moisture content, this lumber is highly susceptible to attack from moulds and fungi which cause a characteristic discolouration known as sapstain. While its effects are primarily aesthetic, sapstain does have the potential to reduce the market value of export lumber. Thus, in order to meet the stringent lumber quality guidelines for export markets, the forest products industry has come to rely upon the treatment of fresh-milled lumber with chemical fungicides known as antisapstains. Didecyldimethylammonium chloride (DDAC) is the principal active component of most antisapstain formulations currently registered and used by the industry in British Columbia (Henderson 1992).

As with many wood preservatives, there exists concern over the toxicity of DDAC to nontarget organisms in the environment. Of particular concern is the potential toxicity of DDAC to organisms in the aquatic environment, as mills using this chemical frequently occupy sites in close proximity

Received June 30, 1996. Accepted May 1, 1996.
J12975

A.W. Wood, Blair D. Johnston, A.P. Farrell, and C.J. Kennedy.[1] Department of Biological Sciences, Simon Fraser University, Burnaby, BC V5A 1S6, Canada.

[1] Author to whom correspondence should be addressed.

© 1996 NRC Canada

to aquatic ecosystems (Envirochem Special Projects Inc. 1992). Upon exposure to rainfall, leachate from lumber treated with DDAC may enter adjacent fish-bearing waters through lumberyard storm sewers. Leachate studies with DDAC-treated lumber have shown initial leachates to be between 48 and 73.2 $mg \cdot L^{-1}$, with later leachates in the range of 6 $mg \cdot L^{-1}$ (Henderson 1992), while storm-sewer outfall measurements in the Fraser River have revealed DDAC concentrations as high as 1.5 $mg \cdot L^{-1}$ (Envirochem Special Projects Inc. 1992). Existing information, upon which current waste management regulations are based, indicates that DDAC is acutely toxic to fish, with a 96-h LC_{50} value of 0.704 $mg \cdot L^{-1}$ as determined by static bioassay methods (Henderson 1992). There is currently no published information on the sublethal toxicity of DDAC to aquatic vertebrates.

Sublethal toxicity testing became an integral component of the chemical hazard evaluation process when it became increasingly evident that the fitness of organisms may be compromised by exposure to toxicants at concentrations well below those that directly cause lethality (Sprague 1971). Previous sublethal toxicity tests have revealed that many environmental pollutants, including former antisapstains such as 2-(thiocyanomethylthio)-benzothiazole (TCMTB) and chlorophenols, exert considerable sublethal effects upon various fish species (Mitrovic et al. 1968; Howard 1975; Johansen and Geen 1990; Schwaiger et al. 1992; MacKinnon and Farrell 1992; Nikl and Farrell 1993). Commonly studied indicators of sublethal toxicity include primary and secondary biochemical stress indicators such as plasma corticosteroid, lactate, and glucose levels, haematocrit, haemoglobin, and liver glycogen levels, as well as tertiary performance indicators such as critical swimming speed and disease resistance. These parameters represent a convenient and reliable means of evaluating the stress responses of fish to environmental perturbation in an ecologically relevant context (Adams 1990).

The primary objectives of this study were to determine the 96-h median lethal concentration of DDAC for juvenile rainbow trout (*Oncorhynchus mykiss*) using a flow-through exposure apparatus, and to evaluate the sublethal toxicity of DDAC to rainbow trout after acute (24 h) exposure. For the latter, a suite of biochemical stress indicators was chosen, together with an evaluation of effects on swimming performance and disease resistance. In addition, scanning electron microscopic analyses of gill lamellae were performed to assess the effects of acute DDAC exposure on gill morphology.

Materials and methods

Test animals and water supply

Juvenile rainbow trout (mean fork length 9.66 ± 0.10 cm; mean weight 8.67 ± 0.28 g) of mixed sex were obtained from West Creek Trout Farms, Aldergrove, B.C., and maintained for 1 mo in indoor 750-L fibreglass holding tanks at a density of approximately 0.8 $g \cdot L^{-1}$. The water supply consisted of recirculated, dechlorinated municipal water (10–15°C; pH 6.8–6.9; hardness 5.2–6.0 mg $CaCO_3 \cdot L^{-1}$; dissolved O_2 > 95% saturation). Fish were exposed to a photoperiod simulating spring conditions (10 h light : 14 h dark) using fluorescent light, and were fed ad libitum five times per week on a diet of commercial pellets (Biodiet Grower, Warrenton, Ore.) until 24 h prior to an experiment.

Test chemical

DDAC is a photolytically stable, nonvolatile salt which constitutes the active ingredient in the commercial antisapstain Bardac®2280. Bardac®2280 (80% DDAC, 10% ethanol, and 10% water) has a specific gravity of 0.891 at 25°C, a flash point of 42°C, and is highly soluble in water (Lonza Inc. 1985). Stock solutions of the appropriate DDAC concentrations were prepared using double-distilled, deionized water. Nominal concentrations, based on the technical-grade DDAC content of the Bardac®2280, were prepared through appropriate dilution of the stock solution.

Exposure apparatus

The apparatus for toxicant exposure consisted of a modified version of the flow-through respirometer system described in detail by Johansen and Geen (1990). Exposure vessels used for the 96-h LC_{50} determination consisted of six 8-L glass cylinders, while sublethal exposures were conducted in four 65-L glass aquaria. All exposure vessels were submersed in constant-temperature water baths (12.0 ± 1.0°C) and enclosed by opaque polyethylene blinds to prevent external disturbances. Toxicant delivery to each vessel was accomplished through computer control of an intermittent-flow delivery pump system. The delivery system was calibrated prior to the study with a series of dye dilutions using Trypan Blue (Sigma, St. Louis, Mo.). At the start of each experiment, toxicant concentrations within the exposure chambers were brought to desired nominal levels by manual injection of the appropriate quantity of stock solution. Injections were performed at various points along each vessel to facilitate mixing of the toxicant, and care was taken to minimize fish disturbance.

Fish were allowed an acclimation period within the exposure chambers for a period of 48 h prior to the start of each bioassay. All trials were conducted in accordance with bioassay guidelines outlined by the American Public Health Association (1976) and Sprague (1973).

Acute lethality test

To determine the 96-h LC_{50} and its 95% confidence limits, six groups of 11 fish were exposed to a logarithmic series of concentrations (0.0, 0.16, 0.25, 0.40, 0.63, and 1.0 $mg \cdot L^{-1}$) which bracketed the published 96-h LC_{50} (static bioassay) value of 0.704 $mg \cdot L^{-1}$ (Environment Canada 1989, *cited in* Henderson 1992). An additional bioassay was performed using six groups of 11 fish exposed to a linear series of concentrations (0.0, 0.2, 0.3, 0.4, 0.5, and 0.6 $mg \cdot L^{-1}$). In each bioassay, mortalities were counted and removed every 24 h. The 96-h LC_{50} value was determined using graphical logarithmic-probability (log-probit) analysis (Zar 1974) as detailed in Sprague (1973), and 95% confidence limits were calculated according to Litchfield and Wilcoxon (1949).

Sublethal toxicity tests

Four experiments were performed to investigate the sublethal toxicity of DDAC to rainbow trout. These experiments examined effects on the following parameters: biochemistry, swimming performance, gill morphology, and disease resistance. Treatment groups ($n = 10$ for biochemistry, swimming performance, and gill morphology; $n = 15 \times 2$ for disease challenge) were randomly selected for exposure to one of the following DDAC concentrations: 0, 0.1, 0.2, or 0.4 $mg \cdot L^{-1}$. The biochemical, disease challenge, and gill morphology analyses were performed after 24-h DDAC exposures, while effects on swimming performance were assessed after DDAC exposure durations of 12, 24, and 48 h. The concentrations and durations of exposure to DDAC in this study are representative of conditions likely to be encountered in the field (Envirochem Special Projects Inc. 1992).

Biochemistry

Immediately following the toxicant exposure, 65 mL of anaesthetic (50% 2-phenoxyethanol (Sigma, St. Louis, Mo.) in distilled water)

© 1996 NRC Canada

was injected into each 65-L aquarium to minimize handling stress on the fish (Janz et al. 1991). Unconsciousness was rapid (<20 s) and each fish was quickly removed with a dip net, blotted dry, and its weight and length recorded. A blood sample was obtained from the caudal vasculature in heparinized capillary tubes. A 4.0-μL aliquot of whole blood was immediately assayed for haemoglobin concentration using a commercial assay kit (Sigma, St. Louis, Mo.) and the remaining blood centrifuged for 3 min at 1800*g*. Following centrifugation, haematocrit and leucocrit percentages were determined and the plasma was separated for further analyses. Plasma cortisol levels were determined using a commercial radioimmunoassay kit (Incstar, Stillwater, Minn.). Spectrophotometric analysis was used to determine plasma levels of lactate and glucose (Sigma, St. Louis, Mo.).

The liver of each fish was dissected out, weighed, frozen on dry ice, and stored at –25°C. The hepatic somatic index (HSI) was calculated using the following formula: HSI = liver wt. × 100·body wt.$^{-1}$. As well, a subsample of white muscle tissue was removed with a scalpel, weighed, and stored at –25°C until assayed. Tissue glycogen was determined using the method of Sweeting (1989).

Swimming performance

Fish were transferred to the swimming performance testing apparatus immediately after exposure, and without the use of anaesthetic. The apparatus consisted of a 1500-L ovoid fibreglass raceway tank (outside length 343 cm, depth 41 cm, raceway width 46 cm), varying on the design described by MacKinnon and Farrell (1992). Each straight section contained an enclosed cylinder (length 100 cm, diameter 31 cm) with a fixed mesh screen at the upstream end and a removable screen at the downstream end. Water velocity was controlled by two variable-output propulsion motors (Mercury Thruster T50). Vanes in the curved sections of the tank reduced rotational disturbances caused by the motor propellers, ensuring uniform flow through the cylindrical testing tubes. Water velocity was calibrated using a portable flowmeter (Valeport) prior to the period of experimentation. This calibration was verified after completion of the swimming performance tests.

Critical swimming speed (U_{crit}) was measured in bodylengths per second (BL·s^{-1}) (Brett 1964). Initial water velocity was approximately 1.5 BL·s^{-1}, to which each group of fish was acclimated for a period of 1.6 h. Following this acclimation period, the water velocity was increased by 1.2–1.4 BL·s^{-1} for two 10-min intervals, followed thereafter by 20-min intervals using velocity increments of 0.5–0.6 BL·s^{-1}. This was continued until all fish were exhausted. Fish were determined to be exhausted when they ceased swimming, became pinned to the removable rear screen, and did not respond to gentle prodding. At this point they were removed and the fork length (centimetres) and swimming time (minutes) were noted.

Gill morphology

Three fish from each treatment group in the 24-h swimming performance experiment were selected for gill examination by scanning electron microscopy. Fish chosen were the first, fifth, and last fish to fatigue in each treatment group, with the intent of avoiding a bias in sensitivity. The second gill arch on the left side was removed from each selected fish and fixed using standard fixation techniques (Bozzola and Russell 1992). The gills were then partially dehydrated with a graded series of ethanol concentrations, followed by a graded series of amyl acetate concentrations. Following this, all remaining water was removed by critical-point drying. The gills were then plated with gold in preparation for viewing with a scanning electron microscope (ETEC Autoscan).

Control for fixation artifacts was provided through the preparation of gills from three fish from the same stock which were neither exposed to DDAC nor subjected to a swimming performance challenge. Fixation protocols for these specimens were exactly the same as those described above.

Disease challenge

The pathogen used in the disease challenge experiments was *Vibrio anguilarum*, the bacterium responsible for the highly infectious fish disease vibriosis. Primary isolates of *V. anguilarum* were cultured from rainbow trout known to have died from vibriosis. Bacterial suspensions in sterile phosphate-buffered saline were prepared from isolated *V. anguilarum* grown for 18 h at 20°C on tryptic soy agar plates (TSA; Difco Laboratories), supplemented with 0.5% NaCl.

Fish in each treatment group were fin-clipped (pelvic fin removal) for identification before exposure to their respective DDAC concentrations. After termination of the 24-h toxicant exposure, fish were gently removed from the toxicant exposure vessels with a dip net, immersed for 20 min in aerated dechlorinated municipal water, and then immersed for 20 min in an aerated solution of phosphate-buffered saline containing 9.5×10^6 CFU *V. anguilarum*·mL^{-1}. All fish were then placed into a single 750-L tank receiving flow-through, dechlorinated municipal water and fed ad libitum three times per week. Mortality was monitored daily for 14 d, and dead fish were removed and frozen at –20°C until necropsy.

Kidney and liver tissue samples were aseptically taken and cultured on NaCl-supplemented TSA plates. Vibriosis was confirmed as the cause of death if tissue smears were found to contain Gram-negative, rod-shaped bacteria.

Data analysis

All values are reported as mean ± standard error. Haematocrit and leucocrit percentages were arcsin transformed prior to statistical comparison. Differences between mean values for treatment and control groups in each bioassay were statistically compared using an unpaired Student *t*-test. Disease challenge mortality curves for treatment groups were compared with those of controls using *z*-test statistic population proportion comparisons (Devore 1987) and life table comparisons (Hayes 1989). Significance was accepted at the 95% level ($p < 0.05$).

Quality assurance/quality control

At the time of this study, there was concern regarding sample preservation and the accuracy of analytical techniques for the quantitative determination of DDAC in solution. For this reason, all values reported within are nominal concentrations. Since this study was performed, preservation methods has been improved, and the accuracy of analytical techniques for the quantitative determination of DDAC in solution has been verified. Samples are analysed and quantitated by Nitrogen–Phosphorus Detection Capillary Gas Chromatography (NPD-GC) (Strub 1992). Qualitative confirmation of solutions from recent studies using equivalent stock solution, techniques, and apparatus has yielded measured DDAC values averaging 81.5% of nominal values.

Results

96-h LC_{50} determination

The 96-h LC_{50} value for rainbow trout exposed to DDAC under flow-through conditions was determined to be 0.409 mg·L^{-1}, with upper and lower 95% confidence limits of 0.511 and 0.328 mg·L^{-1}, respectively. The first incidence of mortality occurred at a DDAC concentration of 0.3 mg·L^{-1} (9.09%), and 100% mortality occurred after exposure to 0.5 mg DDAC·L^{-1}.

Biochemical analyses

The results of the biochemical analyses are presented in Table 1. There were no significant differences in any of the biochemical parameters evaluated for 24-h exposures to DDAC concentrations less than 0.4 mg·L^{-1}. Significant elevations in

© 1996 NRC Canada

Table 1. Effects of a 24-h sublethal exposure to DDAC on biochemical parameters in rainbow trout.

Parameter	DDAC concentration ($mg \cdot L^{-1}$)			
	0.0	0.1	0.2	0.4
HSI	0.011±0.002	0.011±0.004	0.012±0.003	0.011±0.002
Glucose ($mg \cdot dL^{-1}$)	65.48±3.18	62.72±2.72	63.12±2.36	81.54±4.92*
Lactate ($mg \cdot dL^{-1}$)	49.23±4.79	42.51±2.50	45.83±4.55	61.58±3.02*
LG ($mg \cdot g^{-1}$)	27.12±4.53	23.78±5.10	34.82±2.92	27.98±3.74
Hb ($g \cdot dL^{-1}$)	7.48±0.53	7.42±0.16	7.39±0.23	8.35±0.23
Haematocrit (%)	46.0±1.29	46.3±1.45	42.9±1.82	48.9±1.48
Leucocrit (%)	0.67±0.07	1.02±0.10	0.88±0.10	0.78±0.10
Cortisol ($\mu g \cdot dL^{-1}$)	1.88±0.44	3.19±0.92	0.81±0.11	8.17±2.16*

Note: $n = 10$ for each group. HSI, hepatic somatic index; LG, liver glycogen; Hb, haemoglobin.
*Significantly different from controls ($p < 0.05$).

Table 2. Critical swimming speeds of rainbow trout following 12-, 24-, and 48-h exposures to DDAC.

Duration (h)	DDAC concentration ($mg \cdot L^{-1}$)			
	0.0	0.1	0.2	0.4
12	6.64±0.14	6.73±0.28	5.46±0.28*	6.02±0.15*
24	6.62±0.24	7.32±0.14*	5.04±0.12*	5.15±0.14*
48	6.54±0.20	6.34±0.32	5.99±0.19	5.78±0.11*

Note: Values represent mean values ± standard error. $n = 10$ for each group. *Significantly differenct from controls ($p < 0.05$).

plasma glucose, lactate, and cortisol as compared with controls were observed for treatment groups exposed for 24 h to a DDAC concentration of 0.4 $mg \cdot L^{-1}$. There was also a marginal, although not significant, elevation in haematocrit for fish exposed to 0.4 $mg \cdot L^{-1}$.

Swimming performance

The results of the swimming performance experiments are summarized in Table 2. After a 12-h exposure, critical swimming speeds had decreased significantly from controls at concentrations of 0.2 and 0.4 $mg \cdot L^{-1}$, decreasing 17.6 and 9.2%, respectively. After a 24-h exposure, respective reductions in swimming performance for these concentrations were 23.9 and 22.2%, as compared with controls. Exposure to 0.1 mg DDAC$\cdot L^{-1}$ for 24 h resulted in a 10.6% increase in critical swimming speed, although there were no significant differences from controls after either a 12- or a 48-h exposure.

After a 48-h exposure, reductions in critical swimming speeds after exposure to 0.4 mg DDAC$\cdot L^{-1}$ remained significant, with a mean value of 5.78 ± 0.11 $BL \cdot s^{-1}$. This represented an 11.6% reduction in swimming performance as compared with controls. At concentrations of 0.1 and 0.2 $mg \cdot L^{-1}$, the respective reductions in swimming performance of 3.1 and 8.4% as compared with controls were not statistically significant.

Gill morphology

Scanning electron microscopic analysis of the secondary lamellae of test fish did not reveal any apparent differences in gill ultrastructure between treatment fish and controls (Fig. 1). All membrane surfaces appeared intact, with no evidence of gross lesions or obvious disruptions to gill epithelial integrity. Interlamellar spaces were well defined, showing no evidence of mucous hypersecretion, lamellar fusion, necrosis, or epithelial lifting. A detailed microridge pattern was readily observable on the lamellar surfaces, indicating that the gross integrity of the respiratory membrane surfaces was not compromised by acute sublethal exposure to DDAC.

Disease resistance

The results of the disease challenge are summarized in Fig. 2. The onset of mortality tended to be earlier in the control group versus the treatment groups. After the third and fourth observation days, differences between control fish and fish exposed to 0.2 mg DDAC$\cdot L^{-1}$ were statistically significant, but differences were not significant from the fifth day onwards. Differences between control fish and fish exposed to 0.4 mg DDAC$\cdot L^{-1}$ were significant after the third, fourth, and fifth observation days, but differences ceased to be significant beyond that time. Cumulative mortality after the 14-d observation period was highest in control groups, and decreased in concentration-dependent fashion in the treatment groups, although the differences between treatment groups and controls were not statistically significant.

Discussion

The acute 96-h LC_{50} value determined for DDAC using flow-through conditions (0.409 $mg \cdot L^{-1}$) is 42% lower than the published static 96-h LC_{50} value of 0.704 $mg \cdot L^{-1}$ (Environment Canada 1989, *cited in* Henderson 1992). Such a difference is not unexpected when comparing flow-through versus static toxicity testing methods (Sprague 1973). However, because flow-through conditions may be more representative of field conditions, we recommend that our lower LC_{50} value be used for DDAC effluent criteria development. At present, regulatory standards in British Columbia are based on values determined using static bioassays (Henderson 1992), with insufficient incorporation of safety factors. We do not feel that this offers adequate protection for aquatic ecosystems at

© 1996 NRC Canada

Fig. 1. Electron micrographs showing secondary lamellae of rainbow trout after 24-h DDAC exposure and a swimming performance test. (A) 0.0 mg·L^{-1}; (B) 0.1 mg·L^{-1}; (C) 0.2 mg·L^{-1}; (D) 0.4 mg·L^{-1}. Note the well-defined microridge pattern.

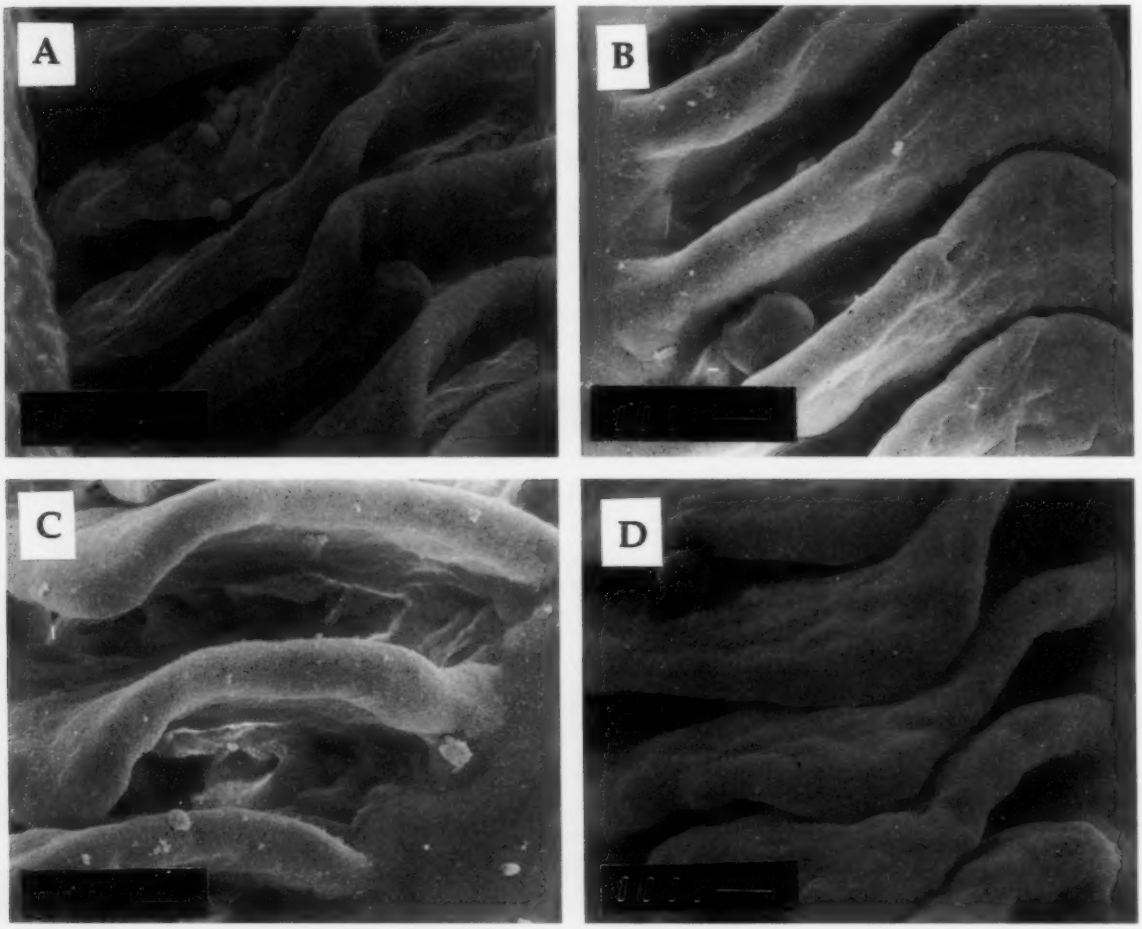

risk of exposure to DDAC. Furthermore, we recommend that sublethal toxicity be considered by those in charge of developing effluent criteria.

It has been suggested that in order to gain a full understanding of the effects of environmental contaminants on fish, it is imperative that sublethal toxicity be investigated (Cairns 1966; Sprague 1971). Sublethal exposure to contaminants, like many environmental stressors, can elicit physiological responses in fish as they attempt to maintain homeostatic balance in the face of environmental change (Barton et al. 1988; Chen 1988; Donaldson and Dye 1975; Thomas 1990; Weisbart et al. 1989). Under certain circumstances, some of these physiological responses may be detrimental to fish, through effects on growth, survival, and/or reproduction (Donaldson 1990; Maule et al. 1989; McLeay and Gordon 1977; Weiner et al. 1986).

This study with DDAC utilized an integrative suite of stress indicators which have frequently been used in sublethal stress analyses of fish (Anderson 1990; Hinton and Laurén 1990; Mallatt 1985; Schreck 1990; Thomas 1990). The indicators chosen for this study were various biochemical stress indicators, swimming performance, gill morphology, and disease resistance. There is no published information regarding the sublethal effects of DDAC at these levels of biological organization, although other industrial pollutants have been shown to elicit significant physiological responses after sublethal exposures (MacKinnon and Farrell 1992; Servizi et al. 1993; Schwaiger et al. 1992).

Stress responses in fish can be classified according to three basic phases: (1) alarm, (2) resistance, and (3) exhaustion. Acute exposure studies, such as the one described here, allow investigators to explore in depth the initial alarm phase of a stress response. The primary physiological response in the alarm phase of a stress response is hypersecretion of catecholamines and corticosteroid hormones, which in turn initiates a cascade of secondary biochemical responses such as hyperglycaemia and hyperlacticaemia, tissue and liver glycogen depletion, and catabolism of tissue proteins (Mazeaud et al. 1977). These responses are believed to facilitate a rapid mobilization of energy reserves, allowing the fish to meet the

© 1996 NRC Canada

Fig. 2. Cumulative mortality of rainbow trout exposed for 24 h to DDAC and experimentally infected with *V. anguilarum* ($n = 30$ for each group (2 replicates of 15)). ■, 0.0 mg·L^{-1}; ▲, 0.1 mg·L^{-1}; ○, 0.2 mg·L^{-1}; ●, 0.4 mg·L^{-1}. *Significantly different from controls ($p < 0.05$).

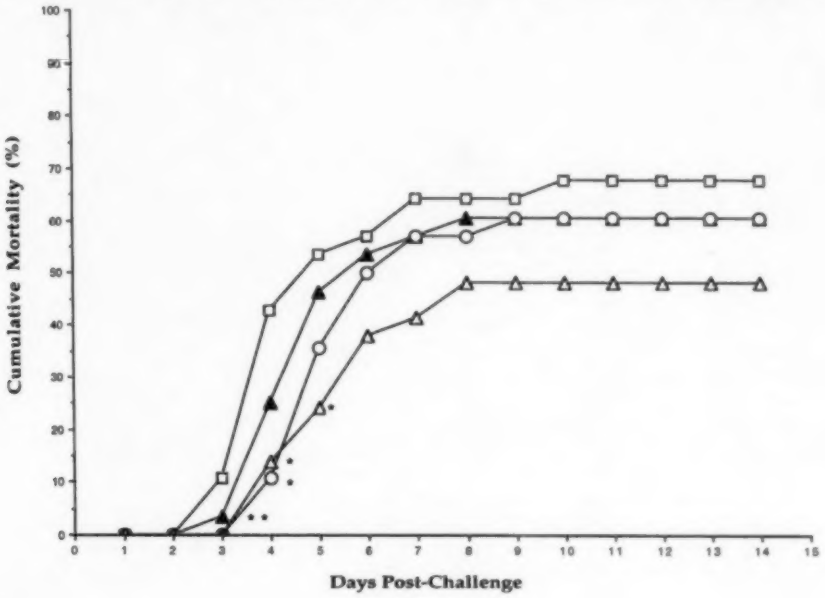

increased energy demands associated with exposure and resistance to stressors (Thomas 1990).

Acute (24 h) exposure to sublethal concentrations of DDAC results in a characteristic primary biochemical stress response in juvenile rainbow trout. Plasma corticosteroid hormone levels were shown to be significantly elevated as compared with controls in trout exposed to the highest treatment concentration (0.4 mg·L^{-1}). Increased plasma corticosteroid levels are believed to stimulate protein catabolism and gluconeogenesis, secondary biochemical responses that function in maintaining the hyperglycaemia associated with catecholamine release (Leach and Taylor 1980). The elevated plasma glucose levels present in fish after a 24-h exposure to 0.4 mg DDAC·L^{-1} indicate that these fish were also experiencing this characteristic secondary stress response. Another secondary biochemical response triggered by increased levels of circulating corticosteroid hormones is plasma hyperlacticaemia. This response was also evident in fish acutely exposed to the highest sublethal concentration of DDAC. Other secondary biochemical indicators (HSI, tissue glycogen, haemoglobin, haematocrit, leucocrit, and liver glycogen levels) did not change significantly after a 24-h exposure.

It is interesting to note that the primary and secondary biochemical stress responses observed in treatment fish only occurred after exposure to a concentration similar to our flow-through 96-h LC_{50} value. It seems likely, then, that the biochemical stress responses elicited after 24 h of exposure to DDAC were simply the prelude to a lethal response, had the exposure continued. A primary stress response was not elicited after a 24-h exposure to DDAC concentrations one-half the 96-h LC_{50} value. These results suggest that the dose–response curve for DDAC is relatively steep, which implies the existence of a well-defined threshold of effect. We feel that this is important information for those in charge of developing effluent criteria for DDAC. The current outflow limit of 0.700 mg·L^{-1} in British Columbia is well above our determined threshold for acute sublethal and lethal effects on rainbow trout, and therefore we feel is inadequate protection for the aquatic ecosystem. The results of this study suggest that a 96-h exposure to the current allowable outflow levels would result in significant if not complete mortality of exposed fish populations.

Fish swimming performance was first suggested as an important index of aquatic sublethal toxicity by Cairns (1966). Because swimming involves the coordinated efforts of a host of physiological mechanisms, measurements of swimming performance can be viewed as a reliable index of general health and stress in fish (Schreck 1990). In addition, fish survivorship is highly dependent on swimming performance, as this character determines the ability to effectively maintain stream position, forage, escape predators, and migrate long distances (Brett 1965). This is of particular importance to diadromous species, many of which make long seaward migrations as juveniles. Decreased swimming performance has been shown to occur after sublethal exposure to a variety of environmental pollutants, such as bleached kraft pulp mill effluent (Howard 1975; McLeay and Brown 1979), TCMTB (Nikl and Farrell 1993), aluminum (Wilson and Wood 1992), and pH (Graham and Wood 1981).

Swimming performance was the most sensitive indicator of DDAC exposure in this study. Even in the absence of a primary stress response, swimming performance was significantly reduced after 12- and 24-h exposures to 50% of the 96-h LC_{50} concentration of DDAC as determined by flow-

© 1996 NRC Canada

through exposure. Short-term exposures to the flow-through 96-h LC_{50} concentration (0.4 $mg \cdot L^{-1}$) also reduced swimming performance, which coincides with the primary stress response observed after a 24-h DDAC exposure. The reductions in swimming performance observed in treatment fish in this study indicate that the physiological systems on which swimming relies have been compromised by exposure to DDAC. This effect was dependent on duration, being greatest after 24 h.

The apparent improvement in swimming performance after a 48-h exposure to sublethal concentrations of DDAC may represent an increased tolerance with exposure. We cannot explain the increase in critical swimming speed after a 24-h exposure to 0.1 mg $DDAC \cdot L^{-1}$.

Commonly cited explanations for toxicant-induced reductions in fish swimming performance relate to disturbances in gill integrity, as these organs represent a primary route of exposure in fishes (Hinton and Laurén 1990). Disruptions to gill integrity occur primarily at the lamellar level, with swelling and fusion of secondary lamellae (clubbing) being particularly well-documented responses to toxicant exposure (Mallatt 1985). These lesions, particularly epithelial desquamation, are believed to result in reduced oxygen transfer across the gill epithelium by increasing the oxygen diffusion distance (Hughes et al. 1979). Disruptions to gill integrity have been observed after exposure to TCMTB (MacKinnon and Farrell 1992), bis(tri-*n*-butyltin)oxide (TBTO) (Schwaiger et al. 1992), phenol (Mitrovic et al. 1968), various synthetic detergents (Abel and Skidmore 1975), and Zephiran®, a cationic quaternary ammonium compound used to treat fish diseases in aquaculture (Byrne et al. 1989). However, Nikl and Farrell (1993) found a nonlinear relationship between alterations in gill morphometry and decreases in critical swimming speed after exposure to TCMTB.

The scanning electron microscopic analyses of exposed gill tissues performed in this study indicate that no gross disruptions to secondary lamellar epithelia occur as a result of sublethal exposure to DDAC. The reductions in swimming performance observed in treatment groups cannot, therefore, be attributed to gross effects on gill epithelial surfaces. Effects on gill membrane biochemistry cannot be ruled out; however, a more sensitive and specific technique than scanning electron microscopic analysis is required to investigate this possibility.

The results of the disease challenge experiments indicate that sublethal exposure of rainbow trout to DDAC marginally increases resistance to infection from *V. anguilarum* in a concentration-dependent fashion, although the differences in mortality between treatments groups and controls were not statistically significant at the end of the 14-d observation period. This is similar to the findings of MacFarlane et al. (1986), who found that striped bass showed increased resistance to the pathogen *Flexibacter columnaris* after exposure to copper and cadmium. The effects of environmental contaminants on fish immunology appear to be variable, however, and are quite possibly toxicant and/or pathogen specific. For example, the resistance of rainbow trout to infectious hematopoietic necrosis virus and the *Yersinia ruckeri* bacterium was observed to decrease after sublethal exposures to copper (Hetrick et al. 1979; Knittel 1981). There also exists extensive documentation on the reduced immunological capacities of fish after experiencing stressful conditions such as handling or reduced water quality (Wedermeyer 1970; Snieszko 1974; Maule et al. 1989).

Reductions in disease resistance have been related to the increased plasma corticosteroid levels associated with a primary stress response (Anderson et al. 1982). Although it is unclear what causes the observed reverse occurrence after exposure to DDAC, despite the presence of a primary stress response, there are indications that significant binding of DDAC to the external surfaces of fish occurs (Springborn Laboratories, Inc. 1990). Even though the fish were immersed for 20 min in aerated fresh water prior to the disease challenge, it is possible that trace residues of DDAC remained on the external surfaces of the fish. The antimicrobial activity of these DDAC residues may have exerted an antiseptic effect during exposure to *V. anguilarum*. The minimal effects on disease resistance came as little surprise, however, as an exposure duration of 24 h is likely too short to produce measurable immune system responses.

In summary, the flow-through 96-h LC_{50} value for DDAC (0.409 $mg \cdot L^{-1}$) was significantly lower than previously determined values for rainbow trout using static bioassay techniques. A 24-h exposure to 0.4 mg $DDAC \cdot L^{-1}$ resulted in significant primary (cortisol), secondary (glucose, lactate), and tertiary (swimming performance) stress responses. Although this concentration is equivalent to the flow-through 96-h LC_{50} value, it is 42% lower than the static 96-h LC_{50} value currently in use for regulatory purposes. The most sensitive indicator of sublethal stress was swimming performance. It was significantly reduced after 12- and 24-h exposures to 50% of the flow-through 96-h LC_{50} value. It is important to note that these reductions in swimming performance occur at exposures equivalent to 21% of the current regulatory limit for DDAC release.

However, given the absence of any detrimental effects at a concentration of 25% of the flow-through 96-h LC_{50} value, we suggest that DDAC has a very steep dose–response relationship for acute exposure durations. To our knowledge, there is no published information on the effects of chronic DDAC exposure.

Acknowledgments

The authors wish to thank Shannon Balfry for her assistance with the disease challenge experiments, Vic Bourne and Kathy Cousins for their assistance with electron microscopy, Dr. R. Sweeting for his technical assistance in the biochemical sampling, Tsai Lin for his guidance with statistics, and Colin Gray for his input on the experimental design. The chemical used in this study was provided by Lonza Inc., and this is appreciated. This study was funded through an operating grant to A.P. Farrell and C.J. Kennedy from the Environment Canada Fraser River Action Plan.

References

Abel, P.D., and Skidmore, J.F. 1975. Toxic effects of an anionic detergent on the gills of rainbow trout. Water Res. **9**: 759–765.

Adams, S.M. 1990. Status and use of biological indicators for evaluating the effects of stress on fish. Am. Fish. Soc. Symp. **8**: 1–8.

American Public Health Association. 1976. Standard methods for the examination of water and waste water. 14th ed. American Public Health Association, New York.

© 1996 NRC Canada

Anderson, D.P. 1990. Immunological indicators: effects of environmental stress on immune protection and disease outbreaks. Am. Fish. Soc. Symp. **8**: 38–50.

Anderson, D.P., Roberson, B.S., and Dixon, O.W. 1982. Immunosuppression induced by a corticosteroid or an alkylating agent in rainbow trout (*Salmo gairdneri*) administered a *Yersinia ruckeri* bacterin. Dev. Comp. Immunol. **6**(Suppl. 2): 197–204.

Barton, B.A., Schreck, C.B., and Fowler, L.G. 1988. Fasting and diet content affect stress-induced changes in plasma glucose and cortisol in juvenile chinook salmon. Prog. Fish-Cult. **50**: 16–22.

Bozzola, J.J., and Russell, L.D. (*Editors*) 1992. Electron microscopy – principles and techniques for biologists. Jones and Bartlett Publishers, Boston, Mass. pp. 16–31.

Brett, J.R. 1964. The respiratory metabolism and swimming performance of young sockeye salmon. J. Fish. Res. Board Can. **21**: 1183–1226.

Brett, J.R. 1965. The relation of size to rate of oxygen consumption and sustained swimming speed of sockeye salmon (*Oncorhynchus nerka*). J. Fish. Res. Board Can. **22**: 1491–1501.

Byrne, P., Speare, D., and Ferguson, H.W. 1989. Effects of a cationic detergent on the gills and blood chemistry of rainbow trout *Salmo gairdneri*. Dis. Aquat. Org. **6**: 185-196.

Cairns, J. 1966. Don't be half-safe – the current revolution in bioassay techniques. Purdue Univ. Eng. Ext. Ser. **1221**: 559–567.

Chen, T.T. 1988. Investigation of effects of environmental xenobiotics to fish at sublethal levels by molecular biological approaches. Mar. Environ. Res. **24**: 333–338.

Devore, J.L. (*Editor*) 1987. Probability and statistics for engineering and the sciences. Brooks/Cole Publishing, Monterey, Calif. pp. 352–355.

Donaldson, E.M. 1990. Reproductive indices as measures of the effects of environmental stressors in fish. Am. Fish. Soc. Symp. **8**: 109–122.

Donaldson, E.M., and Dye, H.M. 1975. Corticosteroid concentrations in sockeye salmon (*Oncorhynchus nerka*) exposed to low concentrations of copper. J. Fish. Res. Board Can. **32**: 533–539.

Envirochem Special Projects Inc. 1992. Lower mainland region antisapstain facilities: assessment of operational practices and environmental discharges study. Vol. 1. Prepared for B.C. Ministry of Environment, Lands and Parks, Victoria, B.C.

Graham, M.S., and Wood, C.M. 1981. Toxicity of environmental acid to the rainbow trout: interactions of water hardness, acid type, and exercise. Can. J. Zool. **59**: 1518–1526.

Hayes, A.W. (*Editor*). 1989. Principles and methods of toxicology. 2nd ed. Raven Press Ltd., New York. pp. 459–461.

Henderson, N.D. 1992. A review of the environmental impact and toxic effects of DDAC. Prepared for Environmental Protection Division, B.C. Ministry of Environment, Lands and Parks, Victoria, B.C.

Hetrick, F.M., Knittel, M.D., and Fryer, J.L. 1979. Increased susceptibility of rainbow trout to infectious hematopoietic necrosis virus after exposure to copper. Appl. Environ. Microbiol. **37**: 198–201.

Hinton, D.E., and Laurén, D.J. 1990. Integrative histopathological approaches to detecting effects of environmental stressors on fishes. Am. Fish. Soc. Symp. **8**: 51–66.

Howard, T.E. 1975. Swimming performance of juvenile coho salmon (*Oncorhynchus kisutch*) exposed to bleached kraft pulpmill effluent. J. Fish. Res. Board Can. **32**: 789–793.

Hughes, G.M., Perry, S.F., and Brown, V.M. 1979. A morphometric study of effects of nickel, chromium and cadmium on the secondary lamellae of rainbow trout gills. Water Res. **13**: 665–679.

Janz, D.M., Farrell, A.P., Morgan, J.D., and Vigers, G.A. 1991. Acute physiological stress responses of juvenile coho salmon (*Oncorhynchus kistuch*) to sublethal concentrations of Garlon 4®, Garlon 3A®, and Vision® herbicides. Environ. Toxicol. Chem. **10**: 81–90.

Johansen, J.A., and Geen, G.H., 1990. Sublethal and acute toxicity of the ethylene glycol butyl ether ester formulation of triclopyr to juvenile coho salmon (*Oncorhynchus kisutch*). Arch. Environ. Contam. Toxicol. **19**: 610–616.

Knittel, M.D. 1981. Susceptibility of steelhead trout *Salmo gairdneri* Richardson to redmouth infection *Yersinia ruckeri* following exposure to copper. J. Fish Dis. **4**: 33–40.

Leach, G.J., and Taylor, M.H. 1980. The role of cortisol in stress-induced metabolic changes in *Fundulus heteroclitus*. Gen. Comp. Endocrinol. **42**: 219–227.

Litchfield, J.T., and Wilcoxon, F. 1949. A simplified method of evaluating dose effect experiments. J. Pharmacol. Exp. Ther. **96**: 99–113.

Lonza Inc. 1985. Product information. Bardac 2250/2280. Lonza Inc., Fair Lawn, N.J.

MacFarlane, R.D., Bullock, G.L., and McLaughlin, J.J.A. 1986. Effects of five metals on susceptibility of striped bass to *Flexibacter columnaris*. Trans. Am. Fish. Soc. **115**: 227–231.

MacKinnon, D.L., and Farrell, A.P. 1992. The effect of 2-(thiocyanomethylthio)-benzothiazole on juvenile salmon (*Oncorhynchus kisutch*): sublethal toxicity testing. Environ. Toxicol. Chem. **11**: 1541–1548.

Mallatt, J. 1985. Fish gill structural changes induced by toxicants and other irritants: a statistical review. Can. J. Fish. Aquat. Sci. **42**: 630–648.

Maule, A.G., Tripp, R.A., Kaattari, S.L., and Schreck, C.B., 1989. Stress alters immune function and disease resistance in chinook salmon (*Oncorhynchus tshawytscha*). J. Endocrinol. **120**: 135–142.

Mazeaud, M.M., Mazeaud, F., and Donaldson, E.M. 1977. Primary and secondary effects of stress in fish: some new data with a general review. Trans. Am. Fish. Soc. **106**: 201–212.

McLeay, D.J., and Brown, D.A. 1979. Stress and chronic effects of untreated and treated bleached kraft pulpmill effluent on the biochemistry and stamina of juvenile coho salmon (*Oncorhynchus kisutch*). J. Fish. Res. Board Can. **36**: 1049–1059.

McLeay, D.J., and Gordon, M.R. 1977. Leucocrit: a simple hematological technique for measuring acute stress in salmonid fish, including stressful concentrations of pulpmill effluent. J. Fish. Res. Board Can. **34**: 2164–2175.

Mitrovic, V.V., Brown, V.M., Shurben, D.G., and Berryman, M.H. 1968. Some pathological effects of sub-acute and acute poisoning of rainbow trout by phenol in hard water. Water Res. **2**: 249–254.

Nikl, D.L., and Farrell, A.P. 1993. Reduced swimming performance and gill structural changes in juvenile salmonids exposed to 2-(thiocyanomethylthio)-benzothiazole. Aquat. Toxicol. **27**: 245–264.

Schreck, C.B. 1990. Physiological, behavioral, and performance indicators of stress. Am. Fish. Soc. Symp. **8**: 29–37.

Schwaiger, J., Bucher, F., Ferling, H., Kalbfus, W., and Negele, R.D. 1992. A prolonged toxicity study on the effects of sublethal concentrations of bis(tri-*n*-butyltin)oxide (TBTO): histopathological and histochemical findings in rainbow trout (*Oncorhynchus mykiss*). Aquat. Toxicol. **23**: 31–48.

Servizi, J.A., Gordon, R.W., Martens, D.W., Lockhart, W.L., Metner, D.A., Rogers, I.H., McBride, J.R., and Norstrom, R.J. 1993. Effects of biotreated bleached kraft mill effluent on fingerling chinook salmon (*Oncorhynchus tshawytscha*). Can. J. Fish. Aquat. Sci. **50**: 846–857.

Snieszko, S.F. 1974. The effects of environmental stress on outbreaks of infectious diseases of fishes. J. Fish Biol. **6**: 197–208.

Sprague, J.B. 1971. Measurement of pollutant toxicity to fish – III: sublethal effects and "safe" concentrations. Water Res. **5**: 245–266.

Sprague, J.B. 1973. The ABC's of pollutant bioassay using fish. Biological methods for the assessment of water quality. ASTM STP S28. American Society for Testing and Materials, Philadelphia, Pa. pp. 6–30.

© 1996 NRC Canada

Springborn Laboratories, Inc. 1990. Bioconcentration and elimination of ^{14}C-residues by bluegill (*Lepomis macrochirus*) exposed to didecyldimethyl-ammonium chloride (DDAC). SLI Rep. No. 89-7-3043. Available from Lonza Inc., Fair Lawn, N.J.

Strub, R.E. 1992. Conservation and Protection Laboratories Internal Methods Development Project. C & P Laboratories, Environment Canada, Pacific and Yukon Division, North Vancouver, B.C.

Sweeting, R.M. 1989. Aspects of growth hormone in the physiology of smoltification and seawater adaptation of coho salmon, *Oncorhynchus kisutch*. Ph.D. thesis, Simon Fraser University, Burnaby, B.C.

Thomas, P. 1990. Molecular and biochemical responses of fish to stressors and their potential use in environmental monitoring. Am. Fish. Soc. Symp. **8**: 9–28.

Wedermeyer, G.A. 1970. The role of stress in the disease resistance of fishes. Am. Fish. Soc. Spec. Publ. **5**: 30–35.

Weiner, G.S., Schreck, C.B., and Li, H.W. 1986. Effects of low pH on reproduction of rainbow trout. Trans. Am. Fish. Soc. **115**: 75–82.

Weisbart, M., Chakraborti, P.K., Gottschall, F., and Freeman, H.C. 1989. Effect of acid environments on cortisol and cortisol receptor activity in Atlantic salmon, *Salmo salar*. Fish Physiol. Biochem. **7**: 267–272.

Wilson, R.W., and Wood, C.M. 1992. Swimming performance, whole body ions, and gill Al accumulation during acclimation to sublethal aluminum in juvenile rainbow trout (*Oncorhynchus mykiss*). Fish Physiol. Biochem. **10**(2): 149–159.

Zar, J.H. (*Editor*). 1974. Biostatistical analysis. Prentice-Hall, Englewood Cliffs, N.J.

© 1996 NRC Canada

Among-lake and within-lake variations of autotrophic pico- and nanoplankton biomass in six Quebec lakes

B. Pinel-Alloul, N. Bourbonnais, and P. Dutilleul

Abstract: The biomass of autotrophic picoplankton (APP) and nanoplankton (ANP) was measured in six lakes from the Laurentian and Eastern Townships regions of Quebec, which vary in trophic status, watershed geology, and water chemistry. We examined the variations in the biomass of both phytoplanktonic components, in relation to changes in limnological variables. Each lake was sampled at three depths, corresponding to the epi-, meta- and hypolimnion strata, and at five times over the summer season. The APP biomass and its contribution to phototrophic biomass of algae <20 μm decreased with lake trophy when expressed as total phosphorus (TP), while ANP dominated the <20 μm algae components in more eutrophic lakes. The critical TP level at which ANP biomass exceeded APP biomass (ANP/APP biomass ratio > 1) was around 20–30 $\mu g \cdot L^{-1}$. The mean values found for APP (75–365 $\mu g \cdot L^{-1}$ or 16–80 $\mu g\ C \cdot L^{-1}$) and ANP (46–249 $\mu g \cdot L^{-1}$ or 7–37 $\mu g\ C \cdot L^{-1}$) biomass in Quebec lakes over our range of trophy (TP: 7–73 $\mu g \cdot L^{-1}$) were of the same order as those reported in other freshwater environments. Most of the variation in APP and ANP biomass was related to among-lake differences in nutrients (NO_3, TP, TDP) and conductivity or pH.

Résumé : Les variations de la biomasse du picoplancton autotrophe (APP) et du nanoplancton autotrophe (ANP) ont été examinées dans six lacs des Laurentides et des Cantons de l'Est (Québec) dont le statut trophique, la géologie du bassin versant et la physico-chimie de l'eau étaient différentes. Les variations de la biomasse des deux composantes du phytoplancton ont été évaluées en fonction des changements dans les caractéristiques limnologiques. Dans chaque lac, l'échantillonnage a été réalisé à trois profondeurs correspondant aux strates épi-, méta- et hypolimnétique et à cinq périodes au cours de l'été. La biomasse de APP et sa contribution à la biomasse totale des algues de taille <20 μm décroît avec le niveau trophique, exprimé en termes de phosphore total (TP), tandis que ANP domine la communauté des algues de taille <20 μm dans les lacs eutrophes. Le seuil critique de TP au dessus duquel la biomasse de ANP excède celle de APP (rapport ANP/APP en biomasse > 1) était d'environ 20–30 $\mu g.L^{-1}$. Les valeurs moyennes des biomasses de APP (75–365 $\mu g \cdot L^{-1}$ ou 16–80 $\mu g\ C \cdot L^{-1}$) et ANP (46–249 $\mu g \cdot L^{-1}$ ou 7–37 $\mu g\ C \cdot L^{-1}$) notées dans les lacs du Québec le long de notre plage de niveau trophique (TP: 7–73 $\mu g \cdot L^{-1}$) étaient du même ordre de grandeur que celles rapportées pour d'autres écosystèmes d'eau douce. La majeure partie de la variation dans la biomasse de APP et ANP était reliée aux variations inter-lacs dans les éléments nutritifs (NO_3, TP, TDP), la conductivité ou le pH.

Introduction

During the last two decades, phytoplankton size fractionation (Malone 1971; Kalff 1972; Munawar et al. 1978; Watson and Kalff 1981; Rai 1982; Carrick and Fahnenstiel 1989) and microbial loop studies (Azam et al. 1983; Stockner and Antia 1986; Fogg 1986; Legendre et al. 1988; Stockner 1991; Stockner and Shortreed 1991; Bertrand and Vincent 1994) have independently highlighted the important role of autotrophic picoplankton (APP) and nanoplankton (ANP) in the planktonic community within oceans, estuaries, and lakes. APP and ANP appear to account for a large proportion of total phytoplankton biomass and productivity in oligomesotrophic systems and play a significant role in carbon transfer to higher trophic levels (Riemann and Sondergaard 1986; Platt and Li 1986; Stockner and Porter 1988; Stockner and Shortreed 1989).

The APP (0.2–2 μm) and ANP (2–20 μm) algal fractions were first defined by Dussart (1965) and latter by Sieburth et al. (1978). APP abundance in oceans and lakes varies from 10^3 to more than 10^6 cells·mL^{-1}, and can account for 10–90% of total phytoplankton biomass or production (Fogg 1986; Stockner and Antia 1986; Stockner 1988, 1991). A large part of this carbon production can be transferred to higher trophic levels by the picoplankton–nanoflagellate–ciliate–zooplankton grazing pathways (Sherr and Sherr 1988, 1992; Carrick and Fahnenstiel 1990; Carrick et al. 1991). ANP is less abundant than APP, with numbers varying from 10^3 to 10^4 cells·mL^{-1} (Pick and Caron 1987; Carrick and Fahnenstiel 1989). However, ANP may also contribute significantly (40–90%) to total phytoplankton biomass and production in marine and oligomesotrophic freshwater systems (Rai 1982; Sager et al. 1988; Carrick and Fahnenstiel 1989). Furthermore, in communities dominated by large herbivores, the nanoplankton–macrozooplankton grazing link constitutes a

Received August 9, 1995. Accepted May 2, 1996.
J13033

B. Pinel-Alloul and N. Bourbonnais. Groupe de Recherche Interuniversitaire en Limnologie et en Environnement Aquatique (GRIL), Département de Sciences biologiques, Université de Montréal, CP 6128, Succ. Centre Ville., Montréal, QC H3C 3J7, Canada.
P. Dutilleul. Department of Plant Science, Faculty of Agricultural and Environmental Sciences, McGill University, Macdonald Campus, 21111 Lakeshore Road, Ste-Anne-de-Bellevue, QC H9X 3V9, Canada.

© 1996 NRC Canada

more direct, two-step carbon transfer to fish than the multistep picoplankton–nanoplankton–zooplankton couplings (Stockner and Shortreed 1989; Mazumder et al. 1990).

The application of epifluorescence microscopy to plankton studies has allowed simultaneous determination of autotrophic APP and ANP by autofluorescence (Pick and Caron 1987; MacIsaac and Stockner 1993; Booth 1993) as well as heterotrophic pico- and nanoplankton cells by using fluorochrome methods (Hobbie et al. 1977; Porter and Feig 1980; Sherr et al. 1993). These methodological improvements led to an understanding of the ecological importance of pico- and nanoplankton autotrophic and heterotrophic components in oceanic and freshwater ecosystems. However, most studies have examined only one component, either the pico- or the nanoplankton, and only a few studies have considered both components at the same time (Landry et al. 1984; Davis et al. 1985; Pick and Caron 1987; Geller et al. 1991; Wehr 1990, 1993). Among the several studies that have been conducted in Canadian lakes and rivers on APP (Hardy et al. 1986; Stockner and Shortreed 1989, 1991; Klut and Stockner 1991; Caron et al. 1985; Fahnenstiel et al. 1986, 1991; Leppard et al. 1987; Fahnenstiel and Carrick 1992; Bertrand and Vincent 1994) and on algae <20 μm (Munawar and Munawar 1975; Munawar et al. 1978; Ross and Duthie 1981; Jordan et al. 1988; Lafond et al. 1990) or ANP (Sager et al. 1988; Carrick and Fahnenstiel 1989), only one study conducted in Lake Ontario assessed the relative importance of pico- and nanoplankton autotrophic and heterotrophic components (Pick and Caron 1987). Our understanding of ecological factors controlling among-lake and within-lake variations in the relative importance of these components across environmental gradients is thus limited.

In particular, the relative importance of APP and ANP along environmental gradients related to lake trophy is still debated. Multilake studies generally revealed strong relationships between lake trophy and phytoplankton sized components. Abundance (or biomass) of algae <20 μm increased along the oligoeutrophic gradient in lake productivity (or in surrogate variables as TP, pH, and conductivity), while its relative contribution to total phytoplankton decreased (Munawar et al. 1978; Watson and Kalff 1981). Some studies strongly suggested that APP abundance (or biomass) and its relative contribution to total phytoplankton decreased with trophic status or nutrients in oligomesotrophic lakes (Pick and Agbeti 1991). In contrast, other studies indicated an increase in APP abundance with lake trophy, although its contribution declined with the trophic gradient (Stockner 1991; Voros et al. 1991).

Within planktonic food webs, both bottom-up and top-down factors may contribute to among-lake and within-lake variations in APP and ANP abundance or biomass. Enclosure experiments demonstrated the role of nutrients or fish and zooplankton trophic cascading forces in structuring the size distribution of planktonic biomass (McQueen et al. 1986; Mazumder et al. 1990; Christoffersen et al. 1993). Studies also reported variations in APP and ANP abundance or relative contribution with vertical, seasonal, or interannual changes in oxygen (Bennett et al. 1990), temperature (Caron et al. 1985; Pick and Caron 1987; Pick and Agbeti 1991; Burns and Stockner 1991; Weisse and Schweizer 1991; Voros et al. 1991; Fahnenstiel and Carrick 1992), light (Pick 1991; Fogg 1991; Fahnenstiel and Carrick 1992), and zooplankton grazing pressure (Weisse and Schweizer 1991; Voros et al. 1991). As stated by Stockner (1988, 1991), more studies on APP and ANP biomass and their relative contribution must be undertaken in ecosystems with varying trophy, in different geographic areas and at various seasons, in order to ensure full documentation of their importance and role in pelagic food webs.

In this paper, we quantify the variation in APP and ANP biomass in six lakes from the Laurentian and Eastern Townships regions of Quebec, which vary in their trophic status, surrounding geology, morphometry, and water chemistry. Our sampling strategy was designed to take into account among-lake, depth, and sampling period sources of variation. Appropriate methods of statistical data analysis were developed to deal with spatiotemporal data which are, by nature, susceptible to be heteroscedastic (heterogeneous in variance) and autocorrelated. We test the influence of environmental variables related to lake trophy and water chemistry on the variation of the autotrophic phytoplankton size components <20 μm (APP and ANP) in several lakes, representative of southern Quebec and northeastern United States regions. We hypothesized that APP and ANP biomass and their relative contribution to phytoplankton <20 μm compartments will change among lakes in relation to lake trophy. APP biomass and its relative contribution will decrease with lake trophy, while ANP biomass and its relative contribution will increase. APP and ANP biomass may also vary within lakes along vertical and temporal gradients in temperature, nutrients, and conductivity.

Materials and methods

Study area and sampling

The six lakes under study cover a wide range of lake trophy as expressed by total phosphorus (TP: 7.2–73 $\mu g \cdot L^{-1}$) and differ by their surrounding geology and landscape (Table 1). The Laurentian lakes are located in the southeastern part of the Precambrian Shield, 80 km north of Montréal (46°N latitude, 74°W longitude). The surrounding watersheds, mainly gneiss-granitic, are covered by morainic parent soils and boreal forest. These lakes have neutral or slightly acidic softwaters and low TP concentration and chlorophyll *a* biomass, indicating an oligomesotrophic status (Table 1). NO_3 concentrations were considerably higher in Lakes Achigan and Pin Rouge than in Lake Echo, while NH_4 concentration was highest in Lake Pin Rouge, a lake that suffered from summer hypolimnetic anoxia. The Eastern Townships lakes are located 100 km south of Montréal (45°N latitude, 72°W longitude) in a well-buffered calcareous sedimentary region covered mostly by deciduous forests. They are characterized by well-mineralized waters and higher nutrient and chlorophyll *a* levels than the Laurentian lakes (Table 1); they can therefore be classified as mesoeutrophic. From the Eastern Townships region, Lake Massawippi presented the highest conductivity and the lowest TP level, a feature indicating hardwater conditions. Higher mean level of NH_4 was noticed in Lake Magog which experienced hypolimnetic anoxia in late summer. Secchi depths varied from 4.5 to 2.3 m (Table 1). In general, the Eastern Townships lakes were slightly more transparent than the Laurentian lakes. In this subset, Lake Achigan and Echo had clear waters, while Lake Pin Rouge was humic.

Subsets of lakes differ also by their morphometry (Table 1). On average, the Eastern Township lakes have greater area and higher mean and maximum depth than the Laurentian lakes. All lakes stratify during summer. Water temperature varied from 16 to 24°C in the epilimnion and from 8 to 10°C in the hypolimnion, except for Lake

© 1996 NRC Canada

Table 1. Morphometric characteristics, water chemical variables, chlorophyll *a* concentration, and water transparency (Secchi depth) for each lake and region studied.

Lakes and regions	Mean depth (m)	Max. depth (m)	Lake area (km^2)	pH	Cond. ($\mu S \cdot cm^{-1}$)	TP ($\mu g \cdot L^{-1}$)	TDP ($\mu g \cdot L^{-1}$)	NO_3 ($\mu g \cdot L^{-1}$)	NH_4 ($\mu g \cdot L^{-1}$)	Chl *a* total ($\mu g \cdot L^{-1}$)	Chl *a* <25 μm ($\mu g \cdot L^{-1}$)	Secchi depth (m)
Achigan	12.3	26.3	5.2	7.5	40.6	8.6	1.1	105.8	7.1	1.9	1.6	4.5
Echo	5.9	9.1	1.8	7.9	98.0	9.6	2.5	8.8	10.4	3.3	3.0	3.5
Pin Rouge	8.7	14.0	0.1	6.4	48.9	7.2	2.2	118.5	43.0	3.0	2.7	2.3
Laurentians	9.0	16.5	2.4	7.6	62.5	8.5	1.9	77.7	20.2	2.7	2.4	3.4
Brompton	12.5	42.3	11.9	6.6	92.1	32.3	8.5	188.1	31.7	3.5	2.7	3.9
Magog	9.8	19.2	10.8	7.0	205.5	73.0	20.4	52.8	129.2	5.1	3.4	3.8
Massawippi	40.2	84.8	17.9	7.5	284.7	15.8	5.4	566.6	20.3	4.5	3.1	4.5
Eastern Townships	20.8	48.8	13.5	7.4	194.1	40.3	11.6	260.1	60.3	4.3	3.1	4.1

Note: Except for lake morphometry, values reported are summer means computed over all measurements taken at the depths and dates of sampling: $n = 15$ for pH, conductivity, and water transparency; $n = 45$ for nutrients and chlorophyll *a*.

Pin Rouge where a stronger and earlier stratification in the spring maintained hypolimnetic waters at 4°C during summer. The metalimnion layer extended from 2 to 6 m in the Laurentian lakes and from 8 to 12 m in the Eastern Townships lakes.

Sampling was carried out in 1990 in the Laurentian lakes and in 1991 in the Eastern Townships lakes. Each lake was sampled five times every 2 wk from June to August. The discrete sampling depths corresponding to the epi-, meta-, and hypolimnion strata were established from temperature and oxygen profiles which were measured at 1-m intervals from the water surface to a few centimetres above the sediments by using a YSI temperature/O_2-meter. Three independent water samples were randomly collected at different sites in the epi-, meta-, and hypolimnion strata using an opaque 6-L Van Dorn sampler. We collected 150-mL subsamples for nutrient analyses and 250-mL subsamples for APP and ANP enumeration; the latter were fixed with glutaraldehyde buffered with 0.1 M sodium cacodylate at pH 7.2 for a final concentration of 1% v/v (Caron et al. 1985; Pick and Caron 1987). Another 1-L subsample was retained in a dark bottle for chlorophyll *a* analysis. pH and conductivity were measured in the field using a portable pH meter (Fisher Acumet, model 620) and conductivity meter (Cole Parmer, model 1484).

Nutrients and pico- and nanoplankton analyses

Water samples collected for dissolved nutrient analysis were filtered through a 25-mm ashed Whatmann GF/F glass filter directly after sampling. Filtered water samples were placed in sterilized 2-mL tubes, previously soaked in nitric acid bath (15% v/v) and rinsed with deionized distilled water; they were stored at –20°C in the dark until analyzed. Nutrients were analyzed within 1 mo; TP and total dissolved phosphorus (TDP) were analyzed using an Alpkem autoanalyzer and a spectrophotometer by the molybdenum blue method after persulfate digestion for TP. NO_3 concentration was determined after conversion to NO_2 by cadmium reduction. Since chlorophyll *a* cannot be considered as a rigourous surrogate of algal biomass (Chow-Fraser et al. 1994), it was only used as another surrogate of lake trophy. Chlorophyll *a* was estimated in total water samples and in water samples screened through a 25-μm Nitex™ net. This <25 μm fraction does not correspond exactly to the pico- and nanoplankton components (<20 μm) but was used to allow comparisons with other chlorophyll *a* estimates available for the same lakes in the Laurentian region (Lafond et al. 1990). Water subsamples (150–500 mL) were filtered on Membrafil Nuclepore™ filters (47-mm diameter, 0.45-μm pore size). Filters were coated with $MgCO_3$ at the end of filtration and stored at –20°C until analyzed. Chlorophyll *a* was determined by spectrophometry according to Strickland and Parsons (1972), after maceration in acetone (90%) for 24 h at 4°C in the dark. Correction for phaeophytin was applied using the Lorenzen (1967) acidification method.

APP and ANP enumeration was performed by autofluorescence using a Leitz Dialux 20 epifluorescence microscope fitted with an HBO 50-W mercury lamp, and standard blue (BP450-490 exciter filter, LP520 barrier filter, FT510 dichromatic beam splitter) and green (BP510-560 exciter filter, LP590 barrier filter, FT580 dichromatic beam splitter) filter sets (Caron et al. 1985; Pick and Caron 1987). One day after sampling, 5–20 mL of preserved water subsamples were filtered through Irgalan Black prestained Nuclepore™ polycarbonate filters (25-mm diameter, 0.2-μm pore size) under low vacuum pressure (<100 mm Hg) (Hobbie et al. 1977; Booth 1993). A backing filter (Membrafil Nuclepore™, 25-mm diameter, 0.45-μm pore size) was used to ensure random distribution of cells on the filter. Slides were prepared with low-fluorescence immersion oil (Cargille type FF) and stored in the dark at 4°C; they were counted within 1 mo in order to minimize the fading of autofluorescence.

Enumeration of APP and ANP cells resulted from microscopic scanning of 10–15 fields across the filter using magnification of 1000× until a minimum of 400 cells per filter were counted to obtain a precision level of ±10% on estimates (Lund et al. 1958).

© 1996 NRC Canada

Fig. 1. Relationships observed for our subsets of lakes (A) between APP and ANP biomass, (B) between the APP and ANP contribution to <20 μm total autotrophic pico- and nanoplankton biomass, and (C) between the ANP/APP ratio and lake trophy expressed by TP concentration. The # symbol corresponds to Lake Ontario data (Pick and Caron 1987).

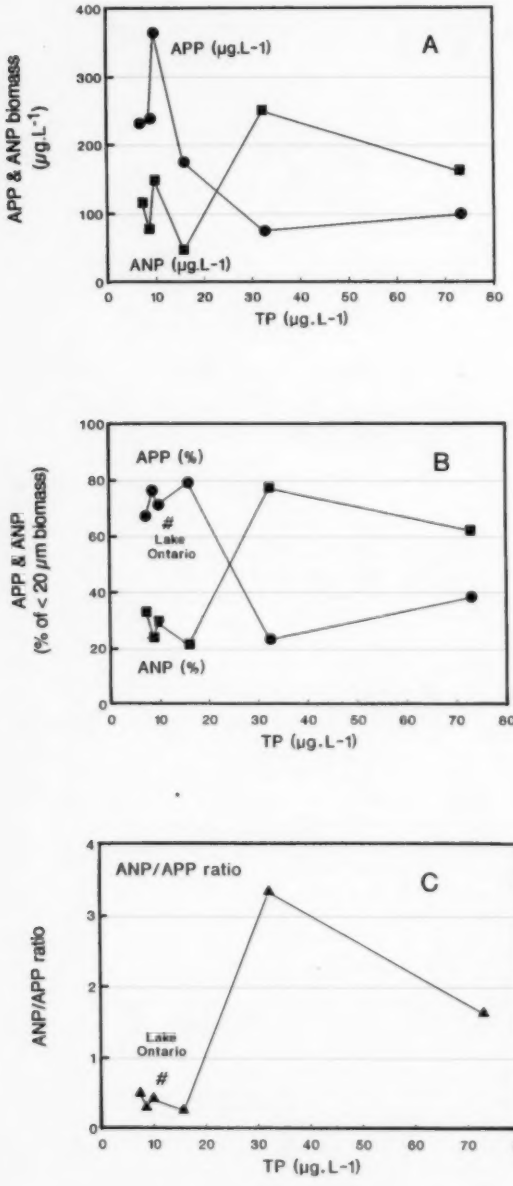

APP (<2 μm) and ANP (2–20 μm) were discriminated by their specific autofluorescence and size based on their longest dimension. Under green excitation, phycobiliprotein-containing cyanobacteria fluoresced bright red (Pick and Agbeti 1991; MacIsaac and Stockner 1993). Under blue excitation, yellow to orange fluorescence was indicative of phycoerythrin-containing cyanobacteria, while red fluorescence distinguished eukaryotes. Total biovolume of each cell type was calculated by multiplying their density (cells per 10^3 millilitres) by their mean biovolume (cubic micrometres) estimated from sizing with an eyepiece ocular micrometer. Wet-weight biomass (micrograms per litre) was calculated by assuming a specific gravity of 1. To allow comparisons with other studies, we converted our biovolume estimates to carbon biomass (micrograms carbon per litre) using the conversion factors 0.22 pg C·μm^{-3} for the picoplankton (Booth 1993) and 0.15 pg C·μm^{-3} for the nanoplankton (Carrick and Fahnenstiel 1989).

Fig. 2. Results of the average linkage cluster analysis of physicochemical data between the six lakes studied in Quebec (Laurentian lakes: AC, Achigan; EO, Echo; PR, Pin Rouge; Eastern Townships lakes: BR, Brompton; MG, Magog; MP, Massawippi) for (A) the epilimnion stratum, (B) the metalimnion stratum, (C) the hypolimnion stratum, (D) means across strata, and (E) means across strata including lake morphometric data. RMS: root mean square.

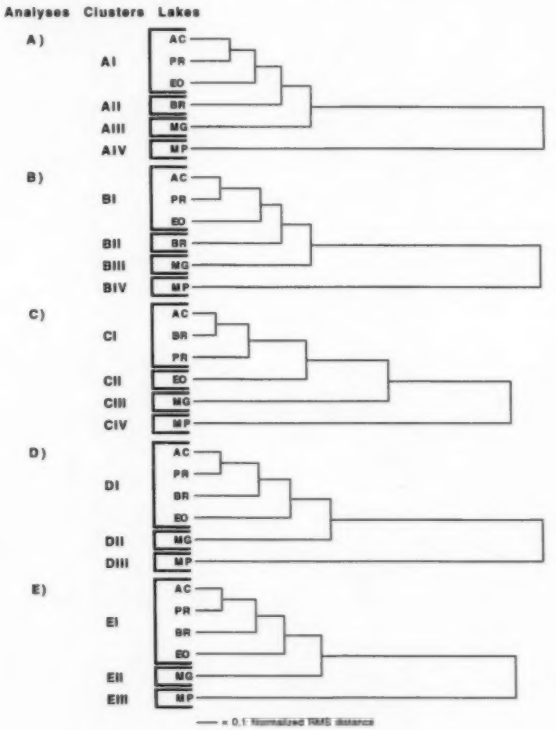

Statistical analyses

The general trends on a multilake basis of the relations between lake trophy (expressed as TP) and APP and ANP variables (biomass, contribution to total APP and ANP biomass, ANP/APP ratio) were investigated first. Thereafter, cluster analysis was carried out to group lakes on the basis of their physicochemical and morphometric characteristics, per sampling depth and across sampling depths; mean values were used when data collected in time or replicates were available. In accordance with the clustering, data from different regions (Laurentian and Eastern Townships) were analyzed separately. Among-lake and within-lake (among sampling depths and periods) variations in APP and ANP biomass were statistically

© 1996 NRC Canada

Table 2. Autotrophic picoplankton (APP) and nanoplankton (ANP) biomass ($\mu g \cdot L^{-1}$ or $\mu g\ C \cdot L^{-1}$) in each lake and region (summer means computed over all biomass estimates at the depths and dates of sampling: $n = 45$), their respective contributions to total autotrophic pico- and nanoplankton <20 μm (%), and ANP/APP ratio.

Lakes and regions	APP ($\mu g \cdot L^{-1}$)	APP ($\mu g\ C \cdot L^{-1}$)	APP (%)	ANP ($\mu g \cdot L^{-1}$)	ANP ($\mu g\ C \cdot L^{-1}$)	ANP (%)	ANP/APP ratio
Achigan	236.8	52.1	76	76.3	11.4	24	0.32
Echo	364.8	80.3	71	149.1	22.4	29	0.41
Pin Rouge	234.3	51.5	67	113.9	17.1	33	0.49
Laurentian lakes (means)	278.6	61.3	71	113.1	17.0	29	0.41
Brompton	74.9	16.5	23	248.8	37.3	77	3.32
Magog	98.5	21.7	38	161.1	24.2	62	1.63
Massawippi	174.4	38.4	79	46.0	6.9	21	0.26
Eastern Townships lakes (means)	115.9	25.5	43 (30)[a]	152.0	22.8	57 (70)[a]	1.31 (2.36)[a]

[a]Considering only Lakes Brompton and Magog.

assessed by factorial ANOVA (Sokal and Rohlf 1995; see also Dutilleul 1993*a*). Among-lake variation was taken into account by the lake factor (factor = classification criterion), while the depth (i.e., strata) and period (i.e., dates of sampling) factors partly account for the within-lake variation. The three water samples randomly collected for a given depth and period within a lake were considered as replicates. The linear correlations between the environmental variables (nutrients, temperature, oxygen, pH, and conductivity) and APP and ANP biomass were statistically assessed for each subset of lakes by *t*-testing based on Pearson's *r*-statistic. Differences in APP and ANP biomass between depths within a lake or between lakes within a region were assessed using *t*-tests for paired observations on normalized data or Mann–Whitney nonparametric *U*-tests (Sokal and Rohlf 1995).

The ANOVA and correlation analysis were modified in order to take the spatiotemporal autocorrelation and heteroscedasticity into account (Cliff and Ord 1981; Dutilleul 1993*a*, 1993*b*; Dutilleul and Legendre 1993; Legendre 1993). Since the number of lakes (three per region) was not greater than the number of spatiotemporal repeated measures (15 = 3 depths × 5 periods), as required by the multivariate approach to the repeated measures ANOVA, we used the modified univariate one (Crowder and Hand 1990; Potvin et al. 1990). The probabilities of significance for the main effects and interactions of the repetition factors (i.e., depth and period) were thus adjusted by application of a correction factor, called epsilon (Box 1954*a*, 1954*b*), that lowers the number of degrees of freedom of the *F*-test statistics. Concerning the correlation analysis, we used a spatiotemporal version of Dutilleul's (1993*b*) modified *t*-test. Basically, the procedure is similar to the modified univariate approach to the repeated measures ANOVA, except that the corrected number of degrees of freedom of the modified *t*-test may be smaller or greater than the uncorrected one. A detailed presentation of the two modified statistical procedures was given by Dutilleul (1994), following Dutilleul (1990).

The cluster analysis, ANOVA, and correlation analysis were performed by using the CLUSTER, GLM, and CORR procedures of SAS (SAS Institue Inc. 1989*a*, 1990), respectively. We used our own computer programs written in the SAS/IML language (SAS Institute Inc. 1989*b*) to implement modifications required by the analysis of spatiotemporal repeated measures. To fulfil the normality assumption underlying the *F*- and *t*-tests in the ANOVA and correlation analysis, Box–Cox–Bartlett's normalizing and variance-stabilizing transformation (Sokal and Rohlf 1995) was carried out by using the VERNORM procedure of the R package (Legendre and Vaudor 1991).

Results

Relations of autotrophic pico- and nanoplankton with lake trophy

Comparative analysis of the APP and ANP biomass and their relative contribution to total autotrophic pico- and nanoplankton components (biomass of cells <20 μm) along the trophic range of the lakes under study revealed negative relationships between TP and APP ($r = -0.68$) and positive relationships between TP and ANP and ANP/APP ratio ($r = 0.40$–0.67) (Fig. 1). Higher APP biomass and lower ANP biomass occurred in oligomesotrophic or hardwater lakes (TP <20 $\mu g \cdot L^{-1}$: Achigan, Echo, Pin Rouge, Massawippi) where the ANP/APP biomass ratio was less than 1. An opposite trend was found in more eutrophic lakes (TP > 30 $\mu g \cdot L^{-1}$: Brompton, Magog) where the ANP/APP biomass ratio was greater than 1. These opposite trends in the relationships of APP and ANP with lake trophy were maintained when their respective contributions to the <20 μm pico- and nanoplankton biomass were considered. APP contribution varied from around 70–80% in the oligomesotrophic or hardwater lakes to around 20–30% in the more eutrophic lakes; ANP contribution showed an opposite trend and dominated with 60–80% of the <20 μm compartment in the more eutrophic lakes. Similar, but weaker, relationships were obtained with the chlorophyll *a* concentrations (total chlorophyll *a* and chlorophyll *a* < 25 μm). Since APP biomass was lower in the large-size lakes of the Eastern Townships, we also found a negative relationship between APP biomass and lake size ($r = -0.67$ and -0.39, respectively, with lake area and maximum depth).

Variation between regions in the limnological conditions, and the APP and ANP biomass

We found significant differences between the two subsets of lakes for most of the physicochemical (except pH) and morphological characteristics (Mann–Whitney *U*-tests: $P < 0.05$–0.001; Table 1). The cluster analysis, based on the physicochemical characteristics, also grouped lakes into two regional subsets (Fig. 2). It must be noted that different methods of cluster analysis corresponding to various criteria were tried; all resulted in very similar results, so that only the average

© 1996 NRC Canada

Table 3. Results of the ANOVA *F*-tests performed on autotrophic picoplankton (APP) and nanoplankton (ANP) biomass to assess statistically the among-lake variation (L) and the differences among lakes in the within-lake variation among depths ($L \times d$) and among periods of sampling ($L \times p$) in the Laurentian and Eastern Townships regions.

Sources of variation	Laurentians APP	Eastern Townships APP	Laurentians ANP	Eastern Townships ANP
L	<0.0001***	<0.0001***	0.0015**	<0.0001***
$L \times d$	0.0082**	<0.0001***	0.7136 ns	0.0256*
$L \times p$	0.0051**	0.0007***	0.4827 ns	0.0207*

Note: The significance probabilities reported are adjusted for spatiotemporal autocorrelation and heteroscedasticity. ns, effect nonsignificant ($P > 0.05$); *effect significant ($0.01 \leq P$ 0.05); **effect highly significant ($0.001 \leq P < 0.01$); ***effect very highly significant ($P < 0.001$).

Table 4. Correlations between autotrophic picoplankton (APP) and nanoplankton (ANP) biomass and the selected limnological variables in the Laurentian and Eastern Townships lakes.

Phytoplankton size class	Region	Environmental variable	Pearson's *r*-statistic	Probability Pr > |r|
APP	Laurentian	pH	0.4538	0.0012**
		Oxygen	0.4162	0.0096**
		NO_3	–0.6053	0.0001***
APP	Eastern Townships	pH	0.6617	0.0001***
		Conductivity	0.4635	0.0016**
ANP	Laurentian	TDP	0.5930	0.0019**
		NO_3	–0.5659	0.0003 ***
ANP	Eastern Townships	Conductivity	–0.5746	0.0011**
		Temperature	0.4014	0.0404 *

Note: The observed significant value of Pearson's *r*-statistic and the corresponding probability from the modified *t*-test are reported; the latter, denoted Pr > |r|, is adjusted for spatiotemporal autocorrelation and heteroscedasticity. Significant levels as in Table 3.

linkage method was retained for graphical purposes. Based on the epi- and metalimnetic physicochemical data (Figs. 2A and 2B), the Laurentian lakes clustered in one group, while the Eastern Townships lakes showed less similarity and were added in the dendogram as three singletons. For the hypolimnion only (Fig. 2C), the cluster analysis indicated that Lake Brompton had some similarity to the Laurentian lakes, especially Lakes Achigan and Pin Rouge, because of its lower conductivity and chlorophyll *a* concentrations. A similar result was obtained when the means across strata were used while either including or excluding morphometric characteristics (Figs. 2D and 2E). In contrast, Lake Massawippi always showed the highest dissimilarity due to its hardwater conditions and greater size. Important differences in APP and ANP mean biomass were also observed between lakes from the two different regions (Table 2). Mean APP biomass and estimated carbon biomass in the Laurentian lakes (Achigan, Echo, Pin Rouge) were more than twice as great as in the Eastern Townships lakes (Brompton, Magog, Massawippi) (Mann–Whitney *U*-test: $P < 0.0001$). In contrast, mean ANP biomass and estimated carbon biomass were slightly higher in the Eastern Townships lakes than in the Laurentian lakes (Mann–Whitney *U*-test: $P = 0.0212$). APP accounted for around 70% of the <20 μm total pico- and nanoplankton biomass (APP + ANP) in the Laurentian lakes where the mean ANP/APP biomass ratio was 0.41. In contrast, APP contribution to the <20 μm biomass was lower (43% in average) in the Eastern Townships lakes and the ANP/APP ratio was greater than 1. The differences between subsets of lakes are even more pronounced after exclusion of Lake Massawippi from the Eastern Townships subset because of its dissimilarity (Fig. 2). It is the largest lake with hardwaters and low phosphorus levels (Table 1), and its APP *and* ANP biomass values as well as its ANP/APP ratio were more similar to those of the Laurentian lakes subset (Table 2). Considering Lakes Brompton and Magog only, APP contributes 30% on average to the biomass of cells <20 μm and the mean ANP/APP ratio increases to 2.36 in the Eastern Townships (Table 2).

© 1996 NRC Canada

Fig. 3. Three-dimensional bar charts of the spatiotemporal variation in autotrophic picoplankton (APP) biomass in the six lakes. Within lakes, space and time are defined by the stratum (EPI, META, HYPO) and the period of sampling (P1–P5) (discrete scale). Strata with the same small letter (a, b, c) are not significantly different ($P \geq 0.05$) in their mean APP biomass; *t*-tests for paired observations were performed between depths across the five periods.

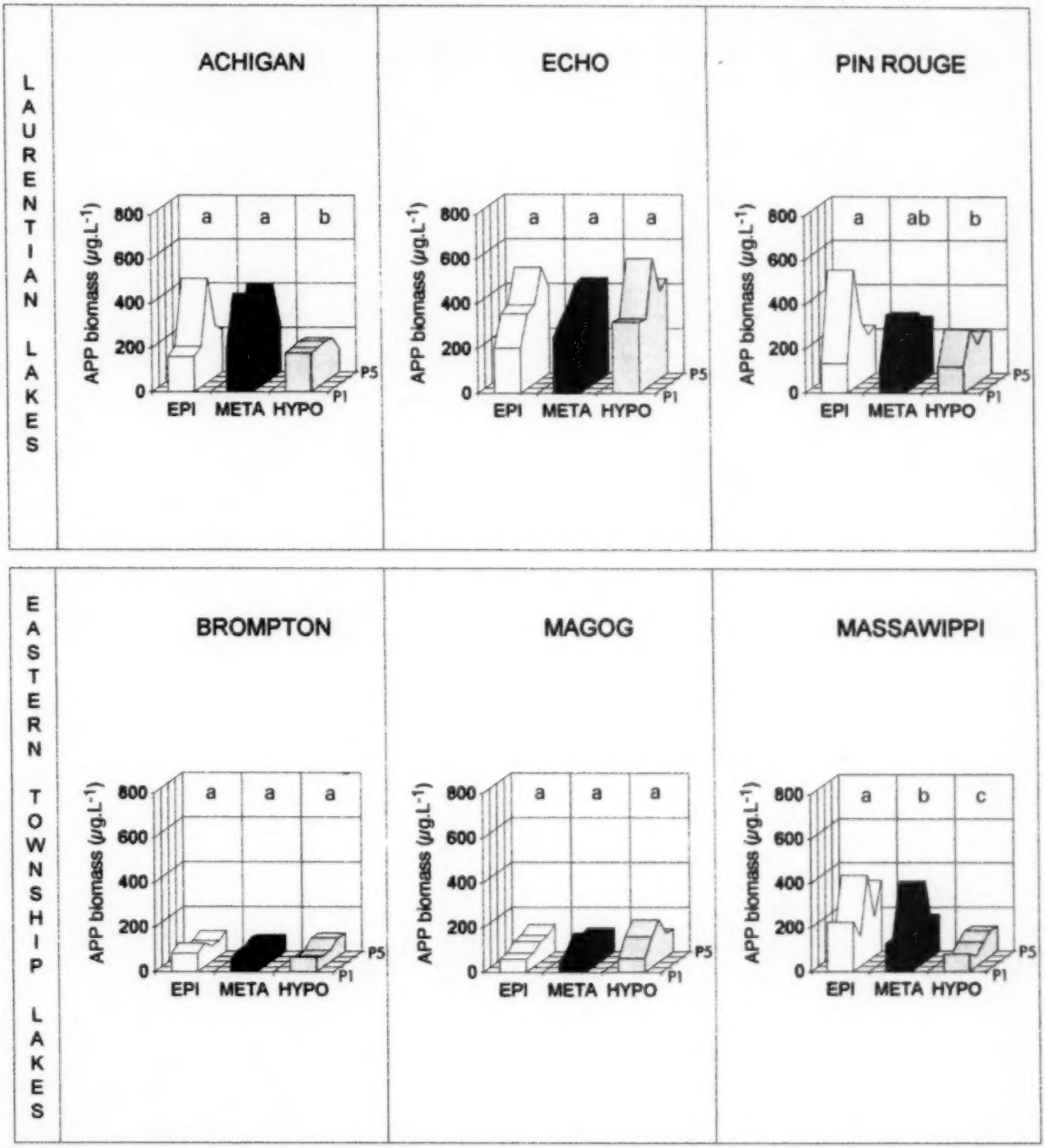

Variation in autotrophic pico- and nanoplankton biomass within each region

Figures 3 and 4 illustrate the variation observed between depths and sampling periods in each lake for APP and ANP biomass, respectively. Among-lake differences are the greatest source of variation within each region (Table 3). For both APP and ANP, we found high among-lake variation ($P \leq 0.0015$), but no systematic within-lake variation due to depth

© 1996 NRC Canada

Fig. 4. Three-dimensional bar charts of the spatiotemporal variation in autotrophic nanoplankton (ANP) biomass in the six lakes. Within lakes, space and time are defined by the stratum (EPI, META, HYPO) and the period of sampling (P1–P5) (discrete scale). Strata with the same small letter (a, b, c) are not significantly different ($P \geq 0.05$) in their mean ANP biomass; *t*-tests for paired observations were performed between depths across the five periods.

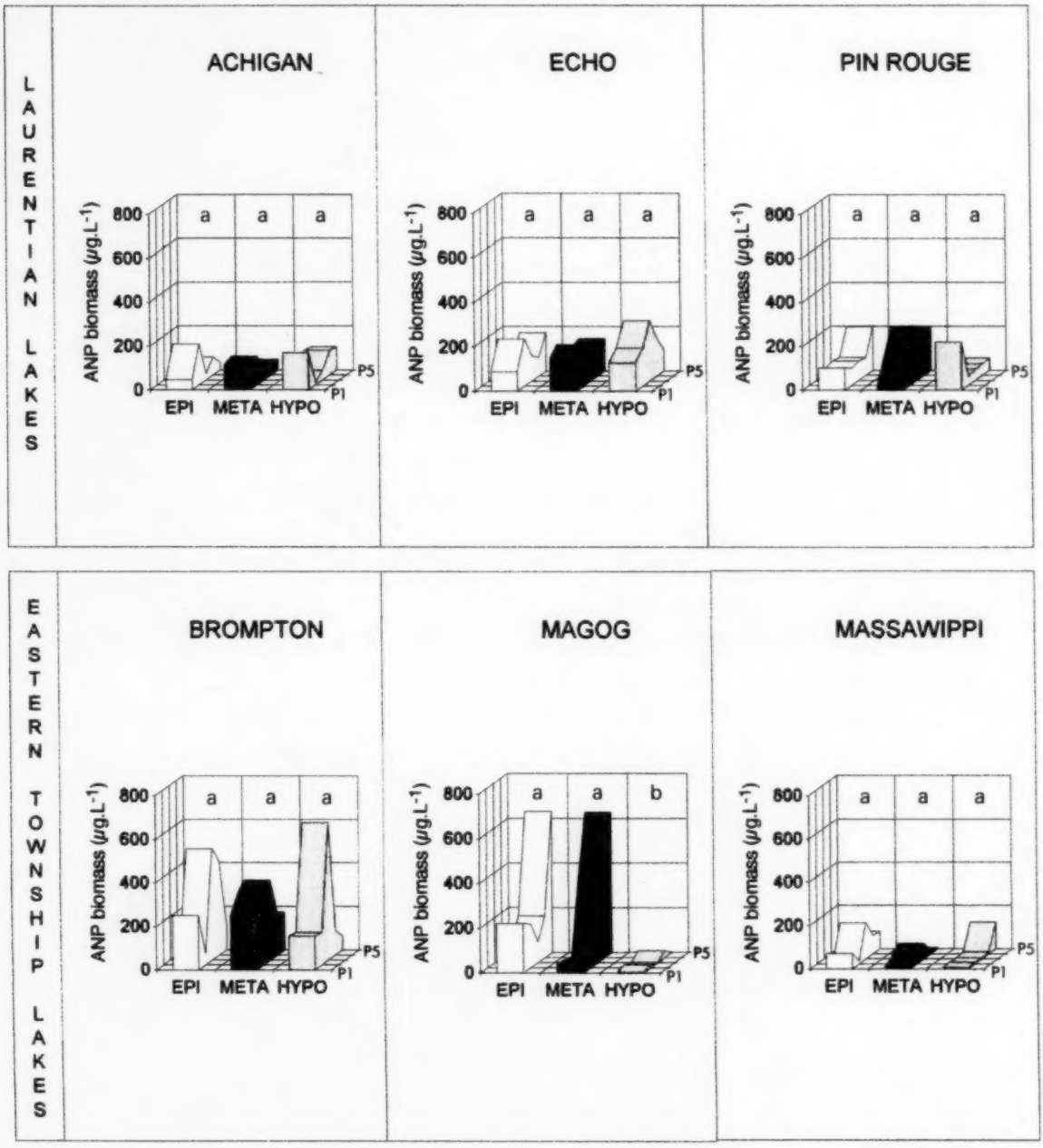

or sampling period ($P > 0.2$) . Additional important variations came from the interactions between the lake factor (L) and the depth (d) and sampling period (p) factors, i.e., the $L \times d$ and $L \times p$ effects (Table 3).

The lake main effects (L) reflect variations between lakes in APP biomass within each region. For instance, in the Laurentians, Lake Echo exhibited the highest mean APP biomass, while Lakes Achigan and Pin Rouge had similar lower values.

© 1996 NRC Canada

In the Eastern Townships, Lake Massawippi showed a higher mean APP biomass than Lakes Brompton and Magog (Table 2). Very highly significant $L \times d$ and $L \times p$ interactions indicated that vertical and temporal variations of APP biomass were not parallel from lake to lake, i.e., differences among depths on one hand and among periods on the other were not constant from lake to lake (Fig. 3). For instance, in the Laurentians, the APP biomass in Lake Achigan was the highest in the epi- and metalimnion and then significantly decreased in the hypolimnion, while there was no variation with depth in Lake Echo and a significant decreasing trend with depth in Lake Pin Rouge. In the Eastern Townships, no significant variation with depth was observed for APP biomass in Lakes Brompton and Magog, while APP steadily decreased with depth in Lake Massawippi, especially in the hypolimnion. Variation in APP biomass between periods of sampling also differed among lakes, as the APP biomass maxima were observed at different periods in each lake.

Among-lake differences were also the most important source of variation for ANP biomass (Table 3). This is especially true in the Laurentian lakes where only the L effect was found to be significant; the absence of $L \times d$ and $L \times p$ interactions indicated homogeneity in biomass along spatial and temporal scales (Fig. 4). The highly significant L effect in the Laurentians reflected a gradient in ANP biomass among lakes, with Lake Echo showing the highest ANP biomass, Lake Achigan the lowest, and Lake Pin Rouge in between (Table 2). Higher variation in ANP biomass occurred in the Eastern Townships where the L effect was found to be very highly significant and the $L \times d$ and $L \times p$ interactions were simply significant (Table 3). Lake Massawippi showed much smaller ANP biomass than Lakes Magog and Brompton (Table 2). No variation with depth was observed in Lakes Brompton and Massawippi, while ANP biomass drastically decreased in the anoxic hypolimnion of Lake Magog (Fig. 4). In the Eastern Townships, ANP biomass was generally the highest in late summer, at the fourth or fifth period of sampling depending on the lake (Fig. 4).

Relationships between APP and ANP biomass and the limnological charateristics

As shown before, lake trophy and size were the most important factors influencing the spatial variation in APP and ANP biomass as well as their relative contribution to the total biomass of cells <20 μm across the two regions. Within each region, several factors were also related to the observed variations in APP and ANP biomass (Table 4). The limnological variables that significantly correlated with APP and ANP biomass were pH, conductivity, oxygen, and NO_3 for the APP biomass and conductivity, temperature, TDP, and NO_3 for the ANP biomass.

For APP, the strongest relationship in the Laurentian lakes was provided by a negative correlation with NO_3 (Table 4). The highest APP biomass was observed in Lake Echo that had very low NO_3 concentrations (<10 $\mu g \cdot L^{-1}$) (Tables 1 and 2), and inverse depth gradients were observed for APP biomass and NO_3 in Lakes Achigan and Pin Rouge. Weaker positive correlations were observed for APP biomass, with oxygen and pH (Table 4). Lake Echo, which had the highest APP biomass (Table 2), showed the highest pH (Table 1), especially in the epi- and metalimnion strata. Higher APP biomass in the warm and oxygenated epilimnia of Lakes Achigan and Pin Rouge, on one hand, and lower APP biomass in the anoxic and cold hypolimnion of Lake Pin Rouge, on the other, may also explain the positive relationship observed with oxygen and temperature. In the Eastern Townships, APP biomass was positively correlated with pH and conductivity (Table 4). Lakes Brompton and Magog had relatively low-mineralized waters (around 100–200 $\mu S \cdot cm^{-1}$) and lower pH (<7.0), and they showed the lowest APP biomass. Conversely, Lake Massawippi, which had hardwaters (conductivity 250–350 $\mu S \cdot cm^{-1}$), presented the highest APP biomass (Tables 1 and 2).

ANP biomass was negatively related to NO_3 and positively correlated with TDP in the Laurentian lakes (Table 4), since the highest ANP biomass was found in Lake Echo where NO_3 concentration was very low (<10 $\mu g \cdot L^{-1}$), while the TDP level was slightly higher than in Lakes Achigan and Pin Rouge (Tables 1 and 2). In the Eastern Townships, ANP biomass was negatively correlated with conductivity (Table 4) because the smallest ANP biomass was found in Lake Massawippi where conductivity was the highest (Tables 1 and 2). A vertical decreasing gradient in water temperature and lower ANP biomass in the hypolimnion of Lake Magog (Fig. 4) resulted in a positive correlation of ANP with water temperature in the Eastern Townships.

Discussion

Although comparisons between studies can be confused by differences in biomass units of reference (chlorophyll, carbon, wet weight, etc.) and size fractionation, our estimates of APP and ANP biomass fall within the ranges reported in other freshwater environments. APP biomass values in Quebec lakes (APP: 75–365 $\mu g \cdot L^{-1}$ or 16–80 $\mu g\ C \cdot L^{-1}$) over our trophic range (TP: 7–73 $\mu g \cdot L^{-1}$) overlap values reported by Stockner (1991) within a similar trophic range (TP: 10–100 $\mu g \cdot L^{-1}$; APP: 21–210 $\mu g\ C \cdot L^{-1}$). ANP biomass values in Quebec lakes (46–249 $\mu g \cdot L^{-1}$ or 7–37 $\mu g\ C \cdot L^{-1}$) generally exceed those reported in the oligotrophic Lake Superior (Munawar et al. 1978), but are similar or slightly lower than those published for Lakes Michigan and Huron (Carrick and Fahnenstiel 1989), which are of the same trophic status (TP: 5 and 8 $\mu g \cdot L^{-1}$) as the Laurentian lakes. In Lake Ontario, Pick and Caron (1987) reported similar estimates for APP (100–400 $\mu g \cdot L^{-1}$) but higher values for ANP (100–700 $\mu g \cdot L^{-1}$).

Studies assessing the relationships between APP abundance or its contribution to total phytoplankton biomass and lake trophy gave conflicting results. Some studies (Burns and Stockner 1991; Hawley and Whitton 1991; Pick and Agbeti 1991) suggested that both APP abundance and its contribution to total phytoplankton decline with lake trophy. In contrast, other studies indicated that APP abundance increased slightly with lake trophy, while its contribution to total phytoplankton biomass decreased (Sondergaard 1991; Wehr 1991; Petersen 1991; Stockner and Shortreed 1991; Stockner 1991). Such contradictory relationships may result from differences in the ranges of lake trophy investigated. For instance, the narrow range of trophy (TP: 1.5–9 $\mu g \cdot L^{-1}$) covered by Stockner and Shortreed (1991) in the oligotrophic coastal lakes of Bristish Columbia, as in the Laurentian lakes,

© 1996 NRC Canada

did not allow the detection of important changes in APP abundance or biomass with phosphorus levels. As stated by Stockner (1991), much work remains to be done on a continuum of lake trophy to remove this uncertainty.

Despite the small number of lakes that we studied in Quebec, variation in APP and ANP biomass was found among lakes in the two regions, in relation to change in lake trophy. We demonstrated that APP biomass and its relative contribution to <20 μm total pico- and nanoplankton biomass decreased with TP, while ANP presented the opposite trend (Figs. 1A and 1B). Consequently, the ANP/APP biomass ratio was lower than 0.5 in the oligomesotrophic or hardwater lakes and higher than 1.5 in the more eutrophic lakes (Fig. 1C). These trends are supported by the results of another study in Lake Ontario (Pick and Caron 1987). Trophic status of Lake Ontario (TP: 10–15 $\mu g \cdot L^{-1}$) is similar to that of the Laurentian lakes and Lake Massawippi, and APP biomass in Lake Ontario accounted for up to 68% of the total phototrophic biomass <20 μm, as in the Laurentian lakes. Our study supports the hypothesis that nutrient enrichment favors a nanoplankton-dominated <20 μm phototrophic community. In our range of lake trophy (TP: 7–73 $\mu g \cdot L^{-1}$), the ANP/APP biomass ratio increased with TP and eutrophic lakes had two times more ANP than APP biomass. The critical level at which nanoplankton outcompetes picoplankton (ANP/APP biomass ratio > 1) was observed for TP levels between 20 and 30 $\mu g \cdot L^{-1}$ (Fig. 1C). This shift from a picoplankton-dominated to a nanoplankton-dominated <20 μm algal community along the trophic gradient has been explained by competitive interactions between APP and ANP for nutrients. More rapid nutrient uptake by the smaller cells in nutrient-limited environments enables APP cells to outcompete ANP or larger cells in oligotrophic systems (Fogg 1986; Sherr et al. 1988; Wehr 1991; Teixeira and Gaeta 1991; Pick and Agbeti 1991). When the nutrient supply increases in eutrophic systems, APP cells lose their competitive advantage, and nano- and microplankton compartments become dominant (Wehr 1990; Lafond et al. 1990; Fogg 1991). Such competitive interactions between APP and ANP have also been documented in enclosure experiments (Wehr 1989). The predominance of algae <20 μm over total phytoplankton that has been previously observed in southern Quebec lakes (Watson and Kalff 1981; Lafond et al. 1990) is confirmed; we found a higher contribution of the chlorophyll <25 μm to total chlorophyll biomass in the oligomesotrophic lakes (Laurentian region: 84–90%) than in the more eutrophic lakes (Eastern Townships region: 67–77%).

Specific nutrients such as N and P can limit the development of APP and ANP in freshwater ecosystems in different ways (Wehr 1989; Suttle and Harrison 1988). Fertilization studies in enclosures suggested that ANP is very N-limited and also P-limited, while APP responds to N but not to P addition. Our empirical study contradicts these trends, since we found negative correlation with NO_3 for both APP and ANP. Differences in the APP and ANP response to nutrients are not always reflected by a significant relationship with the N/P ratio (Wehr 1989), even if other fertilization studies conducted in laboratory or in oligotrophic lakes indicated sensitive responses of algal compartments to N/P ratio (Stockner and Shortreed 1988; Suttle and Harrison 1988). Near-optimum conditions for picocyanobacteria (*Synechococcus*) blooming seem to be associated with high N/P ratios (35:1–45:1). Our study gives little support to the contention that high N/P ratio favors APP, since high APP biomass was observed in lakes with low (Lake Echo: 2:1) as well as higher (Lake Achigan: 13:1; Lake Pin Rouge: 22:1; Lake Massawippi: 37:1) N/P ratios. Only when considering the Eastern Townships lakes does the positive relationship between APP and N/P ratio hold because Lakes Brompton and Magog have lower N/P ratios (7:1; 2.5:1) and lower APP biomass (75–98 $\mu g \cdot L^{-1}$) than Lake Massawippi (N/P: 37:1; APP biomass: 174 $\mu g \cdot L^{-1}$). Based on a small number of lakes, the assessment of a possible N/P ratio effect on the importance of APP and ANP is difficult and may lead to conflicting results. Further studies based on larger samples of lakes are required to assess those relationships.

In our study, many factors may affect the relationships between APP or ANP and nutrients. We analyzed both eukaryotic and prokaryotic APP forms, whose relative abundance and response to nutrients may differ among lakes. Eukaryotic APP usually comprises <10% of total APP, except in humic lakes where the eukaryotic forms tend to be more important than the prokaryotic forms (Stockner 1987; Pick and Agbeti 1991). In our lakes, APP was mainly composed of prokaryotic *Synechococcus* associated with few *Merismopedia* and some eukaryotic cells; we did not observe any higher importance of the latter category in Lake Pin Rouge which was humic. ANP was composed of chlorophytes (mainly *Crucigenia, Scenedesmus, Dictosphearium*), cryptophytes (*Cryptomonas, Rhodomonas*), chrysophytes (*Synura*), cyanophytes (*Lyngbya, Anabaena*), and diatoms (*Melosira, Stephanodiscus*). The relative composition of ANP varied slightly among lakes. Diatoms and chrysophytes were characteristic of Lake Brompton, while cyanophytes were more frequent in Lakes Echo and Magog. Competitive interactions among phytoplankters for the nitrogen forms such as NO_3 and NH_4 may also be of some importance (Suttle and Harrison 1988). Finally, the among-lake variation in ANP biomass observed in each region might derive not only from competition between APP and ANP for different nutrients, but also from interlake variation in zooplankton assemblages, since we found the highest abundances of macrocrustaceans (unpublished data) in Lakes Massawippi, Achigan, and Pin Rouge, where the lowest ANP biomasses were encountered. These relationships with grazers will be investigated in detail in further studies.

There are also methodological caveats that may bias the quantification of APP and ANP biomass and, as a result, of the ANP/APP ratio. For instance, one problem in using epifluorescence to estimate biomass, of ANP in particular, is that what we see is not always the entire cell volume but instead the fluorescence of the chloroplast, which may or may not fill the entire cell, or may not be large enough to illuminate the whole cell. It follows that the ANP biomass and ANP/APP ratio may have been underestimated in a nonsystematic way because of the variation in size of the chloroplast among and within nanoplankton taxa. However, as the size of ANP cells is one order of magnitude larger than that of APP cells, there should be a difference of three orders of magnitude between APP and ANP biomass. We thus consider that this potential underestimation of ANP biomass may have been a source of minor interference, which should not have affected the rela-

© 1996 NRC Canada

tionships observed between APP and ANP biomass, as well as the ANP/APP ratio, and lake trophy.

Within each region, most of the variation in APP and ANP biomass appeared to be driven by lake-specific factors, since no significant systematic variations were found between depths or periods of sampling (Table 3). The variation in APP and ANP biomass was related to changes in conductivity, pH, oxygen, temperature, and nutrients (Table 4). The significant correlations observed between APP or ANP and conductivity in the Eastern Townships lakes resulted from higher APP biomass and higher conductivity in Lake Massawippi or higher ANP biomass and lower conductivity in Lake Brompton, respectively (Tables 1 and 2). Finally, the negative relationship of ANP with NO_3 and its positive correlation with TDP detected in the Laurentian lakes may be explained by the simultaneous occurrence of high ANP biomass and low NO_3 concentration in Lake Echo and from higher ANP biomass in Lakes Echo and Pin Rouge which also had higher TDP concentrations (Tables 1 and 2). Although cyanobacteria show preference for higher pH (Fogg 1986), we hypothesize that the relationships found for APP with pH and conductivity are indirect and reflect a positive relationship with a clearer photic environment and lower trophy. In the Eastern Townships region, APP biomass, conductivity, and pH were higher in Lake Massawippi, which is a hardwater, clear, and less eutrophic lake. In contrast, for the Laurentian region, APP biomass and pH were lower in Lake Pin Rouge, which is a humic lake with brown waters (Tables 1 and 2). In Ontario lakes, significantly higher APP biomass was also reported in enclosures of greater clarity. Low light attenuation is known to favor the development of picocyanobacteria, especially that of cells containing phycoerythrin and utilizing blue–green light more efficiently (Pick 1991; Pick and Agbeti 1991). Only some correlations were found to be related to changes in phytoplankton and limnological variables with depth and period of sampling. The positive correlation observed between APP and oxygen in the Laurentian lakes reflects the simultaneous decrease of APP biomass and oxygen with depth in Lakes Achigan and Pin Rouge. High APP biomass and low NO_3 concentration in Lake Echo (Tables 1 and 2), as well as opposite distributions in depth of APP and NO_3 in Lakes Achigan and Pin Rouge, may explain the negative relationship between APP and NO_3. Finally, vertically decreasing and seasonally increasing temperature gradients may explain the positive relationship observed between ANP biomass and water temperature in the Eastern Townships lakes.

Acknowledgements

The authors are grateful to Joel Desy, Julie Gauthier, Marc Trudel, and Julie Gauvin for technical assistance in sampling. Special thanks go to Dominic Frigon for his assistance in cluster analysis and the drawing of Fig. 2. Dr. Frances Pick provided training in epifluorescence microscopy to N.B. and constructive comments on the manuscript. We also appreciate comments by Antonella Cattaneo and two anonymous reviewers. Financial support for this study was provided by research grants from NSERC and FCAR to B.P.A and P.D. This is a contribution from the GRIL (Groupe de Recherche Interuniversitaire en Limnologie et en Environnement Aquatique) at the Université de Montréal (Quebec, Canada).

References

Azam, F., Fenchel, T., Field J.G., Gray, J.S., Meyer-Reil, L.A., and Thingstad, F. 1983. The ecological role of water-column microbes in the sea. Mar. Ecol. Prog. Ser. **10**: 257–263.

Bennett, S.J., Sanders, R.W., and Porter, K.G. 1990. Heterotrophic, autotrophic, and mixotrophic nanoflagellates: seasonal abundances and bacterivory in a eutrophic lake. Limnol. Oceanogr. **35**: 1821–1832.

Bertrand, N., and Vincent, W.F. 1994. Structure and dynamics of photosynthetic picoplankton across the salt water transition zone of the St. Lawrence River. Can. J. Fish. Aquat. Sci. **51**: 161–171.

Booth, B.C. 1993. Estimating cell concentration and biomass of autotrophic plankton using microscopy. *In* Handbook of methods in aquatic microbial ecology. *Edited by* P.F. Kemp, B.F. Sherr, E.B. Sherr, and J.J. Cole. Lewis Publishers, Boca Raton, Fla. Chap. 24. pp. 199–205.

Box, G.E.P. 1954*a*. Some theorems on quadratic forms applied in the study of analysis of variance problems. I. Effect of inequality of variance in the one-way classification. Ann. Math. Stat. **25**: 290–302.

Box, G.E.P. 1954*b*. Some theorems on quadratic forms applied to the study of analysis of variance problems. II. Effects of inequality of variance and of correlation between errors in the two-way classification. Ann. Math. Stat. **25**: 484–498.

Burns, C.W., and Stockner, J.G. 1991. Picoplankton in six New Zealand lakes: abundance in relation to seasonal and trophic state. Int. Rev. Gesamten Hydrobiol. **76**: 523–536.

Caron, D.A., Pick F.R., and Lean, D.R.S. 1985. Chroococcoid cyanobacteria in Lake Ontario: vertical and seasonal distributions during 1982. J. Phycol. **21**: 171–175.

Carrick, H.J., and Fahnenstiel, G.L. 1989. Biomass, size structure, and composition of phototrophic and heterotrophic nanoflagellate communities in lakes Huron and Michigan. Can. J. Fish. Aquat. Sci. **46**: 1922–1928.

Carrick, H.J., and Fahnenstiel, G.L. 1990. Planktonic protozoa in Lakes Huron and Michigan: seasonal abundance and composition of ciliates and dinoflagellates. J. Great Lakes Res. **16**: 319–329.

Carrick, H.J., Fahnenstiel, G.L., Stoermer, E.F., and Wetzel, R.G. 1991. The importance of zooplankton–protozoan trophic couplings in Lake Michigan. Limnol. Oceanogr. **36**: 1335–1345.

Chow-Fraser, P., Trew, D.O., Findlay, D., and Stainton, M. 1994. A test of hypotheses to explain the sigmoidal relationship between total phosphorus and chlorophyll *a* concentrations in Canadian lakes. Can. J. Fish. Aquat. Sci. **51**: 2052–2065.

Christoffersen, K., Riemann, B., Klysner, A., and Sondergaard, M. 1993. Potential role of fish predation and natural populations of zooplankton in structuring a plankton community in eutrophic lake water. Limnol. Oceanogr. **38**: 561–573.

Cliff, A.D., and Ord, J.K. 1981. Spatial processes. Pion, London.

Crowder, M.J. and Hand, D.J. 1990. Analysis of repeated measures. Chapman and Hall, London.

Davis, P.G., Caron, D.A., Johnson, P.W., and Sieburth, J.M. 1985. Phototrophic and apochlorotic components of picoplankton and nanoplankton in the North Atlantic: geographic, vertical seasonal and diel distributions. Mar. Ecol. Prog. Ser. **21**: 15–26.

Dussart, B.H. 1965. Les différentes catégories de plancton. Hydrobiologia, **26**: 72–74.

Dutilleul, P. 1990. Apport en analyse spectrale d'un périodogramme modifié et modélisation des séries chronologiques avec répétitions en vue de leur comparaison en fréquence. Doctoral dissertation, Département de Mathématique, Université catholique de Louvain, Belgium.

Dutilleul, P. 1993*a*. Spatial heterogeneity and the design of ecological field experiments. Ecology, **74**: 1646–1658.

Dutilleul, P. 1993*b*. Modifying the *t*-test for assessing the correlation between two spatial processes. Biometrics, **49**: 305–314.

© 1996 NRC Canada

Dutilleul, P. 1994. How to deal with the spatio-temporal autocovariance of environmental data in ANOVA and correlation analysis. *In* The Abstracts of the Conference on Environmetrics, Canada Centre for Inland Waters, Burlington, Ont., Canada, August 11–15. The International Environmetrics Society. pp. 64–66.

Dutilleul, P., and Legendre, P. 1993. Spatial heterogeneity against heteroscedasticity: an ecological paradigm versus a statistical concept. Oikos, **66**: 152–171.

Fahnenstiel, G.L., and Carrick, H.J. 1992. Phototrophic picoplankton in Lakes Huron and Michigan: abundance, distribution, composition, and contribution to biomass and production. Can. J. Fish. Aquat. Sci. **49**: 379–388.

Fahnenstiel, G.L., Sicko-Goad, L., Scavia, D., and Stoermer, E.F. 1986. Importance of picoplankton in Lake Superior. Can. J. Fish. Aquat. Sci. **43**: 235–240.

Fahnenstiel, G.L., Carrick, H.J., and Iturriaga, R. 1991. Physiological characteristics and food-web dynamics of *Synechococcus* in Lakes Huron and Michigan. Limnol. Oceanogr. **36**: 219–234.

Fogg, G.E. 1986. Picoplankton: review lecture. Proc. R. Soc. Lond. B Biol. Sci. **228**: 1–30.

Fogg, G.E. 1991. The phytoplankton way of life. New Phytol. **118**: 191–232.

Geller, W., Berberovic, R., Gaedke, U., Muller, H., Pauli, H.R., Tilzer, M.M., and Weisse, T. 1991. Relations among the components of autotrophic and heterotrophic plankton during the seasonal cycle 1987 in Lake Constance. Verh. Int. Ver. Limnol. **24**: 831–836.

Hardy, F.J., Shortreed, K.S., and Stockner, J.G. 1986. Bacterioplankton, phytoplankton, and zooplankton communities in a British Columbia coastal lake before and after nutrient reduction. Can. J. Fish. Aquat. Sci. **43**: 1504–1514.

Hawley, G.R.W., and Whitton, B.A. 1991. Seasonal changes in chlorophyll-containing picoplankton populations of ten lakes in northern England. Int. Rev. Gesamten Hydrobiol. **76**: 545–554.

Hobbie, J.E., Daley, R.J., and Jasper, S. 1977. Use of nucleopore filters for counting bacteria by fluorescence microscopy. Appl. Environ. Microbiol. **33**: 1225–1228.

Jordan, I.T., Ross, P.E., and Pinel-Alloul, B. 1988. Seasonal variations in phytoplankton size structure in Lake Cromwell (Laurentian Shield), Quebec. Hydrobiologia, **169**: 167–182.

Kalff, J. 1972. Net plankton and nanoplankton production and biomass in a north temperate zone lake. Limnol. Oceanogr. **17**: 712–720.

Klut, M.E., and Stockner, J.G. 1991. Picoplankton associations in an ultra-oligotrophic lake on Vancouver Island, British Columbia. Can. J. Fish. Aquat. Sci. **48**: 1092–1099.

Lafond, M., Pinel-Alloul, B., and Ross, P.E. 1990. Biomass and photosynthesis of size-fractionated phytoplankton in Canadian Shield lakes. Hydrobiologia, **196**: 25–38.

Landry, M.R., Haas L.W., and Fagerness, V.L. 1984. Dynamics of microbial plankton communities: experiments in Kaneohe Bay, Hawai. Mar. Ecol. Prog. Ser. **16**: 127–133.

Legendre, L., Demers, S., Delesalle, B., and Harnois, C. 1988. Biomass and photosynthetic activity of phototrophic picoplankton in coral reef waters (Moorea Island, French Polynesia). Mar. Ecol. Prog. Ser. **47**: 153–160.

Legendre, P. 1993. Spatial autocorrelation: trouble or new paradigm? Ecology, **74**: 1659–1673.

Legendre, P., and Vaudor, A. 1991. Le progiciel R: analyse multidimensionnelle, analyse spatiale. Département de sciences biologiques, Université de Montréal, Montréal, Qué.

Leppard, G.L., Urciuolli, D., and Pick, F.R. 1987. Characterization of cyanobacterial picoplankton in Lake Ontario by transmission electron microscopy. Can. J. Fish. Aquat. Sci. **44**: 2173–2177.

Lorenzen, C.J. 1967. Determination of chlorophyll and phaeopigments: spectrophotometric equations. Limnol. Oceanogr. **12**: 343–346.

Lund, J.W.G., Kipling, C., and Le Cren, E.D. 1958. The inverted microscope method of estimating algal numbers and the statistical basis of estimation by counting. Hydrobiologia, **11**: 143–170.

MacIsaac, E.A. and Stockner, J.C. 1993. Enumeration of phototrophic picoplankton by autofluorescence microscopy. *In* Handbook of methods in aquatic microbial ecology. *Edited by* P.F. Kemp, B.F. Sherr, E.B. Sherr, and J.J. Cole. Lewis Publishers, Boca Raton, Fla. Chap. 23. pp. 187–197.

Malone, T.C. 1971. The relative importance of nannoplankton and netplankton as primary producers in tropical oceanic and neritic phytoplankton communities. Limnol. Oceanogr. **16**: 633–639.

Mazumder, A., McQueen, D.J., Taylor, W.D., Lean, D.R.S., and Dickman, M.D. 1990. Micro- and mesozooplankton grazing on natural pico- and nanoplankton in contrasting plankton communities produced by planktivore manipulation and fertilization. Arch. Hydrobiol. **118**: 257–282.

McQueen, D.J., Post, J.R., and Mills, E.L. 1986. Trophic relationships in freshwater pelagic ecosystems. Can. J. Fish. Aquat. Sci. **43**: 1571–1581.

Munawar, M., and Munawar, I.F. 1975. The abundance and significance of phytoflagellates and nannoplankton in the St. Lawrence Great Lakes. Verh. Int. Ver. Limnol. **19**: 705–723.

Munawar, M., Munawar, I.F., Culp, L.R., and Dupuis, G. 1978. Relative importance of nannoplankton in Lake Superior phytoplankton biomass and community metabolism. J. Great Lakes Res. **4**: 462–480.

Petersen, R. 1991. Carbon-14 uptake by picoplankton and total phytoplankton in eight New Zealand lakes. Int. Rev. Gesamten Hydrobiol. **76**: 631–641.

Pick, F.R. 1991. The abundance and composition of freshwater picocyanobacteria in relation to light penetration. Limnol. Oceanogr. **36**: 1457–1462.

Pick, F.R., and Agbeti, M. 1991. The seasonal dynamics and composition of photosynthetic picoplankton communities in temperate lakes in Ontario, Canada. Int. Rev. Gesamten Hydrobiol. **76**: 565–580.

Pick, F.R. and Caron, D.A. 1987. Picoplankton and nanoplankton biomass in Lake Ontario: relative contribution of phototrophic and heterotrophic communities. Can. J. Fish. Aquat. Sci. **44**: 2164–2172.

Platt, T., and Li, W.K.W. (*Editors*). 1986. Photosynthetic picoplankton. Can. Bull. Fish. Aquat. Sci. **214**.

Porter, K.G., and Feig, Y.S. 1980. The use of DAPI for identifying and counting aquatic microflora. Limnol. Oceanogr. **25**: 943–948.

Potvin, C., Lechowicz, M.J., and Tardif, S. 1990. The statistical analysis of ecophysiological response curves obtained from experiments involving repeated measures. Ecology, **71**: 1389–1400.

Rai, H. 1982. Primary production of various size fractions of natural phytoplankton communities in a North German lake. Arch. Hydrobiol. **95**: 395–412.

Riemann, B., and Sondergaard, M. 1986. Carbon dynamics in eutrophic temperate lakes. Elsevier Science Publishers, Amsterdam, The Netherlands.

Ross, P.E., and Duthie, H.C. 1981. Ultraphytoplankton biomass, productivity and efficiency in Lake Matamec, a Precambrian Shield lake. J. Phycol. **17**: 181–186.

Sager, P.E., Rubio, B., and Kirk, J. 1988. The importance of nannoplankton along the trophic gradient in Green Bay, Lake Michigan. Verh. Int. Ver. Limnol. **23**: 376–379.

SAS Institute Inc. 1989*a*. SAS/STAT user's guide, version 6. 4th ed. Vol. 2. SAS Institute Inc., Cary, N.C.

SAS Institute Inc. 1989*b*. SAS/IML software: usage and reference, version 6. 1st ed. SAS Institute Inc., Cary, N.C.

SAS Institute Inc. 1990. SAS procedures guide, version 6. 3rd ed. SAS Institute Inc., Cary, N.C.

© 1996 NRC Canada

Sherr, B.F., Sherr, E.B., and Hopkinson. C.S. 1988. Trophic interactions within pelagic microbial communities: indications of feedback regulation of carbon flow. Hydrobiologia, **159**: 19–26.

Sherr, E., and Sherr, B.F. 1988. Role of microbes in pelagic food webs: a revised concept. Limnol. Oceanogr. **33**: 1225–1227.

Sherr, E., and Sherr, B.F. 1992. Trophic roles of pelagic protists: phagotrophic flagellates as herbivores. Arch. Hydrobiol. Beih. Ergebn. Limnol. **37**: 165–172.

Sherr, E.B., Caron, D., and Sherr, B.F. 1993. Staining of heterotrophic protists for visualization via epifluorescence microscopy. *In* Handbook of methods in aquatic microbial ecology. *Edited by* P.F. Kemp, B.F. Sherr, E.B. Sherr, and J.J. Cole. Lewis Publishers, Boca Raton, Fla. Chap. 26. pp. 213–227.

Sieburth, J.McN., Smetacek, V., and Lenz, J. 1978. Pelagic ecosystem structure: heterotrophic compartments of the plankton and their relationship to plankton size fractions. Limnol. Oceanogr. **23**: 1256–1263.

Sokal, R.R., and Rohlf, F.J. 1995. Biometry. Principles and practice of statistics in biological research. 3rd ed. Freeman, New York.

Sondergaard, M. 1991. Autotrophic picoplankton in temperate lakes: seasonal abundances and importance along a trophic gradient. Int. Rev. Gesamten Hydrobiol. **76**: 505–522.

Stockner, J.G. 1987. Lake fertilization: the enrichment cycle and lake sockeye salmon (*Oncorhynchus nerka*) production. Can. Spec. Publ. Fish. Aquat. Sci. **96**: 198–215.

Stockner, J.G. 1988. Phototrophic picoplankton: an overview from marine and freshwater ecosystems. Limnol. Oceanogr. **33**: 765–775.

Stockner, J.G. 1991. Autotrophic picoplankton in freshwater ecosystems: the view from the summit. Int. Rev. Gesamten Hydrobiol. **76**: 483–492.

Stockner, J.G., and Antia, N.J. 1986. Algal picoplankton from marine and freshwater ecosystems: a multidisciplinary perspective. Can. J. Fish. Aquat. Sci. **43**: 2472–2503.

Stockner, J.G., and Porter, K.G. 1988. Microbial food web in freshwater planktonic ecosystems. *In* Complex interaction in lake communities. *Edited by* S.R. Carpenter. Springer-Verlag, New York. pp. 71–84.

Stockner, J.G., and Shortreed, K.S. 1988. Response of *Anabaena* and *Synechococcus* to manipulation of nitrogen: phosphorus ratios in a lake fertilization experiment. Limnol. Oceanogr. **33**: 1348–1361.

Stockner, J.G., and Shortreed, K.S. 1989. Algal picoplankton production and contribution to food-webs in oligotrophic Bristish Columbia lakes. Hydrobiologia, **173**: 151–166.

Stockner, J.G., and Shortreed, K.S. 1991. Autotrophic picoplankton: community composition, abundance and distribution across a gradient of oligotrophic British Columbia and Yukon Territory lakes. Int. Rev. Gesamten Hydrobiol. **76**: 581–601.

Strickland, J.D.H., and Parsons, T.R. 1972. A practical handbook of seawater analysis. Bull. Fish. Res. Board Can. **67**.

Suttle, C.A., and Harrison, P.J. 1988. Ammonium and phosphate uptake rates, N:P supply ratios, and evidence for N and P limitation in some oligotrophic lakes. Limnol. Oceanogr. **33**: 186–202.

Teixeira, C., and Gaeta, S.A. 1991. Contribution of picoplankton to primary production in estuarine, coastal and equatorial shallow lakes. Hydrobiologia, **209**: 117–122.

Voros, L., Gulyas P., and Nemeth, J. 1991. Occurrence, dynamics and production of picoplankton in Hungarian shallow lakes. Int. Rev. Gesamten Hydrobiol. **76**: 617–629.

Watson, S., and Kalff, J. 1981. Relationships between nanoplankton and lake trophic status. Can. J. Fish. Aquat. Sci. **38**: 960–967.

Wehr, J.D. 1989. Experimental tests of nutrient limitation in freshwater picoplankton. Appl. Environ. Microbiol. **55**: 1605–1611.

Wehr, J.D. 1990. Predominance of picoplankton and nanoplankton in eutrophic Calder Lake. Hydrobiologia, **203**: 35–44.

Wehr, J.D. 1991. Nutrient and grazer-mediated effects on picoplankton and size structure in phytoplankton communities. Int. Rev. Gesamten Hydrobiol. **76**: 643–656.

Wehr, J.D. 1993. Effects of experimental manipulations of light and phosphorus supply on competition among picoplankton and nanoplankton in an oligotrophic lake. Can. J. Fish. Aquat. Sci. **50**: 936–945.

Weisse, T., and Schweizer, A. 1991. Seasonal and interannual variation of autotrophic picoplankton in a large prealpine lake (Lake Constance). Verh. Int. Ver. Limnol. **24**: 821–825.

© 1996 NRC Canada

What is a successful fish? Determinants of competitive success in Arctic char (*Salvelinus alpinus*) in different social contexts

Colin E. Adams and Felicity A. Huntingford

Abstract: In tests between pairs of 0+ Arctic char (*Salvelinus alpinus*) there was a clear relationship between aggressiveness and ability to monopolise a localised and limited food resource. However, indices of competitive ability in pairwise tests in observation arenas where food was highly limited did not predict performance (growth, age of maturation, or reproductive investment) when the same fish were housed under routine husbandry conditions (i.e., at high densities and fed to excess). This is in direct contrast with the results of similar studies conducted on Atlantic salmon (*Salmo salar*), where social suppression of food acquisition occurs despite high food availability. It is suggested that different behavioural traits promote success in different competitive environments and that these do not co-vary at the individual level in char.

Résumé : Lors de tests entre paires d'ombles chevaliers (*Salvelinus alpinus*) d'âge 0+, il est apparu une nette relation entre l'agressivité et la capacité de s'approprier une source limitée de nourriture. Cependant, les indices de la capacité compétitive déterminée lors d'essais par paires dans des enclos d'observation où la quantité de nourriture était très limitée, n'ont pas permis de prédire le rendement (croissance, âge de maturation ou acquisition d'énergie alimentaire en vue de la reproduction) lorsque les mêmes sujets étaient placés en enclos dans des conditions ordinaires d'élevage (c.-à-d. en densité élevée et nourris à satiété). Ces résultats sont opposés à ceux obtenus lors d'études sur le saumon atlantique (*Salmo salar*) où la suppression sociale de la recherche de nourriture s'exerce même quand celle-ci est abondante. On suggère que des traits comportementaux différents favorisent le succès dans des environnements compétitifs différents et qu'ils ne sont pas covariants au niveau des sujets individuels de l'omble chevalier.
[Traduit par la Rédaction]

Introduction

There is now a substantial body of evidence from a range of animal groups, including fish (e.g., Li and Brocksen 1977; Metcalfe 1986; Abbott and Dill 1989; Grant 1990), that the ability of individuals to compete effectively with conspecifics for resources can have a profound effect on rates of growth and on the timing of life-history events (Huntingford & Turner 1987). In Atlantic salmon (*Salmo salar*), a series of experiments conducted over the last decade has elucidated the source of much individual variation in growth rates and in the timing of life-history events (Thorpe 1987; Metcalfe 1993). The timing of smolting (metamorphosis to the seaward migration phase of the life cycle) and age at first sexual maturation have been shown to be regulated by an individual's opportunity for growth (Thorpe 1987, 1989; Adams and Thorpe 1989; Rowe et al. 1991; Simpson 1992; Metcalfe 1993). Opportunity for growth is influenced by a number of abiotic factors such as water temperature and daylength (Thorpe et al. 1989; Metcalfe and Thorpe 1990) but is also strongly affected by an individual's ability to compete for food.

In a number of experiments designed to examine the role of individual competitive ability in determining the timing of life-history events in Atlantic salmon, small groups of fish (2–10) were tested in simple arenas supplied with a limited and highly localised food supply. These experiments have consistently shown that specific individuals are able to acquire favourable feeding sites (close to the food inlet), thereby monopolising the limited food resources (Huntingford et al. 1988, 1990; Metcalfe et al. 1989, 1990). The exact mechanism through which certain individuals are able to outcompete companions in such highly simplified environments is imperfectly understood. Individuals within a cohort that grow poorly and delay smolting (Thorpe 1987) are more readily intimidated by the presence of a competitor (a mirror image of itself) than are faster-growing siblings (Metcalfe 1991). Huntingford et al. (1993) showed that Atlantic salmon parr classified as dominant in small groups initiated more feeding attempts in a later feeding test than did a subordinate companion and that these attempts were more likely to be successful.

In several of the experiments described above, individual

Received September 14, 1994. Accepted May 1, 1996.
J12575

C.E. Adams and F.A. Huntingford. Fish Behaviour and Ecology Group, Division of Environmental and Evolutionary Biology, Institute of Biomedical and Life Sciences, University of Glasgow, Glasgow G12 8QQ, U.K.

© 1996 NRC Canada

salmon that had been screened for competitive ability in pairs or in small groups in highly simplified arenas were subsequently transferred to larger, standard aquaculture holding units containing a large number of conspecifics and an abundant, well-distributed food source (Metcalfe 1989, 1991; Metcalfe et al. 1989, 1990). A consistent finding in such cases is that individuals that were competitively superior in the simplified and low-density environment of the observation arenas also performed better (in terms of faster growth and earlier smolting) in high-density holding tanks. In Atlantic salmon, therefore, the ability to compete at low densities for access to a highly localised food source translates into good performance at high densities and with a more dispersed food supply.

The Arctic char (*Salvelinus alpinus*) is another salmonid species that is commonly housed under aquaculture conditions. Numerous studies have demonstrated great individual variation in growth rates within populations of tank-reared char provided with abundant, well-distributed food sources (see Jobling et al. 1994 for a review). As with Atlantic salmon there is also evidence of social suppression of feeding, despite abundant food. Jobling and Reinsnes (1986) found that char identified as poor growers in groups showed improved growth when housed in isolation. In high-density groups, fish with many bite marks on their fins consumed less food and grew less well than fish without bite marks, particularly at low current speeds when levels of aggression were high (Christiansen and Jobling 1990). These results are consistent with the suggestion that food acquisition and hence growth is being suppressed in unaggressive fish reared in tanks, but as yet there has been no direct behavioural test of this proposal.

In the experiments reported here, we tested the hypothesis that, in Arctic char as in Atlantic salmon, the ability to compete for food at low densities translates into good performance under aquaculture conditions. This was done by relating overt aggression and access to food in fish competing in pairs for a highly localised food supply to their rates of growth, age of maturation and an index of reproductive investment when subsequently housed under standard aquaculture conditions.

Methods

Provenance and husbandry of char

The char used in this study were laboratory-reared offspring of wild-caught resident Arctic char of the pelagic morph from Loch Rannoch, Perthshire, Scotland (Walker et al. 1988). Ova were hatched in standard incubating troughs at the University Field Station, Rowardennan, Loch Lomondside, Scotland. At first feeding they were fed a mixture of homogenised liver and a commercially prepared diet. Following first feeding, fry were transferred to standard fry tanks (1 m in diameter) where they were fed an appropriate size of pelleted food, delivered automatically and to excess.

Pairwise competition trials

About 7 mo after first feeding (October 1991), pairs of fish of similar size (mean ± weight differential = 0.5 g ± 0.05) covering the full range of current sizes (1.2–15.3 g) were weighed and marked with a single alcian blue tattoo mark on the dorsal surface either anterior or posterior to the dorsal fin to allow identification during behavioural observations. Each pair was then placed in a small cylindrical tank (30 cm in diameter; 15 L) with a constant flow of water and left to acclimatise for 48 h, during which they remained unfed. They were then observed for three periods of 5 min (separated by approximately 3 h) during which four favoured food items (bloodworm) were introduced at approximately 90-s intervals. Each aggressive interaction (including chase, attack, nip, and charge, following Noakes 1980 and Adams et al. 1995) was recorded and the originator of the aggression noted. Two measures of individual competitive ability were taken for each fish, namely aggression rate (thetotal number of aggressive acts of all categories delivered) and food acquisition rate (the total number of worms eaten). The degree of polarisation of performance was measured by the difference in the number of attacks delivered and in the number of food items obtained. Seventy pairs of fish were tested in this way.

Following each trial the fish were given permanent individual identification codes using a series of alcian blue tattoo marks on the ventral surface (Kelly 1967; Metcalfe et al. 1989, 1990). After completion of the behavioural trials, the tested fish were housed together in a standard 1-m holding tank, where they were fed to excess on a commercial pelleted diet from an automatic feeder that scattered food across the surface of the tank.

Performance indicators

The fish were screened at intervals up to December 1992, when they were killed by means of an overdose of anaesthesia and three aspects of performance were monitored.

(1) Specific growth rate (SGR)

Growth was calculated as

$$\ln \text{final weight} - \ln \text{initial weight/time elapsed (days)}$$

for the 167-d period between the termination of behavioural trials and the end of July 1992 (when maturing fish would be starting to lose condition).

(2) Investment in gonadal tissue

This was determined immediately prior to spawning in December 1992, approximately 20 mo after first feeding. Fish were killed and their gonads removed by dissection to enable calculation of an individual gonadosomatic index (GSI), where

$$\text{GSI} = \text{wet gonad weight/total wet somatic weight.}$$

(3) Maturation status

Most of the fish fell into two distinct groups with respect to GSI. Those that showed no externally visible signs of maturity (particularly the development of breeding colouration) had GSIs of less than 0.1% for males and 0.8% for females. In contrast, fish with external signs of maturity had GSIs in excess of 4.8% for males and 4.6% for females. Three females had GSIs in the range 1.1–1.4%, but had considerably enlarged ovaries compared with immature fish and were thus classified as maturing.

Statistical analysis

Making use of the matched experimental design, behaviour in the observation arena and performance in the holding tank were examined by paired *t*-tests with respect to aggression rate, food acquisition, and initial size, for pairs in which both fish were alive at the end of the experiment and for which behaviour in the pairwise tests was significantly polarised. All proportional data were arcsin transformed prior to significance testing.

Results

Aggression, relative size, and immediate access to food in pairwise tests

Aggression was relatively frequent in the pairwise tests, occurring with a median rate of four aggressive acts (range

© 1996 NRC Canada

0–52) per 15 min. Fish varied in their tendency to initiate attacks, and in 27 (39%) of the trials there was a significant difference in aggression rate between individuals greater than that expected by chance (binomial test, $P < 0.05$). Over all trials there was no correlation between the frequency with which attacks were initiated and the frequency with which they were received ($R = -0.03$, $N = 70$, NS), suggesting that individual aggressors did not suffer from an elevated rate of retaliatory attacks. There was no evidence that aggression during trials was dependent on gender; in two of the seven cases in which there were significantly more aggressive acts initiated by one individual and in which the competition was between a male and a female fish (determined retrospectively by dissection), the female was the more aggressive individual (binomial test, $N = 7$, $P = 0.227$).

Food acquisition was also non-uniform, with one member of the pair acquiring more pellets than would be expected if acquisition was random in 41 cases (binomial test $P = 0.02$ for 10 food items). Once again, gender was not an influential factor, females acquiring more food in 7 of the 15 trials in which food intake was significantly different from random and in which the pair consisted of a male and a female (binomial test, $N = 15$, $P = 0.50$).

There was a strong association between individual aggression rate and food acquisition. On average, the more aggressive fish of a pair acquired significantly more food (mean number of pellets acquired = 8.71 versus 3.26 pellets, $N = 62$, $T = 6.18$, $P < 0.001$). Size did not significantly influence either level of aggression (mean weight = 6.31 g in both the more and the less aggressive fish, $N = 62$, $T = 0.01$, NS) or the amount of food acquired (mean body weight = 5.98 and 5.87 g in fish getting more and less food, respectively, $N = 64$, $T = 1.21$, NS). These relationships were confirmed by a significant positive correlation across all fish between absolute levels of aggression and food acquisition ($R = 0.36$, $N = 140$, $P < 0.001$) and by the absence of a significant correlation between weight and either aggression ($R = 0.08$, $N = 140$, NS) or food intake ($R = 0.07$, $N = 140$, NS).

Subsequent performance in aquaculture conditions

Specific growth rates over the period from December 1991 to July 1992 were variable, with a mean of 1.05% per day (±0.02 SE; range = 0–1.45% per day). Table 1 shows a complete absence of significant differences in daily specific growth rate between fish based on their relative aggressiveness, relative food intake, or relative size in the pairwise tests. There was no correlation between the absolute size of fish at the time of pairwise testing and subsequent growth rates ($R = -0.047$, $N = 140$, NS). Equally, there was no relationship between differences in growth rates in matched pairs and the degree of polarisation of either aggression ($R = -0.083$, $N = 16$, NS) or food intake ($R = 0.097$, $N = 28$, NS) in the pairwise tests.

Maturation rates (Table 2) were high for both males (91%, $N = 57$) and females (89%, $N = 52$) and did not differ significantly between the sexes ($\chi^2 = 0.28$, 1 df, NS). There was no relationship between status in the pairwise tests and the proportion of fish of either sex that matured. GSIs of maturing fish (Table 3) ranged from 4.8 to 11.4% for males and from 1.1 to 10.3% for females, but this too was unrelated to relative aggression, relative food intake, or relative size in the pairwise tests.

Table 1. Mean daily specific growth rates (SGR) in holding tanks for pairs of fish that differed significantly in the pairwise tests, with respect to aggression, food acquisition, and relative size, where the larger fish was heavier by at least 10%.

High aggression	Low aggression	*N*	*T*	*P*
0.84	0.72	16	1.44	0.17
High food	**Low food**	***N***	***T***	***P***
0.82	0.73	28	1.40	0.17
Larger	**Smaller**	***N***	***T***	***P***
0.78	0.75	28	0.3	0.77

Discussion

Although overt aggression directed from one conspecific towards another occurred at an average rate of 3.5 acts per minute, individuals varied considerably in this respect. In the conditions of low food availability prevailing in the observation arenas in these tests, the most aggressive fish in each pair tended to get more food and the absolute level of combativeness influenced the degree to which food was monopolised. This accords with data from previous work on Arctic char which suggest that these fish can aggressively monopolise access to a limiting food supply (Adams et al. 1995). It also agrees with studies of other salmonid species in which competitively superior individuals gain preferential access to food (Metcalfe et al. 1989, 1990). The lack of effect of size on performance in the pairwise tests also agrees with studies of Atlantic salmon (Huntingford et al. 1990).

In spite of the clear association between aggression and access to food in the pairwise tests, we found absolutely no evidence that the ability to monopolise food under these conditions translated into higher than average performance when the fish were housed at high density and given a less restricted food supply (in terms of both quantity and spatial distribution). This result is in direct contrast with those from Atlantic salmon parr, where fish that compete well for food in small groups with a limited, localised food supply subsequently grow well when fed to excess at high density in standard aquaculture production units (Metcalfe 1989; Metcalfe et al. 1989, 1990). Our finding that competitive ability in pairs does not predict performance at high density and food availability in Arctic char is surprising given the strong circumstantial evidence of social suppression of food acquisition presented by Jobling and his collaborators who have shown improved growth of individuals that exhibit poor growth in groups, when housed in isolation (Jobling and Reinsnes 1986; Christiansen and Jobling 1990; Jobling et al. 1994).

There are at least two possible hypotheses that could explain why competitive ability in the pairwise tests did not predict performance at high densities in the present experi-

© 1996 NRC Canada

Table 2. Probability of maturation (%) for male and female fish in relation to status in pairwise tests, with respect to aggression, food acquisition, and relative size.

	High aggression	Low aggression	df	χ^2	*P*
Males	100	50	1	1.04	0.48
Females	80	56	1	0.40	0.70
	High food	Low food	df	χ^2	*P*
Males	94	80	1	0.18	0.80
Females	79	93	1	0.27	0.90
	Larger	Smaller	df	χ^2	*P*
Males	94	73	1	0.01	0.90
Females	100	75	1	0.77	0.50

Table 3. Mean gonadosomatic index (GSI) in male and female fish in relation to status in the pairwise tests, with respect to aggression, food intake, and relative size.

	High aggression	Low aggression	*N*	*T*	*P*
Males	6.01	4.37	12	0.87	0.48
Females	7.42	6.41	13	1.40	0.21
	High food	Low food	df	*T*	*P*
Males	6.29	6.64	28	1.10	0.28
Females	7.59	6.75	30	1.31	0.20
	Larger	Smaller	*N*	*T*	*P*
Males	6.64	7.32	28	1.20	0.25
Females	7.15	7.56	27	0.75	0.46

ments. Firstly, it may arise from a sampling problem, given that only two fish were used in the initial tests. Relative food acquisition may be a function of relative aggression status, so that in a larger group and competing with individuals with a wide range of ability, actual performance may diverge from that expected from the result of exposure to a single competitor. This seems unlikely, given the fact that pairwise aggression tests do predict performance in aquaculture conditions in Atlantic salmon (Metcalfe et al. 1989). In any event, if this hypothesis were true, then one would expect pairs with a wide difference in competitive ability in the observation arena to show a wider difference in performance, which was not the case.

An alternative hypothesis is that different behavioural traits may promote success in different competitive environments, and that these traits do not co-vary at the individual level. It is known than many species of fish, including salmonids, adjust their methods of resource acquisition to their relative costs and benefits. For example, in brook trout (*Salvelinus fontinalis*) (McNicol and Noakes 1981) and Arctic char (Christiansen and Jobling 1990; Adams et al. 1995), aggressive rates are low when current speed is high, with the consequence that the cost of fighting outweigh the benefits. Similarly, in zebra fish when food is evenly dispersed in space and time, and therefore costly to defend, territoriality breaks down and individuals scramble for food (Grant 1993). In the natural environment of these species, different feeding habitats offer different competitive environments in which, for the economic reasons outlined above, different resource acquisition strategies may be successful. We therefore suggest that in Arctic char, in the conditions prevailing in our pairwise tests (a restricted, highly predictable, and defendable food supply and a single opponent), the resource acquisition strategy that promotes effective competition (aggressive monopolisation of food) is different from that required to gain a high rate of food intake in the holding tanks, where food arrives in relatively large, reasonably dispersed clumps and where there are numerous competitors. In these conditions, other traits, such as the ability to predict the arrival of food and to hold station in a favourable site, might be more important. If we assume that individuals have different, but relatively persistent behavioural profiles (this is the case for a number of fish species, including threespine stickleback (*Gasterosteus aculeatus*) (Huntingford 1976)), then this could explain the fact that the pairwise tests did not predict subsequent performance in the holding tanks. Resolution of this issue requires direct behavioural observation of char at high densities.

It then becomes necessary to explain why competitive ability carried out at low food availability does predict subsequent performance in juvenile salmon (Metcalfe et al. 1990). One possibility is that, for salmon, the economics of resource defence are sufficiently similar at high and low food availability to favour the ability to monopolise food aggressively in both circumstances. A factor that may push the economics of aggressive resource defence "into the black" for salmon is the fact that individuals that perform well during a critical period during their first summer are known to smolt at least 12 mo before those that perform poorly during this period (Metcalfe et al. 1986, 1988; Thorpe 1987). A marginal increase in growth performance can therefore result in considerably enhanced fitness and so might be worth the extra cost involved.

An understanding of the nature of competitive interactions between conspecifics held at high densities, particularly interactions involving aggression, is of crucial importance in the husbandry and welfare of fish in aquaculture systems. Environments that encourage the expression of overt aggression have been shown to result in elevated rates of wounding in steelhead trout (*Oncorhynchus mykiss*, Abbott and Dill 1985) and in Arctic char (Christiansen et al. 1991) and may lead to an increased incidence of other pathological conditions (Turnbull 1992).

Acknowledgements

Thanks to Ron Greer and Andy Walker for help in obtaining and rearing experimental char. This study was funded by the U.K. Natural and Environmental Research Council under grant No. GR3/7607.

© 1996 NRC Canada

References

Abbott, J.C., and Dill, L.M. 1985. Patterns of aggressive attacks in juvenile steelhead trout (*Salmo gairdneri*). Can. J. Fish. Aquat. Sci. **42**: 1702–1706

Abbott, J.C., and Dill, L.M. 1989. The relative growth of dominant and subordinate juvenile steelhead trout (*Salmo gardneri*) fed equal rations. Behaviour **108**: 104—113.

Adams, C.E., and Thorpe, J.E. 1989. Photoperiod and temperature effects on early development and reproductive investment in Atlantic salmon (*Salmo salar* L.). Aquaculture, **79**: 403–409.

Adams, C.E., Huntingford, F.A., Krpal, J., Jobling, M., and Burnett, S.J. 1995. Exercise, agonistic behaviour and food acquisition in Arctic char *Salvelinus alpinus*. Environ. Biol. Fishes, **43**: 213–218.

Christiansen, J.S., and Jobling, M. 1990. The behaviour and relationship between food intake and growth in juvenile Arctic char *Salvelinus alpinus* subjected to sustained exercise. Can. J. Zool. **68**: 2185–2191.

Christiansen, J.S., Jorgensen, E.H., and Jobling, M. 1991. Oxygen consumption in relation to sustained exercise and social stress in Arctic char *Salvelinus alpinus*. J. Exp. Zool. **260**: 149–156.

Grant, J.W.A. 1993. Whether on not to defend? The influence of resource distribution. *In* Behavioural ecology of fishes. *Edited by* F.A. Huntingford and P. Torricelli. Harwood Academic Publishers, Chur, Switzerland. pp. 137–155.

Huntingford, F.A. 1976. The relationship between anti-predator behaviour and aggression among conspecifics in the three-spined stickleback, *Gasterosteus aculeatus*. Anim. Behav. **24**: 245–260.

Huntingford, F.A., and Turner, A.K. 1987. Animal conflict. Chapman and Hall, London.

Huntingford, F.A., Metcalfe, N.B., and Thorpe, J.E. 1988. Feeding motivation and response to predation risk in Atlantic salmon parr adopting different life-history strategies. J. Fish Biol. **32**: 77–84.

Huntingford, F.A., Metcalfe, N.B., Thorpe, J.E., Graham, W.D., and Adams, C.E. 1990. Social dominance and body size in Atlantic salmon parr, *Salmo salar* L. J. Fish Biol. **36**: 877–881.

Huntingford, F.A., Metcalfe, N.B., and Thorpe, J.E. 1993. Social status and feeding in Atlantic salmon *Salmo salar* parr: the effect of visual exposure to a dominant. Ethology, **94**: 201–206.

Jobling, M., and Reinsnes, T.G. 1986. physiological and social constraints on growth in Arctic char, *Salvelinus alpinus* L.: an investigation of factors leading to stunting. J. Fish Biol. **28**: 379–384.

Jobling, M., Jorgensen, E.H., Arnesen, A.M., and Ringo, E. 1994. Feeding growth and environmental requirements of Arctic char: a review of aquaculture potential. Aquacult. Int. **1**: 20–46.

Kelly, W.H. 1969. Marking freshwater and marine fish by injected dyes. Trans. Am. Fish. Soc. **96**: 163–175.

Li, H.W., and Brocksen, R.W. 1977. Approaches to the analysis of energetic costs of intraspecific competition for space by rainbow trout (*Salmo gairdneri*). J. Fish Biol. **11**: 329–341.

McNicol, R.E., and Noakes, D.L.G. 1981. Territories and territorial defence in juvenile brook char, *Salvelinus fontinalis* (Pisces: Salmonidae). Can. J. Zool. **59**: 22–28.

Metcalfe, N.B. 1986. Intraspecific variation in competitive ability and food intake in salmonids: consequences for energy budgets and growth rates. J. Fish Biol. **28**: 525–531.

Metcalfe, N.B. 1989. Differential response to a competitor by Atlantic salmon adopting alternative life-history strategies. Proc. R. Soc. Lond. Ser. B Biol. Sci. **236**: 21–27.

Metcalfe, N.B. 1991. Competitive ability influences seaward migration age in Atlantic salmon. Can. J. Zool. **69**: 815–817.

Metcalfe, N.B. 1993. Behavioural causes and consequences of life history variation in fish. Mar. Behav. Physiol. **23**: 205–217.

Metcalfe, N.B., and Thorpe, J.E. 1990. Determinants of geographical variation in age of seaward migrating Atlantic salmon. J. anim. Ecol. **59**: 135–145.

Metcalfe, N.B., Huntingford, F.A., and Thorpe, J.E. 1986. Seasonal changes in feeding motivation of juvenile Atlantic salmon (*Salmo salar*). Can. J. Zool. **64**: 2439–2446.

Metcalfe, N.B., Huntingford, F.A., and Thorpe, J.E. 1988. Feeding intensity, growth rates and the establishment of life-history patterns in juvenile Atlantic salmon. J. Anim. Ecol. **57**: 463–474.

Metcalfe, N.B., Huntingford, F.A., Graham, W.D., and Thorpe, J.E. 1989. Early social status and the development of life-history strategies in Atlantic salmon. Proc. R. Soc. Lond. Ser. B Biol. Sci. **236**: 7–19.

Metcalfe, N.B., Huntingford, F.A., Thorpe, J.E., and Adams, C.E. 1990. The effects of social status on life-history variation in juvenile salmon. Can. J. Zool. **68**: 2630–2636.

Noakes, D.G.L. 1980. Social behaviour of young chars. *In* chars: salmonid fish of the genus *Salvelinus*. *Edited by* E.K. Balon. Dr. W. Junk Publishers, The Hague, The Netherlands. pp. 683–701.

Rowe, D.K., Thorpe, J.E, and Shanks, A.M. 1991. The role of fat stores in the maturation of male Atlantic salmon (*Salmo salar*) parr. Can. J. Fish. Aquat. Sci. **48**: 405–413.

Simpson, A.L. 1992. Differences in body size and lipid reserves between maturing and non- maturing Atlantic salmon parr, *Salmo salar* L. Can. J. Zool. 70: 1737–1742.

Thorpe, J.E. 1987. Environmental regulation of growth patterns in juvenile Atlantic salmon. p. *Edited by* Summerfelt and G.E. Hall. Iowa State University Press, Ames, Iowa. pp. 463–474.

Thorpe, J.E. 1989. Developmental variation in salmonid populations. J. Fish Biol. **35**: 295–303.

Thorpe, J.E., Adams, C.E., Miles, M.S., and Keay, D.S. 1989. Some influences of photoperiod and temperature an opportunity for growth in juvenile Atlantic salmon *Salmo salar* L. Aquaculture, **82**: 119–126.

Turnbull, J.F. 1992. Studies on dorsal fin rot in farmed Atlantic salmon, *Salmo salar*, parr. Ph.D. thesis, University of Stirling, U.K.

Walker, A.F., Greer, R.B., and Gardner, A.S. Two ecologically distinct forms of Arctic char *Salvelinus alpinus* (L.) in Loch Rannoch, Scotland. Biol. Conserv. **43**: 43–61.

© 1996 NRC Canada

Distributions of oxygen, carbon, and respiratory activity in the deep layer of the Gulf of St. Lawrence and their implications for the carbon cycle[1]

C. Savenkoff, A.F. Vézina, T.T. Packard, N. Silverberg, J.-C. Therriault, W. Chen, C. Bérubé, A. Mucci, B. Klein, F. Mesplé, J.-E. Tremblay, L. Legendre, J. Wesson, and R.G. Ingram

Abstract: The Gulf of St. Lawrence (GSL) is a semi-enclosed sea with an estuarine circulation forced by runoff from the St. Lawrence and Great Lakes drainage systems and balanced by a deep inflow of oceanic waters through the Laurentian Channel. Based on samples collected between July 1992 and June 1994 during Phase I of the CJGOFS program conducted in the Gulf of St. Lawrence, we present new data on the carbon and nutrient chemistry as well as respiratory activity in the deep waters. Organic carbon fluxes estimated from sediment trap data, deepwater respiratory activity, and benthic respiration measurements are consistent with those obtained from the changes in the dissolved oxygen concentration of the deep waters along the Laurentian Channel. These flux estimates suggest that approximately 10% of the local primary production reaches the deep layer (>200 m) and the sediments in the GSL. The vertical carbon budget is almost balanced in the eastern part of the gulf, but approximately half of the carbon produced in the surface layer of the northwestern gulf cannot be accounted for. The difference in hydrodynamic and biological conditions prevailing in both areas may explain our observations.

Résumé : Le golfe du Saint-Laurent (GSL) est une mer semi-fermée avec une circulation estuarienne forcée par l'écoulement issu des systèmes de drainage des grands lacs et du Saint-Laurent, et balancée par une entrée profonde d'eau océanique via le chenal Laurentien. A partir des échantillons récoltés entre juillet 1992 et juin 1994, pendant la Phase I du programme CJGOFS effectué dans le golfe Saint-Laurent, nous présentons de nouvelles données sur la chimie du carbone et des sels nutritifs ainsi que sur l'activité respiratoire dans les eaux profondes. Nous avons pu démontrer que les flux de carbone organique évalués à partir des données de pièges à sédiment, des mesures de l'activité respiratoire dans les eaux profondes et de la respiration benthique sont compatibles avec ceux obtenus à partir des changements dans la concentration en oxygène dissous des eaux profondes le long du chenal laurentien. Ces estimations suggèrent qu'environ 10% de la production primaire locale atteint les eaux profondes (>200 m) et les sédiments du GSL. Le bilan vertical de carbone est presque équilibré dans la partie est du golfe, mais approximativement la moitié du carbone produit dans la couche de surface du nord-ouest du golfe n'est pas prise en compte par notre modèle. Des différences entre les conditions hydrodynamiques et biologiques qui caractérisent les deux régions pourraient expliquer nos observations.

Introduction

Ocean biogenic cycles play a key role in controlling atmospheric CO_2 levels. The formation of organic carbon through photosynthesis (primary production) reduces the partial pressure of CO_2 in the surface waters and establishes a concentration gradient across the air—sea interface that in turn induces a positive flux of CO_2 from the atmosphere to the surface waters. A fraction of the newly produced biogenic material sinks or is actively transported out of the surface waters into deeper waters where it can be remineralized to CO_2 or sequestered in the sediments. This combination of processes

Received November 1, 1995. Accepted May 1, 1996.
J13146

C. Savenkoff, A.F. Vézina, T.T. Packard, N. Silverberg, and J.-C. Therriault. Department of Fisheries and Oceans, Maurice Lamontagne Institute, P.O. Box 1000, Mont-Joli, QC G5H 3Z4, Canada.
W. Chen. Department of Oceanography, Dalhousie University, Halifax, NS B3H 4J1, Canada.
C. Bérubé. Centre Océanographique de Rimouski, Université du Québec à Rimouski, Rimouski, QC G5L 3A1, Canada.
A. Mucci. Department of Earth and Planetary Sciences, McGill University, Montréal, QC H3A 2K6, Canada.
B. Klein, F. Mesplé, J.-E. Tremblay, and L. Legendre. GIROQ, Université Laval, Québec, QC G1K 7P4, Canada.
J. Wesson and R.G. Ingram. Department of Atmospheric and Ocean Sciences, McGill University, Montréal, QC H3A 2K6, Canada.

[1] This paper is a contribution to the research programs of the Maurice Lamontagne Institute (Ocean Productivity Division, Department of Fisheries and Oceans, Canada) and of GIROQ (Groupe Interuniversitaire de Recherches Océanographiques du Québec).

© 1996 NRC Canada

is referred to as the "biological pump" (Longhurst and Harrison 1989). The efficiency of this pump depends on the rate of carbon loss from the surface waters by the downward transport of organic matter, both in particulate and in dissolved forms. Determining the rates and pathways by which carbon fixed by photosynthesis is stored, metabolized, and exported or sequestered is an essential first step towards predicting its behaviour under scenarios of changing atmospheric CO_2 concentrations.

The margins of the world's oceans are characterized by high and variable phytoplankton production relative to the open sea (Platt and Subba Rao 1975) and could account for up to one third of the global marine production (Mantoura et al. 1991). However, the fate of carbon in ocean margins, its export to the deep sea or local oxidation and burial, remains a contentious issue (Falkowski et al. 1988; Walsh 1991). Because much of the recent research on the carbon cycle was concentrated on the open ocean, relatively little is known about carbon cycling in margin areas.

The Gulf of St. Lawrence (GSL) is a semi-enclosed sea with an estuarine circulation forced by runoff from the St. Lawrence and Great Lakes drainage systems. It represents a good example of a productive margin area. At Cabot Strait, the main outflow of relatively fresh surface waters is balanced by a deep inflow of oceanic waters from the North Atlantic. This return flow follows the Laurentian Channel, which is a deep trough (250–500 m) that terminates 900 km inland at the confluence of the St. Lawrence Estuary and the Saguenay Fjord. Along the way, nutrients and oxygen concentrations, respectively, increase and decrease gradually, due to the decomposition of organic matter that locally sinks into the deep layer (Coote and Yeats 1979). In this relatively simple system, the study of nutrient variations along an upstream–downstream gradient can help to elucidate remineralization processes. Furthermore, with some knowledge of the velocity of the deepwater inflow, first-order carbon remineralization rates can be estimated.

In this paper, we present new data on the carbon and nutrient chemistry as well as respiratory activity in the deep waters of the GSL. These data from a deep continental margin environment were acquired over a 2-yr period during Phase I of the Canadian Joint Global Ocean Flux Study (CJGOFS) program. In particular, we compare carbon oxidation rates at depth obtained from the measurements of respiratory activity with those derived from the longitudinal gradients in chemical profiles. We also compare these oxidation rates with the rate of primary production in the overlying waters and of vertical particle fluxes at depth, assuming that they are the dominant source of organic matter to the deep layer. In addition, recent measurements of dissolved organic carbon (DOC) concentrations are used to infer the role of the DOC pool in the remineralization and sequestration of organic carbon in the GSL. Finally, after scaling the carbon fluxes in the deep waters and sediments (remineralization, accumulation, burial) to rates of local primary production, we present a first-order budget of carbon fluxes in the GSL.

Materials and methods

Study area

The GSL is connected to the Atlantic Ocean via Cabot Strait and the Strait of Belle Isle (Fig. 1). Cabot Strait is an order of magnitude wider and deeper than the Strait of Belle Isle and is the only significant passage for the penetration of deep North Atlantic waters into the gulf (Koutitonsky and Bugden 1991). The bathymetry of the GSL is dominated by the Laurentian Channel, a glacially overdeepened trough system (Fig. 1), that starts at the Atlantic Ocean margin and enters the gulf through Cabot Strait before branching into the St. Lawrence Estuary to the northwest and the Esquiman Channel to the northeast. A branch of the Esquiman Channel, the Anticosti Channel, separates Anticosti Island from the north shore of the gulf. At its eastern end, the Anticosti Channel is about 110 km wide with a maximum depth of about 250 m. The bathymetry then converges towards the west to a narrow 30-km passage where depths exceed 100 m only in the midchannel area (Koutitonsky and Bugden 1991). Similar changes in width and depth of the Laurentian Channel occur at the confluence of the St. Lawrence Estuary and Saguenay Fjord. In both areas, these topographic features and tidal currents induce persistent upwellings that bring colder intermediate waters to the surface (Therriault and Lacroix 1976; Greisman and Ingram 1977; Pingree and Griffiths 1980; Koutitonsky et al. 1987).

The waters of the Laurentian Channel may be divided vertically into three layers (Bugden 1981): (1) a surface layer, which displays large seasonal variations in temperature and salinity in response to vernal changes in surface heat flux and freshwater discharge, (2) an intermediate cold layer extending from about 50 to 150 m depth (centered at approximately 80 m) with lesser seasonal variations, and (3) a deep, warmer continuous water mass occupying the greater depths of the lower St. Lawrence Estuary and the GSL, which undergoes only longer term changes. In winter, the surface and intermediate layers merge into one uniform layer over most of the gulf (Forrester 1964; Bugden 1981).

Bugden (1991) showed that conditions prevailing in the deeper waters of the GSL result from a slow and relatively steady inward advection of water from outside the gulf in addition to weak vertical diffusion. These deeper waters in the Laurentian Channel are a mixture of Labrador Current (Forrester 1964; Dickie and Trites 1983) and North Atlantic waters (Bugden 1991) in proportions that vary over time scales of several years. The mean advection velocity in the deeper Laurentian Channel is on the order of 0.5 $cm \cdot s^{-1}$ and appears to be relatively constant (Bugden 1991).

Field sampling

This study is based on data collected at three stations in the Laurentian Channel (Fig. 1) during nine cruises (not all stations were visited during each cruise). Sampling occurred between July 1992 and June 1994 in all months except January, February, and March (Tables 1 and 2). Station 1 is located in the Anticosti Gyre, about 100 km east of the boundary between the St. Lawrence Estuary and the GSL, and is characterized by high primary production (Steven 1975, see review of de Lafontaine et al. 1991; this study: 1057 mg $C \cdot m^{-2} \cdot d^{-1}$). Station 2 is located in the Anticosti Channel and Station 3 is in the Laurentian Channel west of Cabot Strait. These stations are in regions of low primary production (Steven 1975, see review of de Lafontaine et al. 1991; this study: 522 and 227 mg $C \cdot m^{-2} \cdot d^{-1}$ for station 2 and station 3, respectively).

During the first four cruises, a Secchi disk was used to estimate the light attenuation coefficient and the optical depths. During the subsequent five cruises, underwater irradiance was measured at stations sampled during the daytime with a photosynthetically active radiation (PAR) quantum meter (QSP 200PD, Biospherical Instruments). Samples from six optical depths (100, 50, 25, 15, 10, and 1% of the surface irradiance) and up to 11 depths below the photic zone (defined as extending to the depth where 1% of the surface incident radiation remains) were collected at sunrise using 8-L Niskin bottles mounted on a CTD-rosette. The depths sampled in the aphotic layer were usually as follows: 50, 75, 100, and 150 m (intermediate water) and 200, 250, and, station depth permitting, 300, 350, 400, 450, and 500 m (deep water). An additional sample was collected at 10–20 m

© 1996 NRC Canada

Fig. 1. Map of the GSL showing the three station locations during the CJGOFS cruises.

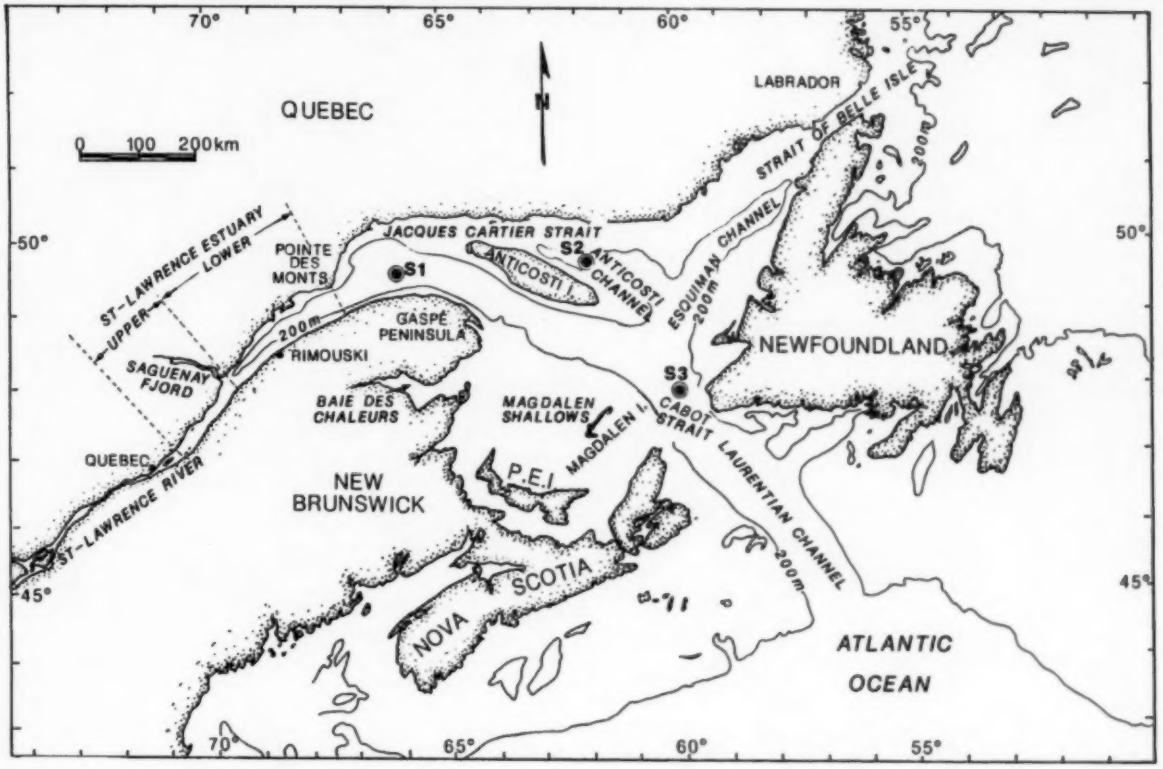

Table 1. Stations sampled during the cruises carried out during the CJGOFS program in the GSL.

Cruise No.	Date	Stations sampled	Vessel
1	23–31 July 1992	1, 3	*Fogo Isle*
2	31 August – 12 September 1992	1, 2, 3	*Fogo Isle*
3	25 September – 6 October 1992	1, 2, 3	*Fogo Isle*
4	6–17 December 1992	1, 2, 3	CSS *Hudson*
5	24 May – 4 June 1993	1	*Fogo Isle*
6	8–19 July 1993	1	*Fogo Isle*
7	22 November – 4 December 1993	1	CSS *Parizeau*
8	10–22 April 1994	1, 2	*Sir Wilfrid Laurier*
9	13–24 June 1994	1, 2, 3	CSS *Hudson*

above the bottom. Samples for the determination of dissolved oxygen, DOC, and dissolved inorganic carbon (DIC) were drawn directly from the Niskin bottles. Samples for the measurements of phytoplankton biomass, primary production, inorganic nutrient concentration, CHN content of suspended particulate matter, and microorganism respiratory activity were prefiltered through a Nitex screen (200-μm mesh size).

Physical and chemical variables

At each station, vertical profiles of irradiance, temperature, salinity, density, and turbidity were determined at 2-h intervals down to 5–10 m above the bottom with a SeaBird® model SBE25 CTD instrument.

The dissolved oxygen concentration was determined by the Winkler method as described by Aminot and Chaussepied (1983) using the automated titration system developed by Jones et al. (1992). Nitrate (NO_3) concentration was determined on fresh samples using a Technicon autoanalyser II (Parsons et al. 1984). Water samples for phosphate (PO_4) and silicate (SiO_4) concentrations were frozen for later onshore analysis.

Primary production

Primary production was determined using the ^{14}C method described in Parsons et al. (1984). Subsamples from the six euphotic depths were incubated with 370 kBq of $NaH^{14}CO_3$ for 24 h, starting at sunrise, in two deck incubators. Water temperatures were maintained at those of the upper and lower parts of the euphotic zone, and irradi-

© 1996 NRC Canada

Table 2. Characteristics of the sampling stations in the GSL.

Station				Depth	Distance from
No.	Name	Latitude	Longitude	(m)	Cabot Strait (km)
1	Anticosti Gyre	49°40.00′N	66°00.00′W	360	570
2	Anticosti Channel	49°40.00′N	62°00.00′W	275	410
3	Cabot Strait	47°40.30′N	60°00.00′W	525	0

ances at the six sampling depths were simulated using combinations of blue and neutral-density filters. At the end of the incubation, samples were filtered through 25-mm Whatman GF/F glass fiber filters. After the addition of 0.05 N HCl to the filters and subsequent evaporation, 10 mL of Ready-Safe scintillation cocktail was added. The activity, corrected for quenching and background radiation, was determined after the cruise using a LKB Minibeta scintillation counter.

Respiratory electron transport system (ETS) activity in the water column

For respiration measurements, we used the ETS method, an enzymatic approach that determines the capacity of the respiratory chain to transfer electrons from the physiological substrates (NADH, NADPH, succinate) to oxygen (Packard 1971, 1985). The sample volumes were 4 and 11.5 L for the euphotic and aphotic layers, respectively. Samples for the ETS activity measurements were vacuum filtered (30 kPa or 0.3 atm) through 47-mm Whatman GF/F glass fiber filters. The filters were then stored in liquid nitrogen to preserve the enzyme activity (Ahmed et al. 1976). The assay procedure in the shore laboratory was performed following the methods described in Packard and Williams (1981) and Packard et al. (1983), respectively, for the euphotic and aphotic samples. The ETS activity was corrected from the incubation temperature (18°C) to in situ temperature using an Arrhenius activation energy of 15.8 kcal·mol^{-1} found by Packard et al. (1975). However, recent work in polar areas (temperature < 3°C) showed lower activation energy values of 11.5 and 12.0 kcal·mol^{-1} for the microplankton of the Barents Sea (Martinez 1991) and the Weddell Sea (Martinez and Estrada 1992), respectively. We used the mean (11.8 kcal·mol^{-1}) of these two values for the samples collected in the layer with an in situ temperature below 3°C (the intermediate waters in our study).

To convert ETS activity to respiration in the surface layer, we used the following regression equation from Aristegui and Montero (1995):

$$\log_{10} \text{respiration} = 0.357 + 0.750 \log_{10} \text{ETS activity}$$

where respiration and ETS activity are expressed in milligrams of O_2 per cubic metre per day. This equation was obtained from a large data set (n = 197) on respiration and ETS activity from plankton communities (<225 μm) of different surface oceanic areas: the east and central North Atlantic, the Baltic Sea, the Gulf of California, and the Antarctic Ocean (Aristegui and Montero 1995). To facilitate comparison with primary production, we used a respiratory quotient of 1 to convert moles of O_2 uptake to moles of CO_2 produced in the euphotic layer (Packard 1979). Multiplying by 12 converts these units to milligrams of carbon per cubic metre per day. Primary production and ETS activity values were integrated over the euphotic zone using the trapezoidal method.

In the aphotic zone, the ETS activity was converted into respiration rates (R) following the procedure described by Packard et al. (1988; R/ETS activity = 0.09). We then used a $\Delta O/\Delta C$ molar ratio of 138/106 (Redfield et al. 1963) to convert respiration values to metabolic CO_2 production.

Respiration in benthic samples

Sediment cores (10-cm internal diameter) were collected in December 1993 and June 1994 with a Bowers and Connelly multicorer (Barnett et al. 1984). Only cores showing an undisturbed sediment–water interface were used for chemical analyses. One core was immediately used to measure the distribution of dissolved oxygen in the pore water with a Diamond General 737 polarographic microelectrode at the in situ temperature. The flux of oxygen into the sediments was calculated from the concentration gradient assuming transport by molecular diffusion.

Three other cores were used for direct O_2-uptake flux measurements. Immediately upon recovery, the cores with the overlying water were placed in a water bath set to the in situ temperature. Plexiglas lids equipped with an O-ring, a magnetic stirring bar whose height above the sediment surface could be adjusted, and two Teflon valves for sampling were put in place while making sure that no air was present under the lid. The incubator could hold six cores placed around a central stirring motor and was equipped with a horseshoe magnet that drove the magnetic stirring bar in each core tube at 30 rpm. At regular intervals, a 50-mL water sample was drawn into a gas-tight glass syringe for oxygen analysis by the Winkler method. When a sample was collected, it was immediately replaced by an equal volume of bottom water of known oxygen concentration. This procedure ensured that during the incubation, contaminating air was not introduced, that the volume of water remained constant, and that the oxygen concentration did not diminish significantly. Hall et al. (1989) have demonstrated the importance of maintaining the oxygen supply to obtain consistent and relevant data. Hulth et al. (1994) described a procedure by which the oxygen concentrations in the sample water and the replacement water are used to calculate benthic respiration.

CHN of suspended particulate matter

Samples for CHN determination of suspended particulate matter content were collected on precombusted 25-mm Whatman GF/F filters, stored frozen, and analysed ashore with a Perkin-Elmer elemental analyser (model 2400 CHN).

DOC in water column samples

A 45-mL seawater sample was filtered through a 47-mm Whatman GF/F glass fiber filter; a 100-μL aliquot was then used for DOC analysis using the modified high-temperature catalytic oxidation method described by Chen and Wangersky (1993*a*, 1993*b*). DOC was only measured during the last two cruises (April and June 1994).

DIC in water column samples

Water column samples were drawn directly from the Niskin bottles into rinsed 125-mL polyethylene bottles and allowed to overflow. A few crystals of mercuric chloride ($HgCl_2$) were added to the bottles before they were capped leaving no headspace gas. Samples were kept at ~4°C until analysis.

A weighed amount of water (~10 g) was taken from each of the bottles with a syringe, to avoid gas exchange with the atmosphere, and injected directly into the gas stripper of a CO_2 coulometer. The

© 1996 NRC Canada

Fig. 2. Vertical distribution of salinity and temperature at station 1 for cruises 2–9, at station 2 for cruises 2, 3, 4, 8, and 9, and at station 3 for cruises 1–4 and 9. The line shows the average values for each parameter below 50 m.

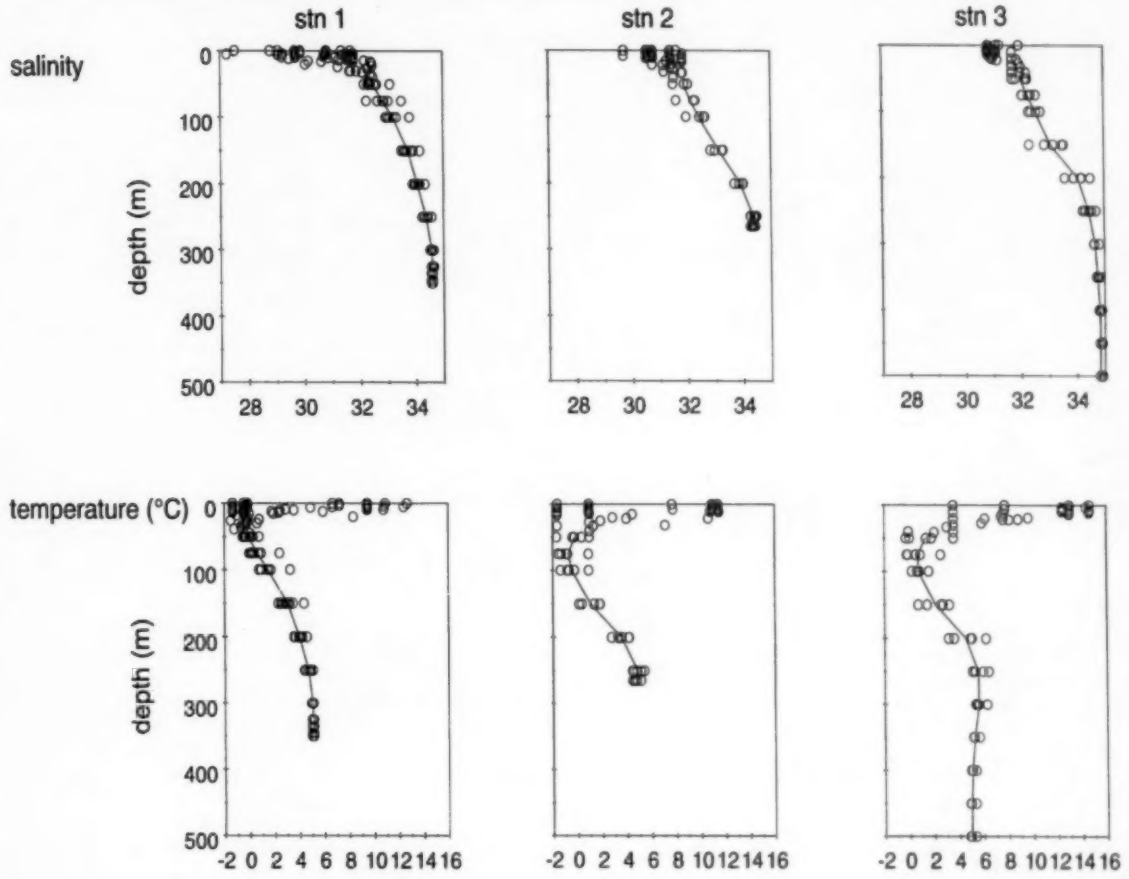

total DIC concentration, ΣCO_2, of the sample was determined following acidification with 2 mL of 2 N HCl and coulometric titration of the evolved CO_2. Total alkalinity, A_t, was determined by potentiometric titration with a standardized dilute HCl solution. The precision of the ΣCO_2 and A_t analyses is 0.2 and 0.4%, respectively.

The carbonate system speciation and pH were calculated from the analytical data (i.e., ΣCO_2 and A_t) using boric acid and carbonic acid stoichiometric dissociation constants based on the total hydrogen ion concentration scale, pH_T (Hansson 1973; Millero 1979) at in situ salinities, temperatures, and pressures (Millero 1983). The borate ion contribution to the total alkalinity was estimated from the total boron concentration at the measured salinity (Culkin 1965). The partial pressure of CO_2 (Pco_2) in equilibrium with the solution was calculated using the carbon dioxide solubility constants of Weiss (1974) at 1 atm total pressure. ΣCO_2 was measured and Pco_2 estimated for samples collected only during the last two cruises (April and June 1994).

Results

Vertical distribution of physical and chemical variables

At all stations, between-cruise variations in salinity and temperature decreased with depth with very little change detected below 200 m (Fig. 2). This is reflected in the temperature–salinity diagram, which contains all the data collected below 50 m (Fig. 3). The changes were mainly observed in the intermediate waters (left of the 200-m isobath, Fig. 3) and correspond to the presence of a temperature minimum that varied in shape and intensity among the three stations. The characteristics of the deep waters (right of the 200-m isobath, Fig. 3) were similar for stations 1 and 2, while we measured slightly higher temperatures for the same salinity range at station 3.

The concentrations of SiO_4, PO_4, and NO_3 increased with depth and with distance from Cabot Strait (Fig. 4), i.e., nutrient levels at station 3 (Cabot Strait) were lower than at station 1 (Anticosti Gyre). Nutrient concentrations at station 2 (Anticosti Channel) were intermediate (Fig. 4), but the distance from Cabot Strait to the Anticosti Channel is considerably less than that from Cabot Strait to the Anticosti Gyre (Fig. 1; Table 2). At station 1, SiO_4 concentrations increased with depth whereas NO_3 and PO_4 remained virtually constant in the deeper waters. Such striking differences in the vertical distribution of nutrients were not observed at the other sta-

© 1996 NRC Canada

Fig. 3. Temperature–salinity diagram of stations 1 (black circles), 2 (black triangles), and 3 (white circles). The lines show the mean distributions at the three stations. The 200-m isobath represents the transition between the intermediate and deep waters. The constant density surfaces ($kg \cdot m^{-3}$) are also shown.

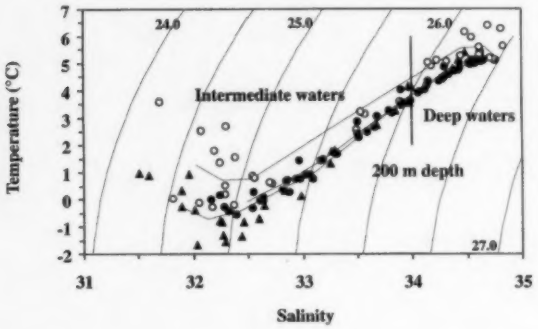

tions. SiO_4 profiles showed more variations at all stations, and the largest variations for all nutrients were observed at station 1 (Fig. 4). The distribution of dissolved oxygen concentrations showed a pattern inverse to that of the nutrients (Fig. 4).

Changes in chemical characteristics in the deep waters

The changes in the chemical characteristics in the intermediate and deep waters (Tables 3 and 4) were calculated by averaging the values for each depth across the cruises to generate a mean profile (solid lines on Figs. 2, 4, and 5). The mean profiles were then integrated over the intermediate layer (50–200 m) or the deep layer (200–350 m at station 1 and 200–265 m at station 2), and the uncertainties at each depth were propagated using standard formulas (Colquhoun 1971). Depth intervals characterized by a single measurement were not used in our calculations. Each integrated value was then divided by the thickness of the corresponding layer.

As previously mentioned, PO_4, NO_3, and SiO_4 concentrations increased from Cabot Strait to the Anticosti Gyre and from Cabot Strait to Anticosti Channel in the intermediate and deep layers (Tables 3 and 4). The same pattern was observed for particulate organic carbon (POC), particulate oganic nitrogen (PON), and DOC (Table 3 and 4). The opposite trend was found for oxygen concentrations (Tables 3 and 4), with a marked decrease in the deep layer from Cabot Strait (station 3; 172 μM) toward the west (station 1; 85 μM) and north (station 2; 126 μM) (Table 4). Furthermore, the mean respiratory ETS activity of the microorganisms is statistically invariant throughout the channel (Table 4; Fig. 5).

We assume that little or no water from other sources was incorporated into the deep inflowing layer of the Laurentian Channel, as supported by the constancy of the salinity and density with increasing distance at any particular depth (Fig. 3). We calculated the changes in chemical characteristics between stations 3 and 1 (transect 3-1) and between stations 3 and 2 (transect 3-2) for a deep layer of fixed thickness (200–350 m for transect 3-1, and because of the limited depth at station 2, the comparison was made for the 200–265 m depth range for transect 3-2). The net changes in the concentrations of PO_4, NO_3, SiO_4, and oxygen in the deep layer correspond to $\Delta O/\Delta Si/\Delta N/\Delta P$ ratios of 280/36/7/1 and 298/32/17/1, respectively, from Cabot Strait to the Anticosti Gyre and between Cabot Strait and the Anticosti Channel.

Bugden (1991) showed that both temporal and along-channel temperature changes appear to be compensated by salinity changes so that the density at 250 m depth is essentially constant. In our study, water at 200, 265, and 350 m had densities of 27.0 ± 0.1, 27.2 ± 0.1, and 27.4 ± 0.1 $kg \cdot m^{-3}$, respectively. The standard deviation represented the cruise-to-cruise variability rather than a difference in density from Cabot Strait and Anticosti Gyre or Channel. Moreover, Yeats (1988) has shown that oxygen and nutrient concentrations vary linearly with distance along the Laurentian Trough. These different results led us to develop a first-order carbon budget assuming a rectangular channel, no significant diffusion across the 200-decibar level, and uniform transport with depth or salinity (slab transport model) in the GSL.

Carbon fluxes in the GSL

We calculated the areal CO_2 production ($Q_{CO_2}^{3-i}$) below the 200-decibar level between Cabot Strait and the Anticosti Channel (transect 3-2) and between Cabot Strait and the Anticosti Gyre (transect 3-1) as

$$\bar{Q}_{CO_2}^{3-i} = \frac{v}{L} \cdot \left[\int_{z=200}^{z=z_{max}} \bar{O}_2^i \, dz - \int_{z=200}^{z=z_{max}} \bar{O}_2^3 \, dz \right] \cdot \frac{106}{138} \cdot 12$$

where v is the mean horizontal velocity in the deep waters along the Laurentian Channel (0.5 $cm \cdot s^{-1}$; Bugden 1991), L is the length of the channel (4.1×10^5 m for transect 3-2 and 5.7×10^5 m for transect 3-1), $\bar{O}_2^i$ is the mean O_2 profile at station 1 or 2, $\bar{O}_2^3$ is the mean O_2 profile at station 3, z_{max} is the maximum depth of integration (265 m for transect 3-2 and 350 m for transect 3-1), and O_2 consumption is converted to CO_2 production using Redfield stoichiometric ratios ($\Delta O_2/\Delta C$ = 138/106; Redfield et al. 1963). This calculation yields values of CO_2 production that are twice as high along transect 3-1 than along transect 3-2 (Table 5); however, this discrepency is due to the difference in the thickness of the deep layers along the two transects (Table 5): in volumetric terms, the oxidation rates in the water column are the same.

We observed higher concentration of POC at depth at stations 1 and 2 than at station 3 (Table 4). Using the gradient in POC concentrations observed along the two transects, we calculated a POC accumulation rate in the deep water equivalent to 2 and 7% of the carbon oxidation rate along transect 3-2 and transect 3-1, respectively (Table 5).

We obtained an estimate of the mean annual primary production over both transects by averaging the measurements of primary production made at the end-member points of those transects and integrating each mean value over an annual cycle (Table 5). We assumed that primary production was zero when the GSL is covered with ice, i.e., in January, February, and March. These primary production values reflect the interannual and the seasonal variations for each transect. The high primary production estimated along transect 3-1 (Table 5) is similar to values reported by Steven (1975) in the northwestern GSL and in the Gaspé Current (table 1 of de Lafontaine et al. 1991, p. 105). Our calculation assumes a gradual linear change of mean annual primary production

© 1996 NRC Canada

Fig. 4. Vertical distribution of SiO_4, PO_4, NO_3, and dissolved oxygen concentrations at station 1 for cruises 2–9, at station 2 for cruises 2, 3, 4, 8, and 9, and at station 3 for cruises 1–4 and 9. The line shows the average values for each parameter below 50 m.

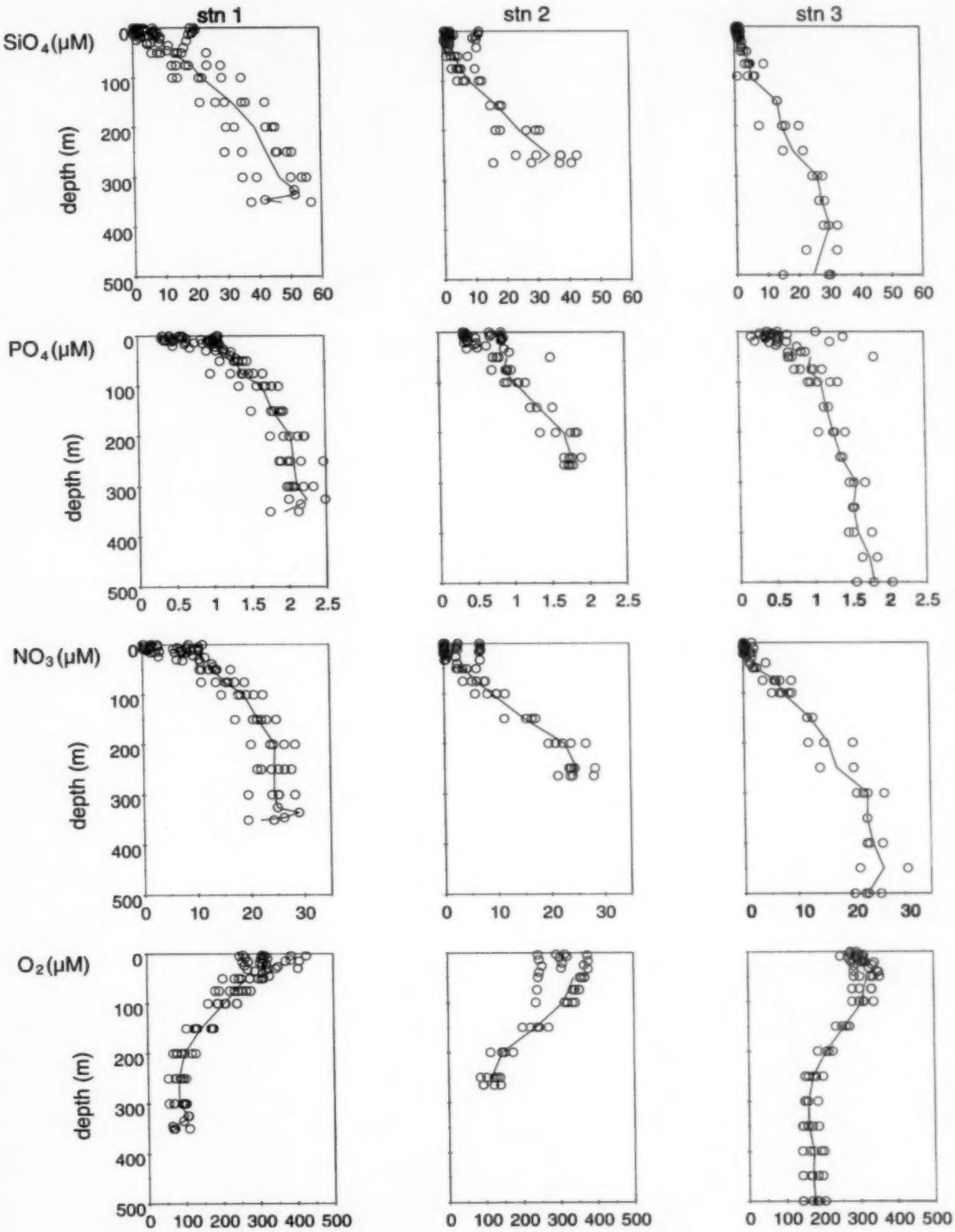

© 1996 NRC Canada

Fig. 5. Vertical distribution of total DIC concentration (ΣCO_2), respiratory ETS activity, POC, and PON at station 1 for cruises 2–9, at station 2 for cruises 2, 3, 4, 8, and 9, and at station 3 for cruises 1–4 and 9. The line shows the average values for each parameter below 50 m.

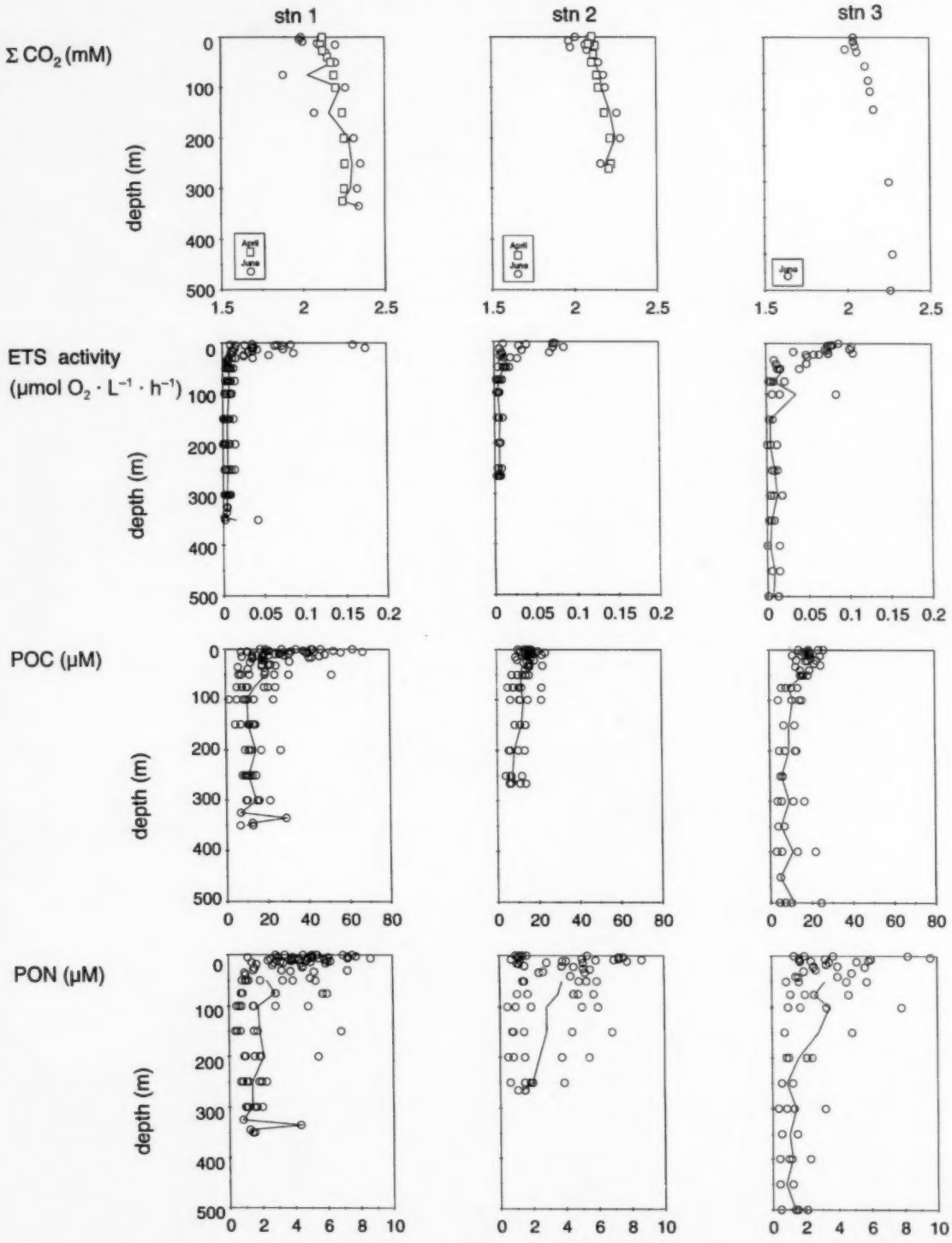

© 1996 NRC Canada

Table 3. Characteristics of the intermediate water layers.

	Anticosti Gyre station 1	Anticosti Channel station 2	Cabot Strait station 3
Layer (m)	50–200	50–200	50–200
Salinity	33.4±0.1	32.8±0.1	32.9±0.1
Temperature (°C)	2.2±0.2	0.7±0.3	1.9±0.4
PO_4 concentration (μM)	1.7±0.1	1.2±0.1	1.1±0.1
NO_3 concentration (μM)	19.7±1.0	12.4±0.9	9.9±0.8
SiO_4 concentration (μM)	26.7±2.8	13.2±1.4	9.3±1.0
Oxygen concentration (μM)	177±11	262±13	276±7
ΣCO_2 concentration (mM)	2.18±0.04	2.20±0.02	2.18
ETS activity (μmol $O_2 \cdot L^{-1} \cdot d^{-1}$)	0.16±0.04	0.15±0.02	0.35±0.19
POC concentration (μM)	12.6±2.4	11.5±1.6	10.4±1.5
PON concentration (μM)	2.1±0.7	3.0±0.9	2.8±0.9
C/N ratio	6±2	4±1	4±1
DOC concentration (μM)	74.7±5.9	59.3±4.4	41.3

Note: All the data were calculated from mean profiles presented in Figs. 2, 4, and 5, which were integrated and then divided by the thickness of the associated water layer; SD is also indicated. The ΣCO_2 and DOC concentrations were based on measurements carried out during the last two CJGOFS cruises (April and June 1994) with the exception of station 3 (June 1994).

Table 4. Characteristics of the deepwater layers.

	Anticosti Gyre station 1	Cabot Strait station 3	Anticosti Channel station 2	Cabot Strait station 3
Layer (m)	200–350	200–350	200–265	200–265
Salinity	34.4±0.0	34.5±0.1	34.2±0.1	34.3±0.2
Temperature (°C)	4.8±0.1	5.3±0.3	4.3±0.3	5.2±0.5
PO_4 concentration (μM)	2.1±0.1	1.4±0.0	1.7±0.1	1.3±0.1
NO_3 concentration (μM)	24.1±1.2	20.1±1.4	23.9±1.4	17.0±2.4
SiO_4 concentration (μM)	44.0±3.9	21.9±1.5	30.0±4.2	17.3±2.8
Oxygen concentration (μM)	85±8	172±7	126±12	186±10
ΣCO_2 concentration (mM)	2.29±0.03	2.26	2.22±0.03	2.26
ETS activity (μmol $O_2 \cdot L^{-1} \cdot d^{-1}$)	0.17±0.10	0.21±0.05	0.13±0.03	0.18±0.06
POC concentration (μM)	12.5±1.7	7.4±1.6	7.9±1.9	7.1±1.7
PON concentration (μM)	1.5±0.3	1.2±0.4	2.1±0.9	1.2±0.4
C/N ratio	8±2	6±2	4±2	6±2
DOC concentration (μM)	70.6±3.2	33.1	47.5±10.7	33.8

Note: All the data were calculated from mean profiles presented in Figs. 2, 4, and 5, which were integrated and then divided by the thickness of the associated water layer; SD is also indicated. The ΣCO_2 and DOC concentrations were based on measurements carried out during the last two CJGOFS cruises (April and June 1994) with the exception of station 3 (June 1994).

along those transects. An annual composite of coastal zone colour scanner (CZCS) images collected in 1979, 1980, and 1981 indicates that this is a reasonable assumption (Fuentes-Yaco et al., Maurice Lamontagne Institute, unpublished data), since the mean annual chlorophyll fields show no significant variations along transect 3-2 and a gradual increase from east to west along transect 3-1.

The sum of carbon oxidation and POC accumulation values in the deep waters amounted to 10% of the primary production in the surface waters along both transects (Table 5). Along transect 3-2, the deepwater and benthic respiration rates added up to a flux similar to that obtained from CO_2 production estimated from oxygen gradients (Table 5). In contrast, the sum of the respiration rates along transect 3-1 was about 60% of the CO_2 production inferred from concentration gradients.

The particle flux at 150 m was measured repeatedly at station 1, and the average particle flux agreed with the deepwater and benthic respiration measurements (Table 5). The particle flux at 150 m was measured only once at station 2; that single measurement (78 mg $C \cdot m^{-2} \cdot d^{-1}$) falls within the range of values obtained for station 1. As a default, the average particle flux for station 1 was compared with the total deep respiration at station 2 and found again to agree with the

© 1996 NRC Canada

Table 5. Organic carbon fluxes measured and estimated during the different CJGOFS cruises (mean ± SE [SD/$\sqrt{n}$]; n in parentheses). Primary production and euphotic respiration were integrated from 0 m to 1% of the surface irradiance. Vertical particle flux was estimated with individual sediment trap measurements at 150 m depth. We also present deepwater and benthic respiration, CO_2 production derived from gradients in oxygen concentration, and POC accumulation from the values measured in the associated deep layer at Cabot Strait.

	Cabot Strait to Anticosti Gyre transect 3-1	Cabot Strait to Anticosti Channel transect 3-2
Carbon fluxes measured in the euphotic layer		
Euphotic zone depth (m)	26±2(13)	29±4(9)
Primary production (mg $C \cdot m^{-2} \cdot d^{-1}$)	835±472(11)	418±226(8)
Euphotic respiration (mg $C \cdot m^{-2} \cdot d^{-1}$)	348±46(13)	366±52(9)
Carbon fluxes measured in the deep layer		
Deep layer thickness (m)	150	65
Particle flux (mg $C \cdot m^{-2} \cdot d^{-1}$)	45±12(5)	
Deepwater respiration (mg $C \cdot m^{-2} \cdot d^{-1}$)	22±2(40)	8±1(24)
Benthic respiration (mg $C \cdot m^{-2} \cdot d^{-1}$)	33±3(24)	39±3(26)
Total respiration (mg $C \cdot m^{-2} \cdot d^{-1}$)	56±4	47±3
Carbon fluxes calculated from changes in chemical composition of the deep layer		
Travel time (yr)	3.5	2.5
CO_2 production (mg $C \cdot m^{-2} \cdot d^{-1}$)	94±7	39±6
POC accumulation (mg $C \cdot m^{-2} \cdot d^{-1}$)	7±2	1±1

deepwater and benthic respiration measurements (Table 5). In contrast with inferences from oxygen gradients, the direct measurements of particle flux (although few in number) and respiration imply that the proportion of the primary production that was remineralized in the deep waters along transect 3-1 is half that along transect 3-2 (Table 5).

In both areas, benthic respiration was the major contributor to O_2 consumption and CO_2 production (Table 5). Benthic respiration accounted for 59% of total deep respiration along transect 3-1 and 83% of the total along transect 3-2. Along transect 3-2, benthic respiration was exactly equivalent to CO_2 production estimated from the oxygen gradient. Carbon recycling at or near the sediment–water interface is thus the major component of deep respiration in these waters.

During the last two cruises (April and June 1994), we measured a net decrease of 0.04 mM in the concentrations of ΣCO_2 within the same deepwater layer from Cabot Strait to the Anticosti Channel and a net increase of 0.03 mM from Cabot Strait to the Anticosti Gyre (Table 4). This net increase corresponded to a $\Delta C/\Delta P$ ratio of 65/1 ($\Delta C/\Delta O_2$ = 65/140; Redfield ratio: 106/138). This CO_2 production observed along transect 3-1 was in agreement with the observed decrease in oxygen (≈60 μM) and corresponds to an estimated CO_2 production of close to 46 μM, approximately 2% of the total DIC concentration (≈2.3 mM). These observations are in agreement with the results obtained by Tan and Walton (1978).

Data obtained from the last two cruises (April and June 1994) indicate that along-channel increases in deepwater DOC parallel decreases in oxygen and increases in nutrients (Table 4). We estimated a DOC accumulation rate of 53 mg $C \cdot m^{-2} \cdot d^{-1}$ along transect 3-1 and 13 mg $C \cdot m^{-2} \cdot d^{-1}$ along transect 3-2. Since the apparent oxygen utilization (AOU) increases along transects 3-2 and 3-1, some refractory DOC fractions probably accumulate in the deep waters of the GSL, especially along the more productive transect 3-1. We also have evidence of DOC utilization on a smaller scale: a net decrease in the DOC concentration was measured from April to June in the deep layer (below 200 m) at stations 1 and 2 with a concomitant increase in the AOU (Fig. 6).

Discussion

Regeneration of nutrients in the GSL

The spatial distribution patterns of nutrients and oxygen from Cabot Strait to the Anticosti Gyre and from Cabot Strait to the Anticosti Channel are similar to those observed by Coote and Yeats (1979) for nutrients and by Dunbar et al. (1980) for oxygen, in accordance with the accepted model of deepwater circulation in the gulf (Bugden 1991). The $\Delta O/\Delta Si/\Delta N/\Delta P$ ratios (280/36/7/1 along transect 3-1 and 298/32/17/1 along transect 3-2) estimated from the net changes in the concentrations of PO_4, NO_3, SiO_4, and oxygen in the deep layer are very similar to those obtained previously in the GSL. Coote and Yeats (1979) calculated $\Delta O/\Delta Si/\Delta N/\Delta P$ ratios of 288/40/7/1 (average of their two ratios) for waters collected at 250 m depth between Cabot Strait and the estuary. More recently, Yeats (1988) revised these ratio estimates by including more data. He found $\Delta O/\Delta C/\Delta Si/\Delta N/\Delta P$ ratios of 267/108/30/4.6/1. In all cases, with the exception of the ratios including ΔN, the estimated ratios were close to the values of Redfield et al. (1963; $\Delta O/\Delta C/\Delta N/\Delta P$ ratios of 267/106/16/1), suggesting that the chemical changes were due to remineralization of organic matter produced in the surface layer.

© 1996 NRC Canada

Fig. 6. Vertical distribution of DOC (circles) and AOU (triangles) at stations 1 (left panel) and 2 (right panel) during the cruises in April (black symbols) and June 1994 (white symbols).

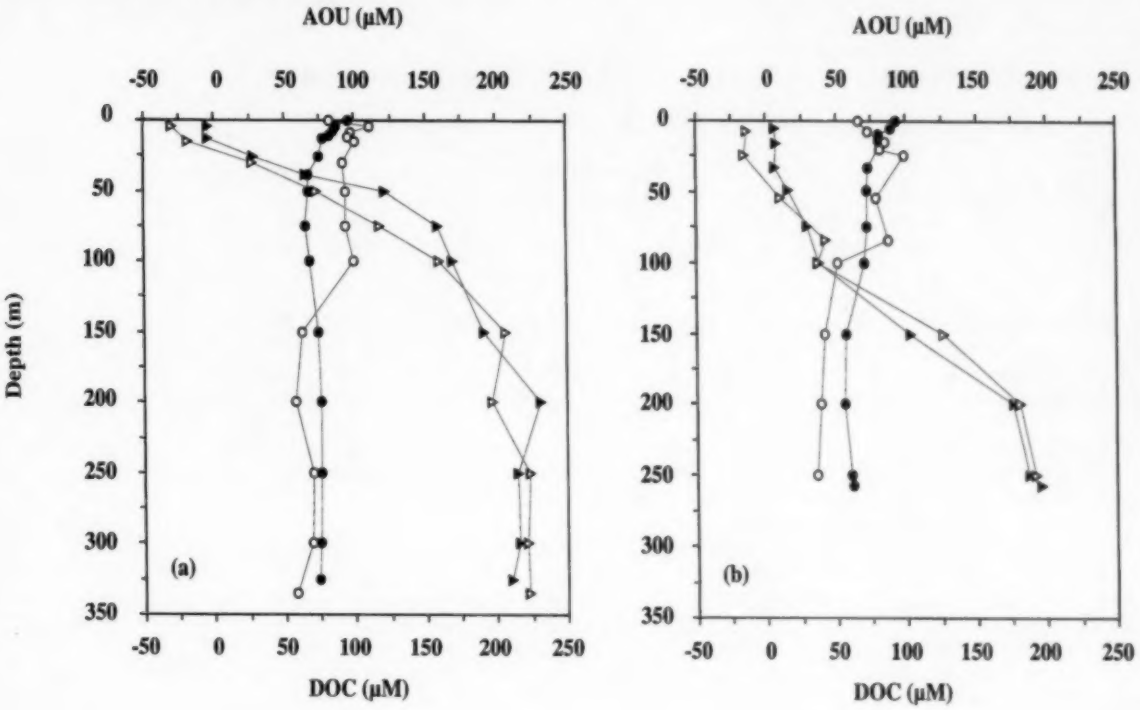

The consistency of oxygen and nutrient concentration gradients in the studies by Yeats (Coote and Yeats 1979; Yeats 1988; data collected from 1971 to 1975) and in the present study (data collected from 1992 to 1994) indicates that the average rates of regeneration processes in the deep waters between Cabot Strait and the estuary are stable over several decades. Our data indicate that this stability is also observed in the deep waters between Cabot Strait and the Anticosti Channel and is supported by a more complete seasonal and interannual data set (from April to December).

First-order carbon remineralization rates in the GSL

The fate of organic matter settling out of the euphotic zone into deeper waters is to be decomposed and eventually oxidized back to CO_2, ingested, partially remineralized, and incorporated into living organisms, or sequestered as refractory components in the sediments. The portion that is remineralized (and hence available for eventual return to the euphotic zone) is assumed to be equivalent to the fraction of the primary production called the new production, when averaged over appropriate time and space scales (Eppley and Peterson 1979; Eppley 1989). In this study, we estimated metabolic CO_2 production at depth from oxygen gradients along the Laurentian Channel and from measurements of respiration in the deep waters and sediments. These independent estimates indicate that about 10% of local primary production reaches and is remineralized in the deep waters (>200 m) and the sediments of the GSL. Our measurements agree with the vertical structure of remineralization that has been observed elsewhere, particularly in the open ocean. Empirical models relating vertical particle flux to depth indicate that between 7 and 20% of the primary production would be found at 200 m depth (Suess 1980; Betzer et al. 1984; Martin et al. 1987).

The agreement between the CO_2 production estimated directly from respiration measurements and indirectly from oxygen gradients for transect 3-2 is remarkably good and indicates that rate process measurements in the deep waters can be extrapolated to large space and time scales. The agreement is reasonable for transect 3-1. Differences in the deep-water velocity of the two branches of the Laurentian Channel would, however, affect our calculations. A better understanding of the circulation of the deep Laurentian waters is required to improve carbon budgets in the deep waters.

Based on measurements of respiratory activity, the remineralization in the surface layer is estimated to be 42 and 88% of the primary production along transect 3-1 and transect 3-2, respectively (Table 5). Adding the respiration estimated for the intermediate layer (from 0.1% optical depth to 200 m; 6 and 11% of the primary production) increases these values to 48 and 99% of the primary production. Finally, addition of the amount of carbon remineralized in the deep waters gives a closed carbon budget for transect 3-2 (110% of the primary production), but accounts for only 55% of the primary production along transect 3-1. These values compare favourably with the work of Lucotte et al. (1991), who estimated that 70% of photosynthetic carbon is recycled in the water column

© 1996 NRC Canada

of the lower St. Lawrence Estuary. Their results were based on the concentration and isotopic carbon composition of suspended particulate matter and surface sediments of the lower St. Lawrence Estuary. Similarly, Pocklington (1988) calculated that 76% of the organic matter within the gulf is remineralized to inorganic nutrients.

Hydrodynamic and biological characteristics prevailing in both areas

That we can nearly balance the vertical particle flux, the in situ measurements of respiration, and the O_2/CO_2 divergence along transect 3-2 but not transect 3-1 is in agreement with their contrasting physical and biological characters. Station 1 is located in a region of strong vertical shear, with a predominant gulfward flow of the fresher surface layer and landward flow of the intermediate and deep layers. The residual outflow veers around the Gaspé Peninsula towards the Magdalen Shallows. Much of the production in this region may be exported to the shelf, with minimal sedimentation in the deep waters of the Laurentian Channel. In contrast, station 2 is in the northern gulf regime, with a predominantly landward surface flow of marine waters. Shear with the deeper layers is probably smaller and the surface organic production is more likely to settle into the deep channel underneath.

Other chemical indicators also reflect the impact of the more estuarine character of transect 3-1. The distribution of nutrients is consistent with a gradual increase due to regeneration from organic matter mineralization as the deep water travels from Cabot Strait to the estuary. SiO_4 has been observed to exhibit stronger increases than other nutrients, with concentrations above 30 μM in the estuary (Coote and Yeats 1979; Levasseur and Therriault 1987; this study). This has been attributed to the ability of the estuarine circulation to trap SiO_4 more efficiently than PO_4 and NO_3. While PO_4 and NO_3 are rapidly flushed out of the estuary due to their longer residence time in the surface layer, where most of the regenerative processes are occurring (Savenkoff et al. 1995), the incorporation of SiO_4 into rapidly sinking particles (diatom theca and fecal pellets) allows a rapid transfer to bottom waters where the residual circulation is in the upstream direction (Ingram 1979).

The nutrient gradients in the deep waters of transect 3-1 could also be affected by hydrodynamic processes unique to the area surrounding station 1. Previous studies revealed the presence of a quasi-permanent geostrophic cyclonic eddy to the west of Anticosti Island, the Anticosti Gyre (see review by Koutitonsky and Bugden 1991). This feature links several dynamic processes, including the outflow from the St. Lawrence Estuary along the south shore, the transverse motion (most often southward) at the mouth of the estuary, and the enhanced coastal jet (Gaspé Current), with its associated instabilities sometimes moving offshore, as well as wind-induced coastal upwelling along the north shore, all of which exhibit considerable synoptic variability (Benoit and El-Sabh 1985; Koutitonsky and Bugden 1991). These hydrodynamic structures lead to a complex circulation of the water masses and influence the spatial distribution of nutrients. They could also explain the relatively large variations in nutrient distributions at station 1.

Another factor that could explain the unbalanced budget along transect 3-1 is the transfer of organic carbon from the primary producers to higher trophic levels, which is not accounted for in our model. The transfer of primary production to large grazers becomes more efficient as the production increases and is dominated by large cells such as diatoms (e.g., Ryther 1969; Malone 1971). The transfer is also enhanced when the physical structure that stimulates the high primary production is stable, giving time for the slow-growing copepods and other mesozooplankton to exploit the fast-growing phytoplankton (Le Fèvre and Frontier 1988; Thibault et al. 1994). Such a pattern accurately describes the environment at station 1: primary production is consistently higher in the western GSL than in the east (Steven 1975; de Lafontaine et al. 1991). This high primary production is largely associated with the Gaspé Current frontal zone, a quasi-permanent feature in the area (Levasseur et al. 1992). Furthermore, Plourde and Runge (1993) found that the spawning of *Calanus finmarchicus* was synchronized with the timing of the phytoplankton bloom in the lower St. Lawrence Estuary. Therefore, it is reasonable to believe that proportionately more of the primary production is transferred to higher trophic levels at station 1 and horizontally exported to the shelf than at station 2, leaving less for degradation in the deep waters.

Important role of benthic respiration

Our results also highlight features of carbon cycling common to both transects that should be given more attention in shelf systems. One is the predominant role of benthic organisms in oxygen consumption in the deep waters. This phenomenon has been reported in the deep North Pacific Ocean (Jahnke and Jackson 1987) but is even more important in the GSL due to the thinness of the deep layer (100–200 m) relative to the average sinking velocity of the large particles carrying the particulate carbon downwards. Most of the organic carbon entering the deep layer from above sinks rapidly to the underlying sediments, where it is consumed or sequestered, thus limiting the amount of degradation and remineralization of organic carbon in the water column. The highest benthic respiration rate was measured at the shallower station 2, where higher benthic fauna densities were observed and more intense bioturbation processes occur (Grehan et al. 1994).

DOC: a significant and dynamic component of the carbon cycle

Another feature common to both transects is the role of DOC in carbon cycling. Recent studies have shown inverse relations between DOC and AOU (Kepkay and Wells 1992; Amon and Benner 1994), suggesting that DOC is used in consuming oxygen and producing CO_2 (Williams and Druffel 1988; Toggweiler 1989). Our observations during the April and June cruises support this interpretation. Some of the water column respiration thus originates from DOC diffusing from its more concentrated sources in upper water column or sediment pore waters (Colombo et al. 1996*a*, 1996*b*) in addition to that derived from sedimenting organic particles. Furthermore, we observed an along-channel increase in DOC from Cabot Strait to both stations 1 and 2 that parallels the AOU change. Unfortunately, the DOC concentrations we report were based on measurements made only during the last two CJGOFS cruises (April and June 1994). Therefore, we cannot exclude the possibility of an interannual variation in

© 1996 NRC Canada

the DOC concentration at station 3; the same holds for ΣCO_2. Nevertheless, our results suggest that refractory forms of DOC accumulate in the deep waters of the GSL, particularly under the richer waters of transect 3-1 (DOC accumulation: 53 and 13 mg $C \cdot m^{-2} \cdot d^{-1}$, respectively, along transect 3-1 and 3-2). The accumulation of DOC along transects 3-1 reflects a carbon flux equivalent to 56% of CO_2 production and raises the proportion of the primary production consumed in the deep waters from 11 to 18%. Obviously, DOC is a significant and dynamic component of the carbon cycle in this system, although its precise role in sequestering carbon originating from the atmosphere remains to be elucidated.

Summary and conclusion

We found good agreement between direct estimates of carbon remineralization from measurements of respiratory activity and indirect estimates from oxygen gradients along the Laurentian Channel. These estimates imply that approximately 10% of local primary production reaches the deep waters (>200 m) and sediments of the GSL. Respiration measurements show that the benthos plays a predominant role in oxygen consumption below 200 m. Spatial and temporal patterns of DOC distribution suggest that this material serves both as a long-term sink for carbon in the deep waters and a significant source for carbon oxidation on a smaller scale. Finally, our data indicate that the vertical carbon budget is balanced between Cabot Strait and the Anticosti Channel (oligotrophic zone) but that approximately half of the carbon produced in the surface layer west of Anticosti Island (northwestern gulf, mesotrophic zone) cannot be accounted for at this time. This is most likely related to the hydrodynamic (estuarine circulation, presence of a quasi-permanent geostrophic cyclonic gyre linked to the Gaspé Current) and biological (higher primary production and its transfer to higher trophic levels) characteristics of the northwestern gulf. We anticipate that our understanding of the carbon cycle in the GSL will improve as we integrate more information concerning the fate of primary production in the northwestern gulf and of the circulation of the deep waters of the Laurentian Channel.

Acknowledgements

This study was carried out as a contribution to the CJGOFS program with financial support from both the Natural Sciences and Engineering Research Council of Canada and the Department of Fisheries and Oceans, Canada. We acknowledge the help of T. Arakaki, M.-L. Dubé, A. Gagné, C. Guignard, and C. Lovejoy for technical assistance. We thank the captains and crews of the various research vessels used during the field work for this study, *Fogo Isle*, CSS *Hudson*, CSS *Parizeau* (Department of Fisheries and Oceans), and the Canadian Coast Guard icebreaker *Sir Wilfrid Laurier*, for their cooperation. We are grateful to L. Devine Castonguay for reading the manuscript and offering comments, as well as for providing the final figures. We also thank Dr. P. Mackas and one anonymous referee for their comments and reviews of the manuscript.

References

Ahmed, S.I., Kenner, R.A., and King, F.D. 1976. Preservation of enzymic activity in marine plankton by low-temperature freezing. Mar. Chem. **4**: 133–139.

Aminot, A., and Chaussepied, M. 1983. Manuel des analyses chimiques en milieu marin. CNEXO, Brest.

Amon, R.M.W., and Benner, R. 1994. Rapid cycling of high-molecular-weight dissolved organic matter in the ocean. Nature (Lond.), **369**: 549–552.

Aristegui, J., and Montero, M.F. 1995. The relationship between community respiration and ETS activity in the ocean. J. Plankton Res. **17**: 1563–1571.

Barnett, P.R.O., Watson, J., and Conelly, D. 1984. A multiple corer for taking virtually undisturbed samples from shelf, bathyal and abyssal sediments. Oceanol. Acta, **7**: 399–408.

Benoit, J., and El-Sabh, M.I. 1985. Structure and seasonal characteristics of the Gaspé Current. J. Geophys. Res. **90**: 3225–3236.

Betzer, P.R., Showers, W.J., Laws, E.A., Winn, C.D., Ditullio, G.R., and Kroopnick, P.M. 1984. Primary productivity and particulate fluxes on a transect of the equator at 153°W in the Pacific Ocean. Deep-Sea Res. **31**: 1–11.

Bugden, G.L. 1981. Salt and heat budgets for the Gulf of St. Lawrence. Can. J. Fish. Aquat. Sci. **38**: 1153–1167.

Bugden, G.L. 1991. Changes in the temperature-salinity characteristics of the deeper waters of the Gulf of St. Lawrence over the past several decades. *In* The Gulf of St. Lawrence: small ocean or big estuary? *Edited by* J.-C. Therriault. Can. Spec. Publ. Fish. Aquat. Sci. 113: 139–147.

Chen, W., and Wangersky, P.J. 1993*a*. High-temperature combustion analysis of dissolved organic carbon produced in phytoplankton cultures. Mar. Chem. **41**: 167–171.

Chen, W., and Wangersky, P.J. 1993*b*. A high-temperature catalytic oxidation method for the determination of marine dissolved organic carbon and its comparison with the UV photo-oxidation method. Mar. Chem. **42**: 95–106.

Colombo, J.C., Silverberg, N., and Gearing, J.N. 1996*a*. Biogeochemistry of organic matter in the Laurentian Trough: I — Composition and vertical flux of rapidly settling particles. Mar. Chem. **51**: 277–294.

Colombo, J.C., Silverberg, N., and Gearing, J.N. 1996*b*. Biogeochemistry of organic matter in the Laurentian Trough: II — Bulk composition of the sediments and relative reactivity of major components during early diagenesis. Mar. Chem. **51**: 295–314.

Colquhoun, D. 1971. Lectures in biostatistics. Oxford University Press, London.

Coote, A.R., and Yeats, P.A. 1979. Distribution of nutrients in the Gulf of St. Lawrence. J. Fish. Res. Board Can. **36**: 122–131.

Culkin, F. 1965. The major constituents of sea water. *In* Chemical oceanography. Vol. I. *Edited by* J.P. Riley and G. Skirrow. Academic Press, London. pp. 121–162.

de Lafontaine, Y., Demers, S., and Runge, J. 1991. Pelagic food web interactions and productivity in the Gulf of St. Lawrence: a perspective. *In* The Gulf of St. Lawrence: small ocean or big estuary? *Edited by* J.-C. Therriault. Can. Spec. Publ. Fish. Aquat. Sci. 113: 99–123.

Dickie, L., and Trites, L.M. 1983. The Gulf of St. Lawrence. *In* Estuaries and enclosed seas. *Edited by* B.H. Ketchum. Elsevier, Amsterdam, The Netherlands. pp. 403–425.

Dunbar, M.J., MacLellan, D.C., Filion, A., and Moore, D. 1980. The biogeographic structure of the Gulf of St. Lawrence. McGill Univ. Mar. Sci. Centre Ms. Rep. No. 32.

Eppley, R.W. 1989. New production: history, methods, problems *In* Productivity of the ocean: present and past. *Edited by* W.H. Berger, V.S. Smetacek, and G. Wefer. John Wiley and Sons Ltd., Chichester, England. pp. 85–99.

Eppley, R.W., and Peterson, B.J. 1979. Particulate organic matter flux and planktonic new production in the deep ocean. Nature (Lond.), **282**: 677–680.

© 1996 NRC Canada

Falkowski, P.G., Flagg, C.N., Rowe, G.T., Smith, S.L., Whitledge, T.E., and Wirick, C.D. 1988. The fate of a spring phytoplankton bloom: export or oxidation? Continental Shelf Res. **8**: 457–484.

Forrester, W.D. 1964. A quantitative temperature-salinity study of the Gulf of St. Lawrence. Bedford Inst. Oceanogr. Rep. No. BIO-64-11.

Grehan, A.J., Scaps, P., Desrosiers, G., Juniper, K., and Stora, G. 1994. Vertical macrofaunal distribution in the soft sediments of the Gulf of St. Lawrence and the Scotian continental margin: a preliminary assessment of intersite differences in bioturbation potential. Vie Milieu **44**: 101–107.

Greisman, P., and Ingram, R.G. 1977. Nutrient distribution in the St. Lawrence Estuary. J. Fish. Res. Board Can. **34**: 2117–2123.

Hall, P.O.J., Anderson, L.G., Rutgers van der Loeff, M.M., Sundby, B., and Westerlund, S.F.G. 1989. Oxygen uptake kinetics in the benthic boundary layer. Limnol. Oceanogr. **34**: 734–746.

Hansson, I. 1973. A new set of acidity constants for carbonic acid and boric acid in seawater. Deep-Sea Res. **20**: 461–478.

Hulth, S., Blackburn, T.H., and Hall, P.O.J. 1994. Arctic sediments (Svalbard): consumption and microdistribution of oxygen. Mar. Chem. **46**: 293–316.

Ingram, R.G. 1979. Water mass modification in the St. Lawrence Estuary. Naturaliste can. **106**: 45–54.

Jahnke, R.A., and Jackson, G.A. 1987. Role of sea floor organisms in oxygen consumption in the deep North Pacific Ocean. Nature (Lond.), **329**: 621–623.

Jones, E.P., Zemlyak, F., and Stewart, P. 1992. Operating manual for the Bedford Institute of Oceanography automated dissolved oxygen titration system. Can. Tech. Rep. Hydrogr. Ocean Sci. **138**: iv + 51 p.

Kepkay, P.E., and Wells, M.L. 1992. Dissolved organic carbon in North Atlantic surface waters. Mar. Ecol. Prog. Ser. **80**: 275–283.

Koutitonsky, V.G., and Bugden, G.L. 1991. The physical oceanography of the Gulf of St. Lawrence: a review with emphasis on the synoptic variability of the motion. *In* The Gulf of St. Lawrence: small ocean or big estuary? *Edited by* J.-C. Therriault. Can. Spec. Publ. Fish. Aquat. Sci. 113: 57–90.

Koutitonsky, V.G., Wilson, R.E., Ulmann, D., and Toro, C. 1987. SWK3D: an enhanced version of the VANERN three-dimensional hydrodynamical model for applications to stratified semi-enclosed seas. INRS-Océanologie, Sci. Rep. for Can. Hydrogr. Ser., Maurice Lamontagne Institute, Mont-Joli, Que.

Le Févre, J., and Frontier, S. 1988. Influence of temporal characteristics of physical phenomena on plankton dynamics, as shown by north-west European marine ecosystems. *In* Toward a theory on biological-physical interactions in the world ocean. *Edited by* E.J. Rothschild. Kluwer, Dordrecht, The Netherlands. pp. 245–272.

Levasseur, M., and Therriault, J.-C. 1987. Phytoplankton biomass and nutrient dynamics in a tidally induced upwelling: the role of the NO_3:SiO_4 ratio. Mar. Ecol. Prog. Ser. **39**: 87–97.

Levasseur, M.E., Fortier, L., Therriault, J.-C., and Harrison, P.J. 1992. Phytoplankton dynamics in a coastal jet frontal region. Mar. Ecol. Prog. Ser. **86**: 283–295.

Longhurst, A.R., and Harrison, W.B. 1989. The biological pump: profiles of plankton production and consumption in the upper ocean. Prog. Oceanogr. **22**: 47–122.

Lucotte, M., Hillaire-Marcel, C., and Louchouarn, P. 1991. First-order organic carbon budget in the St. Lawrence Lower Estuary from ^{13}C data. Estuarine Coastal Shelf Sci. **32**: 297–312.

Malone, T.C. 1971. The relative importance of nanoplankton and netplankton as primary producers in the California Current system. Fish. Bull. **69**: 799–820.

Mantoura, R.F.C., Martin, J.-M., and Wollast, R. 1991. Ocean margin processes in global change: report of the Dahlem Workshop on Ocean Margin processes in global change, March 18–23, 1990, Berlin. Dahlem Workshop Reports: Physical, Chemical and Earth Sciences Research Reports, 9. John Wiley and Sons, Ltd., Chichester, England.

Martin, J.H., Knauer, G.A., Karl, D.M., and Broenkow, W.W. 1987. VERTEX: carbon cycling in the northeast Pacific. Deep-Sea Res. **34**: 267–285.

Martinez, R. 1991. Biomass and respiratory ETS activity of microplankton in the Barents Sea. *In* Proceedings of the Pro Mare Symposium on Polar Marine Ecology, Trondheim, 12–16 May 1990. *Edited by* E. Sakshaug, C.E.E. Hopkins, and N.A. Oritsland. Polar Res. **10**: 193–200.

Martinez, R., and Estrada, M. 1992. Respiratory electron transport activity of microplankton in the Weddell Sea during early spring: influence of the ice cover and the ice edge. Polar Biol. **12**: 275–282.

Millero, F.J. 1979. The thermodynamics of the carbonic acid system in seawater. Geochim. Cosmochim. Acta, **43**: 1651–1661.

Millero, F.J. 1983. Influence of pressure on chemical processes in the sea. *In* Chemical oceanography. Vol. 8. 2nd ed. *Edited by* J.P. Riley and R. Chester. Academic Press, New York. pp. 1–88.

Packard, T.T. 1971. The measurement of respiratory electron-transport activity in marine phytoplankton. J. Mar. Res. **29**: 235–244.

Packard, T.T. 1979. Respiration and respiratory electron transport activity in plankton from the Northwest African upwelling area. J. Mar. Res. **37**: 711–742.

Packard, T.T. 1985. Measurement of electron transport activity of microplankton. *In* Advances in aquatic microbiology. Vol. 3. *Edited by* H. Jannasch and P.J. Leb. Williams. Academic Press, New York. pp. 207–261.

Packard, T.T., and Williams, P.J. Leb. 1981. Rates of respiratory oxygen consumption and electron transport in surface seawater from the northwest Atlantic. Oceanol. Acta, **4**: 351–358.

Packard, T.T., Devol, A.H., and King, F.D. 1975. The effect of temperature on the respiratory electron transport system in marine plankton. Deep-Sea Res. **22**: 237–249.

Packard, T.T., Garfield, P.C., and Martinez, R. 1983. Respiration and respiratory enzyme activity in aerobic and anaerobic cultures of the marine denitrifying bacterium *Pseudomonas perfectomarinus*. Deep-Sea Res. **30**: 227–243.

Packard, T.T., Denis, M., Rodier, M., and Garfield, P. 1988. Deep-ocean metabolic CO_2 production: calculations from ETS activity. Deep-Sea Res. **35**: 371–382.

Parsons, T.R., Maita, Y., and Lalli, C.M. 1984. A manual of chemical and biological methods for seawater analysis. Pergamon Press, New York.

Pingree, R.D., and Griffiths, D.K. 1980. A numerical model of the M2 tide in the Gulf of St. Lawrence. Oceanol. Acta, **3**: 221–225.

Platt, T., and Subba Rao, D.V. 1975. Primary production of marine microphytes. *In* Photosynthesis and productivity in different environments. *Edited by* J.P. Cooper. IBP 3, Cambridge University Press, Cambridge. pp. 249–280.

Plourde, S., and Runge, J.A. 1993. Reproduction of the planktonic copepod *Calanus finmarchicus* in the lower St. Lawrence Estuary: relation to the cycle of phytoplankton production and evidence for a *Calanus* pump. Mar. Ecol. Prog. Ser. **102**: 217–227.

Pocklington, R. 1988. Organic matter in the Gulf of St. Lawrence. *In* Chemical oceanography in the Gulf of St. Lawrence. *Edited by* P.M. Strain. Can. Bull. Fish. Aquat. Sci. 220: 49–58.

Redfield, A.C., Ketchum, B.H., and Richards, F.A. 1963. The influence of organisms on the composition of seawater. *In* The sea. Vol. 2. *Edited by* M.N. Hill. Interscience, New York. pp. 26–77.

Ryther, J.H. 1969. Photosynthesis and fish production in the sea. Science (Wash., D.C.), **166**: 72–76.

Savenkoff, C., Vézina, A.F., Chanut, J.-P., and Gratton, Y. 1995. Respiratory activity and CO_2 production rates of microorganisms in the lower St. Lawrence Estuary. Continental Shelf Res. **15**: 613–631.

© 1996 NRC Canada

Steven, D.M. 1975. Biological production in the Gulf of St. Lawrence. *In* Energy flow — its biological dimension. *Edited by* T.W. Cameron and L.W. Billingsley. Royal Society of Canada, Ottawa, Ont. pp. 229–248.

Suess, E. 1980. Particulate organic carbon flux in the oceans–surface productivity and oxygen utilization. Nature (Lond.), **288**: 260–263.

Tan, F.C., and Walton, A. 1978. Stable isotope studies in the Gulf of St. Lawrence, Canada. *In* Stable isotopes in the earth sciences. *Edited by* B.W. Robinson. N.Z. Dep. Sci. Ind. Res. Bull. 220: 27–37.

Therriault, J.-C., and Lacroix, G. 1976. Nutrients, chlorophyll and internal tides in the St. Lawrence Estuary. J. Fish. Res. Board Can. **33**: 2747–2757.

Thibault, D., Gaudy, R., and Le Fèvre, J. 1994. Zooplankton biomass, feeding and metabolism in a geostrophic frontal area (Almeria–Oran front, western Mediterranean). Significance to pelagic food webs. J. Mar. Syst. **5**: 297–311.

Toggweiler, J.R. 1989. Is the downward dissolved organic matter (DOM) flux important in carbon transport? *In* Productivity of the ocean: present and past. *Edited by* W.H. Berger, V.S. Smetacek, and G. Wefer. John Wiley and Sons Ltd., Chichester, England. pp. 65–83.

Walsh, J.J. 1991. Importance of continental margins in the marine biogeochemical cycling of carbon and nitrogen. Nature (Lond.), **350**: 53–55.

Weiss, R.F. 1974. Carbon dioxide in water and seawater: the solubility of a non-ideal gas. Mar. Chem. **2**: 203–215.

Williams, P.M., and Druffel, E.R.M. 1988. Dissolved organic matter on the ocean: comments on a controversy. Oceanogr. Mag. **1**: 14–17.

Yeats, P.A. 1988. Distribution and transport of suspended particulate matter. *In* Chemical oceanography in the Gulf of St. Lawrence. *Edited by* P.M. Strain. Can. Bull. Fish. Aquat. Sci. 220: 15–28.

© 1996 NRC Canada

Nitrification and methane oxidation at the sediment surface in Hamilton Harbour (Lake Ontario)

Réal Roy, Roger Knowles, and Murray N. Charlton

Abstract: Nitrification and methane oxidation in profundal and littoral sediment surfaces of a polluted system were investigated by means of pore water analyses, enumeration of methanotrophic and nitrifying bacteria, and slurry experiments. Sediment CH_4 concentrations (0.38–3.4 mM) were generally higher than NH_4^+ concentrations (0.35–1.4 mM) at the profundal site but not at the littoral site where CH_4 and NH_4^+ concentrations were 0.10–0.93 and 0.12–0.46 mM, respectively. Methanotroph counts (10^5 cfu·mL^{-1}) were at least an order of magnitude higher than those of NH_4^+-oxidizing bacteria (10^3–10^4 MPN·mL^{-1}). Dissolved O_2 profiles indicated a penetration of 0.5–2.0 mm (profundal) and 2.5–6.0 mm (littoral) which suggests that actual oxidation of CH_4 and NH_4^+ was restricted to this oxic layer. Calculated fluxes of CH_4 (0–23 mmol·m^{-2}·d^{-1}), NH_4^+ (0–2.5 mmol·m^{-2}·d^{-1}), and O_2 (–14 mmol·m^{-2}·d^{-1}) through the surface sediment suggested that CH_4 consumption could account for a more important fraction of the estimated O_2 consumption than could nitrification. We conclude that (*i*) CH_4 metabolism may be more important than nitrification as a sink of hypolimnetic O_2 in Hamilton Harbour, and (*ii*) CH_4 may suppress nitrification by competition for O_2 and NH_4^+ between methanotrophs and nitrifiers.

Résumé : La nitrification et l'oxidation du méthane à la surface de sédiments profonds et littoraux d'un système pollué ont été étudiées par l'analyse des eaux interstitielles, le dénombrement des bactéries méthanotrophes et nitrifiantes et des expériences sur des sédiments dilués. Dans les sédiments profonds les concentrations en CH_4 (0,38–3,4 mM) étaient en général plus élevées que celles en NH_4^+ (0,35–1,4 mM) contrairement aux sédiments littoraux où les concentrations en CH_4 et en NH_4^+ variaient respectivement de 0,10–0,93 et de 0,12–0,46 mM. Les bactéries méthanotrophes (10^5 ufc·mL^{-1}) étaient plus nombreuses que les bactéries oxidatives de NH_4^+ (10^3–10^4 NPP·mL^{-1}). La pénétration de l'O_2 dans les sédiments profonds et littoraux étaient respectivement de l'ordre de 0,5–2,0 et de 2,5–6,0 mm suggérant que l'oxidation du CH_4 et de NH_4^+ était limitée à cette couche oxique. Les flux calculés de CH_4 (0–23 mmol·m^{-2}·d^{-1}), NH_4^+ (0–2,5 mmol·m^{-2}·d^{-1}) et O_2 (–14 mmol.m^{-2}·d^{-1}) suggèrent que la consommation du CH_4 pourrait représenter une fraction plus importante de la consommation estimée d'O_2 que la nitrification. Nous concluons que (*i*) le métabolisme du CH_4 semble être plus important que la nitrification dans la consommation hypolimnétique d'O_2 dans le port de Hamilton et (*ii*) devrait plutôt supprimer la nitrification par une compétition pour l'O_2 et le NH_4^+ entre les bactéries méthanotrophes et les bactéries nitrifiantes plutôt que de stimuler la nitrification par les méthanotrophes.

Introduction

Because of similarities in the physiology of methanotrophs and nitrifiers, which carry out methane oxidation and nitrification, respectively, these two bacterial groups occupy similar niches in natural environments (Bédard and Knowles 1989). They are usually active at the oxic–anoxic boundary layer where NH_4^+ and CH_4, resulting from mineralization of organic matter in the anoxic subsurface, diffuse up to oxic zones. These strictly aerobic microbial populations may have great importance for summer hypolimnetic O_2 depletion in Hamilton Harbour. The complex interaction between methanotrophs and nitrifiers may also be critical for the outcome of nitrogen cycling in freshwater sediments, since nitrification is usually a key rate-limiting step in this cycle. Inhibition of CH_4 oxidation by NH_4^+ (Bosse et al. 1993; Steudler et al. 1989) and suppression of nitrification by CH_4 (Megraw and Knowles 1987; Roy and Knowles 1994) occur in various natural systems. Besides the well-known competitive inhibition at the ammonia monooxygenase active site, inhibition of nitrifiers by CH_4 may also occur by competition between methanotrophs and nitrifiers for O_2 and NH_4^+ (Megraw and Knowles 1987; Roy and Knowles 1994). At low CH_4 concentrations, methanotrophs may also contribute to nitrification in soil and sediments (Megraw and Knowles 1989; Roy and Knowles 1994).

Whether CH_4 suppresses or stimulates nitrification depends on the concentration gradients and fluxes of the substrates NH_4^+ and CH_4. We have previously reported high NH_4^+ and CH_4 concentrations in Hamilton Harbour (at the western extremity of Lake Ontario) when compared with other freshwater ecosystems, but we did not consider sedi-

Received December 6, 1995. Accepted May 1, 1996.
J13196

R. Roy[1] **and R. Knowles.** Microbiology Unit, Department of Natural Resource Sciences, Macdonald Campus of McGill University, 21111 Lakeshore Rd., Ste-Anne-de-Bellevue, QC H9X 3V9, Canada.
M. N. Charlton. Lakes Research Branch, National Water Research Institute, P.O. Box 5050, Burlington, ON L7R 4A6, Canada.

[1] Present address: Max-Planck Institut für terrestrische Mikrobiologie, Karl-von-Frisch-Straße, 35043, Marburg, Germany.

© 1996 NRC Canada

ment–water gradients and fluxes of the substrates and dissolved O_2 (Roy and Knowles 1994). Although Jones and Simon (1981) and Sweerts et al. (1991) have reported contrasts in profiles of NH_4^+ and CH_4 concentrations at littoral and profundal sediment–water interfaces, they did not specifically interpret these results in terms of interactions between the methanotrophs and nitrifiers. We hypothesized that determination of CH_4 and NH_4^+ fluxes in relation to potential nitrification and methane oxidation as a function of sediment depth would allow assessment of the potential role played by CH_4 in the nitrogen cycle.

To test this, we examined CH_4 and NH_4^+ concentration profiles and calculated fluxes at the littoral and profundal sediment surfaces in a polluted freshwater ecosystem: Hamilton Harbour.

Materials and methods

Study site and sediment sampling

Sediment cores were sampled monthly with Plexiglas tubes (inside diameter 65 mm) at a littoral (2 m depth) site (910) and a profundal (23 m depth) site (906) in Hamilton Harbour, Ontario, Canada, five times from June to November 1992 and in October 1993. In addition, two profundal sites (903 and 907) were also sampled in June and July 1992. A detailed description of Hamilton Harbour and the field measurements is reported elsewhere (Roy et al. 1994). Sediment cores were extruded and sliced at 5-mm intervals using a hydraulic extruder. When O_2 microprofiles were measured, it was prior to extrusion and slicing.

O_2 microprofiles

Profiles of dissolved O_2 in sediment pore water were measured at both sites with a needle electrode, non-Clark type with a built-in Ag/AgCl reference electrode (No. 768-20R, Diamond General, Ann Arbor, Mich., U.S.A.), micropositioner, and meter (No. 1201, Diamond General). Before measurement, the electrode was polarized (–0.720 V) overnight, and immediately prior to readings the electrode was calibrated using filtered lake water from Hamilton Harbour equilibrated with air and N_2, respectively. The electrode was recalibrated before every new profile. We performed three profiles on each of two replicate cores equilibrated at 25°C from each site sampled. Dissolved O_2 concentrations were calculated on the basis of 275 μM at air saturation (21.8% v/v).

Microbial assays

Potential microbial activities were measured by dispensing sediment (5 mL) from a given depth of a given duplicate core from each site into either a 50-mL Erlenmeyer flask with an equal volume of sterile distilled water to obtain 1:1 slurry dilution or a 125-mL Erlenmeyer flask with 45 mL of sterile distilled water to obtain a 1:10 slurry dilution. Flasks were capped with serum stoppers (Suba-Seal Works, William Freeman and Co., Barnsley, U.K.). For potential nitrification and CH_4 oxidation assays, 0.1 M $(NH_4)_2SO_4$ was added to a final slurry concentration of 4 mM NH_4^+ for both 1:1 and 1:10 slurries. All flasks were shaken, evacuated three times (15 min each), and backfilled with air to eliminate dissolved gases in the pore water. To each flask, 0.5 mL of pure CH_4 (Matheson, Montréal, Qué., Canada) was added by syringe after withdrawal of an equal volume of the gas phase to give approximately a 1 kPa final partial pressure (equivalent to 13.9 μM dissolved or 23.5 $\mu mol \cdot flask^{-1}$ for the 50-mL Erlenmeyer flasks (1:1 slurries)). For potential denitrification and CH_4 production rate determinations, flasks were backfilled with ultrapure helium (Linde, Union Carbide, Montréal, Qué., Canada) instead of air with no addition of NH_4^+ or CH_4. However, in the case of potential denitrification determination, 0.1 M $NaNO_3$ was added to a final slurry concentration of 5 mM, and 5 mL of C_2H_2 was added to a final partial pressure of 10 kPa (Roy et al. 1994). CH_4 production rates reported here were measured as the accumulated CH_4 in the headspace 72 h after initiation of the incubation. All flasks were wrapped with aluminum foil to avoid light exposure. Flasks were incubated on a gyratory shaker (250 rpm, 25°C) except for anaerobic assays for the determination of CH_4 production and denitrification potential rates, where flasks were incubated statically at 20°C (Roy et al. 1994). Nitrification was measured by NH_4^+ disappearance and NO_2^- and NO_3^- production in the pore water and N_2O production in the gas phase. CH_4 oxidation and CH_4 production were measured as CH_4 disappearance or production, and denitrification as N_2O production in the presence of C_2H_2 in the headspace (Roy and Knowles 1994).

Enumeration of NH_4^+-oxidizers, NO_2^--oxidizers, and methanotrophs

Determination of abundance of NH_4^+-oxidizers and NO_2^--oxidizers was by Most Probable Number (MPN) methods (Alexander 1965; Schmidt and Belser 1982) and of methanotrophs was by a membrane filter colony count (Megraw and Knowles 1989). In the case of the NO_2^--oxidizers, we determined both the NO_2^--sensitive, which include organotrophic NO_2^--oxidizers, and the NO_2^--insensitive chemolithotrophic NO_2^--oxidizers (Laanbroek and Schotman 1991).

Analytical procedures

Gases were determined by gas chromatography as described previously (Roy and Knowles 1994; Roy et al. 1994). Gas concentrations were calculated taking into account the dissolved gas by using the Ostwald solubility coefficient (Wilhelm et al. 1977). Rates of production of gases were calculated as already described (Roy et al. 1994).

Pore water was extracted from sediment samples by centrifugation of sediment from a given depth within a core (Roy et al. 1994). Pore water from 1:1 and 1:10 slurries was also extracted by centrifugation (Roy and Knowles 1994). NH_4^+, NO_2^-, and NO_3^- concentrations in pore water were determined by colorimetric methods described elsewhere (Roy and Knowles 1994). Particulate carbon (PC) and particulate sulfur (PS) were determined on the dried and ground pellet of the centrifuged sediment by a combustion method on a LECO automated carbon-sulfur analyzer (Roy et al. 1994). Particulate organic carbon (POC) was determined in a similar manner, except that dried sediments were acidified with 10% phosphoric acid and dried to eliminate carbonates (Roy et al. 1994).

CH_4 concentrations in sediment cores were measured at the time of onshore extrusion and slicing of the sediment cores (Roy and Knowles 1994). Concentrations were calculated according to Roy and Knowles (1994). Concentrations were corrected by dividing by the average sediment porosity at a given depth and site in order to yield CH_4 concentrations in the pore water. Sediment porosity was determined by gravimetry (Roy and Knowles 1994).

Numerical procedures

Statistical analyses and tests

Basic statistics reported in this work ($[CH_4]$, $[NH_4^+]$, $[O_2]$, total particulate carbon, (TPC), total particulate organic carbon, (TPOC), total particulate sulfur, (TPS), and potentials of methane oxidation, nitrification, denitrification, and CH_4 production) were computed using the computer software Systat 5.01 (Systat Inc., Evanston, Ill., U.S.A.). Distribution normality was tested by the Lilliefors corrected method of the Kolmogorov–Smirnov test (Sokal and Rohlf 1981). Since all variables were not normally distributed based on this test, log transformations were attempted. These transformed data also failed to meet the normality criterion. With the same software the nonparametric Kruskal–Wallis test was performed using as grouped criteria core replicates (2), sampling sites (2), sediment depth (12), and sampling time (5). Wherever the probability (P) level associated

© 1996 NRC Canada

with a statistical decision is mentioned in the following sections, it refers to the result of the Kruskal–Wallis test.

Although the nonnormality of the distributions makes it statistically inappropriate to use parameters such as mean and standard error of the mean (SEM), we have used them because these parameters are expressed in biologically or chemically meaningful units unlike the ranks which have no units.

CH_4, NH_4^+, and O_2 fluxes

CH_4, NH_4^+, and O_2 fluxes (J) in the surface of the sediment were calculated according to Fick's law, modified for sedimentary systems (Lerman 1979):

$$J = \phi D_s dC/dz$$

where ϕ is the sediment porosity, D_s is the specific diffusion constant (D_0) of a given chemical in sediment, and dC/dz is the concentration gradient. The sediment porosity was an average for each site determined by gravimetry on cores from sites 906 and 910. Diffusion constants (D_0) (y) for NH_4^+, CH_4, and O_2 vary linearly with temperature (x). At a given temperature, D_0 was interpolated using the equations found by linear regression of data provided by Li and Gregory (1974) in Lerman (1979): $y = (0.03978x + 0.97649) \times 10^{-5}$ $cm^{-2} \cdot s^{-1}$ for NH_4^+, $y = (0.04230x + 0.70650) \times 10^{-5}$ $cm^{-2} \cdot s^{-1}$ for CH_4, and $y = (0.56x + 0.94) \times 10^{-5}$ $cm^{-2} \cdot s^{-1}$ for O_2. From these diffusion constants in water (D_0) it was possible to calculate the diffusion constants in sediment (D_s) according to the equation $D_s = D_0/\theta^2$ (Lerman 1979). Iversen and Jørgensen (1993) proposed an empirical formula to determine the tortuosity (θ^2) for a given sediment:

$$\theta^2 = 1 + n(1-\phi)$$

where $n = 2$ for sand (910) and $n = 3$ for clay-silts (906).

By means of second- and third-order regression of concentrations on depth, we determined second- and third-degree equations describing concentration profiles in sediments. Then we used these equations to derive dC/dz for $z = 0$, which corresponds to the sediment surface. The regression coefficients and the associated Pearson correlation coefficients (r^2) were computed uaing Sigmaplot 5.0 (Jandel Scientific). The statistical significance of these coefficients was determined using the critical values provided in table 25 of Rohlf and Sokal (1981).

Curve fitting

An exponential decay function was fitted successfully to the decrease in potential CH_4 production rates with sediment depth using the Sigmaplot software (Jandel Scientific, California, U.S.A.). The function was of the form

$$f(x) = ae^{(-bx)}.$$

This function was fitted to y, the dependent variable, which stood for the summer average potential rates of CH_4 production measured at each sediment depth (0–60 mm by 5-mm increments) at each site. The independent variable (x) was the depth (millimetres). Convergence of the data and the function was achieved. The constants and their respective standard errors obtained were: $a = 1.106 \pm 0.040$ (906) and 0.208 ± 0.099 (910) and $b = 0.221 \pm 0.010$ (906) and 0.221 ± 0.132 (910).

Using these constants, it was then possible to calculate a depth at which the potential CH_4 production rates were reduced by 90 and 99% by solving for x in the following manner:

$$x = \{\ln (f(x)/a)\}/-b.$$

Using published sedimentation rates, it was then possible to estimate a time scale required for the decrease in the CH_4 source.

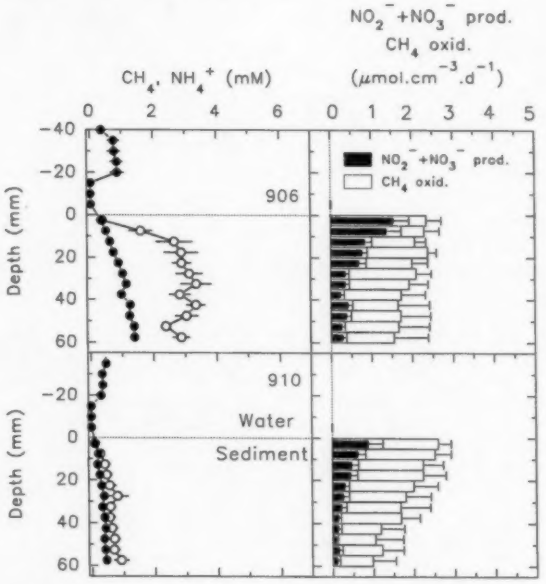

Fig. 1. Vertical profiles of porewater concentrations of NH_4^+ (●) and CH_4 (○) and of potential nitrification (closed bars) and CH_4 oxidation (open bars) in profundal (906) and littoral (910) sediments. Profiles were measured on duplicate cores retrieved at each site from June to November 1992. Error bars are ±1 SEM

Results

Profiles of CH_4 and NH_4^+ concentration, and potential CH_4 oxidation and nitrification

At profundal (906) and littoral (910) sites, pore water CH_4 and NH_4^+ concentrations increased significantly ($P \leq 0.001$) with depth during the study period, June–November 1992, and were higher at the profundal than at the littoral site (Fig. 1). At the profundal site the CH_4 concentrations in sediment pore water were generally much higher than the NH_4^+ concentrations, unlike the littoral site where CH_4 concentrations in the sediment pore water were similar to those of NH_4^+. CH_4 oxidation and nitrification potential rates decreased significantly ($P \leq 0.001$) with sediment depth at both sites. These activities were not significantly ($P > 0.05$) lower at the profundal site. It should also be noted that, in general, potential CH_4 oxidation was higher than nitrification at every depth.

Abundance of methanotrophs and nitrifiers

Methanotroph counts varied from 1×10^5 to 8×10^5 cfu·mL^{-1} throughout the top 6 cm of sediments at the profundal site (Fig. 2). Abundance of NH_4^+-oxidizers and NO_2^--oxidizers (NO_2^--insensitive) at the same profundal site varied from $10^{2.2}$ to 10^3 MPN·mL^{-1}. NO_2^--sensitive NO_2^--oxidizers were in the order of 10^7 MPN·mL^{-1} (data not shown).

Dissolved O_2 microprofiles

Profiles of dissolved O_2 at profundal and littoral sites showed variations within and between cores (Fig. 3). At the profundal site the dissolved O_2 in the overlying water was about half

© 1996 NRC Canada

Fig. 2. Abundance of methanotrophic and nitrifying (NH_4^+-oxidizing and NO_2^--oxidizing/NO_2^--insensitive) bacteria in profundal sediment (906) of Hamilton Harbour as determined on cores sampled on July 20, 1994. Error bars are ±1 SEM.

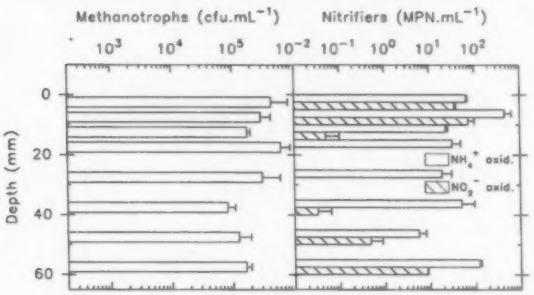

Fig. 3. Profiles of dissolved O_2 concentrations in duplicate cores (●, ○) retrieved at profundal (906) and littoral (910) sites on October 5 and 7, 1993, respectively. Each data point is the average of three profiles performed at different places in one sediment core from a given site. Measurements were carried out at room temperature (25°C) and without stirring. Error bars are ±1 SEM.

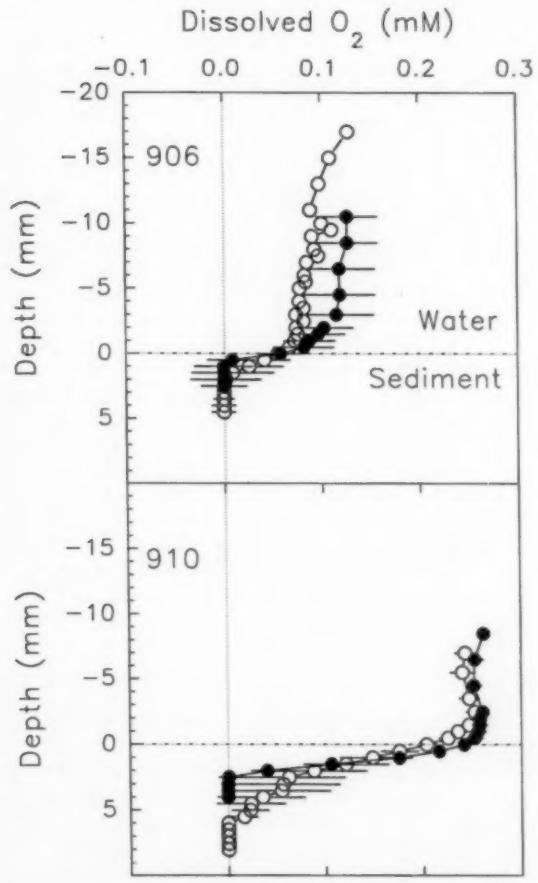

Fig. 4. Profiles of TPC (○), POC (●), and PS (▽), measured on duplicate cores retrieved at a profundal (906) and a littoral (910) site, and profiles of potential rates of denitrification and CH_4 production measured in anaerobic slurries from duplicate cores from the same sites. Each data point is the average of five monthly sampling measurements done between June and November 1992. Error bars are ±1 SEM.

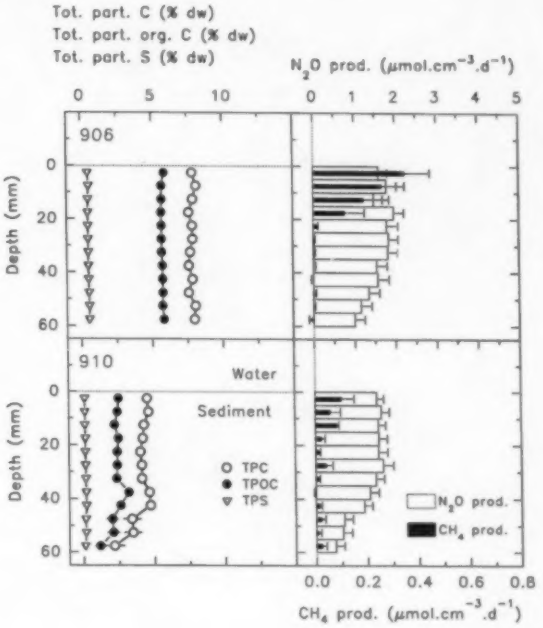

that at the littoral site, suggesting higher rates of O_2 consumption at the profundal site. O_2 penetration was also shallower at the profundal site (0.5–2.0 mm) when compared with the littoral site (2.5–6.0 mm), and actual CH_4 oxidation and nitrification are likely to be restricted to this oxic layer. Based on such O_2 profiles, it was possible to calculate O_2 fluxes on duplicate cores at each site. Such calculations indicated that O_2 fluxes from the water to the sediment were 14.4 ± 3.9 mmol·m^{-2}·d^{-1} in profundal sediment cores and 14.6 ± 2.5 mmol·m^{-2}·d^{-1} in littoral sediment cores.

PC, CH_4 production, and denitrification

PC and POC did not vary significantly ($P > 0.05$) with depth, at least in the 0-to 6-cm layer, at either profundal or littoral sites (Fig. 4). The former had significantly ($P \leq 0.001$) higher levels of PC (7.5 %) and POC (5%) than the littoral site (3.0 and 1.5%, respectively). In general, particulate inorganic carbon (PIC) represented a fraction of 1.5–2.0% of the dry matter at both sites.

At the profundal site, potential CH_4 production was higher in the surface 20 mm and rates decreased sharply and significantly ($P \leq 0.001$) below this depth. They were also higher than at the littoral site but not significantly ($P > 0.05$) so. Potential denitrification rates were slightly higher at the profundal site ($P \leq 0.05$) and moderately decreased with depth ($P = 0.05$).

© 1996 NRC Canada

Fig. 5. Temperature (●, ○) and dissolved O_2 (▼, ▽) in the water column (1 m above the sediment) and calculated fluxes of CH_4 (▲, △) and NH_4^+ (■, □) at a profundal (closed symbols) and a littoral (open symbols) site during summer 1992. Each flux data point was calculated from the regression of concentration on depth for means of duplicate cores. Error bars represent ±1 SE of mean flux based on the standard error of the b coefficient calculated from second-order regression of the type $y = ax^2 + bx + c$.

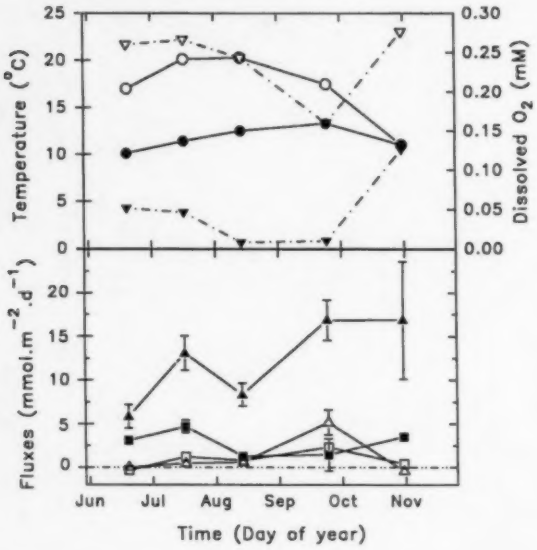

Sediment surface CH_4, NH_4^+, and O_2 fluxes

Based on the concentration profiles of CH_4 and NH_4^+ measured at profundal and littoral sites, fluxes of these chemicals at the sediment surface were calculated. Second-order regression of the concentrations on the sediment depth with $n = 12$ were all highly significant ($P \leq 0.01$) based on the r^2 of each regression (0.771–0.988) except for the regression of CH_4 concentration on depth for the November sampling (r^2 = 0.642, $P \leq 0.05$). CH_4 fluxes at the profundal site were the highest throughout most of the summer (Fig. 5). They increased from 5.86 mmol·m^{-2}·d^{-1} in June 1992 to 16.9 mmol·m^{-2}.d^{-1} in September and November 1992 following the increase of temperature and the decrease of dissolved O_2 in the water column. NH_4^+ fluxes at this site were lower and varied from 1.26 to 4.02 mmol·m^{-2}·d^{-1}. At the littoral site, CH_4 and NH_4^+ fluxes were similar throughout the season, except in September when the CH_4 flux (5.18 mmol·m^{-2}·d^{-1}) was higher than the NH_4^+ flux (1.57 mmol·m^{-2}·d^{-1}). Incubation at 15°C of whole cores sampled at each site indicated that release of CH_4 and NH_4^+ from the sediment to the overlying water was a small fraction (0.1–5%) of the calculated fluxes (data not shown). We conclude that most of the calculated flux was probably consumed in the oxic layers of the sediments.

Discussion

Concentrations of CH_4 and NH_4^+ in sediment pore water were higher at the profundal than at the littoral site. This can be explained by the summer stratification in such dimictic lakes, where anoxic conditions often prevail in profundal or hypolimnetic sites. These conditions lead to a decrease in oxidative activities, such as nitrification and CH_4 oxidation, and to an increase in anoxic activities such as fermentation and CH_4 production, hence greater accumulation of NH_4^+ and CH_4 in hypolimnetic sediments. Unlike a report of Jones and Simon (1981), but similar to a report for Lake Vechten (Sweerts et al. 1991), we found that CH_4 concentrations were generally higher than NH_4^+ concentrations, especially at the profundal site.

Increases in CH_4 and NH_4^+ concentrations with depth in freshwater sediment have been reported (Jones and Simon 1981; Sweerts et al. 1991), representing a steady state with CH_4 and NH_4^+ sources and sinks at the sediment subsurface and surface, respectively. CH_4 oxidation by methanotrophs is the main CH_4 sink. It occurs mostly at the sediment surface as indicated by the profiles of O_2 and potential rates of CH_4 oxidation. Nitrification and NH_4 assimilation, as NH_4^+ sinks, may be involved in the decrease of NH_4^+ at the sediment surface. Under active methanotrophic conditions at sufficiently high CH_4 concentrations (>119 μM), it was previously shown that assimilation of NH_4^+ by methanotrophs may contribute significantly to NH_4^+ disappearance in slurries of sediment from Hamilton Harbour (Roy and Knowles 1994). In that study, we found that with 119 μM dissolved CH_4 (8.6 kPa) added daily to the flasks, about 350 μM NH_4^+·d^{-1} was assimilated by methanotrophic activities. Here we found that CH_4 concentrations in the 0- to 5–mm depth of the profundal sediment averaged 383 μM, representing a potential sink of 1.13 mM NH_4^+·d^{-1}. This sink is three times the average NH_4^+ concentration in the 0–5 mm depth for the same site (347 μM) and suggests that NH_4^+ immobilization by methanotrophs may be a significant sink for NH_4^+ in these sediments.

Potential nitrification was generally lower than CH_4 oxidation potential even though the concentrations of NH_4^+ (4 mM) were much higher than the dissolved CH_4 concentrations (13.9 μM) in all assays. It should be noted that rates of CH_4 oxidation were 10 and 100 times higher than those reported for water and sediment of Lake Washington (Lidstrom and Somers 1984). These rates of CH_4 oxidation would be even higher if we consider that the NH_4 concentration (4 mM) in the slurry assays would inhibit CH_4 oxidation by 20% as reported elsewhere (Roy and Knowles 1994). Counts of CH_4-oxidizers in sediment cores from the profundal site were higher than NH_4^+-oxidizer counts. This may be considered as an indication that methanotrophs could suppress nitrification by NH_4^+-oxidizing bacteria as previously observed in sediment slurries under CH_4 concentrations ≥84 μM (Roy and Knowles 1994). This suppression was found in the latter study, as well as in a humisol (Megraw and Knowles 1987), to be caused by competition for O_2 and NH_4^+ between CH_4- and NH_4^+-oxidizing bacteria. These data provide further circumstantial evidence of effective competition for O_2 and NH_4^+ by methanotrophs against NH_4^+-oxidizing bacteria.

Although we did not determine actual rates of nitrification and CH_4 oxidation in sediment cores, O_2 microprofiles suggest that these activities are likely to be restricted to the top 5 mm. The fact that CH_4 oxidation and nitrification potentials extend below the zone of disappearance of O_2 in the sedi-

© 1996 NRC Canada

ments may be explained by the distribution of microorganisms by bioturbation of benthic micro- and meiofauna active in the top 4 cm of these sediments, and also by a tolerance of methanotrophs (Roslev and King 1994) and nitrifying bacteria (Abeliovich and Vonshak 1992; Hynes and Knowles 1982) to anoxic conditions.

The distribution of potential methanogenic activities indicates that the most important source of CH_4 is in the top 20 mm of the profundal sediment. No significant variations in pH (data not shown) or PC and POC occurred to account for the decrease in CH_4 production below 20 mm. However, we speculate that this higher CH_4 production rate near the surface is likely related to the activity of fermentative bacteria on less refractory organic carbon in this zone. Potential methanogenesis at the profundal site is higher than at the littoral site, consistent with the higher content of TPC at the profundal site. TPC was found to be a significant predictor of potential CH_4 production in a previous study (Roy et al. 1994).

Calculated CH_4 fluxes were always higher at the profundal site. At this site they were also higher than NH_4^+ fluxes. The latter did not vary much throughout the summer. At the littoral site, CH_4 flux was higher than NH_4^+ flux on only one occasion, in September at the end of summer stratification. Higher CH_4 fluxes are likely to support a greater activity of methanotrophs, which may lead to a significant fraction of the NH_4^+ flux being immobilized by active methanotrophs rather than being nitrified by the nitrifying bacteria. Significant methanotrophic nitrification is unlikely at the profundal site, but this could be a possibility at the littoral site for most of the season except at the end of the summer stratification when the CH_4 flux is higher than the NH_4^+ flux.

Calculated fluxes of O_2, CH_4, and NH_4^+ for Hamilton Harbour littoral and profundal sediments were within the ranges reported for Lake Vechten littoral and profundal sediments (Sweerts et al. 1991) and mass balance calculations of O_2 consumption and CH_4 and NH_4^+ production in Lake St. George hypolimnion (Bédard and Knowles 1991). Comparing CH_4 fluxes with O_2 fluxes for Hamilton Harbour, if all the CH_4 flux is consumed by the methanotrophs, these bacteria would account for 100% of the O_2 consumed in the profundal site compared with only 2% at the littoral site, similar to findings for Lake Vechten (Sweerts et al. 1991).

These flux calculations suggest that CH_4 oxidation is likely to be the major O_2 sink in Hamilton Harbour sediments. This sink, on the other hand, is related to the methanogenic activity which defines the size of the CH_4 reservoir. CH_4 production is the last step in the mineralization of organic carbon by successive microbial populations. Methanogens are dependent on fermentative bacteria for their source of H_2, CO_2, and/or acetate. We found that sediment profiles of potential CH_4 production rates followed a single exponential decay function ($f = ae^{(-bx)}$) (where f is the potential CH_4 production and x the sediment depth) with parameters $a = 1.106 \pm 0.040$ (site 906) and 0.208 ± 0.099 (site 910) and $b = 0.221 \pm 0.010$ (site 906) and 0.221 ± 0.132 (site 910) (see Materials and methods for a description of the procedure followed). It is likely that the decrease in potential CH_4 production with depth indicates the decrease in nonrefractory carbon. It is tempting to use the decay function as an approximation of the mineralization of nonrefractory organic carbon in this system by relating the decrease in potential CH_4 production rates to a sediment depth which can then be subtituted to a time scale by using sedimentation rates. It would then be possible to estimate a time lag in the response of the Hamilton Harbour system to a decrease in organic matter inputs to the sediment. Such an estimation may be useful in evaluating measures to correct the depletion of hypolimnetic O_2 in Hamilton Harbour, which is a major consequence of the deterioration of this system following industrialization (Polak and Haffner 1978). Using the decay function along with estimates of sedimentation rates in the Harbour (3.33 mm sediment·yr^{-1} (Nriagu et al. 1983) and 4.07 mm sediment·yr^{-1} (Mayer and Johnson 1994)), we estimated that a reduction of 90% in the potential rate of CH_4 production at the profundal site would take 2.8 ± 0.3 yr and a 99% reduction would take 5.6 ± 0.6 yr. A reduction to a similar level at the littoral site would take 0.8 ± 0.1 and 3.6 ± 0.4 yr, respectively. This may be taken as an indication of the time frame required for the system to respond to a decrease in inputs of organic matter causing lower CH_4 production rates and reducing the sediment methanotrophic O_2 sink.

We conclude that CH_4 metabolism in Hamilton Harbour sediment is likely to be as important in the overall nitrogen cycle as it is for benthic O_2 consumption. CH_4 oxidation by methanotrophs can suppress nitrification by competing for O_2 as found in sediment slurry experiments (Roy and Knowles 1994) and further supported by the data presented here. Nitrification may be the main source of NO_3^- for denitrifying bacteria in freshwater sediment with low pore water NO_3^- concentration (Rysgaard et al. 1993). This is the case in Hamilton Harbour (Roy et al. 1994). Because local loss of fixed nitrogen occurs mainly through denitrification, nitrification is a key link in the nitrogen cycle in Hamilton Harbour. By suppressing nitrification, active methanotrophs may play a key role in the nitrogen cycle of such eutrophic systems. Another effect of methanotrophic activity on the nitrogen cycle may be through a substantial immobilization of NH_4^+, or even of NO_3^- produced from nitrification as found previously (Roy and Knowles 1994). The high calculated CH_4 fluxes reported here support such a hypothesis. Immobilization would therefore short-circuit the nitrogen cycle. The magnitude of this immobilization *in situ* remains to be determined. The high CH_4 concentration observed here also suggests that significant CH_4-dependent nitrification is unlikely. A differential inhibitor that would be specific to the ammonia monooxygenase with little effect on the methane monooxygenase would allow such a determination. Allylsulfide, a recently discovered mechanism-based inhibitor of the ammonia monooxygenase of *Nitrosomonas europaea* (Juliette et al. 1993), affects CH_4 oxidation much less than nitrification in Hamilton Harbour sediment (Roy and Knowles 1995) and so far appears to fit the description of a differential inhibitor (Bédard and Knowles 1989).

Acknowledgments

This work was supported by grants from the Natural Sciences and Engineering Research Council of Canada (NSERC) (Great Lakes University Research Fund) to R.K. and M.N.C., and NSERC and FCAR postgraduate fellowships to R.R. We thank R. LeSage for technical assistance. We also thank C. Dumont and J. Hillsdon for carrying out the enumerations of nitrifying bacteria and methanotrophic bacteria, respectively.

© 1996 NRC Canada

References

Abeliovich, A., and Vonshak, A. 1992. Anaerobic metabolism of *Nitrosomonas europaea*. Arch. Microbiol. **158**: 267–270.

Alexander, M. 1965. Most-Probable-Number method for microbial populations. Methods of soil analysis. Part 2. Chemical and microbiological properties. *Edited by* C.A. Black. American Society for Agronomy, Madison, Wis. pp. 1467–1472.

Bédard, C., and Knowles, R. 1989. Physiology, biochemistry, and specific inhibitors of CH_4, NH_4^+, and CO oxidation by methanotrophs and nitrifiers. Microbiol. Rev. **53**: 68–84.

Bédard, C., and Knowles, R. 1991. Hypolimnetic O_2 consumption, denitrification, and methanogenesis in a thermally stratified lake. Can. J. Fish. Aquat. Sci. **48**: 1048–1054.

Bosse, U., Frenzel, P., and Conrad, R. 1993. Inhibition of methane oxidation by ammonium in the surface layer of a littoral sediment. FEMS Microbiol. Ecol. **13**: 123–134.

Hynes, R.K., and Knowles, R. 1982. Effect of acetylene on autotrophic and heterotrophic nitrification. Can. J. Microbiol. **28**: 334–340.

Iversen, N., and Jørgensen, B.B. 1993. Diffusion coefficients of sulfate and methane in marine sediment: influence of porosity. Geochim. Cosmochim. Acta, **57**: 571–578.

Jones, J.G., and Simon, B.M. 1981. Differences in microbial decomposition processes in profundal and littoral lake sediments, with particular references to the nitrogen cycle. J. Gen. Microbiol. **123**: 297–312.

Juliette, L.Y., Hyman, M.R., and Arp, D.S. 1993. Mechanism-based inactivation of ammonia monooxygenase in *Nitrosomonas europaea* by allylsulfide. Appl. Environ. Microbiol. **59**: 3728–3735.

Laanbroek, H.J., and Schotman, J.M.T. 1991. Effect of nitrite concentration and pH on Most Probable Number enumerations of non-growing *Nitrobacter* spp. FEMS Microbiol. Ecol. **85**: 269–278.

Lerman, A. 1979. Geochemical processes: water and sediment environment. John Wiley and Sons, New York.

Li, Y.-H., and Gregory, S. 1974. Diffusion of ions in seawater and deep-sea sediments. Geochim. Cosmochim. Acta, **38**: 703–714.

Lidstrom, M.E., and Somers, L. 1984. Seasonal study of methane oxidation in Lake Washington. Appl. Environ. Microbiol. **47**: 1255–1260.

Mayer, T., and Johnson, M.G. 1994. History of anthropogenic activities in Hamilton Harbour as determined from the sedimentary record. Environ. Pollut. **86**: 341–347.

Megraw, S.R., and Knowles, R. 1987. Active methanotrophs suppress nitrification in a humisol. Biol. Fertil. Soils **4**: 205–212.

Megraw, S.R., and Knowles, R. 1989. Methane-dependent nitrate production by a microbial consortium enriched from a cultivated humisol. FEMS Microbiol. Ecol. **62**: 359–366.

Nriagu, J.O., Wong, H.K.T, and Snodgrass, W.J. 1983. Historical records of metal pollution in sediments of Toronto and Hamilton harbours. J. Great Lakes Res. **9**: 365–373.

Polak, J., and Haffner, G.D. 1978. Oxygen depletion of Hamilton Harbour. Water Res. **12**: 205–215.

Rohlf, F.J., and Sokal, R.R. 1981. Statistical tables. 2nd ed. W.H. Freeman, New York.

Roslev, P., and King, G. 1994. Survival and recovery of methanotrophic bacteria starved under oxic and anoxic conditions. Appl. Environ. Microbiol. **60**: 2602–2608.

Roy, R., and Knowles, R. 1994. Effects of methane metabolism on nitrification and nitrous oxide production in polluted freshwater sediment. Appl. Environ. Microbiol. **60**: 3307–3314.

Roy, R., and Knowles, R. 1995. Differential inhibition by allylsulfide of nitrification and methane oxidation in freshwater sediment. Appl. Environ. Microbiol. **61**: 4278–4283.

Roy, R., Legendre, P., Knowles, R., and Charlton, M.N. 1994. Denitrification and methane production in sediment of Hamilton Harbour (Canada). Microb. Ecol. **27**: 123–141.

Rysgaard, S., Risgaard-Petersen, N., Nielsen, L.P., and Revsbech, N.P. 1993. Nitrification and denitrification in lake and estuarine sediments measured by the ^{15}N dilution technique and isotope pairing. Appl. Environ. Microbiol. **59**: 2093–2098.

Schmidt, E.L., and Belser, L.W. 1982. Nitrifying bacteria. *In* Methods of soil analysis. Part 2. Chemical and microbiological properties. 2nd ed. *Edited by* A.L. Page. American Society of Agronomy and Soil Science Society of America, Madison, Wis. pp. 1027–1042.

Sokal, R.R., and Rohlf, F.J. 1981. Biometry. 2nd ed. W.H. Freeman, New York.

Steudler, P.A., Bowden, R.D., Melillo, J.M., and Aber, J.D. 1989. Influence of nitrogen fertilization on CH_4 uptake in temperate forest soils. Nature **341**: 314–316.

Sweerts, J.-P.R.A., Bär-Gilisen, M.-J., Cornelese, A.A., and Cappenberg, T.E. 1991. Oxygen consuming processes at the profundal and littoral sediment-water interface of a small meso-eutrophic lake (Lake Vechten, The Netherlands). Limnol. Oceanogr. **36**: 1124–1133.

Wilhelm, E.R., Battino, R., and Wilcock, R.J. 1977. Low pressure solubility of gases in liquid water. Chem. Rev. **2**: 219–262.

© 1996 NRC Canada

New techniques for 3-D video tracking of fish swimming movements in still or flowing water

Nicholas F. Hughes and Lon H. Kelly

Abstract: We describe three new techniques to track fish swimming movements in 3-D, in either still or flowing water. The first technique uses two or more video cameras to track a single point in 3-D. This method is more general, simpler, more flexible, and more precise than the widely used stereo method. Its use of a 3-D calibration quadrat frees the investigator to arrange cameras and adjust zoom lenses as he or she pleases, in contrast with the rather stringent requirements of the stereo method. It also allows a simple one-step rectification of all sources of systematic errors such as perspective effects, refraction at the air–water interface, and spherical distortion by the lens. The second technique expands the first to allow tracking of the fish's midline in 3-D. This simplifies tracking of the fish's center of mass and should facilitate the application of models that describe how swimming thrust is produced by a fish's body movements. The third technique allows estimation of swimming speed for fish foraging in flowing water, where there is significant velocity shear, permitting more accurate estimates of energy expenditure.

Résumé : Nous décrivons trois nouvelles techniques pour suivre dans trois dimensions les mouvements de poissons placés en eaux dormantes ou mouvantes. Avec la première, nous faisons appel à au moins deux caméras vidéo pour suivre les déplacements tridimensionnels d'un point unique. Cette méthode est plus générale, plus simple, plus souple et plus précise que la méthode stéréoscopique usitée. Comme elle utilise un quadrat tridimensionnel de référence, elle donne le loisir au manipulateur de disposer les caméras et d'ajuster les lentilles à focale variable à sa guise, ce qui n'est pas le cas avec la méthode stéréoscopique qui, elle, est plutôt contraignante. Cette première technique permet de corriger en une seule opération simple les erreurs systématiques de toutes les sources comme les effets de perspective, la réfraction à l'interface air–eau et la déformation sphérique attribuable aux lentilles. La deuxième technique, fondée sur la précédente, permet de suivre en trois dimensions les déplacements de l'axe longitudinal des poissons, ce qui simplifie la poursuite de leur centre de masse et qui devrait faciliter l'application de modèles décrivant comment le poisson produit sa poussée motrice par ses mouvements. La troisième technique permet d'estimer la vitesse de nage de poissons en quête de nourriture dans des eaux mouvantes où existe un fort cisaillement attribuable à la vitesse de l'eau. Ainsi, il est possible d'obtenir des évaluations plus précises de leur dépense d'énergie.
[Traduit par la Rédaction]

Introduction

The purpose of this paper is to describe some new techniques for 3-D video tracking of a fish's swimming movements. We developed these techniques during our research on the prey interception maneuvers performed by drift-feeding stream fishes, and we explain the techniques with this application in mind. However, it should be possible to apply the techniques to a broad range of questions about fish swimming in still or moving water, in either laboratory or field situations.

The three techniques we describe are as follows. First is a new way to track points in 3-D. This technique is more general than the stereocinematographic method described by Boisclair (1992) and, as a consequence, has several significant advantages, including increased simplicity, flexibility, and precision, issues that we will address in detail later. Second, we describe a way to track the 3-D location of the fish's undulating midline. This allows a much more complete visualization of swimming movements than can be provided by tracking single identifiable points, such as the fish's nose or tail. By using the midline, we also simplify tracking the fish's center of mass, and subsequent calculation of acceleration rates and turn radii. This technique should facilitate the application of models that describe the forces involved in fish propulsion (e.g., Lighthill 1971) to 3-D maneuvers; currently these analyses have been restricted to 2-D (see Webb 1975, Blake 1983, and Videler 1993 for an introduction to the kinematics, hydrodynamics, and energetics of fish swimming). Finally, we show how to estimate the speed of a drift-feeding stream fish through the water, as it maneuvers across velocity shear in its foraging area, permitting more accurate estimates of its swimming costs.

We describe each of these three techniques in turn, followed by a discussion of their advantages and disadvantages in comparison with existing techniques.

Received December 30, 1994. Accepted May 2, 1996.
J12687

N.F. Hughes. Behavioral Ecology Research Group, Department of Biological Sciences, Simon Fraser University, Burnaby, BC V5A 1S6, Canada.
L.H. Kelly. P.O. Box 82840, Fairbanks, AK 99708, U.S.A.

Can. J. Fish. Aquat. Sci. **53**: 2473–2483 (1996).

I. Tracking points in 3-D[1]

The technique we describe here is based on the observation that "...3-D coordinates may be determined from *any* two

[1] Computer programs to perform the analyses described in this paper are freely available from the authors, e-mail: fnnfh@aurora.alaska.edu or fflak@aurora.alaska.edu.

© 1996 NRC Canada

Fig. 1. Field setup used to video tape the prey-interception maneuvers of a 26.6-cm fork length Arctic grayling (*Thymallus arcticus*) on August 3 and 7, 1993. The channel on Twelvemile Creek, Alaska, was a fairly uniform 120 cm wide and at least 30 cm deep, with a shallow bowl-shaped depression about 45 cm deep in the center. A large alcove in one wall contained a Sony V801 camcorder, mounted in an Amphibico underwater housing, and pointed into the channel from the side. A second V801 camcorder was mounted overhead. The 3-D quadrat was momentarily positioned in the stream channel (as shown) before or after filming fish maneuvers to calibrate the two camera views and to establish a coordinate system with which to describe fish movements. The upper face of the quadrat was positioned at the water surface and the x-axis was aligned with the direction of flow; (x,y,z)-coordinates of six corners of the quadrat are labelled. The upper face of the quadrat defines the plane $z = 30$, at the water surface. The plane $z = 0$ is 30 cm below the water surface. Discharge through the channel was controlled, and prey-interception maneuvers were filmed at both fast (maximum velocities of about 40 cm·s^{-1}) and slow flows (maximum velocities of about 20 cm·s^{-1}). Inset A: side view of the three balls, ballasted to float at different depths, that were used to map water flow in the experimental channel.

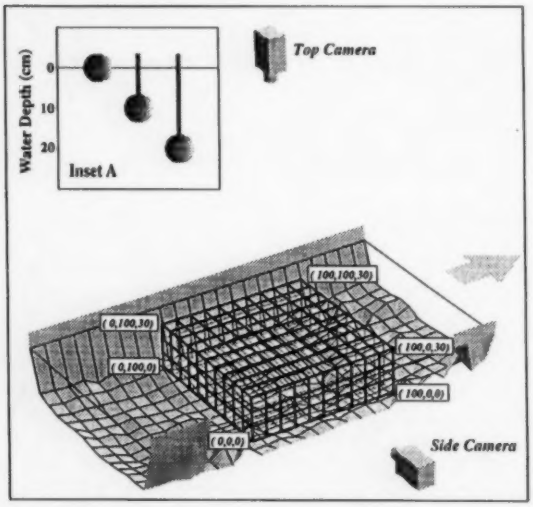

or more 2-D perspective views, provided these views are known" (Potel and Wassersug 1981). The truth of this fact notwithstanding, we have been unable to find any account of how it might be implemented in practice; we show how it can be developed into a simple, flexible, and precise 3-D tracking system.

We rely on a cagelike 3-D reference quadrat to provide the information necessary to calibrate the 2-D views of the cameras (Fig. 1). After the location and zoom settings of the cameras have been determined, this quadrat is momentarily placed in the cameras' field of view, and its image is captured on video tape. Information extracted from images of the quadrat is used to calculate the directions of lines of sight from each of the cameras to a point of interest. The 3-D coordinate at which the lines of sight from two or more cameras intersect is our estimate of the 3-D location of that point. In this section we describe these steps, evaluate the size and source of errors in our application of the technique to drift-feeding stream fish, and provide a note on the hardware we used for video analysis.

Lines of sight

To visualize how we define lines of sight, refer to the setup described in (Fig. 1) and imagine that the 3-D quadrat (Fig. 1) is still in place, and that the fish is swimming inside it. The line of sight from the overhead camera to the fish's nose is defined by the coordinates at which it passes through the upper and lower surfaces of the quadrat. By definition, the upper camera looks directly along this line of sight, so these coordinates correspond to the apparent position of the fish's nose in the upper and lower surfaces of the quadrat (examination of Fig. 2 should help visualize this). Likewise, the line of sight from the side camera to the fish's nose is defined by the coordinates at which it passes through the near and far surfaces of the quadrat. The challenge is to determine the 3-D coordinates describing these lines of sight from 2-D video images, in which the quadrat is no longer present, or has yet to be introduced.

To appreciate how we convert 2-D screen to 3-D quadrat coordinates, it helps to understand the details of these two coordinate systems. 2-D screen coordinates are used to describe the location of a point of interest on the digitized image. We displayed images in a rectangular "view" on the screen that was 640 pixels wide and 480 pixels high, so if the tip of the fish's nose was 300 pixels from the left edge of this view and 200 pixels from the bottom edge, its view coordinate (x_v,y_v) would be (300,200). Now, imagine that the 3-D quadrat, as seen from overhead, is visible in a displayed image (Fig. 2). Each of the nodes on the quadrat would have a 2-D view coordinate, but it would also have a known 3-D coordinate (x_q,y_q,z_q), expressed in terms of centimetres in the real world. In fact, since the quadrat *is* the calibration object, it defines the real-world coordinate system (Fig. 1).

By determining the 2-D screen coordinates of each of the 122 nodes in the quadrat's near face, we obtain the data we need to fit a regression model that estimates either x_q or y_q, from a linear combination of x_v and y_v, (z_q is already known to be 30, by definition). We then repeat this process for the far face of the quadrat (z_q is now 0, by definition, since the quadrat is 30 cm high). The regression model we used was developed by Buckley (1992), for rectification in remote sensing applications; the 10 parameters p_1–p_{10} are estimated by least squares:

$$(1)\qquad x_q = p_1 + p_2x_v + p_3y_v + p_4x_v^2 + p_5x_vy_v + p_6y_v^2 + p_7x_v^3 + p_8x_v^2y_v + p_9x_vy_v^2 + p_{10}y_v^3$$

$$(2)\qquad y_q = p_1 + p_2x_v + p_3y_v + p_4x_v^2 + p_5x_vy_v + p_6y_v^2 + p_7x_v^3 + p_8x_v^2y_v + p_9x_vy_v^2 + p_{10}y_v^3.$$

The four sets of parameters that result can be used to convert a 2-D screen coordinate into the two 3-D quadrat coordinates that define the points at which a line of sight pierces the near and far surfaces of the quadrat (or, more ex-

© 1996 NRC Canada

Fig. 2. Top and side views of the nodes making up the near and far surfaces of 3-D quadrat, as seen by the cameras in Fig. 1. This illustrates how a line of sight from a camera to a point on the image can be described by the coordinates at which it passes through the planes containing these faces. The 3-D quadrat and 2-D screen coordinates of the four corner nodes in each face are show (near face in bold italic, far face in italic). Quadrat coordinates are expressed in terms of centimetres in the real world, as defined by the quadrat; screen coordinates are expressed as pixels from bottom left corner of the 640 × 480 pixel area in which the image is displayed. Data for all the nodes in a face can be used to fit a regression model with which to estimate the 3-D coordinate at which a line of sight pierces the plane containing that face (see text).

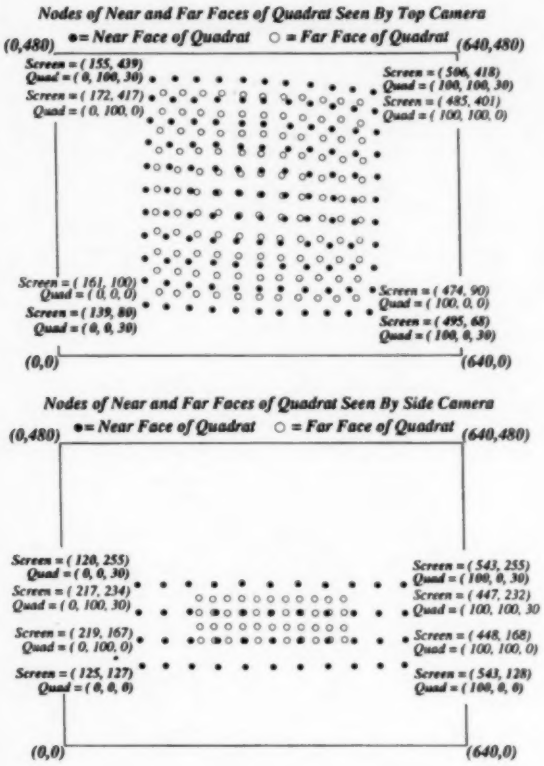
Nodes of Near and Far Faces of Quadrat Seen By Top Camera
(0,480)
●= Near Face of Quadrat ○ = Far Face of Quadrat
(640,480)
Screen = (155, 439)
Quad = (0, 100, 30)
Screen = (172, 417)
Quad = (0, 100, 0)
Screen = (506, 418)
Quad = (100, 100, 30)
Screen = (485, 401)
Quad = (100, 100, 0)
Screen = (161, 100)
Quad = (0, 0, 0)
Screen = (139, 80)
Quad = (0, 0, 30)
Screen = (474, 90)
Quad = (100, 0, 0)
Screen = (495, 68)
Quad = (100, 0, 30)
(0,0)
(640,0)
Nodes of Near and Far Faces of Quadrat Seen By Side Camera
(0,480)
●= Near Face of Quadrat ○ = Far Face of Quadrat
(640,480)
Screen = (120, 255)
Quad = (0, 0, 30)
Screen = (217, 234)
Quad = (0, 100, 30)
Screen = (219, 167)
Quad = (0, 100, 0)
Screen = (125, 127)
Quad = (0, 0, 0)
Screen = (543, 255)
Quad = (100, 0, 30)
Screen = (447, 232)
Quad = (100, 100, 30
Screen = (448, 168)
Quad = (100, 100, 0)
Screen = (543, 128)
Quad = (100, 0, 0)
(0,0)
(640,0)

actly, pierces the *planes* containing the near and far surfaces of the quadrat). The same process can then be used for the side view. The only difference here is that the near and far surfaces of the quadrat lie in planes defined by $y = 0$ and $y = 100$, respectively (Fig. 1), so the regression models are used to estimate x_q and z_q coordinates.

The application of this rectification technique does a lot for us. It removes nearly all systematic error due to differences in scaling, translation, and rotation of the quadrat coordinate system relative to the view coordinate system, radial distortion by the camera lens, perspective effects, and refraction at the water surface ($R^2 > 0.9995$ for all eight fits of the model needed to rectify the four quadrat surfaces shown in Fig. 2).

Intersection of lines of sight

The position of a feature of interest can be fixed in 3-D by finding the intersection of the lines of sight for top and side views. Of course the lines will rarely intersect exactly and so in fact you have to find the center of the shortest possible "bridge" between the two. This method works as long as the two lines are not parallel. It is vital that the top and side views are synchronous. We synchronized our cameras using the RC timecode feature of the V801 camcorder, which gives a unique number to each frame on the tape.

To find the shortest possible bridge between two lines of sight, we make use of the fact that this is the only possible bridge perpendicular to both of the lines of sight. When the two lines are not parallel, there is only one solution to this geometry problem, which we solved following Johnson and Kiokemeister (1969).

Parametric equations describing the (x, y, z) locations of the two lines of sight can be written

$$(3) \qquad line_1 : x = a + ht,\ y = b + kt,\ z = c + lt$$

$$(4) \qquad line_2 : x = a' + h't',\ y = b' + k't',\ z = c' + l't'$$

where (a, b, c) and (a', b', c') are known (x, y, z)-coordinates of points on $line_1$ and $line_2$, respectively, (h, k, l) and (h', k', l') are vectors describing the directions of the two lines, and t, and t' are scalars that can have any value. We need to find values for t and t' that will give us the location at which the bridge touches $line_1$ and $line_2$, respectively. We know the coordinates of a pair of points on each line of sight ($p_{1,1}$ and $p_{1,2}$ for $line_1$ and $p_{2,1}$ and $p_{2,2}$ for $line_2$). We can use the first member of each pair as our known points on $line_1$ and $line_2$, so $(a, b, c) = p_{1,1}$ and $(a', b', c') = p_{2,1}$. We can calculate the vectors describing the directions of the lines as $(h, k, l) = p_{1,2} - p_{1,1}$ and $(h', k', l') = p_{2,2} - p_{2,1}$.

Next we make use of the fact that two vectors $\boldsymbol{v}_1$ and $\boldsymbol{v}_2$ are perpendicular only when $\boldsymbol{v}_1 \cdot \boldsymbol{v}_2 = 0$ to set up two equations describing line segments that connect $line_1$ and $line_2$:

$$(5) \qquad (a + ht - a' - h't')h + (b + kt - b' - k't')k + (c + lt - c' - l't')l = 0$$

$$(6) \qquad (a + ht - a' - h't')h' + (b + kt - b' - k't')k' + (c + lt - c' - l't')l' = 0.$$

Equation 5 describes all possible connecting lines that are perpendicular to $line_1$; only one of these solutions will also be perpendicular to $line_2$. Equation 6 similarly describes all possible connecting lines that are perpendicular to $line_2$. t and t' are the only unknowns. By solving for values of t and t' that satisfy both equations simultaneously, and then substituting t and t' into equations 3 and 4, we can locate a point on $line_1$ (p_3) and a point on $line_2$ (p_4) that are connected by a bridge perpendicular to both lines of sight.

Solutions for t and t' are

$$(7) \qquad t = -\frac{df}{m+n} - \frac{eg}{m+n}$$

$$(8) \qquad t' = -\frac{di}{m+n} - \frac{ej}{m+n}$$

© 1996 NRC Canada

where

$$d = (ah' - a'h' + bk' - b'k' + cl' - c'l')$$

$$e = (ah - a'h + bk - b'k + cl - c'l)$$

$$f = hh' + kk' + ll'$$

$$g = -h'^2 - k'^2 - l'^2$$

$$i = h^2 - k^2 - l^2$$

$$j = -(hh') - kk' - ll'$$

$$m = -(h'^2k^2) - h^2k'^2 - h'^2l^2 - k'^2l^2 - h^2l'^2 - k^2l'^2$$

$$n = 2kk'll' + 2hh'll' + 2hh'kk'.$$

The midpoint of this bridge, and our best estimate of the intersection between $line_1$ and $line_2$, is $p_3 + 0.5(p_4 - p_3)$.

Errors in locating points

To give an idea of the size of errors made in determining the 3-D location of points, we estimated the location of 44 points along the four edges of the quadrat parallel to the x-axis. This approach quantifies errors that result from incorrect digitizing of points, disruption of the image by surface ripples in the overhead view, and imprecision of rectification regressions. It does not quantify errors due to inaccuracies in quadrat construction. The mean error in locating the positions of these points was 0.47 cm; the standard deviation was 0.27 cm.

Errors in synchronizing video frames from the two cameras will also produce errors in fixing the location of moving targets. The size of this error e will be proportional to the size of the synchronization error s and the velocity of the target u, so that $e \leq 0.5\ su$. With a frame rate of 30 frames per second, it should be possible to keep synchronization errors to less than 1/60 of a second. The size of any synchronization error can be determined by plotting the length of the bridge between lines of sight against velocity of the target. For accurate analysis, distances and velocities should be measured in either the x, y, or z direction. The slope of this relationship is equal to the synchronization error in seconds. Using this method, we could not detect any synchronization error in the analyses performed in this paper.

Image analysis hardware

We used the built-in video capabilities of a NeXTdimensions computer to digitize video images. We used a Sony V801 camcorder to play back the tapes. By linking a serial port of the computer with the LANC port on the camcorder via a Sony VBOX, we could control the camcorder from the computer using the Sony VISCA protocol. To improve the quality of the digitized image, we passed the signal from the camcorder to the video-in port on the computer via a NovaMate timebase corrector. This helped to improve the signal produced by the camcorder in freeze-frame mode. Digitizing and processing a maneuver lasting 10 s at 0.1 s resolution with this setup takes about half an hour, most of which time is spent advancing frame by frame through the video tape. A medium such as CD ROM, which allows rapid random access to frames, could speed up this process greatly.

II. Tracking the fish's midline in 3-D

In this section, we describe how to track the movements of the fish's midline, an imaginary line that runs down the center of the fish's body from its nose to the fork of its tail. Our approach to this problem depends on the assumption that the swimming fish bends laterally, but not dorsally or ventrally, a reasonable assumption for most species. The first step, then, is to determine the orientation of the plane that contains this midline. Next, looking at the overhead view, we digitize a series of points along the center of the fish's body, from nose to tail, and convert these into lines of sight. The intersections between the plane and these lines of sight describe the fish's midline in 3-D. We used just two points, the fish's nose and the fork of its tail, to determine the plane of its midline. This allows the fish to pitch but requires that we assume it does not roll around a straight line between these two points. If a third point on the midline, about midway between the nose and the tail, is used, it is not necessary to make this assumption, and it is possible to describe any roll that occurs. The main challenge when using the third point is that it requires very accurate digitizing; otherwise, large errors estimating the roll of the fish will be made, particularly when the fish's body is nearly straight.

Finding the plane of the midline

The plane containing the fish's midline can be defined by the standard equation $hx + ky + lz = d$, where (h,k,l) is a vector normal to the plane and d is a constant found by multiplying the normal vector by any (x,y,z) point on the plane. When using two points to define this plane we first find two vectors $\boldsymbol{v}_1$ and $\boldsymbol{v}_2$. $\boldsymbol{v}_1$ describes the direction between the nose and tail of the fish ($p_1 = (a,b,c)$ and $p_2 = (a',b',c')$, respectively); $\boldsymbol{v}_2$ is perpendicular to $\boldsymbol{v}_1$ and parallel to the plane $z = 0$. $\boldsymbol{v}_1 = (v_{1,1}, v_{1,2}, v_{1,3}) = p_2 - p_1$, and $\boldsymbol{v}_2 = (v_{2,1}, v_{2,2}, v_{2,3}) = (v_{1,2}, -v_{1,1}, 0)$. The normal vector (h,k,l) and the scalar constant d are then

$$h = -v_{2,2}v_{1,3} + v_{1,2}v_{2,3} \quad (9)$$

$$k = v_{2,1}v_{1,3} - v_{1,1}v_{2,3} \quad (10)$$

$$l = -v_{2,1}v_{1,2} + v_{1,1}v_{2,2} \quad (11)$$

$$d = ha + kb + lc. \quad (12)$$

If three points ($(a,b,c) = p_1$, $(a',b',c') = p_2$, $(a'',b'',c'') = p_3$) along the midline of the fish are known, then we can calculate $\boldsymbol{v}_1$ and $\boldsymbol{v}_2$ as $\boldsymbol{v}_1 = p_2 - p_1$, and $\boldsymbol{v}_2 = p_3 - p_2$. Then the normal vector (h,k,l) and the scalar constant d can be calculated using equations 9–12.

Intersection of lines of sight with plane

The intersection of the lines of sight from the overhead camera with the plane of the fish's midline can be found as follows. If $p_1 = (a,b,c)$ and $p_2 = (a',b',c')$ describe a line of sight, $\boldsymbol{v}_1 = (v_{1,1}, v_{1,2}, v_{1,3}) = p_2 - p_1$ describes the direction of this line of sight, (h,k,l) is a vector normal to

© 1996 NRC Canada

Fig. 3. Top and side views of four prey-interception maneuvers by a 26.6-cm fork length Arctic grayling on August 7, 1993. In maneuvers *a* and *b* the fish intercepted a prey that would have passed about 40–45 cm to the right of its focal point. Maneuver *a* was performed at slow flow and maneuver *b* at fast flow; interception took 5.3 and 2.0 s, respectively. In maneuvers *c* and *d* the fish captured prey that would have passed about 25–35 cm directly over its focal point. Maneuver *c* was performed at slow flow and manever *d* at fast flow; interception took 3.9 and 1.1 s, respectively. Peak flows in the channel were 15–20 cm·s^{-1} at slow flow and 35–40 cm·s^{-1} at fast flow. Labels show the number of seconds elapsed since the beginning of the maneuver.

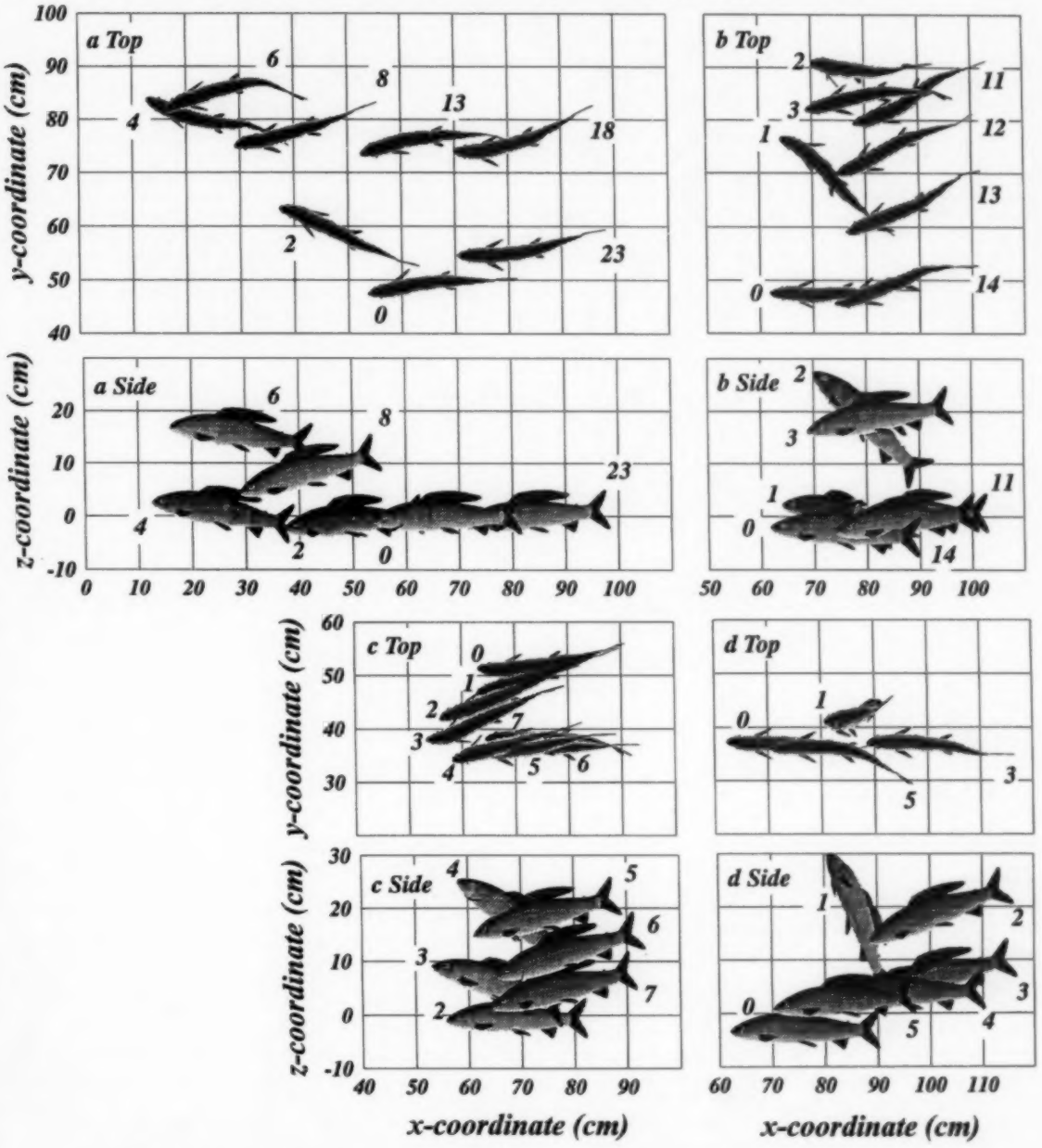

the plane, and d is the scalar constant, then the point on the fish's midline p_3 can be calculated as

$$p_3 = p_1 - \nu_1 \left(\frac{-d + ah + bk + cl}{\nu_{1,1}h + \nu_{1,2}k + \nu_{1,3}l} \right). \quad (13)$$

Figure 3 shows the picture of prey-interception maneuvers the application of these techniques can provide. Inspection of these maneuvers shows how important a 3-D description is to adequately describe the maneuvers; for example, the movements involved in overhead prey capture would be quite in-

© 1996 NRC Canada

Fig. 4. Velocity vectors in the fish's foraging area at slow flow, calculated from video tapes of ballasted balls floating at different depths (Fig. 1, Inset A). Each panel represents a horizontal slice through the fish's foraging area, starting at the surface (the slice defined by the plane $z = 30$ cm) and extending to the stream bed at 10-cm intervals. Note that the z-coordinate of the plane decreases with increasing depth; this is because of the right-handed coordinate system used to describe the foraging area (Fig. 1). The negative value of $z = -10$ simply means that this plane is 10 cm below the origin of the reference coordinate system established by the quadrat. Velocity vectors have a variable x and y component but the z component is assumed to be zero (i.e., there is no vertical water movement). The key indicates the magnitude of 0, 10, and 20 cm·s^{-1} vectors, but the length of the vectors in the panels varies continuously.

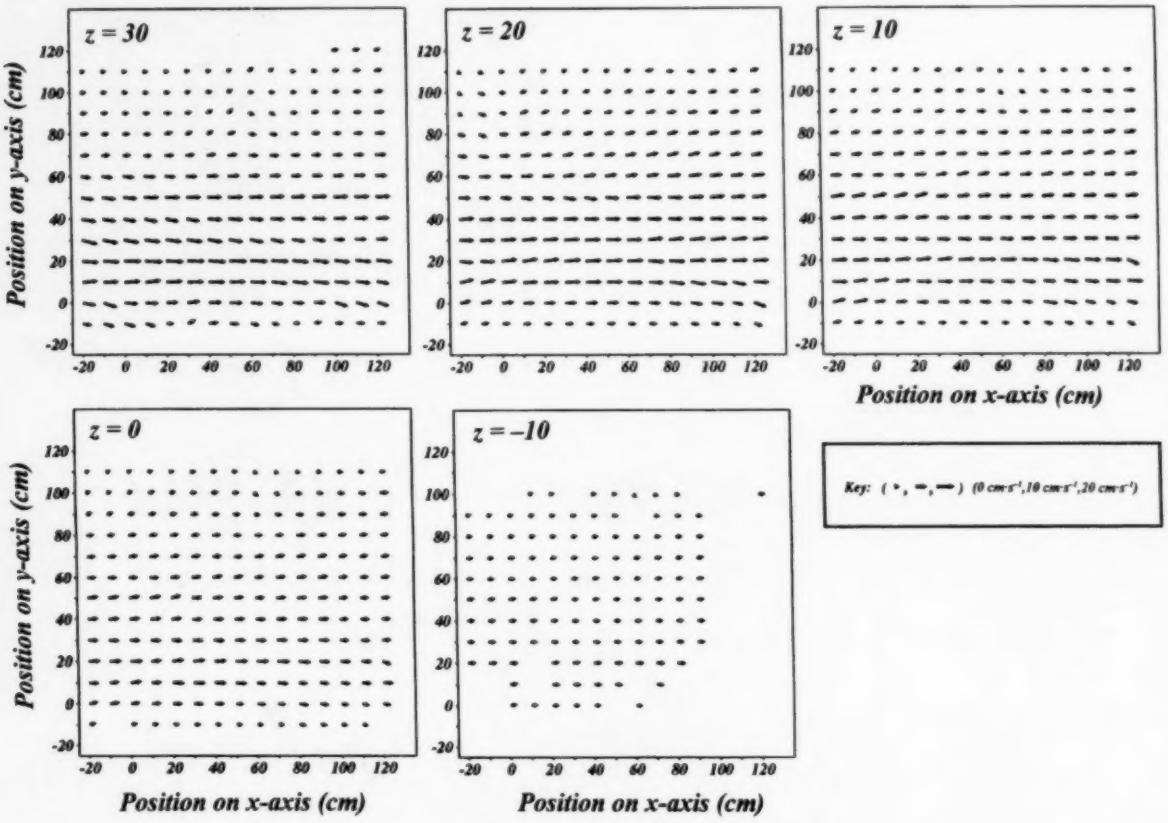

accurate if analysis was restricted to the x–y plane (overhead view).

III. Measuring swimming speed in moving water

Measuring swimming speed relative to the water, rather than relative to the ground, is essential for the accurate estimation of swimming costs. For example, consider a fish that moves 40 cm over the ground in the y direction during 1 s, in a stream where the water velocity is 50 cm·s^{-1} in the direction of the positive x-axis. The fish's speed relative to the ground is 40 cm·s^{-1}, but this is obviously not the correct value to use to calculate its swimming costs! In fact, we need to calculate how far the fish has moved through the water during this 1 s period. This can be calculated as the length of the vector obtained by subtracting downstream displacement by the current (50,0,0) from the movement of the fish over the ground (0,40,0). In this case the vector will be (−50,40,0); Pythagoras' theorem shows that this vector has a length of 64 cm·s^{-1}, which is the correct value to use when calculating swimming costs.

In principle this technique is simple to apply, but in practice it is complicated by the fact that water velocity can change rapidly over short distances within the fish's foraging area. For example, a fish may start a maneuver at its focal point, where the water velocity is typically low, often only 5–10 cm·s^{-1}, and then maneuver through areas where the velocity is much higher, perhaps 100 cm·s^{-1}. In this section, we show how to account for this velocity shear, by making a detailed map of water velocity in the fish's foraging area, and then referring to this map when converting measurements of the fish's movements over the ground into estimates of its speed through the water.

Modelling flow in the channel

To determine the pattern of water flow in the channel, we video taped plastic balls from overhead as they floated down

© 1996 NRC Canada

Fig. 5. Top and side views of two prey-interception maneuvers (Fig. 3, maneuvers *a* and *b*), transformed to remove the effect of downstream displacement by the current on the fish's position. Numbers show the seconds since the beginning of the maneuver. The distance between successive locations of the fish reflects the distance that the fish moved through the water rather than its movement relative to the stream bed.

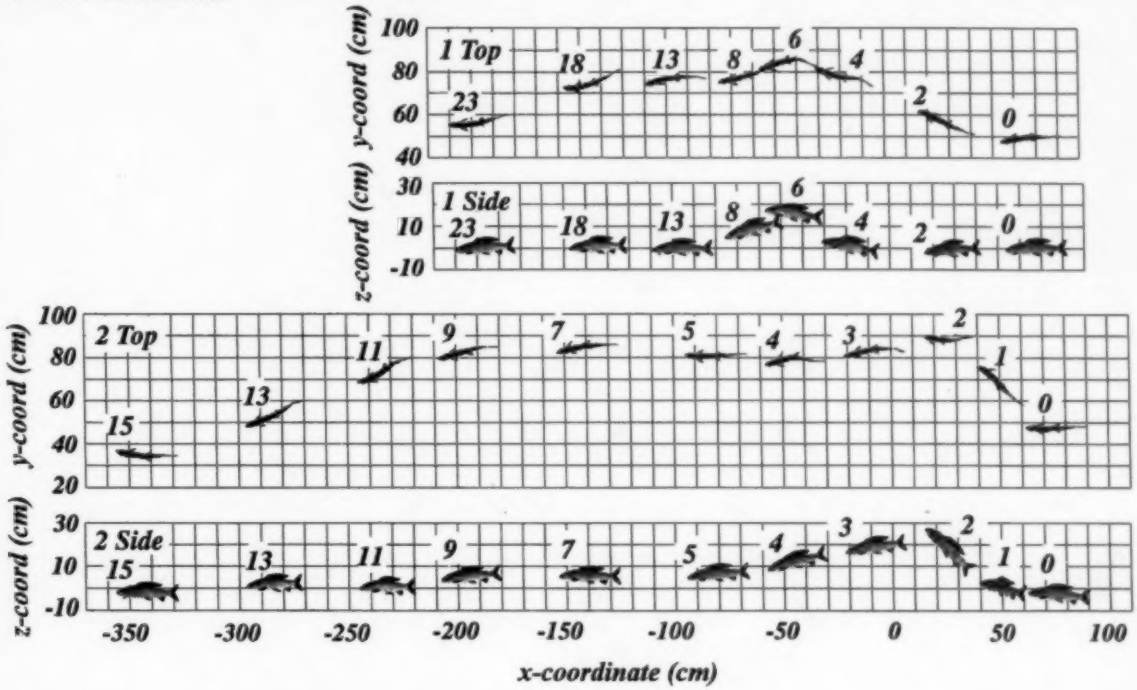

the channel (Fig. 1). These balls were ballasted to float at either 0, 10, or 20 cm depth using a slender balsa wood antenna and lead ballast, each type of ball giving us information on flow at a different depth in the channel. By floating each type of ball from about 20 different starting points, distributed across the width of the channel, it was possible to get quite a complete picture of flow in a short time, although later analysis of the video tape was time consuming, requiring about 3 h of digitizing and analysis. The random frame access provided by a CD ROM of the video would speed this up by an order of magnitude.

We converted the video taped data to velocity measurements as follows. First we determined the (x, y, z) location of the balls at half-second intervals. This could be done using just the overhead view, since the depth (and hence the z-coordinate) of the ball was known. We then broke up the line segments joining successive locations into subsegments 5 cm long. Finally, we calculated the velocity of the ball, in both x and y directions, as it travelled each of these subsegments. Velocity in the z direction was assumed to be 0. Each of the resulting velocity vectors was assigned the midpoint of the subsegment as its location. Using this procedure, each ball provided velocity vectors at 5-cm intervals along its path.

The use of the balls to obtain current velocity data is not a crucial part of the this technique. We could just as well have used a current meter. The main advantage was that it took much less time in the field (20–40 min rather than 2–3 h using a current meter), while accuracy was comparable with a newly calibrated electromagnetic meter. The balls also provided 2-D velocity vectors, which are difficult to get with the current meters commonly employed by aquatic ecologists.

We modelled the spatial distribution of flow by visualizing the channel divided into cubes 10 cm on a side. The axes of these cubes were aligned with the axes of the quadrat coordinate system, and the center of the top layer of cubes was level with the water surface at $z = 30$ cm, so the centers of successively deeper layers were at $z = 20$ cm, $z = 10$ cm, $z = 0$ cm, and $z = -10$ cm (see Fig. 1). Next, we assigned all the velocity vectors obtained from the balls to a cube, based on the vector's position. When more than one vector was assigned to a cube, these were averaged. Finally, we populated empty cubes with velocity vectors by linear interpolation along rows or columns of cubes, first in the y direction and then in the z direction. During interpolation, we assumed zero flow at the water–streambed boundary. Figure 4 shows the picture of flow that this provided.

Accounting for downstream displacement

To account for the effect of downstream displacement by the current, we determined the 3-D location of the fish's center of mass at 0.1-s intervals during the course of each maneuver (the fish's center of mass, for a fish shaped like a trout, can be conveniently determined as a point on the fish's midline one third of the distance between the fish's nose and its tail, Webb 1978). We then used our 3-D map of water velocity to estimate how far the fish was swept downstream during each 0.1-s periods. This allowed us to describe the maneuver such that the distance between successive positions of the fish rep-

© 1996 NRC Canada

Fig. 6. Speed versus time data for eight prey-interception maneuvers performed by a 26.6-cm fork length Arctic grayling at fast and slow flows. Four maneuvers were analysed at each flow level (top four and bottom four panels, respectively). In two of these the fish captured prey that would have passed almost directly overhead, about 25–35 cm above its focal point (left panels). In the other two the fish captured a prey that would have passed its focal point about 40–45 cm to its right (right panels). In each case the speed of the fish was estimated from the position of its center of gravity at 0.1-s intervals (after removing the effect of downstream displacement) smoothed with a moving average of 3. The maneuver begins when the fish sets off from its focal point to capture a prey and ends when it has returned to its focal point. The moment of prey capture is marked (pc).

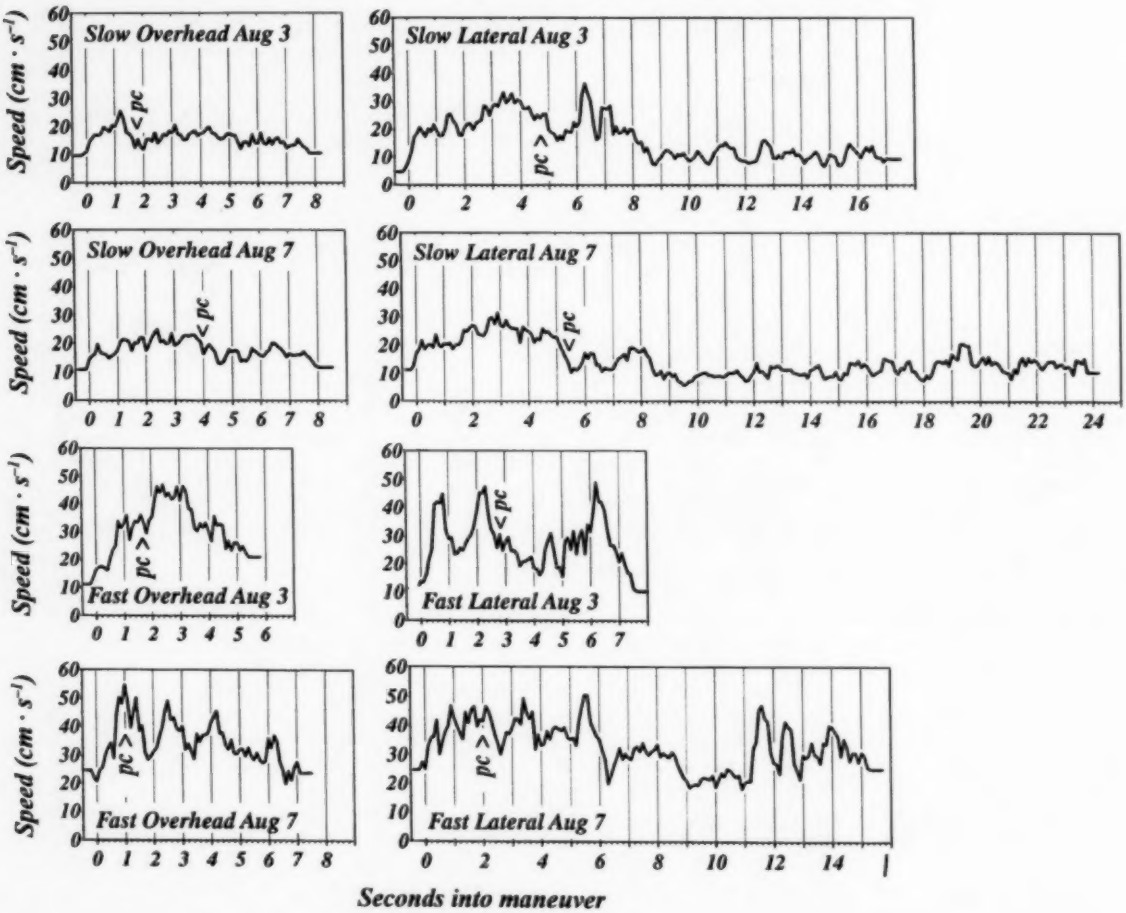

resents the distance the fish travelled through the water, rather than the distance it travelled relative to the ground (Fig. 5). As we showed at the beginning of this section, this is the kind of description we need to calculate the fish's swimming speed during a maneuver (Fig. 6) and its swimming costs (Hughes and Kelly 1996).

Discussion

This discussion focuses on the pros and cons of our techniques and their application in comparison with alternatives already available. Much of this attention is devoted to an evaluation of our method of tracking points in 3-D versus the stereo method, which has been widely used to determine the 3-D structure of fish shoals and bird flocks, and to measure the length and orientation and movements of fish (Cullen et al. 1965; Major and Dill 1978; Dill et al. 1981; Klimley and Brown 1983; Van Long et al. 1985; Van Long and Aoyama 1985; Aoki et al. 1986; Boisclair 1992). We devote less attention to our methods of tracking the fish's midline in 3-D and measuring the fish's swimming speed in velocity shear. This is because there are apparently no other techniques available to perform these tasks. We conclude with a mention of one possible application for these techniques, the investigation of adaptive design of prey-interception maneuvers by drift-feeding stream fishes, currently the subject of our own research interests.

Comparison with the stereo method

The method we describe for tracking points in 3-D differs from the stereo method in a number of ways. And since the

© 1996 NRC Canada

stereo method is currently the only really practical method for tracking fish movements in 3-D described in the literature (Boisclair 1992), it is appropriate to consider the pros and cons of these two alternative approaches. Note: Huse and Skiftesvik (1990) have also described a technique for tracking slow-moving larval fish in the laboratory. It requires specialized equipment for computer-controlled movement of the video camera and focusing ring. While their technique may have advantages in some situations, we will not consider it further here.

The stereo method uses a simple algorithm (Thompson 1966) to calculate the the 3-D location of an object from its position on the images captured by the two cameras. For this simple algorithm to work the optical axes of the two cameras must be aligned (Major and Dill 1978 did this using a laser). The separation of the optical axes and the distance from the second nodal point of the lens to the film plane must also be known. This latter quantity can be estimated empirically, or calculated from a knowledge of the camera's focal length (Klimley and Brown 1983). Additionally the lenses of the cameras must not distort the image; otherwise, a calibration field should be used to correct this distortion (e.g., Dill et al. 1981). If the fish are being filmed through an air–water interface (i.e., the cameras are in a waterproof box or above the water), refraction must be also taken into account, and this requires a knowledge of the geometry of the cameras relative to the air–water interface (e.g., Dill et al. 1981).

Our method frees the investigator from all these requirements of the stereo methods, and has no significant extra requirements of its own. The reason is that it conceptually subsumes the stereo method, being considerably more general. As a consequence, it will usually have greater simplicity, flexibility, and precision than the stereo method. In fact, it can be used in a way that "looks like" the stereo method, but requires no demanding camera alignment, or knowledge of lens characteristics. Several of the most significant practical advantages of our approach are detailed below.

The investigator can position the cameras as he or she pleases. This contrasts with the rather stringent requirements of the stereo method, and can be used to obtain a significant increase in precision. To illustrate this improvement, consider the expected precision of the technique we describe here with the stereo technique described by Boisclair (1992), in a situation similar to that illustrated in Fig. 1. In the technique we describe, one camera can be positioned to look down at the fish while the other views from the side. Using the stereo method, we would mount the stereo array in either the overhead or side position, with a separation of 10 cm between cameras (Boisclair 1992). Camera to target distances are approximately 2 m. Assume that the only errors in fixing the location of a target in 3-D are made when measuring the location of the target on images produced by the two cameras. If this error had magnitude corresponding to an x-mm shift of the actual target, in the plane of the image, then some simple geometry shows that the method we describe would err in locating the target by between 0 and $\sqrt{x^2+x^2}$ mm. The approximate error of the stereo method would be between x and $xd/(0.5s+x)$ mm, where d is the camera to subject distance and s is the separation between the optical axes of the cameras. If $x = 5$ mm, then the errors for the method we describe would range between 0 and 7 mm, while errors for the stereo method would range between 5 and 182 mm. In other words the maximum error would be about 26 times larger with the stereo method. Examination of the equations describing the size of errors shows that the technique we describe will be more precise than the stereo method whenever the distance between the cameras and the subject is large, in comparison with the distance between the two cameras in the stereo array. In practice, this will often be the case when filming feeding fish because the cameras must be close together so they have the overlapping fields of view essential for stereo analysis, and yet far enough from the fish to encompass its foraging area within their field of view.

Flexibility in positioning the cameras also means they can be arranged to provide complementary views of the subject. For example, in our investigations of prey-interception maneuvers by drift-feeding fish, we positioned one camera to provide an overhead view and one to provide and underwater side view (Fig 1). The importance of having these complementary views when analysing individual maneuvers cannot be overemphasized because in situations where the fish's movements were directly towards or away from one of the cameras, it can be virtually impossible for a human observer to detect the start and finish of the maneuver, or even whether a maneuver occurred at all. This makes it very hard to isolate individual maneuvers for analysis. By simultaneously playing back tapes of both views, this task becomes simple, but with a stereo system the problem would be hard to avoid.

A second way that our method can improve precision is to allow the investigator to use any convenient zoom setting, which can be different for each camera. For example, if the cameras have to be mounted far from the subject, they can be independently zoomed in so the fish's foraging area fills the view, allowing more precise digitizing of the fish's movements in later analysis. At best this would be inconvenient with the stereo method, which is designed to work with two cameras of equal, and fixed, focal lengths.

Precision can also be increased by the use of more than two cameras. This would also allow the investigator to track animals in situations where two cameras cannot always keep the subject (or part of a subject) in view, drift-feeding damsel fish around a coral head, for example, or detailed movement of a fish's body and fins during turning maneuvers. The stereo algorithm is not amenable to these kinds of adaptations.

Both precision and accuracy are promoted by our use of advanced rectification techniques (Buckley 1992). These correct for several sources of systematic distortions that occur when capturing a 3-D scene as a 2-D image, including the effects of scaling, translation, and rotation of the quadrat coordinate system relative to the image coordinate system, radial distortion by the camera lens, perspective effects, and refraction at the water surface. The combined use of the 3-D quadrat, our selected rectification techniques, and the algorithms used to establish the 3-D location of points in space allow a one-step unified correction of all these sources of error. Correction of these errors is more complex when using the stereo method (e.g., Dill et al. 1981).

Increased precision of fixing points in 3-D is particularly desirable when estimating acceleration rates. This is because errors due to framing rate decrease as framing rate increases, while errors due to imprecision in fixing points in 3-D in-

© 1996 NRC Canada

crease with framing rate (Harper and Blake 1989). As a consequence of this trade-off, there is an optimal frame rate which minimizes errors. The more precisely points can be fixed in 3-D the higher the optimal framing rate and the smaller the error in measuring acceleration rates.

Finally, since the method we describe is more general than the stereo method, it can be used in a "stereolike" way, while simultaneously avoiding the difficulties inherent in the stereo method. To achieve this, two cameras are mounted a set distance apart on a beam (alignment not crucial) and the zoom setting for each camera decided upon. Once arranged the cameras are used to capture an image of a 3-D quadrat. Preferably the quadrat should be at about the same range as the expected subjects and nearly fill the field of view. The investigator can then relocate the camera array and film subjects of interest, without any further use of the quadrat. As long as the relative positions of the two cameras and their zoom settings are not changed, the 3-D location of the subjects can be determined later, using the method we describe here. The only limitation is that investigators cannot film through the air–water interface, as they can when imaging a 3-D quadrat in the area of interest *after* camera position and lens zoom has been fixed (this is because of refraction), but this limitation also applies to the stereo method.

Advantages of tracking the fish's midline

Tracking the fish's midline provides a much more versatile description of the fish's swimming movement than tracking a single point on its body. For example, for trout-shaped fish, the location of the center of mass can be conveniently determined as a point one third the distance between the fish's nose and tail (Webb 1978). Tracking the center of mass is the best way to estimate acceleration rates and turn radii. One could argue that the center of mass should be tracked as a single point, but this is impractical because it requires that a point on the fish that lies directly over the center of mass be selected in both camera views, and it is often very hard to decide where this point might be.

Tracking the fish's midline in 3-D should also make it possible to apply models that predict thrust from the fish's undulatory swimming movements (Lighthill 1971). Currently, researchers in these fields get their fish to swim in a single plane (usually the horizontal) and then use a 2-D analysis (e.g., Webb 1983). While this has the advantage of simplicity, it does mean that they cannot apply their methods to 3-D maneuvers. We hope that our technique will make such an application possible, and bring new approaches and expertise to the study of these maneuvers.

Finally, tracking the fish's midline simply allows better visualization of fish swimming movements than tracking a single point. This in itself should help us to understand their maneuvers.

Potential applications

The utility of the techniques we describe in this paper will ultimately depend on their value in addressing significant questions in fish biology. One area of particular interest requires all three techniques, the study of adaptive design of prey-interception maneuvers by drift-feeding stream fish. This is a complex subject, but may hold the key to a range of longstanding and unsolved questions about the ecology of drift-feeding fish, including questions about prey choice, food intake rates, energy budgets, and habitat selection. How might an understanding of prey-interception maneuvers help us fathom such a broad range of ecological questions? The answer is that both prey-interception time and cost of prey capture are important parameters in standard foraging models (Stephens and Krebs 1986). Prey-interception time enters these models as handling time (a time cost), and cost of capture is subtracted from the prey's assimilable energy content to calculate the net energy value of the prey (note: Hughes and Kelly 1996 describe a technique for calculating swimming cost from a description of maneuver geometry and dynamics). However, given our current state of knowledge, we have no idea what handling times or capture costs to put into this kind of foraging model, so we are unable to predict prey choice and intake rates, or make well-explained predictions of which habitats would maximize a fish's energy intake rate. The reason for this state of affairs is that interception time and capture costs can be adaptively traded off against one another by the fish, and so become quite fluid. The outcome of this trade-off probably depends on a number of factors, including water velocity, fish size, and prey abundance (in the maneuvers analysed in this paper the fish intercepted prey considerably more quickly in faster water; see Hughes and Kelly 1996). For these reasons, we think study of the adaptive design of prey-interception maneuvers, and the development of predictive models, is really essential if we are to understand drift-feeding fish. We hope that future study of this, and other questions, will prove the value of the techniques we have described in this paper.

Acknowledgements

This research was partly supported by an International Post-Doctoral Fellowship awarded to N.F.H. by the Natural Sciences and Engineering Research Council of Canada, to work with Larry Dill at the Behavioral Ecology Research Group, Simon Fraser University, and by Larry Dill's NSERC operating grant A6869. This support is gratefully acknowledged. The Alaska Cooperative Fish and Wildlife Research Unit and the Institute of Arctic Biology, both at the University of Alaska Fairbanks, provided logistical support for field activities. We thank L.M. Dill, D. Boisclair, and one anonymous reviewer for comments that helped us improve the manuscript.

References

Aoki, I., Inagaki, T., and Van Long, L. 1986. Measurements of the three-dimensional structure of free-swimming pelagic fish schools in a natural environment. Bull. Jpn. Soc. Fish. **52**: 2069–2077.

Blake, R.W. 1983. Fish locomotion. Cambridge University Press, Cambridge, U.K. 208 p.

Boisclair, D. 1992. An evaluation of the stereocinematographic method to estimate fish swimming speed. Can. J. Fish. Aquat. Sci. **49**: 523–551.

Buckley, B.J. 1992. Second and third order polynomial rectification routines. The Center for Remote Sensing, Michigan State University, East Lansing, Mich.

Cullen, J.M., Shaw, E., and Baldwin, H.A. 1965. Methods for measuring the three-dimensional structure of fish schools. Anim. Behav. **13**: 534–543.

Dill, L.M., Dunbrack, R.L., and Major, P.F. 1981. A new stereopho-

© 1996 NRC Canada

tographic technique for analyzing the three-dimensional structure of fish schools. Environ. Biol. Fishes, **6**: 7–13.

Harper, D.G., and Blake, R.W. 1989. A critical examination of the use of high-speed film to determine the maximum acceleration of fish. J. Exp. Biol. **142**: 465–471.

Hughes, N.F., and Kelly, L.H. 1996. A hydrodynamic model for estimating the energetic costs of swimming maneuvers from a description of their geometry and dynamics. Can. J. Fish. Aquat. Sci. **53**. This issue.

Huse, I., and Skiftesvik, A.B. 1990. A PC-aided video based system for behaviour observation of fish larvae and small aquatic invertebrates. Aquacult. Eng. **9**: 131–142.

Johnson, R.E., and Kiokemeister, F.L. 1969. Calculus with analytical geometry. Allyn and Bacon, Boston, Mass.

Klimley, A.P., and Brown, S.T. 1983. Stereophotography for the field biologist: measurements of lengths and three-dimensional positions of free-swimming sharks. Mar. Biol. **74**: 175–185.

Lighthill, M.J. 1971. Large-amplitude elongated-body theory of fish locomotion. Proc. R. Soc. Lond. Ser B Biol. Sci. **179**: 125–138.

Major, P.F., and Dill, L.M. 1978. The three-dimensional structure of airborne bird flocks. Behav. Ecol. Sociobiol. **4**: 111–122.

Potel, M.J., and Wassersug, R.J. 1981. Computer tools for the analysis of schooling. Environ. Biol. Fishes, **6**: 15–19.

Stephens, D.W., and Krebs, J.R. 1986. Foraging theory. Princeton University Press, Princeton, N.J.

Thompson, M.M. (*Editor*). 1966. Manual of photogrammetry. 3rd ed. American Society of Photogrammetry, Washington, D.C.

Van Long, L., and Aoyama, T. 1985. Photographic measurement for obtaining the length, aspect and bearing of free-swimming fish from their spatial position. Bull. Jpn. Soc. Fish. **51**: 191–195.

Van Long, L., Aoyama, T., and Inagaki, T. 1985. A stereo photographic method for measuring the spatial position of fish. Bull. Jpn. Soc. Fish. **51**: 183–190.

Videler, J.J. 1993. Fish swimming. Chapman and Hall, London, U.K.

Webb, P.W. 1975. Hydrodynamics and energetics of fish propulsion. Bull. Fish. Res. Board. Can. **190**: 1–159.

Webb, P.W. 1978. Fast-start performance and body form in seven species of teleost fish. J. Exp. Biol. **74**: 211–226.

Webb, P.W. 1983. Speed, acceleration, and manoeuverability of two teleost fishes. J. Exp. Biol. **102**: 115–122.

© 1996 NRC Canada

A hydrodynamic model for estimating the energetic cost of swimming maneuvers from a description of their geometry and dynamics

Nicholas F. Hughes and Lon H. Kelly

Abstract: In this paper, we describe a model that allows estimation of the energy expenditure of a maneuvering fish from a knowledge of its changes in speed and direction. This model utilizes speed–time data and measurements of the timing and radii of turns. We use hydrodynamic theory to estimate the swimming thrust produced by fish during the accelerations, decelerations, coasting, and turns involved in a maneuver, expressing this thrust in terms of the speed at which it would carry a fish swimming at a constant speed in a straight line. This allows us to estimate energy expenditure by referencing well-established, empirically derived relationships between fish size, water temperature, swimming speed, and oxygen consumption. Application of this model to prey interception maneuvers by drift-feeding Arctic grayling (*Thymallus arcticus*) gave estimates of energy expenditure ranging from 2.6 to 10 (mean 4.7) times higher than the traditional method, which assumes fish pay a cost equivalent to steady swimming at their average speed. These results compare favorably with recent respirometry studies showing that actual oxygen consumption by maneuvering fish can reach as much as 6–14 times the values predicted by the traditional method.

Résumé : Dans cet article, nous décrivons un modèle permettant d'estimer la dépense énergétique d'un poisson qui manoeuvre à partir de la mesure de ses changements de vitesse et de direction. Ce modèle est alimenté par des données vitesse–temps et des mesures du moment et du rayon de braquage. Nous avons recours à la théorie de l'hydrodynamique pour estimer la poussée du poisson durant les accélérations, les décélérations, la nage à vitesse constante et les changements de direction qui constituent une manoeuvre; les résultats sont exprimés en termes de la vitesse qu'aurait le poisson s'il nageait en ligne droite et à vitesse constante. En se reportant à des relations empiriques bien établies entre la taille des poissons, la température de l'eau, la vitesse de nage et la consommation d'oxygène, on peut estimer la dépense énergétique. L'application de ce modèle aux manoeuvres d'interception des proies dérivantes par l'ombre arctique (*Thymallus arcticus*) a conduit à des évaluations de la dépense énergétique dont la valeur est de 2,6 à 10 fois (moyenne de 4,7) supérieure aux résultats obtenus par la méthode classique, qui prend comme hypothèse que le poisson en chasse dépense environ la même quantité d'énergie que lorsqu'il nage à sa vitesse moyenne constante. Ces résultats concordent bien avec ceux de récentes études respirométriques montrant que la consommation réelle d'oxygène par les poissons qui manoeuvrent peut être 6 à 14 fois plus élevée que les valeurs prévues par la méthode classique.
[Traduit par la Rédaction]

Introduction

Swimming maneuvers, involving changes in speed and direction, are one of the hallmarks of fish behavior; they contribute to the fish's fitness by parlaying energy expenditure into food acquisition, predator avoidance, and reproductive activities. However, despite this vital role in transducing energy into fitness, there are actually no theories, or empirically derived relationships, that relate the characteristics of a maneuver to its energetic cost. This lack seriously handicaps investigations into the energetics of fish behavior, particularly studies of the way fish swimming behavior is designed to enhance fitness.

The traditional approach to estimating the energy expenditure of maneuvering fish actually neglects the costs of turning and changing speed altogether, and simply assumes that a maneuvering fish pays the same cost as one swimming in a straight line at the same average speed (Ware 1975, 1978; Kerr 1982; Feldmeth 1983). Even more egregiously, most studies of drift-feeding stream fishes also neglect the influence of prey interception maneuvers on average speed, and simply estimate energy expenditure using the velocity at which the fish swims at its focal point (Feldmeth and Jenkins 1973; Bachman 1981; Fausch 1984; Hughes and Dill 1990; Hill and Grossman 1993; but see Puckett and Dill 1985 and Godin and Rangley 1989 for attempts to improve on this).

Recent work has shown that the traditional practice of equating maneuver costs with the cost of swimming in a straight line at the same average speed can seriously underestimate energy expenditure. For example, when Krohn and Boisclair (1994) measured the oxygen consumption of brook trout (*Salvelinus fontinalis*) maneuvering in aquaria, they found that swimming costs were about six times higher than would be predicted using Brett and Glass's (1973) relationships between *steady* swimming speed and oxygen consumption. A study of the literature by Boisclair and Tang

Received September 27, 1995. Accepted May 2, 1996.
J13090

N.F. Hughes. Behavioral Ecology Research Group, Department of Biological Sciences, Simon Fraser University, Burnaby, BC V5A 1S6, Canada.
L.H. Kelly. P.O. Box 82840, Fairbanks, AK 99708, U.S.A.

© 1996 NRC Canada

(1993) supports this finding, suggesting that maneuvering fish can pay a cost 6–14 times higher than expected using the traditional method. Their analysis also suggested that this cost multiple increases with the complexity of the maneuver and depends on fish size.

Unfortunately, respirometry studies have not been sufficent to establish the relationship between the characteristics of swimming maneuvers and energy expenditure because the amount by which the energy expenditure of a maneuvering fish exceeds that calculated with the traditional method depends on the way characteristics such as speed, turning, and acceleration are blended to form the complete maneuver (Boisclair and Tang 1993). This means that respirometry-based estimates can only be extrapolated from the laboratory to the field if the blend of maneuver characteristics is consistent (Tang and Boisclair 1993; Krohn and Boisclair 1994). Since the swimming behavior of fish in the laboratory and field often differs markedly, such extrapolation is risky (Tang and Boisclair 1993; Krohn and Boisclair 1994). A related problem is that maneuver characteristics in their experimental treatments were highly correlated, preventing them from developing empirical relationships between individual characteristics and energy expenditure. These difficulties led Krohn and Boisclair (1994) to state, "Future research efforts should therefore be directed toward developing direct relationships between spontaneous swimming costs and swimming characteristics."

The goal of this paper is to follow Krohn and Boisclair's (1994) suggestion by developing a theoretical model that allows the estimation of swimming costs from a description of maneuver characteristics. We use hydrodynamic theory to estimate the swimming thrust produced by fish during the accelerations, decelerations, coasting, and turns involved in a maneuver (see Weihs 1974, 1981; Webb 1975, 1991; Blake 1983*a*; and Videler 1993 for an introduction to the hydrodynamics of fish swimming). Following Weihs (1974), we express this thrust in terms of the speed at which it would carry a fish swimming at a constant speed in a straight line. This allows us to estimate energy expenditure by referencing well-established, empirically derived relationships between fish size, water temperature, swimming speed, and oxygen consumption, notably Brett's study on the sockeye salmon (*Oncorhynchus nerka*) summarized in Brett and Glass (1973).

To our knowledge, this is the first model to make a priori predictions of swimming costs from the characteristics of a fish's swimming maneuvers. This model can be used *as is* to estimate the energy expenditure of maneuvering fish. It can also be tested using respirometry experiments. These tests should allow us to improve and refine the model, working towards a reliable way of estimating the energy expenditure of maneuvering fish more efficiently than we could using respirometry alone.

We also compare the estimates of energy expenditure produced by our model with the estimates produced by the traditional method of equating maneuver costs with the cost of swimming in a straight line at the same average speed. We do this by analysing the descriptions of maneuver geometry and dynamics of Arctic grayling (*Thymallus arcticus*) intercepting prey at two different water velocities, as described in our companion paper (Hughes and Kelly 1996). The purpose of this comparison is to see if our model provides significantly different estimates than the traditional approach and to assess whether the magnitude of its predictions compares favorably with the conclusions of Boisclair and Tang (1993) and Krohn and Boisclair (1994).

The model

We begin this section by developing a model with which we can estimate the fish's swimming thrust at each stage in a maneuver. Next we show how to convert these values of thrust into estimates of energy expenditure. The terms we use to define swimming characteristics are as follows, after Webb (1991) and Krohn and Boisclair (1994). Steady swimming is swimming at a relatively constant speed in a straight line. Unsteady swimming involves significant linear or centripetal acceleration. Spontaneous swimming comprises voluntary movements of the fish as it goes about its day to day activities. Spontaneous swimming can therefore involve both steady and unsteady swimming.

Estimating thrust

We express the thrust of either a steady-swimming, accelerating, decelerating, and/or turning fish in terms of the speed at which it would equilibrate if it was swimming steadily in a straight line. It should then be reasonable to use this expression of thrust to estimate the fish's swimming cost by referring to Brett and Glass' (1973) speed–cost relationships for steady-swimming fish.

Steady swimming

As a starting point, consider the thrust produced by a fish swimming in a straight line at a constant speed of u cm·s^{-1} (steady swimming). In this situation the fish's thrust and drag are equal (so the fish neither accelerates nor decelerates) and we can use the conventional equation for hydrodynamic drag (D) to describe thrust (T):

$$(1) \qquad T = D = cu^2$$

where u is the fish's speed and the constants $c = \frac{1}{2}\rho\alpha AC_d$, ρ = density of water, and α = factor by which the drag on swimming fish ($\alpha = 3$) exceeds the drag on coasting fish ($\alpha = 1$); A = surface area of fish C_d = drag coefficient.

Under these circumstances, u can be used to make accurate estimates of the fish's steady-swimming costs simply by referring to empirically derived speed–cost relationships (Brett and Glass 1973). This is because the fish in Brett's respirometry studies were also swimming steadily at constant speed.

Acceleration and deceleration

First we will consider fish that are accelerating or decelerating while swimming on a straight path. Our goal is to estimate the thrust of the fish (in terms of u) from speed–time data. We do this by fitting a hydrodynamic equation that predicts the fish's speed at a given time to the observed data. We derive this equation as follows, beginning with Newton's second law of motion, which describes the way that the difference between the fish's thrust and drag and the fish's apparent mass m (mass of fish plus added mass due to entrained water, taken as 1.2 fish weight after Webb 1983) influence its acceleration a:

$$(2) \qquad T - D = ma.$$

© 1996 NRC Canada

We define u_i as the fish's speed at the start of the period t_0, u_t as the fish's speed t s into the period, and u_f as speed at which the fish will equilibrate (i.e., $T = D$ at u_f). From equation 1, we can see that $T = cu_f^2$ and $D = cu_t^2$. Expressing a as du_t/dt (change in speed with time), and substituting these definitions into equation 2 we can write

$$cu_f^2 - cu_t^2 = m\frac{du_t}{dt}.$$

This can be rearranged in a convenient form for integration:

$$\frac{m}{c}\int_{u_i}^{u_t}\frac{du_t}{u_f^2 - u_t^2} = \int_{t_0}^{t} dt.$$

By evaluating this integral, we obtain the desired relationship between u_t and t:

$$(3)\qquad u_t = u_f\frac{Q - e^{-t/\tau}}{Q + e^{-t/\tau}}$$

where

$$Q = \frac{u_f + u_i}{u_f - u_i} \text{ and } \tau = \frac{m}{2cu_f}.$$

Equation 3 can be used to predict the speed–time relationship for an accelerating or decelerating fish at different values of u_i and u_f (Fig. 1). By fitting this equation to observed speed–time data, we can estimate the fish's thrust, in terms of u_f (see later for details).

However, if the fish is accelerating, decelerating, or turning, it is probably unreasonable to substitute this value of u_f directly into Brett and Glass' (1973) model to estimate swimming costs. This is because, during unsteady swimming, fish apparently labor against a drag about three times larger than they do during steady swimming (Webb 1991). Harper and Blake (1988) also suggested that unsteady swimming is more demanding, but modelled this as a reduction in the efficiency of the caudal fin. To account for this added drag, we must first modify equation 3 by calculating τ as $m/(2wcu_f)$ where the "Webb Factor" (w) has a value of 3 to account for the threefold increase in resistance during unsteady swimming. Next, the value of u_f estimated using equation 3 must be converted into the speed u at which the fish would travel if it was producing the same amount of thrust but steady swimming in a straight line. Since the thrust of an unsteady-swimming fish is $T = wcu_f^2$ and the thrust of a steady-swimming fish is $T = cu^2$, this can be found by solving $cu^2 = wcu_f^2$, which gives

$$(4)\qquad u = \sqrt{wu_f^2}.$$

We propose that this value of u be used to estimate swimming costs using the relationships in Brett and Glass (1973).

Coasting is a special case of deceleration that deserves mention. A coasting fish minimizes its drag by holding its body straight and its fins against its body. This behavior is of considerable interest because by burst-and-coast swimming, a fish can theoretically reduce its swimming costs below what it would pay to steady swim at the same average speed (Weihs 1974; Videler and Weihs 1982; Blake 1983*b*; but see Alexander 1989 for a slightly different interpretation). The dynamics of a coasting fish can be modelled using equation 3 by setting α and w to 1 and u_f to a very small but nonzero number. Costs should be calculated using $u = 0$.

Fig. 1. Top: Theoretical speed–time curve generated with equation 3 for an accelerating salmonid, with a fork length of 26.6 cm, that has an initial speed (u_i) of 25 cm·s^{-1} and a final speed (u_f) of 75 cm·s^{-1}. Bottom: Theoretical speed–time curve for the same fish decelerating from an initial speed (u_i) of 75 cm·s^{-1} towards a final speed (u_f) of 25 cm·s^{-1}. In both cases, swimming is assumed to be unsteady throughout.

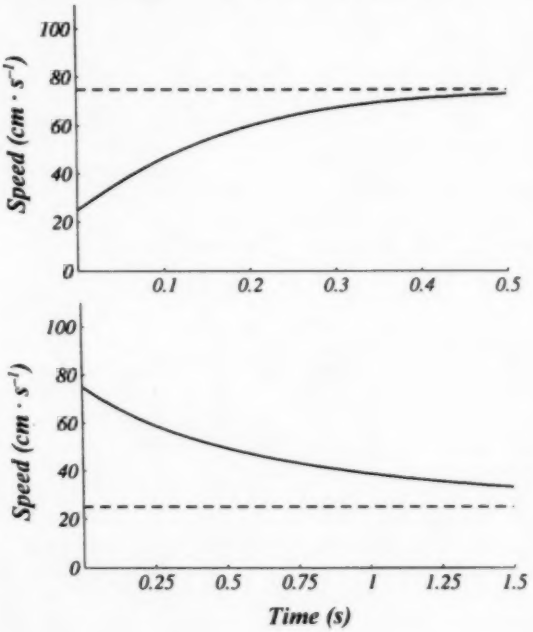

Turning

Now consider a turning fish. Again our goal is to estimate the thrust of the fish in terms of the speed u at which this thrust would carry the fish if it was steady swimming in a straight line. But this fish will have to work harder than one swimming at the same speed in a straight line because it has to overcome centrifugal force. Theoretically the extra thrust it needs to produce is directly proportional to its apparent mass, and to the square of its speed, and inversely proportional to the radius of its turn (Weihs 1981). If the fish produces this thrust with asymmetrical beats of its caudal fin, we can use a relationship developed by Weihs (1981) to estimate the multiple by which the thrust required to swim around a turn (T_t) exceeds the thrust needed to swim at the same speed in a straight line (T_s). For a given fish, this multiple depends only on turn radius:

$$(5)\qquad \frac{T_t}{T_s} = \sqrt{1 + \left(2\frac{V^{1/3}}{RC_{Dt}}(1+\lambda)\right)^2}$$

where V is the volume of the fish (approximated by fish weight for a neutrally buoyant fish), R is the instantaneous

© 1996 NRC Canada

radius of the curved path, C_{Dt} is the drag coefficient based on two-thirds power of volume as reference area (C_{Dt} can be calculated from C_d as $\alpha AC_d/V^{2/3}$), and λ is the added mass coefficient of the fish (taken as 0.2 after Webb 1983).

If we have speed–time data for the turn, and we know the fish's turn radius, we can now estimate the fish's thrust in terms of u. The first step is to estimate u_f using equation 3 after calculating τ as $m/(2(T_t/T_s)wcu_f)$; next the steady straight-line swimming speed u that would be obtained by the fish is found by solving $cu^2 = (T_t/T_s)wcu_f^2$, which gives

$$u = \sqrt{\frac{T_t}{T_s} wu_f^2}. \quad (6)$$

We assume that turning fish are unsteady swimming, so $w = 3$. This approach to modelling the resistance encountered in turns relies on the fact that both the force needed to overcome centrifugal force and the force needed to overcome hydrodynamic drag increase as the square of the fish's swimming speed. We propose that this value of u is used to estimate swimming costs using the relationships in Brett and Glass (1973).

Energy expenditure

We use relationships from Brett and Glass (1973) to convert the values of u into estimates of the swimming cost paid by the fish in each segment of a maneuver. By summing estimates of cost for all the segments, we can calculate costs for the entire maneuver. To simplify these calculations, we have fitted a linear regression model to data digitized from the three contour diagrams in Brett and Glass' (1973) paper, so that the fish's maximum sustainable swimming speed u_{ms} (centimetres per second), standard metabolic rate SMR (milligrams O_2 per kilogram per hour, oxygen consumption at rest), and active metabolic rate AMR (milligrams O_2 per kilogram per hour, oxygen consumption at u_{ms}) can be estimated for different combinations of fish size and water temperature. Details of the regression models used, and estimated parameters, are given in the Appendix. If the fish's weight is W (grams) and the oxycaloric equivalent is OQ (joules per milligram O_2, taken as 14.1 after Videler 1993), then the cost SC (joules) of a fish swimming for time t (seconds) can be calculated using an equation that implements the graphical method described by Brett and Glass (1973):

$$SC = \frac{t}{3600} \frac{W}{1000} OQ \left(e^{\ln(SMR) + u \frac{\ln(AMR) - \ln(SMR)}{u_{ms}}} \right). \quad (7)$$

Note that because of the way u is calculated (equations 4 and 6), it may be bigger than u_{ms} even in situations when the fish's actual speed through the water is less than u_{ms}. In this situation the investigator should be aware that the regressions for SMR and AMR are being used outside the range to which they are known to apply. In this case, costs will probably be underestimated, since swimming at high speeds seems to be particularly expensive (Puckett and Dill 1984).

Applying the model

In this section, we apply the model we have just described to estimate the energy expended by a drift-feeding Arctic grayling intercepting prey at high and low flows. Our purpose here is simply to illustrate the steps needed to use our model, and to compare its estimates relative to those of other methods. We analyse eight maneuvers, four at each flow level. In two of these four maneuvers the fish intercepts prey that would have passed about 40–45 cm to the right of its focal point (lateral capture); in the other two, it intercepts prey that would have passed almost directly over its focal point, at a distance of about 25–35 cm (overhead capture). Hughes and Kelly (1996) detail the methods used to obtain data on the geometry and dynamics of these maneuvers. Data on mean swimming speeds and elapsed times for interception and return legs are given in Table 1.

We compare the predictions of our model with two other methods. In the first of these, energy expenditure is estimated by assuming the fish pays the cost of steady swimming at its average speed during prey interception and return to its focal point. This could be called the traditional method, since it is the way swimming costs have usually been calculated in the past. In the second method, energy expenditure is estimated by assuming that the fish pays the cost of *unsteady* swimming at $u = \sqrt{wu_f^2}$ during prey interception and return to its focal point where u_f is the observed average speed during either interception or return and w is the factor by which drag during spontaneous swimming is thought to exceed drag on a steady-swimming fish (taken as 3 after Webb 1991). This method accounts for the generally greater drag encountered during spontaneous swimming, but not, explicitly, for the costs associated with acceleration or turning, or the energy savings that may result from coasting.

Fitting speed–time curves

To fit theoretical speed–time curves, it is necessary to determine the radii and timing of turns executed during the course of the maneuver. We did this using the technique illustrated in Fig. 2. Subsequently we treated segments involving turns separately, so that we could account for the additional costs involved, as we described earlier.

The values of u_i and u_f that fit the theoretical curves to the observed data can be estimated in a couple of different ways. For the estimates in this paper, we used trial and error to interactively fit the data (Fig. 3); all other parameters were calculated a priori as follows. The fish's fork length is Fl (centimetres), its total length Tl (centimetres), and its weight W (grams); $m = 1.2 \cdot W$, where $\log_{10}(W) = -2.03 + 3.03 \cdot \log_{10}(\text{Fl})$, (Hughes and Dill 1990); $A = 0.28 \cdot \text{Tl}^{2.11}$, using Webb's (1976) relationship for rainbow trout; $C_d = 0.072 \cdot \text{Re}^{-0.2}$ where Re is Reynolds number calculated as $\text{Re} = \text{Tl} \cdot u/v$ (Webb 1991); u is the fish's swimming speed, taken as 25 cm·s^{-1} for the purpose of calculating C_d, and v is the kinematic viscosity of water (approximately 0.01 cm^{-2}·s^{-1}). For the fish in this example, Fl = 26.6 cm, Tl = 28.3 cm, m = 233 g, A = 324 cm^2, and $C_d = 0.008$. We have also tried estimating u_i and u_f using the Levenberg–Marquart method for nonlinear least squares (Press et al. 1988). This technique has the advantage of objectivity, but has the disadvantage that it does not necessarily give enough weight to the first and last data points in a segment of the maneuver. Both methods give generally similar results, but the interactive method provides a more satisfying fit.

© 1996 NRC Canada

Table 1. Time taken and average swimming speeds for an Arctic grayling (26.6 cm Fl) during prey interception and return to its focal point.

	Interception time (s)	Return time (s)	Total time (s)	Avg. interception speed ($cm \cdot s^{-1}$)	Avg. return speed ($cm \cdot s^{-1}$)	Avg. total speed ($cm \cdot s^{-1}$)
Overhead capture						
Slow flow, Aug. 3	1.5	6.1	7.6	18	16	16
Slow flow, Aug. 7	3.9	4.0	7.9	20	16	18
	2.7 ± 2.4	**5.1 ± 2.1**	**7.8 ± 0.3**	**19 ± 2**	**16 ± 0**	**17 ± 1**
Fast flow, Aug. 3	1.6	3.6	5.2	28	35	33
Fast flow, Aug. 7	1.1	5.8	6.9	40	34	36
	1.4 ± 0.5	**4.7 ± 2.2**	**6.1 ± 1.7**	**34 ± 12**	**35 ± 1**	**35 ± 3**
Lateral capture						
Slow flow, Aug. 3	4.7	12.2	16.9	24	14	17
Slow flow, Aug. 7	5.3	18.3	23.6	24	12	15
	5.0 ± 0.6	**15.2 ± 5.6**	**20.3 ± 6.6**	**24 ± 0**	**13 ± 2**	**16 ± 2**
Fast flow, Aug. 3	2.7	4.7	7.4	32	26	28
Fast flow, Aug. 7	2.0	13.1	15.1	40	32	33
	2.4 ± 0.7	**8.9 ± 8.3**	**11.3 ± 7.6**	**36 ± 8**	**29 ± 6**	**31 ± 5**

Note: Prey are either captured at a distance of about 25–30 cm almost directly overhead or about 40–45 cm laterally to the right of the fish's focal point. Each of these prey capture locations is represented by two maneuvers at slow flow (peak velocities in channel 15–20 $cm \cdot s^{-1}$) and two maneuvers at high fast flow (peak velocities in channel 35–40 $cm \cdot s^{-1}$). Mean values and 95% confidence intervals for each of the four maneuver/flow combinations are summarized in bold type.

Fig. 2. Our technique for measuring the timing and radii of turns. A 3-D representation of the path followed by the fish's center of mass (points at 0.1-s intervals) is rotated on a computer monitor until the turn of interest (solid points) lies in the horizontal plane (by aligning solid points with horizon in side view, see Hearn and Baker 1994 for the required transformation techniques). The top panel shows the rotated maneuver in plan view, and the bottom panel shows it in side view; axes units are pixels. Once in this configuration, it is possible to determine the time at which the turn begins, and ends, and to measure the turn radii using a digital protractor. Symbols show the fish's body angle at the start and finish of the turn. The data illustrated here were acquired using techniques described by Hughes and Kelly (1996) and describe the slow lateral maneuver performed by a 26.6-cm Fl Arctic grayling on August 3, 1993. The turn being measured is turn 3 in Fig. 3.

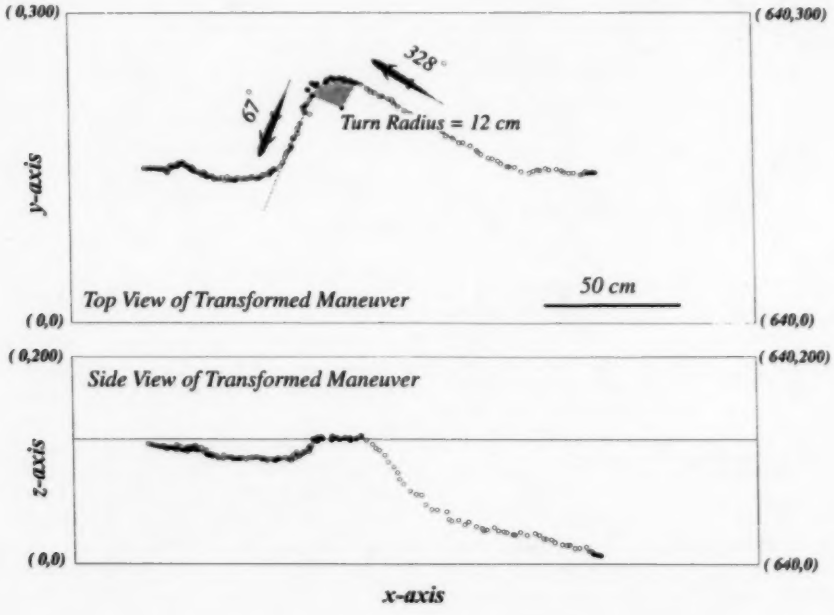

© 1996 NRC Canada

Fig. 3. Estimating u_i and u_f by fitting theoretical speed–time curves to observed speed–time data. Curves were generated using equation 3 and constants given in the text; values of u_i and u_f were estimated by interactively matching theoretical curves with the data by eye. Vertical lines divide the maneuver into discrete segments and individual speed–time curves were fitted to each segment. The resulting estimates of u_i and u_f are shown. The solid bars along the top of the figure show the duration and radius of the four turns executed during the maneuver (t_1–t_4). To allow correct calculation of thrust in later analysis, each turn was analysed as an integral part of one or more segments. The data illustrated here were acquired using techniques described by Hughes and Kelly (1996) and describe the slow lateral maneuver performed by a 26.6-cm Fl Arctic grayling on August 3, 1993.

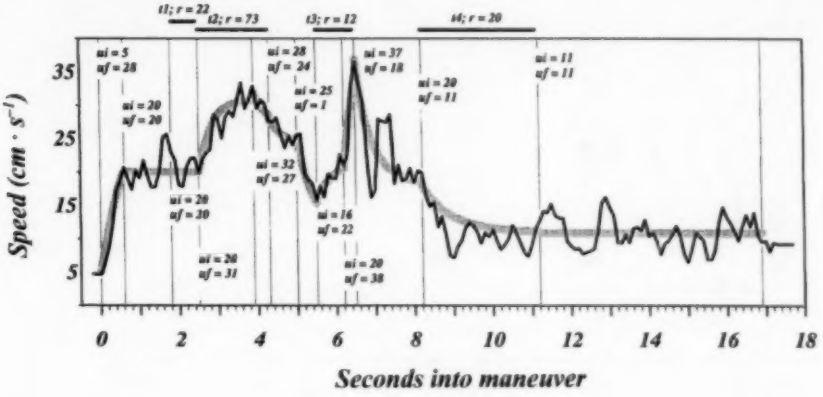

The question of how to divide the maneuver into segments for analysis is a much more puzzling and important question than whether to fit the data by eye or by using least squares. For example, at what scale should fluctuations in speed over time be divided into discrete segments, and fit with a series of curves, and at what scale should these fluctuations be lumped into the same segment and fit with a single curve? The choice that is made is going to have a considerable influence on the cost calculated. To illustrate this, consider the last 8 s of the maneuver illustrated in Fig. 3. In this segment of the maneuver, there are periodic fluctuations in the fish's speed, apparently due to fluctuating thrust during the course of individual tail beats. We judged this segment to be steady swimming, and calculated costs accordingly. However, we could have judged it to be unsteady swimming and fit individual curves to each rise and fall in the speed–time data. This would undoubtedly have produced a much higher estimate of energy expenditure. We have little doubt that we made the right choice for this segment, but there are other situations where the decision is more equivocal. We dealt with this issue by familiarizing ourselves with fluctuations in the speed–time data during steady swimming (e.g., the last 8 s of the maneuver in Fig. 3) and then used this as a standard, judging sections of the speed–time data with higher or more irregular amplitude to be unsteady.

Estimating energy expenditure

Our estimates of net energy expenditure (Table 2) range from 2.6 to 10 times higher than estimates made assuming steady-swimming costs throughout the maneuvers (the mean is 4.7 times higher). Our method also gives estimates between 1.3 and 3.3 times higher than estimates made assuming unsteady swimming throughout the maneuvers (the mean is 1.9 times higher). This comparison suggests that about half of the increase in the cost estimates of our method, over the traditional steady-swimming method, is due to our assumption of increased drag during unsteady swimming (the Webb Factor). The rest of the increase results from the extra work that our method ascribes to accelerations and turns. Of course, the proportion of energy expended to accelerate and turn will depend on the geometry and dynamics of the maneuver, so this rough apportioning of costs applies specifically to the maneuvers analysed in this example.

Estimates of the extra energy required to capture prey in fast versus slow flow are also affected by the method we use. Our method suggests that this increase is larger than either of the other methods, in both absolute and relative terms. The traditional method gives the most modest estimates of the extra energy expended.

Discussion

The purpose of this paper is to describe a theoretical model that can be used to estimate the energy expenditure of fish from a knowledge of maneuver characteristics, and to provide a comparison between the estimates produced by this model and more traditional approaches. In keeping with these objectives, we focus this discussion on the pros and cons of our model and the magnitude of its cost estimates in relation to the other approaches.

One desirable feature of our model is that it accounts for all three of the sources of resistance that the swimming fish must overcome, resistance due to hydrodynamic drag, resistance due to linear acceleration, and resistance due to centripetal acceleration (Webb 1991). In theory, this means that our model should make accurate estimates of thrust and en-

© 1996 NRC Canada

Table 2. Estimated net energy expenditure during prey-interception maneuvers by a 26.6-cm Fl Arctic grayling.

	(*i*) Net energy expenditure (J)	(*ii*) Net energy expenditure (J)	(*iii*) Net energy expenditure (J)
Overhead capture			
Slow flow, Aug. 3	1.28	0.47	0.69
Slow flow, Aug. 7	0.51	0.22	0.48
	0.90 ± 0.75	**0.35 ± 0.25**	**0.58 ± 0.21**
Fast flow, Aug. 3	1.94	0.30	0.91
Fast flow, Aug. 7	5.84	0.48	1.43
	3.89 ± 3.82	**0.39 ± 0.18**	**1.17 ± 0.51**
Lateral capture			
Slow flow, Aug. 3	1.74	0.44	0.96
Slow flow, Aug. 7	1.01	0.51	1.09
	1.38 ± 0.72	**0.48 ± 0.07**	**1.03 ± 0.13**
Fast flow, Aug. 3	2.20	0.37	0.92
Fast flow, Aug. 7	3.35	1.01	2.74
	2.78 ± 1.13	**0.69 ± 0.63**	**1.83 ± 1.78**

Note: Prey are either captured almost directly overhead (25–30 cm distance) or 40–45 cm laterally to the right of the fish's focal point. Each of these prey capture locations is represented by two maneuvers at slow flow (peak water velocities 15–20 $cm \cdot s^{-1}$) and two maneuvers at fast flow (peak water velocities 35–40 $cm \cdot s^{-1}$). Energy costs are estimated in three different ways: (*i*) using the method described in this paper, (*ii*) assuming the fish paid the costs of steady swimming at its average speed during the prey-interception and return legs, and (*iii*) assuming the fish paid the cost of unsteady swimming during the prey interception and return legs. Net energy cost is calculated by subtracting the cost that the fish would have paid for standard metabolism during the course of the maneuver from the gross cost of swimming during the maneuver. Mean values and 95% confidence intervals for each of the four maneuver/flow combinations are summarized in bold type.

ergy expenditure. In practice, however, there are a number of possible pitfalls. To begin with, accurate estimation of thrust is contingent on accurate estimates of resistance, and this is no easy matter, particularly for hydrodynamic drag. In fact the model relies on at least two rough approximations about the magnitude of hydrodynamic drag, α (the factor by which drag on a swimming fish exceeds drag on a coasting fish) and w (the factor by which drag during unsteady swimming exceeds drag during steady swimming). We assume that α is either 1 for a coasting fish or 3 for a swimming fish and that w is either 1 for a steady-swimming fish or 3 for an unsteady-swimming fish. These assumptions mean that our calculation of drag involves a multiplication by either 1 (for a coasting fish), 3 (for a steady-swimming fish), or 9 (for an unsteady swimming fish). Of course it is unlikely that drag exists only at these three distinct levels — it probably varies continuously over a range, depending on the fish's body movements. However, our assumptions on α and w are currently "state of the art" (e.g., Webb 1991), and so, until further research is conducted, they are probably the best values to use. Assumptions about resistance due to linear acceleration and turns may also have to be revised (Webb 1991). These limitations should certainly be borne in mind when using our model, but, on the positive side, we hope that the model will galvanize research that improves our ability to estimate the swimming thrust of fish in the field, and also proves amenable to the incorporation of this new knowledge.

A second desirable feature of our model is that it allows estimates of thrust to be converted into estimates of cost using established relationships between steady-swimming speed and oxygen consumption. This can be seen as a kind of calibration procedure that should give accurate results for steady-swimming fish and, hopefully, prevent estimates from straying too far from reality for maneuvering fish. An additional advantage of this, over techniques that estimate energy consumption from work = force × distance (e.g., Harper and Blake 1988), is that it accounts for changes in the efficiency of the fish's muscles with contraction speed and temperature (R.W. Blake, personal communication). However, it is worth pointing out that our estimates of thrust could be converted into estimates of work using methods similar to those described by Harper and Blake (1988).

One of the biggest difficulties in applying our model is deciding how to divide the speed–time data into segments for curve fitting, and the related matter of deciding whether swimming is steady or unsteady, or when the fish is coasting. These decisions can have a big impact on estimates of swimming costs. The method we used to make these decisions (described in the previous section on fitting speed–time curves) is just a reasoned rule of thumb. The issue deserves further study. Perhaps futher work on estimates of α and w will make the model less sensitive to these decisions.

Alternative approaches to estimating energy expenditure from data on maneuver geometry and dynamics may be worth looking into in future. For example, it may be worth-

© 1996 NRC Canada

while to develop Harper and Blake's (1988) approach, perhaps using numerical integration, rather than the curve-fitting approach we have described here. It would also be an interesting challenge to estimate energy consumption from a description of the fish's undulatory swimming movements (e.g. Lighthill 1971). Webb (1991) pointed out that this require an analysis of whole-body movements when swimming is unsteady (as opposed to a description of movements by just the trailing edge of the caudal fin for steady swimming), and suggested that this is impractical. This may be a prudent assessment, but to us it would seem possible to use a high-speed computerized video system to describe 3-D movements of the fish's midline (perhaps using the techniques described in Hughes and Kelly 1996) and perform the required analyses.

When applied to Arctic grayling maneuvering at two different water velocities, our model produced cost estimates ranging from 2.6 to 10 times (average 4.7) the estimates made using the traditional method. This demonstrates that it does not simply use a more complex analysis to provide similar results. At present it is not possible to make a precise judgement of the improvement that this represents, since we do not know the actual cost paid by the fish to perform the maneuvers we analysed. However, we do know that maneuvering fish can pay up to 6–14 times the cost predicted by the traditional method, with the actual value depending on the characteristics of the maneuver and fish size (Boisclair and Tang 1993; Krohn and Boisclair 1994). This suggests that the cost estimates produced by our model are reasonable, and a significant improvement over the traditional method. A rigorous test of our model would be to compare its predictions of energy expenditure with experimentally determined values for fish swimming in situations that promote a range of different maneuver designs.

Acknowledgements

This research was partly supported by an International Post-Doctoral Fellowship awarded to N.F.H. by the Natural Sciences and Engineering Research Council of Canada, to work with Larry Dill at the Behavioral Ecology Research Group, Simon Fraser University, and by Larry Dill's NSERC operating grant A6869. This support is gratefully acknowledged. The Alaska Cooperative Fish and Wildlife Research Unit and the Institute of Arctic Biology, both at the University of Alaska Fairbanks, provided logistical support for field activities. We thank L.M. Dill, D. Boisclair, and one anonymous reviewer for comments that helped us improve the manuscript and Leigh Palmer of the SFU Physics Department for showing us how to derive Equation 3.

References

Alexander, R. McN. 1989. Optimization and gaits in the locomotion of vertebrates. Physiol. Rev. **69**: 1199–1227.

Bachman, R.A. 1981. A growth model for drift-feeding salmonids: a selective pressure for migration. *In* Proceedings of Salmon and Trout Migratory Behavior Symposium. *Edited by* E.L. Brannon and E.O. Salo. University of Washington, Seattle, Wash. pp. 128–135.

Blake, R.W. 1983*a*. Fish locomotion. Cambridge University Press, Cambridge, U.K.

Blake, R.W. 1983*b*. Functional design and burst-and-coast swimming in fishes. Can. J. Zool. **61**: 2491–2494.

Boisclair, D., and Tang, M. 1993. Empirical analysis of the influence of swimming pattern on the net energetic cost of swimming in fishes. J. Fish Biol. **42**: 169–183.

Brett, J.R., and Glass, N.R. 1973. Metabolic rates and critical swimming speeds of sockeye salmon (*Oncorhynchus nerka*) in relation to size and temperature. J. Fish. Res. Board Can. **30**: 379–387.

Fausch, K.D. 1984. Profitable stream positions for salmonids: relating specific growth rate to net energy gain. Can. J. Zool. **62**: 441–451.

Feldmeth, C.R. 1983. Cost of aggression in trout and pupfish. *In* Behavioral energetics W.S. Aspey and S.I. Lustick. Ohio State University Press, Columbus, Ohio. pp. 117–138.

Feldmeth, C.R., and Jenkins, T.M. 1973. Measurement of the energy expenditure of rainbow trout in a small mountain stream. J. Fish. Res. Board. Can. **30**: 1755–1759.

Godin, J.-G.J., and Rangley, R.W. 1989. Living in the fast lane: effects of cost of locomotion on foraging behaviour in juvenile Atlantic salmon. Anim. Behav. **37**: 943–954.

Harper, D.G., and Blake, R.W. 1988. Energetics of piscivorous predator–prey interactions. J. Theor. Biol. **134**: 59–76.

Hearn, D., and Baker, M.P. 1994. Computer Graphics. Prentice Hall, Englewood Cliffs, N.J.

Hill, J., and Grossman, G.H. 1993. An energetic model of microhabitat use for rainbow trout and rosyside dace. Ecology, **74**: 685–698.

Hughes, N.F., and Dill, L.M. 1990. Position choice by drift-feeding salmonids: model and test for Arctic grayling *(Thymallus arcticus)* in subarctic mountain streams, interior Alaska. Can. J. Fish. Aquat. Sci. **47**: 2039–2048.

Hughes, N.F., and Kelly, L.H. 1996. New techniques for 3-D video tracking of fish swimming movements in still or flowing water. Can. J. Fish. Aquat. Sci. **53**. This issue.

Kerr, S.J. 1982. Estimating activity budgets for actively predatory fishes. Can. J. Fish. Aquat. Sci. **39**: 371–379.

Krohn, M.M., and Boisclair, D. 1994. Use of a stereo-video system to estimate the energy expenditure of free-swimming fish. Can. J. Fish. Aquat. Sci. **51**: 1119–1127.

Lighthill, M.J. 1971. Large-amplitude elongated-body theory of fish locomotion. Proc. R. Soc. Lond. Ser. B Biol. Sci. **179**: 125–138.

Press, W.H., Flannery, B.P., Teukolski, S.A., and Vetterling, W.T. 1988. Numerical recipes in C. Cambridge University Press, Cambridge, U.K.

Puckett, K.J., and Dill, L.M. 1984. Cost of sustained and burst swimming of juvenile coho salmon (*Oncorhynchus kisutch*). Can. J. Fish. Aquat. Sci. **41**: 1546–1551.

Puckett, K.J., and Dill, L.M. 1985. The energetics of feeding territoriality in juvenile coho salmon (*Oncorhynchus kisutch*). Behaviour, **92**: 97–111.

Tang, M., and Boisclair, D. 1993. Influence of the size of enclosures on the swimming characteristics of juvenile brook trout (*Salvelinus fontinalis*). Can. J. Fish. Aquat. Sci. **50**: 1786–1793.

Videler, J.J. 1993. Fish swimming. Chapman and Hall, London, U.K.

Videler, J.J., and Weihs, D. 1982. Energetic advantages of burst-and-coast swimming of fish at high speeds. J. Exp. Biol. 97: 169–178.

Ware, D.M. 1975. Growth, metabolism and optimal swimming speed of a pelagic fish. J. Fish. Res. Board. Can. 32: 33–41.

Ware, D.M. 1978. Bioenergetics of pelagic fish: theoretical changes in swimming speed and ration with body size. J. Fish. Res. Board. Can. 35: 220–228.

Webb, P.W. 1975. Hydrodynamics and energetics of fish propulsion. Bull. Fish. Res. Board Can. 190: 1–159.

Webb, P.W. 1976. The effect of size on the fast-start performance of rainbow trout *Salmo gairdneri*, and a consideration of piscivorous predator–prey interactions. J. Exp. Biol. 65: 157–177.

© 1996 NRC Canada

Webb, P.W. 1983. Speed, acceleration, and manoeuverability of two teleost fishes. J. Exp. Biol. 102: 115–122.

Webb, P.W. 1991. Composition and mechanics of routine swimming of rainbow trout, *Oncorhynchus mykiss*. Can. J. Fish. Aquat. Sci. 48: 583–590.

Weihs, D. 1974. Energetic advantages of burst swimming of fish. J. Theor. Biol. 48: 215–229.

Weihs, D. 1981. Effects of swimming path curvature on the energetics of fish motion. Fish. Bull. U.S. 79: 171–176.

Appendix

Tables A1, A2, and A3 give parameters for calculating maximum sustained speed u_{ms} (centimetres per second), standard metabolic rate SMR (milligrams O_2 per kilogram per hour), and active metabolic rate AMR (milligrams O_2 per kilogram per hour) of sockeye salmon (*O. nerka*) of different weights W (grams) at different water temperatures T (degrees Celsius), based on 222 points digitized from each of the three contour diagrams in figs. 3 and 4 in Brett and Glass (1973) for fish between 1 and 10 000 g. The regression model fitted was

$$u_{ms},\ \text{SMR, or AMR} = b_1 + b_2 \log_e(W) + b_3 \log_e(W)^2 + b_4 \log_e(W)^3 + b_5 \log_e(W)^4.$$

Table A1. Parameters for calculating maximum sustained speed u_{ms}.

T (°C)	b_1	b_2	b_3	b_4	b_5	R^2
0	16.0807	9.7663	−0.9914	0.1493	0.0005	1.00
1	16.8226	11.0578	−1.8682	0.3386	−0.0115	1.00
2	17.5645	12.3492	−2.7451	0.5279	−0.0235	1.00
3	18.3064	13.6407	−3.6220	0.7173	−0.0355	0.99
4	19.0483	14.9322	−4.4989	0.9066	−0.0475	0.99
5	19.7902	16.2237	−5.3757	1.0959	−0.0596	0.98
6	21.7221	14.5830	−4.4013	0.9199	−0.0487	0.99
7	23.6541	12.9423	−3.4270	0.7439	−0.0378	0.99
8	25.5861	11.3016	−2.4526	0.5680	−0.0270	1.00
9	27.5181	9.6609	−1.4782	0.3920	−0.0161	1.00
10	29.4501	8.0202	−0.5038	0.2160	−0.0053	1.00
11	31.2651	7.6782	−0.1090	0.1486	−0.0008	1.00
12	33.0801	7.3363	0.2857	0.0813	0.0036	1.00
13	34.8951	6.9943	0.6804	0.0140	0.0080	1.00
14	36.7101	6.6524	1.0751	−0.0534	0.0125	1.00
15	38.5251	6.3104	1.4699	−0.1207	0.0169	1.00
16	38.0136	6.7590	1.1385	−0.0551	0.0127	1.00
17	37.5021	7.2076	0.8072	0.0106	0.0085	1.00
18	36.9906	7.6561	0.4759	0.0763	0.0043	1.00
19	36.4791	8.1047	0.1445	0.1419	0.0001	1.00
20	35.9676	8.5533	−0.1868	0.2076	−0.0040	1.00
21	35.2118	9.1098	−0.4654	0.2510	−0.0064	1.00
22	34.4561	9.6662	−0.7441	0.2945	−0.0088	1.00
23	33.7004	10.2227	−1.0227	0.3379	−0.0112	1.00
24	32.9446	10.7792	−1.3014	0.3814	−0.0135	1.00
25	32.1889	11.3357	−1.5800	0.4248	−0.0159	1.00

© 1996 NRC Canada

Table A2. Parameters for calculating standard metabolic rate SMR.

T (°C)	b_1	b_2	b_3	b_4	b_5	R^2
0	45.5499	−1.6385	−0.3505	0.0251	−0.0005	1.00
1	49.6992	−3.7997	0.2781	−0.0489	0.0025	1.00
2	53.8485	−5.9608	0.9068	−0.1228	0.0055	1.00
3	57.9978	−8.1219	1.5355	−0.1968	0.0084	1.00
4	62.1471	−10.2830	2.1641	−0.2708	0.0114	1.00
5	66.2965	−12.4441	2.7928	−0.3448	0.0144	1.00
6	71.9988	−12.7830	2.6376	−0.3210	0.0135	1.00
7	77.7011	−13.1218	2.4824	−0.2972	0.0126	1.00
8	83.4034	−13.4606	2.3272	−0.2735	0.0117	1.00
9	89.1057	−13.7995	2.1720	−0.2497	0.0108	1.00
10	94.8080	−14.1383	2.0168	−0.2259	0.0099	1.00
11	103.7160	−13.7171	1.3149	−0.1193	0.0051	1.00
12	112.6230	−13.2959	0.6130	−0.0127	0.0002	1.00
13	121.5310	−12.8747	−0.0889	0.0938	−0.0046	1.00
14	130.4390	−12.4535	−0.7908	0.2004	−0.0094	1.00
15	139.3460	−12.0323	−1.4927	0.3070	−0.0142	1.00
16	151.8810	−12.9877	−1.6820	0.3381	−0.0156	1.00
17	164.4150	−13.9431	−1.8713	0.3692	−0.0170	1.00
18	176.9500	−14.8985	−2.0607	0.4003	−0.0184	1.00
19	189.4840	−15.8539	−2.2500	0.4314	−0.0198	1.00
20	202.0190	−16.8093	−2.4393	0.4625	−0.0212	1.00
21	218.9340	−19.3705	−1.6324	0.2911	−0.0107	1.00
22	235.8480	−21.9317	−0.8255	0.1196	−0.0002	1.00
23	252.7630	−24.4929	−0.0186	−0.0518	0.0103	1.00
24	269.6780	−27.0541	0.7884	−0.2233	0.0207	1.00
25	286.5920	−29.6153	1.5953	−0.3947	0.0312	1.00

Table A3. Parameters for calculating active metabolic rate AMR.

T (°C)	b_1	b_2	b_3	b_4	b_5	R^2
0	439.7440	0.8350	−0.5782	0.1335	−0.0096	0.86
1	450.7300	1.1548	−0.9083	0.1983	−0.0136	0.94
2	461.7160	1.4747	−1.2384	0.2630	−0.0176	0.96
3	472.7020	1.7945	−1.5684	0.3278	−0.0216	0.97
4	483.6880	2.1143	−1.8985	0.3925	−0.0255	0.97
5	494.6740	2.4341	−2.2286	0.4573	−0.0295	0.97
6	531.4340	2.5550	−1.8418	0.2961	−0.0199	1.00
7	568.1940	2.6759	−1.4550	0.1349	−0.0102	1.00
8	604.9530	2.7968	−1.0683	−0.0263	−0.0006	1.00
9	641.7130	2.9177	−0.6815	−0.1874	0.0090	1.00
10	678.4730	3.0387	−0.2948	−0.3486	0.0187	1.00
11	741.4360	7.4827	−6.8461	0.7548	−0.0356	1.00
12	804.3990	11.9268	−13.3975	1.8581	−0.0899	1.00
13	867.3620	16.3708	−19.9489	2.9615	−0.1442	1.00
14	930.3250	20.8149	−26.5003	4.0649	−0.1985	1.00
15	993.2880	25.2589	−33.0516	5.1682	−0.2528	1.00
16	977.5690	20.0484	−27.7516	4.2329	−0.2033	1.00
17	961.8510	14.8378	−22.4515	3.2974	−0.1538	1.00
18	946.1330	9.6273	−17.1515	2.3621	−0.1044	1.00
19	930.4150	4.4168	−11.8514	1.4267	−0.0549	1.00
20	914.6970	−0.7937	−6.5514	0.4913	−0.0054	1.00
21	906.5870	−0.9270	−6.8678	0.6507	−0.0175	1.00
22	898.4780	−1.0602	−7.1842	0.8101	−0.0295	1.00
23	890.3680	−1.1935	−7.5006	0.9696	−0.0416	1.00
24	882.2590	−1.3268	−7.8171	1.1290	−0.0536	1.00
25	874.1490	−1.4600	−8.1335	1.2884	−0.0657	0.99

© 1996 NRC Canada

Dynamics of juvenile sea scallop (*Placopecten magellanicus*) and their predators in bottom seeding trials in Lunenburg Bay, Nova Scotia

M.A. Barbeau, B.G. Hatcher, R.E. Scheibling, A.W. Hennigar, L.H. Taylor, and A.C. Risk

Abstract: Thousands of juvenile sea scallop (*Placopecten magellanicus*) were released on the sea bed in summer and winter at two sites (a topographically open and an enclosed site) along the southwestern coast of Nova Scotia, Canada. Seeded and wild scallops and their predators (sea stars *Asterias vulgaris* and *A. forbesi* and rock crab *Cancer irroratus*) were monitored by video and diver surveys over 17 mo. Following release, the density of seeded scallops rapidly decreased, and stabilized after 1–8 wk; variation in final densities was greater between sites than between seasons of seeding. Seasonal temperature affected the rate at which the final densities were attained. Seeding effectively doubled scallop density at each site. Survivorship was ~10% due to loss from crab predation and dispersion of seeded scallops at the open site and ~1% due to mainly crab predation at the enclosed site. Temporal variation in abundance and spatial distribution of predators was not correlated with that of seeded scallops, suggesting that predatory mortality of seeded scallops was due to a functional response, rather than an aggregative response of predators. Growth of seeded scallops was similar at both sites. The dynamics of the seeded scallop populations reflected the interaction of predation, dispersion, and growth.

Résumé : Des milliers de juvéniles du pétoncle géant (*Placopecten magellanicus*) ont été lâchés en deux endroits sur le fond de la mer (un secteur à la topographie ouverte, un autre à la topographie fermée) le long de la côte sud-ouest de la Nouvelle-Écosse, Canada, à deux saisons, soit en été et en hiver. Les pétoncles indigènes et introduits ainsi que leurs prédateurs (les étoiles de mer *Asterias vulgaris* et *A. forbesi* ainsi que le crabe *Cancer irroratus*) ont fait l'objet d'une surveillance vidéo et d'examens visuels par des plongeurs sur une période de 17 mo. La densité des pétoncles introduits a diminué rapidement après les lâchers et s'est stabilisée au bout d'une à 8 sem; à la fin du projet, l'écart de densité entre les stations était plus grand que celui entre les saisons d'ensemencement. La température saisonnière influe sur la vitesse à laquelle la densité finale est atteinte. L'ensemencement a permis de doubler effectivement la densité des pétoncles à chaque endroit. Le taux de survie a été d'environ 10 % sur le site ouvert, à cause de la prédation exercée par le crabe et de la dispersion des pétoncles introduits, et d'environ 1 % sur l'autre site, principalement à cause de la prédation par le crabe. Il n'existe pas de corrélation entre les variations dans le temps de l'abondance et de la distribution spatiale des prédateurs et celles du pétoncle introduit; cela suggère que la mortalité par prédation de ce dernier est attribuable à une réponse fonctionnelle plutôt qu'à une réponse par agrégation des prédateurs. Le développement des pétoncles introduits était sensiblement le même aux deux endroits. La dynamique des populations de pétoncles introduits reflétait les interactions entre la prédation, la dispersion et le développement.
[Traduit par la Rédaction]

Introduction

With increased interest in aquaculture of bivalves, two methods are presently being evaluated: suspended culture, in which bivalves are placed in cages or attached to lines suspended in the water column, and bottom culture, in which juvenile bivalves are released (seeded) onto the sea bed and harvested once they reach commercial size (Quayle and Newkirk 1989; Shumway 1991; Boghen 1995). Bottom culture is less labour- and cost-intensive than suspended culture, but produces lower yields due to increased rates of mortality and dispersion. Bottom culture also results in slower growth rates than suspended culture (MacDonald 1986; Wildish et al. 1988; but see Kleinman et al. 1996). Bottom culture preceded by a period of growth in suspended culture (intermediate culture) may prove to be the most economically viable culture method for scallops (Ventilla 1982; Wildish et al. 1988; Couturier et al. 1995).

Bottom culture of scallops has had varying success in previous seeding trials, with survivorship ranging from 0 to 80% (Ventilla 1982; Minchin 1991; Tettelbach and Wenczel 1993; Bull 1994; Dao et al. 1994; Goshima and Fujiwara 1994; Halary et al. 1994). Low survivorship of seeded scallops may result from one or more causes of mortality which include predation (Volkov et al. 1983; Minchin 1991; Spencer 1992; Cliche et al. 1994; Halary et al. 1994; Hatcher et al. 1996),

Received July 20, 1995. Accepted May 1, 1996.
J13010

M.A. Barbeau,[1] R.E. Scheibling, A.W. Hennigar, L.H. Taylor, and A.C. Risk. Department of Biology, Dalhousie University, Halifax, NS B3H 4J1, Canada.
B.G. Hatcher. Department of Oceanography, Dalhousie University, Halifax, NS B3H 4J1, Canada.

[1] Corresponding author. New address: Woods Hole Oceanographic Institution, Coastal Research Lab, Mail Stop 2, Woods Hole, MA 02543-1525, U.S.A. e-mail: mbarbeau@whoi.edu

© 1996 NRC Canada

Fig. 1. Lunenburg Bay, Nova Scotia, Canada, showing location of Sites 2 and 3 where bottom seeding trials with juvenile sea scallop (*P. magellanicus*) were conducted. Site 1 indicates the location of the pilot study detailed in Hatcher et al. (1996).

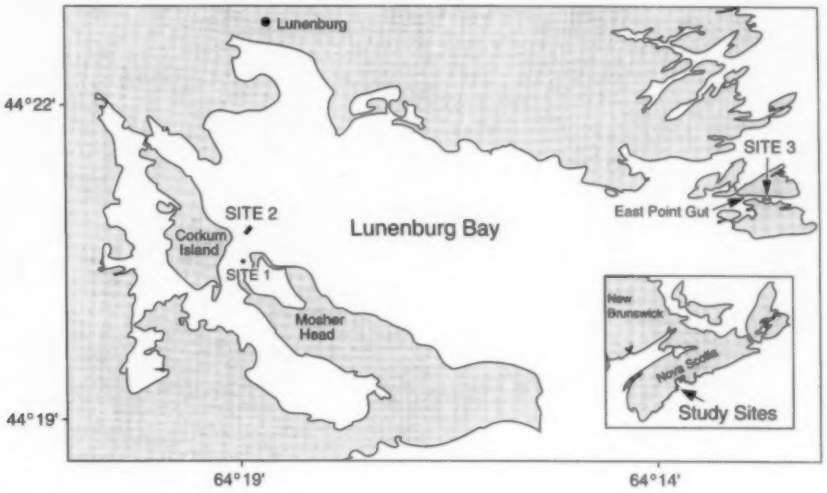

interspecific competition (Halary et al. 1994), and adverse environmental conditions, such as extreme temperatures, low salinity, heavy sedimentation (Tettelbach et al. 1990), strong wave action (Kalashnikov 1991; Tettelbach and Wenczel 1993), and toxic algal blooms (Tettelbach and Wenczel 1993). As well, loss of seeded scallops may be due to dispersion from sites and be related to high initial densities of seeded scallops (Volkov et al. 1983; Hatcher et al. 1996), inappropriate substratum type (Dupouy 1983; Picard and Vigneau 1992), local hydrodynamics (Morgan et al. 1980; Hatcher et al. 1996), and high water temperatures (Morgan et al. 1980; Carsen et al. 1996*b*; Hatcher et al. 1996).

Predation is usually the main cause of loss of seeded scallops, especially when the scallops are of small size and (or) in poor condition (Morgan et al. 1980; Lake et al. 1987; Minchin 1991; Barbeau et al. 1994; Halary et al. 1994). However, the effect of predators is multifaceted. Predation rates may increase with increased scallop density due to greater consumption rates of individual predators (a functional response) and (or) enhanced local densities of predators (an aggregative numerical response) (Taylor 1984; Barbeau et al. 1994). The magnitude of the predator effect also depends on the size distribution of predators at a given site in relation to that of seeded scallops (Lake et al. 1987; Minchin 1991; Barbeau and Scheibling 1994*a*). In addition, predators trigger escape swimming in many scallop species, which causes scallops to disperse (Thomas and Gruffydd 1971; Peterson et al. 1982; Dadswell and Weihs 1990).

The sea scallop (*Placopecten magellanicus*) is an important commercial species in fisheries and aquaculture in the northeastern United States and eastern Canada (Brand 1991; Couturier et al. 1995). In coastal environments most suitable for bottom culture, sea stars (*Asterias vulgaris* and *A. forbesi*) and rock crab (*Cancer irroratus*) are the major predators of sea scallop (Naidu and Cahill 1986; Barbeau et al. 1994; Cliche et al. 1994; Hatcher et al. 1996). This study builds on a previous pilot seeding trial in Nova Scotia, in which 10 000 juvenile sea scallops were released in autumn and followed for ~1 yr (Hatcher et al. 1996). The pilot study demonstrated that enhancement of wild scallop populations was possible, but it did not identify the reasons for successful seeding. Here, we report on four subsequent seeding trials, in which 13 000 – 21 000 juvenile sea scallops were seeded in summer and winter at two sites in the same locale. Our objectives were to determine the effects of site and season on mortality, movement, and growth of seeded scallops, and to estimate the relative contribution of predation and dispersion to losses of seeded scallops. As well, we suggest recommendations for enhanced success in future bottom seeding operations.

Material and methods

Study sites

The seeding experiments were conducted at two contrasting locations near Lunenburg, Nova Scotia, Canada (Fig. 1). The sites were selected to meet the following criteria based on a pilot study (Hatcher et al. 1996): a 1-ha area of relatively uniform cobble and silt sea bed, experiencing similar weather conditions and moderate currents (>0.1 and <1.0 $m \cdot s^{-1}$), and supporting a wild population of scallops. Logistic constraints limited the depth of the sites to <10 m and the distance offshore to <1 km. The two sites were chosen to maximize the contrast between topographically bounded and open-water culture conditions: Site 2 was an exposed portion of a large embayment, 600 m away from the pilot site (Site 1), and Site 3 was a narrow channel between islands at the mouth of the bay, 4.8 km away from Site 2.

Site 2 (44°20.7′N, 64°18.8′W) was centred on a 100-m-long transect running on a true bearing of 40° at a depth (at mean low tide) of 7.9–8.8 m along this transect. The longitudinal axis of the 100 × 50 m survey area was parallel to the dominant vector of the ebb tide current which runs out of Corkum Island Channel. The site was exposed to the ocean swell and easterly wind-generated waves, but the currents were dominated by the tidal flows filling and emptying the shallow coves to the southwest. Current velocities ranged from 0 at slack water to 0.58 $m \cdot s^{-1}$ at peak flow, as measured using one or two electromagnetic current meters (model S4, Inter Ocean

© 1996 NRC Canada

Table 1. Summary of the surveys and seeding schedule at Sites 2 and 3 in Lunenburg Bay.

Site	Surveys and seeding	Date	Day
2	–2	19 July 1991	–46
	–1	29 Aug. 1991	–5
	Summer seeding	3 Sept. 1991	0
	1	4 Sept. 1991	1
	2	9 Sept. 1991	6
	3	6–7 Nov. 1991	64–65
	4	16 Mar. 1992	195
	Winter seeding	18 Mar. 1992	197
	5	20 Mar. 1992	199
	6	26 Mar. 1992	205
	7	23 Apr. 1992	233
	8	26 May 1992	266
	9	10 Aug. 1992	342
	10 (diver census)	16–18 Nov. 1992	440–442
3	–1	27 Aug. 1991	0
	Summer seeding	27 Aug. 1991	0
	1 (quadrat sampling)	28 Aug. 1991	1
	2	5 Sept. 1991	9
	3	22 Nov. 1991	87
	4	24 Feb. 1992	181
	Winter seeding 1	5 Mar. 1992	191
	5	5–6 Mar. 1992	191–192
	6	17 Mar. 1992	203
	Winter seeding 2	18 Mar. 1992	204
	7	31 Mar. 1992	217
	8	16 Apr. 1992	233
	9 (diver census)	22 Oct. 1992	422

Note: Surveys were video transects except for survey 10 at Site 2 and surveys 1 and 9 at Site 3.

Systems, San Diego, Calif.) located on the transect and 0.6 m above the sea bed. The semidiurnal tides ranged from 0.7 to 2.1 m for neap and spring tides, respectively. Mean daily water temperature measured near the sea bed by diver gauge, min–max in situ thermometer, Ryan thermograph, or digital recording thermometer (Hobo Temp Corp.) ranged from –1.3 to 18.3°C during the 17-mo study. Tidal period variation in water temperature could exceed 6°C, as the cold bottom waters of the bay intruded under the warmer surface water on flood tides in summer and autumn, and as colder water in winter or warmer water in summer flowed out of the nearby shallow coves. Salinity as measured by the S4 current meters ranged from 29.1 to 31.4 ppt near the sea bed during the study. The site was located on a mixed substrate consisting of shell fragments and medium to fine granite slate and cobbles on silty sediment. Most shell fragments and cobbles were coated with crustose coralline algae (*Clathromorphum* sp., *Lithothamnium* sp., *Phymatolithon* sp.). Kelp (*Laminaria longicruris* and *Agarum cribosum*) cover as estimated from video surveys was 8–16%, depending on season. Approximately 100 m west and 100 m southeast off the centre of Site 2, the substratum changes to predominantly sand and silt–size sediments as it shoals towards the shore of Corkum Island and Mosher Head. Towards the north and east quadrants of the survey area, the substratum changes gradually to silt-clay-size sediments as it deepens towards the centre of the bay at depths exceeding 15 m.

Site 3 (East Point Gut, 44°21.1′N, 64°12.8′W) was centred on a 100-m-long transect running on a true bearing of 85° at a depth of 4.8 m along this transect. The longitudinal axis of the 100 × 25 m survey area extended along the centre of the channel, parallel to the major axis of the current flow, and the survey area spanned the width of the narrowest section of the channel. The site was protected from ocean swell and large wind-generated waves. Tidal currents on the channel were superimposed on lower frequency, horizontal pressure gradient currents driven by differential winds in the bays to the west (Lunenburg Bay) and east (Mahone Bay) of the channel. The resulting current was often strong enough to prevent tidal reversal in current direction, producing several days of unidirectional flow through the channel. Current velocities ranged from 0.1 at slack water to 0.48 $m \cdot s^{-1}$ at peak flow. The tidal range was 0.7–1.9 m for neap and spring tides, respectively. The water temperature regime was less variable than at Site 2, with tidal variation rarely exceeding 3°C. During the study, the ranges in daily mean temperature and salinity near the sea bed were similar to those at Site 2. The substratum at Site 3 was compositionally similar to that at Site 2, but had a higher silt fraction and was less uniform. It graded from a mixture of shell fragments and medium-size granite cobbles on the north side to silty sediment towards the south shore. Kelp (*L. longicruris*) and seagrass (*Zostera marina*) covered 2–8% of the sea bed, depending on season.

Seeding

Juvenile scallops were seeded at Sites 2 and 3 in late summer 1991 and in late winter 1992 (Table 1). For the summer seeding, scallops were obtained from spat collectors in Passamaquoddy Bay, New Brunswick, through a commercial supplier (The Great Maritime

© 1996 NRC Canada

Scallop Trading Co.) and from an experimental hatchery at Sandy Cove, Nova Scotia (Fisheries Resource Development Limited). At each site, 16 000 wild-collected and 5600 hatchery-reared scallops were mixed and released within a 20 × 60 m area from a chute on a 7-m Cape Islander boat. For the winter seeding, all juvenile scallops were obtained from the commercial supplier. At Site 2, 18 000 scallops were released within a 30 × 20 m area by SCUBA divers. At Site 3, 13 000 scallops (initially 9000 followed by 4000, 2 wk later) were released within a 20 × 15 m area. In all cases, scallops were seeded during slack water, between 13:00 and 16:00 Atlantic Standard Time.

Prior to the seeding trials, scallops were held in the laboratory in 250- or 2100-L tanks with flowing ambient seawater for 1–4 wk and drip-fed to maintain a cultured algae concentration of $\sim 1 \times 10^4$ cells·mL^{-1} (a mixture of T-*Isochrysis galbana*, *Thalassiosira pseudonana*, and *Chaetoceros mülleri*). For the summer seeding, 10–15% of wild-collected and hatchery-reared scallops were tagged using plastic bee tags (2.6-mm diameter, 0.02-mm thickness, 0.0014 g, Steele & Brodie Ltd., Hampshire, England) in the laboratory. To tag the scallops, a small area of the upper valve of a scallop was cleaned with a cotton swab and acetone (care was taken not to expose the scallop's mantle edge to acetone) and dried with an airjet. Two numbered and coloured tags were glued to the valve using cyanoacrylate glue. During the tagging procedure, individual scallops spent <3 min out of the water.

Distribution and abundance of scallops and predators

The distribution and abundance of wild and seeded scallops, and their major predators, sea stars and rock crabs, were sampled by diver-held video camera (Sony CCD-V801 Hi-8 video camera recorder in an Amphibico housing) in 0.5-m-wide × 100-m long transects running parallel at 5-m intervals at Site 2 and 2.5- or 5-m intervals at Site 3. The transects were sampled before seeding and at approximately 1 d, 1 wk, 1–3 mo, 6 mo, and 1 yr after seeding (Table 1). A rod attached to the camera housing was used to keep the camera 0.6 m above the sea bed and centred on the transect line which was graduated at 1-m intervals. Calibration quadrats (0.25 m^2, n = 14–48) were set within the video transects in most surveys and censused immediately before or after the passage of the camera. The video tapes were analysed with a video cassette recorder (Sony EV-S900 VCR) and colour monitor (Sony KV-20EXR2). Scallops and predators were counted in successive 1-m (0.5 m^2), 2-m (1 m^2), 5-m (2.5 m^2), and 10-m (5 m^2) sections of the video transects. Given the restrictions to sampling in the subtidal environment, this design was chosen to maximize sample size (although contiguous quadrat sampling presents the possibility of nonindependence). Seeded scallops could be distinguished from wild scallops by their size, shape, and lack of silt or epibionts on their shells. Based on the calibration quadrats, only the counts of seeded scallops needed to be adjusted; the mean ± SD adjustment coefficient was 1.274 ± 0.224 (n = 9 surveys). Three surveys were done without video: on day 1 at Site 3, the study area was surveyed using 0.25-m^2 quadrats (n = 50), and on days 440–442 at Site 2 and day 422 at Site 3, all scallops, sea stars and crabs were collected and counted. Abundance of seeded scallops was used to calculate survivorship.

Standardized Morisita's Index (SMI) of distribution was calculated for each quadrat size (0.5, 1, 2.5, and 5 m^2) (Krebs 1989). An appropriate quadrat size was chosen to minimize the variance in the densities of each species. Negative exponential interpolation algorithms (Wilkinson 1989) were used to plot the density contours of scallops and predators for each survey date. Because the same transects were monitored at each survey, changes in the density of wild scallops, sea stars, and crabs were tested using a one-way repeated measures analysis of variance (ANOVA) or a Friedman test if the assumption of homogeneity of variance was not met, even after log or square root transformation of the data. The assumption of equal covariance in the repeated measures ANOVA was tested using the sphericity test (Crowder and Hand 1990). Because the data were nonspherical, the degrees of freedom were adjusted using Greenhouse–Geisser estimate ϵ. Multiple comparisons of means are not presented.

At each survey date, displacements of seeded scallops were measured as the distance between each scallop and the centre of the release area (displacements of scallops on the seeding dates were not measured). The change in scallop displacement after each seeding was tested using a one-way ANOVA, with survey as the fixed factor, and the GT2-method for multiple comparison of means (Sokal and Rohlf 1981). Diffusion coefficients (C_x and C_y) were calculated as $(\sigma^2_{x,s+1} - \sigma^2_{x,s})/[2(t_{s+1} - t_s)]$ and $(\sigma^2_{y,s+1} - \sigma^2_{y,s})/[2(t_{s+1} - t_s)]$, where σ^2_x and σ^2_y were the variances in displacement in the along-channel (x) and across-channel (y) directions, t was time in days, and s was survey number (Bowden 1983). Loss due to dispersion of scallops out of the study area was calculated as a flux in both the along-channel (F_x) and across-channel (F_y) directions: $F_x = -C_x(\Delta\text{density}/\Delta x)$ and $F_y = -C_y(\Delta\text{density}/\Delta y)$, where $\Delta\text{density}/\Delta x$ and $\Delta\text{density}/\Delta y$ were the changes in seeded scallop density over the last 10 or 20 m at the edge of the site. The daily flux of scallops out of a site was estimated by multiplying the directional fluxes by the perimeter of the site: $(100F_x + 200F_y)$ for Site 2 and $(50F_x + 200F_y)$ for Site 3. The total flux between surveys was estimated as the daily flux multiplied by the number of days between surveys.

Key-factor analysis was used to estimate the relative contribution of dispersion and predatory mortality to loss of seeded scallops from a site (Varley and Gradwell 1960). The k-values of the different factors ($k_{\text{dispersion}}$, $k_{\text{sea star}}$, and k_{crab}) reflect the intensity or rate of loss, and their summation should be equivalent to the observed total loss (k_{total}). Loss due to dispersion was estimated as described in the paragraph above. Loss due to predation was estimated from the results of tethering experiments with juvenile scallops, concurrent with the seeding trials at Sites 2 and 3 (Barbeau et al. 1994). In the tethering experiments, predators could be identified by the scallop shell remains. The tethering procedure did not significantly affect crab predation rates, but increased sea star predation rates 17 times in laboratory experiments (Barbeau and Scheibling 1994b). Therefore, sea star predation rates estimated from the tethering experiments were divided by 17. The k-values were calculated for each k-factor as $\log_{10}$(estimated scallop abundance at a survey) – $\log_{10}$(estimated scallop abundance at the next survey after a k-factor has acted). Total loss (k_{total}) was calculated using the scallop abundances recorded in the surveys. The k-values were not calculated for the first interval after seeding, due to lack of dispersion estimates.

Size frequency distributions

Random samples of wild scallops were measured (±1 mm accuracy) by divers at each site before seeding (Site 2: 2 and 5 August 1991; Site 3: 26 July 1991). Scallop shell height (Sh) was measured from the middle of the dorsal hinge to the furthest ventral shell edge. Tagged scallops and a random sample of seeded scallops were measured (0.1 mm accuracy) using vernier calipers before the summer and winter seedings, and at the end of the study for both sites. For Site 2, seeded and wild scallops were measured from the video tapes for most surveys and calibrated against a scale bar. Growth rates of seeded scallops at Site 2, based on modal size progression, were estimated using linear regression.

Random samples of sea stars and crabs were measured (±1 mm accuracy) by divers during July–August 1991 and September–October 1992 at Sites 2 and 3. On 6 May 1992, crabs were measured from traps placed at Site 3. Sea stars and crabs were also measured from the video tapes for all surveys at both sites and calibrated against a scale bar. Sea star radius (R) was measured from the tip of an average ray to the mouth and crab carapace width (CW) as the distance between the tips of the two most distal marginal teeth. The predators were then classified into size classes (for sea stars, small: <30, medium: >30 and <50, and large: >50 mm R; for crabs, small: <50,

© 1996 NRC Canada

Fig. 2. Spatial distribution of seeded juvenile sea scallop (*P. magellanicus*) over 12 mo at Site 2. The outer box represents the site. The area defined by the broken lines represents the area surveyed. The inner box represents the area where the scallops were seeded. The number of days after the summer seeding are not in parentheses and those after the winter seeding are in parentheses. Note that the area surveyed was moved 10 m southeast and 20 m northeast prior to the survey on day 64. See Table 1 for survey number and date.

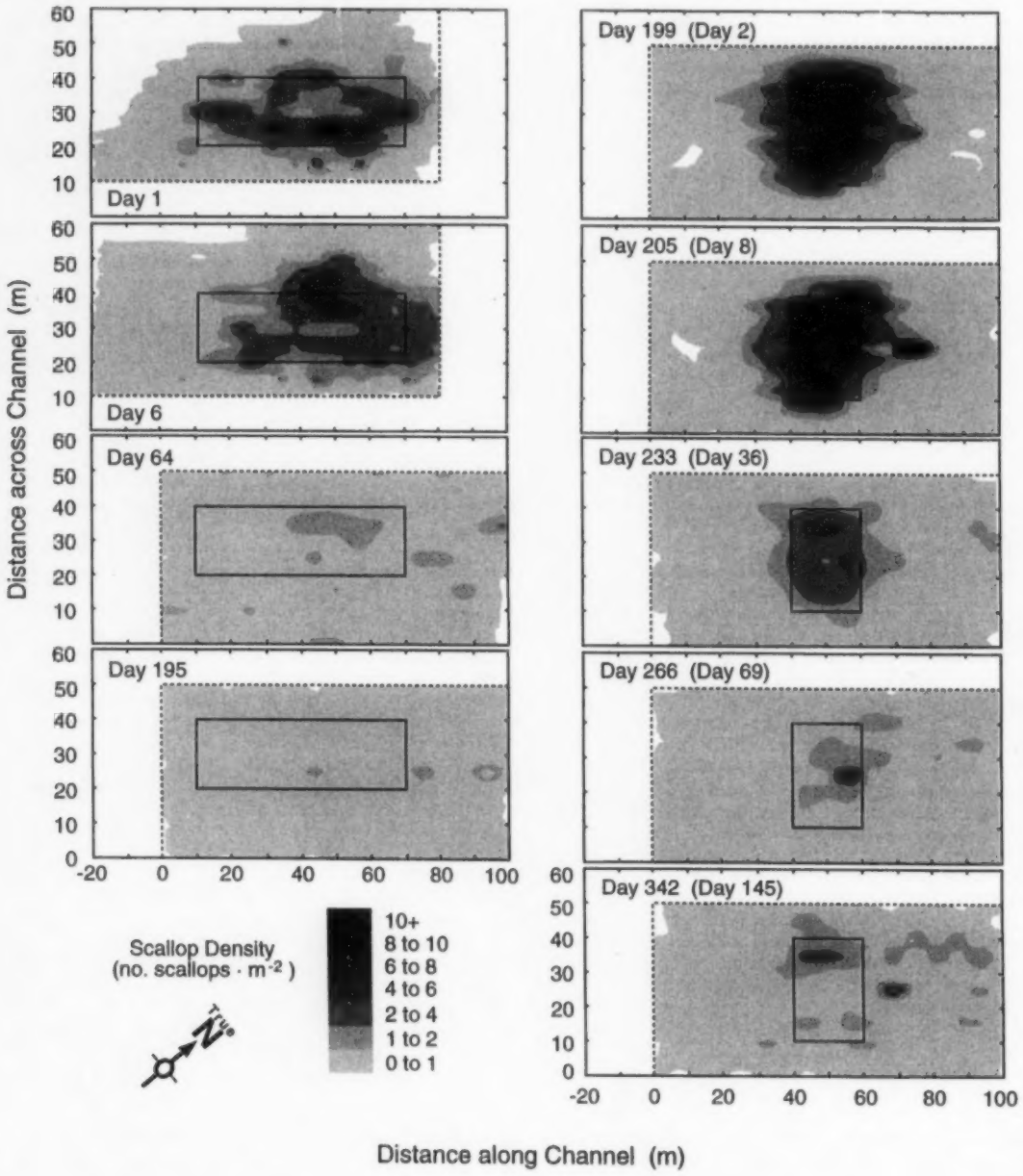

medium: >50 and <90, large: >90 mm CW), and the change in frequency of animals in each size class over time was examined using two-way *G*-tests.

Predator activity and diet

Predator activity and diet were recorded at various times during the study by SCUBA divers. Predator activity was categorized as quiescent (not moving and not feeding), searching (moving and not feeding), or feeding. The change in frequency of predators in each activity category over time was examined using two-way *G*-tests. On the four seeding dates, an underwater camerahead linked to a time-lapse (3 frames·10 s^{-1}) video recorder (Fuhrman Diversified

© 1996 NRC Canada

Fig. 3. Spatial distribution of seeded juvenile sea scallop (*P. magellanicus*) over 8 mo at Site 3. The outer box represents the site and the inner box, the area where the scallops were seeded. The number of days after the summer seeding are not in parentheses and those after the winter seeding are in parentheses. See Table 1 for survey number and date.

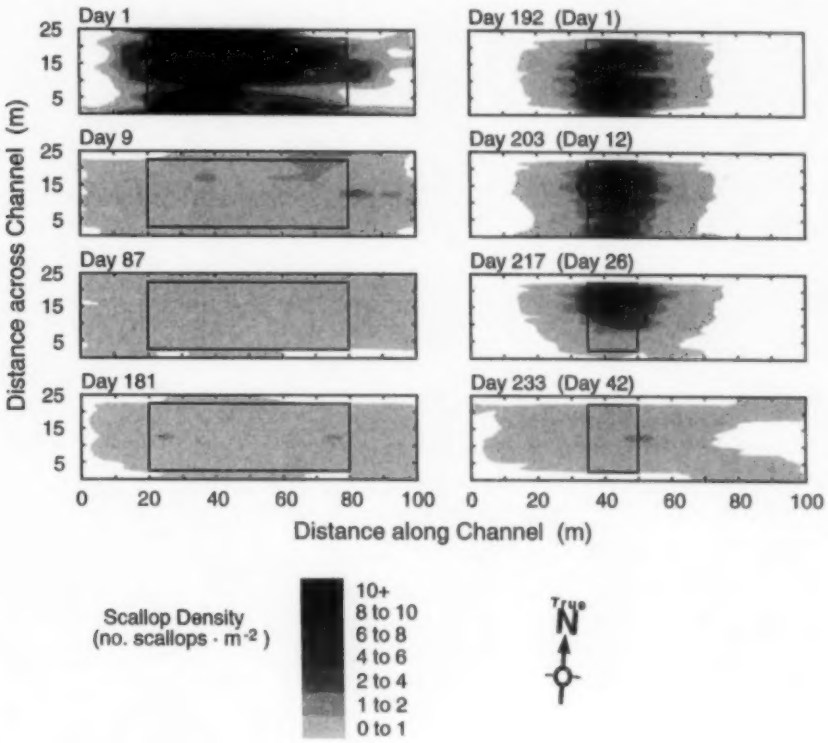

Inc., La Porte, Tex.) was used to monitor predator activity for 16–52 h. The infrared-sensitive camerahead was mounted on a scaffolding to give a field of view of 0.34 m^2 and was surrounded by two banks of infrared lights which were triggered on at dusk and off at dawn. The video recordings were used to quantify the number and duration of visits by predators into the field of view.

Results

Distribution and abundance of scallops and predators

The distribution of seeded scallops was aggregated at each of the four spatial scales (0.5, 1.0, 2.5, 5.0 m^2, Site 2: 0.500 < SMI < 0.530; Site 3: 0.270 < SMI < 0.579) on each survey date, except for the survey immediately prior to the winter seeding (survey 4) at both sites. In the fourth survey, seeded scallops at Site 2 were less aggregated (0.107 < SMI < 0.500) than in previous and subsequent surveys, and seeded scallops at Site 3 had a uniform or random distribution (–0.717 < SMI < 0.157). For the summer seeding, the initial aggregation of seeded scallops in the release area quickly spread over the site and disappeared within 64 d at Site 2 and 9 d at Site 3 (Figs. 2 and 3). The dynamics were slower for the winter seeding: the initial seeding aggregation disappeared after 69 d at Site 2 and 26 d at Site 3. In surveys 7 (day 233) and 9 (day 342) at Site 2, the slightly higher densities at 35 m across channel and 45–55 m along channel were due to the introduction of an additional 1250 scallops for a growth experiment (Kleinman et al. 1996). Densities of seeded scallops, whether averaged over the whole site or only the area occupied by the seeded population, also decreased rapidly after seeding to ~1 scallops·2.5 m^{-2} at Site 2 and 0.1 scallops·2.5 m^{-2} at Site 3 (Figs. 4, 5*a*, and 5*b*). The summer-seeded scallops showed a steeper decline in density than the winter-seeded scallops. Survivorship declined rapidly and stabilized at ~10% of the original number of seeded scallops at Site 2, and ~1% at Site 3, for both the summer and winter seedings (Figs. 5*c* and 5*d*).

Displacement of seeded scallops (Fig. 6) increased significantly over time after each seeding (Site 2, summer seeding: $F = 97.06$, df = 3, 1500, $p < 0.001$; Site 2, winter seeding: $F = 84.52$, df = 4, 2276, $p < 0.001$; Site 3, summer seeding: $F = 11.47$, df = 3, 254, $p < 0.001$; Site 3, winter seeding: $F = 68.68$, df = 3, 1655, $p < 0.001$). Displacement increased immediately following the summer seeding, but levelled off as water temperature decreased. Conversely, mean displacement was low following the winter seeding, but increased as water temperature increased. Estimated fluxes of seeded scallops away from Site 2 varied between 4 and 380 scallops·d^{-1}. Estimated fluxes of seeded scallops away from Site 3 varied between 0 and 112 scallops·d^{-1}, and were very low (<25 scallops·d^{-1}) in the across-channel direction, since the survey area was generally bordered by the shore. Key-factor analysis

© 1996 NRC Canada

Fig. 4. Mean ± SD density of seeded and wild sea scallop (*P. magellanicus*), sea star (*Asterias* spp.), and rock crab (*C. irroratus*) calculated over the whole surveyed area of (*a*) Site 2 and (*b*) Site 3. Circles indicate data obtained from video survey, except for the data point on day 1 at Site 3, which was obtained from diver quadrat survey. Squares indicate data (day 440 at Site 2 and day 422 at Site 3) obtained from diver censuses. Quadrat size for the different species was chosen to minimize variance. n = 100–220 for scallop and sea star (except for seeded scallop on day 1 at Site 3, n = 10) and n = 50–110 for crab. Arrows indicate the days when a site was seeded with juvenile scallop. See Table 1 for survey number and date.

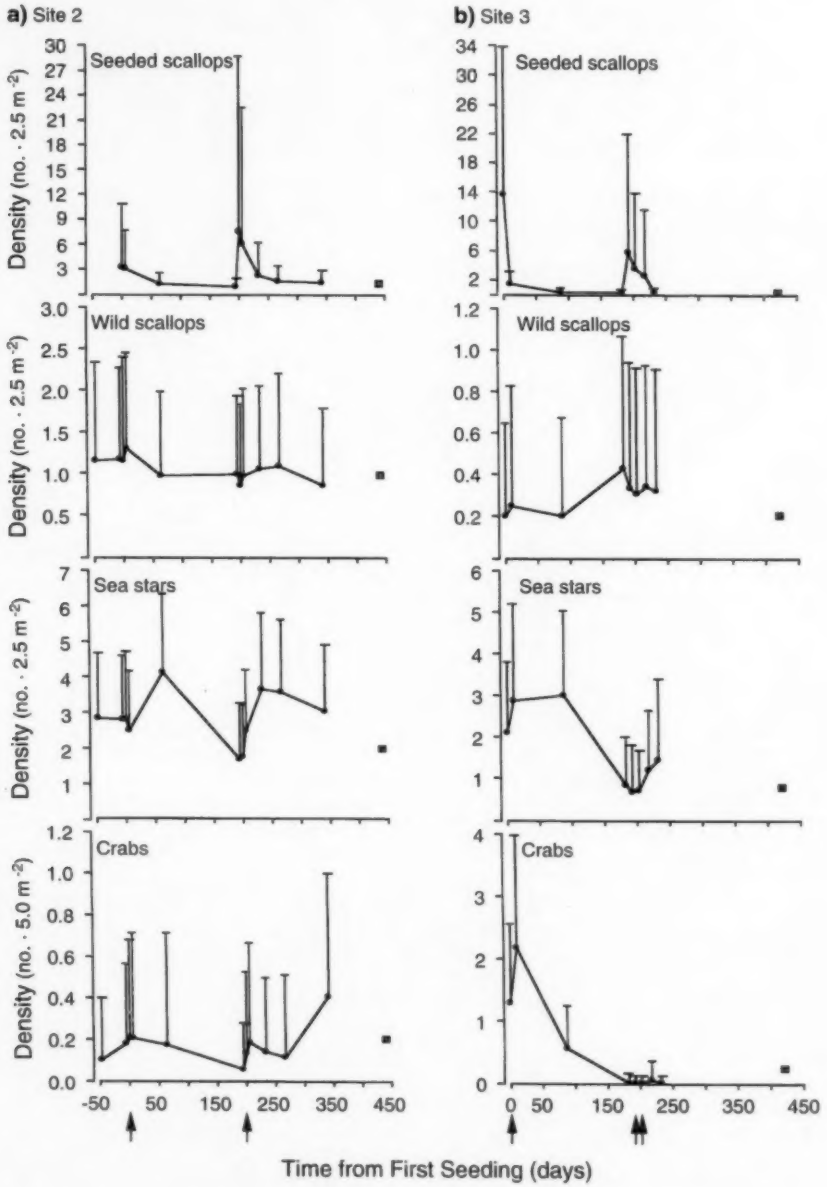

showed that dispersion and crab predation accounted for most of the loss of summer-seeded scallops at Site 2 (Fig. 7). Crab predation accounted for most of the loss of winter-seeded scallops at Site 2 and of both summer- and winter-seeded scallops at Site 3, although the estimated losses due to dispersion and predation combined were less than the total loss measured from the video surveys.

The distribution of wild scallops varied greatly for all spa-

© 1996 NRC Canada

Fig. 5. (*a* and *b*) Mean ± SD density and (*c* and *d*) survivorship of seeded sea scallop (*P. magellanicus*) at Sites 2 and 3. Scallop density was calculated over the area occupied by the seeded populations. Data were obtained from video survey, except for the data points on day 440 at Site 2 and days 1 and 422 at Site 3, which were obtained from diver surveys. w1 and w2 indicate the first and second winter seeding at Site 3. Arrows indicate the days when a site was seeded with juvenile scallop. See Table 1 for survey number and date.

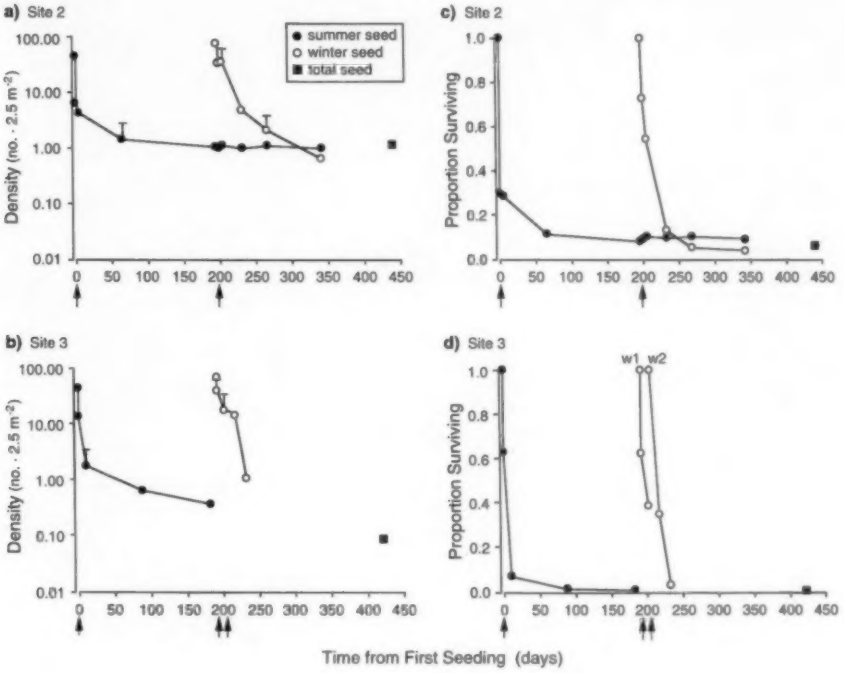

tial scales and survey dates (–0.747 < SMI < 0.506), but on average was random at both Site 2 (SMI = 1.33 ± 0.327 (SD)) and Site 3 (SMI = 1.08 ± 0.408). Density of wild scallops was relatively constant over time with a mean (±SE) of 1.05 ± 0.13 scallops·2.5 m^{-2} at Site 2 and 0.29 ± 0.07 scallops·2.5 m^{-2} at Site 3 (Fig. 4), although the density at Site 2 was significantly higher in surveys –1 (day –5) and 2 (day 6) than in other surveys (Site 2: $F = 3.71$, df = 10, 2190, $\epsilon = 0.855$, $p < 0.001$; Site 3: $F = 1.83$, df = 7, 693, $\epsilon = 0.855$, $p > 0.05$).

Sea stars were usually aggregated at Site 2, but occasionally had a uniform or random distribution at the different spatial scales and survey dates (–0.512 < SMI < 0.501; mean ± SD: 0.391 ± 0.201). Sea stars at Site 3 were aggregated at all spatial scales and survey dates (0.117 < SMI < 0.505; mean ± SD: 0.486 ± 0.069). However, sea star aggregation did not coincide with seeded scallop aggregation (Figs. 8 and 9). Sea star density (Fig. 4) showed significant temporal variation (Site 2: $F = 39.02$, df = 10, 2190, $\epsilon = 0.937$, $p < 0.001$; Site 3: $F = 47.55$, df = 7, 693, $\epsilon = 0.880$, $p < 0.001$). Sea star density did not correlate with seeded scallop density, either for the same survey dates (Site 2: $r = -0.498$, df = 7, $p > 0.05$; Site 3: $r = -0.524$, df = 5, $p > 0.05$) or for sea star survey dates lagged by one behind seeded scallop survey dates (Site 2: $r = 0.307$, df = 6, $p > 0.05$; Site 3: $r = 0.489$, df = 5, $p > 0.05$).

Crab distribution varied greatly at all spatial scales and survey dates (–1.000 < SMI < 0.520), but on average was random at Site 2 (SMI = –0.218 ± 0.606 (SD)) and Site 3 (SMI = –0.002 ± 0.568; indices were not calculated for surveys 4, 5, 6, and 8 because of low abundance). Crab density (Fig. 4) showed significant temporal variation at both sites (Site 2: Friedman $X^2 = 19.03$, df = 10, $p < 0.05$; Site 3: $X^2 = 114.84$, df = 7, $p < 0.001$). Crab density did not correlate with seeded scallop density for the same survey dates (Site 2: $r = -0.072$, df = 7, $p > 0.05$; Site 3: $r = -0.210$, df = 5, $p > 0.05$), but correlated significantly for crab survey dates lagged by one behind seeded scallop survey dates at Site 3 only (Site 2: $r = -0.007$, df = 6, $p > 0.05$; Site 3: $r = 0.864$, df = 5, $p < 0.05$). At Site 3, 558 crabs were trapped and removed between 28 April and 16 October 1992 (days 245 and 416).

Size frequency distributions

In the survey prior to the summer seeding, only 4% of the wild scallops were within the size range of the seeded scallops at Site 2 and none was within this range at Site 3 (Fig. 10). At Site 2, cohorts of summer- and winter-seeded scallops could be followed until August 1992 when the two modes joined together. Growth of summer-seeded scallops as measured by modal progression was initially rapid at Site 2 and then slowed in winter (Fig. 11). Growth of winter-seeded scallops paralleled that of the summer-seeded scallops in winter. Overall at Site 2, the growth rate was 0.078 ± 0.008 (SE) mm·d^{-1} ($r^2 = 0.948$, df = 1, 5, $p < 0.001$) for summer-seeded

© 1996 NRC Canada

Fig. 6. Mean ± SD displacement (squares) of seeded sea scallop (*P. magellanicus*) and average monthly water temperature (dotted line) at (*a*) Site 2 and (*b*) Site 3. Displacement of scallops on the seeding day was not available. Letters indicate the results of multiple mean comparisons (displacements with the same letter did not differ significantly). Arrows indicate days when the sites were seeded with juvenile scallop. n = 25–1118 for displacement. See Table 1 for survey number and date.

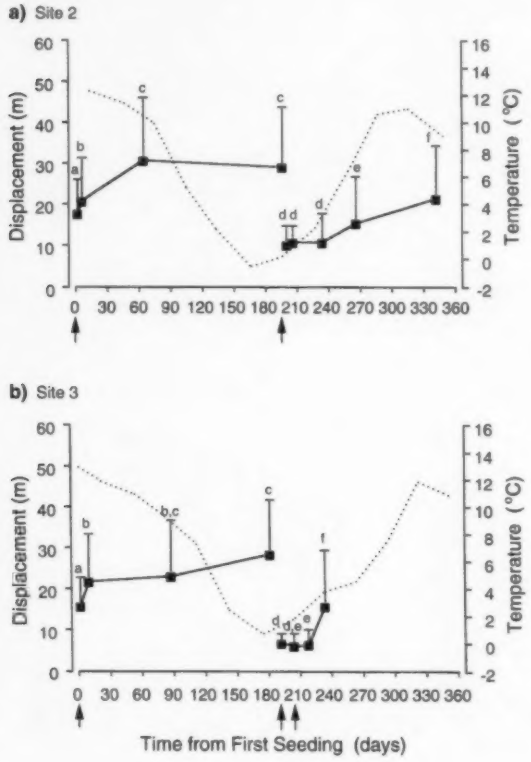

scallops and 0.059 ± 0.006 mm·d^{-1} (r^2 = 0.979, df = 1, 2, p < 0.05) for winter-seeded scallops.

Of the total number of scallops tagged for the summer seeding, 3.3% at Site 2 and 0.4% at Site 3 were recovered 14–15 mo later (Fig. 10). At Site 2, the ratio of wild-collected to hatchery-reared tagged scallops released in September 1991 (2.2:1.0) was similar to that recovered in November 1992 (1.8:1.0). Also, the growth rates of tagged wild-collected (0.087 ± 0.012 mm·d^{-1} (SD)) and hatchery-reared (0.088 ± 0.014 mm·d^{-1}) scallops at Site 2 were not significantly different (t = –0.35, df = 81, p > 0.50). The growth rate of tagged scallops at Site 3 was 0.079 ± 0.023 mm·d^{-1}.

The mean ± SD size of sea stars before the summer seeding was 35 ± 11 mm R (n = 678, range: 6–150 mm R) at Site 2 and 49 ± 31 mm R (n = 349, range: 12–205 mm R) at Site 3. The proportion of sea stars in three different size classes (Figs. 12*a* and 12*c*) showed significant temporal variation at both sites (Site 2: G = 248.91, df = 24, p < 0.001; Site 3: G = 231.01, df = 18, p < 0.001).

The mean ± SD size of crabs before the summer seeding was 73 ± 24 mm CW (n = 70, range: 13–120 mm CW) at Site 2 and 64 ± 18 mm CW (n = 81, range: 23–100 mm CW) at Site 3. Within each site, the proportion of crabs in the three different size classes (Figs. 12*b* and 12*d*) varied significantly over time (Site 2: G = 88.43, df = 22, p < 0.001; Site 3: G = 143.74, df = 10, p < 0.001 (sampling dates with <10 individuals were excluded from the analysis)).

Predator activity and diet

Sea star activity patterns varied significantly throughout the year (Site 2: G = 140.79, df = 14, p < 0.001; Site 3: G = 742.64, df = 20, p < 0.001) (Table 2). Sea stars spent a higher proportion of time quiescent in winter than in summer. Sea stars fed mainly on detritus and periwinkles, although they were observed feeding on scallops immediately postseeding (Table 2). Very few sea stars were observed on the time-lapse video (Fig. 13) because of their low movement velocities. Sea stars spent 79.4 ± 8.0 (SE, n = 13) min within the field of view.

The activity patterns of crabs based on diver surveys were generally difficult to interpret because few crabs (usually <10) were observed, except at Site 3, on 27 August 1991, when 15% of crabs (n = 136) were feeding on scallops immediately after seeding. On other occasions, crabs were generally quiescent (buried or not) or searching. The time-lapse video showed high crab activity during the day in summer, particularly at Site 3 (Figs. 13*a* and 13*b*). There was a 5- to 6-h time-lag before crabs responded to the input of scallops in winter (Figs. 13*c* and 13*d*). At Site 3 in winter, crabs were active only at night, but at Site 2, they were active throughout the day and night. Crabs spent 6.7 ± 0.2 (SE, n = 109) min within the field of view. They were observed feeding on seeded scallops on all dates. A few lobsters were observed at night in summer.

Discussion

Predation

Predation was the major cause of loss of seeded scallops in our study which is consistent with previous seeding trials with scallops (Morgan et al. 1980; Volkov et al. 1983; Minchin 1991; Cliche et al. 1994; Wilson and Brand 1994) and other bivalves (Flagg and Malouf 1983; Peterson 1990; Spencer 1992). Temporal variation in the abundance and distribution of sea stars and crabs did not coincide with that of seeded scallops, suggesting that increased predation was mainly due to a functional response rather than an aggregative numerical response of these predators. The video sampling may have underestimated crab abundances, since crabs are highly motile and may be active only at night (as observed in winter at Site 3), and a numerical response may have gone undetected. However, small-scale experiments using tethered scallops at Sites 1, 2, and 3 also indicated a functional response by crabs to increased scallop density. In these experiments, crab predation rates appeared to be density dependent and sea star predation rates density independent, suggesting that crabs are more important predators of recently seeded scallops than sea stars (Barbeau et al. 1994; M.A. Barbeau et al., unpublished data). Other seeding trials with *P. magellanicus* (Cliche et al. 1994; Hatcher et al. 1996) also showed no agreement between the distribution and abundance of seeded

© 1996 NRC Canada

Fig. 7. Estimated contribution of predation and dispersion to total loss of seeded sea scallop (*P. magellanicus*) from Sites 2 and 3. Data points for loss of scallops between the seeding day and 1 d post were excluded. The inserted plots compare estimated with observed loss for the summer and winter seedings (the diagonal line gives the expectation if the losses match perfectly). Arrows indicate days when a site was seeded with juvenile scallop. See Table 1 for survey number and date.

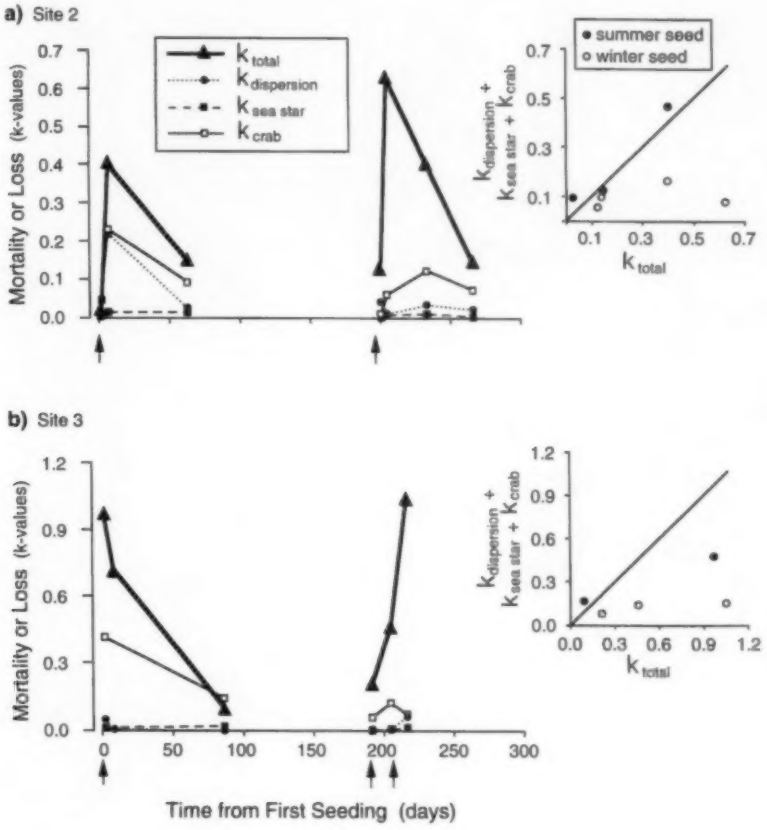

scallops and predatory sea stars and crabs whereas seeding trials with *Patinopecten yessoensis* (Volkov et al. 1983) and *Pecten maximus* (Wilson and Brand 1994) showed an aggregative numerical response by sea stars.

Laboratory experiments indicated that size-selective predation of scallops by sea stars and crabs varies with predator size (Elner and Jamieson 1979; Lake et al. 1987; Barbeau and Scheibling 1994*a*). Larger sea stars and crabs can consume larger prey than smaller predators. Sea star predation is greater on small juvenile scallops (<15 mm Sh) than larger ones (>20 mm Sh) because larger scallops have a more effective escape response to sea stars (Barbeau and Scheibling 1994*a*; Barbeau et al. 1994). In contrast, large juvenile and even adult scallops remain vulnerable to crab predation (Elner and Jamieson 1979; Lake et al. 1987; Minchin 1991; Pohle et al. 1991; Barbeau and Scheibling 1994*a*; Barbeau et al. 1994). Thus, prior inspection of the size distribution of predators at a site may indicate an appropriate scallop size to seed in a sea-star-dominated area, but may be less useful in a crab-dominated one. Temporal variation in the size distribution of predators, as observed at both Sites 2 and 3, complicates the issue.

Temporal variation in predator activity may determine the survivorship of seeded scallops and the rate at which scallop density stabilizes. Sea stars foraged mainly during warmwater months and were quiescent during cold months. Laboratory and field experiments showed that temperature was a primary variable affecting sea star activity and predation rates (Barbeau and Scheibling 1994*c*; Barbeau et al. 1994). Crabs were highly active in summer, but less so in winter. For example, crabs responded immediately to the input of seeded scallops in summer, but only after a time-lag of 5–6 h in winter. The high daytime activity and low nighttime activity of crabs in summer may be due to the nighttime activity of lobsters, which are important crab predators (Elner and Campbell 1987). In winter, the reversal of diel activity pattern of crabs at Site 3, and the absence of a diel pattern at Site 2, may reflect lower lobster abundance due to fishing (Hudon 1994). Tethering experiments concurrent with our seeding trials indicated a significant interaction between site and water tem-

© 1996 NRC Canada

Fig. 8. Spatial distribution of sea star (*Asterias* spp.) over 13 mo at Site 2. The outer box represents the site. The area defined by the broken lines represents the area surveyed. The inner box represents the area where the scallops were seeded. Time from first seeding in days in given for each plot. Note that the area surveyed was moved 10 m southeast and 20 m northeast prior to the survey on day 64. See Table 1 for survey number and date.

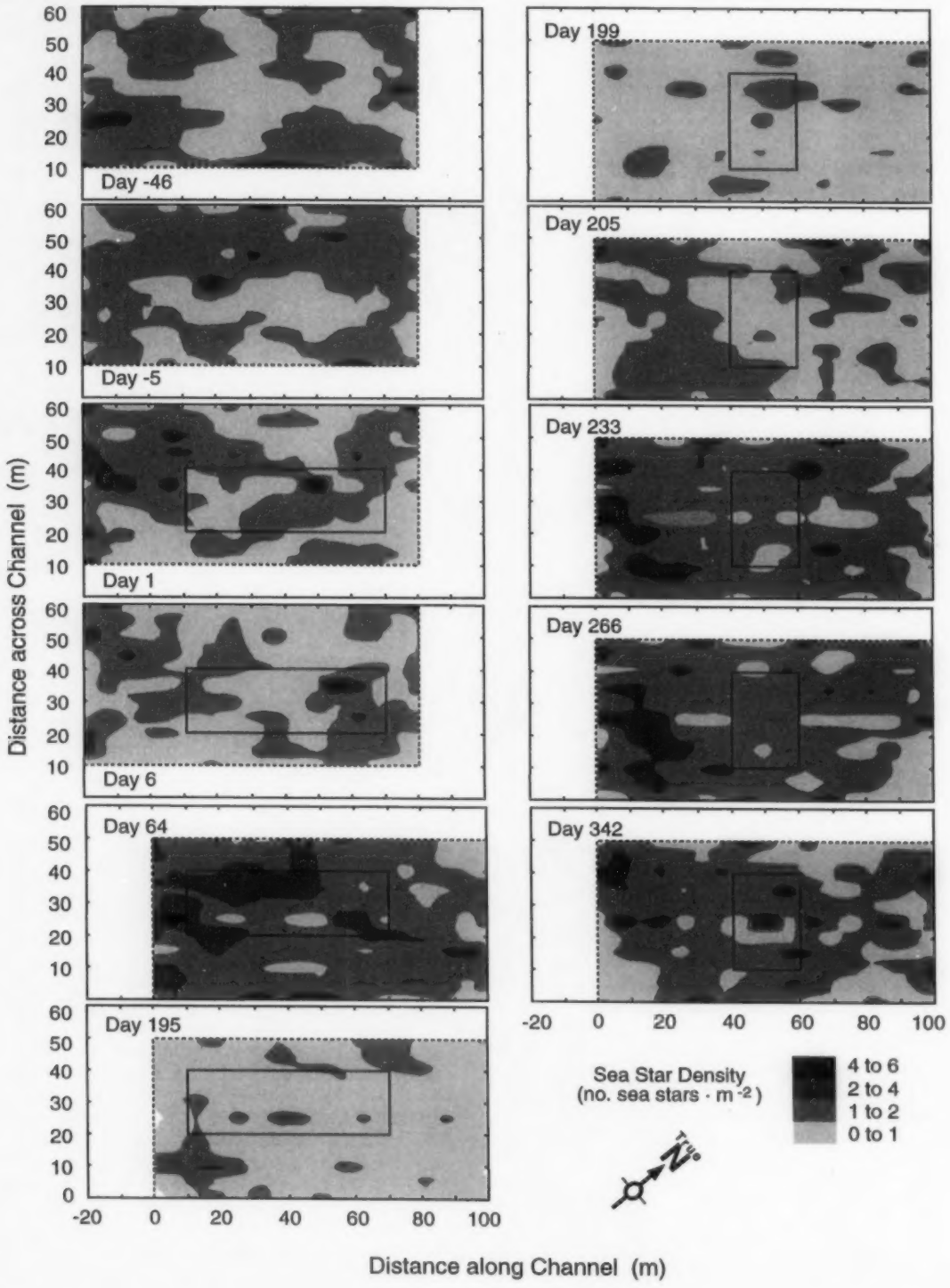

© 1996 NRC Canada

Fig. 9. Spatial distribution of sea star (*Asterias* spp.) over 8 mo at Site 3. The outer box represents the site and the inner box the area where the scallops were seeded. Time from first seeding in days is given above each plot. See Table 1 for survey number and date.

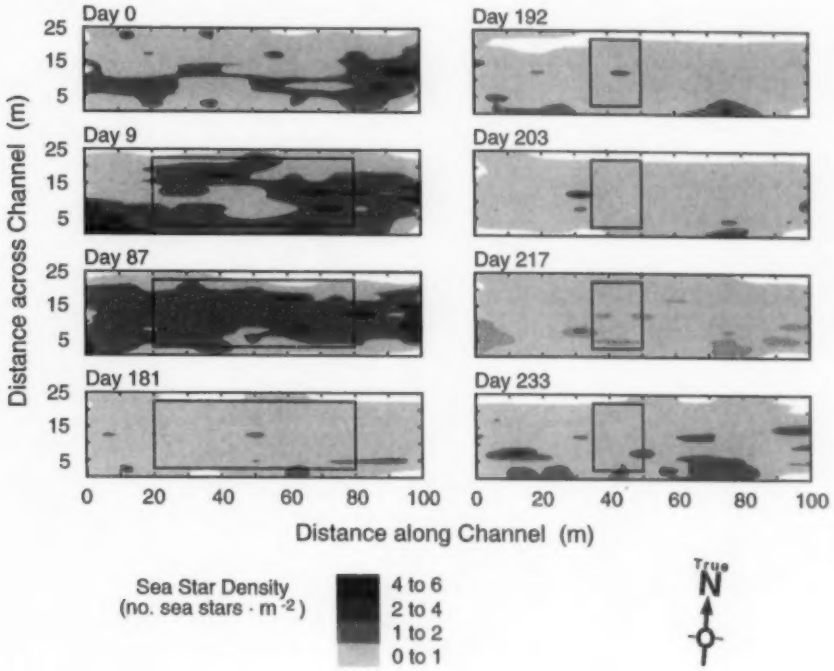

perature on crab predation rates, such that predation increased with temperature at Site 2, but was high and independent of temperature at Site 3 (Barbeau et al. 1994). This site effect may be the result of the different site topographies: Site 3 is adjacent to extensive rocky shore with may provide shelter for crabs (Auster and Malatesta 1991) whereas Site 2 is a more open site. Crab density was higher at Site 3 than at Site 2, at least in summer.

Dispersion

Dispersion was an important cause of loss of scallops from Site 2 (especially after the summer seeding) but not Site 3, which is more enclosed. Small-scale experiments conducted concurrently with the seeding trials at Sites 2 and 3, in which marked scallops were released at point sources and monitored regularly, indicated that only ~50% of scallops showed a net movement direction consistent with the main current vectors (Carsen et al. 1996*b*). In the previous seeding trials at Site 1 and off the Magdalen Islands, dispersion of seeded scallops did not coincide with the primary current vectors (Cliche et al. 1994; Hatcher et al. 1996). Experiments in the field and in laboratory flumes showed that the swimming displacement of small scallops (10–30 mm Sh) was significantly related to flow direction and velocity, but that of larger scallops (30–80 mm Sh) was not (Carsen et al. 1996*a*). Taken together, these studies indicate that local hydrodynamics are not a good predictor of dispersion of seeded scallops across the sea bed. Scallop dispersion may be better represented as a diffusion process rather than an advection process (Bowden 1983). Predators are an important trigger of scallop swimming (Thomas and Gruffydd 1971; Peterson et al. 1982; Manuel and Dadswell 1993), and the interaction between predator activity and currents may better explain the direction and distance of juvenile scallop movement (A.E. Carsen et al., unpublished data). In this respect, predatory sea stars may be a more important trigger for dispersal than crabs, since scallops often swim after contact with sea stars, but often close their valves after contact with crabs (Barbeau and Scheibling 1994*a*).

Displacement of recently seeded scallops at Sites 1, 2, and 3 and movement activity of scallops in concurrent point-source release experiments were higher in summer than winter (Carsen et al. 1996*b*; Hatcher et al. 1996). These results may reflect the effect of water temperature on scallop swimming and (or) seasonal activity of predators in triggering swimming. Previous studies have shown that scallop swimming is highly affected by water temperature. For example, response times after contact with predatory sea stars and gastropods decreased with increasing temperature in the bay scallop (*Argopecten irradians*) (Ordzie and Garofalo 1980), and valve clapping rates increased with temperature in *P. magellanicus* and *Argopecten irradians* (Manuel and Dadswell 1993; Olson and Marsh 1993).

Growth

Growth rates of scallops may show large variations among sites, seasons, and depth due to variations in food and temperature (Bricelj and Shumway 1991; Emerson et al. 1994).

© 1996 NRC Canada

Fig. 10. Size frequency distribution of sea scallop (*P. magellanicus*) (both seeded and wild) on different dates at (*a*) Site 2 and (*b*) Site 3. Scallops in July and August 1991, summer and winter seed, and tagged summer-seeded scallops recovered in October and November 1992 were measured manually; other scallops were measured from the video tapes. Solid triangle = mean and open triangle = median of the distribution.

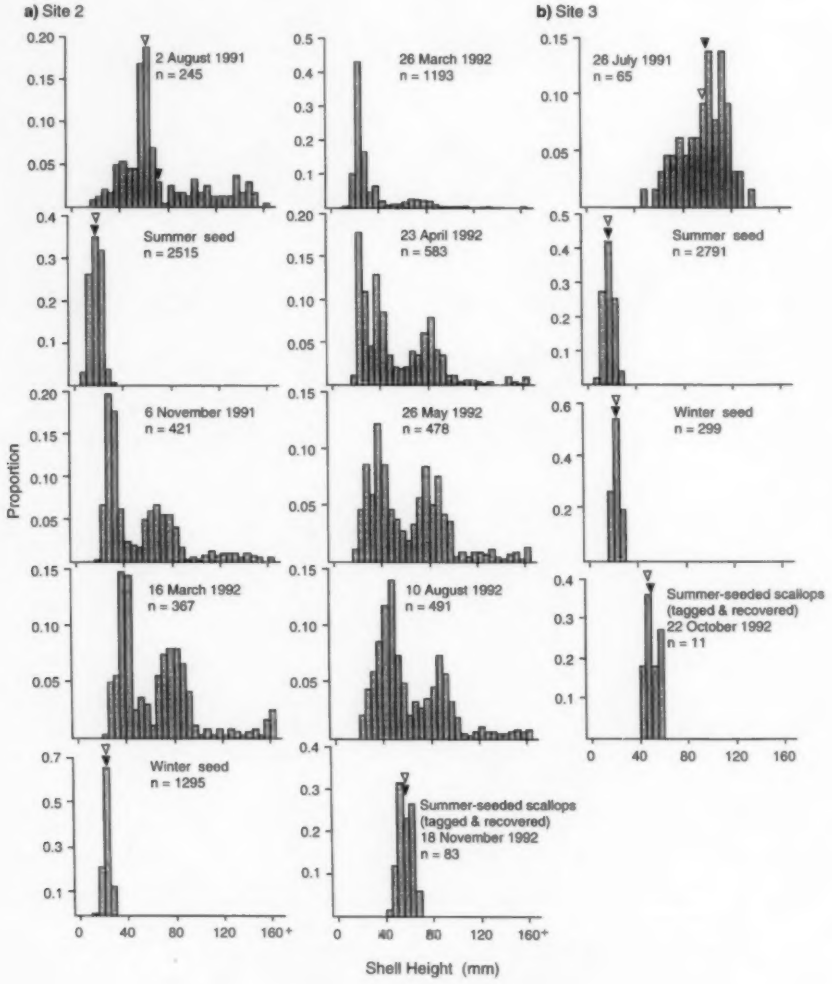

Growth rates of the summer-seeded scallops from two different sources (wild-collected and hatchery-reared) at Sites 2 and 3 were similar to that previously recorded at Site 1 (0.09 $mm \cdot d^{-1}$, Hatcher et al. 1996). However, concurrent small-scale field experiments with more precise and frequent measurements showed that growth rates were generally significantly greater at Site 2 than at Site 3, probably due to higher chlorophyll content at Site 2 (Kleinman et al. 1996). These experiments also showed that shell and tissue growth rates peaked in mid-summer and were lowest in winter (Kleinman et al. 1996), which is consistent with our observations for seeded scallops at Site 2. Lower growth rates for scallops on the sea bed compared with those suspended in the water column are often cited as a disadvantage of bottom culture compared with suspended culture (Tremblay 1988; Wildish et al. 1988; Couturier et al. 1995). However, Kleinman et al. (1996) showed that free-ranging scallops on the sea bed of Sites 1, 2, and 3 generally exhibited growth rates similar to or greater than scallops placed in pearl nets suspended 3 m above bottom at the same sites and with a scallop density equivalent to <40% areal coverage.

Interaction between predation, dispersion, and growth

Immediately following release, density of seeded scallops rapidly decreased in the study area due to predation and dispersion, and stabilized after 1–8 wk. Variation in final scallop densities was greater between sites than between seasons of seeding. Seasonal temperature mostly affected the rate at which the final densities were attained. Seeding effectively doubled the scallop density from 0.42 to $0.95 \cdot m^{-2}$ at

© 1996 NRC Canada

Fig. 11. Growth curves (mean ± SD Sh) of summer- and winter-seeded sea scallop (*P. magellanicus*) at Site 2. n = 65–2515. Arrows indicate the days when the site was seeded with juvenile scallop. See Table 1 for survey number and date.

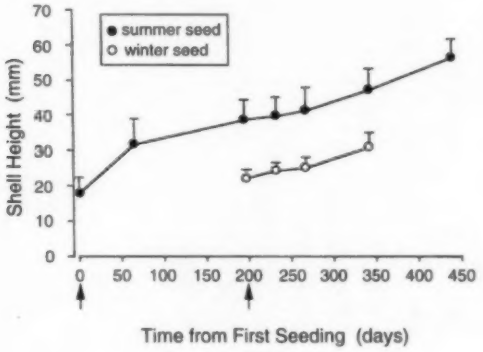

Site 2, from 0.12 to 0.21·m^{-2} at Site 3, and from 0.8 to 1.7·m^{-2} at Site 1 (Hatcher et al. 1996). These densities are within the range observed in wild scallop beds (Orensanz et al. 1991).

The survivorship of seeded scallops stabilized at considerably lower levels at Site 2 (~10%) and Site 3 (~1%) than in the previous seeding trial at Site 1 (~40% after 13 mo, Hatcher et al. 1996). Spat source (wild-collected versus hatchery-reared) did not significantly affect survivorship, as indicated by marked and recovered scallops at Site 2. The large difference in survivorship at Site 1 compared with that at Sites 2 and 3 may be due to several operational differences between the seeding trials. Firstly, seeding was conducted in late autumn at Site 1, a few weeks before the water temperature decreased below 5°C. This provided a short period of relatively warm water temperature for the scallops to disperse, followed by a long period of reduced predation. Secondly, the scallops were initially seeded at a high density (250 scallops·m^{-2}) which may have swamped predators. However, laboratory and field studies indicate that crabs have the potential to decimate dense scallop populations, since encounter rate between crabs and scallops is the major determinant of crab predation rate (Barbeau and Scheibling 1994*a*) and crabs showed a strong functional response to increased scallop densities (Barbeau et al. 1994). Thirdly, tethering assays run concurrently with the seeding trial at Site 1 showed that crab predation was minimal and that sea star predation was the major cause of mortality, which contrasts with our seeding trials at Sites 2 and 3. Crab predation also was suggested as the main cause of low survivorship of sea scallops in seeding trials off the Magdalen Islands, based on scallop shell fragments observed during postseeding surveys (Cliche et al. 1994). Variation in survivorship of seeded *P. maximus* at four sites off the coast of Ireland also was attributed to crab predation (Minchin 1991).

The size of the site and seeded area within the site may influence how various processes affect survival of seeded scallops. For example, if the seeded area is large, predation may be more important at the borders of the area than towards the centre and overall survivorship may be high. Alternatively, predators may show an aggregative numerical response if a large area is seeded, resulting in low scallop survival. Loss due to dispsersion may be minimal in a relatively small seeded area within a large site, but may be important in a relatively large seeded area.

The relative contribution of predation and dispersion to loss of seeded scallops from a site has always been difficult to resolve (Morgan et al. 1980; Cliche et al. 1994; Dao et al. 1994; Hatcher et al. 1996). In this study, predation and dispersion rates were estimated, and key-factor analysis used to determine the relative importance of each. However, the total estimated loss ($k_{\text{dispersion}} + k_{\text{sea star}} + k_{\text{crab}}$) of seeded scallops did not add up to the total observed loss (k_{total}) in three of the four seeding trials. Possible sources of error in the estimation of k-values are as follows. Firstly, k-values for predation were based on tethering experiments which are known to have artifactual problems (Barbeau and Scheibling 1994*b*; Barbeau et al. 1994). Also, a small proportion of tethered scallops had an unassigned cause of mortality that was not included in the estimates. Secondly, although previous and concurrent studies (Cliche et al. 1994; Carsen et al. in 1996*a*, 1996b; Hatcher et al. 1996) indicated that dispersion of seeded scallops was best represented by diffusion, some advection by water currents (particularly of small scallops) probably occurred and may have affected k-values for dispersion. In addition, sources of uncertainty inherent in estimating the variables needed for the diffusion equation, such as the coefficient of diffusion and the gradient of scallop density at the border of a site, may have contributed to error in the estimates of k-values. Thirdly, there may have been causes of loss other than dispersion and predation by crabs and sea stars, although considering our extensive monitoring, we believe this is unlikely. Finally, key-factor analysis assumes no interaction between the different causes of loss, although we expect that these interactions exist and may contribute to the discrepancy between the sum of loss terms and the total observed loss.

The stabilization of seeded scallop populations at a certain density and survivorship reflects the interaction of growth, predation, and dispersion. As scallops grow, their vulnerability to different predators changes (Barbeau and Scheibling 1994*a*; Barbeau et al. 1994). Larger scallops escape from sea stars less often by swimming than do smaller scallops (Barbeau and Scheibling 1994*a*), and this may lower their dispersion rate. Scallop swimming behaviour also changes as scallops grow. Only scallops >10 mm Sh can overcome drag to swim effectively (Manuel and Dadswell 1993) and scallops attain a hydrodynamic optimum at 40–80 mm Sh (Dadswell and Weihs 1990). As previously noted, the movement of smaller scallops is positively affected by water flow direction and velocity, but movement of larger scallops is not (Carsen et al. 1996*a*, 1996*b*). Hence, dispersion is affected by scallop size as well as by predator activity. But as scallops disperse and become less densely aggregated, predation particularly by crabs diminishes. Further investigation of interactions between predator activity, scallop movement, and scallop growth should identify the conditions for maximizing survivorship of seeded scallops.

Implications for aquaculture

Based on our seeding experiments in combination with the

© 1996 NRC Canada

Fig. 12. Proportion of sea star (*Asterias* spp., small: <30, medium: >30 and <50, and large: >50 mm *R*) and rock crab (*C. irroratus*, small: <50, medium: >50 and <90, and large: >90 mm CW) abundance in different size classes over 15 mo at Sites 2 and 3. S–2 to S9, video surveys (see Table 1); M, manual or diver surveys; TR, crab trap measurements. The number of animals upon which the proportions were based is given above each bar. For Site 3, the penultimate bar represents sea stars measured from the video survey on 16 April 1992 and crabs measured from traps on 6 May 1992.

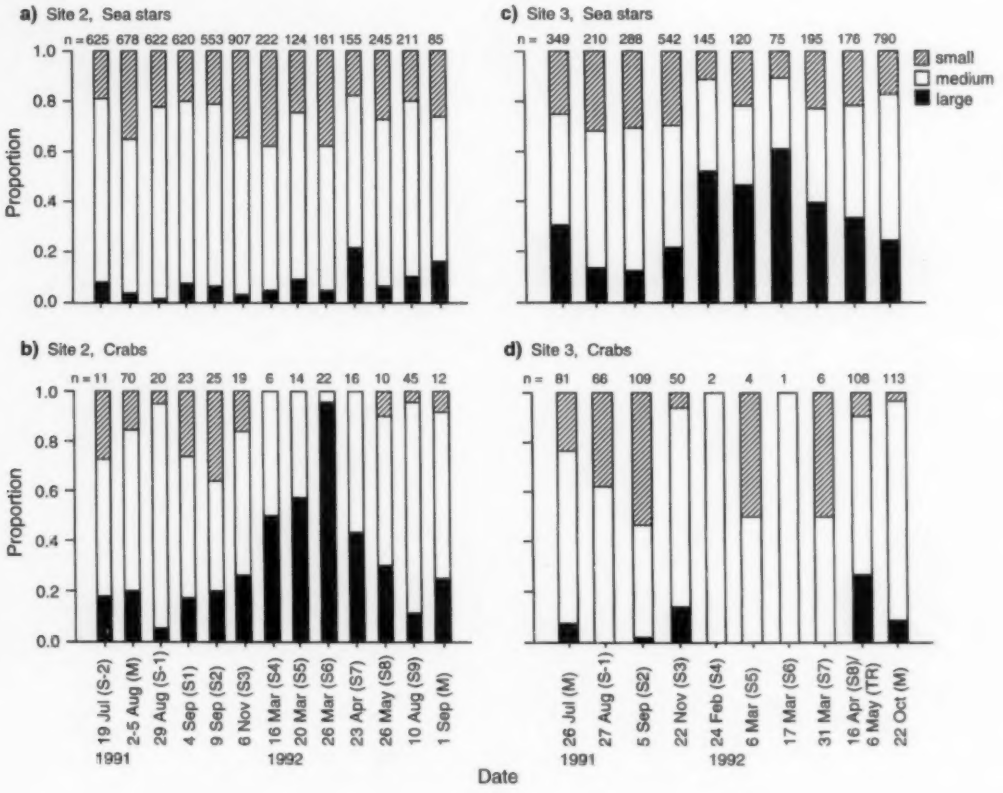

small-scale field and laboratory experiments, we have several recommendations for bottom culture. (1) Seeding large sizes of juvenile scallops minimizes predation by sea stars, although predation rates will greatly increase if the scallops are stressed due to handling and (or) temperature shock. Large juvenile scallops, however, remain vulnerable to crab predation. (2) To lower predation by crabs, scallops should be seeded at low density to reduce encounter rates, since crabs show a functional response to increased scallop density. Alternatively, crab densities could be lowered through predator erradication procedures such as trapping (Minchin 1991; Spencer 1992). (3) Seeding at low water temperature or immediately prior to a period of low temperature reduces predation (particularly by sea stars) and dispersion. However, variation between sites greatly exceeds that between seasons of seeding. In addition, the effect of temperature on crab predation may be overshadowed by the effects of crab and (or) scallop density. (4) Selecting an appropriate site with a suitable substratum is of primary importance; otherwise, scallops may actively disperse or die due to sedimentation or wave action (Picard and Vigneau 1992; Tettelbach and Wenczel 1993; Halary et al. 1994). Furthermore, the size of a site and presence of spatial refuges for predators may influence the relative importance of predation and dispersion to scallop survival. Our study, combined with the results from seeding trials in other locations, provides a significant data base for the development of bioeconomic models for bottom culture of scallops (e.g., Paquotte and Fleury 1994) in eastern Canada and elsewhere.

Acknowledgements

We thank T. Balch, A. Carsen, H. Hunt, S. Kleinman, S. Lothian, A. Metaxas, P. McKenna, K. Richard, and A. Windust for assistance in tagging scallops and (or) SCUBA diving. We are grateful to W. Flower and L. Mosher for the use of their wharves. We also thank two anonymous reviewers for helpful comments on the manuscript. The research was funded by an NSERC Networks of Centres of Excellence Grant (Ocean Production Enhancement Network) and an NSERC research grant to R.E. Scheibling. M.A. Barbeau was supported by an Atlantic Canada Opportunities Agency grant to R.K. O'Dor while writing the manuscript.

© 1996 NRC Canada

Table 2. Sea star (*Asterias* spp.) activity and dietary patterns based on diver surveys during a 14-mo period at Sites 2 and 3.

			Activity			Prey type						
Site	Date	*n*	Quiescent	Searching	Feeding	Detritus	Periwinkles	Mussels	Scallops	Slipper shells	Crabs	Sea stars
2	29 Aug. 91	127	0.57	0.31	0.12	0.73	0.20	0.07	—	—	—	—
	27 Feb. 92	58	0.74	0.00	0.26	1.00	—	—	—	—	—	—
	16 Mar. 92	71	0.87	0.06	0.07	0.80	—	—	—	—	—	0.20
	19 Mar. 92	54	0.87	0.02	0.11	0.33	—	0.17	0.50	—	—	—
	5 May 92	61	0.56	0.26	0.18	0.45	0.27	0.09	—	—	0.18	—
	26 May 92	60	0.33	0.50	0.17	0.30	0.20	—	—	—	0.50	—
	1 Sept. 92	85	0.49	0.19	0.32	0.78	0.11	0.07	0.04	—	—	—
	15 Sept. 92	28	0.14	0.57	0.29	0.63	0.25	—	—	—	0.13	—
3	27 Aug. 91	472	0.44	0.27	0.29	0.28	0.25	0.20	0.19	0.09	—	—
	29 Jan. 92	109	0.84	0.00	0.16	0.82	0.06	—	—	0.12	—	—
	24 Feb. 92	56	0.95	0.02	0.04	0.50	0.50	—	—	—	—	—
	4 Mar. 92	52	0.88	0.06	0.06	1.00	—	—	—	—	—	—
	5 Mar. 92	60	0.95	0.00	0.05	0.33	0.33	—	0.33	—	—	—
	6 Mar. 92	53	0.92	0.00	0.08	0.25	—	—	0.75	—	—	—
	9 Mar. 92	29	0.86	0.00	0.14	1.00	—	—	—	—	—	—
	8 Apr. 92	26	0.46	0.00	0.54	0.50	0.14	0.14	—	—	0.21	—
	28 Apr. 92	75	0.44	0.40	0.16	0.17	0.33	0.17	—	—	0.33	—
	1 Sept. 92	71	0.13	0.58	0.30	0.24	0.43	0.24	—	0.05	—	0.05
	22 Oct. 92	400	0.07	0.68	0.26	0.36	0.59	0.02	—	0.03	—	—

Note: Data are the proportion of total sea stars in each activity and the proportion of feeding sea stars for each prey type; *n* is the total number of sea stars observed. The prey species include periwinkle (*Littorina littorea*), mussels (*Modiolus modiolus* and *Mytilus edulis*), scallop (*P. magellanicus*), slipper shell (*Crepidula fornicata*), crabs (*C. irroratus* and *Carcinus maenas*), and sea star. Sea stars were classified as feeding on detritus when their stomach was everted and no obvious prey species could be observed.

© 1996 NRC Canada

Fig. 13. Time-lapse video observations of rock crab (*C. irroratus*), sea star (*Asterias* spp.), and American lobster (*Homarus americanus*) activity immediately prior to and post summer and winter seedings at Sites 2 and 3. Activity was measured as the number of animals entering the 0.34-m^2 video field of view. The thick horizontal line on the *x*-axis indicates nighttime. Arrows indicate the times when a site was seeded with juvenile scallop.

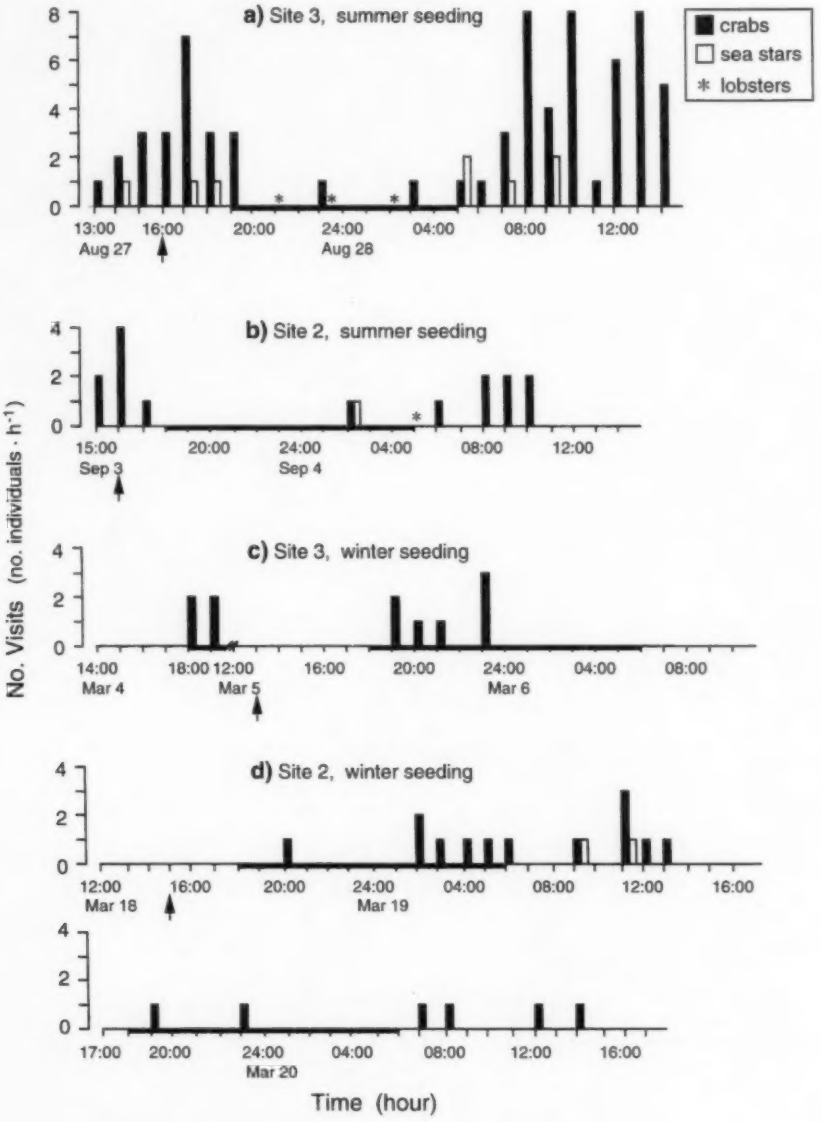

References

Auster, P.J., and Malatesta, R.J. 1991. Effects of scale on predation patterns. *In* An international compendium of scallop biology and culture. *Edited by* S.E. Shumway and P.A. Sandifer. World Aquaculture Workshops No. 1. World Aquaculture Society, Baton Rouge, La. pp. 198–203.

Barbeau, M.A., and Scheibling, R.E. 1994*a*. Behavioral mechanisms of prey size selection by sea stars (*Asterias vulgaris* Verrill) and crabs (*Cancer irroratus* Say) preying on juvenile sea scallops (*Placopecten magellanicus* (Gmelin)). J. Exp. Mar. Biol. Ecol. **180**: 103–136.

Barbeau, M.A., and Scheibling, R.E. 1994*b*. Procedural effects of prey tethering experiments: predation of juvenile scallops by crabs and sea stars. Mar. Ecol. Prog. Ser. **111**: 305–310.

Barbeau, M.A., and Scheibling, R.E. 1994*c*. Temperature effects on predation of juvenile sea scallops (*Placopecten magellanicus* (Gmelin)) by sea stars (*Asterias vulgaris* Verrill) and crabs (*Cancer irroratus* Say). J. Exp. Mar. Biol. Ecol. **182**: 27–47.

Barbeau, M.A., Scheibling, R.E., Hatcher, B.G., Taylor, L.H., and

© 1996 NRC Canada

Hennigar, A.W. 1994. Survival analysis of tethered juvenile sea scallops *Placopecten magellanicus* in field experiments: effects of predators, scallop size and density, site and season. Mar. Ecol. Prog. Ser. **115**: 243–256.

Boghen, A.D. (*Editor*). 1995. Cold-water aquaculture in Atlantic Canada. 2nd ed. The Canadian Institute for Research on Regional Development, Moncton, N.B.

Bowden, K.F. 1983. Physical oceanography of coastal waters. John Wiley & Sons, New York.

Brand, A.R. 1991. Scallop ecology: distributions and behaviour. *In* Scallops: biology, ecology and aquaculture. *Edited by* S.E. Shumway. Elsevier, Amsterdam, The Netherlands. pp. 517–584.

Bricelj, V.M., and Shumway, S.E. 1991. Physiology: energy acquisition and utilization. *In* Scallops: biology, ecology and aquaculture. *Edited by* S.E. Shumway. Elsevier, Amsterdam, The Netherlands. pp. 305–346.

Bull, M.F. 1994. Enhancement and management of New Zealand's "Southern Scallop" fishery. *In* Proceedings of the 9th International Pectinid Workshop, Nanaimo, B.C., Canada, April 22–27, 1993. Vol. 2. *Edited by* N.F. Bourne, B.L. Bunting, and L.D. Townsend. Can. Tech. Rep. Fish. Aquat. Sci. **1994**: 131–136.

Carsen, A.E., Hatcher, B.G., and Scheibling, R.E. 1996*a*. Swimming trajectories of sea scallops (*Placopecten magellanicus*) as a function of size and current velocity: a comparison of laboratory and field measurements. J. Exp. Mar. Biol. Ecol. (In press)

Carsen, A.E., Hatcher, B.G., Scheibling, R.E., Hennigar, A.W., and Taylor, L.T. 1996*b*. Effects of site and season on movement frequencies and displacement patterns of juvenile sea scallops (*Placopecten magellanicus*) under natural hydrodynamic conditions in Nova Scotia, Canada. Mar. Ecol. Prog. Ser. **128**: 225–238.

Cliche, G., Giguère, M., and Vigneau, S. 1994. Dispersal and mortality of sea scallops, *Placopecten magellanicus* (Gmelin, 1791), seeded on the sea bottom off Iles-de-la-Madeleine. J. Shellfish Res. **13**: 565–570.

Couturier, C., Dabinett, P., and Lanteigne, M. 1995. Scallop culture in Atlantic Canada. *In* Cold-water aquaculture in Atlantic Canada. 2nd ed. *Edited by* A.D. Boghen. The Canadian Institute for Research on Regional Development, Moncton, N.B. pp. 297–340.

Crowder, M.J., and Hand, D.J. 1990. Analysis of repeated measures. Chapman & Hall, London.

Dadswell, M.J., and Weihs, D. 1990. Size-related hydrodynamic characteristics of the giant scallop, *Placopecten magellanicus* (Bivalvia: Pectinidae). Can. J. Zool. **68**: 778–785.

Dao, J.C., Barret, J., and Muzellec, M.L. 1994. Seeding-recapture of scallop (*Pecten maximus*) by commercial dredging in Bay of Brest during the fishing season 1991–92. *In* Proceedings of the 9th International Pectinid Workshop, Nanaimo, B.C., Canada, April 22–27, 1993. Vol. 2. *Edited by* N.F. Bourne, B.L. Bunting, and L.D. Townsend. Can. Tech. Rep. Fish. Aquat. Sci. **1994**: 16–22.

Dupouy, H. 1983. La pectiniculture à Saint-Pierre et Miquelon. Sci. Pêche Bull. Inst. Pêches Marit. **337**: 17–29.

Elner, R.W., and Campbell, A. 1987. Natural diets of lobster *Homarus americanus* from barren ground and macroalgal habitats off southwestern Nova Scotia, Canada. Mar. Ecol. Prog. Ser. **37**: 131–140.

Elner, R.W., and Jamieson, G.S. 1979. Predation of sea scallops, *Placopecten magellanicus*, by the rock crab, *Cancer irroratus*, and the American lobster, *Homarus americanus*. J. Fish. Res. Board Can. **36**: 537–543.

Emerson, C.M., Grant, J., Mallet, A., and Carver, C. 1994. Growth and survival of sea scallops *Placopecten magellanicus*: effects of culture depth. Mar. Ecol. Prog. Ser. **108**: 119–132.

Flagg, P.J., and Malouf, R.E. 1983. Experimental plantings of juveniles of the hard clam *Mercenaria mercenaria* (Linné) in the waters of Long Island, New York. J. Shellfish Res. **3**: 19–27.

Goshima, S., and Fujiwara, H. 1994. Distribution and abundance of cultured scallop *Patinopecten yessoensis* in extensive sea beds as assessed by underwater camera. Mar. Ecol. Prog. Ser. **110**: 151–158.

Halary, C., Royer, Y., Corlouer, J.P., and Dao, J.C. 1994. Effects of predation and competition on scallop *Pecten maximus* seabed cultivation in Saint Brieuc Bay: preliminary results. *In* Proceedings of the 9th International Pectinid Workshop, Nanaimo, B.C., Canada, April 22–27, 1993. Vol. 2. *Edited by* N.F. Bourne, B.L. Bunting, and L.D. Townsend. Can. Tech. Rep. Fish. Aquat. Sci. **1994**: 39–50.

Hatcher, B.G., Scheibling, R.E., Barbeau, M.A., Hennigar, A.W., Taylor, L.H., and Windust, A.J. 1996. Dispersion and mortality of a population of sea scallop (*Placopecten magellanicus*) seeded in a tidal channel. Can. J. Fish. Aquat. Sci. **53**: 38–54.

Hudon, C. 1994. Large-scale analysis of Atlantic Nova Scotia American lobster (*Homarus americanus*) landings with respect to habitat, temperature, and wind conditions. Can. J. Fish. Aquat. Sci. **51**: 1308–1321.

Kalashnikov, V.Z. 1991. Soviet Union. *In* Scallops: biology, ecology and aquaculture. *Edited by* S.E. Shumway. Elsevier, Amsterdam, The Netherlands. pp. 1057–1082.

Kleinman, S., Hatcher, B.G., Scheibling, R.E., Taylor, L.H., and Hennigar, A.W. 1996. Shell and tissue growth of juvenile sea scallops, *Placopecten magellanicus*, in suspended and bottom culture in Lunenburg Bay, Nova Scotia. Aquaculture, **142**: 75–97.

Krebs, C.J. 1989. Ecological methodology. Harper & Row Publishers, New York.

Lake, N.C.H., Jones, M.B., and Paul, J.D. 1987. Crab predation on scallop (*Pecten maximus*) and its implication for scallop cultivation. J. Mar. Biol. Assoc. U.K. **67**: 55–64.

MacDonald, B.A. 1986. Production and resource partitioning in the giant scallop *Placopecten magellanicus* grown on the bottom and in suspended culture. Mar. Ecol. Prog. Ser. **34**: 79–86.

Manuel, J.L., and Dadswell, M.J. 1993. Swimming of juvenile sea scallops, *Placopecten magellanicus* (Gmelin): a minimum size for effective swimming? J. Exp. Mar. Biol. Ecol. **174**: 137–175.

Minchin, D. 1991. Decapod predation and the sowing of the scallop, *Pecten maximus* (Linnaeus, 1758). *In* An international compendium of scallop biology and culture. *Edited by* S.E. Shumway and P.A. Sandifer. World Aquaculture Workshops No. 1. World Aquaculture Society, Baton Rouge, LA. pp. 191–197.

Morgan, D.E., Goodsell, J., Matthiessen, G.C., Garey, J., and Jacobson, P. 1980. Release of hatchery-reared bay scallops (*Argopecten irradians*) onto a shallow coastal bottom in Waterford, Connecticut. Proc. World Maricult. Soc. **11**: 247–261.

Naidu, K.S., and Cahill, F.M. 1986. Culturing giant scallops in Newfoundland waters. Can. MS Rep. Fish. Aquat. Sci. 1876.

Olson, J.M., and Marsh, R.L. 1993. Contractile properties of the striated adductor muscle in the bay scallop *Argopecten irradians* at several temperatures. J. Exp. Biol. **176**: 175–193.

Ordzie, C.J., and Garofalo, G.C. 1980. Behavioral recognition of molluscan and echinoderm predators by the bay scallop, *Argopecten irradians* (Lamarck) at two temperatures. J. Exp. Mar. Biol. Ecol. **43**: 29–37.

Orensanz, J.M., Parma, A.M., and Iribarne, O.O. 1991. Population dynamics and management of natural stocks. *In* Scallops: biology, ecology and aquaculture. *Edited by* S.E. Shumway. Elsevier, Amsterdam, The Netherlands. pp. 625–713.

Paquotte, P., and Fleury, P.G. 1994. Production costs in French scallop culture. *In* Proceedings of the 9th International Pectinid Workshop, Nanaimo, B.C., Canada, April 22–27, 1993. Vol. 2. *Edited by* N.F. Bourne, B.L. Bunting, and L.D. Townsend. Can. Tech. Rep. Fish. Aquat. Sci. **1994**: 66–75.

Peterson, C.H. 1990. On the role of ecological experimentation in resource management: managing fisheries through mechanistic understanding of predator feeding behaviour. *In* Behavioural

© 1996 NRC Canada

mechanisms of food selection. *Edited by* R.N. Hughes. Springer-Verlag, New York. pp. 821–846.

Peterson, C.H., Ambrose, W.H. Jr., and Hunt, J.H. 1982. A field test of the swimming response of the bay scallop (*Argopecten irradians*) to changing biological factors. Bull. Mar. Sci. **32**: 939–944.

Picard, P., and Vigneau, S. 1992. Essais d'ensemencement de péton-cle géant sur les fonds à potentiel pectinicole aux Iles-de-la-Madeleine. Rapport annuel. Roche ltée Groupe-Conseil, Sainte-Foy, Québec, Canada.

Pohle, D.G., Bricelj, V.M., and Garcia-Esquivel, Z. 1991. The eelgrass canopy: an above-bottom refuge from benthic predators for juvenile bay scallops *Argopecten irradians*. Mar. Ecol. Prog. Ser. **74**: 47–59.

Quayle, D.B., and Newkirk, G.F. 1989. Farming bivalve molluscs: methods for study and development. World Aquaculture Society, Baton Rouge, La.

Shumway, S.E. (*Editor*). 1991. Scallops: biology, ecology and aquaculture. Elsevier, Amsterdam, The Netherlands.

Sokal, R.R., and Rohlf, F.J. 1981. Biometry. W.H. Freeman and Company, New York.

Spencer, B.E. 1992. Predators and methods of control in molluscan shellfish cultivation in north European waters. *In* Aquaculture and the environment. *Edited by* N. De Pauw and J. Joyce. European Aquaculture Society Special Publication No. 16, Ghent, Belgium. pp. 309–337.

Taylor, R.J. 1984. Predation. Chapman & Hall, New York.

Tettelbach, S.T., and Wenczel, P. 1993. Reseeding efforts and the status of bay scallop *Argopecten irradians* (Lamarck, 1819) populations in New York following the occurrence of "brown tide" algal blooms. J. Shellfish Res. **12**: 423–431.

Tettelbach, S.T., Smith, C.F., Kaldy, J.E. III, Arroll, T.W., and Denson, M.R. 1990. Burial of transplanted bay scallops *Argopecten irradians irradians* (Lamarck, 1819) in winter. J. Shellfish Res. **9**: 127–134.

Thomas, G.E., and Gruffydd, Ll.D. 1971. The types of escape reactions elicited in the scallop *Pecten maximus* by selected sea-star species. Mar. Biol. **10**: 87–93.

Tremblay, M.J. (*Editor*). 1988. A summary of the proceedings of the Halifax sea scallop workshop, August 13–14, 1987. Can. Tech. Rep. Fish. Aquat. Sci. 1605.

Varley, G.C., and Gradwell, G.R. 1960. Key factors in population studies. J. Anim. Ecol. **29**: 399–401.

Ventilla, R.F. 1982. The scallop industry in Japan. Adv. Mar. Biol. **20**: 309–382.

Volkov, Y.P, Dadaev, A.A., Levin, V.S., and Murakhveri, A.M. 1983. Changes in the distribution of Yezo scallop and starfishes after mass planting of scallops at the bottom of Vityaz' Bay (Sea of Japan). Sov. J. Mar. Biol. **8**: 216–223.

Wildish, D.J., Wilson, A.J., Young-Lai, W., DeCoste, A.M., Aiken, D.E., and Martin, J.D. 1988. Biological and economic feasibility of four grow-out methods for the culture of giant scallops in the Bay of Fundy. Can. Tech. Rep. Fish. Aquat. Sci. **1658**.

Wilkinson, L. 1989. SYGRAPH: the system for graphics. SYSTAT Inc., Evanston, Ill.

Wilson, U.A.W., and Brand, A.R. 1994. Nowhere to hide? Predator impact on seeded scallops. *In* Proceedings of the 9th International Pectinid Workshop, Nanaimo, B.C., Canada, April 22–27, 1993. Vol. 2. *Edited by* N.F. Bourne, B.L. Bunting, and L.D. Townsend. Can. Tech. Rep. Fish. Aquat. Sci. **1994**: 118.

© 1996 NRC Canada

Low-frequency acoustic imaging of Pacific salmon on the high seas

Redwood W. Nero and Michael E. Huster

Abstract: Near-surface fish are visible in high-resolution acoustic images of the sea surface obtained from the Gulf of Alaska in late February 1992. Images were made using time domain beamforming of data taken using explosive sources and a horizontal-line-array (HLA) receiver. Images are of high resolution to a range of 4 km. Targets in the images are determined to be Pacific salmon based on the historical absence of other large fish and a match of a peak in their scattering spectra near 500 Hz with predictions of swimbladder resonance. Scattering levels indicate that the salmon occur singly or in small groups of two to four individuals. Counts of 114 salmon/km^2 are comparable with historical estimates of 160 salmon/km^2. Salmon were seen in daytime images, but at night, only a few weak targets were observed. At night the salmon are hypothesized to have migrated very close to the sea surface where they became acoustic dipoles and were acoustically invisible to the HLA. The spatial arrangement of salmon in the images suggests that at small spatial scales (2–200 m), they are uniformly distributed whereas at larger spatial scales (400–2000 m), they are aggregated.

Résumé : Les poissons nageant à faible profondeur sont visibles sur des images acoustiques grande définition de la surface de la mer prises dans le golfe de l'Alaska à la fin février 1992. Ces images ont été obtenues par la mise en forme temporelle des faisceaux de données générées au moyen de sources de détonation et au moyen d'un récepteur à réseau linéaire horizontal d'éléments d'antenne. Les images sont à grande définition jusqu'à 4 km. On dit que les cibles sur les images sont des saumons du Pacifique compte tenu de l'absence historique de tout autre poisson de grande taille dans ce secteur et à cause de la concordance entre un pic dans les spectres de diffusion situé près de 500 Hz et des prévisions de la résonnance de la vessie natatoire. Les degrés de diffusion observés indiquent que le saumon se tenait seul ou par petits groupes de deux à quatre. Les dénombrements de 114 saumons/km^2 sont comparables aux évaluations historiques de 160 saumons/km^2. Le saumons sont visibles sur les photos de jour, mais seuls quelques-uns d'entre eux sont faiblement observables sur les photos de nuit. On suppose que la nuit, ils migraient pour venir très près de la surface où ils devenaient des dipôles acoustiques et étaient invisibles avec le récepteur. Sur les images, la répartition spatiale du saumon suggère qu'à petite échelle (2–200 m) il est distribué uniformément, mais qu'à grande échelle (400–2000 m), il est agrégé.
[Traduit par la Rédaction]

Introduction

Direct observation of salmon on the high seas is rare. We document the probable occurrence of salmon close to the sea surface using low-frequency, high-resolution acoustic imaging. The occurrence of salmon in these images was incidental, obtained during the Space and Naval Warfare Systems Command's seventh Critical Sea Test experiment (CST 7). The primary objective of this experiment was to measure scattering from the sea surface in very high sea states. Late winter in the Gulf of Alaska was chosen as the time and place to encounter high seas. However, several periods of low wind speed were encountered, during which the sea surface scattering measurements were contaminated by fishlike scatterers (Ogden and Erskine 1994). These fish were initially assumed to be salmon because 95% of the large (>20 cm) fish in the epipelagic offshore waters of the Gulf of Alaska are probably salmon (Rogers 1987).

Received October 6, 1995. Accepted May 1, 1996.
JI3101

R. W. Nero. Naval Research Laboratory, Stennis Space Center, MS 39529-5004, U.S.A.
M.E. Huster. AETC, Inc., Suite 900, 8910 University Center Ln., San Diego, CA 92122, U.S.A.

Most observations of salmon at sea provide only indirect distribution information, having been obtained from gill nets, drift nets, longlines, purse seines, and trawls, along with some limited visual sightings (Godfrey et al. 1975; French et al. 1976; Neave et al. 1976; Major et al. 1978; Takagi et al. 1981; Groot and Margolis 1991). Recent tracking experiments (Ogura and Ishida 1992, 1995) provide valuable insights into salmon behavior. However, all methods either provide limited data or are biased by the particular sampling characteristics of the gear. Salmon at sea reportedly occur at low density in small groups or schools of several individuals, and occur close to the sea surface (Ogura and Ishida 1992, 1995; Welch and Ishida 1993). These characteristics make high-seas salmon poor targets for conventional fisheries acoustics. We show that acoustic images made using explosive sound sources and a horizontal-line-array (HLA) can provide direct measures of the spatial distribution and abundance of salmon.

This study serves two purposes: first, it eliminates any possible confusion for the CST 7 surface scattering experiment by determining the biological and acoustic characteristics of likely fish scatterers; second, it provides unique direct observation of the spatial distributions of salmon and insight into their diel behavior. No test fishing was carried out to absolutely identify the observed targets. However, given the high percentage of salmon in the region, we start with the assump-

© 1996 NRC Canada

Fig. 1. Schematic showing the HLA geometry and ray paths. θ is the grazing angle.

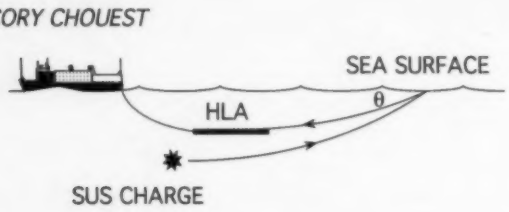

tion that the targets are caused by salmon. Then we show, through bioacoustic modeling of swimbladder resonance, that the acoustic signature of salmon matches the acoustic data. Finally, an analysis of a priori knowledge of salmon and other potential targets leads us to conclude, with a high degree of certainty, that the observed targets are indeed salmon. The results presented below include reverberation images of large regions of the sea surface showing salmon, measurements of the sound scattering characteristics of single salmon and small groups of salmon, and estimates of salmon numbers per unit area.

Materials and methods

Measurements

The CST 7 experiment took place from 24 February through 1 March 1992, in an area centered at 48°45′N, 150°00′W. This location was approximately 350 km west of ocean station "P"in the Gulf of Alaska. Acoustic measurements described in this paper were made from the M/V *Cory Chouest*. In addition to the acoustic experiments, a large suite of environmental data was collected for studies of atmosphere – sea surface interactions. In general, conditions were rough, with sustained wind speeds of 18 m/s and wave heights reaching 5 m. Further information and a summary of meteorological conditions are available in Hanson and Erskine (1992).

The acoustic measurements used explosives as sound sources (Navy SUS: Signal, Underwater Sound) and a 122-element HLA to receive the echoes. The SUS contained 1.8 kg of cyclotol explosive. The HLA was towed behind the ship at a depth of 125–270 m with the first hydrophone approximately 1000 m aft of the ship's stern (Fig. 1). SUS sequences, termed runs, consisted of between four and nine shots with 5 min between shots. The SUS were detonated at a depth between 500 and 550 m between the ship and the HLA. The explosion from a SUS at depth does not provide a "flat" source spectrum but one rather scalloped in shape due to sound pulses caused by bubble oscillations characteristic of charges detonated at depth. This discontinuous nature of the SUS source spectra required that, for best results, the received signals be processed for those frequency bands with the most energy for each particular shot. Hence, the frequency bands that were processed vary by several hertz from shot to shot.

Signals from each shot were processed by two methods. In the first case, a study was made of the dependence of the average sound scattering from a large region of the sea surface on grazing angle (angle of incidence with the sea surface, Fig. 1), sea surface roughness, and frequency. This study did not require high angular resolution, so a 16-hydrophone subaperture of the main array was used to form 17 beams going from aft endfire to forward endfire. Data from the broadside beam and five beams on either side were used to determine average scattering strengths. Each beam sees both sides of the array because an HLA has depth–left–right ambiguity. Azimuthal coverage at the sea surface was approximately 160°, +40° to –40° off the broadside axis on the left and right sides of the array. Range binning of the data and calculated propagation paths allowed the determination of grazing angles. This analysis provided average scattering from the sea surface over a range of grazing angles for nine frequency bands between 70 and 1000 Hz. The sea surface scattering results are reported in Ogden and Erskine (1994).

In the second case, a study was made of the spatial characteristics and frequency content of the scattering from the rough sea surface. To obtain high angular resolution, this experiment used data from all 122 hydrophones of the main array. Data were processed using AETC's nearfield Wideband Acoustic Scattering Processor (WASP, Adair and Huster 1993). The WASP was used to characterize direct path near-surface scatter with high spatial resolution and large bandwidth (21 frequency bands between 80 and 1500 Hz). The processor is a time domain, delay-and-sum beamformer which takes the nearfield wavefront curvature into account and compensates for distortions in array shape. The beamformer's output was mapped to Cartesian coordinates at a 5-m^2 pixel size and the intensity displayed on a grayscale. Scattering was mapped to a plane at the sea surface on one side of the array. Images end when the bottom echo was received, which corresponds to approximately 4 km range.

To extract acoustic information from the suspected salmonlike targets, 14-high resolution images were examined for targets within a subsection +35° to –35° off the broadside axis, and within a range of 1500–2750 m. This region had the least noise and best target resolution. Single targets were identified by eye. Pixels constituting a single target were manually selected using an interactive data display-selection program. Two characteristics of this procedure ensured a relatively consistent selection of targets. First, the extreme dynamic range of the data in the decibel scale results in almost any targetlike feature being easily separated from the background. Targets at least 5 dB above background were selected. Noise sources were easily dismissed, as they were evident as radial spokes in the images. Second, the same operator selected the targets from all images without prior knowledge of image sequence, time of day, or location during the experiment. After designation of pixels as belonging to a target, scattering data for a single target were integrated to give target strength and spectral composition. Target densities per unit area were corrected for the left–right ambiguity by dividing by 2.

Verification of the suspected fishlike targets was provided by comparing the target spectra of the observed resonance responses with those predicted by a model of swimbladder scattering. Model fits were performed by eye for lack of a suitable test for comparing mismatched frequency spectra. This model used as input data giving the probable size distribution of salmon expected in the central Gulf of Alaska in February–March, their vertical position, and swimbladder behavior.

Swimbladder modeling

Omnidirectional scattering from the swimbladder dominates the scattering from a fish at frequencies less than and somewhat above the swimbladder's monopole resonance frequency (Love 1978). The resonance frequency is primarily dependent on bladder size and depth in the water. We use the swimbladder model of Love (1978) to calculate the expected level and frequency spectra of sound scattered from fish swimbladders. This model is robust; it was used successfully to model swimbladders of fish in several widely different ocean environments (Love 1993; Thompson and Love 1996). In this model, swimbladders are treated as air-filled spheres inside a viscous spherical shell. The spherical assumption is reasonable; Feuillade and Werby (1994) have recently shown that scattering functions of spheroids with aspect ratios of 10 are not appreciably different from those of spheres except for a 10–15% increase in resonance frequency (also noted by Weston 1967). Our model includes a 10% increase in resonance frequency.

In applying the swimbladder model, several assumptions were made on the size and depth of the suspected swimbladders. Fish

© 1996 NRC Canada

were assumed to maintain their swimbladder gas at a pressure nearly equal to the ambient hydrostatic pressure. To maintain neutral buoyancy, a swimbladder volume needs to be about 5% of a fish's volume for salt water (Alexander 1993). However, this volume is subject to the effects of pressure as a fish changes depth (Blaxter and Batty 1990). Salmonids and herring are physostomes, fish containing a connection between the swimbladder and esophagus. Thorne and Thomas (1990) have suggested a "big gulp" hypothesis based on observations of herring in Puget Sound. They suspect that herring may attain neutral buoyancy at depth by gulping a volume of air at the surface, forcing it into the swimbladder, and swimming down to a preferred depth. If salmon do this, then they may be neutrally buoyant at depths well below the surface. Salmonids also appear capable of secreting gas into the swimbladder. Sundnes and Sand (1975) observed a captive charr, without access to the surface, increase its swimbladder volume by 44% over 20 h.

For lack of better information on salmon behavior, we examined four combinations created by two extremes of swimbladder behavior and two extremes of depth behavior. For swimbladders, we assumed (*a*) constant mass of gas: swimbladders compress from the surface according to Boyle's Law with no compensation for their decreasing volume and (*b*) constant volume: swimbladder volumes are maintained at 5% of a fish's volume by either a "big gulp" or by gas secretion. For depth behavior, we used a 40-m maximum depth range (based on a subsequent examination of multipaths) and assumed (*c*) a uniform distribution of fish from the surface to 40 m depth and (*d*) all the fish at 40 m depth. The results of the four combinations of these assumptions illustrate the extremes in the expected resonance from potential salmon targets. Finally, by liberally varying depth and swimbladder behavior, we provide a best fit to the measurements. This exercise is used to hypothesize the depth range and swimbladder behavior of the suspect salmon.

This modeling used a length distribution of salmon expected for March based on information contained in documents published by the International North Pacific Fisheries Commission (Godfrey et al. 1975; French et al. 1976; Neave et al. 1976; Major et al. 1978; Takagi et al. 1981). This historical distribution contained salmon with fork lengths from 18 to 68 cm with a mean of 38 cm. Variability in swimbladder size with fish length was included (Ona 1990; Love 1993).

Spatial analysis

The spatial information contained in the images was examined in two ways. First, a test of dispersion (Clark and Evans 1954) was applied to nearest-neighbor distances calculated from the x (across array) and y (along array) position data for targets in the images. This test was performed to determine if the spatial arrangement of targets was uniform, random, or aggregated. Targets near the image edges were included, as this test is not sensitive to edge effects (Cressie 1993). Second, the scaled neighbor-K function (Meir et al. 1995) was used to characterize the spatial scale at which the target distribution patterns were uniform, random, or aggregated. This function uses the spatial data in each image and 99 random simulations of target position. The average number of targets contained in successively larger radii drawn around each target is determined for the original image and each of the 99 simulations. The ratio of the mean of the real data to the mean of the simulated data is the scaled neighbor-K. Values near 1 indicate a random pattern, below 1 a uniform pattern, and above 1 an aggregated pattern. The minimum and maximum number of targets for the simulated data are also scaled by dividing by the mean of the simulation, and they provide upper and lower bounds from which to gauge departures from randomness (Meir et al. 1995).

To compensate for the left–right ambiguity in the images, nearest-neighbor distances were corrected for the entire ensonified area using a factor of $\sqrt{2}$. This is based on the formula for the expected average nearest-neighbor distance under the assumption of a random distribution (Clark and Evans 1954). This correction is accurate if the distribution is random and is approximate if the distributions are uniform or aggregated. This correction was not applied to the scaled neighbor-K function.

Results

Twenty-four HLA–SUS surface scatter runs were examined for biological scattering. All runs were processed for average sea surface scattering in relation to grazing angle; in six high-sea state runs, surface scattering totally dominated over volume scattering (Ogden and Erskine 1994). The remaining 18 runs (Table 1) were at lower sea states where fish might contaminate measurements of sea surface scattering. For these runs, sea surface conditions had abated with wind speeds less than 15 m/s and wave heights at or below 3.6 m. In Ogden and Erskine's (1994) analysis of average scattering versus grazing angle, several runs showed excessive scattering at frequencies of 400–800 Hz and grazing angles less than 10°. Figure 2 shows this excess scattering for Run 23C at 8° grazing angle. In this case the greatest excess in comparison with the empirical Chapman–Harris curve (Chapman and Harris 1962) for surface scattering occurred at 500 Hz. Scattering from the rough sea surface or bubble clouds could not explain these observations (Ogden and Erskine 1994). Pacific salmon of approximately 40 cm length occurring within 40 m of the surface would be resonant near 500 Hz; they were suggested as the cause of this scattering (Nero 1993).

The presence or absence of fish (Table 1), based on an examination of excess scattering near 500 Hz at shallow grazing angles, indicated a significant dependence of fish presence on whether runs were conducted during the day or night (2×2 contingency table, $p \leq 0.001$). Runs were considered day if they occurred between 1h before sunrise and 1h after sunset. All other runs were considered night. Examination of the exact positions of runs, all within 20 km of the test center, did not show any spatial pattern which could explain the reduced numbers of salmon during night. Wind speed and wave height were not significantly different between day and night (Mann–Whitney test, $p \geq 0.2$). These results suggest that the fish became less visible to the HLA at night because of some aspect of their behavior.

Several explanations are possible as to why fish were visible to the HLA during day but less so at night. First, and least likely, is that the salmon expelled all the air from their swimbladders and became weak targets. Second, and also unlikely, is that the fish swam beyond the range of the HLA (4000 m depth or range). Third, the salmon became hidden in the rough sea surface. Geometrical considerations indicate that, at shallow grazing angles and wave heights of 2–3 m, this explanation would only account for reduced ensonification of at most half the salmon. A fourth, and more plausible explanation, is that when a salmon occurs within a metre of the sea surface, it becomes an acoustic dipole. An acoustic dipole occurs when two out-of-phase monopole sources are separated by a distance much shorter than their radiated wavelength (Clay and Medwin 1977, p. 452). This general phenomenon as it pertains to underwater acoustics is termed Lloyd's Mirror (Albers 1965, p. 49). In our case the salmon swimbladder and its acoustic reflection in the sea surface would be the two out-of-phase sources. For the frequency of interest (500 Hz), the separation distance between the swim-

© 1996 NRC Canada

Table 1. Presence and absence of fishlike targets in relation to local time, sea condition, and the classification of runs as day or night.

Run	Local time		Average wind speed (m/s)	Significant wave height (m)	Day/night	Fish
	Begin	End				
1A	18:00	18:30	8.0	3.0	D	No
3C	02:00	02:30	15.0	3.0	N	No
5B	09:05	09:35	9.0	3.1	D	No
11C	04:45	05:15	13.0	3.6	N	No
13C	14:35	15:05	6.0	3.7	D	Yes
18B	12:25	12:55	6.0	3.2	D	Yes
19C	18:55	19:25	7.5	3.0	N	No
20B	23:55	00:25	10.0	2.6	N	No
21C	06:20	06:50	10.5	3.0	D	Yes
23C	14:30	15:00	8.0	2.9	D	Yes
24B	19:25	19:55	5.0	2.1	N	No
25C	01:45	02:15	4.1	2.3	N	No
25D	02:20	02:50	3.0	2.2	N	No
26B	06:50	07:20	5.0	1.9	D	Yes
29E	23:50	00:20	8.0	2.4	N	No
34A1	03:30	04:30	9.0	2.9	N	No
34A2	04:30	05:30	10.0	2.9	N	No
34A3	05:30	06:20	10.0	2.9	D	Yes

Note: Sunrise/sunset times were 06:55/17:33 at the beginning of the experiment and 06:42/17:43 at the end of the experiment. Runs from 1 h before sunrise to 1 h after sunrise are considered day.

Fig. 2. Surface scattering results for Run 23C at 8° grazing angle as a function of frequency (after Ogden and Erskine 1994). Points are the measured surface scattering with ±3 dB bars representing uncertainties due to shot-to-shot variability. The broken line is the reference curve representing Chapman–Harris prediction for a wind speed of 8 m/s at 8° grazing angle.

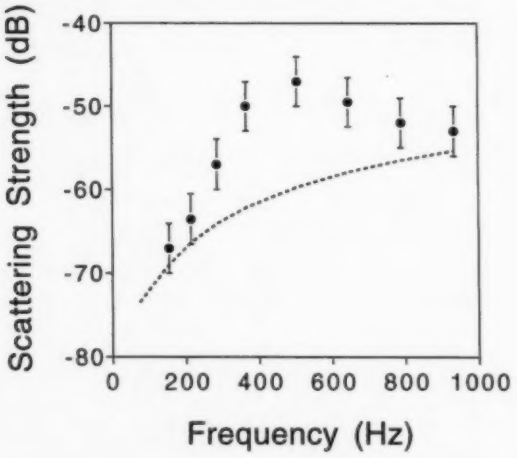

bladder and its reflection would need to be 1 m or less. Under these conditions the acoustic energy radiated by the swimbladder will be canceled by its surface reflection in the direction of the HLA. This is the most plausible explanation of why many salmon were invisible to the HLA at night. This observation also agrees with anecdotal observations of salmon caught within 1 m of the float line of high-seas drift nets (D.W. Welch, Pacific Biological Station, Nanaimo, B.C., personal communication) and the ultrasonic tracking studies showing salmon at the sea surface during the night (Ogura and Ishida 1992 1995).

High-resolution acoustic images were made of 14 SUS shots distributed over six runs using the WASP. In example day and night images, targets, presumably salmon schools, are evident as distinct white blips (Fig. 3). Azimuthal smearing of the schools at greater range reflects the sampling geometry of the HLA and limitations of the beamforming. Radial spokes are attributed to distant noise sources. The difference in number of schools visible in the daytime and nighttime shots is evident. Higher resolution blowups (Fig. 4) show 2-km^2 subsections of three shots taken during the day, at dawn, and night.

Limited information on the target depth of salmon during day was obtained by examination of the four possible ray paths that exist between the source, target, and receiver. One is a direct path, two include one surface reflection, and the fourth contains two surface reflections. As fish targets occur deeper in the water, the time delays between the paths increase. Examination of this multipath spread can allow a determination of target depth. In this study, multipath spread of the targets was either small or had a blended appearance. This small amount of multipath spread indicates that the salmon targets were at most 40 m from the sea surface during the day. This observation matches the depth of fish deter-

© 1996 NRC Canada

Fig. 3. High-resolution scattering image to a range of 4 km mapped to Cartesian coordinates for a scattering image from day and a scattering image from night. Grayscale gives target strength per 5-m^2 resolution cell.

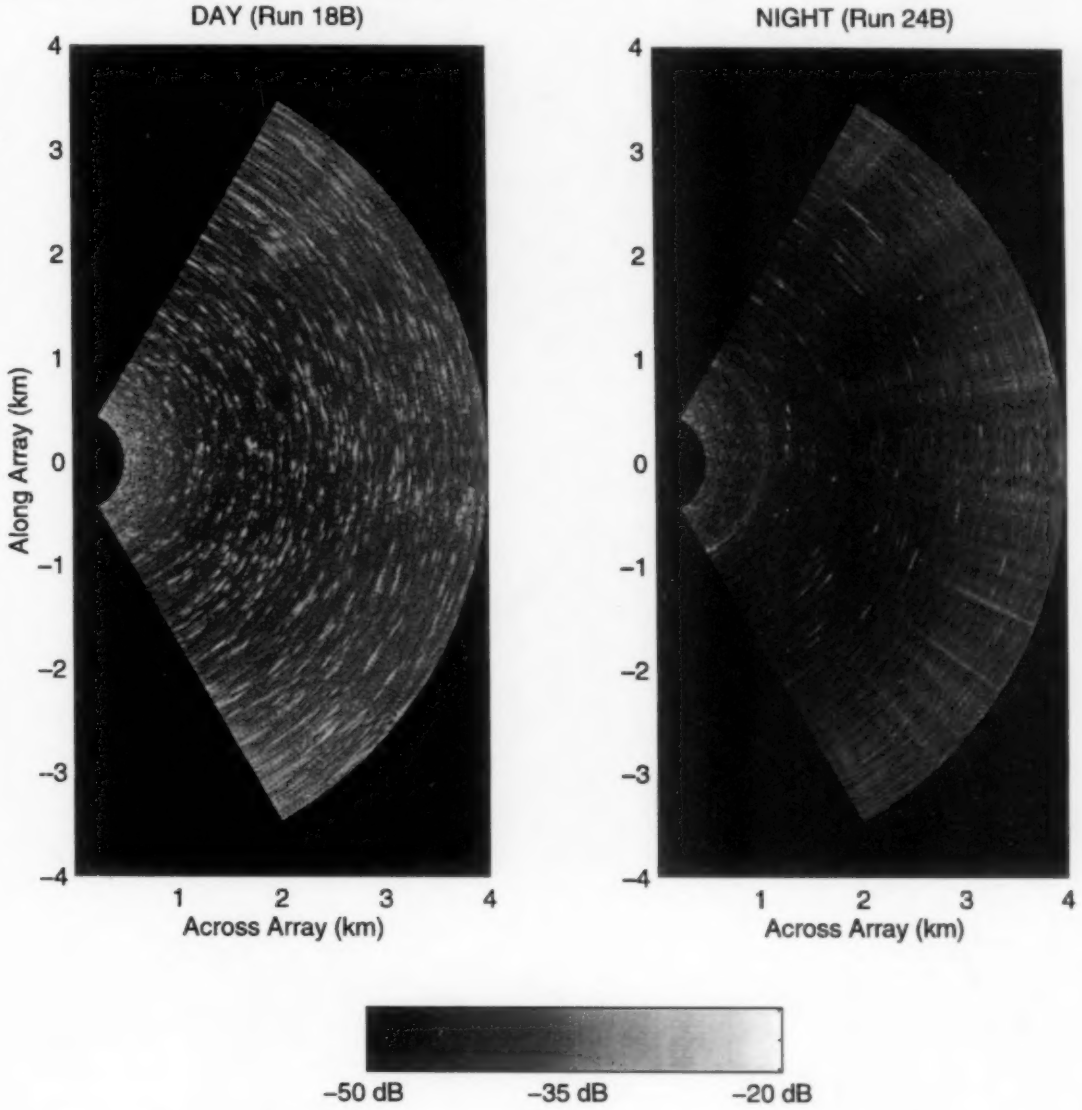

mined from ultrasonic tracking of salmon (Ogura and Ishida 1995).

The spectra of individual targets could not be directly interpreted because of the high variability in spectral shape due to interference between the previously described multipaths. An example of 176 targets detected in Run 18B shot 1 is shown in Fig. 5. These targets show high variability in spectral shape, and the range is about 20 dB. Multipath interference would be expected to produce both abnormally strong and weak targets. Averaging many spectra should minimize these effects; therefore, only average spectra were compared with the scattering spectra predicted by the model of swimbladder resonance.

Figure 6A shows the effect of four extremes of swimbladder compression and depth behavior on swimbladder resonance. Fish maintaining constant swimbladder volume have resonance peaks at lower frequency than those with swimbladders compressing. Fish spread from the surface to 40 m depth have a lower resonance than those occurring just at 40 m depth. None of these extreme examples exactly fits the average spectra for targets obtained during day and dawn (Figs. 6B and 6C); however, they do demonstrate the range of possibilities. Adjustment of the depth at which swimbladder compression began and the depth distribution of fish in the upper 40 m allowed good fits between the swimbladder model and the average spectra for targets obtained during the

© 1996 NRC Canada

Fig. 4. Blowups of 2-km^2 subsections of high-resolution scattering images. Images are for day, dawn, and night. Grayscale as in Fig. 3.

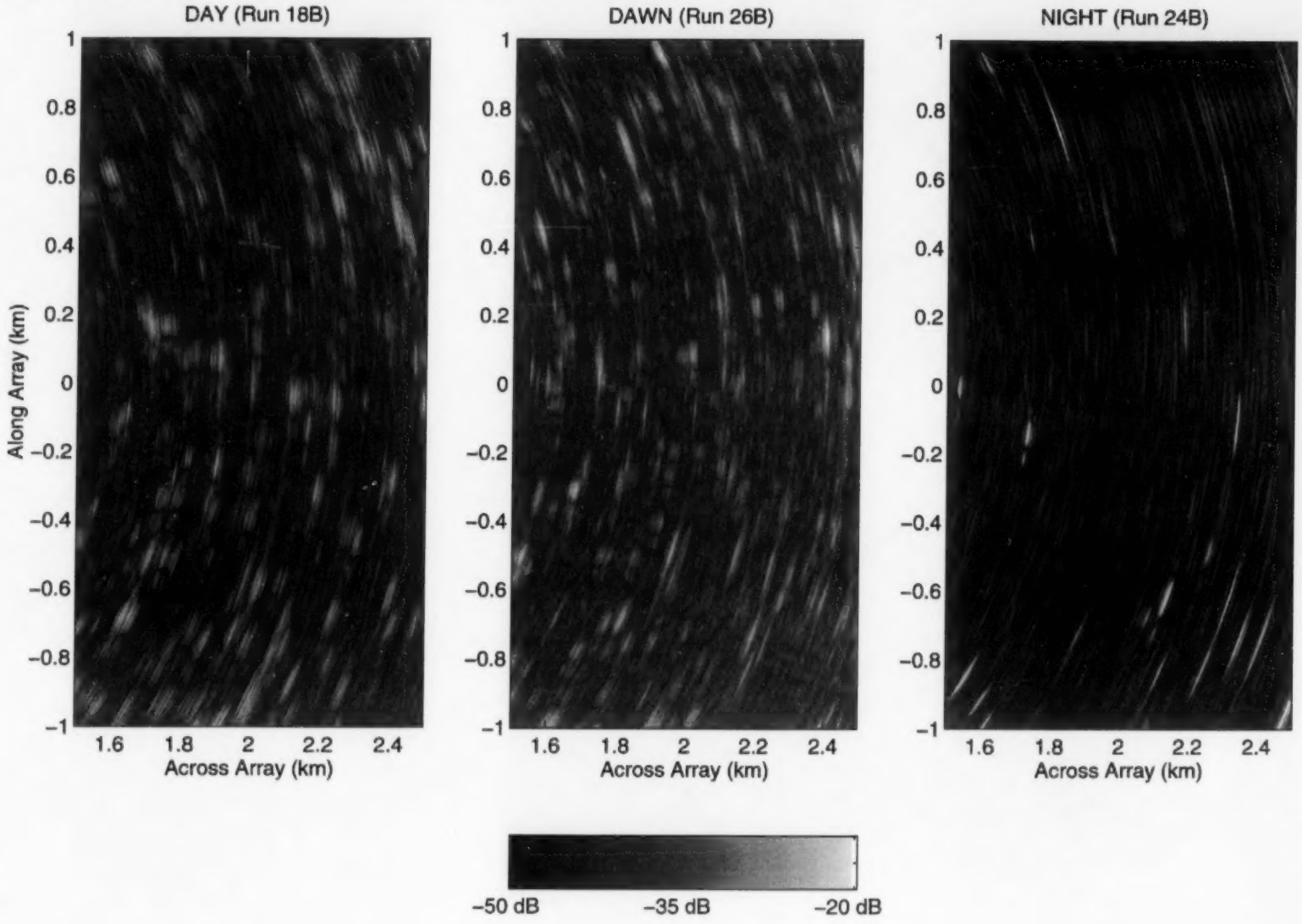

© 1996 NRC Canada

Fig. 5. Overlay of 176 individual target spectra obtained during Run 18B, Shot 1.

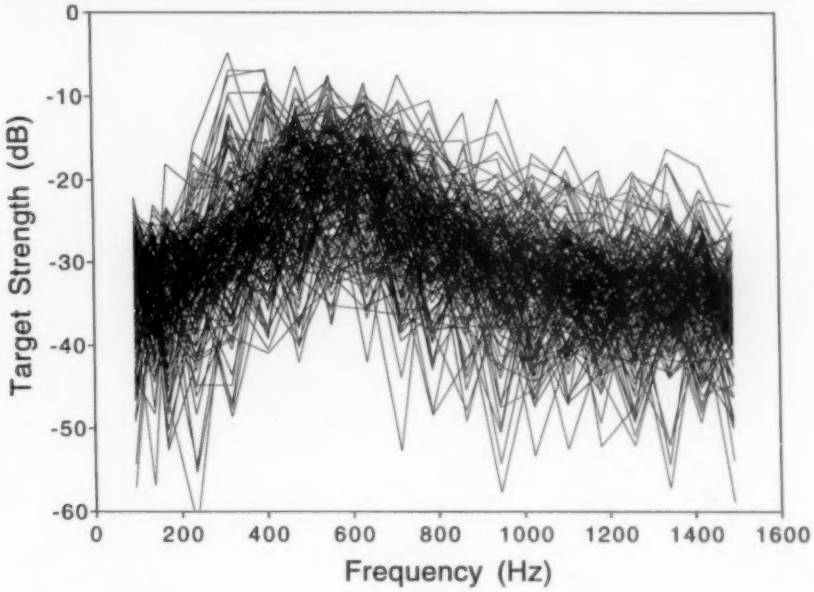

day and dawn (Figs. 6B and 6C). In both cases, swimbladder compression was begun at 10 m depth. The average day spectra were fit with four fish at 30–40 m depth (average target strength (TS) = –17 dB at 450 Hz). Dawn targets were fit with two fish at 20–40 m depth (average TS = –20 dB at 450 Hz). The few targets seen at night showed little indication of a resonance peak, and a model fit was not attempted (Fig. 6D). These targets may have been salmon but, if so, their scattering spectra were likely distorted by their close proximity to the sea surface. Target densities are summarized in Table 2, where fish density is calculated as the product of target density and the average number of salmon per target. The mean density of salmon calculated from the two midday runs, 18B and 23C, is 114 fish/km^2.

The test of dispersion showed that salmon in all day shots departed significantly from a random distribution pattern ($p \leq 0.0002$) with targets tending to be somewhat uniform (Table 2). Targets in three of four night shots did not depart significantly from random (p = 0.2–0.6), with only one night shot showing a slightly uniform distribution (p = 0.02). The average distance between neighboring schools was near 100 m during the day and 160 m for the targets detected at night.

The results of the scaled neighbor-K function are shown in Fig. 7 for the first day shot of Run 18B. The original data are shown in Fig. 7a and one of 99 simulated images in Fig. 7b. The numbers of schools contained in successively larger radii drawn around each school are shown in Figs. 7C and 7D for the real and simulated data, respectively. The scaled neighbor-K function, the result of dividing the real by the simulation, is below the lower limit of the simulation for scales of approximately 2.2 (edge of a 5-m^2 pixel) to 200 m (Fig. 7E). This suggests that a uniform distribution pattern was present at these small spatial scales. This result occurred in all day and dawn images and confirms the result of the test of dispersion. The uniform pattern is also apparent in the x–y positions of the data in comparison with the x–y positions of the simulation. For example, in the data for Run 18B (Fig. 7A), none of the schools overlap and most are separated by the diameter of at least one plotting symbol, while in the random simulation of Run of 18B (Fig. 7B), a number of schools overlap, occurring in small clusters. All four images from night did not show a departure below the lower limits of the simulation, indicating that uniform patterns were not as evident during the night as they were during the day. Aggregation, evident as a departure of the scaled neighbor-K function above the upper limits of the simulation, was seen at scales of 400–2000 m for several dawn shots (three out of four images) and for several night shots (three out of four images).

Discussion

The fishlike targets detected during CST 7 are believed to be salmon. Large fish in the Gulf of Alaska in March are expected to be primarily pink, chum, and sockeye salmon (Rogers 1987; Ware and McFarlane 1989; Groot and Margolis 1991). The swimbladder model indicates that these fish would be strong acoustic targets, with an individual's target strength near –20 dB at frequencies near the swimbladder resonance of 400–600 Hz, depending on depth and swimbladder volume. The presence of a low-frequency resonance and a strong diel pattern and the lack of other likely low-frequency scatterers lead us to conclude that the observed scattering was caused by salmon.

Other sources of low-frequency biological scattering were not likely. Scattering from mesopelagic fish probably occurred during CST 7; however, because of their small size, their contribution to volume scattering below 1000 Hz would be far less than that of salmon. Preliminary model estimates

© 1996 NRC Canada

Fig. 6. Swimbladder model results and target spectra. (A) Swimbladder model: solid line, constant volume with fish at 0–40 m depth; broken line, constant volume with fish at 40 m depth; dot-dashed line, swimbladders compressing with fish at 0–40 m depth; dotted, line, swimbladders compressing with fish at 40 m depth; (B) fit of the swimbladder model to the average scattering spectra for midafternoon; (C) fit to dawn; (D) fit to night. In Figs. 6B and 6C, the solid line is the model and the broken line is the average of all spectra obtained during one shot.

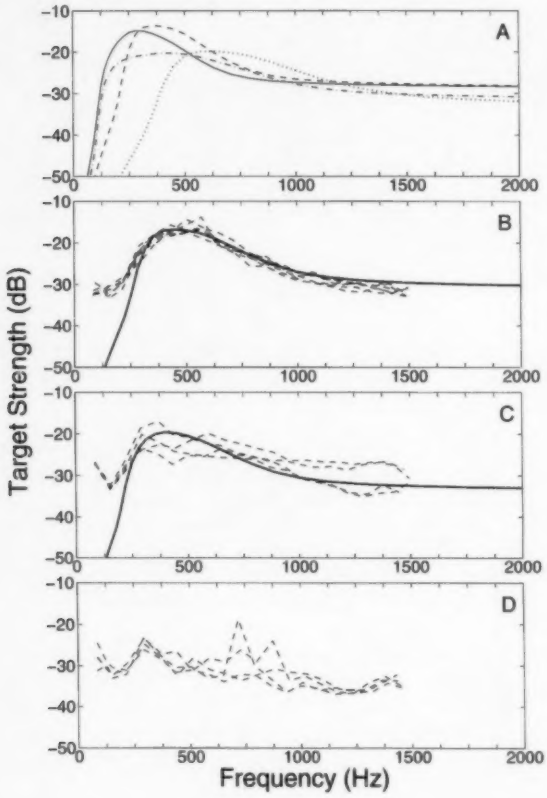

based on mesopelagic fish size and abundance data (Frost and McCrone 1979) gave layer strengths near –84 dB at 1000 Hz, with levels decreasing with decreasing frequency by 12 dB per octave. Pacific saury are the only other potentially important scatterer that could occur in the Gulf of Alaska during March (B. Frost, School of Oceanography, University of Washington, Seattle, Wash., personal communication). They would be about 20–30 cm in length and would occur in the upper 50 m in waters as cool as those observed during the experiment (6–7°C), but would be more prevalent in waters of 12–18°C. If saury were present, they would be expected to exhibit a resonance peak near 900 Hz. Other species occurring in the region during winter are pollack and herring. These species, although abundant near the continental shelf and slope, are not expected in the central part of the Gulf of Alaska (Ware and McFarlane 1989). Fish such as mackerel and pomfret occur in the warm surface waters of the Gulf of Alaska in summer but migrate south during winter (Neave and Hanavan 1960); these species are not expected to return to the Gulf of Alaska by March.

Quantitative density estimates of salmon are unavailable for the Gulf of Alaska. A rough approximation of average densities of pink, chum, and sockeye in the Gulf of Alaska was determined by dividing estimates of stock biomass by fish weight and ocean area. This assumes a uniform distribution over a very wide area. Stock biomass was taken from a review of fisheries production in the Northeast Pacific by Ware and McFarlane (1989). They examined historic catch and life-history information in the "Central Subarctic Domain" (3.1 million km^2). Salmon sizes in March were obtained from documents published by the International North Pacific Fisheries Commission (Godfrey et al. 1975; French et al. 1976; Neave et al. 1976; Major et al. 1978; Takagi et al. 1981). Fish length was converted to weight and this information was used as described above to estimate average fish densities (individuals per square kilometre): pink, 83; sockeye, 39; chum, 38; total 160 ind./km^2. This value is comparable with the mean-density of 114 fish/km^2 calculated from the two midday runs, 18B and 23C, and is quite good considering the broad assumptions used in both estimates.

Our conclusion that salmon occurred in the upper 40 m agrees with most previous studies. Salmon in the open ocean are generally considered to frequent the upper 50 m, with the greatest concentrations occurring in the upper 10 m (Ware and McFarlane 1989; Groot and Margolis 1991). Most observations are from research and commercial catches conducted during spring, summer, and fall using gill nets, drift nets, longlines, purse seines, and trawls. A recent study using ultrasonic tracking of sockeye, chum, pink, and chinook salmon in the central Bering Sea during June and early July showed average depths ranging from 6 to 29 m with pink salmon spending approximately 76% of the time in the upper 10 m (Ogura and Ishida 1995). At times, these fish occurred within 1 m of the surface. Anecdotal observations from driftnet catches indicate that, at night, salmon frequent the upper 10 m with many caught within 1–2 m of the surface. Drift nets were not set during day, as the catches were poor (D.W. Welch, Pacific Biological Station, Nanaimo, B.C., personal communication). The preceding information would suggest that, during CST 7, salmon would most likely have occurred in the upper 10–40 m during day and within 10 m of the sea surface at night.

The small average school size obtained on CST 7, two to four individuals, concurs with observations from gillnet that catches and sonar echograms (Takagi et al. 1981; Suzuki and Sonoda 1972). Welch and Ishida's (1993) analysis of catch data from Japanese research gill nets indicates that catches were spatially uncorrelated at spacing greater than 15 m, suggesting that the size of a school is somewhat less than 15 m. Catch numbers from a 250-m section of net ranged from single fish to a maximum of 56 fish with the majority between two and six fish. These observations suggest that during CST 7, salmon probably occurred in small schools of several to a few dozen fish. Just a few fish per target matches previous studies which suggest that salmon occur singly, in pairs, or in small schools of up to at most 24 fish (Takagi et al. 1981; Welch and Ishida 1993).

This study provides significant new information on the distribution of salmon at sea. Interpretation of salmon catch from nets is dependent on the statistical nature of the distribution of

© 1996 NRC Canada

Table 2. Target information, including results of the test of dispersion.

Run	Time of day	No. of SUS shots	Target density (no./km^2)	Avg. fish per target	Fish density (no./km^2)	D (m)	p
26B	Dawn	2	36.3	2	73	100	0.0002
34A3	Dawn	2	39.9	2	80	98	≤0.0002
18B	Noon	2	29.9	4	120	111	≤0.0002
23C	Mid afternoon	4	26.8	4	107	114	0.0002
24B	Night	2	13.0	n/a	n/a	149	0.02 and 0.2
25D	Night	2	8.4	n/a	n/a	165	0.5 and 0.6

Note: D is the average distance between nearest neighbors, and p is the probability of the observed result under the assumption of a random dispersion pattern.

salmon on the high seas. Recent tracking experiments (Ogura and Ishida 1992, 1995) and studies of the statistical distribution of salmon at sea from gillnet catches (Welch and Ishida 1993) have begun to address their spatial distribution and behavior. Welch and Ishida (1993) found that the catch of salmon from 250-m sections of gill net was best described by the negative binomial distribution. Knowledge of this distribution is useful to guide future sampling efforts and the statistical treatment of results from gill nets. Their results describe the statistical nature of the encounter between the salmon and the gill nets. In this study, we go one step further and show a close approximation of the actual in situ spatial arrangement of the salmon at several spatial scales.

Uniform areal distribution patterns of small salmon schools were observed at small spatial scales (2–200 m). These patterns may have an acoustic or biological origin. Although the density estimates of salmon from the HLA are unbiased, the spatial patterns could be biased. The acoustic sampling, subsequent beamforming, and visual selection of schools from the acoustic images could have resulted in closely spaced schools being combined as single schools, resulting in a uniform pattern at small scales. The alternative biological explanation is that the uniform distribution may have been caused by the behavior of the salmon. Could schools of salmon be repelling one another? This would suggest a behavioral mechanism to optimize their spatial distribution at the sea surface, presumably for feeding on widely dispersed prey. It also may suggest a scarcity of salmon predators in the open sea. Fish schools are usually hypothesized as a defense against predators (Pitcher and Parrish 1993). The survival rate of salmon at sea is high (85% annual survival rate, Groot and Margolis 1991) and would suggest that these fish have little need for schooling as a defense against predators.

At much larger spatial scales (400–2000 m), aggregations occurred among the few targets, possibly schools, which were observed during night. One possibility is that salmon form large-scale loose aggregations near the sea surface at night. These aggregations may be related to subtle ocean features, be they either physical or biological, occurring at scales of 400–2000 m.

The acoustic technology demonstrated here provides a reasonable estimate of fish density. Such technology could aid in the monitoring of many high-seas pelagic fish stocks, especially those that are widely dispersed and close to the sea surface. Conventional fisheries echosounders are difficult to modify to survey the surface because of their limited range and angular resolution. Many near-surface fish avoid moving vessels (Gunderson 1993). Horizontal-looking sonars are generally single-frequency systems and lack low-frequency broadband information, shown here to be extremely useful in target classification. Presently the assessment or study of high-seas salmon is expensive in terms of ship time because of the small number of fish sampled per day at sea. This is exemplified by a recent survey of the W.E. *Ricker* (Morris and Welch 1992), where the number of tows or sets, and the number of salmonids caught were as follows: 10 rope trawls, 9; nine gillnet sets, 74; two longline sets, 5. Trawls were for 1 h, gillnet sets were overnight, and longline sets were for 3–4 h. In comparison, one noon shot with the HLA gave quantitative results from an area of 4 km^2, with a count of 120 targets, presumed to be 420 salmon. Of course the identity of these targets is not absolutely known; in any survey program, nets are still required to identify targets and to provide basic biological data. In addition, some modification in the HLA technique may be required for routine fisheries assessment. A smaller more easily deployed HLA with a smaller sound source may be required for practical use in fisheries assessments.

Finally, relationships between salmon and surface oceanography are important in understanding the ecology of high-seas salmon. The salmon observed in this study were inferred to have occurred very close to the sea surface while feeding at night. Such close proximity to the sea surface and recent hypotheses on their thermal limits (Welch et al. 1995) suggest that these fish are highly susceptible to the effects of changes in the near-surface oceanographic conditions. In the future, fine-scale observations with instrumentation like the HLA could prove especially useful when combined with detailed environmental observations.

Acknowledgments

We are indebted to F.T. Erskine and P.M. Ogden for providing several sets of acoustic data that were used in producing the high-resolution images. R.H. Love kindly provided guidance in interpreting scattering data. We thank R. Kieser and an anonymous reviewer for constructive comments on the manuscript. Funding was provided by the Office of Naval Research and the Space and Naval Warfare Systems Command.

© 1996 NRC Canada

Fig. 7. Scaled neighbor-*K* function. (A) Original position data from Image 18B, Shot 1; (B) random simulation of 18B, Shot 1; (C) average number of schools within progressively larger radii of each school for the data; (D) average (solid line) and minimum and maximum (broken lines) number of schools within progressively larger radii for the simulation; (E) scaled neighbor-*K* (solid line) and scaled minimum and maximum (broken lines).

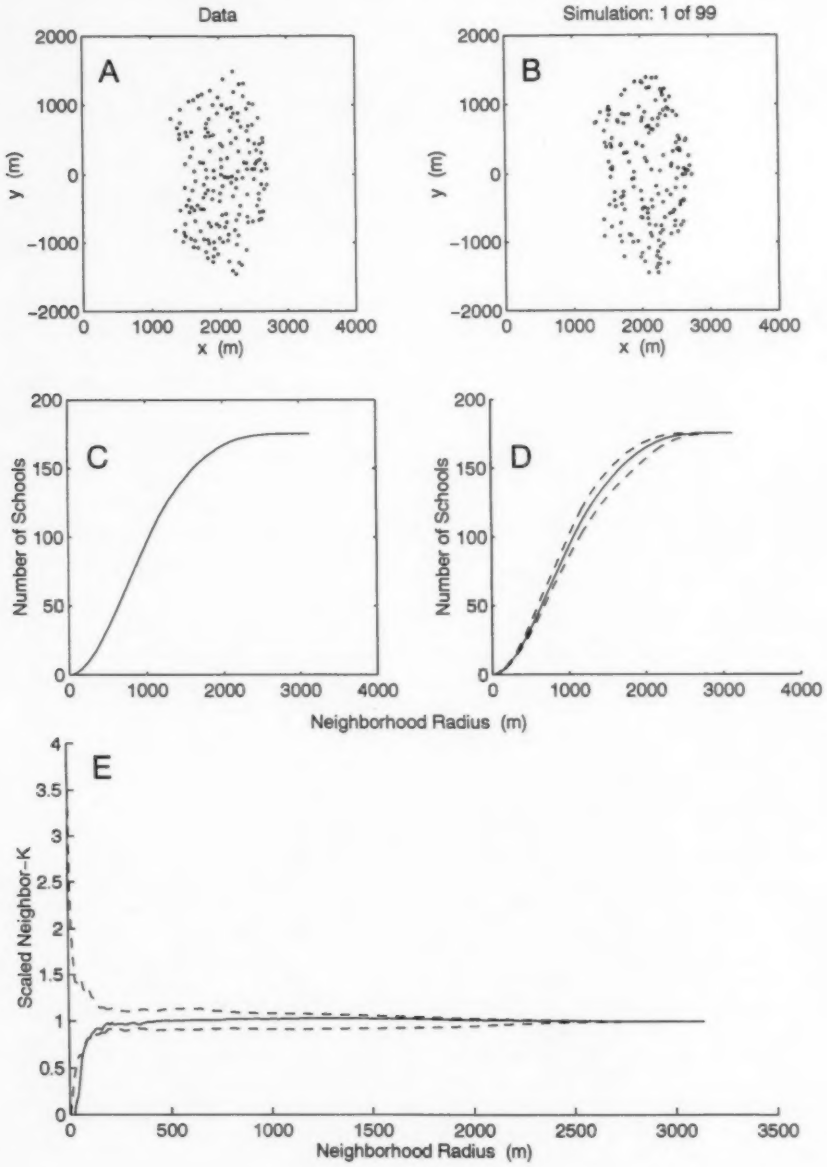

References

Adair, R.G., and Huster, M.E. 1993. High resolution surface reverberation imaging during CST 7 Phase 2. *In* Critical Sea Test 7, Phase 2: principal investigators' results; Gulf of Alaska surface scattering and air–sea interaction experiment. *Edited by* F.T. Erskine and J.L. Hanson. Johns Hopkins University, Applied Physics Laboratory, Laurel, Md, Report STD-R-2258. pp. 4–1–4–84.

Albers, V.M. 1965. Underwater acoustics handbook II. Pennsylvania State University Press, University Park, Pa.

Alexander, R.M. 1993. Buoyancy. *In* The physiology of fishes. *Edited by* H.E. Evans. CRC Press, Boca Raton, Fla. pp. 75–97.

Blaxter, J.H.S., and Batty, R.S. 1990. Swimbladder "behavior" and target strength. Rapp. P.-v. Réun. Cons. Int. Explor. Mer, **189**: 233–244.

Chapman, R.P., and Harris, J.H. 1962. Surface backscattering

© 1996 NRC Canada

strengths measured with explosive sound sources. J. Acoust. Soc. Am. **34**: 1592–1597.

Clark, P.J., and Evans, F.C. 1954. Distance to nearest neighbor as a measure of spatial relationships in populations. Ecology, **35**: 445–453.

Clay, C.S., and Medwin, H. 1977. Acoustical oceanography: principles and applications. John Wiley & Sons, Inc., New York.

Cressie, N.A.C. 1993. Statistics for spatial data. John Wiley & Sons, Inc., New York.

Feuillade, C., and Werby, M.F. 1994. Resonances of deformed gas bubbles in liquids. J. Acoust. Soc. Am. **96**: 3684–3692.

French, R., Bilton, H., Osako, M., and Hartt, A. 1976. Distribution and origin of sockeye salmon (*Oncorhynchus nerka*) in offshore waters of the north Pacific ocean. Int. North Pac. Fish. Comm. Bull. no. 34.

Frost, B.W., and McCrone, L.E. 1979. Vertical distribution, diel vertical migration, and abundance of some mesopelagic fishes in the eastern subarctic Pacific Ocean in summer. Fish. Bull. **76**: 751–770.

Godfrey, H., Henry, K.A., and Machidori, S. 1975. Distribution and origin of coho salmon in offshore waters of the north Pacific ocean. Int. North Pac. Fish. Comm. Bull. 31.

Groot, C., and Margolis, L. (*Editors*). 1991. Pacific salmon life histories. University of British Columbia Press, Vancouver, B.C.

Gunderson, D.R. 1993. Surveys of fisheries resources. John Wiley & Sons, Inc., New York.

Hanson, J.L., and Erskine, F.T. 1992. An experiment to study the influence of the air–sea boundary zone on underwater acoustic reverberation. Proceeding of MTS'92: Global Ocean Partnership. Marine Technology Society, Washington, D.C.

Love, R.H. 1978. Resonant acoustic scattering by swimbladder-bearing fish. J. Acoust. Soc. Am. **64**: 571–580.

Love, R.H. 1993. A comparison of volume scattering strength data with model calculations based on quasisynoptically collected fishery data. J. Acoust. Soc. Am. **94**: 2255–2268.

Major, R.L., Ito, J., Ito, S., and Godfrey, H. 1978. Distribution and origin of chinook salmon (*Oncorhynchus tshawytscha*) in offshore waters of the north Pacific ocean. Int. North Pac. Fish. Comm. Bull. no. 38.

Meir, E., Greene, C.H., and Zamon, J.E. 1995. Analytical techniques for detecting and characterizing small-scale zooplankton patchiness in acoustic data sets. Paper presented at the ICES International Symposium on Fisheries and Plankton Acoustics, Aberdeen, 12–16 June 1995. Book of abstracts. p. 76.

Morris, J.F.T., and Welch, D.W. 1992. Data report from the Canadian high seas salmon cruise to the eastern North Pacific, February 27th – March 25th 1992. Can. Data Rep. Fish. Aquat. Sci. 884.

Neave, F., and Hanavan, M.G. 1960. Seasonal distribution of some epipelagic fishes in the Gulf of Alaska region. J. Fish. Res. Board Can. **17**: 221–233.

Neave, F., Yonemori, T., and Bakkala, R.G. 1976. Distribution and origin of chum salmon in offshore waters of the north Pacific ocean. Int. North Pac. Fish. Comm. Bull. 35.

Nero, R.W. 1993. Volume reverberation from fish during CST 7 phase 2. *In* Critical Sea Test 7, Phase 2: principal investigators' results; Gulf of Alaska surface scattering and air–sea interaction experiment, *Edited by* F.T. Erskine and J.L. Hanson. Johns Hopkins University, Applied Physics Laboratory, Laurel, Md. Report STD-R-2258. pp. 7–1–7–24.

Ogden, P.M., and Erskine, F.T. 1994. Surface and volume scattering strength measurements using broadband explosive charges in the Critical Sea Test 7 experiment. J. Acoust. Soc. Am. **96**: 2908–2920.

Ogura, M., and Ishida, Y. 1992. Swimming behavior of coho salmon, *Oncorhynchus kisutch*, in the open sea as determined by ultrasonic telemetry. Can. J. Fish. Aquat. Sci. **49**: 453–457.

Ogura, M., and Ishida, Y. 1995. Homing behavior and vertical movements of four species of Pacific salmon (*Oncorhynchus* spp.) in the central Bering Sea. Can. J. Fish. Aquat. Sci. **52**: 532–540.

Ona, E. 1990. Physiological factors causing natural variations in acoustic target strength of fish. J. Mar. Biol. Assoc. U.K. **70**: 107–127.

Pitcher, T.J., and Parrish, J.K. 1993. Functions of shoaling behaviour in teleosts. *In* Behaviour of teleost fishes. 2nd ed. Edited by T.J. Pitcher. Chapman and Hall, New York. pp. 363–439.

Rogers, D.E. 1987. Pacific salmon. *In* The Gulf of Alaska physical environment and biological resources. *Edited by* D.W., Hood, and S.T. Zimmerman. National Oceanic and Atmospheric Administration, Washington, D.C. pp. 461–478.

Sundnes, G., and Sand, O. 1975. Studies of physostome swimbladder by resonance frequency analyses. J. Cons. Int. Explor. Mer, **36**: 176–182.

Suzuki, T., and Sonoda, H. 1972. On the schooling of salmon in the North Pacific Ocean observed by salmon fish finder. Hokkaido Univ. Facul. Fish. Bull. **23**(2): 77–81. (In Japanese, English summary)

Takagi, K., Aro, K.V., Hartt, A.C., and Dell, M.B. 1981. Distribution and origin of pink salmon (*Oncorhynchus gorbuscha*) in offshore waters of the north Pacific ocean. Int. North Pac. Fish. Comm. Bull. 40.

Thompson, C.H., and Love, R.H. 1996. Determination of fish size distributions and areal densities using broadband low-frequency measurements. ICES J. Mar. Sci. **53**: 197–201.

Thorne, R.E., and Thomas, G.L. 1990. Acoustic observations of gas bubble release by Pacific herring (*Clupea harengus pallasi*). Can. J. Fish. Aquat. Sci. **47**: 1920–1928.

Ware D.M., and McFarlane, G.A. 1989. Fisheries production domains in the northeast pacific ocean. *In* Effects of ocean variability on recruitment and an evaluation of parameters used in stock assessment models. *Edited by* R.J. Beamish and G.A. McFarlane. Can. Spec. Publ. Fish. Aquat. Sci. **108**: 359–379.

Welch, D.W., and Ishida, Y. 1993. On the spatial distribution of salmon in the sea: application of the negative binomial distribution, and the influence of sampling effort. Can. J. Fish. Aquat. Sci. **50**: 1029–1038.

Welch, D.W., Chigirinsky, A.I., and Ishida, Y. 1995. Upper thermal limits on the oceanic distribution of Pacific salmon (*Oncorhynchus* spp.) in the spring. Can. J. Fish. Aquat. Sci. **52**: 489–503.

Weston, D.E. 1967. Sound propagation in the presence of bladder fish. Underwater acoustics. Vol 2. *Edited by* V.M. Abbers. Plenum, New York. pp., 55–88.

© 1996 NRC Canada

Eye development in Atlantic halibut (*Hippoglossus hippoglossus*): differentation and development of the retina from early yolk sac stages through metamorphosis

A.M. Kvenseth, K. Pittman, and J.V. Helvik

Abstract: The eye and retina in Atlantic halibut (*Hippoglossus hippoglossus*), from early yolk sac stages through metamorphosis, were examined after dissection by light microscope, and, for selected stages, by transmission electron microscope. At hatching the eyes were transparent and the retina undifferentiated. The retina differentiated slowly in sectors, and appeared functional around 150 degree-days (d°) posthatching (about 50% yolk absorption). This timing coincided with the development of functionality in other organs and observations of ability to feed. At the commercial time of first feeding (about 210 d° or 70% yolk absorption) the eyes were fully pigmented. Eye migration started at approximately 80 days posthatching, concurrent with the reorganization of the cones in the outer retina from single rows into a square-type cone mosaic. At 130 days, when metamorphosis was complete, the retina contained groups of rods and appeared to be mature, but until this stage, cones were the primary photoreceptor. The formation of a cone mosaic, recruitment of rods, and increasing size of the eye all indicated increased visual sensitivity at the time of settling. The results suggest that in culture, larvae can see to feed after 150 d°, and at settling, they can be successfully fed under dim light.

Résumé : L'oeil et la rétine de flétans (*Hippoglossus hippoglossus*), des premiers stades de la larve vésiculée jusqu'à la métamorphose, ont été examinés après dissection au microscope optique et, pour certains stades, au microscope électronique à transmission. À l'éclosion, les yeux sont transparents et la rétine n'est pas encore différenciée. Elle se différencie lentement par secteurs et paraît être fonctionnelle environ 150 degrés-jours (d°) après l'éclosion (vitellus absorbé à environ 50 %). Ce moment coïncide avec l'entrée en fonction d'autres organes et la capacité observée de s'alimenter. Au moment du premier repas en élevage commercial (environ 210 d° ou 70% d'absorption du vitellus), les yeux ont complètement acquis leur pigmentation. Leur migration commence environ 80 jours après l'éclosion, au moment de la réorganisation des cônes vers la surface de la rétine, soit d'un alignement en rangées simples à une mosaïque de carrés formés de ces cônes. Au bout de 130 jours, une fois la métamorphose complétée, la rétine contient des groupes de bâtonnets et paraît être complètement fonctionnelle, mais jusqu'à ce stade, les cônes constituent les principaux photorécepteurs. La formation d'une mosaïque de cônes, le recrutement des bâtonnets et le grossissement de l'oeil pointent tous vers une sensibilité visuelle accrue au moment de la migration vers le fond. Les résultats suggèrent qu'en conditions d'élevage, les larves voient assez bien pour s'alimenter au bout de 150 d° et qu'au moment de s'installer au fond, elles voient assez bien pour s'alimenter sous une lumière tamisée.
[Traduit par la Rédaction]

Introduction

The Atlantic halibut (*Hippoglossus hippoglossus*) is a promising species for farming in temperate waters (Tilseth 1990). Despite its abundance in the North Atlantic, capture of larvae are rare, and information regarding the natural history of the early life stages is scarce. Nevertheless, the eggs, larvae, and fry of this bathypelagic spawner experience significant changes in ambient temperature and light during development (Haug 1990).

Light impinges on the early life stages of halibut in several ways, by regulating egg bouyancy (Mangor-Jensen 1995), synchronizing hatching (Helvik and Walther 1992), affecting activity during the yolk sac stage (Skiftesvik et al. 1990), and repositioning the larvae in the water column as negative phototaxy turns to positive phototaxy (Mangor-Jensen and Naas 1993). Since the eyes become fully pigmented first at about 150 degree-days d° posthatching (halfway through the yolk sac stage, slightly prior to first feeding), many of these responses seem to be mediated extraretinally, although retinal involvement may be present at some stages.

Descriptions of halibut eye development have been restricted to observations of the pigmentation, diameter, and eye displacement from hatching through metamorphosis (Blaxter et al. 1983; Pittman et al. 1990*b*). The timing of photoreceptor development was regarded as a critical clue for

Received October 3, 1995. Accepted May 23, 1996.
J13093

A.M. Kvenseth and K. Pittman. Department of Fisheries and Marine Biology, University of Bergen, Bergen High Technology Center, N-5020 Bergen, Norway.
J.V. Helvik. Laboratory of Marine Molecular Biology, University of Bergen, Bergen High Technology Center, N-5020 Bergen, Norway.

© 1996 NRC Canada

differentiating retinally and nonretinally mediated responses to light in this primarily visual feeder. Additional information on the timing of reorganization of retinal structures could provide insight into the natural photic environment and suitable culture techniques. The purpose of this study was to describe the histomorphological development of the eye from hatching through metamorphosis, and determine milestones in the ontogeny of visual perception in the halibut.

Materials and methods

Larvae and juveniles were obtained from Sea Farm Aga A/S, a commercial halibut farm situated in western Norway.

Yolk sac larvae were kept in darkness in 3.5-m^3 silos, as described by Rabben et al. (1987), in water temperatures varying between 5.5 and 7.0°C throughout the season (March–May). The larval age in degree-days was calculated from the daily temperature recordings. Yolk sac larvae were sampled from the top of the silos and brought out in daylight before being killed and fixed at 25, 50, 90, 110, 150, and 210 d° (end of yolk sac (EYS) is about 300 d°). The halibut were fixed in a mixture of 5% glutaraldehyde and 0.2 M phosphate buffer in Ringers solution.

At 210 d° (30 days) larvae were transferred to the feeding units, 70-m^3 black plastic bags, floating in a closed seawater system, as described by Berg and Øiestad (1986). The larvae were exposed to natural light, with a daylength of 16 h in early May to a maximum of 19 h in late June. Naturally occurring zooplankton was filtered from the seawater and introduced to the bags, together with Selco-enriched Artemia nauplii. The temperature in the bags varied with depth and throughout the season from 12°C in the upper metre and 7.5°C at the bottom of the bag in early May to 19 and 17°C in June. In July the temperature was homogenously 15°C. Because of the variation in temperature, an estimation of degree-days was impossible and larval age in days from hatching was used for these later stages. Larvae were sampled at night, with a dip net, at ages of 35, 45, 55, 60, 70, 80, 90, and 100 days.

Close to the completion of metamorphosis, larvae were collected from the bags, transferred to 1-m^2 square tanks on shore, and weaned onto a commercial dry feed. The temperature in the tanks varied from 11 to 15°C in July. The light regime followed the natural daylight. Juvenile fish were sampled at 110 and 130 days, together with 1-yr-old fish from the previous season.

Morphology

Fixed fish from all stages were decapitated, and the heads were rinsed in buffer, dehydrated in ethanol, and embedded in Historesin™ (Reichert-Jung). Serial sections of the eyes, 1.5 and 3 μm thick, were cut sagittally and transversally to the body axis on a Reichert-Jung 2050 supercut microtome. The sections were stained with toluidine blue and studied under a Leica Aristoplan light microscope.

On the basis of light microscopy, three stages, 110, 150, and 210 d°, were selected for examination by transmission electron microscope. Larvae were postfixed in 1% OsO_4, dehydrated in acetone, and embedded in Epon 812. Sections, 40 nm thick, were cut on a Reichert-Jung Ultracut E microtome, stained with uranyl acetate and lead citrate, and studied under a Jeol Jem 100S transmission electron microscope.

Results

Gross morphology

At hatching the eyes were transparent and symmetrically placed on the larval head (Fig. 1*i*). Eye pigmentation was first visible about 50 d° posthatching as a bar stretching from the pupil opening to the temporal (towards the tail) edge of the eye. Pigmentation proceeded slowly, sector by sector, through the next 3 wks before the eyes became fully pigmented about 210 d° (Figs. 1*iv* and 1*vii*). At about 55 days (EYS) the eyes acquired a silvery appearance with a dorsal melanin shading. Eye migration was first observed about 60 days posthatching and was completed at about 130 days (Figs. 1*x*, 1*xiii*, and 1*xv*).

Retinal differentation

Retinal differentation in the yolk sac stage

Around 25 d°, most of the neural retina consisted of a pseudostratified layer of apparently undifferentiated, spindle-shaped neuroblastic cells, and the cells of the monolayered pigment epithelium contained no melanin granules (Figs. 1*ii* and 1*iii*). In the temporal part of the retina, vitread (towards the corpus vitreum in the center of the eye) to the pigment epithelium, a group of cells could be distinguished from the neuroblasts by their darker staining nuclei. A bundle of axons went through the retina as a primary formation of the optic nerve, indicating an early differentiation of ganglion cells.

Around 50 d° the amount of cells containing dark-staining nuclei had expanded, and the adjacent pigment epithelium contained few melanin granules. The neuroblastic layer had become bisected (Fig. 2A), but the cells of the two layers could not be morphologically distinguished under the light microscope.

Around 90 d°, all retinal layers could be recognized in the central part of the retina (Fig. 2B), and the amount of melanin granules in the pigment epithelium had increased in areas corresponding with the macroscopically visible eye pigmentation. In the visual cell layer, photoreceptor inner segments had expanded through the external limiting membrane and were discernible as pale expansions of the sclerad (outward in the direction of the sclera) part of the photoreceptor precursors.

The outer nuclear layer consisted of a regular row of columnar, dark-staining nuclei, and vitread to these a thin outer plexiform layer was discernible. In the inner nuclear layer, the scleradmost part consisted of a single row of cells with flattened nuclei, indicating differentiated horizontal cells. The vitread part of the inner nuclear layer contained numerous rounded cells with large, light-staining nuclei and very little cytoplasm, resembling amacrine cells. The bipolar cells could not be morphologically distinguished from neuroblasts at this stage.

The inner plexiform layer was thin and contained some displaced amacrine or ganglion cells. The cells of the ganglion cell layer were rounded and clearly differentiating. There were two morphologically distinct types: cells with smaller, dark-staining nuclei situated near the inner plexiform layer and cells with larger, lighter-staining nuclei situated more vitread in the ganglion cell layer. The nerve fibre layer was visible on the vitreal surface of the retina.

Around 110 d° the bipolar cells had attained a more mature appearance. The optic nerves from both eyes crossed completely in the optic chiasma and continued into the opposite brain hemisphere (Fig. 3).

Around 150 d° (Figs. 1*v* and 1*vi*) the photosensitive outer segments of the photoreceptors could be observed for the first time and were about 5 μm long (Figs. 1*vi* and 4). Concomitantly the retinal pigment epithelium extended pigmented processes between these outer segments, in the ventral part of

© 1996 NRC Canada

Fig. 1. Overview of the development of the eye and retina in the larval, postlarval, and juvenile halibut. The age is given in the first column, gross morphology in the second column, and a general description of behaviour and rearing system in the third column. Eye development, in the fourth column, shows transverse (*viii* and *xiv*) and sagittal (*ii* and *v*) sections through the eye showing the sectoral development of the retina, or sections through the retinal periphery (photoreceptor layer) (*xi* and *xvi*) showing the rearrangement of the cones from rows of single cones (*xi*) into a regular mosaic of double and single cones (*xiv*). The sagittal sections are paralell to the larva's length axis, the nasal end pointing to the left, while the transverse sections are at right angles to the length axis. Letters on photographs in fourth column: L, lens; ef, embryonal fissure. Retinal development, in the fifth column, shows transverse sections through the layers of the retina illustrating their differentiation and

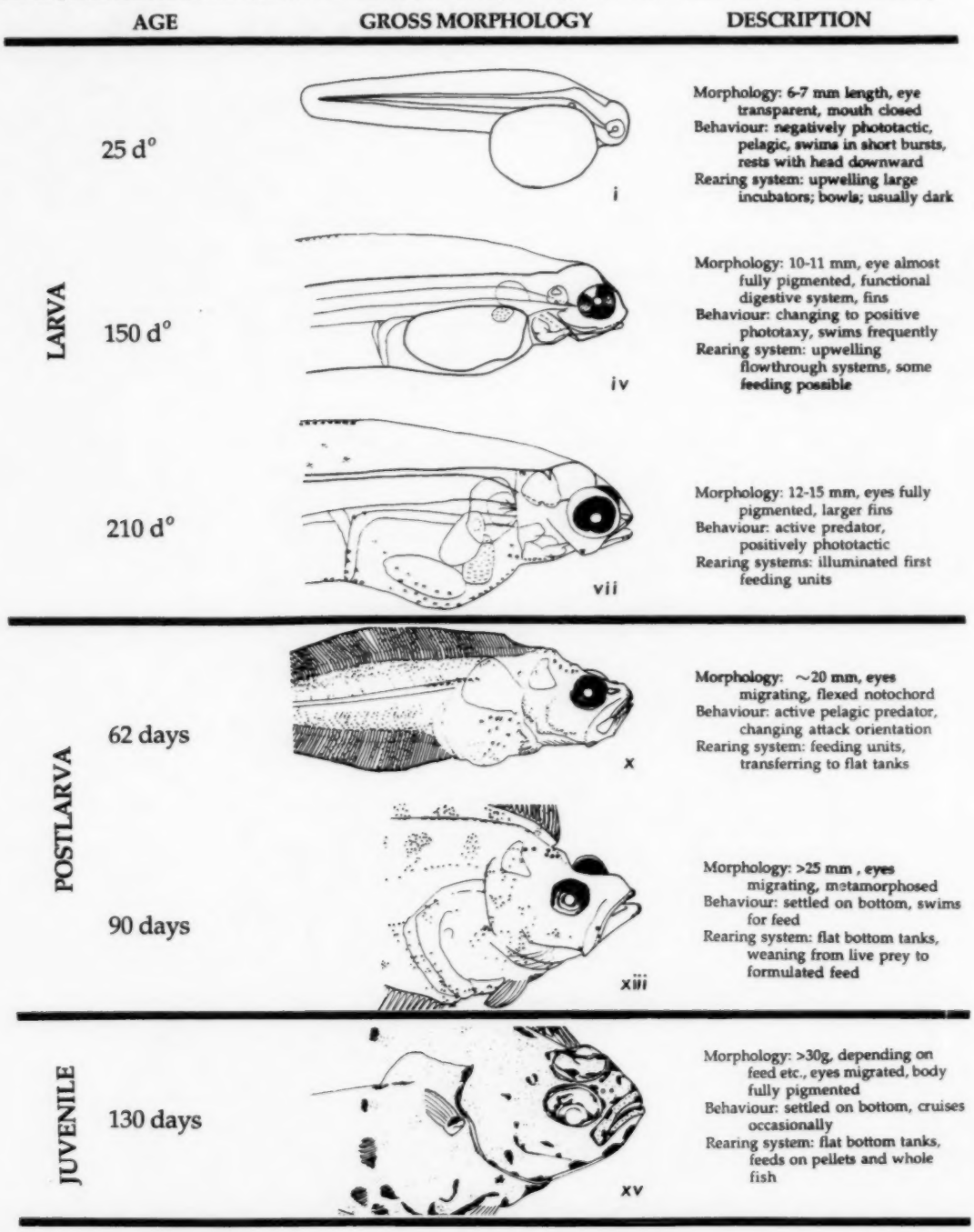
AGE
GROSS MORPHOLOGY
DESCRIPTION
LARVA
25 d°
i
Morphology: 6-7 mm length, eye transparent, mouth closed
Behaviour: negatively phototactic, pelagic, swims in short bursts, rests with head downward
Rearing system: upwelling large incubators; bowls; usually dark
150 d°
iv
Morphology: 10-11 mm, eye almost fully pigmented, functional digestive system, fins
Behaviour: changing to positive phototaxy, swims frequently
Rearing system: upwelling flowthrough systems, some feeding possible
210 d°
vii
Morphology: 12-15 mm, eyes fully pigmented, larger fins
Behaviour: active predator, positively phototactic
Rearing systems: illuminated first feeding units
POSTLARVA
62 days
x
Morphology: ~20 mm, eyes migrating, flexed notochord
Behaviour: active pelagic predator, changing attack orientation
Rearing system: feeding units, transferring to flat tanks
90 days
xiii
Morphology: >25 mm , eyes migrating, metamorphosed
Behaviour: settled on bottom, swims for feed
Rearing system: flat bottom tanks, weaning from live prey to formulated feed
JUVENILE
130 days
xv
Morphology: >30g, depending on feed etc., eyes migrated, body fully pigmented
Behaviour: settled on bottom, cruises occasionally
Rearing system: flat bottom tanks, feeds on pellets and whole fish

© 1996 NRC Canada

Fig. 1 *(concluded).*

expansion, the relative proportion of each retinal layer changing with development stage. Letters below photographs in fifth column: a, pigment epithelium; b, visual cell layer; c, outer nuclear layer, d, outer plexiform layer; e, inner nuclear layer; f, inner plexiform layer; g, ganglion cell layer; h, nerve fiber layer. Letters on photographs in fifth column: c, cones; os, outer segment of cones; r, rods. The section through the retina of the postlarval stage (*xii*) was from a larva fixed in Bouin's fluid, while the rest were fixed with phosphate-buffered glutaraldehyde.

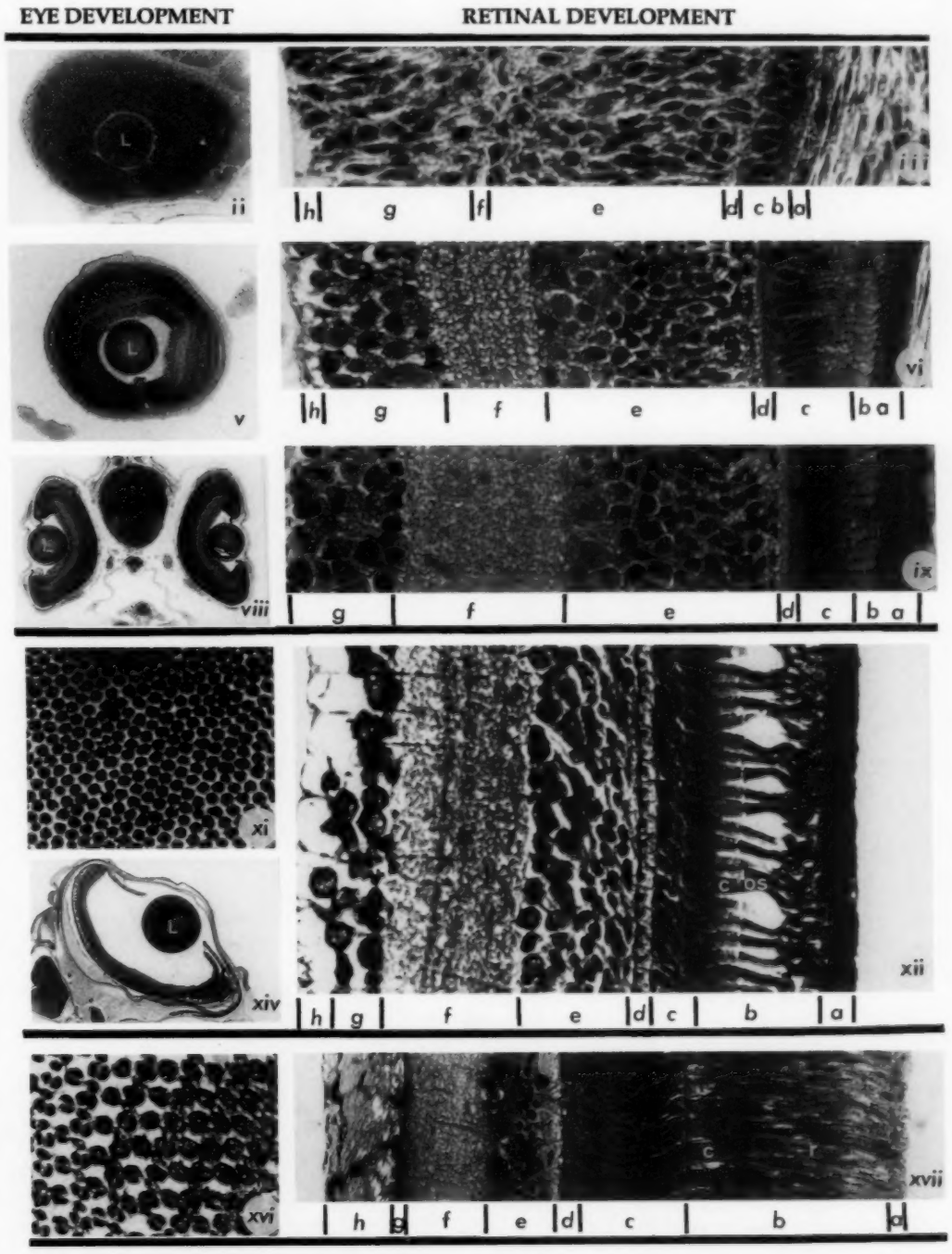

© 1996 NRC Canada

Fig. 2. Retinal differentiation at (A) 50 d° showing the bisection of the neuroblast layer (arrows) and (B) 90 d° showing the development of all layers, except the photoreceptors. gcl, ganglion cell layer; ipl, inner plexiform layer; inl, inner nuclear layer; opl, outer plexiform layer; onl, outer nuclear layer; elm, external limiting membrane; pe, pigment epithelium; in the internal nuclear layer: a, amacrine cells; b, bipolar cells; h, horizontal cells.

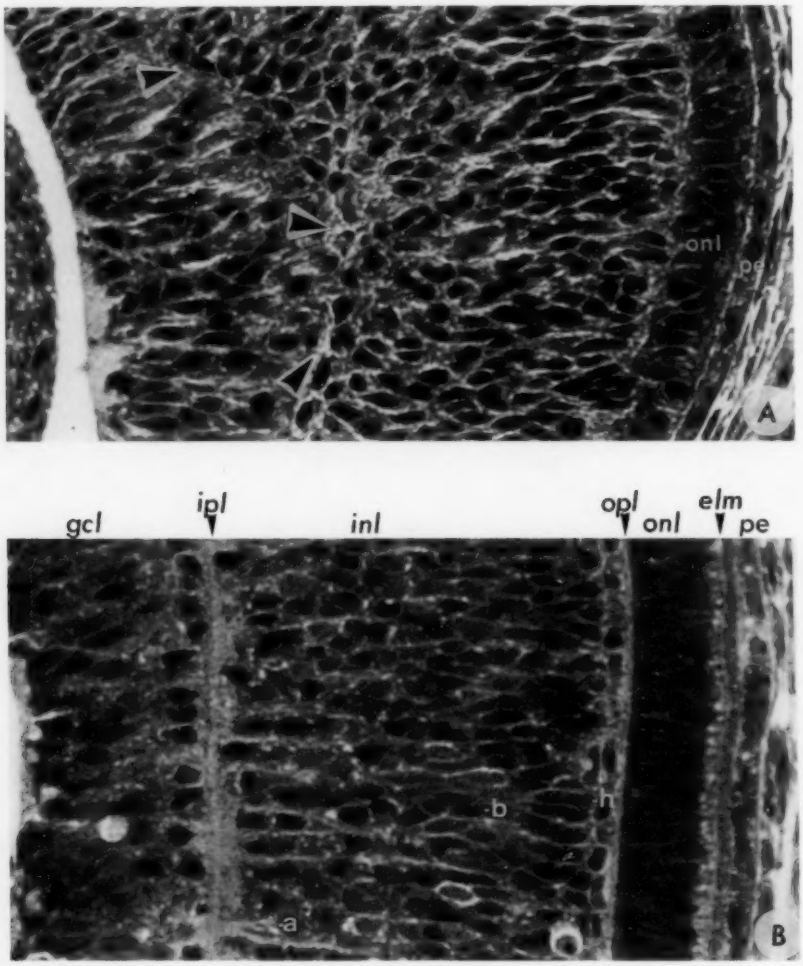

the retina only. The presence of an area, a part of the retina where photoreceptors were more densely packed, was also apparent in the temporal part of the retina at this stage. The area was characterized by a displacement of photoreceptor nuclei and a thickening of the inner plexiform layer.

Around 210 d° (Fig. 1 *viii*) the length of the outer segments had increased threefold, to 15 μm, and pigmented processes from the pigment epithelium interdigitated with outer segments all over the retina (Fig. 1*ix*). Only one type of photoreceptor could be distinguished on a morphological basis at this stage of development.

Total retinal thickness did not change significantly during the later stages of retinal cell differentiation (90–120 d°). However, throughout this period, all layers of the central part of the neural retina exhibited significant directional alterations in thickness, with the nuclear layers becoming narrower and the plexiform and visual cell layers becoming thicker (Table 1).

A distinct variation in retinal differentiation between sectors equidistant from the posterior pole of the eye was revealed by sagittal sections (Figs. 1*ii* and 1*iv*) and confirmed by transversal sections. The development of the temporal part of the retina clearly preceded that of the rest of the retina, while the development of the dorsotemporal part was delayed. The temporal retina corresponded to the part of the eye that was pigmented first (at about 50 d°), while the dorsotemporal part was pigmented last (between 150 and 210 d°). The ora terminalis of the temporal part also seemed to lack neuroblastic cells from about 90 d°, when all retinal layers could otherwise be recognised.

© 1996 NRC Canada

Fig. 3. Crossing of the optic nerves at 110°d. OC, optic chiasma.

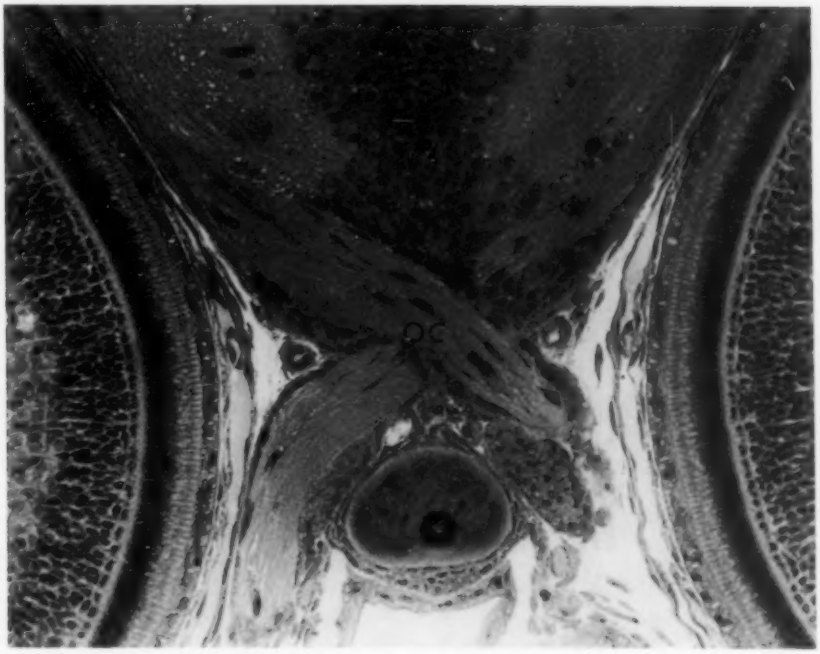

Retinal differentation and reorganisation in postlarval stages

During the post-larval stages the photoreceptors were organized in densely packed rows of single cones (Figs. 1*xi* and 1*xii*). At about 70 days posthatching, just before the onset of eye migration, the photoreceptors had begun reorganization into a square mosaic of double and single cones, with four double cones surrounding a central single cone (Fig. 1*xvi*). No cones could be found in the corners of the mosaic. The reorganization was most advanced in the periphery of the retina (near the ora) and had reached the center of the retina at 100 days posthatching.

Development of rods

Rods were first observed in 130-day-old juveniles as groups of slender photoreceptors with long outer segments, a small ellipsoid and a thin myoid part, between the single and double cones (Fig. 1*xvii*). Two morphologically different types of nuclei were present simultaneously in the outer nuclear layer. A few large, light-staining nuclei, characteristic of cones, were found adjacent to the external limiting membrane whereas numerous small, dark-staining nuclei, characteristic of rods, were found in the vitread part of the outer nuclear layer.

The outer eye muscles are first apparent at 90°d, when the muscle cells have a large central nucleus and no transverse striations. At 110°d, striations were visible, although differentiated muscle cells were first found in one larva at 150°d.

A falsiform process enters the eye via the embryonal fissure. By 210°d, this process is pigmented and lies close to the lens. As the embryonal fissure is displaced from the ventral (larval) position to a temporal (postlarval) position, the falsiform process attains a horizontal orientation. In juvenile fish, there is a thin pigmented connection between the process and the ventral portion of the eye. Evidence of a ligament joining the process and the ventral lens appears first at 55 days. There is no clear distinction between the vascularized falsiform process and the retractor lentis muscle. In juvenile fish, this muscle appears to have the characteristics of smooth muscle cells.

Discussion

In the Atlantic halibut, initial retinal differentiation proceeds slowly from an undifferentiated mass of cells at hatching to an apparently functional state between 150 and 210 d° (half to two thirds yolk absorption). The histological development closely agrees with macroscopic observations of pigment patterns, in that photoreceptor outer segments are present when the eyes are pigmented. The results corroborate Blaxter's (1983) earlier assumptions of a functional visual system when the eyes of fish are fully pigmented.

The general organ development of Atlantic halibut is remarkably slow (Rollefsen 1934; Lønning et al. 1982; Pittman et al. 1990*a*). Retinal development is similarly langorous, particularly in comparison with other marine flatfish such as the plaice, whose retina is differentiated at hatching (Sandy and Blaxter 1980), the turbot and sole, whose retinae differentiate within a few days (Neave 1984), or even the Pacific halibut (*Hippoglossus stenolepis*) with complete retinal pigmentation at about 40 d°, despite a duration of the yolk sac stage similar to that of the Atlantic halibut (McFarlane et al. 1991).

A notable feature of halibut eye development is the sectoral advancement of cell differentiation prior to becoming func-

© 1996 NRC Canada

Fig. 4. Photosensitive outer segments of the photoreceptors at 150 d° (25000×). Part of the inner segments with abundant mitochondria can be seen. OS, outer segment of photoreceptors; M, mitochondria.

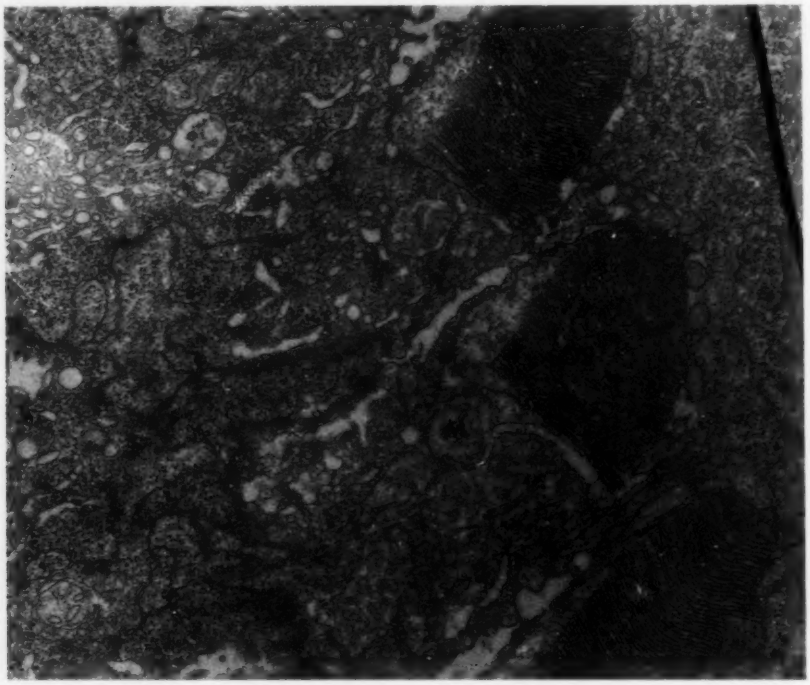

tional, with the presence of a temporal area having densely packed photoreceptors in a sector of advanced differentiation, coinciding with a dorsotemporal region of retarded differentiation. Although an area temporalis is also found in herring (Blaxter and Jones 1967), this is found at 150 d° in halibut whereas it is evident at metamorphosis in herring. If functional perception exists in this area, it would mean that the larvae are endowed with acute vision in a forward direction at a very early stage.

Other evidence of non-uniform development was found in the processes of the pigment epithelium and the early formation of the outer plexiform layer. Although the retinae of fish are diverse in both form and function (Ali and Anctil 1976), we are not aware of any other fish exhibiting such a specific pattern of eye development. If indeed an adaptation to the natural environment may be found in the characteristics of the visual system, as summarized by Muntz (1990), then it is possible that not only quantity but also direction of light during ontogenesis may be important to the halibut.

The differentiation of the ganglion cell layer indicates a possible connection between the retina and the optic tectum about 40 d° prior to the appearance of the outer segments of the photoreceptors, agreeing with previous studies of the simultaneous development of receptor systems in both the retina and the brain (Powers and Raymond 1990). Thus, transmission of light-induced impulses to the optic tectum is possible from the moment the photoreceptors become functional.

At 150 d°, pigment processes interdigitated with the photoreceptor outer segments in the ventral retina, extending to the entire retina by 210 d°, suggesting development of pigment migration between these stages. This is in accordance with Neave's (1984) work on flatfish such as plaice and turbot, showing pigment migration long before metamorphosis at the time of or somewhat later than first feeding. However, Blaxter and Staines (1970) found no pigment migration before metamorphosis in a number of marine fish larvae. According to Neave (1984), this discrepancy may be due to differences in light levels during experiments, as the fish in Blaxter and Staines' (1970) study experienced maximum light levels of 10^2 metre candela, compared with a maximum of 10 000 lx in Neaves' study. It is possible that younger larvae need higher light intensities to trigger the retinomotor reaction.

Focussing the eye requires movement of the lens, which is possible through the retractor lentis muscle, found at 55 days in halibut larvae. O'Connell (1981) found a similar trend in anchovy larvae which first developed outer eye muscles, then the functional visual system, and finally the retractor lentis. This would indicate the possibility of greater prey capture efficiency from that point, and perhaps greater prey selectivity in optimal feeding regimes.

Photoreceptor reorganization occurred around metamorphosis and settling, when the single cones grouped into a regular mosaic of four double cones surrounding one single cone, slightly prior to the appearance of rods. The square mosaic has been found in a number of flatfish species (Engström and Ahlberth 1963). The cone mosaic is thought to

© 1996 NRC Canada

Table 1. Relative changes in thickness of retinal layers in yolk sac larvae.

	Larval age (d°)				
Retinal layer	90	110	135	150	210
GCL	28.6 (2.8) *a*	25.6 (2.6) *ab*	21.8 (4.0) *bcd*	19.3 (2.2) *cd*	18.2 (2.9) *d*
IPL	4.5 (0.9) *a*	7.9 (3.2) *ab*	10.6 (4.2) *b*	15.1 (2.1) *c*	23.7 (1.4) *d*
INL	48.8 (2.3) *a*	47.0 (3.3) *a*	46.1 (1.0) *a*	39.4 (2.6) *b*	31.4 (1.3) *c*
OPL	1.3 (0.4) *a*	1.5 (0.4) *a*	1.8 (0.5) *ab*	2.3 (0.6) *bc*	2.8 (0.2) *c*
ONL	9.5 (0.4) *a*	10.0 (1.7) *a*	9.7 (0.7) *a*	9.5 (1.1) *ab*	6.3 (0.8) *c*
VCL	3.9 (0.3) *a*	5.0 (1.9) *a*	6.1 (1.9) *a*	10.2 (1.4) *b*	13.7 (1.7) *c*

Note: At least five larvae were sampled for each mean (SD). Different letters indicate significant differences ($p < 0.05$). GCL, ganglion cell layer; IPL, inner plexiform layer; INL, inner nuclear layer; OPL, outer plexiform layer; ONL, outer nuclear layer; VCL, visual cell layer.

either increase photoreception at low light intensities (Engström 1963), increase the effective visual acuity (Wagner 1978), or enable the fish to perceive polarized light (Cameron and Pugh 1991; Land 1991). Any or all of these functions, as well as the increasing absolute size of the eye itself, would increase the visibility of prey items over a broader range of environments. The timing of the reorganization is in agreement with Sandy and Blaxter (1980) and supports the general trend for flatfish of increased visual sensitivity around the time of settling.

Rods, the more light sensitive of the photoreceptors, appeared at the end of metamorphosis, around 130 days posthatching. This is in accordance with other observations on marine fish larvae, showing rod formation around metamorphosis in plaice (Blaxter 1968), sole (Sandy and Blaxter 1980), and a number of other species (Blaxter and Staines 1970; Blaxter 1975).

This reorganization and further development slightly prior to settling may allow the halibut to perceive objects in lower ambient light levels than in previous stages, and lends credence to growth studies showing better growth rates in small juvenile halibut under light intensities of 1 and 10 lx than of 500 lx (Hole and Pittman 1995).

Ecological aspects

The results indicate that halibut larvae may perceive a gradient in light from about 150 d°, allowing them to finely adjust their position in the water column. However, prior to that time, larvae rest head downward in water and the dorsotemporal sector of delayed development remains transparent, possibly permitting downwelling light to impinge directly on the optic nerve, or to directly reach the inner eye circumventing the normal frontal approach to the lens. This may increase the amount of photons available for photoreception. The existence of an extraretinal photoreception in fish has been suggested in many studies, and may be due to dermal (Wales 1975), pineal (Tamura and Hanyu 1979, *cited in* Guthrie 1990), or perhaps this form of photosensitivity.

Increased visibility of the transparent larvae due to eye pigmentation increases their vulnerability to predation (Langsdale 1993). In comparison with other fish species, the halibut develops pigmentation rather late, perhaps as an adaptation to a pelagic existence relatively high in the water column, or to an existence near other visual ichthyoplanktivores, such as in the deep scattering layer.

General implications for culture

Light is probably an important zeitgeber and depth indicator in the natural environment of the halibut. Reactions to light prior to 150 d° posthatching must be mediated by nonretinal light-sensitive organs, such as the pineal organ. A structure resembling the pineal exists prior to hatching (J.V. Helvik, upublished data), and has been shown in other species by Østholm et al. (1987).

The speed of reaction to light may be slower before than after retinal development, as found in sole by Champalbert et al. (1991). This is supported by short experiments on the development of phototaxy in halibut, where Mangor-Jensen and Naas (1993) found positive phototaxy within 10 min of exposure in larvae older than 160 d°.

The development of a functional retina and the mobility of the pigment to cover the cones occur at a time (150 d°) when larval halibut have been observed to capture prey (Harboe et al. 1990) and when the digestive system appears to be histologically functional (Kjørsvik and Reiersen 1992). External eye muscles also become differentiated at this point, and there are coinciding changes in behaviour and in the RNA/DNA ratio (Skiftesvik et al. 1990). The results of this study support statements by the above authors that the halibut may be ready for exogenous feeding at the time of eye pigmentation, or halfway through the yolk sac stage.

Increased photosensitivity at settling would indicate that successful feeding of halibut juveniles can be conducted under very dim light. However, other aspects of the reaction to the photic environment, such as behavioural influences and physiological responses to daylength, may influence the choice of lighting in commercial rearing situations.

Acknowledgements

The authors would like to thank Stolt Sea Farm A/S for the donation of material and Dr. Are Nylund for patient help with analysis. This study was funded by the University of Bergen, Bergen, Norway.

References

Ali, M.A., and Anctil, M. 1976. Retinas of fishes: an atlas. Springer Verlag, Berlin.

Berg, L., and Øiestad, V. 1986. Growth and survival studies of halibut (*Hippoglossus hippoglossus*) from hatching to beyond meta-

© 1996 NRC Canada

morphosis carried out in mesocosms. Int. Counc. Explor. Sea C.M. 1986/F16.

Blaxter, J.H.S. 1968. Light intensity, vision and feeding in young plaice. J. Exp. Mar. Biol. Ecol. **2**: 293–307.

Blaxter, J.H.S. 1975. The eyes of larval fish. *In* Vision in fishes. *Edited by* M.A. Ali. Plenum Press, New York. pp. 427–443.

Blaxter, J.H.S., and Jones, M.P. 1967. The development of the retina and retinamotor responses in the herring. J. Mar. Biol. Assoc. U.K. **47**: 677–697.

Blaxter, J.H.S., and Staines, M. 1970. Pure-cone retinae and retinamotor responses in larval teleosts. J. Mar. Biol. Assoc. U.K. **50**: 449–460.

Blaxter, J.H.S., Danielsen, D., Moksness, E., and Øiestad,V. 1983. Description of the early development of the halibut *Hippoglossus hippoglossus* and attempts to rear the larvae past first feeding. Mar. Biol. **73**: 99–107.

Cameron, D.A., and Pugh, E.N. Jr. 1991. Double cones as a basis for a new type of polarization vision in vertebrates. Nature (Lond.), **353**: 161–164.

Champalbert, G., Macquart-Moulin, C., Patriti, G., and Chiki, D. 1991. Ontogenetic variations in the phototaxis of larval and juvenile sole *Solea solea* L. J. Exp. Mar. Biol. Ecol. **149**: 207–225.

Engström, K. 1963. Cone types and cone arrangements in teleost retinae. Acta Zool. (Stockholm), **44**: 179–243.

Engström, K., and Ahlberth, I.B. 1963. Cone types and cone arrangements in some flatfishes. Acta Zool. (Stockholm), **44**: 119–129.

Guthrie, D.M. 1990. The physiology of the teleostean optic tectum. *In* The visual system of fish. *Edited by* R. Douglas and M. Djamgoz. Chapman and Hall, London. pp. 279–336.

Harboe, T., Næss, T., Naas, K.E., Rabben, H., and Skjolddal, L. 1990. Age of Atlantic halibut larvae (*Hippoglossus hippoglossus* L.) at first feeding. Int. Counc. Explor. Sea C.M. 1990/F:53.

Haug, T. 1990. Biology of the Atlantic halibut *Hippoglossus hippoglossus* (L., 1758). Adv. Mar. Biol. **26**: 1–70.

Helvik, J.V., and Walther, B.T. 1992. Photoregulation of the hatching process of halibut (*Hippoglossus hippoglossus*) eggs. J. Exp. Zool. **263**: 204–209.

Hole, G., and Pittman, K. 1995. Effects of light and temperature on growth in juvenile halibut (*Hippoglossus hippoglossus* L.). Proceedings of the ICES Symposium on Mass Rearing of Juvenile Fish, June 21–23, 1993, Bergen, Norway. ICES Mar. Symp. Ser. **210**: 197. (Abstract)

Kjørsvik, E., and Reiersen, A.L. 1992. Histomorphology of the early yolk-sac larvae of the Atlantic halibut (*Hippoglossus hippoglossus* L.) — an indication of the timing of functionality. J. Fish Biol. **41**: 1–19.

Land, M.F. 1991. Polarizing the world of fish. Nature (Lond.), **353**: 118–119.

Langsdale, J.R.M. 1993. Developmental changes in the opacity of larval herring, *Clupea harengus*, and their implications for vulnerability to predation. J. Mar. Biol. Assoc. U.K. **73**: 225–232.

Lønning, S., Kjørsvik, E., Haug, T., and Gulliksen, B. 1982. The early development of the halibut, *Hippoglossus hippoglossus* (L.), compared with other marine teleosts. Sarsia, **67**: 85–91.

Mangor-Jensen, A. 1995. Effects of light exposure on buoyancy of halibut eggs. J. Fish Biol. **47**: 18–25.

Mangor-Jensen, A., and Naas, K.E 1993. Phototaxis of halibut larvae (*Hippoglossus hippoglossus* L.). *In* Physiological and biochemical aspects of fish larval development. *Edited by* B.T. Walther and H.J. Fyhn. University of Bergen, Bergen, Norway. pp. 132–138.

McFarlane, G.A., Jensen, J.O.T., Andrews, W.T., and de Groot, E.P. 1991. Egg and yolk sac larval development of the Pacific halibut (*Hippoglossus stenolepis*). Int. Pac. Halibut Comm. Tech. Rep. No. 24.

Muntz, W.R.A. 1990. Stimulus, environment and fishes. *Ediited by* R. Douglas and M. Djamgoz. *In* The visual system of fish. Chapman and Hall, London. pp. 491–511.

Neave, D.A. 1984. The development of visual acuity in larval plaice (*Pleuronectes platessa* L.) and turbot (*Scophthalmus maximus* L.). J. Exp. Mar. Biol. Ecol. **78**: 167–175.

O'Connell, C.P. 1981. Development of organ systems in the Northern anchovy, *Engraulis mordax*, and other teleosts. Am. Zool. **21**: 429–446.

Østholm, T., Brännäs, E., and van Veen, Th. 1987. The pineal organ is the first differentiated light receptor in the embryonic salmon *Salmo salar* L. Cell Tissue Res. **249**: 641–646.

Pittman, K.A., Bergh, Ø., Opstad, I., Skiftesvik, A.B., Skjolddal, L., and Strand, H. 1990*a*. Development of eggs and yolk sac larvae of halibut (*Hippoglossus hippoglossus*). J. Appl. Ichthyol. **6**: 142–160.

Pittman, K.A., Skiftesvik, A.B., and Berg, L. 1990*b*. Morphological and behavioural development of halibut (*Hippoglossus hippoglossus*) larvae. J. Fish Biol. **37**: 455–472.

Powers, M.K., and Raymond, P.A. 1990. Development of the visual system. *In* The visual system of fish. *Edited by* R. Douglas and M. Djamgoz. Chapman and Hall, London. pp. 419–442.

Rabben, H., Jelmert, A., and Huse, I. 1987. Production experiment of halibut fry (*Hippoglossus hippoglossus*) in silos. Int. Counc. Explor. Sea C.M. 1987/F:42.

Rollefsen, G. 1934. The eggs and larvae of the halibut (*Hippoglossus vulgaris*). Det Kongelige Norske Vitenskabers Selskaps Forhandlinger BD, **7**: 20–23.

Sandy, J.M., and Blaxter, J.H.S. 1980. A study of retinal development in larval herring and sole. J. Mar. Biol. Assoc. U.K. **60**: 59–71.

Skiftesvik, A.B., Opstad, I., Bergh, Ø., Pittman, K., and Skjolddal, L. 1990. Effects of light on the development, activity and mortality of halibut (*Hippoglossus hippoglossus*) yolk sac larvae. Int. Counc. Explor. Sea C.M. 1990/F:43.

Tilseth, S. 1990. New marine fish species for cold-water farming. Aquaculture, **85**: 235–245.

Wagner, H. 1978. Cell types and connectivity patterns in mosaic retinas. Adv. Anat. Embryol. Cell Biol. **55**: 1–81.

Wales, W. 1975. Extraretinal photosensitivity in fish larvae. *In* Vision in fishes. *Edited by* M.A. Ali. Plenum Press, New York. pp. 445–450.

© 1996 NRC Canada

An extravariation model for improving confidence intervals of population size estimates from removal data

You-Gan Wang and Neil R. Loneragan

Abstract: We propose a new model for estimating the size of a population from successive catches taken during a removal experiment. The data from these experiments often have excessive variation, known as overdispersion, as compared with that predicted by the multinomial model. The new model allows catchability to vary randomly among samplings, which accounts for overdispersion. When the catchability is assumed to have a beta distribution, the likelihood function, which is refered to as beta-multinomial, is derived, and hence the maximum likelihood estimates can be evaluated. Simulations show that in the presence of extravariation in the data, the confidence intervals have been substantially underestimated in previous models (Leslie–DeLury, Moran) and that the new model provides more reliable confidence intervals. The performance of these methods was also demonstrated using two real data sets: one with overdispersion, from smallmouth bass (*Micropterus dolomieu*), and the other without overdispersion, from rat (*Rattus rattus*).

Résumé : Nous proposons un nouveau modèle pour estimer une population à partir de prises successives dans le cadre d'une expérience d'enlèvement. Les données générées par ces expériences sont souvent entachés de variations très marquées, décrites par le terme de surdispersion, par rapport aux données obtenues à partir du modèle multinomial. Le nouveau modèle permet de laisser varier au hasard la capturabilité d'un prélèvement à l'autre, ce qui règle le problème de la surdispersion. Lorsqu'on prend comme hypothèse que la capturabilité suit la distribution bêta, la fonction de probabilité, du type bêta-multinomiale, est dérivée et les évaluations du maximum de vraisemblance peuvent être calculées. On montre, par simulation, que lorsqu'il y avait trop de variation dans les données, les intervalles de confiance ont été substantiellement sous-estimés dans les modèles précédents (Lesley–DeLury, Moran), et que le nouveau modèle en fournit qui sont plus fiables. L'efficacité de cette méthode a été démontrée aussi au moyen de deux ensembles de données réelles : l'un avec surdispersion, dans le cas de l'achigan à petite bouche (*Micropterus dolomieu*), et l'autre sans surdispersion, dans le cas du rat (*Rattus rattus*).
[Traduit par la Rédaction]

Introduction

Removal experiments are often used in biological research to estimate the abundance of animals in a population (Seber 1973; Ricker 1975). In these types of experiments, an area is sampled repeatedly over a relatively short period of time and the population size is estimated from the change in catch rates. The data generated from a removal experiment consist of a sequence of catch numbers and the corresponding efforts. The population is assumed to be closed in the sense that no emigration, immigration, or natural mortality occurs during the experiment, and all catches are removed from the population (Otis et al. 1978; Schnute 1983).

Typically, the catches from a removal experiment can be expressed by a sequence $(C_1, C_2, \ldots, C_k)$, where C_i is the ith catch and k is the number of samples taken. For the convenience of further discussion, we list below the notation used in this paper:

- N: initial population size before sampling
- k: number of samples
- q_i: capture efficiency at time i
- p_i: $q_i \prod_{j=1}^{i-1}(1-q_j)$ and $p_1 = q_1$, the marginal proportion of the ith sampling
- γ_i: $q(1-q)^{i-1}$, the value of p_i when all q_i's are equal
- C_i: number of animals caught from the ith sampling
- T_i: $\sum_{j=1}^{i} C_j$, the cumulative catch up to (including) time i
- N_i: $N - T_i$ and $N_0 = N$, the population size after ith sampling
- c_i: expected value of C_i, $E(C_i) = E(q_i N_{i-1}) = p_i N$
- t_i: expected value of T_i, $\sum_{j=1}^{i} c_j$

We are interested in estimating the parameter N, and possibly the parameter q, as well. If we assume that the capture efficiencies are independent of the population size:

$$(1) \qquad E(C_i|N_{i-1}) = q_i N_{i-1},\ N_i = N_{i-1} - C_i,\ i = 1, 2, \ldots, k.$$

In this study, we assume, for simplicity, that effort is constant during each sampling interval, although the methods discussed here can easily be extended to allow for variable effort if the relationship between catchability and effort is specified.

Many methods already exist to analyse data from removal

Received November 20, 1995. Accepted May 1, 1996.
J13162

Y.-G. Wang.[1] CSIRO IPPP Biometrics Unit, Division of Fisheries, P.O. Box 120, Cleveland, Queensland 4163, Australia.
N.R. Loneragan. CSIRO Division of Fisheries, P.O. Box 120, Cleveland, Queensland 4163, Australia.

[1] Author to whom correspondence should be addressed.
e-mail: wan032@qld.ml.csiro.au

© 1996 NRC Canada

experiments. The performance of these methods has been tested in many ways (e.g., Seber 1973; Ricker 1975; Otis et al. 1978; Schnute 1983; Crittenden 1983). Two fundamental methods for analysing removal data are the regression method, which will be referred to as the Leslie–DeLury (L–D) method (Leslie and Davis 1939; DeLury 1947; Ricker 1975), and the multinomial likelihood (ML) method (Moran 1951; Schnute 1983; Loneragan et al. 1995).

A major complication in the estimation arises when the variation in the data exceeds the nominal level of variation from the multinomial models, a phenomenon known as overdispersion. A simple way to address this situation is to assume that the catchabilities (capture efficiencies) $(q_1, q_2, \ldots, q_k)$ are different parameters (Otis et al. 1978). However, this will create an oversaturated model (with $k+1$ parameters and k data points) and makes estimation impossible. In general, too many parameters in the model often result in unreliable estimates of N with very wide confidence intervals (cf. Otis et al. 1978). To reduce the number of parameters, Schnute (1983) suggested a parametric function to govern the q_i's.

However, in some cases, catchability cannot be specified in a deterministic way. This paper suggests a way of modelling extravariation that provides an alternative to the model of deterministic catchability outlined by Schnute (1983). Our "extravariation" model assumes that catchabilities vary randomly over occasions, and it improves the estimates of the confidence intervals when there is overdispersion in the data.

The model's performance was compared with that of two commonly used models: the L–D model and the multinomial model of constant catchability. Real data from smallmouth bass (*Micropterus dolomieu*) (Ricker 1975) and rat (*Rattus rattus*) (Schnute 1983) were also used to test the performance of the various models.

Two existing fundamental models

L–D model

If the proportion of the population removed during each sampling period is assumed to be have the same expectation, i.e., $q_i = q$ for all i, we have

$$(2) \qquad E(C_i|T_{i-1}) = q(N - T_{i-1}).$$

Here, T_0 is defined as 0. Parameter estimates can be obtained by regression of the catch against the cumulative catch in the form of $Y = a + bX$ with $a = qN$ and $b = -q$ (Ricker 1975, p. 151). Calculation of confidence intervals is given by DeLury (1951) and Ricker (1975).

A weighted regression may result in a better estimate of N, and $(1/N_i)$ can be used as the weighting function where a preliminary estimate of N is obtained by eye (Zippin 1956). We suggest using the unweighted regression analysis to obtain a preliminary estimate of N first for the weighting function. The formulae for calculating confidence limits using weighted regression are given in Appendix A.

Multinomial model

If we assume that each catch is sampled from a binomial distribution with a probability parameter q_i and a population parameter $N - T_{i-1}$, the catch vector C will have a multinomial distribution with parameters $(N, p_1, p_2, \ldots, p_k)$, where $p_i = q_i \sum_{j=1}^{i-1}(1-q_j)$. The probability function of C under this general multinomial model can be written as (2.4) in Schnute (1983):

$$(3) \qquad p(C|q_1, q_2, \ldots, q_k) = \frac{N!}{(N-T_k)!} \times \prod_{i=1}^{k} \frac{q_i^{C_i}(1-q_i)^{N-T_i}}{C_i!}.$$

A special and important case, considered by Moran (1951), is when the q_i's are assumed to be a constant, q, and the log-likelihood becomes

$$(4) \qquad l_{\mathrm{MULT}}(N, q) = \log \frac{N!}{(N-T_k)!} + T_k \log(q) + \sum_i (N - T_i)\log(1-q) - d$$

where d is a constant $\sum_i \log(C_i)$, independent of the parameters. Maximum likelihood estimates can be obtained from the estimating Eq. (C.2) (see Appendix C). For a given N, let $l_{\mathrm{MULT}}(N)$ be the maximum value of $l_{\mathrm{MULT}}(N, q)$ evaluated at the optimal q. The function $l_{\mathrm{MULT}}(N)$ is known as a profile likelihood function of N (McCullagh and Nelder 1989, p. 254). A confidence interval for $\hat{N}$ can be obtained based on the fact that $-2\log l(N)/l(\hat{N})$ is approximately $\chi^2(1)$ distributed (Schnute 1983; Bedrick 1994).

Extravariation model

To account for the extramultinomial variation in the data, we assume that the capture efficiencies q_i are random variables, independent and identically distributed.

Likelihood function

The joint likelihood of C can be written as

$$(5) \qquad p(C) = p(C_1)p(C_2|C_1)\cdots p(C_k|C_1, C_2, \ldots, C_{k-1}).$$

If we assume that the distribution of q_i, $f(q)$, is beta with parameters (α, β), this allows considerable flexibility (Johnson and Kotz 1970):

$$(6) \qquad f(q) = \frac{q^{\alpha-1}(1-q)^{\beta-1}}{B(\alpha, \beta)}$$

where $B(\alpha, \beta)$ is the beta function $\int_0^1 x^{\alpha-1}(1-x)^{\beta-1}dx$. Therefore:

$$(7) \qquad p(C_i|C_1, C_2, \ldots, C_{i-1}) = \int p(C_i|q, C_1, C_2, \ldots, C_{i-1})f(q)dq = \binom{N-T_{i-1}}{C_i} \int q^{C_i}(1-q)^{N-T_i} \times \frac{q^{\alpha-1}(1-q)^{\beta-1}}{B(\alpha, \beta)}\, dq = \binom{N-T_{i-1}}{C_i} \frac{B(\alpha_i, \beta_i)}{B(\alpha, \beta)}$$

© 1996 NRC Canada

where $\alpha_i = \alpha + C_i$ and $\beta_i = \beta + N - T_i$. From Eqs. (5) and (7) we obtain the log-likelihood function of C as

$$(8) \qquad l_{NEW}(N, \alpha, \beta) = \log \frac{N!}{(N - T_k)!} + \sum_{i=1}^{k} \log \left(\frac{B(\alpha_i, \beta_i)}{B(\alpha, \beta)} \right) - d.$$

In the case of fixed catchability, i.e., $q_i = q$ for all i, or when $\alpha + \beta \to \infty$ and $\alpha/(\alpha + \beta) = q$, the likelihood function (Eq. (8)) becomes that of the multinomial model given by Eq. (4).

If $l_{NEW}(N)$ is the profile likelihood function (Eq. (8)) evaluated at optimum values of (α, β)), the approximate 95% confidence limits can be obtained by solving the equation $-2 \log\{l(N)/l(\hat{N})\} = 3.84$.

Variance components

Under the general multinomial model (Eq. (3)), the variance of C_i is $Np_i(1 - p_i)$. Therefore, for Moran's multinomial model, the variance of C_i is

$$(9) \qquad V_1(C_i) = N\gamma_i(1 - \gamma_i)$$

in which $\gamma_i = (1 - q)^{i-1}q$.

In the extravariation model, q_i is assumed to be a random variable with a mean q and a variance σ^2. Recall that $p_i = q_i \prod_{j=1}^{i-1}(1 - q_j)$. The variance of C_i is

$$(10) \qquad V_2(C_i) = E\{\text{var}(C_i|p_i)\} + \text{var}\{E(C_i|p_i)\} = V_1(C_i) + N(N - 1)\text{var}(p_i)$$

in which

$$(11) \qquad \text{var}(p_i) = E(p_i^2) - \{E(p_i)\}^2 = \{(1 - q)^2 + \sigma^2\}^{i-1}(q^2 + \sigma^2) - \gamma_i^2.$$

If q_i is assumed to have a beta distribution with parameters (α, β), we have $q = \alpha/(\alpha + \beta)$ and $\sigma^2 = q(1 - q)/(\alpha + \beta + 1)$.

Note that $V_2(C_i)$ consists of two components: the variance by the multinomial model $V_1(C_i)$ and the extravariation.

Simulation studies

To investigate the performance of the different models, catch data were generated from Monte Carlo simulations. The population N was assumed to be 1000 and three different values of q were chosen: 0.1, 0.2, and 0.5. Three sweep numbers (k = 10, 5, and 3) were used. The values of k were chosen to be smaller for larger values of q, as is the case in typical removal experiments. Estimates of N were obtained by three methods: the weighted L–D method, the ML method based on Moran's (1951) multinomial model, and the new method based on the extravariation model.

If we rewrite $\text{var}(C_1)$ as $(1 + \tau)Nq(1 - q)$, where $\tau = (N - 1)\sigma^2/(q(1 - q))$, τ can be used as an index of overdispersion. The values of τ were chosen to be 0.0, 0.5, and 1.0. The case of $\tau = 0$ corresponds to Moran's multinomial model.

The catchability (capture efficiency) was sampled each time from a beta distribution with parameters calculated from the values of (q, τ). A catch was then obtained by sampling from the remaining population with the catchability obtained from the beta distribution.

Table 1. Mean ($\hat{N}$) and standard error (SE) of estimates of N, and 95% coverage probability for N = 1000 ($p(N)$) by the L–D regression model, the Moran multinomial model, and the extravariation model (New) (q = catchability, k = number of sweeps, τ = level of extravariation).

q	k	τ	var(q) × 1000	Model	$\hat{N}$	(SE)	$p(N)$
				L–D	1007.0	(87.1)	0.945
0.1	10	0.0	0.00	Moran	1005.0	(86.4)	0.939
				New	1004.7	(86.7)	0.952
				L–D	1006.4	(94.7)	0.953
0.1	10	0.5	0.045	Moran	1005.8	(94.9)	0.909
				New	1003.7	(93.9)	0.942
				L–D	1019.3	(117.2)	0.957
0.1	10	1.0	0.090	Moran	1019.6	(117.6)	0.891
				New	1016.6	(116.3)	0.934
				L–D	1007.9	(77.8)	0.952
0.2	5	0.0	0.000	Moran	1005.0	(77.0)	0.953
				New	1004.3	(77.5)	0.965
				L–D	1008.9	(89.5)	0.954
0.2	5	0.5	0.080	Moran	1006.9	(88.9)	0.919
				New	1005.5	(88.5)	0.944
				L–D	1015.2	(102.6)	0.947
0.2	5	1.0	0.160	Moran	1014.1	(102.0)	0.872
				New	1011.7	(101.6)	0.925
				L–D	999.3	(22.6)	0.840
0.5	3	0.0	0.000	Moran	997.9	(22.4)	0.948
				New	997.7	(22.6)	0.958
				L–D	1001.1	(25.5)	0.809
0.5	3	0.5	0.125	Moran	999.8	(25.3)	0.921
				New	999.6	(25.3)	0.937
				L–D	1003.3	(28.8)	0.757
0.5	3	1.0	0.250	Moran	1003.6	(28.6)	0.887
				New	1001.4	(28.5)	0.922

The estimates, together with corresponding 95% confidence intervals, were evaluated by the three methods for each simulated catch sequence of 1000 simulations. To assess the reliability of the confidence intervals, we calculated 95% coverage probability (the proportion of the number of simulations in which the 95% confidence interval covers the true value of N = 1000).

The performance of the three methods was quite similar for the point estimate of N (Table 1). Although the L–D method performs well when q is small (i.e., 0.1, 0.2 in our simulations), the confidence intervals are substantially underestimated when q is 0.5. It is interesting to note that the L–D method does not seem to be affected by the extent of overdispersion (τ) in the data, while Moran's method does, as one might expect (Table 1). The 95% coverage probabilities also clearly suggest that, in the case of overdispersion, the confidence limits of Moran's model are too optimistic and can be substantially underestimated (Table 1). The standard er-

© 1996 NRC Canada

Fig. 1. Observed and predicted catches of smallmouth bass. The Pearson χ^2 test shows overdispersion in the catch data.

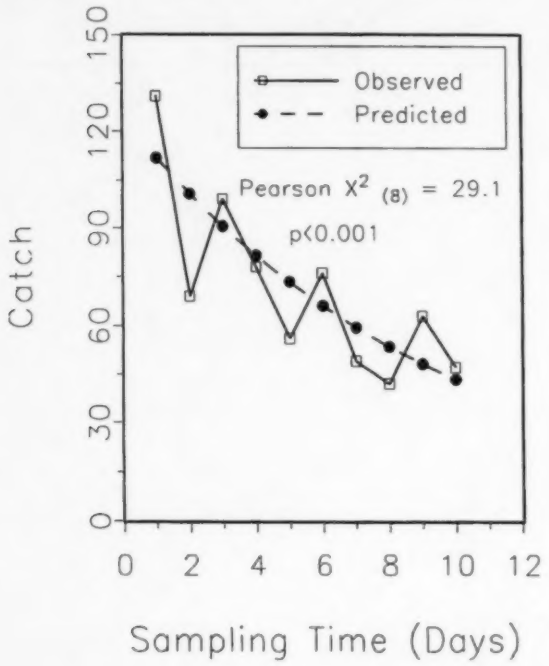

rors produced by the three methods are similar because they were calculated from the 1000 point estimates. In practice, it is unlikely that the same experiment could be repeated many times, and therefore, one may rely on the likelihood ratio statistics to evaluate the uncertainty of the estimate and its confidence intervals. The performance of the new method was reliable in all aspects.

Applications

Smallmouth bass data

Ricker (1975, p.151) described a removal experiment which estimated the population size of smallmouth bass in Little Silver Lake, Lanark County, Ontario. The successive catch numbers were 131, 69, 99, 78, 56, 76, 49, 42, 63, and 47, making a total catch of 710. Using the unweighted L–D regression method, Ricker estimated N as 1078, with a 95% confidence interval of (814, 2507).

To find out whether there is an overdispersion problem in the data, we calculated the Pearson χ^2 statistic using the estimates from Moran's model of constant catchability. It was 29.1 with 8 degrees of freedom, corresponding to a p-value <0.001 (Fig. 1). This strongly indicates that Moran's multinomial model is inappropriate and that the variation in the data is significantly in excess of that predicted by the multinomial model (Fig. 1). Therefore, the extravariation model was used. Although the estimates of N by these methods differ slightly, there were substantial differences in the widths of the confidence intervals (Table 2). The variances of C_i were evaluated under the multinomial model and the new model. The ratios of the two variances for the 10 catches were found to be (3.83, 3.58, 3.35, 3.14, 2.95, 2.78, 2.63, 2.49 2.37, 2.25). Therefore the inflation factor for the first catch τ is 2.83, i.e., 283% higher than the nominal variance.

Table 2. Estimates of the population of smallmouth bass, confidence intervals (CI), and catchability (q) by different methods (also shown are deviance reduction (DR) from Moran's model, degrees of freedom (df), and the corresponding p-value).

Method	$\hat{N}$	(95% CI)	q	DR	df	p
L–D (Ricker)	1078	(814, 2507)	0.1068			
L–D (weighted)	1112	(852, 2016)	0.0966			
Moran	1124	(979, 1357)	0.0958	0	0	1.000
Otis	∞	(1018, ∞)	0.0000	2.15	1	0.142
New	1134	(917, 1785)	0.0935	9.25	1	0.002

Fig. 2. Scaled deviance functions of three different models. The horizontal lines indicate 95% confidence intervals.

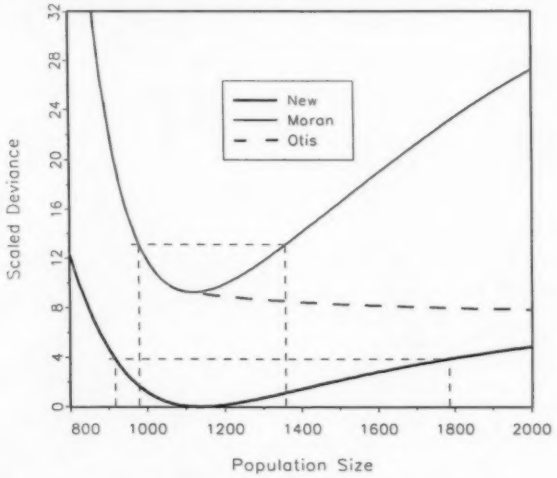

We further analysed the data using the model of Otis et al. (1978), which requires the same number of parameters as the extravariation model (see Appendices B and C). Unfortunately, it gave the estimate of N as ∞. The deviance functions (−2 log (profile likelihood)) of N from different models were evaluated (Fig. 2). The corresponding 95% confidence intervals were obtained using likelihood ratio statistics (Schnute 1983) (Table 2).

The reduction of the deviance by the extravariation model with one extra degree of freedom is 9.25 ($p < 0.002$), a substantial improvement over the other methods. On the other hand, there is little reduction by the Otis model (Table 2).

Rat data

Schnute (1983) reanalysed the rat data in Leslie and Davis (1939). The 18 successive catches are C = (49, 32, 31, 34, 16, 33, 22, 27, 17, 19, 18, 16, 18, 12, 14, 12, 17, 7). Schnute (1983) obtained the maximum likelihood estimate of N as 522.3 using Moran's multinomial model (see also Moran 1951). The corresponding Pearson χ^2 value is 17.8 with 16 degrees of freedom (p = 0.34). These results suggest that the variation in the data is within the range predicted by

© 1996 NRC Canada

the multinomial model with constant capture efficiency and therefore there is no overdispersion problem. Using the new extravariation model, we obtained the same estimate of N as using Moran's model. Based on the profile log-likelihood function of the catch, the 95% confidence interval was found to be (468, 607).

The programs are written in GAUSS and are available from the first author.

Discussion

The catches at successive times during a removal experiment are always correlated because the catch at time i depends on how many were being caught before time i. As pointed out by Schnute (1983), the ML method allows for this correlation between the catches.

Otis et al. (1978) also proposed a series of models to account for the individual heterogeneity of catchability, which appears to have great similarity to the model proposed here. However, their models are actually different versions of the multinomial models, and cannot be used to explain extravariation in the catches (Appendix B). Their models were also found to be unreliable (Appendix B) and did not provide a sensible estimate of N for the smallmouth bass data.

Carle and Strub (1978) also proposed a method to make Moran's ML more robust. However, their model assumes constant capture probability at different times, and is therefore inappropriate for overdispersed data.

Schnute (1983) realized that the assumption of constant capture efficiency over time might not be valid in practice, and proposed that a steadily decreasing or increasing function for the capture efficiency at time i be

$$q_i = q_1 + (q - q_1)(1 - a^{i-1}) \tag{12}$$

where q_1 is the initial capture efficiency, q is the limit of the efficiency as i becomes large, and a is a parameter measuring the change rate from q_1 to q. He referred to this as Model 3, and it included his Model 1 (the same as Moran's model of constant capture efficiency: $a = 1$) and Model 2 (constant capture efficiency except the initial one: $a = 0$) as special cases. He further evaluated the likelihood function based on the binomial model of capture for estimating the parameters. In Schnute's model, the capture efficiency is determined by a parametric function. In our model, it is governed by a stochastic law which has a parametric distribution.

When we are interested in estimating the catch efficiency from multiple experiments, we can analyse the pooled data by multiplying the likelihoods together. But it is not obvious for the L–D regression method, which is based on the catch versus the cumulative catch. Crittenden (1983) examined the effect of variability in q and found that the variance of the catch was a quadratic function of the expected catch. He therefore used a quadratic weighting function in the regression and found that his method was more efficient than the conventional weighting one, but still showing some positive bias in its estimate of the initial population. This may be due to the violation of the assumptions in the regression. As pointed out by Pollock (1991, p. 232), this approach is not recommended because the likelihood can be very right-skewed, and the χ^2 approximation for the confidence intervals can be unsatisfactory, necessitating an adjustment.

Overdispersion is a phenomenon with many causes, each of which should be modelled in its own way to obtain the most appropriate analysis. We have developed a model that allows for the catchability to vary randomly; the model is natural and easy to interpret and it is a counterpart of the deterministic model of Schnute (1983). If there is evidence that the catchability changes systematically, a deterministic model may be more appropriate. A more realistic model is to assume that catchability is random and that its expectation varies among sweeps. However, parameter estimation for this model has to rely on multiple removal experiments.

In practice, the Pearson χ^2 test can be used first to see if the multinomial model can adequately describe the data, and if extravariation is found, the beta-multinomial model may be used. It is possible that in somes cases the catchability may change in a deterministic way and Schnute's model would be more appropriate.

The likelihood ratio statistic would then be useful to determine the most appropriate model for the estimation (Schnute 1983). However, likelihood statistics are available only for likelihood-based methods, which makes the regression methods less attractive for the analysis of removal data. On the other hand, it may be difficult to justify the distribution used, although the distribution we used for q_i (beta distribution) is quite flexible.

Existing methodology for overdispersion is to inflate the variance by a dispersion parameter and to apply a quasi-likelihood approach that requires specification of a mean–variance relationship (Wang 1996). However, such a relationship cannot be uniquely specified when both the population parameter (N) and probabilities (q's) are unknown. Therefore, it is of great interest to develop distribution-free methods to account for overdispersion in removal data.

Not much attention has been paid to the effect of overdispersion in fisheries research, although the effect of overdispersion in general is well known in statistical literature (e.g., Cox 1983; Roberts et al. 1987). In estimating the recapture rate of marked fish, Bayley (1993) found that the standard errors of the parameters were substantially lower when overdispersion is ignored. Our simulation results are consistent with his findings, albeit in a different context.

Risk evaluation of fisheries management strategies is based on the uncertainties associated with parameter estimates. Incorrect confidence intervals will result in inappropriate estimates of the risk associated with management decisions. The proposed extravariation model will therefore prove useful because of its ability to account for overdispersion in the removal data when estimating a population size.

Acknowledgments

We are grateful to Dr. Mervyn R. Thomas for his support and encouragement on this work and Drs. David Die and Yongshun Xiao for helpful comments on an early version of the manuscript. We also thank Dr. Nick Ellis for his assistance in some programming for this work.

References

Bayley, P.B. 1993. Quasi-likelihood estimation of marked fish recapture. Can. J. Fish. Aquat. Sci. **50**: 2077–2085.

Bedrick, E.J. 1994. Maximum-likelihood estimation for the removal method. Can. J. Stat. **22**: 285–293.

© 1996 NRC Canada

Carle, F.L., and Strub, M.R. 1978. A new method for estimating population size from removal data. Biometrics, **34**: 621–630.

Crittenden, R.N. 1983. An evaluation of the Leslie–DeLury method and of a weighted method for estimating the size of a closed population. Fish. Res. **2**: 149–158.

Cox, D.R. 1983. Some remarks on overdispersion. Biometrika, **70**: 269–274.

DeLury, D.B. 1947. On the estimation of biological populations. Biometrics, **3**: 145–167.

DeLury, D.B. 1951. On the planning of experiments for the estimation of fish populations. J. Fish. Res. Board. Can. **8**: 281–307.

Johnson, N.I., and Kotz, S. 1970. Continuous univariate distributions — 2. Houghton Mifflin, Boston, Mass. pp. 37–54.

Leslie, P.H., and Davis, D.H.S. 1939. An attempt to determine the absolute number of rats in a given area. J. Anim. Ecol. **8**: 94–113.

Loneragan, N.R., Wang, Y.-G., Kenyon, R.A., Staples, D.J., Vance, D.J., and Heales, D.S. 1995. Estimating the efficiency of a small beam trawl for sampling tiger prawns *Penaeus esculentus* and *P. semisulcatus* in seagrass by removal experiments. Mar. Ecol. Prog. Ser. **118**: 139–148.

McCullagh, P., and Nelder, J.A. 1989. Generalized linear models. Chapman and Hall, London.

Moran, P.A.P. 1951. A mathematical theory of animal trapping. Biometrika, **38**: 307–311.

Otis, D.L., Burnham, K.P., White, G.C., and Anderson, D.R. 1978. Statistical inference from capture data on closed animal populations. Wildl. Monogr. 62. The Wildlife Society, Inc., Washington, D.C.

Pollock, K.H. 1991. Modeling capture, recapture, and removal statistics for estimation of demographic parameters for fish and wildlife populations: past, present and future. J. Am. Stat. Assoc. **86**: 225–238.

Ricker, W.E. 1975. Computation and interpretation of biological statistics of fish populations. Bull. Fish. Res. Board Can. 191.

Roberts, G., Rao, J.N.K., and Kumar, S. 1987. Logistic regression analysis of sample survey data. Biometrika, **74**: 1–12.

Schnute, J. 1983. A new approach to estimating populations by the removal method. Can. J. Fish. Aquat. Sci. **40**: 2153–2169.

Seber, G.A.F. 1973. The estimation of animal abundance and related parameters. Griffin, London.

Wang, Y.-G. 1996. A quasi-likelihood approach for ordered categorical data with overdispersion. Biometrics, **52**: (In press)

Zippin, C. 1956. An evaluation of the removal method of estimating animal populations. Biometrics, **12**: 163–189.

Appendix A: Confidence interval of $\widehat{N}$ for the weighted L–D method

For the convenience of readers, we present general expressions of the L–D estimates and corresponding standard errors when a weighting function is used. The estimation can be written in the regression form of $C = X\beta + \epsilon$, where C is the vector of catch ($k \times 1$), X is a ($k \times 2$) matrix with the ith row being $(1, T_{i-1})$, and β is a vector of two parameters qN and $-q$. The estimate of β is $\hat{\beta} = (X'X)^{-1}X'C$ under the assumption that the error vector ϵ is independently distributed with mean 0 and a common variance σ^2.

DeLury (1951) obtained the confidence limits based on the approximation of t-distribution to $\mathbf{b}'\hat{\beta}/\hat{s}$, where $\mathbf{b} = (1, N)$ and $\hat{s}$ is the standard error of the numerator (see also Ricker 1975). If the regression is weighted by a diagonal matrix W:

$$\text{(A.1)} \quad \hat{\beta} = (X'WX)^{-1}X'WC \text{ and } \hat{s}^2 = \mathbf{b}'(X'WX)^{-1}\mathbf{b}\hat{\sigma}^2$$

where $\hat{\sigma}^2 = \{C'W(C - X\hat{\beta})\}/(k-2)$. Assuming $\hat{\beta}$ can be approximated by a binormal distribution, the $(1-\alpha)$ confidence limits can be expressed as the two roots of the qudratic function

$$\text{(A.2)} \quad (\mathbf{b}'\hat{\beta})^2 = \hat{s}^2 t^2_{\alpha, k-2}$$

where $t_{\alpha,k-2}$ is the critical value of a t-distribution with $k-2$ degrees of freedom at significance level (two sided) α. If W is the identity matrix, the expressions derived here become identical to those given in Ricker (1975, p. 150).

Appendix B. Approach of Otis et al. (1978)

The above multinomial model assumes that each animal has the same constant catchability. To account for the heterogeneity of individuals, one may assume that the individual catchability is a random variable with a distribution function $\pi(q)$ (Otis et al. 1978). In this case, the capture efficiency at time i becomes the conditional expectation given that the animal has not been captured before:

$$\text{(B.1)} \quad q_i = \frac{\int_0^1 x(1-x)^{i-1}\pi(x)dx}{\int_0^1 (1-x)^{i-1}\pi(x)dx}.$$

From a Bayesian point of view, q_i is a posterior mean when the prior distribution is $\pi(x)$.

In the model of Otis et al. (1978), C has a multinomial distribution with marginal probabilities $\lambda_i = E\{q(1-q)^{i-1}\}$ $(1 \le i \le k)$. The variance of C_i is thus $N\lambda_i(1-\lambda_i)$, which does not differ from $V_1(C_i)$ substantially. If $\pi(x)$ is taken to be beta(a, b), we have

$$\text{(B.2)} \quad \lambda_i = ab(b+1)\ldots(b+i-2)/\{(a+b)(a+b+1)(a+b+2)\ldots(a+b+i-1)\}.$$

To make use of the ML method, one needs to specify the function form of $\pi(\cdot)$ to obtain the likelihood of the observed catches. If $\pi(x)$ is assumed to be a beta distribution with parameters (a, b), we have $q_i = a/(a+b+i-1)$, and from Eq. (3) the likelihood function of the catch C is

$$\text{(B.3)} \quad l_{\text{OTIS}} = \log \frac{N!}{(N-T_k)!} + T_k \log(a) + \sum_{i=1}^{k}(N - T_i)\log(b+i-1) - \sum_{i=1}^{k}(N - T_{i-1})\log(a+b+i-1) - d.$$

Appendix C. Estimating functions of Moran's and Otis' models

If $l(N, q)$ is the log-likelihood function of the catch C which is assumed to follow some distribution, the ML estimates of (N, q) satisfy the following equations:

$$\text{(C.1)} \quad \begin{cases} l(N, q) - l(N-1, q) = 0 \\ \partial l/\partial q = 0. \end{cases}$$

© 1996 NRC Canada

From Eq. (B.3), we obtain the estimating equations for Moran's model:

$$\text{(C.2)}\quad \begin{cases} N = \dfrac{T_k}{1-(1-q)^k} \\ q = \dfrac{T_k}{kN - \sum_{i=1}^{k-1} T_i} \end{cases}.$$

From Eq. (B.3), we obtain the estimating equations for Otis' model:

$$\text{(C.3)}\quad \begin{cases} N = \dfrac{T_k}{1-\prod_{i=1}^{k} \dfrac{b+i-1}{a+b+i-1}} \\ a = \dfrac{T_k}{\sum_{i=1}^{k} \dfrac{N-T_{i-1}}{a+b+i-1}} \\ \vdots \\ \sum_{i=1}^{k} \dfrac{N-T_{i-1}}{a+b+i-1} = \sum_{i=1}^{k} \dfrac{N-T_i}{b+i-1} \end{cases}.$$

© 1996 NRC Canada

Gulf of Mexico Offshore Operations Monitoring Experiment (GOOMEX), Phase I: Sublethal responses to contaminant exposure — introduction and overview

Mahlon C. Kennicutt II, Roger H. Green, Paul Montagna, and Pasquale F. Roscigno

Abstract: The Gulf of Mexico Offshore Operations Monitoring Experiment (GOOMEX) is a three-phase study to test and evaluate a range of biological, biochemical, and chemical methodologies to detect and assess chronic sublethal biological impacts in the vicinity of long-duration activities associated with oil and gas exploration and production. A chronic impact is defined as an effect on the biota caused by exposure to the long-term accumulation of chemicals in the environment. The basic program, comprising four field activities over a 2-yr period, was designed to detect nearfield impacts and contaminant gradients extending out from each site. Five test sites were evaluated and three selected as most appropriate for long-term study: MU-A85, MAI-686, and HI-A389. The sampling design included a radial pattern with stations at 30–50, 100, 200, 500, and 3000 m distance and employed a dose–response model to test the hypotheses that biological, chemical, and biochemical variations are due to platform-derived contaminants. Study components included contaminant (trace metals and hydrocarbons) analysis in sediments, pore waters, and biological tissues; assemblage analysis of benthic meiofauna, infauna, and epifauna, assessment of community health based on life history and reproduction studies; and the induction of detoxification responses.

Résumé : L'Expérience de surveillance des opérations extracôtières dans le golfe du Mexique, dite « GOOMEX », est une étude en trois étapes visant à vérifier et à évaluer une gamme de méthodes biologiques, biochimiques et chimiques de détection et d'évaluation des effets biologiques sublétaux chroniques au voisinage d'activités de longue durée, associées à la prospection et à la production de pétrole et de gaz. Un effet chronique s'entend d'un effet sur le biote d'une exposition à l'accumulation prolongée de produits chimiques dans l'environnement. Le programme de base, comportant quatre activités sur le terrain en 2 ans, vise à détecter les effets des contaminants à proximité de chaque site et leurs gradients en s'en éloignant. Cinq sites d'essai ontété évalués, et trois ont été choisis comme les plus appropriés pour une étude à long terme : MU-A85, MAI-686 et HI-A389. Dans le plan d'échantillonnage de géométrie radiale, où les stations étaient réparties à des distances de 30–50, 100, 200, 500 et 3 000 m, le modèle dose–réponse retenu visait à vérifier les hypothèses selon lesquelles les variations biologiques, chimiques et biochimiques tiennent aux contaminants de plate-forme. Les volets de l'étude comprenaient l'analyse des contaminants (hydrocarbures et métaux à l'état de traces) dans les sédiments, les eaux interstitielles et les tissus biologiques, l'analyse d'assemblages de la méiofaune, de l'endofaune et de l'épifaune benthiques, l'évaluation de la santé du milieu d'après des études du cycle biologique et de la reproduction et l'induction de réponses de détoxification.
[Traduit par la Rédaction]

Introduction

The most significant unanswered questions related to the environmental impacts of offshore oil and gas development and production are those involving chronic, low-level stresses on ecosystems. These stresses result from discharges, spills, and leaks associated with the long-term development of energy resources on the continental shelf (Boesch et al. 1987; Aurand 1988; Ahlfeld 1990; Kendall 1990). A three-phase program, called the Gulf of Mexico Offshore Operations Monitoring Experiment (GOOMEX), is being conducted to test and evaluate a range of biological, biochemical, and chemical methodologies that may indicate whether the local environment around platforms is responding to chronic, sublethal exposure to discharged contaminants. A multidisciplinary team of scientists was assembled to implement Phase I of the program (Table 1). Work elements included ancillary physical, chemical, and sedimentological variables, analysis of contaminants (trace metals and hydrocarbons) in sediments, pore waters, and biological tissues; assemblage analysis of benthic meiofauna, macroinfauna, and megafauna, meiofaunal and megafaunal invertebrate life history and reproduction studies, and the presence and intensity of inducible detoxification responses in megafaunal biota (Table 2).

Received October 2, 1995. Accepted September 13, 1996.
J13407

M.C. Kennicutt II. Geochemical and Environmental Research Group,Texas A&M University, 833 Graham Rd., College Station, TX 77845, U.S.A.
R.H. Green. Department of Zoology, University of Western Ontario, London, ON N6A 5B7, Canada.
Marine Science Institute, University of Texas, 750 Channel View
P. Montagna. Dr., Port Aransas, TX 78373, U.S.A.
P.F. Roscigno. Minerals Management Service, 1201 Elmwood Park Blvd., New Orleans, LA 70123-2394, U.S.A.

© 1996 NRC Canada

Table 1. Summary of the GOOMEX team of investigators.

Work element activity	Principal investigator	Collaborators
Program Manager	M.C. Kennicutt II[a]	R. Darnell (deputy)[b]
Study design	R. Green[c]	P. Montagna[d]
Field logistics	R. Fay[e]	J. Jobling,[a] H. Barnett[a]
Data management	G. Wolff[a]	
Physical oceanography	F. Kelly[a]	S. Sweet[a]
Sedimentology	R. Rezak[b]	
Contaminant chemistry		
Hydrocarbons	J. Brooks[a]	T. Wade[a]
Metals	B.J. Presley[b]	P. Boothe[b]
Meiofauna	P. Montagna[d]	G. Street[d], R. Kalke[d]
Macroinfauna	D. Harper[c]	S. Powers[c]
Megafauna		
Invertebrates	E. Powell[f]	B. Ormond-Wilson,[c] M. Ellis[f]
Demersal Fish	R. Darnell,[b] J. McEachran,[h] J. Fournie[a]	H. Konstantinou,[h] L. Courtney
Detoxification	S. Safe[i]	S. McDonald,[a] K. Willet[i]
Pore water toxicity	S. Carr[j]	P. Montagna[d]

[a]Geochemical and Environmental Research Group, Texas A&M University, College Station, Tex.
[b]Department of Oceanography, Texas A&M University, College Station, Tex.
[c]Department of Zoology, University of Western Ontario, London, Ont.
[d]University of Texas Marine Science Institute, Port Aransas, Tex.
[e]Department of Marine Biology, Texas A&M University at Galveston, Galveston, Tex.
[f]Haskin Shellfish Research Laboratory, Rutgers University, Port Norris, N.J.
[g]Environmental Protection Agency, Gulf Breeze, Fla.
[h]Department of Wildlife and Fisheries Sciences, Texas A&M University, College Station, Tex.
[i]Department of Physiology and Pharmacology, Texas A&M University, College Station, Tex.
[j]National Biological Service.

The program involved an intensive sampling of the study sites and utilization of a variety of analytical techniques to produce a comprehensive data set to test the programmatic hypotheses. Field and laboratory methods are summarized in Tables 3 and 4. All study components were linked by common study and sampling designs to ensure an integrated synthesis. A comprehensive summary of the samples collected is provided in Table 5.

The objective of GOOMEX Phase I was to test a variety of variables representing all levels of biological organization for suitability as indicators to detect chronic, sublethal biological responses to long-term production activities. The central question is whether the variables measured are significantly different near a platform as compared with away from the platform and can these differences be attributed to the release of contaminants from the platform. While contaminants were identified as the primary agent of concern, it was recognized that the physical presence of the structure will lead to other alterations in the local environment. For example, disposal of coarse materials to the surrounding sediments also sets the stage for a shift in community structure. The outcome of these events is commonly referred to as rig ecology. Differences in various parameters or variables related to distance from the platform can only be fully understood in the context of cause, effect, and biological significance. Any two places on the continental shelf can be demonstrated to be different, if the areas are analyzed to a sufficient level of detail. Tacit in the design of the GOOMEX program is an effort to provide correlative support for cause and effect at several levels of biological organization and provide a focus for the scope of future studies. Concordance amongst independent biological responses was evaluated to determine if it supported the interpretations. Another guiding principle was biological significance. The goals of monitoring are to detect resource degradation or damage and to provide guidance on how to prevent or reverse the undesired response.

Detection of impacts or biological effects responding to contaminant exposure requires confirmation that the exposure has taken place and that the observed "biological patterns" are beyond those attributable to natural variations (Carney 1987). Biological response to exposure can be highly variable in both mechanism and intensity. Biological changes can have a short time span (i.e., induced detoxification or reduced reproductive effort in an individual) or a long time span (i.e., compositional shifts in communities). Impact can be expected to manifest itself differently from species to species and from population to population due to differences in the history of exposure and the response to exposure.

Based on the objectives, the GOOMEX Phase I study was designed to collect a data set to provide statistical tests of two interrelated hypotheses. The null hypotheses tested were as follows:

H_0: There are no differences in any sedimentological, chemical, community, population, reproductive, toxic, or detoxification measures between seasons, among platforms (or platform groups), or with distance or direction away from platforms (or platform groups).

H_0: There are no functional relationships between chemical

© 1996 NRC Canada

Table 2. Summary of GOOMEX Phase I work elements.

Work element	Variables
	Independent variables: sediments/water column
Physiochemical	Salinity, oxygen, nutrients, light transmittance, and temperature
Sedimentology	Grain size, carbon content (organic and inorganics), minerology, redox condition
Contaminants	Hydrocarbons and metals
	Independent variables: biota
Contaminants	Hydrocarbons and metals in fish livers, fish stomach contents, and invertebrate soft tissues
Physiological	Percent moisture and lipid content
	Independent variables: pore waters
Contaminants	Hydrocarbons and trace metals
	Dependent variables
Meiofauna[a]	Abundance, diversity, community structure, nematode trophic dynamics, life history and reproduction, and genetic diversity
Macroinfauna[b]	Abundance, diversity, community structure
Megafauna: invertebrates	Catch per unit effort, size and frequency, histopathology, reproductive effort, reproductive development, and detoxification response[c]
Megafauna: fish	Fish food analysis, histopathology, and detoxification response[d]

[a]Also pore water toxicity testing: bioassays with meiobenthic species.
[b]Also pore water toxicity testing: sea urchin fertilization and embryological development test.
[c]Detoxification response: AHH activity, in vitro rat hepatoma H-4IIE cell assays.
[d]Detoxification response: EROD and AHH activity, biliary PAH metabolites, P4501A and mRNA levels, laboratory dosing experiments.

contaminant gradients and community, population, reproductive, toxic, or detoxification measures.

To test the first hypothesis, univariate analysis of variance (ANOVA) for all variables being measured at all stations in the study design was the method of choice. The categorical variables in such a design, particularly distance from a platform, are surrogates of the contaminant gradients that might exist among and within platform stations. Therefore, the approach to test the second hypothesis was a multivariate approach.

Study design

Two study designs formed the basis of the GOOMEX Phase I program. Both rely on a dose–response model but differ in the details of the sampling design. The first design provided for an assessment of the benthos by using a quantitative boxcorer to sample sediments and resident organisms adjacent to platforms. The sampling plan was designed to detect near-field impacts and contaminant gradients extending out from a platform. The sampling design included a radial pattern to ≥3000 m distance to define the platform's contamination gradient. The sediment sampling design included five radii, five distances per radii, and two or three pseudoreplicates, i.e., replicates from within boxcores, at each station (Fig. 1). The number of stations was maximized to test for directional and distance patterns. With four sampling events, this led to a total of 600 or 900 samples for the three study sites (Table 5). Twenty-five stations comprised the sampling grid at each site (5 distances × 5 radii at 50, 100, 200, 500, and ≥3000 m distance; Fig. 1). Control sites were provided by extension of the radii beyond the distance of measurable contaminants, generally ≥3000 m distance. Controls were chosen to be as similar in setting to the near-field stations as possible to minimize differences due to non-platform-related variations.

The second study design employed a Near (or impacted) versus Far (or unimpacted) pairwise comparison of indicators of contaminant exposure. Due to the need for large amounts of biomass for the various work elements, boxcorers were insufficient as a collection technique. Therefore, biomass sample collection relied primarily on otter trawls. Samples were taken as close as possible to the platform (<100 m) and at a comparison station (≥3000 m). The studies utilizing this design employed laboratory techniques that were generally time intensive and/or relatively untested so that they were only evaluated at the presumed extremes of exposure.

The study design is based on a dose–response model. Contaminant concentrations are expected to decline exponentially with distance away from a platform. Biological variables should respond to the contaminant gradient; thus, the magnitude of the response is expected to decrease with increasing distance from a platform. These five distances away from the platform were chosen on a log scale. This model indicates that contaminant concentration and organism abundance variables should be transformed using the natural logarithm. Percentage data, e.g., percent sand, or toxicity test results

© 1996 NRC Canada

Table 3. Summary of field methods.

Work element	Description	Reference(s)
Boxcorer	Ocean Instruments BX-600 deep ocean corer	Hessler and Jumars 1974; Jumars 1975
Trawling	Otter trawl:mesh 4.04 cm, mouth opening 17.58 m, bridle 67.58 m, wood doors (1.83 × 0.92 m), time 10–15 min, speed 0.5 kt	—
Navigation	DGPS (±3 m)	
Continuous profiles	Seabird SEACAT Profiler, Sea-Tech transmissometer	—
Discrete water samples	5-L Niskin bottle; nutrients, frozen (–20°C), plastic bottles; salinity: glass bottles	
Sedimentology grain size, mineralogy	Refrigerated (4°C), plastic bags	
Redox potential	Combination platinum electrode	Whitfield 1969
TOC, TIC	Frozen (–20°C), glass jars	NOAA 1993
Contaminants: sediments		
Hydrocarbons	Frozen (–20°C), glass jars	NOAA 1993
Metals	Frozen (–20°C), plastic jars	
Contaminants: tissues		
Hydrocarbons	Disected, frozen, glass jars	NOAA 1993
Metals	Dissected, frozen, plastic jars	NOAA 1993
Meiofauna		
Abundance, diversity, life history, reproduction	1.9-cm i.d. core tube, depth 0–2 cm, anesthetized with 7% $MgCl_2$ (5 min), preserved 10% buffered formalin; two replicates	Montagna 1991; Hulings and Gray 1971
Genetic diversity	Depth 0–2 cm, preserved in EDTA–buffered alcohol, stored at 4°C	Dessauer et al. 1990
Macroinfauna	Depth 9–10 cm, sieve: 0.5 mm, preserved 5% buffered seawater–formalin	Harper et al. 1981, 1991
Megafauna	Stored at 4°C until fixation in isoane $MgCl_2$ or seawater, egg sacs: immediately frozen in LN_2, dimensions measured, sex determined, stage of reproductive development described	King 1948; Chamerlain and Lawrence 1983; Hill et al. 1989; Hard 1942
Immunological probe	Egg sacs frozen in LN_2	Choi et al. 1994
Contaminants (fish livers, fish stomach contents, invertebrate soft tissues)	Dissected, frozen (–20°C) in precleaned teflon-lined jars	NOAA 1993
Toxicology	Kept alive until processing, dissected, frozen in LN_2, bile removed into vacutainers and stored at –20°C	Bradford 1976

received a special treatment, the "arcsin square root" transformation. Log transformation of some of the variables was appropriate for another reason. An important assumption in ANOVA is that sample variances are homogeneous. This means that the variance of a parameter for each sample should be the same. A common feature of benthic organism abundance and chemical concentration data is that the mean and variance are correlated, and thus violate the assumption of homogeneity of variances. It is common in these cases to use a logarithmic transformation. The data from the first two cruises were tested and it was found that the variances of contaminant variables and organism abundances were stabilized by log transformation.

Univariate analyses

Four different views were used to interpret the GOOMEX Phase I sampling design (Table 6). The following describes the statistical model and the decomposed models used to test the first hypothesis and explore interactions among the sources of variation in the design. The models are given in SAS (SAS Institute Inc. 1990) notation. Interaction terms (·) are used to indicate that the variables are crossed. For crossed variables, every level of a variable occurs in every level of the other variable. For example, every platform (P) was sampled on every cruise (C). Nested terms, designated with parentheses, are used to indicate that the variables are hierarchical. For hierarchical variables, the nested term occurs only once in each level. For example, each radius is unique to a platform. Radius *A* at one platform has no relationship to radius *A* at another platform. In this sense, radii (R) are also random variables and represent a form of replication. In contrast, platforms and distance (D) from a platform are fixed variables. The terms random and fixed are important in determining the expected mean squares, and thus the appropriate denominators for *F*-tests.

First, in the overall design analysis, all platforms (P) and all cruises (C) were included (Table 7). This analysis demonstrated that platforms are heterogeneous, and that the model is best decomposed to perform analyses "by P", i.e., at each individual study site. R is nested within P. Here, distance (D)

© 1996 NRC Canada

Table 4. Summary of laboratory methodologies.

Variable	Method	Reference(s)
Nutrients		
NO_3	Autoanalyzer	Armstrong et al. 1967
PO_4	Autoanalyzer	Murphy and Riley 1962
SiO_3	Autoanalyzer	Brewer and Riley 1966
Salinity	Guideline 8400 Autosal	Unesco Technical Papers in Marine Science 1981
Dissolved O_2	MicroWinkler technique	Carpenter 1965
Grain size	Settling/gravimetric	Folk 1974: NOAA 1993
Mineralogy	X-ray diffraction	—
TOC/TIC	Leco total combustion	NOAA 1993
Redox Eh	Platinum electrode	Whitfield 1969
Hydrocarbons	GC/FID, GC/MS	NOAA 1993
Metals	INAA, CVAAS, AES	NOAA 1993; USEPA 1991
Meiofauna	Concentration techniques	Pfannkuche and Thiel 1988
Taxonomy	Counting	Sherman et al. 1984
Nematode feeding type	Mouth morphology	Wieser 1953; Romeyn and Bouwman 1983
Nematode biomass	Body measurements	Andrassy 1956
Harpacticoid life history and reproduction	Microscopy	Webb and Montagna 1993
Diversity	Computational	Ludwig and Reynolds 1988
Genetic variability	PCR/RFLP	Avise 1994; Bucklin et al. 1992; Nei 1987
Macroinfauna	Microscopy	Harper et al. 1981, 1991
Megafauna		
Invertebrates		
Reproductive effort	Histology	Preece 1972; Bell and Lightner 1988; Freeman and Bracegirdle 1971
Immunological probe		Choi et al. 1994
Demersal fish		—
Histopathology	Macrophage aggregates	Hinton et al. 1992; Blazer et al. 1994
Fish food	Visual inspection	Darnell 1958; Rogers 1977
Detoxification		
Microsomal protein	Centrifugation	Bradford 1976
EROD activity	Assay	Pohl and Fouts 1980
AHH activity	Assay	Nebert and Gelboin 1968
Rat hepatoma H-4IIE	Assay	
mRNA	Assay	Chomczynski and Sachi 1987
PAH metabolites	HPLC/fluorescence	Krahn et al. 1984, 1986*a*, 1986*b*
Pore water toxicity	Assays	Carr 1993; Carr and Chapman 1992

and C are crossed with both P and R(P). R is a random effect, and C, P, and D are fixed effects. P is tested against R(P), and D and P·D against D·R(P), C and P·C are tested against D·C·R(P). R(P), D·R(P), C·R(P), and D·C·R(P) are tested against replicate error. Second, the platform-by-platform analysis model was used to test and describe distance and direction effects at each platform, given that the total design model, which includes P in it, shows significant interactions involving P (Table 7). This is a fully crossed model because levels of R are now sampled at all C and D. Although R is now a crossed variable, it is still a random effect. So, C is tested against C·R, R is tested against a composite error term, and D is tested against R·D. The double interaction terms C·R, C·D, and R·D are tested against the triple interaction term C·R·D. The triple interaction term is tested against replicate error. The by-cruise analysis was used when seasonal or interannual interactions were occurring (Table 7). It is necessary to analyze each cruise separately if there are significant seasonal or temporal interactions. By-cruise·platform analyses had only limited usefulness. It was only useful for specific questions about R and D patterns at a specific platform at a specific time (Table 7). It implies that there is no generality. This model was used to discover directional (i.e., R) effects at specific platforms that were different during each cruise. All terms were tested against the error term.

For trawling, there were only two stations. There was no need to specify R and D, since there were no replicates and this designation decomposes to just two stations (S), which were designated Near and Far. Each model was modified, and R and D are replaced by S. In these instances, P, C, and S were always crossed variables and fixed effects. Therefore, the effects were always tested against the mean square error

© 1996 NRC Canada

Table 5. GOOMEX Phase I: final sample inventory by work element.

Work element	No. of samples				
	Cruise 1	Cruise 2	Cruise 3	Cruise 4	Total
Physicochemical					
Nutrients	417	252	252	252	1173
Salinity	416	251	251	252	1170
Dissolved O_2	417	252	249	252	1170
CTD's	125	75	75	75	350
Total					3863
Sedimentology					
Grain size	268	150	150	150	718
Mineralogy	125	—	—	—	125
Total organic carbon	268	150	150 (+42)	152	720 (762)
Total carbon	268	150	150 (+42)	152	720 (762)
Redox	268	150	150	152	720
Total					3003 (3087)
Contaminant analyses					
Hydrocarbons					
Sediments	268	150	150 (+42)	152	760
Tissues	283	184	181	199	810
Pore water	30	30	—	—	60
Total					1630
Trace metals					
Sediments	268	150	150 (+42)	152	720 (762)
Tissues	283	184	181	199	847
Pore water	30	30	—	—	60
Total					1627 (1669)
Meiofauna					
Sort	268	150	150	150	718
Taxonomy to species					
Nematodes	268	150	150	150	718
Harpacticoids	268	150	150	150	718
Reproduction	268	150	150	150	718
Life history	268	150	150	150	718
Toxicity testing	—	150	—	—	150
Genetic diversity	—	30	30	—	60
Total					3800
Macroinfauna					
Wash/preserve	405	225	225	225	1080
Sorting					
Polychaete	405	225	225	225	1080
Nonpolychaete	405	225	225	225	1080
Identification					
Polychaete	405	225	225	225	1080
Nonpolychaete	405	225	225	225	1080
Total					5400
Macroinvertebrates					
Histology	200	290	280	229	999
Immunological probe	—	—	74	81	155
Total					1154
Demersal fish					
Histopathology	189	127	126	113	555
Splenic MA image analysis	71	83	126	113	393
Statistical analysis	71	83	126	113	393
Fish food	212	269	238	226	945
Total					2286
Detoxification					
Catalytic enzyme activity	202	147	117	160	626

© 1996 NRC Canada

Table 5 (*concluded*).

Work element	No. of samples				
	Cruise 1	Cruise 2	Cruise 3	Cruise 4	Total
Biliary metabolites	81	103	89	124	397
Rat hepatoma H-4IIE cell bioassays	35	30	30	36	131
P4501A mRNA levels in fish	—	41	86	100	227
Total					1381
Pore water toxicity bioassay	125	75	—	—	200

[a]Depth profiles in the sediment on Cruise 3.

term. In the total design analyses, P, C, and S were crossed. The data set was analyzed by platform, by cruise, and by platform and cruise, when interactions were present.

Multivariate analyses

The univariate analyses are fine for testing the first null hypothesis, where distance from the platform is the most interesting main effect. A second issue is how all the variables measured, and there were almost 200, relate to one another. In addition, many of the variables measured came from a specific sample, meaning that this was a true multivariate sampling design. Also, distance is simply used as a surrogate for the actual environmental gradient at each platform. We expect that the rig effect will cause many of the variables to covary with distance from the platform. Also, the rig effect may not be symmetric around the rig, even though it is easy to sample that way. A directional effect would cause significant interactions, which makes interpretation of the univariate ANOVA very difficult. Concordance of biological responses with increasing measures of contamination would be strong evidence that contaminants are causing the changes that might be observed near platforms. It is obvious that experiment-wise error rates must be controlled; therefore, a huge matrix of *t*-tests is not appropriate. The second null hypothesis can be tested using multivariate statistical techniques. Many exist, but we chose to use principal components analysis (PCA). This allows us to reduce the large data set of 91 abiotic variables to two factors that represent the first and second principal components (PC1 and PC2) that contain most of the variability in the data set. Then regression or correlation analysis can be used where PC1 and PC2 are the independent variables representing the covarying variables that make up the contamination gradient, and biotic responses are the dependent variables. Within the contaminant gradient, there may also be other gradients that covary with distance or direction from platforms, e.g., sediment grain size. The data set was prepared for PCA by merging the means of all the transformed pseudoreplicates according to the boxcore from which the data were derived. This produced a data set with 300 observations (4C × 3P × 5D × 5R), one for each boxcore sample.

Study sites

Initially, five sites were sampled during Cruise 1 (Fig. 2). After evaluation of the Cruise 1 results, three sites were selected for final study. The criteria for site selection included the following: (1) The site must be located in an area with a long history of oil and/or gas development and production must have been active for no less than 10 yr, (2) the site must be located in the western and/or central Gulf of Mexico far enough to the west to be outside the perpetual, confounding influence of the Mississippi River plume, and (3) comparison stations (controls) must be available that are located away from suspected present or past influences of any platform or pipeline and be similar to the near-platform stations in depth, sediment characteristics, physicochemical parameters, ambient current regime, and benthic fauna.

The Mississippi River discharge can cause fluctuations in the physical and sedimentological setting leading to significant confounding, natural variability over time and space. It was deemed important to choose sites outside the confounding influence of the Mississippi River plume to enhance one's ability to recognize a perturbation. In this particular study, "river" influence was primarily judged based on homogeneity of benthic substrate. However, it was recognized that the Mississippi River has substantial influence on water masses throughout the Gulf of Mexico. Given consideration of these criteria and the regional occurrence of major petroleum- producing reservoirs, site selection was restricted to the western Gulf of Mexico which is primarily a gas/condensate-producing region. As such, "oil" platform sites per se were not included in the study. Long-term production activity and water depth were also constraining factors in site selection. Other secondary considerations in site selection included the availability of previous studies at a site and the known presence of a detectable chemical contaminant gradient.

The five sites chosen were Mustang Island Block-A85 (MU-A85), Matagorda Island Block-686 (MAI-686), Matagorda Island Block-622 (MAI-622), High Island Block-A389 (HI-A389), and Galveston Area Block-288 (GA-288; Fig. 2). Due to the short time between GOOMEX Cruises 1 and 2, only preliminary results were available to reduce the number of study sites from five to three as mandated. A primary consideration was the documentation of a gradient in chemical contaminants in sediments surrounding the platform sites. The presence of a detectable spatial contaminant gradient was seen as the most important factor in selecting the final three study sites. The underlying assumption was that the stronger (steeper) the gradient, the greater the likelihood of observing statistically significant biological effects between near- and far-field samples. A comparison of indicators of

© 1996 NRC Canada

Fig. 1. Example of boxcorer and trawl locations at a study site for Cruises 1 (January 1993) and 2 (June 1993).

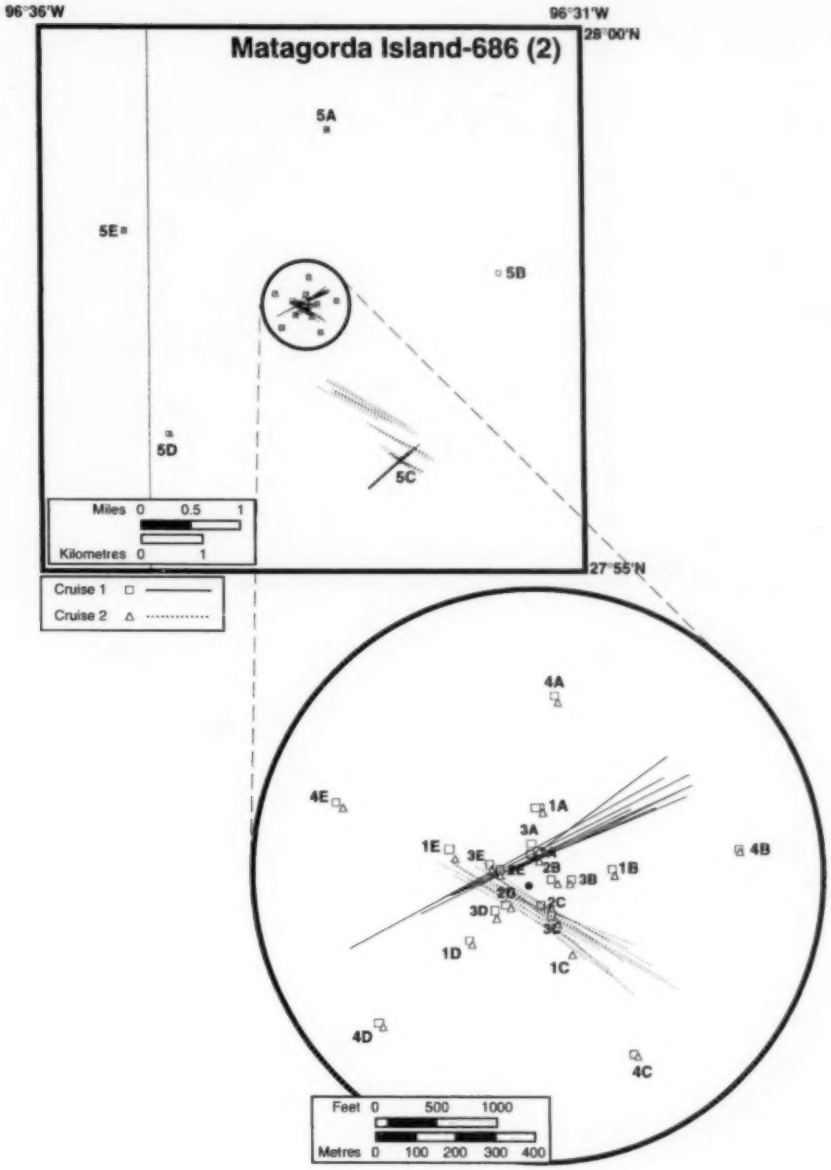

Table 6. Different analysis categories for different subsets to examine the total design and interactions within the design.

Number of cruises (C)	Number of platforms (P)	
	3	1
4	Total design analyses	By-platform analyses
1	By-cruise analyses	By-C·P analyses

hydrocarbon contamination clearly demonstrated that the highest contaminant values were at the MU-A85 and HI-A389 sites. MAI-686 and MAI-622 were similar; however, MAI-686 exhibited elevated alkanes due to the leakage of condensate near the platform. GA-288 exhibited little or no gradient in hydrocarbons. The steepest gradients in barium were at MU-A85 and HI-A389. Metal contaminants at both sites were significantly elevated and clearly related to drilling discharges. GA-288 showed no trend in barium concen-

© 1996 NRC Canada

Table 7. ANOVA designs for statistical analyses (P = platform, R = radius, D = distance, and C = cruise).

Source	df	Test against	df if D is continuous
Overall design analysis (model: Y = C P C·P R(P) C·R(P) D P·D D·R(P) D·C P·D·C D·C·R(P) where R(P), C·R(P), D·R(P), and D·C·R(P) are declared random)			
1 P	3 − 1 = 2	2	2
2 R(P)	(5 − 1)3 = 12	(7 + 8) − 11	12
3 D	5 − 1 = 4	7	1
4 C	4 − 1 = 3	8	4
5 P·D	(3 − 1)(5 − 1) = 8	7	2
6 P·C	(3 − 1)(4 − 1) = 6	8	6
7 D·R(P)	(5 − 1)(5 − 1)3 = 48	11	12
8 C·R(P)	(4 − 1)(5 − 1)3 = 36	11	36
9 D & C	(5 − 1)(4 − 1) = 12	11	3
10 P·D·C	(3 − 1)(5 − 1)(4 − 1) = 24	11	24
11 D·C·R(P)	(5 − 1)(4 − 1)(5 − 1)3 = 144	12	36
12 Rep. error	(3)(4)(5)(5)(2 − 1) = 300		461
Total	(3)(4)(5)(5)(2) − 1 = 599		599
By-platform analysis (model: Y = C R C·R D C·D R·D C·R·D where R, C·R, R·D, and C·R·D are declared random)			
1 C	4 − 1 = 3	4	3
2 R	5 − 1 = 4	4 + 6 − 7	4
3 D	5 − 1 = 4	6	1
4 C·R	(4 − 1)(5 − 1) = 12	7	12
5 C·D	(4 − 1)(5 − 1) = 12	7	3
6 R·D	(5 − 1)(5 − 1) = 16	7	4
7 C·R·D	(4 − 1)(5 − 1)(5 − 1) = 48	8	24
8 Rep. error	(4)(5)(5)(2 − 1) = 100		197
Total	(4)(5)(5)(2 − 1) = 100		249
By-cruise analysis (model: Y = C R C·R D C·D R·D C·R·D where R, C·R, R·D, and C·R·D are declared random)			
1 P	5 − 1 = 4	2	4
2 R(P)	(5 − 1)5 = 20	5	20
3 D	5 − 1 = 4	5	1
4 P·D	(5 − 1)(5 − 1) = 16	5	4
5 D·R(P)	(5 − 1)(5 − 1)5 = 80	6	20
6 Rep. error	(5)(5)(5)(2 − 1) = 125		200
Total	(5)(5)(5)(2) − 1 = 249		
By-cruise·platform analyses (model: Y = R D R·D where R is declared a random effect)			
1 R	5 − 1 = 4	3	4
2 D	5 − 1 = 4	4	1
3 R·D	(5 − 1)(5 − 1) = 16	4	4
4 Rep. error	(5)(5)(2 − 1) = 25		40
Total	(5)(5)(2) − 1 = 49		49

© 1996 NRC Canada

Fig. 2. Location of the five study sites sampled on Cruise 1.

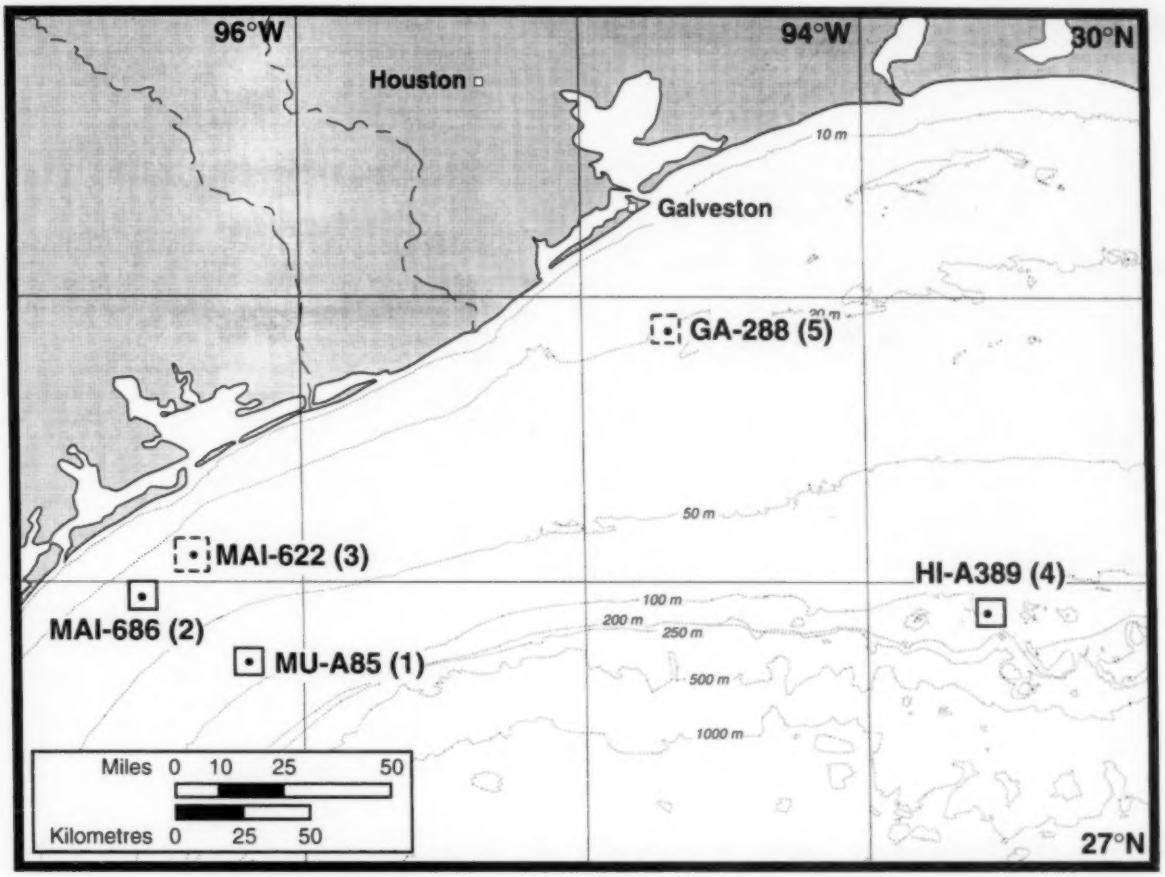

trations and, in fact, the control stations were slightly elevated over background; therefore, this site was eliminated as a location for further study. MAI-686 and MAI-622 were similar in sediment contaminant levels; however, barium variations with distance from the MAI-686 platform were more significant. A more consistent contaminant field was demonstrated at MAI-686 than at MAI-622 with several metals covarying with barium. Primarily because of the existence of chemical gradients, MU-A85, MAI-686, and HI-A389 were chosen as the final study sites.

Matagorda Island Area Block-686 (MAI-686)

A total of 12 wells were drilled from the MAI-686 platform between 1977 and 1981. This gas field produces from depths of 9152 to 12 260 ft (1 ft = 0.3048 m). A summary of the drilling history and associated discharges until 1980 is provided in Table 8. Monthly production of condensate, gas, and water is summarized in Fig. 3.

Mustang Island Area Block-A85 (MU-A85)

In the MU-A85 field, drilling has occurred as recently as 1986, and a total of 18 wells have been spudded. Discharges associated with the first six wells are summarized in Table 9 (Gettleson and Laird 1980). Monthly production of condensate, gas, and water is summarized in Fig. 4. Exploratory well Nos. 1, 2, and 3 were drilled between 1976 and 1978. In most instances, drilling muds and cuttings were discharged near the seafloor due to the proximity of the drill site to Baker Bank, a topographic high that serves as a fishing bank on the outer continental shelf. Pre- and postdrilling sediment barium surveys documented a benthic barium plume extending 1000 m from the drill site.

High Island A389 (HI-A389) – East Flower Garden Bank

The HI-A389 platform has six wells, and current production is 22.0 million million cubic feet per day (MMCFD) of natural gas. A comprehensive history of hydrocarbon development at the site is given in Boland et al. (1983). Preliminary exploratory drilling near the East Flower Garden Bank took place in the spring of 1975. Drilling continued in the fall of 1977 in 129 m of water. Totals of 129 000 L of drilling fluid and 1 035 000 kg of drill cuttings were discharged during October and November 1977. Residues from the fluids and cuttings were detected up to 1000 m from the drill site by

© 1996 NRC Canada

Table 8. Summary of the drilling history and associated discharges at the Matagorda Island Block-686 (MAI-686) site through 1980 (after Boothe and Presley 1985).

Characteristic	MAI-686
Type of drilling activity	Development
Type of wells	Gas
Number of wells	8 (4 additional wells drilled after 1980)
Total well depth (sum of all wells, m)	24 938
Total volume of cuttings discharged (sum of all wells, m^3)[a]	3 130
Drill mud components used (total of all wells in kg × 10^3)[b]	5 334
Total barite used (total of all wells in kg × 10^3, percent of total components used)	4 547 (85)
Total barium used (TBU, total of all wells in kg × 10^3)[c]	2 326
Discharge pipe location bearing in °T from rig (±water surface, m)	022 (–6)
Number of adjacent drilling sites (number of wells drilled within 3000-m radius of study rig)	1 (1)
Nearest adjacent drilling site to study site (m, °T)	1 500 (095)

[a]Estimated as 1.1 times total volume all wells.
[b]Mud systems used: seawater/gel (to 900 m), lignite/lignosulfonate (below 900 m).
[c]Assuming the barite used was 87% $BaSO_4$ and that the percent composition of Ba in $BaSO_4$ was 58.8%.

Fig. 3. Monthly production of condensate, gas, and water at MAI-686.

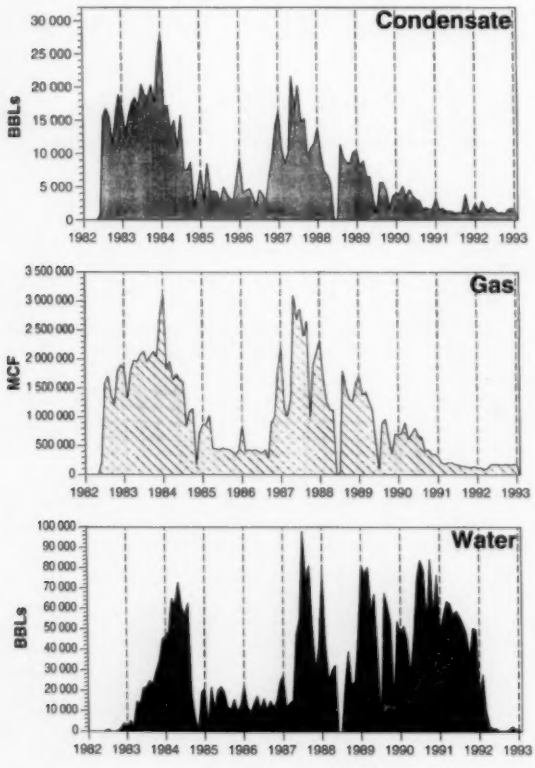

Continental Shelf Associates, Inc. (1985), but not on the reef monitoring stations 2000 m away. Results of the exploratory phases indicated the presence of commercial quantities of natural gas. The present platform was installed in October 1981, approximately midway between the two exploratory wells.

Additional drilling began on 26 April 1982 and continued into 1983. Drilling fluid and cuttings were shunted to within 10 m of the bottom prior to release. This procedure was required because the platform is located within the "shunting and monitoring" zone around the East Flower Garden Bank. Discharges were stopped when operations required oil-based drilling fluids. Oil-based fluid drilling requires a closed system. Cuttings, muds, and discharge water were barged for disposal elsewhere. Six production wells were drilled. The last drilling occurred on 19 April 1983. The depth of the six wells ranged from 1827 to 4313 m. Monthly production of condensate, gas, and water is summarized in Fig. 5.

Study results

The following seven articles provide a review of the major findings and an integrated synthesis of the data produced during Phase I of GOOMEX. Kennicutt et al. set the stage by documenting the abiotic setting around platforms. The hydrographic, sedimentologic, and contaminant conditions around the study sites are described in detail. Contaminant distributions in sediments and organisms provide a first-order evaluation of the degree to which long-term platforms are polluting the surrounding environment. Montagna and Harper provide a detailed description of the benthic ecology around a platform. Meiofaunal and macroinfaunal studies provide the basis for evaluating contaminant effects on life history, community

© 1996 NRC Canada

Table 9. Summary of drilling discharges from the first six wells at Mustang Island Block-A85 (MU-A85) (from Gettleson and Laird 1980).

Well	Amount of muds used (lb)	Percent barite by weight of mud used	Weight of cuttings discharged (lb)[a]	Weight of mud discharged (lb)	Weight of barium discharged (lb)
No.1 Block A-85	4 157 000	—	—	2 536 916[a]	317 765[b]
No.2 Block A-85	1 875 000	—	—	1 144 267[a]	143 327[b]
Platform A Nos. A-3 through A-6 Block A-85	8 798 636	87	7 696 087	509 852[b]	

[a]Estimated from mean (mud discharged/mud used) of Platform A well Nos. A-3, 4, and 5 (A-6 judged atypical).
[b]Estimated from barium content of muds discharged from Platform A well Nos. A-5 and 6.

Fig. 4. Monthly production of condensate, gas, and water at MU-A85.

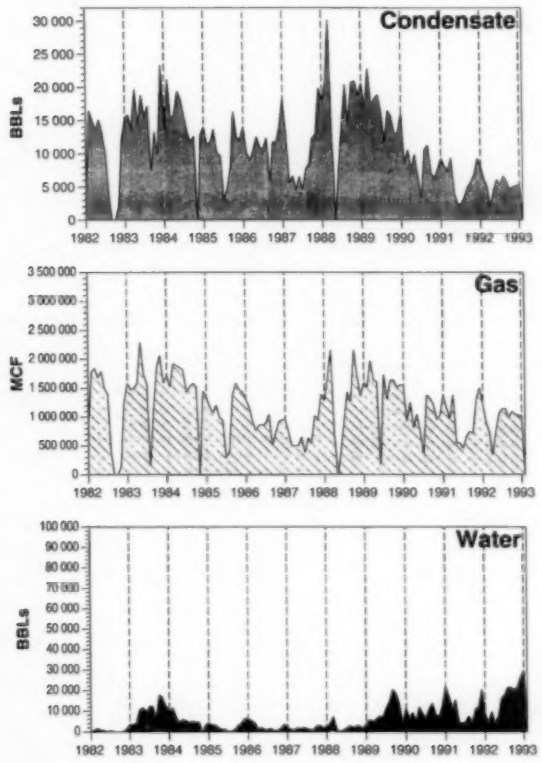

Fig. 5. Monthly production of condensate, gas, and water at HI-A389.

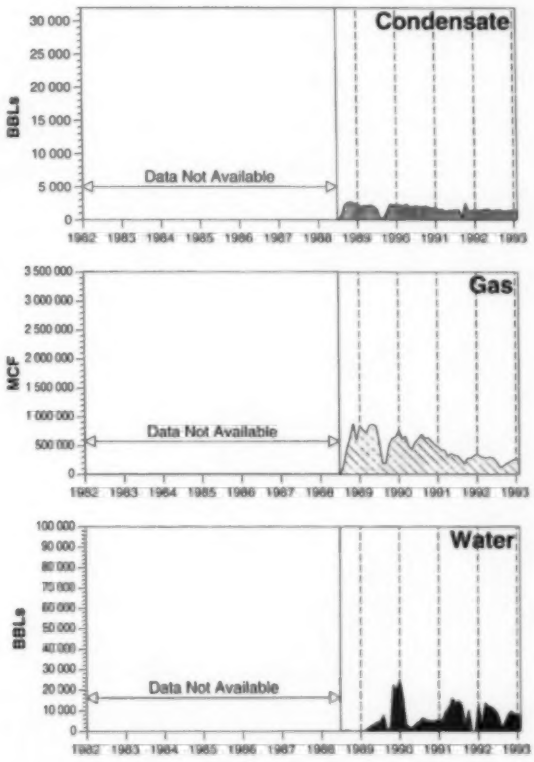

structure, and reproduction. Ellis et al. deal with epibenthic organisms, primarily invertebrates, and provide an assessment of platform effects on reproduction, size, and size frequency and pathologies in megafauna. McDonald et al. provide an evaluation of the induction of detoxification enzyme systems in demersal fish as a response to contaminant exposure. As a link to sediment toxicity, Carr et al. present sediment pore water bioassay results. Green and Montagna evaluate of the generality of results, a test of coherence among diverse work elements (a sediment quality triad approach), an evaluation of heterogeneity of variance as an impact response, and a discussion of study design in general. Finally, Peterson et al. provide a summary of programmatic results and recommendations for future studies.

© 1996 NRC Canada

References

Ahlfeld, T.E. 1990. Changing emphases in OCS studies. *In* Northern Gulf of Mexico Environmental Studies Planning Workshop. Proceeding of a Workshop held in New Orleans, Louisiana, 15–17 August 1989. *Edited by* R.S. Carney. Prepared by Geo-Marine, Inc. OCS Study MMS 90-0018. U.S. Department of the Interior, Minerals Management Service, New Orleans, LA. pp. 11–13.

Andrassy, I. 1956. The determination of volume and weight of nematodes. Acta Zool. **2**: 1–15.

Armstrong, F.A.J., Stearns, C.R., and Strickland, J.D.H. 1967. The measurement of upwelling and subsequent processes by means of the Technicon Auto Analyzer and associated equipment. Deep-Sea Res. **14**: 381–389.

Aurand, D.V. 1988. The future of the Department of the Interior OCS studies program. Oceans '88. Proceedings of a Conference sponsored by the Marine Technology Society and IEEE. Vol. I. IEE Cat. No. 88-CH2585-8, Baltimore, Md.

Avise, J.C. 1994. Molecular markers, natural history and evolution. Chapman and Hall, New York.

Bell, T.A., and Lightner, D.V. 1988. A handbook of normal penaeid shrimp histology. World Aquaculture Society, Baton Rouge, La.

Blazer, V.S., Facey, D.E. Fournie, J.W. Courtney, L.A., and Summers, J.K. 1994. Macrophage aggregates as indicators of environmental stress. *In* Modulators of fish immune responses: Vol. 1, Models for environmental toxicology, biomarkers, immunostimulators. *Edited by* J.S. Stolen and T.C. Fletcher. SOS Publications, Fair Haven, N.J. pp. 169–185.

Boesch, D.F., Bulter, J.N. Cacchione, D.A. Geraci, J.R. Neff, J.M., Ray, J.P., and Teal, J.M. 1987. An assessment of the long-term effects of U.S. offshore oil and gas development activities: future research needs. *In* Long-term environmental effects of offshore oil and gas development. *Edited by* D.F. Boesch and N.N. Rabalais. Elsevier Applied Science, New York. pp. 1–53.

Boland, G.S., Gallaway, B.J., Baker, J.S., and Lewbel, G.S. 1983. Ecological effects of energy development on reef fish of the Flower Garden Banks. Final report to National Marine Fisheries Service, Southeast Fisheries Center, Galveston, Tex. Contract No. NA80-GA-C-00057.

Boothe, P.N., and Presley, B.J. 1985. Distribution and behavior of drilling fluids and cuttings around Gulf of Mexico drilling sites. American Petroleum Institute, Washington, D.C.

Bradford, M.M. 1976. A rapid and sensitive method for quantitation of microgram quantities of protein using the principle of protein–dye binding. Anal. Biochem. **72**: 248–254.

Brewer, P.G., and Riley, J.P. 1966. The automatic determination of silicate silicon in natural waters with special reference to sea water. Anal. Chim. Acta, **35**: 514–519.

Bucklin, A., Frost, B.W., and Kocher, T.D. 1992. DNA sequence variation of the mitochondrial 16S rRNA in *Calanus* (Copepoda; Calanoida): intraspecific and interspecific patterns. Mar. Mol. Biol. Biotechnol. **1**: 397–407.

Carney, R.S. 1987. A review of study deisgns for the detection of long term environmental effects of offshore petroleum activities. *In* Long-term environmental effects of offshore oil and gas development. *Edited by* D.F. Boesch and N.N. Rabalais. Elsevier Applied Science, New York. pp. 651–696.

Carpenter, J. 1965. The accuracy of the Winkler Method for dissolved oxygen analysis. Limnol. Oceanogr. **14**: 135–140.

Carr, R.S. 1993. Survey of Galveston Bay bottom sediments and benthic communities. Galveston Bay National Estuary Program Rep. GBNEP-30.

Carr, R.S., and Chapman, D.C. 1992. Comparison of solid-phase and pore-water approaches for assessing the quality of marine and estuarine sediments. Chem. Ecol. **7**: 19–30.

Chamberlain, G.W., and Lawrence, A.L. 1983. Reproductive activity and biochemical composition of *Penaeus setiferus* and *Penaeus aztecus* in the Gulf of Mexico. Texas A&M Sea Grant College Program TAMU-SG-84-203.

Choi, K.-S., Powell, E.N., Lewis, D.H., and Ray, S.M. 1994. Instantaneous reproductive effort in female American oysters, *Crassostrea virginica*, measured by a new immunoprecipitation assay. Biol. Bull. **186**: 41–61.

Chomczynski, P., and Sachi, N. 1987. Single step method of RNA isolation by acid guanidium thiocyanatephenol – chloroform extraction. Anal. Biochem. **162**: 156–159.

Continental Shelf Associates, Inc. 1985. Environmental monitoring program for Platform "A", lease OCS-G 2759, High Island Area, South Extension, East Addition, Block A-389 near the East Flower Garden Bank. Final Report to Mobil Producing Texas and New Mexico, Inc., Houston, Tex. 3 volumes.

Darnell, R.M. 1958. Food habits of fishes and larger invertebrates of Lake Pontchartrain, Louisiana, an estuarine community. Publ. Inst. Mar. Sci. Univ. Tex. **5**: 353–416.

Dessauer, H.C., Dole, C.J., and Mafner, M.S. 1990. Collection and storage of tissues. *In* Molecular systematics. *Edited by* D.M. Hillis and C. Mortiz. Sinauer Associates, Inc. Sunderland, Mass. pp. 25–39.

Folk, R.L. 1974. Petrology of sedimentary rocks. Hemphill Publishing Company, Austin, Tex.

Freeman, W.H., and Bracegirdle, B. 1971. An atlas of invertebrate structure. Heinemann Educational Books Ltd, London.

Gettleson, D.A., and Laird, C.E. 1980. Benthic barium levels in the vicinity of six drill sites in the Gulf of Mexico. *In* Symposium Research on Environmental Fate and Effects of Drilling Fluids and Cuttings. Proceedings. Vol. II. pp. 739–788.

Hard, W.L. 1942. Ovarian growth and ovulation in the mature blue crab *Callinectes sapidus* Rathbun. Contrib. 46, Bull. Chesapeake Biol. Lab.

Harper, D.E. Jr., McKinney, L.D., Salzer, R.R., and Case, R.J. 1981. The occurrence of hypoxic bottom water off the upper Texas coast and its effects on the benthic biota. Contrib. Mar. Sci. **24**: 53–79.

Harper, D.E. Jr., McKinney, L.D., Nance, J.M., and Salzer, R.R. 1991. Recovery responses of two benthic assemblages following an acute hypxoc event on the Texas continental shelf, northwestern Gulf of Mexico. *In* Modern and ancient continental shelf anoxia. *Edited by* R.V. Tyson and T.H. Pearson. Geol. Soc. Spec. Publ. No. **58**: 49–64.

Hessler, R.R., and Jumars, P.A. 1974. Abyssal community analysis from replicate boxcores in the central North Pacific. Deep-Sea Res. **21**: 185–209.

Hill, J., Fowler, D.L., and VanDen Avyle, M.J. 1989. Species profiles: life histories and environmental requirements of coastal fishes and invertebrates (mid-Atlantic) — blue crab. U.S. Fish Wildl. Serv. Biol. Rep. 82(11.100). U.S. Army Corps of Engineers TR EL-82-4.

Hinton, D.E., Baumann, P.C., Gardner, G.R., Hawkins, W.E., Hendricks, J.D., Murchelano, R.A., and Okihiro, M.S., 1992. Histopathologic biomarkers. *In* Biomarkers: biochemica. *Edited by* R.J. Huggett, R.A. Kimerle, P.M. Mehrle, Jr., and H.L. Bergman. pp. 155–209.

Hulings, N.C., and Gray, J.S. 1971. A manual for the study of meiofauna. Smithson. Contrib. Zool. **78**: 1–84.

Jumars, P.A. 1975. Methods for measurement of community structure in deep-sea macrobenthos. Mar. Biol. **30**: 245–252.

Kendall, J.J. 1990. Detection of effects at long-term production sites. *In* Northern Gulf of Mexico Environmental Studies Planning Workshop. Proceeding of a Workshop held in New Orleans, Louisiana, 15–17 August 1989. *Edited by* R.S. Carney. Prepared by Geo-Marine, Inc. OCS Study MMS 90-0018. U.S. Department of the Interior, Minerals Management Service, New Orleans, La. pp. 23–28.

© 1996 NRC Canada

King, J.E. 1948. A study of the reproductive organs of the common marine shrimp, *Penaeus setiferus* (Linnaeus). Biol. Bull. **94**: 244–262.

Krahn, M.M., Meyers, M.S., Burrows, D.G., and Malins, D.C. 1984. Determination of metabolites and xenobiotics in the bile of fish from polluted waterways. Xenobiotica, **14**: 633–646.

Krahn, M.M., Kittle, L.J. Jr., and MacLeod, W.W. Jr. 1986*a*. Evidence of exposure of fish to oil spilled in the Columbia River. Mar. Environ. Res. **20**: 291–298.

Krahn, M.M., Rhodes, L.D., Meyer, M.S., Moore, L.K., MacLeod, W.D. Jr., and Malins, D.C. 1986*b*. Associations between metabolites of aromatic compounds in bile and the occurrence of hepatic lesions in English sole (*Parophrys vetulus*) from Puget Sound, Washington. Arch. Environ. Contamin. Toxicol. **15**: 61–67.

Ludwig J.A., and Reynolds, J.F. 1988. Statistical ecology: a primer on methods and computing. John Wiley & Sons, New York.

Montagna, P.A. 1991. Meiobenthic communities of the Santa Maria Basin on the California continental shelf. Continental Shelf Res. **11**: 1355–1378.

Murphy, J., and Riley, J.P. 1962. A modified single solution method for determination of phosphate in natural waters. Anal. Chim. Acta, **27**: 31–36.

National Oceanic and Atmospheric Administration (NOAA). 1993. Sampling and analytical methods of the National Status and Trends Program, National Benthic Surveillance, and Mussel Watch Projects 1984–1992. Vols. 1, 2, 3, and 4. NOAA Tech. Memo. NOS ORCA 71.

Nebert, D.W., and Gelboin, H.V. 1968. Substrate-inducible microsomal aryl hydroxylase in mammalian cell culture. I. Assay and properties of induced enzyme. J. Biol. Chem. **243**: 6242–6249.

Nei, M. 1987. Molecular evolutionary genetics. Columbia University Press, New York.

Pfannkuche, O., and Thiel, H. 1988. Sample processing. *In* Introduction to the study of meiofauna. *Edited by* R.P. Higgins and H. Thiel. Smithsonian Institution Press, Washington, D.C. pp. 134–135.

Pohl, R.J., and Fouts, J.R. 1980. A rapid method for assaying the metabolism of 7-ethoxyresorufin by microsomal subcellular fractions. Anal. Biochem. **107**: 150–155.

Preece, A. 1972. A manual for histologic technicians. Little, Brown and Company, Boston, Mass.

Rogers, R.M. Jr. 1977. Trophic interrelationshiips of selected fishes on the continental shelf of the northern Gulf of Mexico. Ph.D. disseration, Texas A&M University, College Station, Tex.

Romeyn, K., and Bouwman, L.A. 1983. Food selection and consumption by estuarine nematodes. Hydrobiol. Bull. **17**: 103–109.

SAS Institute Inc. 1990. SAS/STAT user's guide, version 6, fourth edition. Vol. 2. SAS Institute Inc., Cary, N.C.

Sherman K.M., Meeter, D.A., and Reidenauer, J.A. 1984. A technique for subsampling an abundant taxon while completely sorting other taxa. Limnol. Oceanogr. **29**: 433–439.

Unesco Technical Papers in Marine Science. 1981. Background papers and supporting data on the practical salinity scale 1978. No. 37.

US EPA. 1991. Methods for the determination of metals in environmental samples. EPA/600/4-91/010. Office of Research and Development, Washington, D.C. pp. 227–239.

Webb, D.G., and Montagna, P.A. 1993. Reproductive patterns in meiobenthic Harpacticoida (Crustacea Copepoda) of the California continental shelf. Continental Shelf Res. **13**: 723–739.

Whitfield, M. 1969. E_h as an operational parameter in estuarine studies. Limnol. Oceanogr. **14**: 547–558.

Wieser, W. 1953. Die beziehung zwischen mundhohlengestalt, ernahrungsweise und vorkommen bei freilebenden marinen nematoden. Arch. Zool. **4**: 439–484.

© 1996 NRC Canada

Geochemical patterns in sediments near offshore production platforms

Mahlon C. Kennicutt II, Paul N. Boothe, Terry L. Wade, Stephen T. Sweet, Richard Rezak, F.J. Kelly, James M. Brooks, B.J. Presley, and Denis A. Wiesenburg

Abstract: Patterns of the geochemical characteristics of sediments adjacent to three production platforms (22–150 m water depths) in the northwestern Gulf of Mexico were determined by the presence of the structure, the amount and type of materials discharged from the structure, and the local hydrographic setting. Sediments close to platforms (<500 m) were enhanced in coarse-grain materials primarily derived from discharged muds and cuttings. Hydrocarbon and trace metal (Ag, Ba, Cd, Hg, Pb, and Zn) contaminants were associated with these coarse-grain sediments. Contaminants were asymmetricallly distributed around each platform in response to the prevailing currents. Contaminant concentrations at most locations were below levels thought to induce biological responses. At a few locations close to one platform, trace metal (i.e., Cd, Hg) concentrations exceeded levels thought to induce biological effects. In deep water (>80 m), sediment trace metal contaminant patterns were stable over time frames of years. A few metals (Pb, Cd) exhibited evidence of continued accumulation in sediments over the history of the platform.

Résumé : Les caractéristiques géochimiques des sédiments adjacents à trois plates-formes de production (par 22 à 150 , d'eau) dans le nord-ouest du golfe du Mexique ont été déterminées à partir de la présence de l'ouvrage, de la quantité et du type de matériaux libérés par l'ouvrage, et du contexte hydrographique local. Les sédiments proches des plates-formes (< 500 m) étaient chargés de matériaux grossiers provenant surtout des boues et des débris de forage. Ces sédiments grossiers étaient contaminés par des hydrocarbures et des métaux à l'état de traces (Ag, Ba, Cd, Hg, Pb, et Zn). Les contaminants étaient répartis asymétriquement autour de chaque plate-forme à cause des courants dominants. Leurs concentrations étaient presque partout inférieures aux seuils prévus d'induction d'effets biologiques. À quelques endroits près d'une plate-forme, les concentrations de métaux à l'état de traces (Pb, Cd) dépassaient les seuils d'induction prévus. En eau profonde (> 80 m), les concentrations des métaux à l'état de traces dans les sédiments n'ont pas varié pendant des années. Il s'est avéré que quelques métaux (Pb, Cd) se sont constamment accumulés dans les sédiments depuis la mise à l'eau de la plate-forme.
[Traduit par la Rédaction]

Introduction

Offshore petroleum platforms discharge a variety of materials over the lifetime of a field. These discharges are associated with a number of activities including drilling, ship operations, accidental spills, runoff from the platform, discharge of produced waters and sewage, and other platform practices (sand blasting, painting, welding, etc.; Neff et al. 1987; Aurand 1988; Ahfeld 1990; Kendall 1990). The platform structure also acts as a reef and can generate a flux of materials to the seabed resulting from enhanced biological activity in the surrounding waters. Over a number of years, these various processes lead to alterations in the benthic environment (Southwest Research Institute 1978; Middleditch 1981; Lake Buena Vista Symposium 1981). These benthic alterations would be predicted to produce changes in the associated biology (Neff et al. 1987; Boesch and Rabalais 1987). The Gulf of Mexico Offshore Operations Monitoring Experiment (GOOMEX) Phase I program was designed to test for responses in the resident biota with particular reference to the chronic introduction of toxic contaminants (Kennicutt et al. 1996). Grain size alteration, substrate changes, and organic enrichment are also suspected to exert significant control over changes in biological patterns. Abiotic and biotic patterns near platforms reflect the cumulative, long-term interaction of the structure, materials emanating from the structure, and local oceanographic conditions.

The two most common contaminants associated with platforms are hydrocarbons and metals (Boothe and Presley 1987; Middleditch 1981; Boesch and Rabalais 1987; Continental Shelf Associates, Inc. 1983, 1985). The release of petroleum from a platform to the surrounding environment can occur during drilling as well as in the production phase of a platform's lifetime. Petroleum hydrocarbons are potentially present in a variety of discharges including drilling fluids,

Received October 2, 1995. Accepted September 13, 1996.
J13408

M.C. Kennicutt II, T.L. Wade, S.T. Sweet, F.J. Kelly, and J.M. Brooks. Geochemical and Environmental Research Group, Texas A&M University, 833 Graham Rd., College Station, TX 77845, U.S.A.
P.N. Boothe, R. Rezak, and B.J. Presley. Department of Oceanography, Texas A&M University, College Station, TX 77843, U.S.A.
D.A. Wiesenburg. Center for Marine Science, University of Southern Mississippi, Stennis Space Center, MS 39529, U.S.A.

© 1996 NRC Canada

cuttings, produced water, spills, deck drainage, and other releases (Kendall 1990). Petroleum-derived hydrocarbons released to the environment can be differentiated from naturally occurring background biogenic hydrocarbons (Brassell et al. 1978; Philp 1985; Boehm and Requejo 1986; Kennicutt and Comet 1992). Petroleum contains (1) a homologous series of *n*-alkanes with one to more than 30 carbons with odd and even carbon number *n*-alkanes present in nearly equal amounts, (2) a complex mixture of branched and cycloalkanes, and (3) an extensive suite of polycyclic aromatic hydrocarbons (PAH). Aliphatic hydrocarbons synthesized by organisms (both planktonic and terrestrial) include a suite of normal alkanes with odd numbers of carbons from 15 to 33. Complex branched and cycloalkanes are rare in organisms. Petroleum PAH mixtures are easily differentiated from PAH synthesized by organisms by the structural complexity of the mixture and the presence of substantial amounts of alkyl-substituted PAH. PAH are some of the more toxic components of oil and as such indicate the potential for biological effects. Based on considerations of petroleum chemistry, biological occurrences, and toxicological effects, aliphatic and aromatic hydrocarbons were chosen as tracers of petroleum contamination (Kennicutt 1995).

Trace metals are also released in discharges from offshore drilling activities (Boothe and Presley 1987; Boesch and Rabalais 1987; Lake Buena Vista Symposium 1981). Metal contamination can potentially affect both infauna and epifauna in the vicinity of platforms (Southwest Research Institute 1978). Many trace metals are priority pollutants (Ag, As, Cd, Cr, Cu, Hg, Ni, Pb, Sb, Se, and Zn) and are known to be toxic to organisms. These metals are often a constituent of drill muds (Tornberg et al. 1981; Houghton et al. 1981 Rubinstein et al. 1981). Tin is known to be toxic and is present in antifouling paints used on platform structures. Barium is an ideal tracer of the settlable particulate fraction of discharged drilling fluids and cuttings because it occurs in high concentrations in drilling muds and has a low, natural background in ambient sediments (200–500 ppm dry weight; Chow and Snyder 1981; Boothe and Presley 1985, 1987). Barium (as barite, barium sulfate) is the dominant component of drill mud (up to 90% on a dry weight basis). Aluminum and Fe are major constituents of alumino-silicate minerals and can be used to detect changes in sediment type. Vanadium is another metal of interest because it can occur in significant concentrations in crude oil. Sixteen elements were measured in sediments and seven in pore waters (Ba, Cd, Cu, Hg, Pb, V, and Zn).

Other properties measured in sediments included grain size, mineralogy, organic and inorganic C content, and redox potential. Sediment texture (i.e., grain size) is an important variable in the evaluation of biological assemblage data and contaminant distributions in benthic systems. Numerous studies have shown a strong correlation between biology, chemistry, and sediment texture and quality. In benthic ecosystem studies, cross-correlations between study sites are often dependent on substrate characteristics. Correlation of biological response variables with contaminant exposure can be confounded by the effects of variations in substrate. The organic and inorganic C content of sediments is another important measure of sediment quality. The C content of sediments near platforms may be influenced by organic enrichment (i.e., reef effect), disposal of drill mud and cuttings, and discharges from the platform. The O_2 content of sediment pore water as measured by redox potential is an important factor in determining the quality of the benthic substrate. Redox conditions also play an important role in the mobility and bioavailability of metals.

Methods

The laboratory methods for determining geochemical variables are summarized by Kennicutt et al. (1996). The methods used in this study are those of the NOAA National Status and Trends Program (NOAA 1993). Details of the methods are available in the references cited and the GOOMEX Final Report and will not be repeated here (Kennicutt 1995).

Results

The most dramatic feature of grain size distributions in sediments was the relationship between sand content (percent) and distance from the platform. Sediments out to a distance of 100 m were clearly enhanced in sand content (Fig. 1A). Stations between 200 and 500 m were impacted to varying degrees, depending on water depth, discharge location (i.e., near-bottom shunting), and the amount of materials discharged. The sand content of sediments at the near-field stations was increased above background sediment by 35–60% depending on the site. Indications were that most of this increase in sand-size materials resulted from disposal of cuttings during drilling operations at the platform. Sand content may also be enhanced by winnowing of fine particles by bottom currents, sand disposal during sandblasting activities, and deposition of carbonate skeletal fragments from platform-associated biota. Sediments at the shallowest, highest energy site (MAI-686) exhibited the greatest enhancements in sand content (Fig. 1A). However, the location of the discharges and the magnitude of the volume of the discharged materials were important controls on the sand content of sediments adjacent to the platforms.

An examination of sand fractions using a stereoscopic microscope and reflected light indicated that drill cuttings were present in sediments from the innermost stations at all three sites. The cuttings were characterized as very large rounded quartz-sand grains (two to three times as large as grains in background sediments from the area) and lithoclasts (fossiliferous limestones, chert, and/or fine-grained limestone). In addition, there were some angular, very fine quartz-sand grains presumably derived from sandblasting of the platform during rust-control programs. Small, sand-size metallic spheres were believed to be droplets of molten metal from welders or cutting torches that were quenched by seawater. Also visible was fragmented carbonate skeletal material derived from organisms encrusting the underwater parts of the platform. The most abundant skeletal remains were polychaete worm tubes and barnacles. The enhancement in sand-size particles was clear at all three sites. At HI-A389, an enhanced silt fraction was also evident in a cluster of samples closest to the platform. This indicated the possible addition of silt-sized materials as a result of drilling mud disposal. Sediments at HI-A389 within 50 m of the platform were more than 40% barite in some instances.

Carbon content distributions indicated that multiple pro-

© 1996 NRC Canada

Fig. 1. Areal distribution of (A) sand content and (B) mean total PAH concentrations in sediments as a composite of all four cruises.

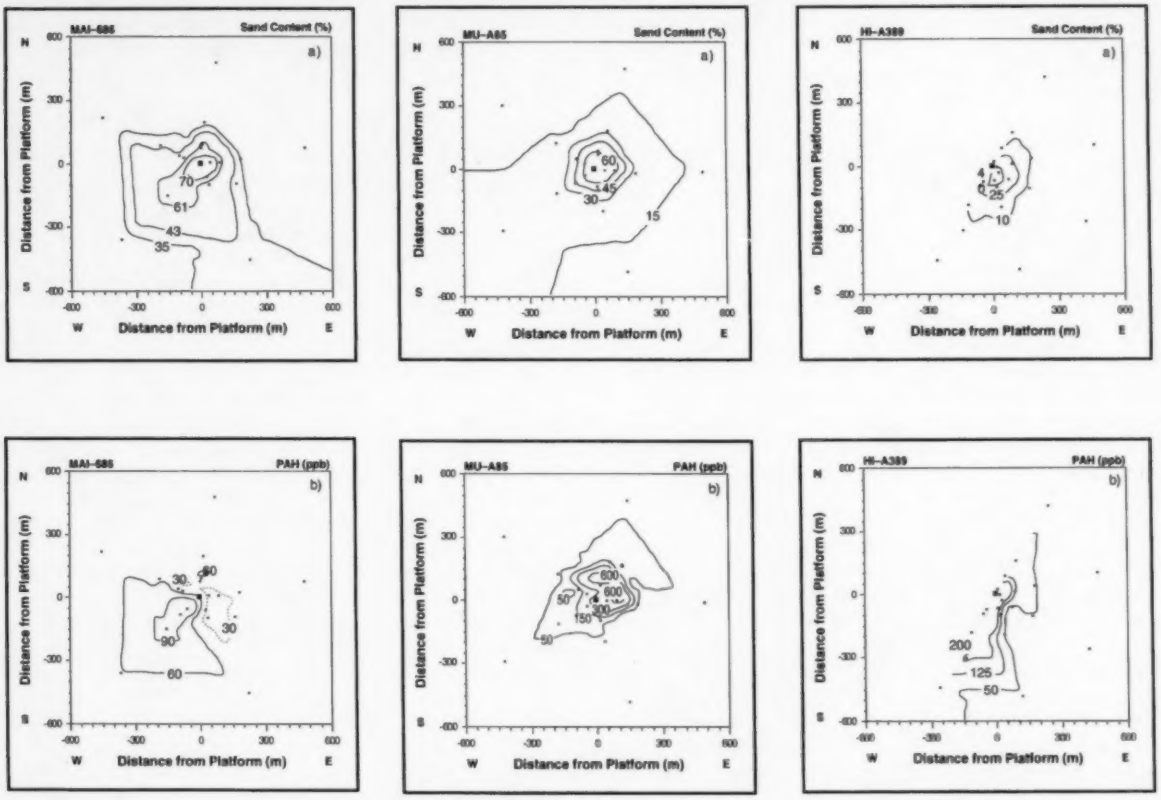

cesses were active. In the most general case, organic C decreased and inorganic C increased near the platform (Table 1). Total organic carbon (TOC) was in part decreased due to the addition of sand. However, TOC decreased by only 30% whereas sand and metals were increased by factors of 5–10 or more, suggesting that there was an additional source of TOC near the platforms. Sediment organic C content can increase due to deposition of organic matter derived from enhanced biological productivity associated with platforms. Enhanced sedimentary microbial populations in response to platform discharges, in particular hydrocarbon-oxidizing bacteria, may also contribute to TOC. Additions of TOC from cuttings is also possible but the significance of this source is unknown. Total inorganic carbon (TIC) content was subject to the sand dilution events as well. Inorganic C is a constituent of debris deposited from platform-associated calcareous biota such as barnacles and serpulids. Cuttings often contain inorganic C and can also be a source of TIC to the sediments. A positive correlation between sediment sand and TIC concentrations was observed.

Sediments from most stations contained little or no evidence of petroleum contamination. Concentrations of the unresolved complex mixture (UCM), total PAH, and total alkanes at most stations were less than 10 ppm, 150 ppb, and 500 ppb, respectively (Table 2). The method detection limit for total PAH in sediment was approximately 100–50 ppb. The areal distribution of the hydrocarbon contaminants was not symmetrical around the platforms, with concentration gradients varying in steepness among radii (Fig. 1B). Concentrations generally reached constant concentrations at distances of 100–200 m from the platform. At MAI-686, extracts from a few stations exhibited gas chromatograms typical of fresh condensate contamination (predominance of lower molecular weight *n*-alkanes and no UCM during all four cruises, suggesting a recent and continuing discharge of hydrocarbons (i.e., pipeline leak or an active seep)). In contrast, the contaminants at most stations at MU-A85 and HI-A389 lacked *n*-alkanes and exhibited a large UCM. Sediment extracts at HI-A389 exhibited a range of compositions probably resulting from differential input from multiple sources of hydrocarbon contamination. One station appeared to be contaminated with a low molecular weight fluid. Other stations exhibited a bimodal UCM suggesting two or more sources of petroleum in the area. Hydrocarbon concentrations were similar between cruises, suggesting that the low-level contamination observed was relatively stable. The greatest variations between cruises were detected at stations nearest to the platform, indicating steep, near-platform gradients and a heterogeneous distribution of hydrocarbons in sediments.

Variations in metal concentrations (on a dry weight basis) among cruises are illustrated for selected metals in Fig. 2.

© 1996 NRC Canada

Table 1. Tukey's multiple comparison test results by distance based on sedimentologic variables.

Variable[a]	Distance				
Overall design					
Sand	50 m	100 m	200 m	500 m	≥3000 m
(%)	(60.5)	(49.2)	(21.9)	(13.8)	(12.6)
TOC	≥3000 m	500 m	200 m	100 m	50 m
(%)	(1.02)	(0.98)	(0.89)	(0.69)	(0.61)
TIC	100 m	50 m	200 m	500 m	≥3000 m
(%)	(1.07)	(1.00)	(0.83)	(0.79)	(0.75)
MAI-686					
Sand	50 m	100 m	200 m	500 m	≥3000 m
(%)	(72.8)	(59.8)	(40.8)	(30.6)	(27.4)
TOC	3000 m	500 m	200 m	100 m	50 m
(%)	(0.79)	(0.78)	(0.65)	(0.42)	(0.35)
TIC	50 m	100 m	200 m	500 m	3000 m
(%)	(0.36)	(0.31)	(0.30)	(0.23)	(0.19)
MU-A85					
Sand	50 m	100 m	200 m	500 m	3000 m
(%)	(67.0)	(54.8)	(20.80)	(12.2)	(11.6)
TOC	3000 m	500 m	200 m	100 m	50 m
(%)	(0.93)	(0.92)	(0.90)	(0.62)	(0.55)
TIC	50 m	100 m	500 m	200 m	3000 m
(%)	(1.02)	(0.86)	(0.79)	(0.78)	(0.77)
HI-A389					
Sand	50 m	100 m	200 m	500 m	5000 m
(%)	(40.3)	(33.4)	(8.5)	(3.9)	(3.5)
TOC	5000 m	500 m	200 m	100 m	50 m
(%)	(1.40)	(1.27)	(1.19)	(1.13)	(1.02)
TIC	100 m	50 m	200 m	500 m	5000 m
(%)	(2.66)	(1.96)	(1.71)	(1.66)	(1.62)

[a]% sand–sand content, % silt–silt content, % clay–clay content.

[b]Detransformed means are presented (x) and means that are underlined are not different at the 0.05 level.

Contour plots are presented for Al concentrations, a major elemental constituent of the alumino-silicate minerals. Cadmium and Ba contour plots are presented to illustrate the typical distribution of metal contaminants. The level of contamination by metals was lowest at MAI-686, intermediate at MU-A85, and highest at HI-A389, the same order observed for hydrocarbon contamination (Table 2). Metals exhibited one of three distributions: (1) metal concentrations increased near the platform (Figs. 2A and 2C), (2) metal concentrations decreased near the platform (Fig. 2B), or (3) metal concentrations showed no detectable change. The metals with near-uniform distributions include Ag, As, Cu, Hg, Sb, Se, and Sn. These metals showed little change relative to distance from the platform. An exception to this relatively uniform pattern was an increase for a few of these metals (Ag, As, and Hg) near the platform at HI-A389 where the very highest metal levels were observed. Since a dilution of the sediments with 35–60% added sand had occurred, uniform concentrations suggest that a platform-related source must have been present to counteract the dilution. Several metals showed a decrease in sediments near the platform including Al, Cr (occasionally), Fe, Ni, and V. The remaining metals (Ba, Cd, Pb, and Zn) increased in concentration in sediments near the platforms. The magnitude of the increase was determined, in part, by the metal content of the materials discharged at each site.

Contamination at a site exhibits significant variability in three dimensions. Subsurface pockets of contaminants may influence biotic patterns in sediments. To assess the three-dimensional distribution of contaminants at each of the study sites, subsurface samples were taken at three depths to a depth of 20 cm along radius "C" during Cruise 3. Discharged drilling muds and cuttings (enriched in Ba) formed a thin veneer of materials that was 10–15 cm thick near the platform and thinned with increased distance from the platform. This pattern was also true for the hydrocarbons, with most of the hydrocarbons residing in the top 2 cm of the sediment column. Two sites (MAI-686 and MU-A85) exhibited subsurface Ba maxima illustrating the heterogeneous distribution of contaminants with depth in the sediment.

© 1996 NRC Canada

Table 2. Ranges in contaminant concentrations in surficial sediments (0–2 cm) from GOOMEX study sites.

	MAI-686	MU-A85	HI-A389
Hydrocarbons			
PAH (ppb)	7.8–588	17.7–6358.5	11.4–1238.1
Aliphatics (ppb)	72–9568	68–13.960	63–15.927
UCM (ppm)	0.0–119.4	0.0–381.8	0.0–406.1
Metals (ppm)			
Ag	0.1–1.7	0.0–1.0	0.0–3.8
Al	17 700–71 000	29 100–121 626	11 359–75 037
As	4.2–21.6	3.6–39.1	3.4–32.2
Ba	653–4680	720–26 250	785–280 220
Cd	0.0–1.6	0.0–2.3	0.1–63.7
Cr	25.5–82.0	37.8–131.0	35.0–171.0
Cu	3.8–48.9	5.5–36.2	9.0–106.1
Fe	11 940–30 280	13 680–69 940	15 400–36 590
Hg	0.0–0.1	0.0–0.3	0.0–3.5
Ni	0.5–28.5	7.5–28.5	9.2–35.4
Pb	0.2–555	15.2–436	0.2–694.8
Sb	0.3–2.4	0.3–5.5	0.4–7.5
Se	0.0–0.3	0.1–0.8	0.2–0.8
Sn	0.2–3.0	0.7–79.5	0.5–3.2
V	43.3–119.5	27.8–208.5	3.41–145.5
Zn	43.1–3850	54.6–1440	65.7–11 444

Discussion

One important observation was that sand content positively correlated with contaminant concentrations. This contrasts with most environmental studies where contaminants are associated with fine-grain particles (Boehm and Requejo 1986). This is a consequence of the origins of the contaminants, the composition of the materials discharged, the rapidity of the initial discharge, and the energetics of sediment transport at the site of deposition. A gradient in sand content is present at all three sites studied; however, the contaminant gradient is quite different among sites. Little or no hydrocarbon contaminant gradient was apparent at MAI-686. This results from differential redistribution of discharged materials based on grain size association, discharge history, and discharge technique. At MAI-686 the Ba anomaly is weak, suggesting loss of silt-sized materials due to winnowing at this shallow site. Timing of discharges, mode of discharge, and the amount of materials discharged are also important influences on sediment characteristics and cannot be fully resolved by the present study.

Principal components analysis (PCA) was performed on sedimentologic and contaminant variables to define interrelationships between sediment texture and contaminant content and to provide an effective representation of the variance in the data. Sediment texture and contaminant content were closely coupled at the platform sites. The contaminant and sedimentologic variables used for final PCA and score calculations were generated by a two-step data reduction procedure. As previously discussed, many contaminant variables (individual PAH and metals) strongly covary. The sediment metal data set is characterized by a strong covariance (both positive and negative) with Ba. At both HI-A389 and MU-A85, several metals (Cd, Hg, Pb, and Zn) showed highly significant, positive correlations with sediment Ba. For metals such as Cd and Hg, the correlation with Ba suggests a common source in the barite ore. In contrast, the lesser correlation of Pb and Zn with Ba suggests that a source other than drilling discharges is important (e.g., produced-water discharges, lubricants, welding operations, etc.). Lead and Zn have been detected in produced waters and are thought to be derived from the corrosion of galvanized structures on the platform or the oil–water separator system (Neff et al. 1987). Other metals (i.e., Al, Fe, Cr, Ni, Se, and V) associated with indigenous sediments show a weak, if any, correlation with Ba. Finally, As, Cu, and Sn are of mixed origins based on correlations with both Ba and sediment metals (e.g., Fe). For Cu, the correlation with Ba was weak except at high Ba concentrations suggesting that the concentration of Cu in the original barite ore was low.

Initial statistical analysis including all of the sedimentologic parameters produced principal components that reflected the high degree of covariation amongst variables. To more succinctly represent the consortium of materials present, significantly covarying parameters were reduced in number by either summing (TOTPAH) or selecting representatives of classes of contaminants as defined by statistical correlations (i.e., Ba as a marker of drill muds). The reduced set of parameters was then analyzed by PCA to produce a set of covariates that could be used to analyze the results from other study work elements (Table 3). PCA conducted at all levels of complexity (all variables, reduced variables, extended sets of variable) produced similar classifications of the data and thus led to equivalent interpretations. The consistency in the conclusions drawn from a variety of statistical treatments illustrates the robustness of

© 1996 NRC Canada

Fig. 2. Areal distribution of mean (A) Ba, (B) Al, and (C) Cd concentrations in sediments of all four cruises.

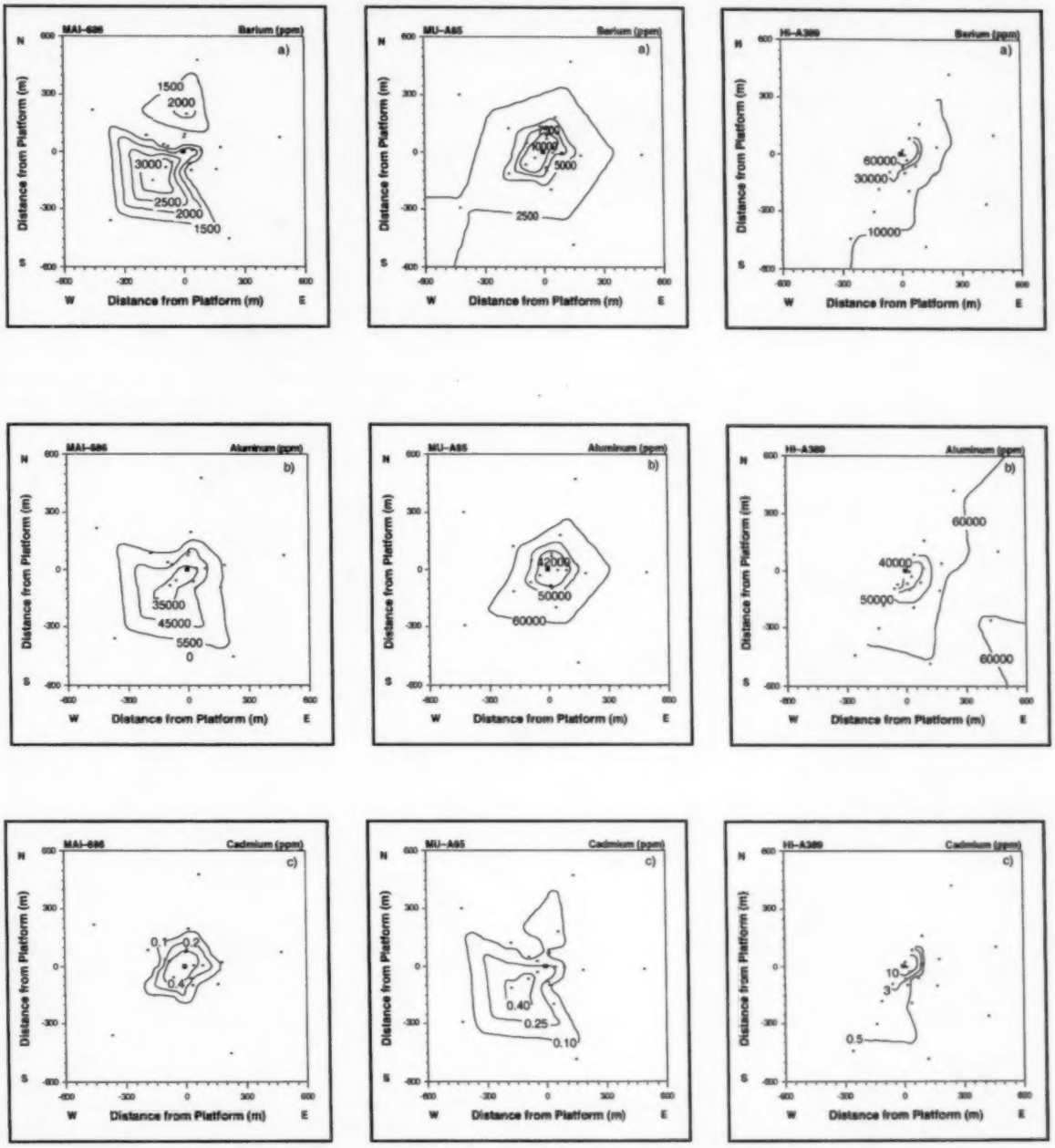

the conclusions to differing approaches to statistical analysis. A crossplot of the first component of the chemical analyses (ChemPC1) versus the second component (ChemPC2) clearly differentiates the stations by distance from platform and by site (Fig. 3). Translated into the variables measured, contamination increased as ChemPC1 increased (i.e., Near stations were more contaminated with hydrocarbons, metals, and sand than Far stations). Grain size decreased with distance from the platform. As ChemPC2 increased, fines increased and the sites were classified based on variables affected primarily by water depth and depositional setting.

As mentioned, many sediment contaminant variables covaried; therefore, a subset of representative contaminant and sedimentologic variables is presented to test the chemistry

© 1996 NRC Canada

Table 3. PCA factor patterns for reduced and combined sediment and contaminant variables (all variables were transformed as summarized under Discussion).

Variable	ChemPC1	ChemPC2
Total PAH	0.60	0.54
Total UCM	0.79	0.38
Total alkanes	0.79	0.20
%sand	0.85	–0.48
%silt	–0.61	0.58
%clay	–0.88	0.30
TOC	–0.50	0.63
TIC	0.08	0.64
Redox potential	–0.26	0.03
Fe	–0.61	0.58
Cd	0.69	0.64
Al	–0.86	–0.05
Ba	0.54	0.71
% of variance	43.6	24.7

Fig. 3. Relationship between ChemPC1 and ChemPC2 for sediment contaminant data coded by distance and grouped by site.

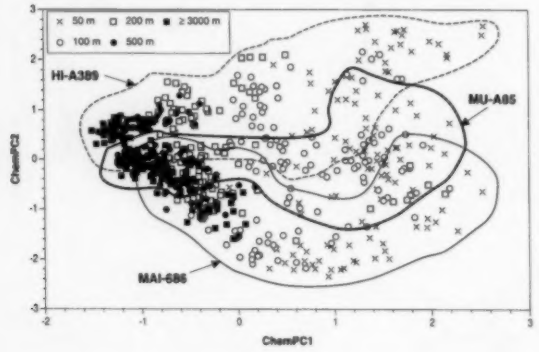

component of the programmatic hypotheses. The overall study design was devised to detect interactions among cruises, platforms, and distances from platforms (Kennicutt et al. 1996). Higher order interactions prohibited a direct interpretation of the main study design elements such as distance. The analysis of hydrocarbons and metals revealed many two- and three-way interactions. Significant interactions due to platform uniqueness were common. Distance and radius interactions were present for all variables, suggesting that many parameters vary not only in relationship to distance from the platform but also among radii within a site. Due to extensive, higher order interactions, more detailed information is provided if the data are tested on a platform-by-platform basis.

On a platform-by-platform basis, significant distance effects were clearly evident at all sites. Significant variations related to distance were independent of the site in that the analysis of data individually at all three sites gives similar and concordant results. Few interactions between cruise and distance were apparent, but distance interactions with radius were significant at all sites for almost all contaminant and sedimentologic variables. This signifies that most "platform-perturbed" variables have a strong directional orientation, since distances are not equivalent along different radii. While distance is a significant determinant in variable variances, direct indicators of contaminants must be used to investigate biological associations (i.e., distance is insufficient as a surrogate for contamination or exposure).

Another approach for identifying differences among sample means is a multiple comparison test. Tukey's multiple comparisons were effective in summarizing and highlighting differences among distances and succinctly illustrated the attributes of each study site. Hydrocarbon-based variables differentiated stations out to 500 m (Table 4). Stations at greater than 500 m distance from the platform were indistinguishable from each other (i.e., background). Barium content differentiated all distances, suggesting a much wider dispersion of Ba (Fig. 2A). Aluminum, a background sediment constituent, reflected a near-field dilution caused by the addition of sand. Iron was diluted 30% compared with a 45% decrease in Al concentrations, suggesting a secondary source of Fe near the platform. Cadmium distributions were similar to those of Ba and differentiated sediments at all distances. The distribution of Ba and Cd was similar to that observed for sand content. However, Ba and Cd increased by a factor of 10 or more over controls whereas sand increased by only a factor of 5. The distance of recognizable differences based on various variables suggested different modes of transport related primarily to the hydraulic properties of the materials. Various size fractions were also influenced to varying degrees by contaminant additions, either enhanced or diluted. To more fully understand the origins of the sediments at the sites, the distribution of contaminant variables as a function of grain size is needed.

PAH were low and not significantly associated with distance from the platform at MAI-686 (Table 4). Other hydrocarbon parameters were somewhat correlated with distance but the association was weak and most likely related to a pipeline leak or seep along an individual radius that was not a site-wide contaminant event. Metals associated with drill muds (Ba and Cd) were only weakly correlated with distance from the platform. However, a concordant ordering of stations was not apparent. Sediment-associated metals (Fe and Al) reflected dilution with sand, and the sand content differentiated sediments out to 3000 m from the platform. At this site the increases and decreases in variables were relatively concordant, suggesting a common depositional event (i.e., Fe and Al concentrations decreased by 40%; sand content increased by a factor of 2.6).

MU-A85 clearly had enhanced contaminant concentrations near the platform. Hydrocarbon concentrations were significantly higher near the platform than away. The effect was most significant to 100 m, with the 200-m stations not significantly different from the 500-m stations other than for the UCM which differentiated sediments to a distance of 500 m. Barium and Cd concentrations differentiated sites to 500 m and, in the case of Ba out to 3000 m. This distribution was similar to changes in sand content. Iron and Al were diluted in response to the increase in sand content close to the platform. At this site, sand and Ba concentrations increased by 5- and 10-fold; however, Fe, Al, and TOC decreased by only 25–50%.

© 1996 NRC Canada

Table 4. Tukey's multiple comparison test results by distance based on contaminant variables.

Variable[a]	Distance[b]				
Overall					
TOTPAH	50 m	100 m	200 m	500 m	≥3000 m
(ppb)	(114)	(73)	(48)	(35)	(35)
Ba	50 m	100 m	200 m	500 m	≥3000 m
(ppm)	(10 217)	(6065)	(4359)	(2019)	(1149)
Cd	50 m	100 m	200 m	500 m	≥3000 m
(ppm)	(0.73)	(0.25)	(0.13)	(0.07)	(0.06)
Al	≥3000 m	500 m	200 m	100 m	50 m
(ppm)	(61 248)	(61 175)	(54 776)	(41 680)	(33 982)
MAI-686					
TOTPAH	3000 m	500 m	200 m	50 m	100 m
(ppb)	(49)	(43)	(40)	(32)	(30)
Ba	200 m	50 m	100 m	500 m	3000 m
(ppm)	(1625)	(1459)	(1323)	(1134)	(1072)
Cd	50 m	200 m	100 m	500 m	≥3000 m
(ppm)	(0.13)	(0.11)	(0.09)	(0.06)	(0.05)
Al	500 m	3000 m	200 m	100 m	50 m
(ppm)	(59 742)	(57 457)	(50 599)	(42 078)	(34 922)
MU-A85					
TOTPAH	50 m	100 m	200 m	500 m	3000 m
(ppb)	(180.9)	(126.4)	(42.3)	(31.7)	(27.1)
Ba	50 m	100 m	200 m	500 m	3000 m
(ppm)	(10 064)	(9263)	(3706)	(1817)	(1094)
Cd	50 m	100 m	200 m	500 m	3000 m
(ppm)	(0.46)	(0.25)	(0.07)	(0.05)	(0.05)
Al	500 m	3000 m	200 m	100 m	50 m
(ppm)	(64 119)	(63 386)	(57 971)	(41 956)	(37 339)
HI-A389					
TOTPAH	50 m	100 m	200 m	500 m	5000 m
(ppb)	(256)	(103)	(65)	(33)	(32)
Ba	50 m	100 m	200 m	500 m	5000 m
(ppm)	(72 605)	(18 196)	(13 756)	(3993)	(1293)
Cd	50 m	100 m	200 m	500 m	5000 m
(ppm)	(6.4)	(0.65)	(0.29)	(0.11)	(0.08)
Al	5000 m	500 m	200 m	100 m	50 m
(ppm)	(63 082)	(59 776)	(56 027)	(41 011)	(30 091)

[a]TOTPAH, sum of all measured PAH.

[b]Detransformed means are presented (x) and means that are underlined are not different at the 0.05 level.

HI-A389 sediment characteristics reflected the intensity of the contaminant discharges, near-bottom shunting, and the low-energy environment of deeper water. Total PAH concentrations differentiate sediments to 500 m and UCM concentrations were significantly different to 5000 m. Barium and Cd concentrations differentiated sediments to a distance of at least 5000 m. As at the other sites, Fe and Al contents reflected dilution by sand.

The data are also compared with sediment data from previous Gulf of Mexico platform monitoring studies conducted at sites with similar drilling histories. This approach aids in determining if the perturbations observed at the three study sites are similar to perturbations observed elsewhere. Also, since some of the previous studies were conducted at sites that were also chosen for this study, changes in sediments over time can be evaluated. As previously discussed, metal concentrations strongly correlate with sediment grain size. For example, some metal concentrations are much higher in fine-grained, clay-rich sediments than in coarse, sandy ones. This relationship is the result of both physical (i.e., surface area) and chemical (alumino-silicate versus quartz minerals) differences among the grain size fractions in typical marine sediments. Even in pristine, unperturbed sediments, metal concentrations will vary considerably solely on the basis of differences in sediment texture. Therefore, sediment contaminant levels must be compared after a normalization taking into account differences in sediment texture. One normalization approach is to relate metal concentrations to Al content.

© 1996 NRC Canada

Fig. 4. Relationship between sediment (A) Fe amd Al concentrations, (B) Fe concentrations and distance from the platform, and (C) Ba concentrations and distance from the platform at MAI-686 at two samplings 14 yr apart.

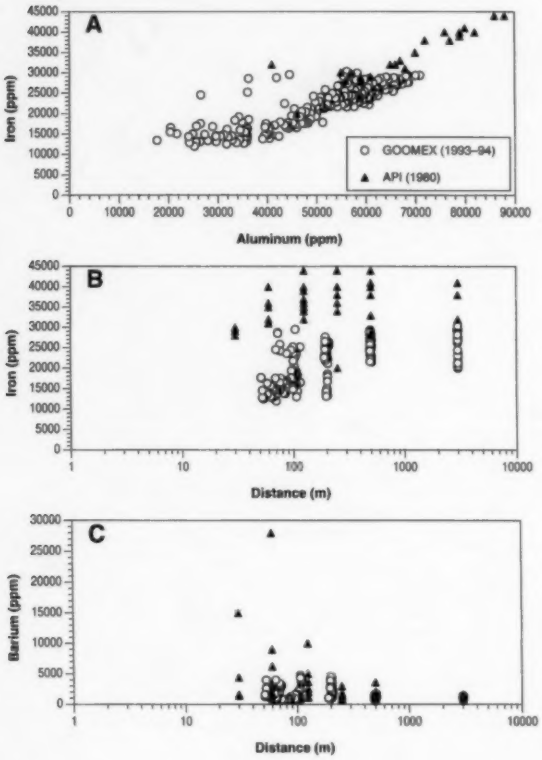

Aluminum is a major component of the minerals comprising most marine sediments (i.e., alumino-silicate clay minerals) and occurs at concentrations at the percent level. It is unlikely that anthropogenic inputs of Al would be sufficient to significantly alter the indigenous concentrations of Al in sediments. Iron is also a percent-level component of sediments and can be used as a normalization factor for trace metal comparisons. However, a suspected source of Fe related to the platform makes these comparisons less useful. The relationships between metal concentrations and Al content are used to evaluate the sediment trace metal perturbations observed in the present study.

Two previous studies were available for comparison. One study sponsored by the American Petroleum Institute (API) sampled sediments (40 stations in a radial pattern) surrounding six drilling sites in 1980 (Boothe and Presley 1985). Barium, Cr, and Fe were determined at all stations and Al, Cd, Cu, Hg, Pb, and Zn at selected stations. A second study, conducted by Continental Shelf Associates, Inc. (CSA), investigated a drilling site at HI-A384 near the West Flower Gardens in 1982 (Continental Shelf Associates, Inc. 1983). Barium and Fe were measured at 44 stations arranged in a similar radial pattern. Chromium was determined at 17 stations. The MAI-686 site was sampled in 1980 as part of the API study and resampled as part of this study (1993–1994). Eight wells had been drilled prior to the 1980 sampling. The characteristics of the ambient sediments have changed significantly during the 14-yr period between samplings. Much of the finer-grained sediment (Al and Fe rich) has been removed (Fig. 4). Aluminum and Fe contents clearly show a significant change in sediment composition with essentially no overlap in compositions between the two sampling events. The relationship between Fe and distance from the platform for the two studies confirms this conclusion. All of the elevated Ba levels observed in 1980 within ≤125 m of the platform are no longer present. Barium levels beyond 125 m are essentially unchanged over the 14-yr period. The concentration of Hg showed the same decline as Ba. The concentrations of Cd, Cu, and Zn also appear to have decreased between the two sampling events but the decrease was less dramatic. Lead is the only element that increased over the 14-yr period, suggesting a continuing, nondrilling discharge source for Pb (Fig. 5). The change in sediment texture between 1980 and 1993–1984 is the result of a continuing process of sediment resuspension and transport at this shallow-water, high-energy site.

Deeper water development and production sites from the 1980 API study (HI-A341 and V-321) were selected for comparison with the two remaining GOOMEX study sites (MU-A85 and HI-A389). The API sites had similar drilling histories (HI-A341: 8 wells, V-321: 25 wells) and sediment types (based on Al and Fe concentrations). These data sets provide a comparison of metal distributions measured soon after the cessation of drilling (API sites) and again 5–10 yr later (GOOMEX sites). The magnitude of the sediment Ba enrichments within each pair of sites is similar (Fig. 6). The only significant difference in Ba enrichment is the anomalous 18–28% Ba enrichment at the HI-A389 site caused by shunting of the drilling discharges within 10 m of the seafloor. The similarity in Ba concentrations suggests that, for sites with similar drilling histories and in deepwater depositional environments (i.e., ≥50–70 m and lower energy), there has been little change in the ambient sediments with time. The temporal stability of Ba at the deeper water sites is also apparent for other elements. Enrichments in Cr, Cd, Cu, Hg, and Zn at the HI-A341 and MU-A85 sites are similar. Again, as observed for the MAI-686 site, the only exception is Pb which is significantly higher at the MU-A85 site, suggesting a continuing input of this element after the cessation of drilling discharges (Fig. 5). The relationship is similar at the more highly contaminated V-321 and HI-A389 sites. Even excluding the high-Ba samples (Fig. 6), Pb levels are several-fold higher at HI-A389 than at V-321 (Fig. 7). In addition, Cd and Zn levels are significantly higher at the HI-A389 site suggesting a continuing input of these metals after cessation of drilling operations.

The CSA study in 1982 (Continental Shelf Associates, Inc. 1983) suggested that the magnitude of surface enrichments from drilling discharges among sites within similar depositional environments (i.e., judged by water depth) was similar regardless of the number of wells drilled. Differences in the amount of drilling resulted in a thicker veneer of metal-enriched sediments overlying the native sediment, but no clear difference in the magnitude of surface enrichment was apparent. This may indicate that the contaminant to inert

© 1996 NRC Canada

Fig. 5. Relationship between sediment Pb concentrations and distance from the platform at two samplings (recent: MAI-686, MU-A85, HI-A389; 14 yr ago: API MAI-686, HI-A341, V-321) (ERL = effects range low; ERM = effects range medium; Long and Morgan 1990).

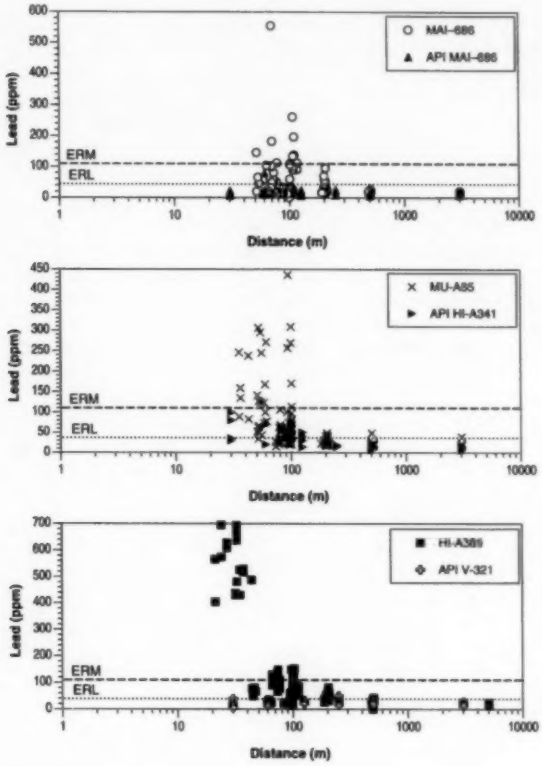

Fig. 6. Relationship between Ba concentrations in sediment collected immediately (HI-A341, V-321, HI-A384) and 5–10 yr after (MU-A85, HI-A389) cessation of drilling activities.

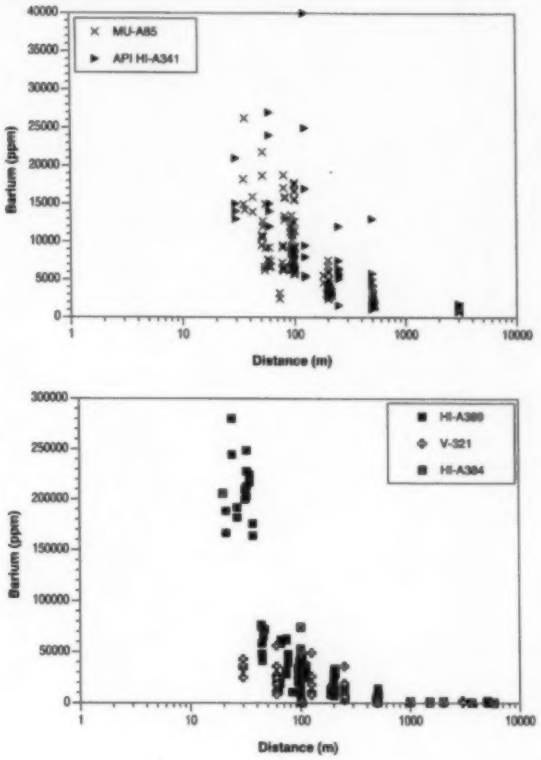

material ratio for the discharges was similar at the sites and this original concentration was the highest value possible at a site. The veneer of materials on top of the indigenous sediments was primarily drilling discharges. The CSA study sampled around a single exploratory well in lease block HI-A384, while six wells were drilled at the GOOMEX HI-A389 site. The two sites are in essentially identical depositional environments and separated by only about 20 km. Both sites are in approximately 120 m of water and both are located in close proximity to a topographic feature (West and East Flower Gardens, respectively). The drilling discharges were also shunted to within 10 m of the seafloor at both sites. The surficial sediment Ba distribution, an indicator of the distribution of the drilling discharge contaminant field, is similar at both sites (Fig. 7). Even the more than 20% Ba enrichment caused by shunting is present at both sites. This comparison is another indication of the stability of the contaminant fields at deeper water sites. The CSA study was conducted immediately after drilling, while the sampling of HI-A389 reported here occurred almost 10 yr after the last drilling event. Although based on only two samples, the levels of Cd and Pb also appeared to be quite similar and elevated above suspected drilling discharge levels at the two sites.

A further evaluation of the contaminant level is provided by a comparison with sediment concentrations known to elicit biological effects. While biological effects were directly measured, comparison with literature values provides an assessment of the potential for effect. The concentration of total PAH at the study sites is presented as a frequency distribution along with sediment PAH concentrations from the National Oceanic and Atmospheric Administration National Status and Trends (NOAA NS&T) Program and the Environmental Protection Agency's Environmental Monitoring and Assessment Program-Near Coastal (EPA-EMAP-NC) Programs (Fig. 7). Sediment total PAH concentrations at the platform sites were generally less than 1000 ppb with only a few exceptions close to the platforms at HI-A389 and MU-A85. The EPA-EMAP-NC data represent 183 sites along the Gulf Coast collected on a probability-based sampling design. As expected the median PAH concentrations in shelf sediments are nearly an order of magnitude lower than in coastal areas of the Gulf. However, at a few locations, PAH concentrations at the platform sites approach the highest values observed in coastal bays. To assess the potential for biological effects from the observed near-field sediment, the contaminant levels observed are compared with the effects threshold data of Long and Morgan

© 1996 NRC Canada

Fig. 7. Comparison of sediment PAH concentrations at GOOMEX sites with the NOAA National Status and Trends (NS&T) and EPA Environmental Monitoring and Assessment (EMAP) databases for coastal Gulf of Mexico sites (ER-L = effects range low; Long and Morgan 1990).

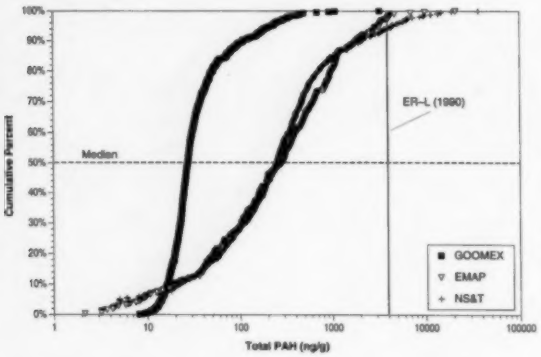

Fig. 8. Percentage of samples from the GOOMEX sites that exceeded the Long and Morgan (1990) (A) 50% and (B) 10% bioeffects criteria.

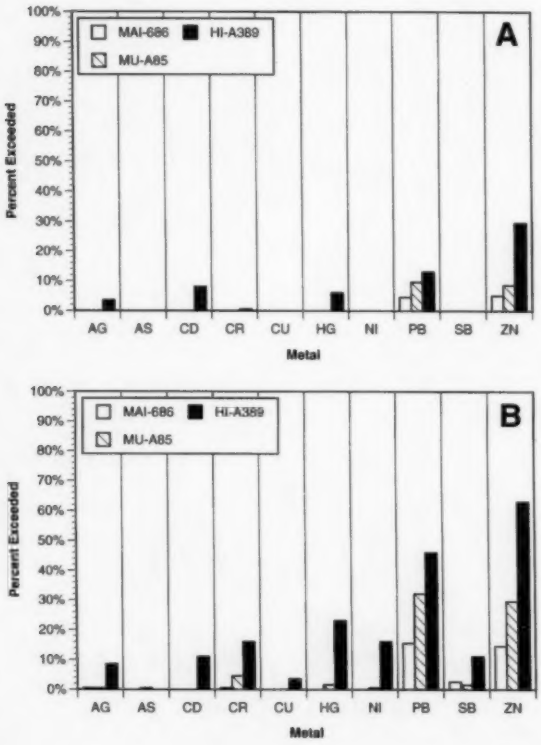

(1990). The PAH values observed at the platform sites are significantly below the Long and Morgan (1990) 10% biological effects criteria of 4000 ppb (Fig. 4). These effects criteria are based on a compilation of the chemical concentrations observed, or predicted, to be associated with biological effects (broadly defined). Note that the definition of total PAH is highly variable and that these values only serve as a semiquantitative guide. The 10% criterion is defined as the level at which biological effects were observed 10% of the time. Long and Morgan (1990) also noted that compounds such as PAH, which may be mutagenic or teratogenic, may not be toxic in acute tests of mortality. The percentages of sediment samples that exceeded the Long and Morgan low (ER-L, 10%) and median (ER-M, 50%) effects ratios in the present study are compared (Fig. 8). Several metals exceed the effects levels in near-field sediments. These comparisons suggest that a significant percentage of sediments at the study sites might elicit biological responses. While these comparisons are informative, they are not definitive for predicting biological effects. Sediment metals may or may not be bioavailable and a detailed evaluation of redox potential and metal speciation is needed to determine a causal link between sediment metals and observed biological effects.

The three-dimensional nature of the contaminant distributions suggests that assessments of exposure might be more accurately expressed as amount per square metre of surface area or cubic metres of sediment volume integrated over a defined near-field area (i.e., out to a distance of 100 m). The sediment column, especially at the deeper water sites (MU-A85, HI-A389), is not well mixed with respect to Ba despite the long time since cessation of drilling activities. This observation confirms that the sedimentary contaminant field is quite stable over time frames of years. Previous research (Boothe and Presley 1985) has shown fine, undisturbed barite laminations in the sediment column up to a decade after the cessation of drilling discharges.

Conclusions

The following conclusions were derived from the geochemical portions of the GOOMEX Phase I study.

(1) All study sites exhibited an enhancement of sand close to the platform (from 25 to 60% enhancement over a few hundred metres).

(2) A suite of contaminants is associated with platforms: trace metals, hydrocarbons, and sand. PCA analysis groups, aliphatic hydrocarbons, PAH, Ag, Ba, Cd, Hg, Pb, Zn, and percent sand as covariates.

(3) The contaminants are closely associated with large-grain-sized materials at platforms in contrast with many other environmental studies where contaminants are associated with fine-grained materials.

(4) Distance and direction (D·R) were the most important main effects in defining contaminant distributions. The directionality of the contaminant field is in response to the oceanographic setting at each site.

(5) Water depth, discharge history, and ambient physical oceanographic conditions control the intensity, direction, and extent of the contaminant field.

(6) Organic C is decreased near platforms, but not in proportion to the sand dilution event, suggesting possible organic enrichment.

(7) Inorganic C increases close to the platform due to platform-related sources such as biogenic debris (calcareous remains) and disposal of carbonate-containing cuttings.

© 1996 NRC Canada

(8) Compared with marine settings impacted by spills and coastal areas that experience long-term non-point-source chronic contamination, sediment hydrocarbon concentrations were low at the sites studied.

(9) Petroleum contamination is high near a platform and decreases rapidly with distance away from the platform.

(10) Sediment PAH are at levels below documented biological effects thresholds for marine biota. In contrast, sediment trace metal concentrations at several locations exceeded levels known to elicit biological effects.

(11) Some sediment parameters (i.e., Al) decreased near the platform due to dilution with sand.

(12) Several metals appear to have sources other than the cutting/drill mud discharged during drilling (i.e., Pb, Zn, and Cd).

(13) An evaluation of the three-dimensional distribution of contaminants suggests that subsurface pockets of contaminants may influence biotic patterns in the overlying sediment.

(14) A comparison of samplings 14 yr apart at the MAI-686 site confirmed an ongoing loss of fine particulates and contaminants due to dynamic redistribution of sediments at this site.

(15) At all three sites, Pb was shown to continue to accumulate in sediments near the platform over a period of years above that attributable to the initial increase due to drill mud and cutting disposal. Lead concentrations increased to levels known to elicit biological responses.

(16) At deeper water sites (>80 m), a comparison of metal enrichments immediately after cessation of drilling and 5–10 yr after the last discharges showed that similar concentrations were observed confirming the relative stability of the contaminant field over time frames of years, possibly decades (an exception is the observed increase in Pb over time).

(17) At MU-A85 and HI-A389, Cr and Fe concentrations were higher in near-field sediments relative to Al than is typical for background sediments. This enhancement suggests that a platform source of these metals is contributing to sediment concentrations.

These patterns in geochemical characteristics provide a basis for the evaluation of the processes that control biological patterns observed at these sites. An important finding that must be considered when describing the relationship between independent and dependent variables is that many environmental factors including water depth, sediment grain size, organic enrichment, toxic response, and seasonality strongly covary, and thus, cause and effect may be difficult to ascertain from field observations alone.

Acknowledgments

This program was funded by the Minerals Management Service (MMS) through National Biological Service (NBS) contract No. 14-35-0001-30582. The financial support of MMS through the New Orleans Office is appreciated. Additional data presented in this paper were generated as a part of the National Oceanic and Atmospheric Administration National Status and Trends (NS&T) Program (contract No. 50-DGNC-0-00447) and the Environmental Protection Agency Environmental Monitoring and Assessment Program-Near Coastal (EMAP-NC, contract No. CR-818-222-01-3).

References

Ahlfeld, T.E. 1990. Changing emphases in OCS studies. *In* Northern Gulf of Mexico Environmental Studies Plannning Workshop. Proceedings of a Workshop held in New Orleans, Louisiana, 15–17 August 1989. *Edited by* R.S. Carney. Prepared by Geo-Marine, Inc. OCS Study MMS 90-0018. U.S. Department of the Interior, Minerals Management Service, New Orleans, La. pp. 11–13.

Aurand, D.V. 1988. The future of the Department of the Interior OCS studies program. Oceans '88. Proceedings of a Conference sponsored by the Marine Technology Society and IEEE. Vol. I. IEE Cat. No. 88-CH2585-8, Baltimore, Md.

Boehm, P.D., and Requejo, A.G. 1986. Overview of the recent sediment hydrocarbon geochemistry of Atlantic and Gulf Coast over continental shelf environments. Estuarine Coastal Shelf Sci. **23**: 29–58.

Boesch, D.F., Bulter, J.N., Cacchione, D.A., Geraci, J.R., Neff, J.M., Ray, J.P., and Teal, J.M. 1987. An assessment of the long-term effects of U.S. offshore oil and gas development activities: future research needs. *In* Long-term environmental effects of offshore oil and gas development. *Edited by* D.F. Boesch and N.N. Rabalais. Elsevier Applied Science, New York. pp. 1–53.

Boothe, P.N., and Presley, B.J. 1985. Distribution and behavior of drilling fluids and cuttings around Gulf of Mexico drilling sites. American Petroleum Institute, Washington, D.C.

Boothe, P.N., and Presley, B.J. 1987. The effects of exploratory petroleum drilling in the northwest Gulf of Mexico on trace metal concentrations in near rig sediments and organisms. Environ. Geol. Water Sci. **9**: 173–182.

Brassell, S.C., Eglinton, G., Maxwell, J.R., and Philip, R.P. 1978. Natural background of alkanes in the aquatic environment. *In* Aquatic pollutants, transformations, and biological effects. *Edited by* O. Huntzinger, L.H. van Lelyveld, and B.C.J. Zoetman. Pergamon Press, Oxford. pp. 69–86.

Chow, T.J., and Snyder, C.B. 1981. Barium in marine environment: a potential indicator of drilling contamination. *In* Proceedings on Research on Environmental Fate and Effects of Drilling Fluids and Cuttings Symposia, Lake Buena Vista, Florida, 21–23 January 1980. pp. 691–722.

Continental Shelf Associates, Inc. 1983. Environmental monitoring program for Exploratory Well No. 3, lease OCS-G 3316, Block A-384, High Island Area, South Extension near the West Flower Garden Bank. Final Report to Union Oil Company, Tequesta, Fla. 2 volumes.

Continental Shelf Associates, Inc. 1985. Environmental monitoring program for Platform "A", lease OCS-G 2759, High Island Area, South Extension, East Addition, Block A-389 near the East Flower Garden Bank. Final Report to Mobil Producing Texas and New Mexico, Inc., Houston, Tex. 3 volumes.

Houghton, J.P., Beyer, D.L., and Thielk, E.D. 1981. Effects of oil well drilling fluids on several important Alaskan marine organisms. *In* Proceedings on Research on Environmental Fate and Effects of Drilling Fluids and Cuttings Symposia, Lake Buena Vista, Florida, 21–23 January 1980. pp. 1017–1043.

Kendall, J.J. 1990. Detection of effects at long-term production sites. *In* Northern Gulf of Mexico Environmental Studies Plannning Workshop. Proceedings of a Workshop held in New Orleans, Louisiana, 15–17 August 1989. *Edited by* R.S. Carney. Prepared by Geo-Marine, Inc. OCS Study MMS 90-0018. U.S. Department of the Interior, Minerals Management Service, New Orleans, La. pp. 23–28.

Kennicutt, M.C. II (*Editor*). 1995. Gulf of Mexico Offshore Operations Monitoring Experiment, Phase I: Sublethal responses to contaminant exposure. Final report. OCS Study MMS 95-0000. U.S. Department of the Interior, Minerals Management Service, Gulf of Mexico OCS Region, New Orleans, La.

Kennicutt, M.C. II, and Comet, P. 1992. Resolution of sediment

© 1996 NRC Canada

hydrocarbon sources: multiparameter approaches. *In* Organic productivity, accumulation, and preservation in recent and ancient sediments. *Edited by* J.K. Whelan and J.W. Farrington. Columbia University Press, New York. pp. 308–337.

Kennicutt, M.C. II, Green, R.H., Montagna, P., and Roscigno, P.F. 1996. Gulf of Mexico Offshore Operations Monitoring Experiment (GOOMEX), Phase I: Sublethal responses to contaminant exposure — introduction and overview. Can. J. Fish. Aquat. Sci. **53**. This issue.

Lake Buena Vista Symposium. 1981. Research on environmental fate and effects of drilling fluids and cuttings, 21–24 January 1980, Lake Buena Vista, Fla. Vols. 1 and 2.

Long, E.R., and Morgan, L.G. 1990. The potential for biological effects of sediment-sorbed contaminants tested in the National Status and Trends Program. NOAA Tech. Memo. NOS OMA 52. U.S. Department of Commerce, National Oceanographic and Atmospheric Administration, Seattle, Wash.

Middleditch, B.S. 1981. Environmental effects of offshore production. The Buccaneer Gas and Oil Field Study. Plenum Press, New York.

National Oceanic and Atmospheric Administration (NOAA). 1993. Sampling and analytical methods of the National Status and Trends Program, National Benthic Surveillance, and Mussel Watch Projects 1984–1992. Vols. 1, 2, 3, and 4. NOAA Tech. Memo. NOS ORCA 71.

Neff, J.M., Rabalais, N.N., and Boesch, D.F. 1987. Offshore oil and gas development activities potentially causing long-term environmental effects. *In* Long-term environmental effects of offshore oil and gas development. *Edited by* D.F. Boesch and N.N. Rabalais. Elsevier Applied Science, New York. pp. 149–173.

Philp, R.P. 1985. Fossil fuel biomarkers: application and spectra. Methods in geochemistry and geophysics. Vol. 23. Elsevier, New York.

Rubinstein, N.I., Rigby, R., and D'Asaro, C.N. 1981. Acute and sublethal effects of whole used drilling fluids on representative estuarine organism. *In* Proceedings on Research on Environmental Fate and Effects of Drilling Fluids and Cuttings Symposia, Lake Buena Vista, Florida, 21–23 January 1980. pp. 828–846.

Southwest Research Institute. 1978. Ecological investigations of petroleum production platforms in the central Gulf of Mexico. Report Prepared for the U.S. Department of Commerce.

Tornberg, L.D., Thielk, E.D., Nakatani, R.E., Miller, R.C., and Hillman, S.O. 1981. Toxicity of drilling fluids to marine organisms in the Beaufort Sea, Alaska. *In* Proceedings on Research on Environmental Fate and Effects of Drilling Fluids and Cuttings Symposia, Lake Buena Vista, Florida, 21–23 January 1980. pp. 997–1016.

© 1996 NRC Canada

Benthic infaunal long-term response to offshore production platforms in the Gulf of Mexico

Paul A. Montagna and Donald E. Harper, Jr.

Abstract: Meiofaunal and macroinfaunal communities around three gas platforms on the continental shelf (29–157 m water depths) in the Gulf of Mexico were assessed for sublethal or persistent effects of chronic exposure to contaminants associated with long-term production. Subsamples of boxcores were collected from five distances (30–3000 m) along five radii from each platform during winter and spring in two years. In contrast with platforms in the North Sea, effects were very localized, extending to 100 m from the platforms. Total polychaete and nonselective deposit-feeding nematode density increased near platforms. Amphipod and harpacticoid abundance and diversity and harpacticoid reproductive success declined near platforms. Organic enrichment, contamination by toxicants (e.g., heavy metals and hydrocarbons), and changes in sediment granulometry are confounded along the gradient of distance from platforms. However, the pattern of community change in both meiofauna and macrofauna around these gas production platforms follows an emerging paradigm of response in which density increases of deposit-feeding polychaetes and nematodes indicate organic enrichment, while density declines of harpacticoids and amphipods indicate toxicity.

Résumé : Les communautés de méio- et de macro-endofaune autour de trois plates-formes d'exploitation gazière situées sur la plateau continental (profondeurs d'eau variant de 29 à 157 m) dans le golfe du Mexique ont fait l'objet d'une étude visant à évaluer les effets sublétaux et persistants de l'exposition chronique à des contaminants liés à l'exploitation à long terme. Des sous-échantillons ont été prélevés à cinq endroits différents (distances variant de 30 à 3 000 m) le long de cinq droites rayonnant autour des plates-formes. L'échantillonnage a eu lieu en hiver et au printemps au cours de deux années différentes. Contrairement à la situation observée dans le cas des plates-formes situées en mer du Nord, les effets étaient très localisés puisqu'ils se sont fait sentir jusqu'à une distance de 100 m des plates-formes. La densité totale de polychètes et de nématodes limivores non sélectifs a augmenté près des plate-formes. L'abondance et la diversité des amphipodes et des harpacticoïdes ont diminué et le taux de reproduction de ces derniers a diminué à proximité des plates-formes. L'enrichissement organique, la contamination par des produits toxiques (p. ex. métaux lourds et hydrocarbures) et des changements touchant la granulométrie des sédiments se confondent le long du gradient de distance par rapport aux plates-formes. Toutefois, les changements touchant les communautés de méio- et de macro-endofaune autour de ces plates-formes d'exploitation gazière suivent un nouveau paradigme de réponse selon lequel l'augmentation de la densité des polychètes et nématodes limivores indique un enrichissement organique, tandis que la diminution de la densité des amphipodes et des harpacticoïdes indique une toxicité. [Traduit par la Rédaction]

Introduction

The development of offshore oil and gas reserves has been accompanied by good support for marine environmental research. This literature has been reviewed, and it is known that the acute effects of oil spills and drilling discharges are localized and unlikely to have regional significance (NRC 1975, 1985). However, much less is known about long-term chronic effects associated with low-level disturbances (Boesch and Rabalais 1987). The goal of the Gulf of Mexico Offshore Operations Monitoring Experiment (GOOMEX) was to develop and recommend sensitive and appropriate techniques for monitoring activities of offshore oil and gas production (Kennicutt et al. 1996*a*). To accomplish this goal, a broad range of biological, biochemical, and chemical methodologies were tested to detect and assess potential chronic, sublethal, and long-term effects of offshore oil and gas production. Other GOOMEX studies report on the detoxification response by fish and invertebrates to contaminant exposure (McDonald et al. 1996), sediment toxicity to invertebrates (Carr et al. 1996), effects on harpacticoid population genetic structure (Street and Montagna 1996), and effects on megaepifaunal reproduction and ecology (Ellis et al. 1996). The present report documents the impacts of contaminant exposure on benthic infauna at the community level.

The benthic infaunal component of the GOOMEX program focused on organisms that live in sediments. There is a wealth of literature in which benthos is used to detect environmental impacts for reasons well detailed by Warwick (1993). Both meiofauna and macrofauna were studied during GOOMEX. Meiofauna are small metazoans, passing through a 500-μm sieve and retained on a 63-μm sieve. Macrofauna

Received March 21, 1996. Accepted September 13, 1996.
J13409

P.A. Montagna. Marine Science Institute, University of Texas, 750 Channelview Dr., Port Aransas, TX 78373, U.S.A.
D.E. Harper, Jr. Marine Laboratory, Texas A&M University, 5007 Avenue U, Galveston, TX 77551, U.S.A.

© 1996 NRC Canada

are larger, being retained on a 500-μm sieve. In 1971, Thiel suggested that the grouping of benthic organisms according to size differences had little taxonomic or ecological justification, except convenience of sample processing (quoted from Thiel 1975). However, the explosive growth of ecological literature since 1971 has shown that meiofauna are different from macrofauna and have different roles in marine ecosystems (for reviews, see Coull and Bell 1979; Coull and Palmer 1984). Even where meiofauna share ecological properties with macrofauna, the processes operate on much smaller spatial and temporal scales (Bell 1980). Although the operational definition of these two groups is based on sieve sizes, the groups are dominated by different phylogenetic taxa. The meiofauna are composed primarily of nematodes and harpacticoid copepods. Macrofauna are composed primarily of polychaetes, mollusks, and peracarid crustaceans (mainly amphipods). Meiofauna and macrofauna have different characteristics that are either advantageous or disadvantageous for detecting environmental gradients (Warwick 1988*b*, 1993). Studying both groups allows detection of changes at different levels, which are a function of different ecological processes, affecting each group. Concordance of a finding among both groups is strong evidence for generality of an effect.

The response variables examined for both the meiofauna and the macrofauna were total abundance, abundance of particular groups that are known to be sensitive or resilient to contamination, and community structure. Additional data were collected for the meiofaunal component. Harpacticoid genetic diversity and life history characteristics were determined to examine some specific sublethal population responses, and nematode biomass and feeding guilds were determined to test for changes in community trophic dynamics. We tested hypotheses relating changes in benthic infauna with respect to distance from the platforms and to chemical contaminant gradients. Abundance changes were examined using analysis of variance (ANOVA) procedures. Community structure changes were examined using univariate analyses on diversity indices and multivariate analysis on the species data. To detect change as a function of contamination, infaunal changes were compared with changes in the environmental setting near the platforms.

Materials and methods

Field methods

Samples for both infaunal groups came from randomly selected subcores within a partitioned "vegematic box core" (Jumars 1975). Each boxcore (area = 0.25 m^2) was subdivided into 25 subcores. Two meiofauna cores (area = 2.8 cm^2, to a depth of 2 cm) were taken from two different subcores of each boxcore. Three subcores (area = 100 cm^2, to a depth of 10 cm) were taken for macrofauna. Samples for community structure measurements were preserved with buffered formalin in the field and analyzed back at the laboratory. Macrofauna were removed from sediment with a 500-μm-mesh sieve in the field, and meiofauna were removed using a 63-μm-mesh sieve in the laboratory. All macrofauna and harpacticoids and nematodes within the meiofauna were identified to the species level or the lowest taxonomic level possible.

Meiofaunal samples received additional treatment. Abundance and biomass of nematode trophic groups were determined to gain insight on how trophic interactions might be affected. Nematodes were chosen because they are numerically dominant and trophically diverse. Nematodes were sorted into feeding groups according to the classification proposed by Wieser (1953). Biomass was calculated from the product of microscopical measurement of body length and width and a conversion value (Andrassy 1956).

Sampling design

Experimental design and data analysis are described in detail in Kennicutt et al. (1996*a*). Briefly, there were four cruises (C_{1-4}: one in summer and winter, in two consecutive years), three platforms (P_{1-3}: MAI-686, MU-A85, and HI-A389, each at progressively deeper water depths), and five distances away from a platform (D_{1-5}: 50, 100, 200, 500, and 3000 m), where each distance was sample on a radial transect from the platform (R_{1-5}). The five radii were symetrical around MAI-686 and MU-A85, but not at HI-A389. At HI-A389, all radii were southeast of the platform deeper than the 100-m depth contour because there is a shallow (~50 m) reef (the Flower Gardens) northwest of the platform. The experimental design is a complex, partially hierarchical design, where the radial transect is a random nested variable within platforms. A total of 25 boxcores were taken at each platform during each cruise (=5 R × 5 D). From each boxcore, two meiofaunal cores and three macrofaunal subcores were taken as samples. The five radii are the true replicates because the subcore samples are pseudoreplicates. Therefore, the expected mean square for each main effect was calculated to determine the appropriate mean square to use as the denominator in the *F*-test. All data were transformed using natural logarithms. Abundance ratios were calculated as the difference of the log-transformed variables. All diversity indices were also calculated using natural logarithms. Calculated variables (i.e., diversity, taxa ratios, and nematode biomass) were calculated on pooled samples from each boxcore. Community structure (of harpacticoids, nematodes, and macrofauna) was analyzed by principal components analysis (PCA). The PCA was done two ways: by species and by family. In all cases the community structure data set was composed of 300 observations, one for each boxcore. Two null hypotheses were tested using the meiofaunal and macrofaunal data:

H_0: There are no differences in any community measures among seasons, platforms (or platform groups), or with distance or direction away from platforms (or platform groups).

H_0: There are no functional responses to chemical contaminant gradients at platforms (or platform groups) by infaunal community measures.

The first hypothesis was tested with a univariate ANOVA for all variables being measured at all stations in the study. Tukey tests were used to find significant differences among means, and linear contrasts were used to test for linear responses with respect to distance from a platform (SAS Institute Inc. 1990). All references to statistical models use SAS notation (SAS Institute Inc. 1990) Graphics of distributions around platforms were constructed using a contouring procedure (SAS Institute Inc. 1990). Over 100 environmental variables were measured from each boxcore (Kennicutt et al. 1996*b*).

The second hypothesis was designed to test for changes with respect to any chemical contaminant gradients that might exist among and within sediments of platforms stations. The second hypothesis is tested using a multivariate approach. In the univariate ANOVA the categorical variables, particularly D (distance from a platform), are just surrogates of the contaminant gradient that might exist around a platform. However, the chemical contaminant concentrations in sediments were meaured and are described in Kennicutt et al. (1996*b*). The chemical data were reduced to two principal components labeled ChemPC1 and ChemPC2. The prefix "Chem" is added to the suffix "PC" to distinguish this result from the PC performed on species data. The first axis, ChemPC1, represents changes in the abiotic setting with respect to distance from platforms, where positive values represent higher concentrations of sand, alkanes, unresolved complex mixture (UCM), Cd, Ba, and PAH. ChemPC1 explained 44% of the variance in the data set. The second axis,

© 1996 NRC Canada

Table 1. Overall average abundance and diversity for meiofauna variables at all platforms, stations, and cruises.

Variable	HI-A389	MAI-686	MU-A85	Mean
Meiofaunal density	734	2571	846	1169
Nematode density	481	1864	482	757
Harpacticoid density	85	283	171	161
Other meiofaunal density	100	369	164	182
Nematode biomass	0.674	1.084	1.280	1.000
NC ratio	5.64	6.60	2.81	5.02
Nematode diversity	2.74	3.12	3.31	3.06
Harpacticoid diversity	2.00	2.56	2.52	2.36

Note: Numbers for density (individuals/10 cm^2) and for biomass (mg wet weight/10 cm^2) are detransformed from $\log_e$. Averages for 200 samples. Diversity values are the Shannon–Weaver index (H') pooled by boxcore (average for 100 samples).

Table 2. Probability values for tests from a hierarchical ANOVA of meiofauna variables for the total design of the sampling program.

No.	Source	df	EMS	Total	NEMA	HARP	OTHE	NC	NBIO	NH'	HH'
1	C	3	1/9	0.0742	0.0054	0.0302	0.0023	0.0021	0.1037	0.0001	0.0001
2	P	2	2/8	0.0001	0.0001	0.0001	0.0001	0.0009	0.0001	0.0001	0.0001
3	P·C	6	3/9	0.0001	0.0001	0.0001	0.0037	0.0048	0.0001	0.0001	0.0010
4	D	4	4/10	0.2102	0.2437	0.0030	0.0001	0.0092	0.1072	0.0001	0.0002
5	C·D	12	5/11	0.0009	0.0005	0.0162	0.0007	0.0726	0.5095	0.1358	0.3798
6	P·D	8	6/10	0.0277	0.0214	0.0724	0.0106	0.0001	0.0383	0.0001	0.0824
7	P·C·D	24	7/11	0.2254	0.0594	0.3382	0.1969	0.0118	0.0425	0.5342	0.7013
8	R(P)	12	8/(9 + 10 – 11)	0.0138	0.0130	0.5065	0.2157	0.0062	0.0181	0.0223	0.7164
9	C·R(P)	36	9/11	0.5058	0.4367	0.2482	0.3336	0.0529	0.4428	0.6341	0.9643
10	D·R(P)	48	10/11	0.0001	0.0001	0.0001	0.4318	0.0001	0.0001	0.0001	0.0001
11	C·D·R(P)	144	11/12	0.0001	0.0302	0.0001	0.0001	0.0285	0.0001		
12	Error	300									

Note: The model includes four cruises (C), three platforms (P), five distances (D), five radii (R), and two replicates: variable = C P C·P D C·D P·D C·P·D R(P) C·R(P) D·R(P) where P, D, and C are fixed and R is random. Performed on log-transformed data. The table gives line number (No.), source for variation, degrees of freedom (df), expected mean squares (EMS) in terms of the numerator and denominator mean square for the F-test, and probability values for the meiofauna variables. Total = total meiofauna density, NEMA = nematode density, HARP = harpacticoid density, OTHE = other meiofauna density, NC = density ratio between nematode and harpacticoid, NBIO = nematode biomass, NH' = nematode diversity, HH' = harpacticoid diversity. Diversity values pooled by boxcore.

ChemPC2, represents differences among the platforms, where positive ChemPC2 values are due to platform HI-A389, neutral values are MU-A85, and negative values are MAI-686. ChemPC2 contained 25% of the variance in the data set. Biological responses were correlated with ChemPC1 and ChemPC2 to determine if a relationship exists between contaminants and responses.

Results

Meiofaunal communities

The overall detransformed average density for the meiofaunal community was 1170 individuals/10 cm^2 in the top 2 cm of sediment (Table 1). Sixty-nine percent of the community was composed of nematodes, which averaged 757 individuals/10 cm^2. Fifteen percent of the community was composed of harpacticoids, which averaged 161 individuals/10 cm^2. The remaining 16% of the community was composed of 11 "other" taxa, which averaged 182 individuals/10 cm^2. The "other" taxa were Kinorhyncha, Polychaeta, Ostracoda, Mollusca, Rhynchocoela, Amphipoda, Isopoda, Tanaidacea, Cumacea, Priapulida, and unknown or unidentifiable soft-body taxa. Nematode biomass averaged 1.00 mg wet weight/10 cm^2. Nematode communities were more diverse (H' of 3.06) than harpacticoid communities (H' of 2.36). Abundance decreased from MAI-686 to MU-A85 to HI-A389 (Table 1). There are two gradients of independent environmental variables correlated with trend. Water depths increase and contaminant concentrations increase along this gradient. Therefore, depth and contamination are confounded, and we cannot simply conclude that differences among platforms represent differences in contamination. Three meiofauna variables do not follow the trend: nematode to copepod (NC) density ratio, nematode biomass, and nematode diversity.

Total sample design analysis was performed to detect interactions among cruises, platforms, and distances from platforms (Table 2). The model is complex, and because our samples were pseudoreplicates, all F-tests are calculated using a random term (i.e., something with R(P) in it) as the denominator (Table 2). The four-way interaction (C·D·R(P)) is the only term that uses the mean square error as the denominator in the F-test (Table 2, line 11). Because samples were within boxcore replicates, the C·D·R(P) interaction represents differences among boxcores, not interactions among

© 1996 NRC Canada

Table 3. Probability values for ANOVA by platform on log-transformed meiofauna variables.

No.	Source	df	EMS	Total	NEMA	HARP	OTHE	NC	NBIO	NH'	HH'
					A. HI-A389						
1	C	3	1/5	0.0072	0.0061	0.0004	0.5966	0.2482	0.3492	0.0001	0.0001
2	D	4	2/6	0.7866	0.6297	0.1997	0.0185	0.0020	0.2881	0.0792	0.0792
3	C·D	12	3/7	0.1753	0.0910	0.0359	0.0136	0.0859	0.0911	0.6117	0.6117
4	R	4	4/(5 + 6 + 7)	0.0681	0.0623	0.5368	0.3555	0.0212	0.0544	0.0001	0.0001
5	C·R	12	5/7	0.4161	0.2214	0.9410	0.4332	0.4438	0.3608	0.4924	0.4924
6	D·R	16	6/7	0.0001	0.0001	0.0001	0.0633	0.0001	0.0001	0.0084	0.0084
7	C·D·R	48	7/8	0.0001	0.0001	0.1130	0.8176	0.0701	0.0648		
8	Error	100									
					B. MAI-686						
1	C	3	1/5	0.0485	0.0493	0.0012	0.0719	0.0014	0.0015	0.0346	0.0001
2	D	4	2/6	0.0006	0.0013	0.0002	0.0003	0.5897	0.0691	0.9026	0.4891
3	C·D	12	3/7	0.0100	0.0041	0.1411	0.1171	0.0569	0.0667	0.1733	0.6617
4	R	4	4/(5 + 6 + 7)	0.4675	0.4221	0.5614	0.7521	0.4589	0.6451	0.9061	0.0117
5	C·R	12	5/7	0.2601	0.3097	0.0966	0.2278	0.0787	0.2102	0.4531	0.5657
6	D·R	16	6/7	0.1943	0.1024	0.2548	0.7152	0.1685	0.3263	0.1433	0.3231
7	C·D·R	48	7/8	0.0001	0.0001	0.0001	0.0001	0.0983	0.0027		
8	Error	100									
					C. MU-A85						
1	C	3	1/5	0.0046	0.0005	0.2466	0.0001	0.0742	0.0356	0.0001	0.0036
2	D	4	2/6	0.0009	0.0005	0.2085	0.0087	0.0233	0.0020	0.1828	0.2399
3	C·D	12	3/7	0.2383	0.0836	0.6441	0.0794	0.0502	0.1761	0.6760	0.5289
4	R	4	4/(5 + 6 + 7)	0.8980	0.7440	0.1570	0.0924	0.7487	0.5303	0.0697	0.1224
5	C·R	12	5/7	0.9074	0.9759	0.2755	0.7657	0.0124	0.9122	0.0422	0.6381
6	D·R	16	6/7	0.9074	0.7324	0.7137	0.6293	0.0035	0.2044	0.0158	0.6677
7	C·D·R	48	7/8	0.0001	0.0001	0.0004	0.0155	0.4840	0.0001		
8	Error	100									

Note: The model includes four cruises (C), five distances (D), five radii (R), and two pseudoreplicates: variable = C R C·R D C·D R·D C·P·D where D and C are fixed and R is random. All abbreviations as in Table 2.

the main effects. Therefore, C·D·R(P) is always significant and signifies that each of the 300 boxcores was different. The C·D·R(P) interaction does not exist for diversity because diversity was calculated per boxcore. Interactions among cruises, platforms, and distances mean that overall analyses cannot be interpreted simply, and a decomposition of the ANOVA model is necessary. P·C interactions were generally strong (Table 2, line 3), occurring for all meiofaunal variables measured, meaning that seasonal and interannual community change was different among platforms. P·C·D interactions did not occur (Table 2, line 7), meaning that distance effects were constant (i.e., parallel) across cruises and among platforms. The D·R(P) interaction is very strong ($P = 0.0001$, Table 2, line 10), except for other meiofauna, indicating that distance effects are different among radii among all platforms. Therefore, it is most useful to analyze each platform independently.

When the data are analyzed by P, the triple interaction (C·D·R) represents differences among the replicate boxcores because it is tested against error mean square (Table 3, lines 7). All main effects are tested against this term or a lower order interaction with R. If effects were asymmetrical about a platform, then we would expect significant interactions to occur. Therefore, the most interesting test is for D·R interactions. The D·R interactions were very strong at HI-A389, but were not present for MAI-686 or MU-A85 (Table 3, lines A6, B6, and C6). This means that the response at HI-A389 is very different from the other two platforms. A nonsignificant D·R interaction means that there was a parallel response among distances, i.e., there were contours or symmetry of response about a platform. In contrast, a significant D·R interaction indicates different responses with distance and direction or an asymmetrical response around a platform. There were asymmetric distributions of meiofauna around HI-A389, but not at the other two platforms. Changes in total meiofauna, nematode, and "other meiofauna" density were statistically significant with respect to distance from the other two platforms (Table 3, lines B2 and C2). The platform MAI-686 had significant differences for harpacticoid density (Table 3B). The platform MU-A85 had significant differences for the NC ratio and nematode biomass (Table 3C). Multiple comparison tests are useless for HI-A389, but valid for the other two platforms.

There was an abundance and diverisity gradient, with den-

© 1996 NRC Canada

Table 4. Tukey multiple comparison test to compare distances for meiofaunal variables at two plantforms.

A. MAI-686					
Distance	3000	500	200	100	50
Total meiofauna density	3868	3534	2477	1976	1681
Distance	3000	500	200	100	50
Nematode density	2818	2589	2589	1786	1451
Distance	3000	500	200	100	50
Harpacticoid density	449	402	297	205	164
Distance	3000	500	200	100	50
Other meiofauna density	534	490	353	278	267
Distance	50	3000	100	500	200
NC ratio	15.2	13.1	12.6	11.3	10.2
Distance	3000	500	200	100	50
Nematode biomass	2.48	1.17	0.98	0.85	0.42
Distances	50	100	200	500	3000
Nematode diversity	3.16	3.13	3.12	3.11	3.10
Distance	3000	500	200	100	50
Harpacticoid diversity	2.75	2.73	2.62	2.44	2.24
B. MU-A85					
Distance	100	500	200	3000	50
Total meiofauna density	1098	892	874	782	647
Distance	100	500	200	3000	50
Nematode density	660	533	525	434	326
Distance	100	50	500	200	3000
Harpacticoid density	212	167	166	162	156
Distance	100	500	3000	200	50
Other meiofauna density	191	180	173	162	125
Distance	200	500	100	3000	50
NC ratio	7.1	6.4	6.2	5.7	4.3
Distance	3000	200	500	100	50
Nematode biomass	2.16	1.75	1.63	1.18	0.23
Distance	100	200	3000	500	50
Nematode diversity	3.45	3.37	3.31	3.27	3.18
Distance	100	500	3000	200	50
Harpacticoid diversity	2.69	2.54	2.51	2.48	2.38

Note: The table finds distance from platform (m) and detransformed mean (n/10 cm^2). Means that are underlined are not different at the 0.05 level.

sity of all taxa and harpacticoid diversity increasing with distance away from platform MAI-686 (Table 4A, Tukey test). Nematode diversity decreased with distance away from the platform. Although the *F*-test for differences among means was not significant for the diversity of nematode biomass (Table 3B), there was a linear relationship between distance and response for these three variables (Table 4A, linear contrast). The trend was not clearly defined at the MU-A85 platform (Table 4B). Nematode density and biomass and "other meiofauna" and total meiofauna density were lowest at the station nearest the platform (50 m), but there was no linear trend with any of the variables and distance from the platform (Table 4B).

The asymmetrical responses at HI-A389 and the more symmetrical responses at MAI-686 and MU-A85 were also detected using a graphical contouring technique (Figs. 1–5). The highest abundance for total meiofauna and nematodes was found southwest of HI-A389 (Figs. 1 and 2). Harpacticoid abundance was highest southeast of HI-A389, but always away from the platform (Fig. 3). The other two platforms had more symmetrical responses. Harpacticoid diversity was always lowest just near the platform, and increased away from the platform (Fig. 4). Nematode diversity increased away from all three platforms (Fig. 5).

The harpacticoid community was very diverse. A total of 154 species of harpacticoids were found. Only nine of the

© 1996 NRC Canada

Fig. 1. Areal distribution of mean total meiofaunal density for all four cruises.

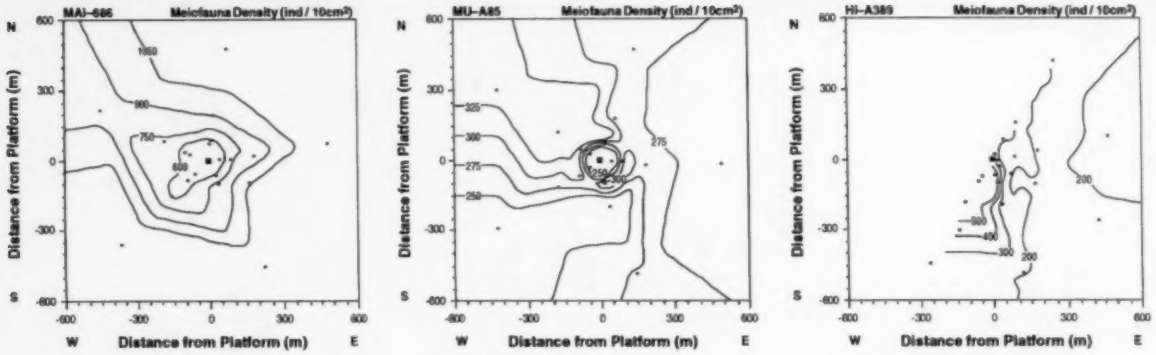

Fig. 2. Areal distribution of mean nematode density for all four cruises.

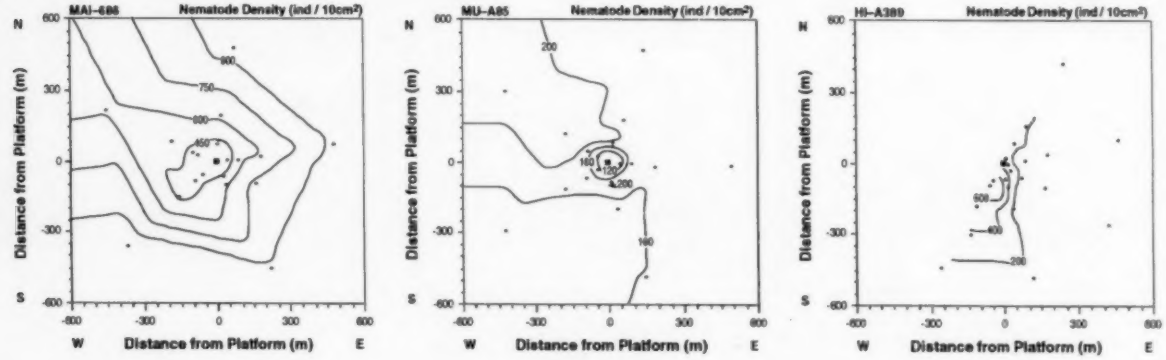

Fig. 3. Areal distribution of mean harpacticoid density for all four cruises.

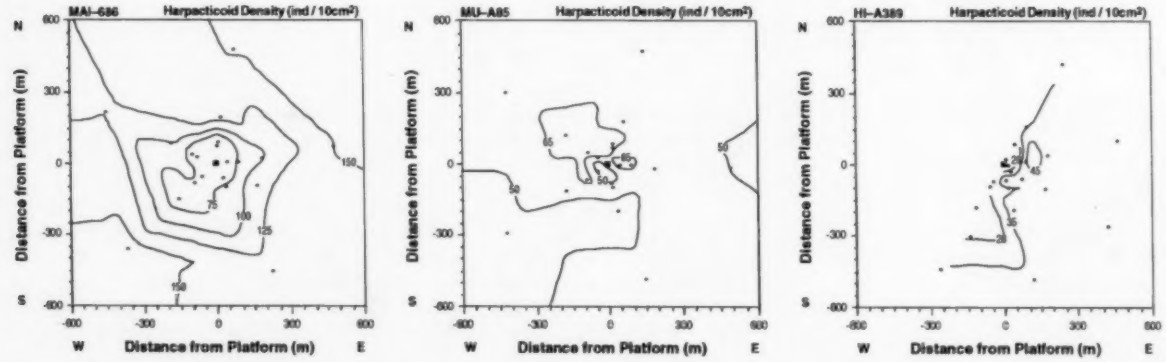

species were easily distinguished as described species. We presume that the rest are either new to science or that the Gulf of Mexico variant is undescribed. Members of the Ectinosomatidae dominated the fauna. This family has long, torpedo-like body shapes, and most members are very small. Two PCAs were performed on the community: one where species were grouped by families (Fig. 6A) and one by species (Fig. 6B). The species PCA indicates that there were large differences in community structure among platforms (Fig. 6B). Platform MU-A85 shared harpacticoid species in common with HI-A389 and MAI-686, which were very different from one another (Fig. 6B). For harpacticoids at the family level,

© 1996 NRC Canada

Fig. 4. Areal distribution of mean harpacicoid diversity (H' to $\log_e$) for all four cruises.

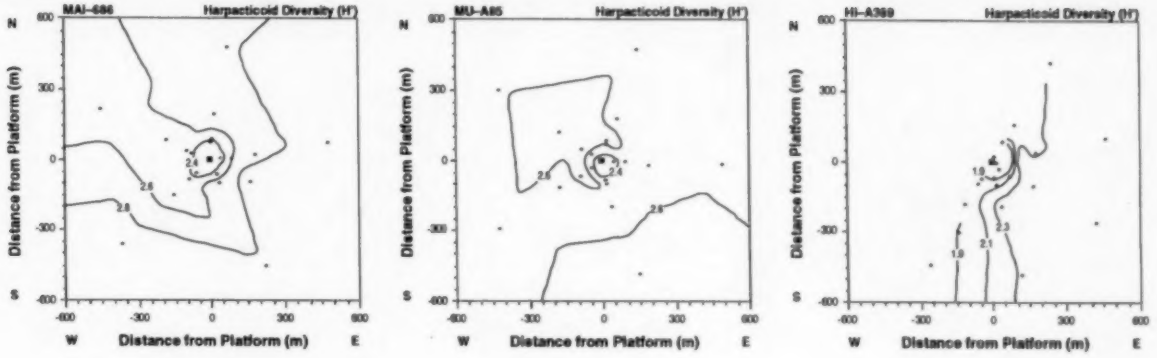

Fig. 5. Areal distribution of mean nematode diversity (H' to $\log_e$) for all four cruises.

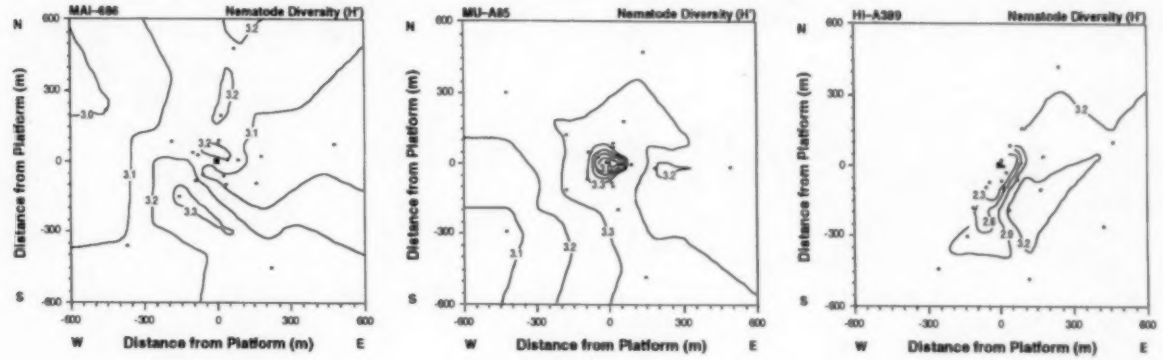

platform differences are still obvious (Fig. 6A), but not as obvious at the species level (Fig. 6B).

The nematode community was also very diverse, containing 130 species. The community was cosmopolitan, with 31 species being similar to known species. Again, we presume that the rest of the species are new to science or that the Gulf of Mexico variants are unknown. Unlike the harpacticoids, no family dominated the nematode fauna. However, dominance by a single species was characteristic of HI-A389 and MAI-686. At HI-A389 the dominant was *Molgolaimus turgofrons* followed by *Sabatieria ornata*, *Linhomoeus gittingsi*, and *Halalaimus meyeri*. At MAI-686 the dominant species was *Desmodora curvispiculum* followed by *Actinonema* sp. 1, *Microlaimus* sp. 1, and *Tricocoma filipjevi*. At MU-A85, dominance was shared by about 12 species. The most abundant (in order) were *Halalaimus thalassinus*, *Pselionema* sp. 1, *Sabatieria punctata*, *Elzalia* sp. 1, and *Cervonema* sp. 3. There was no overlap in the dominant species at the three platforms. Based on PCA, the pattern of community structure was very similar at the family and species level (compare Figs. 7A and 7B). In both cases, the two deeper platforms (MU-A85 and HI-A389) shared some families or species, but the shallowest platform (MAI-686) was very different from the two deep platforms (Fig. 7, PCA). The shallower platform is somewhat more different at the species level.

To find differences with respect to distances from a platform, the PCAs were also computed by platform for families and species. This is necessary because the platforms have different families and species of harpacticoids and nematodes (Figs. 6 and 7), which would confound distance effects.

For both harpacticoid families and species, PC1 is weakly separating distances from platform MAI-686 (Fig. 8). All of the 50-m stations had negative PC1 loading scores for both families and species. For families, the farther stations (>500 m) had positive loading scores (Fig. 8A), but many of these stations had negative scores at the species level (Fig. 8B). At MU-A85 and HI-A389, distance appears to be more heavily loaded on PC2 (Figs. 9 and 10). There were differences in community structure at the species level due to inner rings (50 and 100 m) at the deeper platforms, MU-A85 and HI-A389 (Figs. 9B and 10B). At MU-A85, distance effects are noticeable at the family level (Fig. 9A) with high loadings for PCA1 at stations at 50 and 100 m. At HI-A389, differences at the species level were represented by negative PC1 and PC2 scores (Fig. 10B), and differences at the family level were represented by positive PC2 scores (Fig. 10A).

Nematode species and family trends were very similar to

© 1996 NRC Canada

Fig. 6. PCA of harpacticoids for all platforms. (A) Families; (B) species.

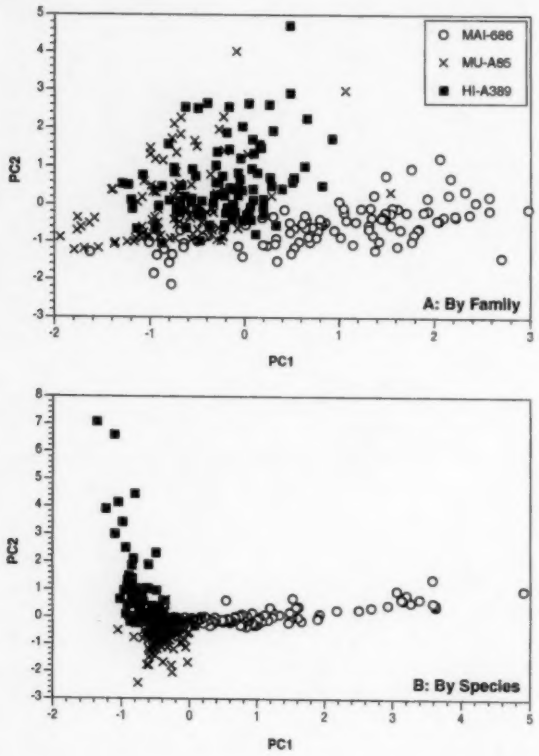

Fig. 7. PCA of nematodes for all platforms. (A) Families; (B) species.

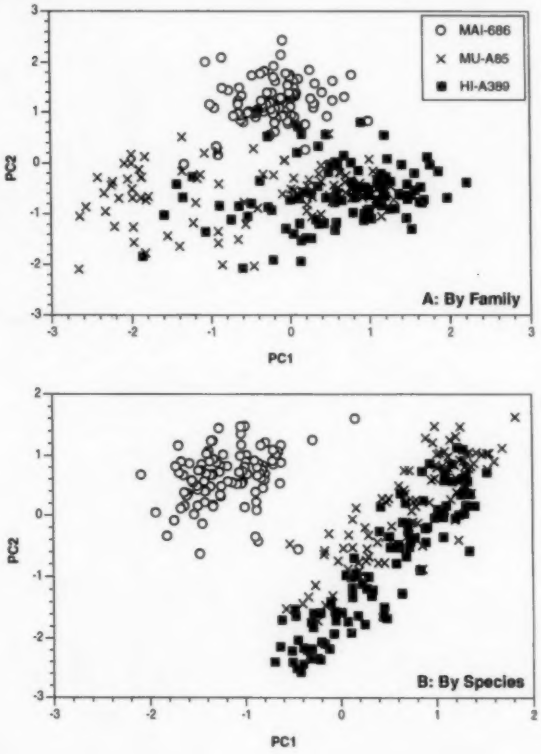

the harpacticoid trends, with the 50- and 100-m stations clustering together at each platform (Figs. 11–13). The distribution at MAI-686 was due to positive PC2 loadings for families (Fig. 11A) and negative PC2 loadings for species (Fig. 11B) at the 50- and 100-m stations. Distances near MU-A85 were positively loaded on PC2 for family (Fig. 12A) and negatively loaded on PC1 for species (Fig. 12B). At MU-A85, the 50- and 100-m stations clustered apart, and separate from all other stations at both the family (Fig. 12A) and species (Fig. 12B) levels. At HI-A389, distance near the platform was negatively loaded on PC1 for both families and species (Fig. 12). There was some overlap of 100-m stations with 50-m stations for both families (Fig. 12A) and species (Fig. 12B).

Although effects on meiofaunal abundance and diversity can be found with respect to distance from platforms, the distance category itself is just a surrogate for changes in the environment related to the platform. In each boxcore from which biological data were obtained, a large suite of environmental variables was also measured (Kennicutt et al. 1996*b*). A PCA was performed on all the environmental variables to extract two principal components axes (ChemPC) that could be used to describe variability in the environmental data set. When the entire data set is analyzed, ChemPC1 is related to the contaminant gradient associated with distance from platforms, and ChemPC2 is related to the differences among the platforms (Kennicutt et al. 1996*b*). Positive values of the ChemPC1 axis represent high levels of a suite of heavy metals (Ba, Cd, Hg, Pb, and Zn) and sand content. Therefore, ChemPC1 increases near platforms. Positive values of the ChemPC2 axis are related to variables that change with the water depth of a platform, i.e., the mud content and total contaminant load at a platform. The water depth gradient is confounded with the contaminant gradient among platforms. The ChemPC axes can be correlated with meiofaunal variables to test the hypothesis that meiofaunal response is due to changes in the environment (Table 5). The advantage of this test is that by relating environmental differences with meiofaunal responses in each sample, we avoid the difficulty of complex interpretations due to significant interactions in the ANOVA tests.

Total meiofauna density and nematode density did not have a significant relationship with ChemPC1 (Table 5). Harpacticoid and other meiofauna density and harpacticoid and nematode diversity had a significant negative relationship with ChemPC1 and ChemPC2. Nematode feeding groups exhibited an interesting pattern. Nonselective deposit and epigrowth feeders increased near platforms, and selective deposit feeders decreased near platforms (Table 5). All meiofauna variables decreased with ChemPC2. This means that, in general, as depth and contamination increase, declines in meiofauna population abundance and diversity will also

© 1996 NRC Canada

Fig. 8. PCA of harpacticoids at platform MAI-686. (A) Families; (B) species.

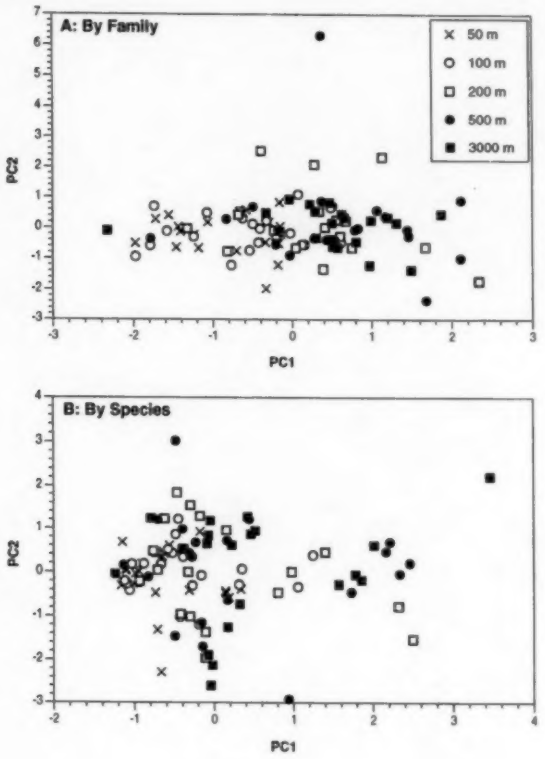

Fig. 9. PCA of harpacticoids at platform MU-A85. (A) Families; (B) species.

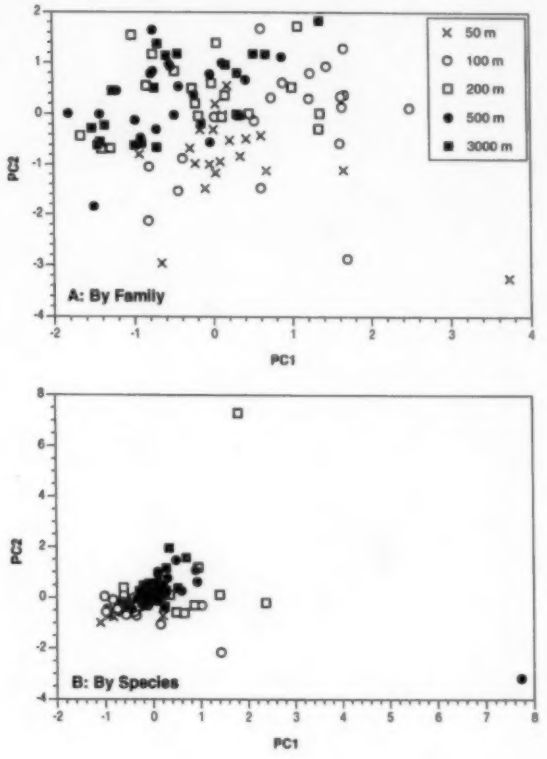

occur. The NC ratio has a positive relationship with all ChemPC factors because harpacticoid abundance declines relative to nematode abundance with depth and with proximity to platforms.

The abiotic PCA was also computed by platform. Positive values of the first component (ChemPC1) are still related to distance effects at each platform. The only variable with a consistent trend of negative correlation with ChemPC1 is other meiofauna density (Table 6). There are negative correlations with increases in the contamination gradient for harpacticoid density and diversity at HI-A389 and MAI-686 (Table 6). Nematode diversity was also negatively correlated with ChemPC1 at HI-A389.

When the abiotic PCA is computed by platform, the meaning of the second component (ChemPC2) changes. Negative values represent winter cruises and positive values represent summer cruises, but loading of variables are different at each platform and strongest at the two shallower platforms. At MAI-686, dissolved oxygen (DO) decreased in winter, but silicate, nitrate, and temperature increased in summer. At MU-A85, DO is the most negative, and salinity, temperature, and silicate are positive. There was no seasonality at the deepest platform (HI-A389). For HI-A389 only, positive values of ChemPC2 are related to increasing silt content of the sediment All meiofauna variables have a negative correlation at MAI-686, indicating that winter density and diversity values were higher than summer values (Table 6). The only exception is the NC ratio which has a positive correlation. There appears to be no seasonality at the middle-depth platform (MU-A85) because none of the correlation values was significant (Table 6).

Macrofaunal communities

Macrofaunal densities averaged about 1000/m^2 overall (Table 7). The community was predominantly composed of polychaetes (66%) and amphipods (8%), with six other higher taxa comprising a total of 26% of the community (Table 7). Of the three platforms, MU-A85, intermediate in depth between MAI-686 and HI-A389, exhibited the largest average number of macrofaunal species and diversity. However, the two dominant groups, the polychaetes and amphipods, were both in greater abundance at MAI-686.

Two indices were computed, the Shannon–Weaver diversity index (H') and a proposed polychaete to amphipod (PA) ratio (Table 7). The PA ratio is analogous to the NC ratio because polychaetes and nematodes are predominantly deposit-feeding worms, and amphipods and harpacticoids are both crustaceans. If the two crustaceans feed on similar food sources, then the PA ratio should be analogous to the NC ratio in terms of trophic structure.

All macrofaunal variables were analyzed by an ANOVA using the overall sample design with all cruises, platforms,

© 1996 NRC Canada

Fig. 10. PCA of harpacticoids at platform HI-A389. (A) Families; (B) species.

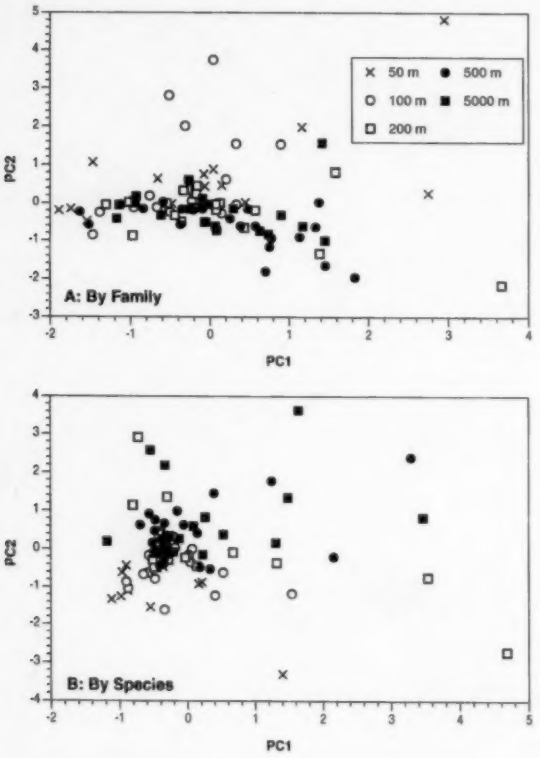

Fig. 11. PCA of nematodes at platform MAI-686. (A) Families; (B) species.

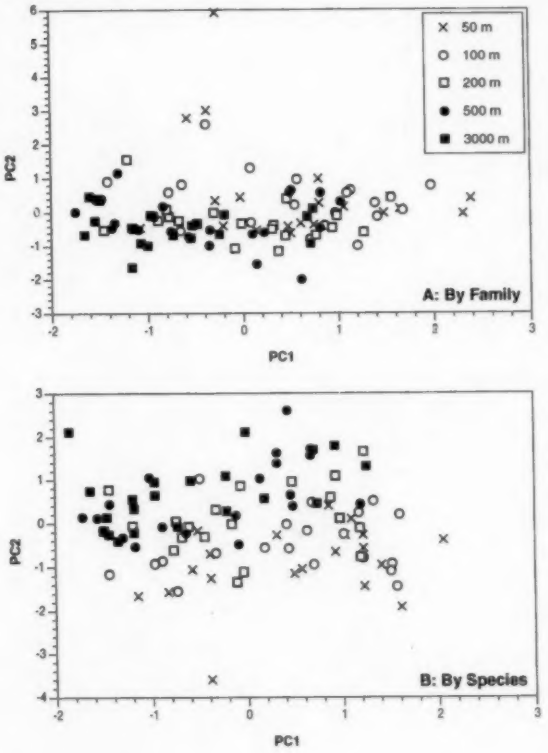

and distances included (Table 8). Ophiuroids were the only taxa that exhibited no significant interactions among P·D (Table 8). However, there were no differences in ophiuroid density with respect to platform, cruise, or distance from platforms. All the other macrofaunal variables had significant P·D interactions. The ANOVA was recomputed by platform to test for distance effects at platforms (Table 9).

At HI-A389, total density of macrofauna was significantly greater at the inner rings (Table 9A), with the 50-m station having a higher density than the 100-m station (Table 10A). Amphipods and foraminifera had significantly higher densities at far stations (1000 and 3000 m). Bivalves, decapods, and polychaetes were higher at near stations (50 and 100 m). Isopods, nemerteans, and ophiuroids were not significantly different among platforms. The PA ratio does not change with respect to distance. Species diversity was lowest at the innermost ring (50 m).

At MAI-686, few taxa had significant differences among distances from the platform (Table 9B). Total abundance was higher at the 50- and 100-m stations than all other stations, which is apparently due to higher numbers of polychaetes, decapods, isopods, nemerteans, and ophiuroids (Table 10B). However, only amphipods and nemerteans exhibited significant density trends; amphipods increased away from MAI-686, while nemerteans increased towards MAI-686. Species diversity decreased away from the platform (Table 10B).

At MU-A85, distance effects were more apparent (Table 9C). Total abundance was higher at 50 and 100 m than all other distances (Table 10C). As in MAI-686, the trend was due to higher numbers of polychaetes, decapods, isopods, nemerteans, and ophiuroids (Table 10C). However, unlike the other platforms, all these trends were significant. Foraminiferans were significantly lower at the three farthest distances, while decapods, isopods, nemerteans, and polychaetes were all in higher abundance at the inner rings. Species diversity did not change among the distances.

The pattern of macrofauna density was symmetrical about the two deeper platforms (MU-A85 and HI-A389), but not around the shallow platform (MAI-686) (Fig. 14). In general, density increased near the platform. Low densities occurred just northeast of platform MAI-686. Diversity patterns were asymmetrical about the two shallower platforms, but symmetrical about the deepest platform (Fig. 15). Although not significant, diversity was lowest near the deepest platform (HI-A389).

There were 649 species found in the macrofaunal community and these biota were used in a PCA among platforms (Fig. 16). The PCA was performed by species (Fig. 16B) and with individuals grouped at the family level (Fig. 16A). Although there were a large number of species, only 22 species were responsible for 25% of the variation in the PCA. A total of 57 species accounted for 50% of the variation, and

© 1996 NRC Canada

Fig. 12. PCA of nematodes at platform MU-A85. (A) Families; (B) species.

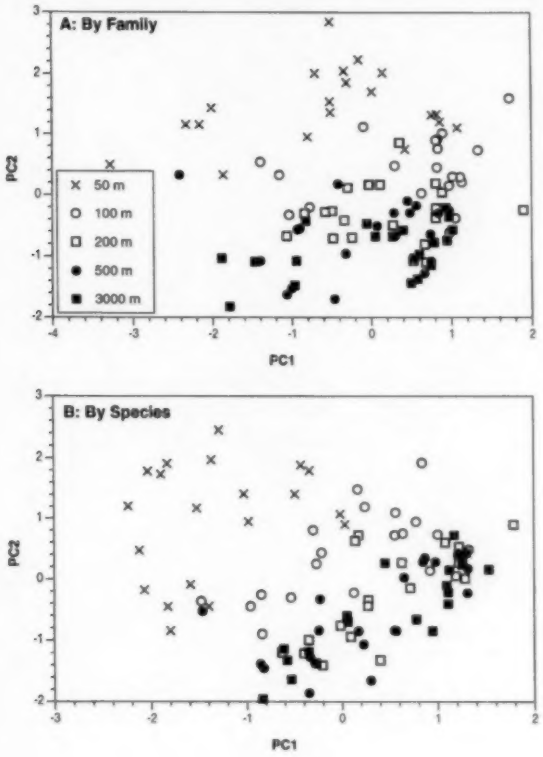

Fig. 13. PCA of nematodes at platform HI-A389. (A) Families; (B) species.

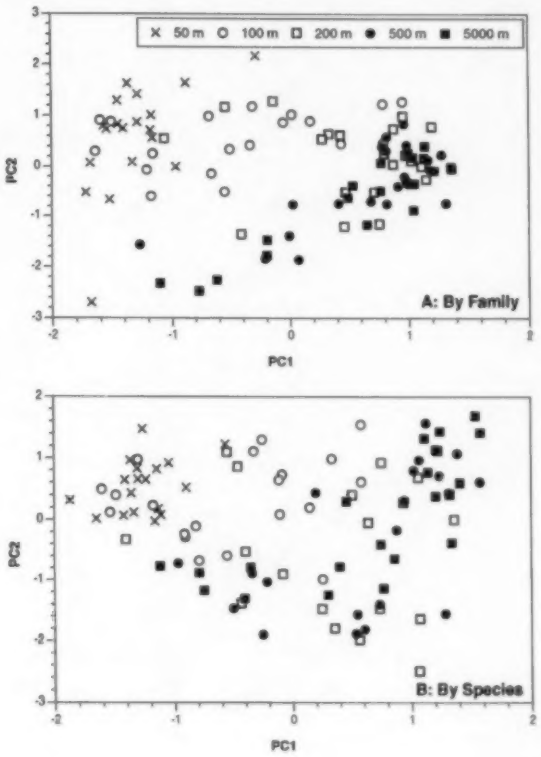

112 species were responsible for 75% of the variation in the data. The fact that less than a quarter of the macrofauna species accounted for three quarters of the variation in the data suggests that trends in macrofauna density were driven by a small number of species, and that the high diversity (approximately 500 of the species collected and identified) did not appreciably change the trend in the data. There were 42 species of amphipods. Of these, 6 accounted for 25% of the variance, 14 for 50% of the variance, and 24 for 75% of the variance. There were 310 species of polychaetes identified in the study. Fifteen of these species accounted for 25% of the variance in the data set and 39 for 50% of the variance, and 75% of the variance can be explained by only 79 species. The vast majority of total macrofauna, amphipods, and polychaetes are not distributed in any consistent species patterns.

There were platform differences in community structure at the species level and this appears to be primarily along PC1 (Fig. 16B). MU-A85 had the highest value along PC1, with HI-A389 intermediate and MAI-686 with the lowest value for both PC1 and PC2. The species that were driving this trend were the spionid polychaetes *Polydora* sp., *Prionospio* sp., *Spiophanes* cf. *missionensis*, and the isopod *Xenanthura brevitelson*. All of these species were associated with midlevel water depths at the MU-A85 platform. For amphipods, there were no strong platform effects. However, amphipod species abundance was lower than for polychaetes, and the small sample size for amphipods could account for the lack of significant trends. The species *Parametopella texensis* and *Phoxocephala* sp. were dominant in determining the factor pattern. Macrofauna had the same trend as the meiofauna, i.e., platform differences were obvious at the species level (Fig. 16B) but not as clear at the family level (Fig. 16A).

To test for species differences at the five distances from a platform, it was necessary to compute the PCA by platform (Figs. 17–19). There were no consistent separations of species by distances for amphipods at any platform. For polychaetes, there was no difference between species for any distances at MU-A85 and MAI-686 and only a weak separation of species by distance along PCA1 for HI-A389. However, at all three platforms, there was more variance at the inner three distances than at the outer two distances. There are no species differences along distances from platforms for any taxa. Differences among distances could not be easily distinguished at the family level at platform MAI-686 (Fig. 17A), MU-A85 (Fig. 18A), or HI-A389 (Fig 19A).

The densities of macrofaunal variables were correlated to abiotic factors (ChemPC1 and ChemPC2, Kennicutt et al. 1996*b*). When data from all platforms are considered, there is a positive relationship between ChemPC1 and total macrofauna density and species richness that is highly significant ($P < 0.0001$) (Table 11). As ChemPC1 (i.e., proximity to platforms) increases, both species abundance and richness

© 1996 NRC Canada

Table 5. Correlation (and significance level in parentheses) between meiofaunal variables and environmental factors.

Variable	ChemPC1	ChemPC2
Meiofauna density	–0.007	–0.472
	(0.9077)	(0.0001)
Nematode density	0.012	–0.431
	(0.8337)	(0.0001)
Harpacticoid density	–0.216	–0.507
	(0.0002)	(0.0001)
Others meiofauna density	–0.141	–0.630
	(0.0145)	(0.0001)
NC ratio	0.276	0.221
	(0.0001)	(0.0001)
Total nematode biomass	0.255	–0.417
	(0.0001)	(0.0001)
Nematode selective deposit feeder biomass	–0.225	–0.295
	(0.0001)	(0.0001)
Nematode non-selective deposit feeder biomass	0.348	–0.365
	(0.0001)	(0.0001)
Nematode epigrowth feeder biomass	0.212	–0.485
	(0.0002)	(0.0001)
Nematode predator biomass	0.029	–0.417
	(0.6141)	(0.0001)
Nematode diversity	–0.339	–0.380
	(0.0001)	(0.0001)
Harpacticoid diversity	–0.282	–0.420
	(0.0001)	(0.0001)

Note: The factors are the axes from the chemical PCA (ChemPC, from Kennicutt et al. 1996*b*).

increase. This trend could be due to the enrichment effect near platforms, and not the contamination effect related to ChemPC1. There is no correlation between ChemPC2 (differences among platforms) and species abundance or richness, and only a slight negative correlation ($P = 0.0242$) with species diversity (H').

The analysis was re-computed by platform to test for distance effects within platforms (Table 12). When platforms are considered independently, the trend is similar to that revealed in the ANOVA. ChemPC1 (proximity to platforms) is strongly correlated with increased species abundance at HI-A389 and MU-A85, and weakly correlated at MAI-686. Species diversity (H') is negatively correlated with ChemPC1 at HI-A389, but positively correlated with ChemPC1 at the other two platforms. The other two platforms are less contaminated than HI-A389, so perhaps organic enrichment is responsible for this trend. ChemPC2 (seasonal difference) is negatively correlated with species abundance and diversity at MAI-686 and MU-A85.

Harpacticoid population studies

Several harpacticoid copepod population studies were performed. The measurements derived from these studies were correlated with the abiotic factors at platforms (ChemPC1 and ChemPC2, Kennicutt et al. 1996*b*). Harpacticoid genetic haplotype diversity decreases with increasing contamination (Table 13). There were no differences among platforms (because there is a lack of correlation for ChemPC2). Also, there were no differences in the responses of five different species. All species had reduced numbers of rare haplotypes near platforms (Street and Montagna 1996). There were no differences in body sizes of harpacticoids near and away from platforms (Lanzotti 1995). Clutch size was significantly positively correlated with ChemPC1 and ChemPC2 (Table 13). Positive correlation of ChemPC1 with clutch size is related to proximity to platforms or increases in egg size along the contaminant gradient. Mean clutch size was also significantly correlated with ChemPC2, which represents platform differences. The number of gravid females increases near platforms, yet there were fewer copepodites (Table 13). Abundance of all life history stages (males, females, gravid females, and copepodites) was significantly negatively correlated with ChemPC2 ($P = 0.0001$). In total, these results indicate that harpacticoid populations are affected by the proximity to platforms. There appears to be a population subdivision at the genetic level, but nothing that is morphologically distinct.

Discussion

Benthic response to gulf platforms

Meiofauna, particularly Harpacticoida, have greater abundances in surfical sediments. Therefore, meiofauna can be affected by deposition of contaminant materials associated with platforms. Among meiofauna, harpacticoids proved to

© 1996 NRC Canada

Table 6. Correlation (and significance level in parentheses) between meiofaunal variables and environmental factors.

Variable	HI-389		MAI-686		MU-A85	
	ChemPC1	ChemPC2	ChemPC1	ChemPC2	ChemPC1	ChemPC2
Meiofauna density	0.164	−0.219	−0.496	−0.167	−0.081	−0.067
	(0.1037)	(0.0287)	(0.0001)	(0.0966)	(0.4241)	(0.5079)
Nematode density	0.208	−0.205	−0.492	−0.140	−0.119	−0.083
	(0.0378)	(0.0411)	(0.0001)	(0.1653)	(0.2400)	(0.4094)
Harpacticoid density	−0.456	−0.452	−0.489	−0.400	0.092	−0.107
	(0.0001)	(0.0001)	(0.0001)	(0.0001)	(0.3645)	(0.2873)
Other meiofauna density	−0.297	0.030	−0.401	−0.080	−0.215	0.0658
	(0.0027)	(0.7654)	(0.0001)	(0.4266)	(0.0319)	(0.5156)
NC ratio	0.497	0.242	0.165	0.467	−0.150	0.0740
	(0.0001)	(0.0152)	(0.1000)	(0.0001)	(0.1363)	(0.4645)
Total nematode biomass	0.480	−0.194	−0.269	−0.220	0.373	0.062
	(0.0001)	(0.0558)	(0.0069)	(0.0276)	(0.0001)	(0.5432)
Nematode selective deposit feeder biomass	0.088	−0.059	−0.539	0.056	−0.490	−0.111
	(0.3900)	(0.5664)	(0.0001)	(0.5831)	(0.0001)	(0.2698)
Nematode nonselective deposit feeder biomass	0.389	−0.037	0.011	−0.370	0.567	0.015
	(0.0001)	(0.7174)	(0.9104)	(0.0002)	(0.0001)	(0.8862)
Nematode epigrowth feeder biomass	0.403	−0.190	−0.428	0.015	0.425	0.096
	(0.0001)	(0.0612)	(0.0001)	(0.8789)	(0.0001)	(0.3439)
Nematode predator biomass	0.055	−0.326	−0.195	−0.251	−0.036	0.118
	(0.5919)	(0.0010)	(0.0522)	(0.0116)	(0.7191)	(0.2430)
Nematode diversity	−0.725	−0.079	0.139	−0.318	−0.067	0.004
	(0.0001)	(0.4358)	(0.1665)	(0.0012)	(0.5096)	(0.9712)
Harpacticoid diversity	−0.556	−0.386	−0.382	−0.390	−0.030	−0.185
	(0.0001)	(0.0001)	(0.0001)	(0.0001)	(0.7701)	(0.0653)

Note: The factors are the axes from the chemical PCA (ChemPC, from Kennicutt et al. 1996*b*) by platform.

be the best indicators of platform effects. This is true for total abundance, species diversity, population structure, and reproductive effort. There appears to be reduced reproductive success of harpacticoids associated with the contaminant gradient at platforms. This effect is indicated by increased reproductive effort near platforms (in terms of more gravid females and greater clutch sizes) coupled with reduced recruitment (indicated by fewer copepodites and adults). Additionally, harpacticoids exhibited toxicity to porewater exposure (Carr et al. 1996). Therefore, harpacticoid abundance, community diversity, genetic diversity, reproductive success, and survivability decline nearer the platforms with an increasing contaminant gradient at all study sites. This appears to be a response to the contamination gradient associated with platforms. Nematode diversity does not appear to be useful for detecting platform effects because there was a discernable trend at only one platform, HI-A389. The NC ratio was an effective indicator only at the HI-A389 platform, suggesting that this is not a good general index of platform effects. Nematode feeding guilds are good indicators of platform effects because the biomass of nonselective deposit feeders increased with the contaminant gradients (Montagna and Li 1996). All platforms have different natural abiotic characteristics in terms of depth, oxygen content, and sediment grain size. Within a platform area, there seems to be little influence due to these environmental characteristics on community structure, but most differences among platforms are probably due to variation and gradients in these natural abiotic components. In general, changes in meiofaunal responses were most noticeable within 50 m of platforms. The strongest response was found at MAI-686. This platform was unique in that there were hypoxic events (extending to a distance of 50 m from the platform) during the summer sampling seasons (Kennicutt et al. 1996*b*). Meiofauna responses at MAI-686 could be due to hypoxia as well as contaminant exposure. The platform HI-A389 is also unique in that the drilling fluids were shunted to the bottom to avoid contamination of nearby shallow coral reefs in the Flower Garden Banks. Therefore, HI-A389 has higher contaminant loads than the other two platforms. It is possible that the lack of assymetrical effects at HI-A389 is due to the bottom-shunted effluent or the abrupt change in the water depth signified by the presence of the coral reef bank. There was little or no general community response at MU-A85.

Macrofaunal density was generally higher at the 50- and 100-m distances than at distances farther away from platforms. Macrofaunal diversity (computed as H') and richness (number of species) were also higher near platforms. The enrichment of macrofauna was generally due to increases in the number of deposit-feeding polychaetes. At first glance, it appears that meiofauna and macrofauna respond differently. It is tempting to suggest that the inverse relationship is due to macrofaunal predation on meiofauna. However, nonselective deposit-feeding nematodes and deposit-feeding polychaetes

© 1996 NRC Canada

Table 7. Overall average abundance and diversity for macrofauna variables at all platforms, stations, and cruises.

Variable	HI-A389	MAI-686	MU-A85	Mean
Macrofauna density	886	956	1013	950
Polychaete density	561	648	586	597
Amphipod density	17	73	44	43
Bivalve density	12	14	32	19
Decapod density	33	19	53	35
Foraminifera density	30	0	17	15
Isopod density	3	0	20	7
Nemertean density	39	57	33	43
Ophiuroid density	6	3	7	6
Polychaete:Amphipod ratio	14.3	7.7	3.3	8.4
Diversity (H')	2.47	2.20	2.82	2.50
Number of species	17.1	14.8	23.3	18.4

Note: Numbers for density (individuals/m^2) are detransformed from $\log_e$. Diversity values are the Shannon–Weaver index (H'). Density averages are for 300 samples, but diversity and species number averages are for 100 boxcores (300 cm^2).

Table 8. Probability values for tests from a hierarchical ANOVA of macrofauna variables for the total design of the sampling program.

Source	Total	POLY	AMPH	BIVA	DECA	FORA	ISOP	NEME	OPHI	PA	H'
C	0.0001	0.0001	0.3355	0.0001	0.0363	0.0001	0.0001	0.0002	0.1702	0.0001	0.0001
P	0.5527	0.5732	0.0001	0.0028	0.0117	0.0001	0.0001	0.1555	0.1966	0.0059	0.0001
P·C	0.0013	0.0005	0.0001	0.0152	0.0934	0.0043	0.0001	0.1143	0.0863	0.0025	0.0208
D	0.0001	0.0001	0.0001	0.0886	0.0001	0.0001	0.0032	0.0001	0.0504	0.0001	0.0156
C·D	0.1582	0.0189	0.0001	0.0284	0.0359	0.0010	0.0374	0.2953	0.3055	0.0002	0.0001
P·D	0.0001	0.0010	0.0002	0.0084	0.0001	0.0011	0.0010	0.0023	0.3109	0.0099	0.0380
P·C·D	0.0248	0.0095	0.0062	0.1520	0.0021	0.0001	0.0211	0.5677	0.6794	0.0050	0.1563
R(P)	0.0516	0.0682	0.8764	0.2728	0.0170	0.6775	0.1233	0.0068	0.3748	0.4886	0.3940
C·R(P)	0.1559	0.0302	0.0195	0.6477	0.1713	0.2184	0.9070	0.7743	0.4626	0.0158	0.3158
D·R(P)	0.2279	0.1894	0.1659	0.1243	0.3938	0.2581	0.0539	0.8492	0.5045	0.1214	0.0001
C·D·R(P)	0.0001	0.0001	0.0001	0.0004	0.0055	0.0097	0.0001	0.0002	0.0183		

Note: The model includes four cruises (C), three platforms (P), five distances (D), five radii (R), and three pseudoreplicates: variable = C P C·P D C·D P·D C·P·D R(P) C·R(P) D·R(P) where P, D, and C are fixed and R is random. Performed on log-transformed data. The table gives source for variation and probability values for the macrofauna variables. The degrees of freedom and expected means squares in terms of the numerator and denominator mean square for the F-test are the same as in Table 2, except that the error degrees of freedom is 600. Total = total macrofauna density, POLY = polychaete density, AMPH = amphipod density, BIVA = bivalve density, NEME = nemertean density, FORA = foraminfera density, ISOP = isopod density, DECA = decapod density, OPHI = ophiuroid density, PA = density ratio between polychaetes and amphipods, H' = pooled diversity by boxcore.

increased in abundance toward platforms. Increased abundance by these two groups was responsible for the community abundance changes. An increase in both macrofaunal and meiofaunal deposit feeders is evidence of trophic enrichment. In this way, there is actually concordance of response between the two benthic groups. Also, lower abundances of some meiofaunal groups, (e.g., harpacticoids) may be due to a contaminant toxicity. Toxic effects on some taxa and enrichment effects on others lead to the conclusion that both enrichment and toxic effects are being detected due to platforms altering the ecology of the continental shelf in a localized area.

Utility of higher taxonomic levels

Analysis of benthic infaunal communities has been widely used in pollution detection and monitoring studies. In GOOMEX, we used ANOVA on diversity indices and PCA on the species data to detect changes. Using these two techniques, we have demonstrated that both meiofaunal and macrofaunal assemblages change among platforms, and with distance from platforms. The use of these techniques is powerful, but expensive due to the labor-intesive effort required. This has inspired efforts to determine if species-level data are really necessary. For meiofauna, at least two approaches have been proposed that do not require taxonomic identifications beyond the target taxa. One method is the NC ratio (Raffaelli and Mason 1981), and the other method is to perform univariate or multivariate analyses using higher taxonomic groupings, e.g., phyla (Raffaelli 1987) or suborder and family (Warwick 1988*b*). Each method works under certain circumstances, but each may not be generally applicable due to a loss of information (Kingston and Riddle 1989).

The NC ratio was originally proposed to detect gradients of

© 1996 NRC Canada

Table 9. Probability values for ANOVA by platform on log-transformed macrofauna variables.

Source	Total	POLY	AMPH	BIVA	DECA	FORA	ISOP	NEME	OPHI	PA	*H'*
					A. HI-A389						
C	0.0001	0.0001	0.0214	0.0666	0.8553	0.0027	0.0269	0.3633	0.2274	0.0024	0.0002
D	0.0001	0.0001	0.0164	0.0044	0.0001	0.0027	0.4362	0.0004	0.1516	0.0001	0.2709
C·D	0.0657	0.0782	0.0156	0.3362	0.0516	0.0001	0.4173	0.8793	0.1606	0.0359	0.0038
R	0.1117	0.0773	0.6756	0.1261	0.1097	0.7003	0.5555	0.0812	0.9403	0.2180	0.8337
C·R	0.8303	0.6924	0.5864	0.6065	0.2821	0.1695	0.9387	0.4763	0.2311	0.2568	0.2090
D·R	0.0278	0.0056	0.2252	0.0853	0.4803	0.2245	0.5345	0.3756	0.7479	0.0198	0.0001
C·D·R	0.0013	0.0085	0.4576	0.0001	0.0830	0.3099	0.1857	0.0661	0.2689		
					B. MAI-686						
C	0.0027	0.0011	0.0408	0.0458	0.9283	0.4262		0.0665	0.0921	0.0019	0.0832
D	0.4071	0.7133	0.0002	0.5994	0.5511	0.4362		0.0018	0.4958	0.0002	0.0010
C·D	0.5207	0.8022	0.0065	0.1864	0.5809	0.4634		0.2906	0.3224	0.0290	0.0919
R	0.1269	0.2268	0.7652	0.4061	0.0872	0.4752		0.0939	0.1565	0.6262	0.0597
C·R	0.0928	0.0255	0.0383	0.6535	0.4951	0.4634		0.5768	0.1442	0.0112	0.4299
D·R	0.6083	0.8467	0.2889	0.2631	0.4989	0.4727		0.8603	0.1919	0.3965	0.3298
C·D·R	0.0001	0.0001	0.0001	0.0001	0.2064	0.4815		0.0004	0.2061		
					C. MU-A85						
C	0.0001	0.0001	0.0001	0.0011	0.0301	0.0274	0.0003	0.0001	0.2361	0.0367	0.0007
D	0.0008	0.0003	0.0070	0.4094	0.0001	0.0038	0.0124	0.0083	0.1550	0.0001	0.1309
C·D	0.0085	0.0001	0.0030	0.0484	0.0052	0.2389	0.0539	0.4416	0.9360	0.0017	0.0455
R	0.7039	0.5916	0.5123	0.8887	0.1150	0.4294	0.2280	0.7458	0.4121	0.5347	0.2932
C·R	0.3283	0.2173	0.5172	0.4512	0.1927	0.4908	0.7242	0.9800	0.8702	0.5406	0.4018
D·R	0.5853	0.6092	0.2572	0.4391	0.3543	0.4712	0.1370	0.6873	0.4459	0.4781	0.5559
C·D·R	0.0004	0.0009	0.3441	0.5559	0.0259	0.0075	0.0015	0.4054	0.0228		

Note: The model includes four cruises (C), five distances (D), five radii (R), and two replicates: variable = C R C·R D C·D R·D C·P·D where D and C are fixed and R is random. The degrees of freedom and expected mean squares are as in Table 3, except that the error degrees of freedom is 200. All abbreviations as in Table 8.

organic enrichment (Raffaelli and Mason 1981). This worked in Scotland (Raffaelli and Mason 1981) and Norway (Amjad and Gray 1983), but not in South Africa (Hennig et al. 1983) or Yugoslavia (Vidaković 1983). Coull et al. (1981) suggested that seasonal variation or nonpollution events could have caused the observed ratios. Subsequent analysis has shown that these criticisms were correct for the Scottish coast, where seasonal variation and sediment grain size caused the ratio to vary inconsistently (Lambshead 1984; Moore and Pearson 1984; Shiells and Anderson 1985). The ratio has also been proposed to detect oil pollution in South Africa (Hennig et al. 1983) and exposure to a gradient of natural petroleum seepage in California (Montagna et al. 1987, 1989). As in the sewage studies, results are not consistent for all oil studies. The ratio declined, rather than increased, with respect to drill cuttings around a platform in the North Sea (Moore et al. 1987) and in experimental mesocosms where drilling muds were added (Leaver et al. 1987). In the GOOMEX study, the NC ratio was of mixed value. In univariate tests, it worked at HI-A389 but the response was not symmetrical about the platform (Table 3A), and it did not work at MU-A85 and MAI-686. However, in the multivariate test, which pools all platforms and stations, it was successful in detecting near-field effects ($P = 0.0001$, Table 5). This was due to the fact that nematode populations generally increase or stay the same size with proximity to platforms, while harpacticoid populations always decrease in size.

The theoretical basis for the NC ratio is that during pollution events, particularly organic enrichment, the number of deposit feeders should increase relative to the number of grazers or predators. A corollary to this theory is that some crustaceans are more sensitive to hypoxia, sulfides, or other toxic materials. We created an analogous ratio for the macrofauna, the PA ratio. At all three platforms the PA ratio was highest at the two closest distances to platforms (50 and 100 m) (Table 10). The consistent trend indicates that the mean PA ratio at each distance from each platform was a more consistent indicator of effects than the mean NC ratio (Table 4). This suggests that the NC ratio should be refined to include only deposit feeders, and this does work better in the GOOMEX data (Peterson et al. 1996).

For both meiofauna and macrofauna, a promising prospect is identification to only the suborder or family level. At the GEEP workshop, all levels of biological organization were studied from the molecular to the community, and all biological components from bacteria to macrofauna were included in both mesocosm and field experiments (Bayne et al. 1988). In the GEEP mesocosm experiment, harpacticoids exhibited a

© 1996 NRC Canada

Table 10. Tukey multiple comparison test to compare distances for macrofaunal variables at three platforms.

A. Platform HI-389					
Distance	50	100	200	500	3000
Total macrofauna density	2091	1298	660	564	505
Distance	50	100	200	500	3000
Polychaete density	1807	1015	504	281	243
Distance	500	200	3000	50	100
Amphipod density	30	23	22	6	5
Distance	50	100	200	3000	500
Bivalve density	43	17	4	2	1
Distance	50	100	500	3000	200
Decapod density	90	34	26	16	14
Distance	3000	500	200	100	50
Foram density	62	37	29	21	7
Distances	100	200	50	500	3000
Isopod density	5	5	2	1	1
Distance	100	50	200	500	3000
Nemertean density	94	44	32	20	19
Distance	500	50	100	3000	200
Ophiuroid density	11	7	5	5	1
Distance	50	100	200	3000	500
PA ratio	3.83	3.29	2.29	1.61	1.55
Distance	100	200	500	3000	50
Diversity (H')	2.77	2.50	2.49	2.45	2.14
B. Platform MAI-686					
Distance	500	50	200	3000	100
Total macrofauna density	1134	1002	960	890	821
Distance	500	50	100	200	3000
Polychaete density	710	689	630	625	589
Distance	500	3000	200	50	100
Amphipod density	156	130	74	34	13
Distance	50	200	500	100	3000
Bivalve density	20	18	14	11	7
Distance	50	200	100	500	3000
Decapod density	25	24	19	15	14
Distance	200	100	50	500	3000
Foraminifera density	1	0.0	0.0	0.0	0.0
Distance	50	100	200	500	3000
Nemertean density	106	63	63	32	31
Distance	3000	500	200	100	50
Ophiuroid density	7	4	4	3	0
Distance	100	50	200	500	3000
PA ratio	2.77	2.40	1.89	1.40	1.34
Distance	50	100	200	500	3000
Diversity (H')	2.44	2.39	2.33	2.02	1.83
C. Platform MU-A85					
Distance	50	100	200	3000	500
Total macrofauna density	1375	1303	886	826	802

© 1996 NRC Canada

Table 10 (*concluded*).

Distance	50	100	200	500	3000
Polychaete density	812	802	566	436	419
Distance	3000	200	500	100	50
Amphipod density	60	55	53	45	12
Distance	100	500	3000	200	50
Bivalve density	39	38	35	26	23
Distance	50	100	200	500	3000
Decapod density	147	75	27	24	24
Distance	500	3000	200	50	100
Foraminfera density	39	28	16	5	1
Distances	50	100	200	500	3000
Isopod density	47	31	12	8	7
Distance	50	100	500	200	3000
Nemertean density	59	39	34	26	16
Distance	50	100	3000	500	200
Ophiuroid density	15	9	7	4	2
Distance	50	100	200	500	3000
PA ratio	3.00	2.46	1.90	1.70	1.58
Distance	100	50	200	3000	500
Diversity (H')	2.94	2.92	2.76	2.73	2.72

Note: The table finds distance from platform (m) and detransformed mean (n/m^2). Means that are underlined are not different at the 0.05 level. If no underline is present, then the Tukey test is not valid due to significant interactions.

Fig. 14. Areal distribution of mean macrofauna density for all four cruises.

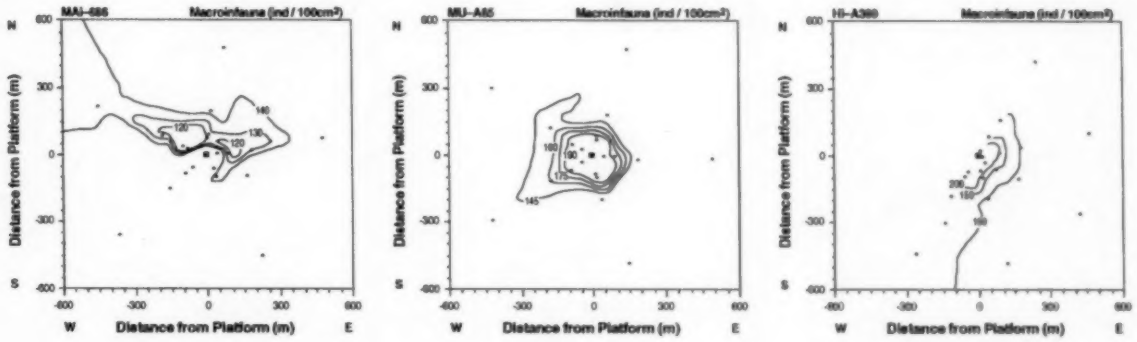

graded response of decreasing diversity with increasing exposure to pollutants, but diversity profiles for nematodes were virtually unaffected Warwick et al. (1988). Diversity was not useful in detecting the pollution gradient in the field study, but community differences were distinct and species-level data gave no more information for discrimination than did nematode suborder or harpacticoid family groupings (Heip et al. 1988). Macrofauna family groupings also were just as adequate for distinguishing the pollution gradient as were species-level data (Warwick 1988*a*). Higher level identifications were found to be just as good as species identifications to detect pollution gradients in the Southern California Bight (Ferraro and Cole 1990) and Trinidad (Agard et al. 1993). For either meiofauna or macrofauna around Gulf of Mexico oil and gas platforms, it does not appear to be sufficient to analyze at the family level only (Figs. 6–13 and 17–19). Too much information is lost to adequately describe among-platform differences, and differences among distances from platforms.

© 1996 NRC Canada

Fig. 15. Areal distribution of mean macrofaunal diversity (H' to $\log_e$) for all four cruises.

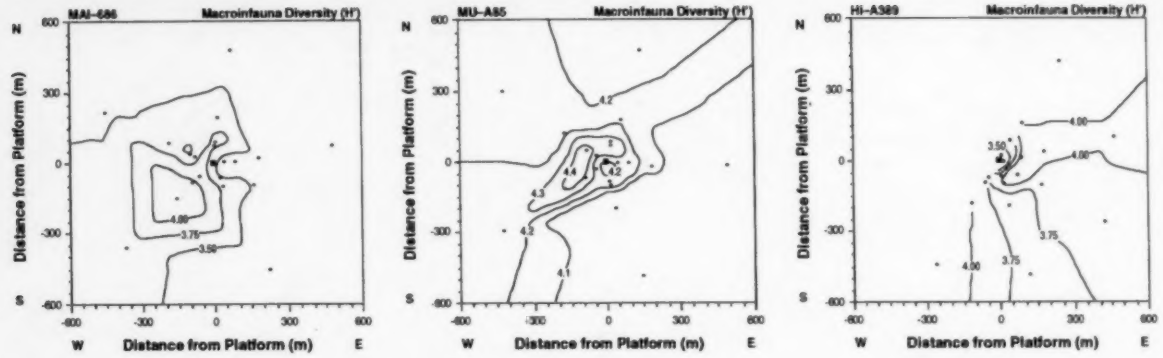

Fig. 16. PCA of macrofauna for all platforms. (A) Families; (B) species.

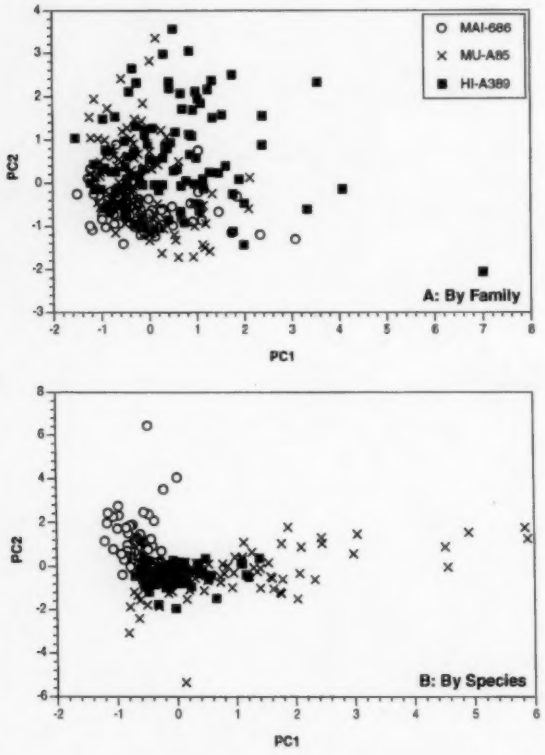

Fig. 17. PCA of macrofauna at platform MAI-686. (A) Families; (B) species.

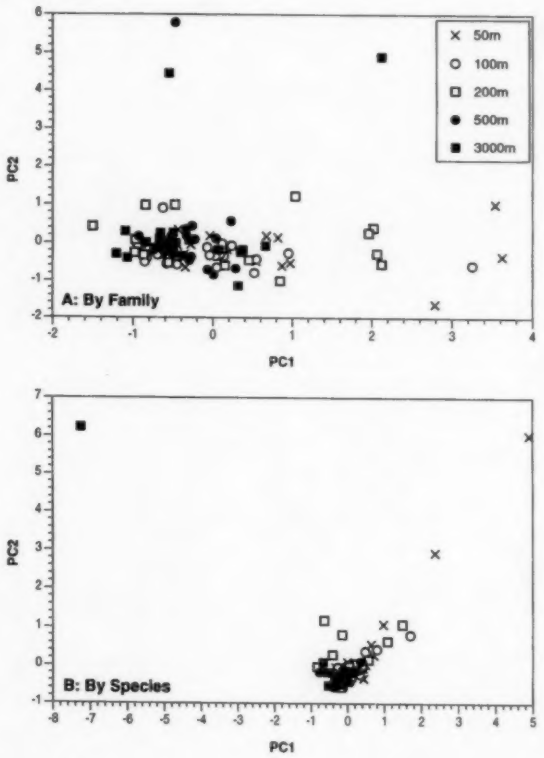

Confounding factors

When several environmental variables strongly covary, it is difficult to identify which factor, factors, or interaction of factors is responsible for the observed biological responses; this is the concept of "confounded variables." Confounding of multiple environmental variables is typical of most anthropogenic discharges into marine environments (Pearson and Rosenberg 1978). In the present study, sand content, concentrations of several metals, Ba, inorganic C, and petroleum hydrocarbons were all elevated in close proximity to platforms. In an analogous study of the impacts of North Sea oil production platforms, Gray et al. (1990) encountered significant covariation in environmental variables with Ba, mud content, and total hydrocarbon concentrations elevated around platforms.

Benthic abundance patterns can also be driven by top-down

© 1996 NRC Canada

Fig. 18. PCA of macrofauna at platform MU-A85. (A) Families; (B) species.

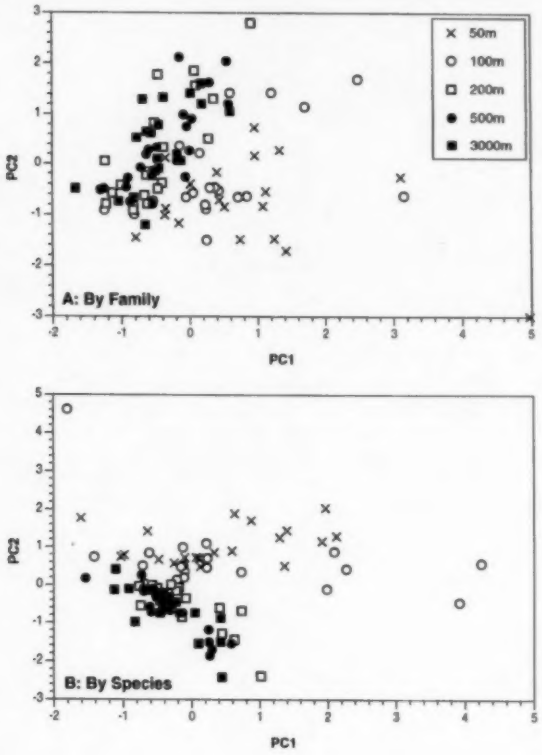

Fig. 19. PCA of macrofauna at platform HI-A389. (A) Families; (B) species.

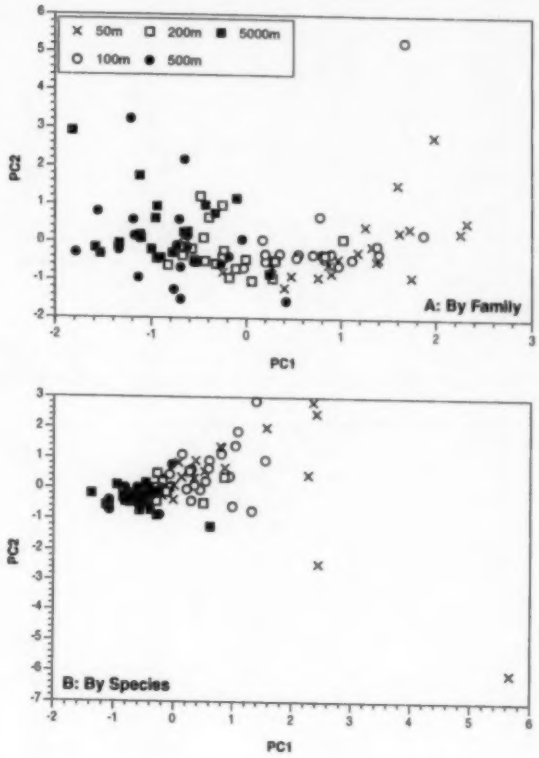

differences in predation pressure as well as by bottom-up differences in food supply and toxicity. Enhancement of species that utilize the hard substrate, i.e., "reef" habitat, of platforms would be expected. Enhanced abundances could also lead to enriched organic matter in the sediments near platforms. There is little evidence of substantial differences between Near and Far stations in the abundance of megaepifaunal invertebrates, but there may be enhancement of some fish species near platforms (Ellis et al. 1996). Analysis of gut contents in small fish showed no differences in dietary composition or in gut fullness between Near and Far stations (Kennicutt 1995). This is consistent with the observation that foraging by reef-associated fishes did not cause a widespread reduction of infaunal densities near an artificial reef (Ambrose and Anderson 1990). Nevertheless, increased abundance in fish near platforms may indicate somewhat greater predation pressure on meiofauna and macroinfauna near platforms. However, demersal fish may not be benthic feeders, as evidenced by the increased polychaete abundances in the near field at all GOOMEX platforms. There may also be a size effect. Meiofauna abundances generally decreased near platforms and macrofauna abundances generally increased. It is possible that some macrofauna are feeding on some meiofauna.

Benthic abundance can also be affected by hypoxia. Hypoxic events are common in the northwestern Gulf of Mexico due to the influence of the Mississippi River.

Table 11. Correlation (and significance level in parentheses) between macrofaunal variables and environmental factors.

Variable	ChemPC1	ChemPC2
Density	0.427	–0.074
	(0.0001)	(0.2027)
Diversity (H')	0.023	–0.130
	(0.6947)	(0.0242)
Number of species	0.253	–0.092
	(0.0001)	(0.1137)

Note: The factors are the axes from the chemical PCA (ChemPC, from Kennicutt et al. 1996*b*).

Hypoxia due to flooding of the Mississippi River was identified as the major factor affecting macrobenthos and meiobenthos near offshore production platforms on the Louisiana continental shelf (Baker et al. 1981). In the present study, care was taken to avoid sampling in these areas to eliminate this possible confounding factor. However, localized hypoxia was encountered during the summer months at the shallowest platform (MAI-686), which is also very far from the Mississippi River influence. This hypoxia is thought to be due to the

© 1996 NRC Canada

Table 12. Correlation (and significance level in parentheses) between macroinfauna variables and environmental factors.

	MAI-686		MU-A85		HI-A389	
Variable	ChemPC1	ChemPC2	ChemPC1	ChemPC2	ChemPC1	ChemPC2
Abundance	0.236	–0.399	0.347	–0.493	0.702	0.148
	(0.0180)	(0.0001)	(0.0004)	(0.0001)	(0.0001)	(0.1404)
Diversity (H')	0.504	–0.220	0.215	–0.345	–0.235	–0.376
	(0.0001)	(0.0277)	(0.0321)	(0.0004)	(0.0186)	(0.0001)
Number of species	0.521	–0.410	0.287	–0.581	0.285	–0.234
	(0.0001)	(0.001)	(0.0037)	(0.0001)	(0.0040)	(0.0191)

Note: The factors are the axes from the chemical PCA (ChemPC, from Kennicutt et al. 1966*b*).

Table 13. Correlation (and significance level in parentheses) between harpacticoid population parameters and environmental factors.

Variables	ChemPC1	ChemPC2
Haplotype diversity	–0.613	–0.053
	(0.0001)	(0.6900)
Clutch volume	–0.126	0.046
	(0.238)	(0.668)
Clutch size	0.220	0.305
	(0.038)	(0.003)
Females	–0.098	–0.443
	(0.092)	(0.0001)
Gravid females	0.194	–0.242
	(0.0007)	(0.0001)
Males	–0.031	–0.382
	(0.589)	(0.0001)
Copepodites	–0.133	–0.242
	(0.022)	(0.0001)

Note: The factors are the axes from the chemical PCA (ChemPC, from Kennicutt et al. 1996*b*).

large amount of biomass associated with the platform and the higher water temperatures in summer. The hypoxia and high density of deposit feeders are clearly an indication of organic enrichment at these sites. Hypoxia is known to be lethal to meiofauna in the Gulf of Mexico (Murrell and Fleeger 1989). Declines of total meiofauna abundance near MAI-686 in conjunction with the high NC and PA ratios indicate that organic enrichment could also influence the trends at this platform.

Distinguishing between effects due to organic enrichment and effects due to contaminant toxicity is difficult, especially when related to oil pollution (Spies et al. 1988). However, the sediment concentrations of 10 metals exceed the Long and Morgan (1990) "effect range-low" values, and at HI-A389 they are higher than the "effect range-median" values (Kennicutt et al. 1996*b*). Sediments near HI-A389 also exhibited toxicity (Carr et al. 1996). The hydrocarbon concentrations in sediments are too low to be important contributors to the observed toxicological effects. These results support the inference that metal toxicity is responsible for some of the responses detected at the platforms.

The major patterns in biological responses to the environmental gradients at the three platforms studied can be interpreted largely as the consequence of organic enrichment and metal toxicity. The pattern of increased sand content should alter the community composition because of differential recruitment, but the trends observed in GOOMEX are largely opposite to the usual biotic response to sediment texture. There is little evidence that fish predation is responsible for differential responses near platforms. The emergence of patterns in benthic meiofaunal and macroinfaunal communities that are broadly consistent with other documented responses to organic enrichment and sediment toxicity, despite the sediment grain-size gradient, leads to the conclusion that sediment grain-size patterns are not a primary cause of the observed biological responses (Peterson et al. 1996).

Contrasts with other platform studies

One detailed sediment quality triad study was performed at a platform near MAI-686. Sediment chemistry, toxicity, and macroinfaunal community structure were measured from 25 to 3000 m away from platform MAI-622 (Chapman et al. 1991). High levels of contaminants were found at 25 m, but there was low toxicity and enrichment in the community density and structure. These results are consistent with findings for macrofauna reported here and for toxicity reported by Carr et al. (1996) for MAI-686 during the GOOMEX study.

Kingston (1992) reviewed the impacts of offshore oil production on the benthos in the Shetland Basin of the North Sea. Oil discharged as drill cuttings was the greatest source of pollution with high levels of hydrocarbon contamination in the sediments near platforms. The infaunal response was similar to that found at the GOOMEX site where there was a decline in abundance of a few species due to a toxic effect and an increase in abundance of a few species due to an organic enrichment effect. Diversity is also depressed near platforms where hydrocarbon contaminants are elevated. In contrast with the Gulf of Mexico, in the Shetland Basin, hydrocarbon contaminant levels were high in sediments at distances between 5 and 10 km away from the installations.

A comprehensive analysis of the effects on macrofauna of 14 oil and gas platforms located in the Norwegian Shelf was recently completed (Olsgard and Gray 1995). One large difference is the use of oil-based drilling muds in the Norwegian Shelf compared with water-based drilling muds at the GOOMEX platforms. Consequently, contamination gradients around the Norwegian Shelf platforms included high lev-

© 1996 NRC Canada

els of hydrocarbons, which were not evident in the Gulf of Mexico. High levels of the metals Zn, Cu, and Cd were also found, consistent with Gulf of Mexico platforms. The gradients also extended out at much greater distances at three of the sites in the Norwegian Shelf. Whereas we detected effects to only 50–100 m radii from platforms, Olsgard and Gray (1995) reported effects out to 2–6 km from the three most contaminated sites. Analysis linking fauna and environmental variables indicated that effects were mainly due to levels of THC, Ba, and Sr and to a lesser extent levels of Zn, Cu, Cd, and Pb. Whereas oil can degrade, the metals that originate in the drill cuttings persist. There was reduced biological impact in areas using water-based drilling muds. Multivariate analysis of community structure was superior to diversity indices in detecting changes.

In the GOOMEX study, it is obvious that the chemical contaminants orginate from the drilling mud discharge, and not from production. Drilling mud discharges can also contribute suspended particulate loads that can cause physical disturbances to bottom fauna. This can disrupt the activities of filter feeders or bury newly settled larvae. Such effects may have been responsible for the cause of declining hard-bottom benthic fauna observed in the Santa Maria Basin, California, platform studies (Hyland et al. 1994).

Conclusion

GOOMEX is a study of the long-term effects of platforms on benthos, but not a long-term study of effects, nor a study of short-term effects. The effects of offshore platforms are complex and often unique due to variation in the local ecology and the technology used (i.e., what drilling muds are used and how fluids are discharged). There is also the confounding nature of the platform as a source of contaminants that can cause toxicity, but also as an artificial reef that can lead to organic enrichment in the environment. This trend is detected by declines in crustaceans, especially harpacticoids, and increases in deposit-feeding nematodes and polychaetes. Population studies on harpacticoids indicate increased toxicity, a loss of genetic divesity, and declines in reproductive success near platforms. At the three GOOMEX platforms (where water-based muds were used) the main chemical contaminants were heavy metals associated with drilling muds. Contamination apparently originates from the drilling activity, especially the discharge of drill cuttings. Hydrocarbon contaminants are relatively minor and there are apparently few effects that can be detected due to the low amount of hydrocarbon contamination associated with production activities. The effects on benthos detected here were very localized, extending out to as little as 100 m from a platform. The effects take the form of toxicity to sensitive organisms and concordant changes in benthic community structure. This implies that platforms are islands of slightly altered benthic communities in the context of large soft-bottom habitat in the Gulf of Mexico continental shelf. The most sensitive community level technique to detect change is multivariate analysis at the species level.

Acknowledgments

Many people contributed to this study. We are indebted to Rick Kalke and Sean Powers for sample collection and laboratory analyses. In addition, Robert Burgess, Mark Lanzotti, Jian Li, Greg Street, Robert Rewolinski, Monica Dozier, Heather Young, Lisa Elune, Jennifer Doerr, Kathy Hancock, Miriam Monsey, and Richard Senker provided assistance in the laboratory. Carrol Simanek organized and managed the data sets. This research was funded by Project RF-8289-9 from the U.S. Department of the Interior, Minerals Management Service, via Subcontract L300033 from the Texas A&M Research Foundation.

References

Agard, J.B.R., Gobin, J., and Warwick, R.M. 1993. Analysis of marine macrobenthic community structure in relation to pollution, natural oil seepage and seasonal disturbance in a tropical environment (Trinidad, West Indies). Mar. Ecol. Prog. Ser. **92**: 233–243.

Ambrose, R.F., and Anderson, T.W. 1990. Influence of an artificial reef on the surrounding infaunal community. Mar. Biol. **107**: 41–52.

Amjad, S., and Gray, J.S. 1983. Use of the nematode-copepod ratio as an index of organic pollution. Mar. Pollut. Bull. **14**: 178–181.

Andrassy, I. 1956. The determination of volume and weight of nematode. Acta Zool. **2**: 1–15.

Baker, J.H., Jobe, W.D., Howard, C.L., Kimball, K.T., Janousek, J., and Chase, P.R. 1981. Part 6. Benthic biology. *In* Ecological investigations of petroleum production platforms in the central Gulf of Mexico. Vol. I. *Edited by* C.A. Bedinger, Jr. Southwest Research Institute, San Antonio, Tex.

Bayne, B.L., Clarke, K.R., and Gray, J.S. 1988. Background and rationale to a practical workshop on biological effects of pollutants. Mar. Ecol. Prog. Ser. **46**: 1–5.

Bell, S.S. 1980. Meiofauna–macrofauna interactions in a high salt marsh habitat. Ecol. Monogr. **50**: 487–505.

Boesch, D.F., and Rabalais, N.N. (*Editors*). 1987. Long-term environmental effects of offshore oil and gas development. Elsevier Applied Science, London.

Carr, R.S., Chapman, D.C., Presley, B.J., Biedenbach, J.M., Robertson, L., Boothe, P., Kilada, R., Wade, T., and Montagna, P. 1996. Sediment porewater toxicity assessment studies in the vicinity of offshore oil and gas production platforms in the Gulf of Mexico. Can. J. Fish. Aquat. Sci. **53**. This issue.

Chapman, P.M., Power, E.A., Dexter, R.N., and Andersen, H.B. 1991. Evaluation of effects associated with an oil platform, using the sediment quality triad. Environ. Toxicol. Chem. **10**: 407–424.

Coull, B.C., and Bell, S.S. 1979. Perspectives of marine meiofauna ecology. *In* Ecological processes in coastal and marine systems. *Edited by* R.J. Livingston. Plenum Publishing Corp., New York. pp. 189–216.

Coull, B.C., and Palmer, M.A. 1984. Field experimentation in meiofaunal ecology. Hydrobiologia, **118**: 1–19.

Coull, B.C., Hicks, G.R.F., and Wells, J.B.J. 1981. Nematode/copepod ratios for monitoring pollution: a rebuttal. Mar. Pollut. Bull. **12**: 378–381.

Ellis, M.S., Wilson-Ormond, E.A., and Powell, E.N. 1996. Effects of gas-producing platforms on continental shelf macroepifauna in the northwestern Gulf of Mexico: abundance and size structure. Can. J. Fish. Aquat. Sci. **53**. This issue.

Ferraro, S.P., and Cole, F.A. 1990. Taxonomic level and sample size sufficient for assessing pollution impacts on the Southern California Bight macrobenthos. Mar. Ecol. Prog. Ser. **67**: 251–262.

Gray, J.S., Clarke, K.R., Warwick, R.M., and Hobbs, G. 1990. Detection of initial effects of pollution of marine benthos: an example from the Ekofisk and Eldfisk oilfields, North Sea. Mar. Ecol. Prog. Ser. **66**: 285–299.

Heip, C., Warwick, R.M., Carr, M.R., Herman, P.M.J., Huys, R., Smol, N., and Van Holsbeke, K. 1988. Analysis of community

© 1996 NRC Canada

attributes of the benthic meiofauna of Frierfjord/Langesundfjord. Mar. Ecol. Prog. Ser. **46**: 171–180.

Hennig, H.F.-K., Eagle, G.A., Fielder, L., Fricke, A.H., Gledhill, W.J., Greenwood, P.J., and Orren, M.J. 1983. Ratio and population density of psammolittoral meiofauna as a perturbation indicator of sandy beaches in South Africa. Environ. Monit. Assess. **3**: 45–60.

Hyland, J., Hardin, D., Steinhauer, M., Coats, D., Green, R., and Neff, J. 1994. Environmental impact of offshore oil development on the outer continental shelf and slope off Point Arguello, California. Mar. Environ. Res. **37**: 195–229.

Jumars, P.A. 1975. Methods for measurement of community structure in the deep-sea macrobenthos. Mar. Biol. **30**: 245–252.

Kennicutt, M.C. II (*Editor*). 1995. Gulf of Mexico Offshore Operations Monitoring Experiment (GOOMEX), Phase I: sublethal responses to contaminant exposure. Final Report. OCS Study MMS 95-0045. U.S. Department of the Interior, Mineral Management Service, Gulf of Mexico OCS Region, New Orleans, La.

Kennicutt, M.C. II, Green, R.H., Montagna, P., and Roscigno, P.F. 1996*a*. Gulf of Mexico Offshore Operations Monitoring Experiment (GOOMEX), Phase I: Sublethal responses to contaminant exposure — introduction and overview. Can. J. Fish. Aquat. Sci. **53**. This issue.

Kennicutt, M.C. II, Boothe, P.N., Wade, T.L., Sweet, S.T., Rezak, R., Brooks, J.M., Presley, B.J., and Wiesenburg, D.A. 1996*b*. Geochemical patterns in sediments near offshore production platforms. Can. J. Fish. Aquat. Sci. **53**. This issue.

Kingston, P.F. 1992. Impact of offshore oil production installations on the benthos of the North Sea. ICES J. Mar. Sci. **49**: 45–53.

Kingston, P.F., and Riddle, M.J. 1989. Cost effectiveness of benthic faunal monitoring. Mar. Pollut. Bull. **20**: 490–496.

Lambshead, P.J.D. 1984. The nematode/copepod ratio some anomalous results from the Firth of Clyde. Mar. Pollut. Bull. **15**: 256–259.

Lanzotti, M. 1995. Sublethal effect of hydrocabon production on harpacticoid copepods in the Gulf of Mexico Outer Continental Shelf. Masters thesis, Marine Science Institute, University of Texas at Austin, Port Aransas, Tex.

Leaver, M.J., Murison, D., Davies, J.M., and Raffaelli, D. 1987. Experimental studies of the effects of drilling discharges. Philos. Trans. R. Soc. Lond. B Biol. Sci. **316**: 625–640.

Long, E.R., and Morgan, L.G. 1990. The potential for biological effects of sediment-sorbed contaminants tested in the National Status and Trends Program. NOAA Tech. Memo. NOS OMA 52. U.S. Department of Commerce, National Oceanographic and Atmospheric Administration, Seattle, Wash.

McDonald, S.J., Willett, K.L., Thomsen, J., Beatty, K.B., Connor, K., Narasimhan, T.R., Erickson, C.M., and Safe, S.H. 1996. Sublethal detoxification responses to contaminant exposure associated with offshore production platforms. Can. J. Fish. Aquat. Sci. **53**. This issue.

Montagna P.A., and Li, J. 1996. Modeling contaminant effects on deposit feeding nematodes near Gulf of Mexico production platforms. Ecol. Model. (In press)

Montagna P.A., Bauer, J.E., Hardin, D., and Spies, R.B. 1987. Temporal variability and the relationship between benthic meiofaunal and microbial populations of a natural coastal petroleum seep. J. Mar. Res. **45**: 761–789.

Montagna, P.A., Bauer, J.E., Hardin, D., and Spies, R.B. 1989. Vertical distribution of microbial and meiofaunal populations in sediments of a natural coastal hydrocarbon seep. J. Mar. Res. **47**: 657–680.

Moore, C.G., and Pearson, T.H. 1984. Response of a marine benthic copepod assemblage to organic enrichment. *In* Proceedings of the Second International Conference on Copepoda. *Edited by*: G. Schriever, H.K. Schminke, and C.-t. Shih. National Museums of Canada, Ottawa, Ont. pp. 369–373.

Moore, C.G., Murison, D.J., Mohdlong, S., and Mills, D.J.L. 1987. The impact of oily discharges on the meiobenthos of the North Sea. Philos. Trans. R. Soc. Lond. B Biol. Sci. **316**: 525–544.

Murrell, M.C., and Fleeger, J.W. 1989. Meiofauna abundance on the Gulf of Mexico continental shelf affected by hypoxia. Continental Shelf Res. **9**: 1049–1062.

NRC (National Research Council). 1975. Petroleum in the marine environment. National Academy Press, Washington, D.C.

NRC (National Research Council). 1985. Oil in the sea: inputs, fates, and effects. National Academy Press, Washington, D.C.

Olsgard, F., and Gray, J.S. 1995. A comprehensive analysis of the effects of offshore oil and gas exploration and production on the benthic communitites of the Norwegian continental shelf. Mar. Ecol. Prog. Ser. **122**: 277–306.

Pearson, T.H., and Rosenberg, R. 1978. Macrobenthic succession in relation to organic enrichment and pollution in the marine environment. Oceanogr. Mar. Biol. Annu. Rev. **16**: 229–311.

Peterson, C.H., Kenicutt, M.C. II, Green, R.H., Montagna, P., Harper, D.E. Jr., Powell, E.N., and Roscigno, P.F. 1996. Ecological consequences of environmental perturbations associated with offshore hydrocarbon production: a perspective on long-term exposures in the Gulf of Mexico. Can. J. Fish. Aquat. Sci. **53**. This issue.

Raffaelli, D. 1987. The behavior of the nematode/copepod ratio in organic pollution studies. Mar. Environ. Res. **23**: 135–152.

Raffaelli, D., and Mason, C.F. 1981. Pollution monitoring with meiofauna, using the ratio of nematodes to copepods. Mar. Pollut. Bull. **12**: 158–163.

SAS Institute Inc. 1990. SAS/STAT user's guide, version 6, fourth edition. Vol. 2. SAS Institute Inc., Cary, NC.

Shiells, G.M., and Anderson, K.J. 1985. Pollution monitoring using the nematode/copepod ratio — a practical application. Mar. Pollut. Bull. **16**: 62–68.

Spies, R.B., Hardin, D.D., and Toal, J.P. 1988. Organic enrichment or toxicology? A comparison of the effects of kelp and crude oil in sediments on the colonization and growth of benthic infauna. J. Exp. Mar. Biol. Ecol. **124**: 261–282.

Street, G.T., and Montagna, P.A. 1996. Loss of genetic diversity in Harpacticoida near offshore platforms. Mar. Biol. **126**: 271–282.

Thiel, H. 1971. Häufigkeit und verteilung der meiofauna in bereich des Island–Färöer–Rückers. Ber. Dtsch. Wiss. Komm. Meeresforsch. **22**: 99–128.

Thiel, H. 1975. The size structure of the deep-sea benthos. Int. Rev. Gesamten Hydrobiol. **60**: 575–606.

Vidaković, J. 1983. The influence of raw domestic sewage on density and distribution of meiofauna. Mar. Pollut. Bull. **14**: 84–88.

Warwick, R.M. 1988*a*. Analysis of community attributes of the macrobenthos of Frierfjord/Langesundfjord at taxonomic levels higher than species. Mar. Ecol. Prog. Ser. **46**: 167–170.

Warwick, R.M. 1988*b*. Effects on community structure of a pollutant gradient — summary. Mar. Ecol. Prog. Ser. **46**: 207–211.

Warwick, R.M. 1993. Environmental impact studies on marine communities: pragmatical considerations. Aust. J. Ecol. **18**: 63–81.

Warwick, R.M., Carr, M.R., Clarke, K.R., Gee, J.M., and Green, R.H. 1988. A mesocosm experiment on the effects of hydrocarbon and copper pollution on a sublittoral soft-sediment meiobenthic community. Mar. Ecol. Prog. Ser. **46**: 181–191.

Wieser, W. 1953. Die beziehung zwischen mundhohlengestalt, ernahrungsweise und vorkommen bei freilebenden marinen nematoden. Arch. Zool. **4**: 439–484.

© 1996 NRC Canada

Effects of gas-producing platforms on continental shelf macroepifauna in the northwestern Gulf of Mexico: abundance and size structure

M.S. Ellis, E.A. Wilson-Ormond, and E.N. Powell

Abstract: Macroepifaunal populations near three active gas-producing platforms were studied as part of the Gulf of Mexico Offshore Operations Monitoring Experiment (GOOMEX) using a near-field (50–100 m), far-field (3 km) collection strategy. When differences in catch per unit effort (CPUE) existed, they were species and site specific. Size effects were not solely due to sexual dimorphism. Differences in size and abundance did not covary. General responses to the presence of platform structure or other characteristics common to gas-producing platforms were not observed. CPUE was site (platform) specific, indicating that epifauna responded to the unique physical and chemical characteristics of each platform. The frequency of significant near-field/far-field differences declined with increasing depth as did the frequency of significant seasonal and time-of-collection differences in size and CPUE, suggesting that platforms affect adjacent community structure more strongly in shallow water and that seasonality and behavior patterns may be important promoters of this effect. Significant differences occurred no less frequently in the most mobile species (penaeid shrimp) than in the much less mobile starfish and scallops. Accordingly, discrete populations of mobile epifauna maintain their coherence for significant periods, which permits differential effects produced by nearness to platforms to be expressed in some of the most mobile invertebrates on the shelf.

Résumé : Les populations de macro-épifaune à proximité de trois plates-formes d'exploitation gazière ont été étudiées dans le cadre de la GOOMEX (*Gulf of Mexico Offshore Operations Monitoring Experiment*) à l'aide d'une stratégie de collecte à champ proche (50–100 m) et à champ éloigné (3 km). Lorsqu'il existait des différences relatives aux prises par unité d'effort (PPUE) et à la taille, ces différences étaient spécifiques de l'espèce et du site. Les effets sur la taille n'étaient pas attribuables uniquement au dimorphiemse sexuel. Les différences touchant la taille et l'abondance ne variaient pas en même temps. On n'a pas observé de réposes générales à la présence de la structure même de la plate-forme ni à d'autres caractéristiques communes aux plates-forme ni à d'autres caractéristiques communes aux plates-formes d'exploitation gazière. Les différences quant à la taille et aux PPUE étaient spécifiques du site (plate-forme), ce qui indique que l'épifaune a réagi aux caractéristiques physiques et chimiques uniques de chacune des plates-formes. La fréquence des différences champ proche-champ éloigné statistiquement significatives a diminué avec l'accroissement de la profondeur, tout comme la fréquence des différences significatives saisonnières et liées au moment du prélèvement, à la fois pour la taille et les PPUE, ce qui indiquerait que les plates-formes influent davantage sur la structure de la communauté adjacents en eau peu profonde et que la saisonnalité et les comportements pourraient être des promoteurs importants de ces effets. Les différences significatives n'étaient pas moins fréquentes chez les espèces plus mobiles (crevettes penaides) que chez les étoiles de mer et les pétoncles beaucoup moins mobiles. En conséquence, des populations discrète de l'épifaune mobile maintiennent leur cohérence pendant des périodes importantes, ce qui permet aux effets différentiels produits par la proximité de la plate-forme de se manifester chez certains des invertébrés les plus mobiles du plateau continental.
[Traduit par la Rédaction]

Introduction

The Gulf of Mexico Offshore Operations Monitoring Experiment (GOOMEX) examined the impact of chronic exposure to chemical contaminants on populations living in close proximity to gas-producing platforms in the Gulf of Mexico. An extensive literature exists documenting the effects of chemical contaminants on macroepifauna subjected to dosing experiments under controlled conditions. Exposure to chemical contaminants results in decreased growth rate, altered reproductive ability, retarded larval development, and altered biochemical composition (e.g., Wang and Stickle 1988; Sindermann 1983; Widdows et al. 1982; Cantelmo et al. 1981); however, little is known concerning the effects of exposure to chemical contaminants on these organisms in their natural environment. Previous studies have documented detrimental effects of exposure to chemical contaminants in populations of meiofauna and macroinfauna found along pollution gradi-

Received July 21, 199. Accepted September 13, 1996.
J13410

M.S. Ellis and E.N. Powell. Haskin Shellfish Research Laboratory, Rutgers University, 6959 Miller Ave., Port Norris, NJ 08349, U.S.A.
E.A. Wilson-Ormond. Texas Department of Health, Environmental Health Services, P.O. Box 8748, Bacliff, TX 77518, U.S.A.

© 1996 NRC Canada

ents (e.g., Warwick 1988; Grassle et al. 1981; Powell et al. 1986); however, these studies typically did not consider the larger, more mobile macroepifauna. Therefore, the goal of the macroepifaunal portion of the GOOMEX program was to identify and describe effects of exposure to contaminant gradients associated with gas-producing platforms on populations of macroinvertebrates under field conditions.

Although measurable contaminant gradients are associated with many gas-producing platforms (e.g., Shinn et al. 1993), platforms may affect the continental shelf biota in a variety of ways. Increased fish densities (Render and Wilson 1994) and the attached epibiota (Bull and Kendall 1994) on the platform structure may affect local predation pressure and food supply. Structure may modify local water flow and variation in sediment type may impact benthic community composition. Hence, this component of the GOOMEX program necessarily examined the effects of a suite of platform-associated variables on macroepifaunal population structure. The assessment was based on a variety of attributes including population size frequency, reproductive state, and population health. In this contribution, we examine the abundance, as measured by catch per unit effort (CPUE), sex ratio, and size-frequency distribution of mobile epifaunal populations associated with gas-producing platforms.

Materials and methods

Mobile epifauna were collected by otter trawl. Two distances were sampled at the extremes of the chemical contamination gradient. The "near-field" station was located within 50–100 m of the platform whereas the "far-field" station, or control, was located approximately 3 km from the platform. Target species were chosen based on the most abundant mobile epifauna collected in the trawls that provided pairwise comparisons between the near- and far-field stations and that also represented a variety of taxa including decapod crustaceans, bivalve molluscs, and echinoderms. Therefore, not only was collection of the same taxa at both the near- and far-field stations important, but the distribution of species among these taxa was also considered in selecting target species.

Three platforms were studied: MAI-686 (Matagorda Island), MU-A85 (Mustang Island), and HI-A389 (High Island). Water depth varied between platforms with MAI-686 located in 29 m of water, MU-A85 in 75 m, and HI-A389 in 130 m. All three platforms have an increased sediment sand content in close proximity to the platforms with mud content increasing with increasing distance from the rigs. As expected from the increased sand content in the near field, sediments near the platforms were depleted in total organic carbon (TOC). Sand enrichment was greatest at the shallowest site and decreased offshore. TOC followed an antithetical trend. Metal contamination was lowest at MAI-686, intermediate at MU-A85, and highest at HI-A389. Generally, hydrocarbon concentrations were near detection limit, at all sites. A more detailed discussion of the contamination gradient within 500 m of the platform is presented elsewhere in this issue (Kennicutt et al., 1996).

Four cruises were conducted: January 1993, June 1993, January 1994, and May 1994. On each cruise, a series of measured (by GPS navigation) otter trawls were conducted, normally at least 10 at each station. Trawling was conducted from 08:00 to 20:00 on the first cruise and from 12:20 to 24:00 on the remaining cruises so that dusk was encompassed to permit the capture of nocturnal and diurnal species.

After retrieving each trawl, the catch was rinsed and sorted. The animals were refrigerated at 4°C, if immediate processing was not possible. All specimens of the target species were counted and measured to the nearest millimetre. The dimensions measured were as follows: bivalves, maximum anterior–posterior length; crabs, maximum carapace width; shrimp, tip of the rostrum to the rear of the carapace; mantis shrimp (stomatopods), maximum length; starfish, central disc width.

For Cruise 2, a maximum of 50 individuals of each species was randomly chosen and measured. On Cruises 3 and 4, all individuals of the target species were measured from every trawl to determine CPUE. CPUE was calculated for each trawl as

$$\text{CPUE} = \frac{\text{total number of individuals caught in a trawl}}{\text{distance trawled} \times \text{width of trawl}}.$$

Sex was determined for all shrimp and crab individuals. Sex of shrimp was based on the presence of the thyleca in females or claspers in males (King 1948). Crabs were sexed based on the appearance of the ventral carapace (Hill et al. 1989). Beginning on Cruise 3, stomatopods and hermit crabs were also sexed externally by visual inspection. Stomatopods were sexed by the presence of claspers at the base of the sixth set of legs, indicating a male, or their absence, indicating a female (Defenbaugh 1976). Hermit crabs were sexed according to the presence of gonopores on the third set of legs, for females, or their absence, for males (Defenbaugh 1976). Scallops are hermaphroditic. Only species of starfish could not be sexed through external examination.

Each dependent variable was analyzed by MANOVA to determine the effect of cruise, distance, and platform on size and CPUE. In some cases, sex and time of collection were included as class variables. In cases where interaction terms between platform or sex and other variables occurred, the analysis was extended to examine each platform and sex individually. All analyses were first run using MANOVA models that included all interaction terms. After the first analysis, interaction terms that were not significant were dropped from the model and the simpler model used to reapportion the error. Dependent variables were transformed by ranking when appropriate.

In some instances, a greater n (number of individuals) was obtained by collectively analyzing species of the same higher taxon. The assumption underlying these groupings is that these species have similar lifestyles and, thus, should react similarly to environmental gradients. Four groupings of species were used: portunid crabs, mantis shrimp, starfish, and penaeid shrimp. In combining species into higher groupings, differences in species size were minimized by normalization to the largest individual. For example, individual species of shrimp were very different in size (i.e., *Penaeus aztecus* is much larger than *Trachypenaeus similis*). The maximum size for each species collected during all four cruises was determined by univariate analysis. The size of each individual was then normalized to this maximum size. Thus, in this analysis, size used as a covariate was defined as the proportion of the maximum size collected for that species, thus allowing species with very different size ranges to be analyzed together.

Results

Species

The species collected at each platform and the degree to which the same species was collected at the near- and far-field stations during the four GOOMEX cruises are summarized in Table 1. Similar species were collected at each platform during each cruise, but some differences in species composition did exist among platforms. In general, many of the same species were collected at MAI-686 and MU-A85 whereas the species collected at HI-A389 were different from those at the other two platforms. This between-platform difference resulted primarily from differences in the locations of the platforms. MAI-686 and MU-A85 are located in relatively shallow water, 29 and 75 m, respectively, whereas HI-A389 is located in much deeper water (130 m), near the edge

© 1996 NRC Canada

Table 1. Target species collected from each platform on each cruise showing the extent of species overlap between the near- and far-field stations.

Species	MAI-686		MU-A85		HI-A389	
	Near	Far	Near	Far	Near	Far
Shrimp						
Penaeus aztecus	1234	1234	1234	1234	1---	
Trachypenaeus similis	1234	-234	-23-	-23-		
Solenocera atlantidis			-234	-234	-234	-234
Sicyonia dorsalis		1-3-		--3-		
Parapenaeus similis					--3-	--3-
Crabs						
Callinectes similis	1234	1234	-2--	-2--		
Portunus spinicarpus			1234	1234	1234	-2--
Portunus gibbesii	1234	1-34				
Myropsis quinquespinosa					12-4	1234
Acanthocarpus alexandria					-234	1234
Hermit crab			1---		1234	-234
Echinoderms						
Astropecten duplicatus	1-34	1-34	1---	--3-		
Astropecten cingulatus			12-4	1234	12-4	-234
Mollusc						
Amusium papyraceum			1234	1234		
Stomatopods						
Squilla empusa	-234	1234	-2--	-2--		
Squilla chydaea	-234	-234	-234	-234	-23-	-2--
Squilla edentata					-23-	-23--

Note: Dashes indicate that the species was not collected at that site on that cruise. Blank spaces under sites indicate that the species was not collected at that site during any of the four GOOMEX cruises.

of the continental shelf. This difference in depth results in a different assemblage of animals being found at HI-A389. The target species collected during the majority of the cruises included three species of shrimp (*Penaeus aztecus, Trachypenaeus similis*, and *Solonocera atlantidis)*, three portunid crabs (*Callinectes similis, Portunus spinicarpus* and *Portunus gibbesii*), two starfish (*Astropecten cingulatus* and *Astropecten duplicatus)*, a scallop (*Amusium papyraceum*), and three species of stomatopods (*Squilla empusa*, *Squilla chydaea*, and *Squilla edentata*). These species were typically collected at both the near- and far-field stations of at least one platform and were representative of each of the major taxa of interest.

Catch per unit effort

CPUE measures species abundance; for example, high values indicate that more individuals were collected per trawl and, thus, that the species is present in higher abundance. CPUE for each of the target species collected at each platform is given in Table 2 (detailed data are presented in Kennicutt 1995). Shrimp were usually the most abundant species collected, regardless of platform, cruise, or station. *Trachypenaeus similis* was collected in extremely high numbers, with CPUE values as high as $5.1 \cdot m^{-2}$ at the near-field station and $10.5 \cdot m^{-2}$ at the far-field station. *Callinectes similis* was the most abundant crab species collected, with CPUE as high as $4.0 \cdot m^{-2}$ at MAI-686 on Cruise 4. Species at the deepwater HI-A389 were usually less abundant than species collected at either of the other two platforms.

Few significant differences in CPUE existed between the near- and far-field stations; however, more species had significantly different CPUE values at MAI-686 (Table 3). Several species at MAI-686 were more abundant at the far-field station, including three species of shrimp and a starfish. Only a crab and a mantis shrimp were more abundant at the near-field station. At MU-A85, the scallop and one species of shrimp were more abundant at the far-field station, and again a species of mantis shrimp was more abundant at the near-field station. One species of crab and one shrimp at HI-A389 were significantly more common at the near-field station. Of the seven species that were collected at more than one platform (*T. similis, P. aztecus, A. duplicatus, S. chydaea, P. spinicarpus, S. atlantidis,* and *A. cingulatus)*, only *T. similis* had significantly different CPUE values at more than one platform. In both cases, *T. similis* was more common at the far-field site.

Many benthic invertebrates are more active from dusk to dawn. CPUE can therefore be biased by the time of collection (Brusher et al. 1972). For this reason, trawling operations

© 1996 NRC Canada

Table 2. CPUE statistics for species collected during Cruises 3 and 4.

Cruise 3: MAI-686

	Penaeus aztecus		*Trachy-penaeus similis*		*Callinectes similis*		*Squilla empusa*		*Squilla chydaea*		*Astropecten duplicatus*	
Trawl	Near	Far	Near	Far	Near	Far	Near	Far	Near	Far	Near	Far
n	17	13	17	7	17	13	17	13	17	13	17	13
Mean	0.015	0.036	1.290	4.928	0.007	0.019	0.084	0.085	0.007	0.047	0.011	0.228
SD	0.015	0.048	1.489	3.406	0.012	0.033	0.081	0.132	0.012	0.054	0.017	0.284

Cruise 3: MU-A85

	Penaeus aztecus		*Solenocera atlantidis*		*Portunus spinicarpus*		*Squilla chydaea*		*Amusium papyraceum*	
Trawl	Near	Far	Near	Far	Near	Far	Near	Far	Near	Far
n	10	14	10	14	10	14	10	14	10	14
Mean	0.052	0.042	0.118	0.071	0.128	0.013	0.066	0.001	0.032	0.113
SD	0.049	0.035	0.118	0.081	0.138	0.014	0.068	0.002	0.021	0.057

Cruise 3: HI-A389

	Solenocera atlantidis		*Parapenaeus similis*		*Portunus spinicarpus*		*Acanthocarpus alexandria*		Hermit Crab		*Squilla chydaea*		*Squilla edentata*	
Trawl	Near	Far	Near	Far	Near	Far	Near	Far	Near	Far	Near	Far	Near	Far
n	6	13	6	13	6	13	6	13	6	13	6	13	6	13
Mean	0.019	0.049	0.148	0.049	0.021	0.001	0.002	0.008	0.009	0.008	0.006	0.001	0.004	0.003
SD	0.031	0.050	0.118	0.063	0.038	0.005	0.003	0.019	0.011	0.015	0.009	0.004	0.006	0.005

© 1996 NRC Canada

Table 2 (*concluded*).

Cruise 4: MAI-686

	Penaeus aztecus		*Trachy-penaeus similis*		*Callinectes similis*		*Portunus gibbesii*		*Squilla empusa*		*Squilla chydaea*		*Astropecten duplicatus*	
Trawl	Near	Far	Near	Far	Near	Far	Near	Far	Near	Far	Near	Far	Near	Far
n	7	10	7	10	7	11	7	10	7	11	7	11	7	10
Mean	0.005	0.106	0.143	0.867	1.951	0.511	0.071	0.026	0.081	0.036	0.007	0.004	0.232	1.325
SD	0.006	0.037	0.126	1.004	1.056	0.262	0.035	0.014	0.047	0.089	0.010	0.006	0.149	0.979

Cruise 4: MU-A85

	Penaeus aztecus		*Solenocera atlantidis*		*Portunus spinicarpus*		*Squilla chydaea*		*Amusium papyraceum*		*Astropecten cingulatus*	
Trawl	Near	Far	Near	Far	Near	Far	Near	Far	Near	Far	Near	Far
n	9	6	9	6	9	6	9	6	9	6	9	6
Mean	0.011	0.025	0.391	0.141	0.019	0.096	0.033	0.004	0.079	0.262	0.013	0.039
SD	0.013	0.016	0.434	0.143	0.020	0.080	0.029	0.006	0.069	0.106	0.021	0.028

Cruise 4: HI-A389

	Solenocera atlantidis		*Myropsis quinquespinosa*		*Acanthocarpus alexandria*		Hermit Crab		*Astropecten cingulatus*	
Trawl	Near	Far	Near	Far	Near	Far	Near	Far	Near	Far
n	11	11	11	11	11	11	11	11	11	11
Mean	0.044	0.015	0.008	0.007	0.006	0.012	0.003	0.002	0.004	0.009
SD	0.062	0.026	0.008	0.009	0.007	0.017	0.004	0.005	0.005	0.015

Note: *n* is the number of trawls performed; mean is the average CPUE (individualism·m^{-3}) for all trawls; SD is the standard deviation. For number of individuals collected, see Tables 6 and 7 (details in Kennicutt 1995).

© 1996 NRC Canada

Table 3. Differences in CPUE for species collected from the near- and far-field stations at each platform.

CPUE is higher at the far-field station	No difference in CPUE between near and far-field	CPUE is higher at the near-field station
	MAI-686	
T. similis ** (•••)	*C. similis*	*P. gibbesii****
S. dorsalis *** (••)	*S. chydaea*	*S. empusa** (•••)
*P. aztecus****		
*A. duplicatus****		
	MU-A85	
*T. similis**	*A. duplicatus*	*S. chydaea****
*A. papyraceum**** (•)	*P. aztecus* (••)	
	S. atlantidis (•••)	
	P. spinicarpus (••)	
	A. cingulatus	
	HI-A389	
	S. atlantidis (•••)	*P. spinicapus***
	M. quinquespinosa	*P. similis** (•)
	A. alexandria	
	Hermit crab	
	A. cingulatus	
	S. chydaea	
	S. edentata	

Note: Asterisks designate the level of significance for species that have different CPUE between the near- and far-field stations: *P = 0.05–0.01; **P = 0.01–0.001; ***P = 0.001–0.0001. Dark circles in parentheses indicate species that have a significant relationship between CPUE and the time-of-day of collection: (•) P = 0.05–0.01; (••) P = 0.01–0.001; (•••) P = 0.001–0.0001. In each case where CPUE was significantly related to time of day, time period 3 (after dusk) had the highest CPUE.

were conducted from noon to midnight to bracket dusk and include trawling time after dark. To determine whether collections, and therefore CPUE, were biased by time of day, the trawls were assigned to one of three equal time periods: 12:00–15:59, 16:00–19:59, and 20:00–24:00. Several species at each platform had significant relationships between time of collection and CPUE (Table 3). In each case, time period 3 (after dusk) had higher CPUE than the other time periods. In fact, in every case except *A. cingulatus* (HI-A389), time period 3 had a higher CPUE, whether significant or not, suggesting that time of day had a significant effect on the numbers of individuals collected and, therefore, that measured abundance increased after dark due to increased activity in epifaunal species. Overall means include trawls throughout the time range and, thus, are underestimates of true abundance.

Size frequency

Summary statistics describing the size distributions of individuals for species collected at both the near- and far-field stations on each cruise are given in Tables 4–7. Size-frequency histograms were constructed for each species from the field measurements of individuals collected at both the near- and far-field stations at each platform. Four examples of size-frequency distributions are presented as histograms for representative species collected on Cruise 4 (Fig. 1). Size distributions were compared in two ways. A MANOVA was used to determine whether significant differences existed in mean size between the near- and far-field stations and between sexes. The size-frequency distributions were also compared by chi-square analysis to determine whether differences existed within the size-frequency distribution between the near- and far-field stations (Table 8).

Size-frequency distributions, examined by chi-square, differed between near-and far-field stations more frequently at MAI-686 than at the other two platforms. Size-frequency distributions were rarely dissimilar at the deepest platform, HI-A389. In several cases, size frequencies were different between near- and far-field stations at one platform, but not at the others. The size-frequency distributions of *P. spinicarpus*, for example, were usually different at MU-A85, but not at MAI-686.

One reason for a difference in size-frequency distribution is that more larger individuals may be present at one station

© 1996 NRC Canada

Table 4. Summary statistics describing the number of individuals analyzed and size for species collected at both sites for at least one platform during Cruise 1.

Platform	Species	Station	Total analyzed	Mean size	Standard deviation
MAI-686	*P. aztecus*	N	10	41.8	6.2
		F	10	43.5	3.6
MAI-686	*T. similis*	N	50	29.4	4.8
		F	52	28.9	4.5
MAI-686	*C. similis*	N	5	55.0	3.4
		F	27	56.9	9.6
MAI-686	*P. gibbesii*	N	10	43.0	7.2
		F	10	44.4	5.4
MAI-686	*A. duplicatus*	N	17	13.0	0.8
		F	15	12.1	1.7
MU-A85	*P. aztecus*	N	14	54.1	5.9
		F	12	57.4	5.8
MU-A85	*P. spinicarpus*	N	38	40.9	6.1
		F	26	47.0	6.0
MU-A85	*A. papyraceum*	N	16	50.9	6.4
		F	50	50.4	5.8
MU-A85	*A. duplicatus*	N	15	15.5	5.5
		F	12	8.3	1.0
HI-A389	*M. quinquespinosa*	N	10	16.7	2.8
		F	11	27.0	7.3

Note: Individuals collected and measured were not separated by sex. N = near-field station; F = far-field station. All measurements are in mm.

than another. As Table 9 shows, in a few cases, larger animals were obtained at the near- or far-field sites.

Many of these species, however, are sexually dimorphic, particularly the penaeid shrimp and portunid crabs (Brusher et al. 1972; Larson et al. 1989). Differences observed between size-frequency distributions could result from a preferential distribution of one sex compared with the other, or because of a true difference in the distribution of individuals of particular sizes, regardless of sex. Thus, significant trends may be produced by a biased distribution of the sexes, but, as importantly, significant trends may be obscured by the sex ratio. Accordingly, size-frequency distributions were constructed for each species and compared by chi-square analysis to determine whether an inherent difference in size frequency exists between the sexes at the same platform and site. Table 10 indicates that several species, particularly shrimp and portunid crabs, had a significant difference in size frequency between the sexes; normally this difference occurred because females were larger. For *T. similis*, for example, females are much larger than males at the far-field station at MAI-686 on Cruise 3 (Fig. 2). Therefore, for some species, differences in size-frequency distributions could result from more females being collected from a site compared with the smaller (or bigger) males, and distance effects could be produced by factors affecting the two sexes differently rather than processes inherently affecting size (e.g. recruitment and growth).

Accordingly, we examined size differences within sexes. At MAI-686, nearly as many species were significantly larger near the platform as far from the platform (Table 11). Female *P. aztecus* and most crabs were larger at the far-field site whereas *T. similis* and starfish were larger near the platform. Some of these differences were sex specific and may have been obscured by the sex ratio in the earlier analysis reported in Table 9. A different pattern occurred at MU-A85. At this platform, no species had larger individuals at the near-field station; in all significant cases, larger individuals were collected at the far-field station. This was true for both sexes of *S. atlantidis*, scallops, the portunid crabs once again, and female stomatopods. The opposite pattern occurred at HI-A389. At this platform, when significant differences existed, larger animals were collected at the near-field station. Species larger near the platform included female (but not male) crabs and the female stomatopods that were larger in the far field at MU-A85. Only at HI-A389 were the statistical results of the combined sexes (Table 9) similar to results obtained when the data were analyzed by sex (Table 11).

These results suggest that, although differences in size exist in some species between sexes (see also Tables 6 and 7 and Fig. 2), the differences in sizes observed between near- and far-field stations are normally related to differences in the size of the individuals of a sex and not just the preferential distribution of sexes between near- and far-field stations. This is further supported by statistical analysis of the data which shows that few significant differences occur in the male to female ratio (Table 12). That is, whereas sexual dimorphism exists, differences in size between the near- and far-field stations are due more to actual differences in the size of individuals, rather than differences that may be attributed to one sex being present in higher abundances than the other. However, in only three cases were trends similar in both sexes (Table 11). Thus, the fewer significant differences in Table 9 when compared with Table 11 can be attributed to the inclusion of

© 1996 NRC Canada

Table 5. Summary statistics describing the number of individuals analyzed and size for species collected at both sites for at least one platform during Cruise 2.

			Number analyzed		Mean size		Standard deviation	
Platform	Species	Station	Male	Female	Male	Female	Male	Female
MAI-686	*P. aztecus*	N	6	15	32.8	33.1	1.3	7.2
		F	21	29	38.0	43.2	6.6	7.6
MAI-686	*T. similis*	N	2	31	18.5	28.7	2.1	3.5
		F	4	83	21.8	29.9	3.5	3.3
MAI-686	*C. similis*	N	127	22	40.6	51.3	9.7	16.1
		F	119	15	40.9	63.2	14.5	6.3
MU-A85	*P. aztecus*	N	23	27	48.8	58.6	5.5	8.4
		F	16	34	50.5	58.9	6.1	7.3
MU-A85	*T. similis*	N	0	3	—	33.7	—	2.1
		F	2	41	22.0	33.8	1.4	2.9
MU-A85	*S. atlantidis*	N	19	29	14.5	20.9	2.0	5.6
		F	14	39	14.1	21.7	2.5	4.7
MU-A85	*C. similis*	N	10	0	42.6	—	13.1	—
		F	9	0	40.6	—	4.5	—
MU-A85	*P. spinicarpus*	N	8	42	47.0	41.0	4.4	5.6
		F	1	73	41.0	36.7	0.0	7.2
HI-A389	*S. atlantidis*	N	21	10	14.6	21.0	1.1	4.9
		F	3	3	15.3	25.0	0.6	8.7
HI-A389	*P. spinicarpus*	N	15	17	52.4	51.9	5.6	5.4
		F	0	2	—	46.5	—	0.7
HI-A389	*M. quinquespinosa*	N	1	2	17.0	24.0	0.0	2.8
		F	7	7	23.0	21.7	4.1	6.5
HI-A389	*A. alexandria*	N	2	3	27.5	24.7	7.8	2.1
		F	13	8	31.3	27.6	8.1	3.9

Platform	Species	Station	Number analyzed	Mean size	Standard deviation
MAI-686	*S. empusa*	N	50	113.8	11.7
		F	50	115.0	14.0
MU-A85	*S. empusa*	N	13	109.8	22.4
		F	11	111.3	15.7
MU-A85	*A. cingulatus*	N	7	15.7	15.7
		F	9	15.3	15.3
MU-A85	*A. papyraceum*	N	50	46.3	11.5
		F	50	35.6	7.7
MU-A85	*P. albida*	N	18	52.9	7.1
		F	50	52.2	6.8
HI-A389	Hermit crab	N	22	11.5	11.5
		F	24	12.9	4.6
HI-A389	*S. empusa*	N	25	111.5	24.6
		F	7	143.0	20.6
HI-A389	*A. cingulatus*	N	5	12.2	7.4
		F	5	15.6	2.3

Note: N = near-field station; F = far-field station. All measurements in mm. Species listed at bottom of table were not sexed based on external characteristics in the field, so the results include both males and females.

one sex whose size distribution was not significantly different between near- and far-field stations. Normally, the size of only one sex was influenced by nearness to the platform.

To determine whether small animals were discriminated against during collection, the size of the organisms in each trawl was compared with the time of day they were collected (Table 13). In all instances when a significant difference occurred, larger animals were caught during the day or at dusk. Whereas the pattern for larger individuals being caught during the day was consistent across all three platforms, the pattern of capture by taxon was not. For example, time of capture had a significant effect on the size of *T. similis* cap-

© 1996 NRC Canada

Table 6. Summary statistics describing the number of individuals collected and size for species collected at both sites for at least one platform during Cruise 3.

			Number collected		Mean size		Standard deviation	
Platform	Species	Station	Male	Female	Male	Female	Male	Female
MAI-686	*P. aztecus*	N	13	9	41.1	39.6	6.0	4.9
		F	24	28	42.5	44.7	5.9	6.2
MAI-686	*T. similis*	N	71	1210	18.2	29.1	2.8	3.9
		F	318	1228	16.2	26.8	3.4	6.4
MAI-686	*C. similis*	N	3	4	44.7	46.5	6.1	6.2
		F	19	9	59.2	47.3	13.2	8.9
MAI-686	*P. gibbesii*	N	0	9	—	46.2	—	4.7
		F	0	57	—	42.5	—	8.4
MAI-686	*S. empusa*	N	67	50	101.7	101.4	12.1	16.1
		F	56	55	93.5	95.8	12.6	19.2
MAI-686	*S. chydaea*	N	4	5	67.8	73.6	6.9	2.7
		F	19	47	66.9	70.4	5.9	9.9
MU-A85	*P. aztecus*	N	10	31	52.2	61.0	2.9	5.7
		F	22	36	54.0	61.9	3.8	6.0
MU-A85	*T. similis*	N	2	7	17.5	25.1	0.7	2.9
		F	3	19	16.0	23.0	0.0	3.8
MU-A85	*S. atlantidis*	N	33	56	14.1	20.2	2.3	5.6
		F	35	57	14.6	20.7	2.5	4.4
MU-A85	*P. spinicarpus*	N	0	91	—	33.9	—	4.7
		F	0	18	—	40.7	—	8.4
MU-A85	*S. chydaea*	N	22	29	84.1	90.4	24.5	18.8
		F	0	1	—	127.0	—	0.0
HI-A389	*S. atlantidis*	N	6	8	15.3	23.1	1.5	4.5
		F	33	39	16.2	22.8	1.6	5.5
HI-A389	*P. similis*	N	7	89	13.0	21.0	1.2	4.3
		F	8	65	13.3	21.3	3.1	4.9
HI-A389	*P. spinicarpus*	N	0	16	—	50.8	—	4.6
		F	0	1	—	31.0	—	0.0
HI-A389	*A. alexandria*	N	1	0	24.0	—	0.0	—
		F	7	3	30.0	26.0	8.2	5.3
HI-A389	Hermit crab	N	2	4	10.0	6.3	1.4	1.5
		F	6	4	11.8	9.8	2.9	2.9
HI-A389	*S. chydaea*	N	1	4	118.0	107.3	0.0	3.6
		F	1	1	105.0	83.0	0.0	0.0
HI-A389	*S. edentata*	N	2	0	98.5	—	31.8	—
		F	3	1	119.3	137.0	11.0	0.0

Platform	Species	Station	Number analyzed	Mean size	Standard deviation
MAI-686	*A. duplicatus*	N	16	8.4	2.4
		F	351	6.6	1.8
MU-A85	*A. papyraceum*	N	27	45.6	8.5
		F	149	50.6	7.1

Note: N = near-field station; F = far-field station. All measurements in mm. Species listed at bottom of table were not sexed based on external characteristics in the field, so the results include both males and females.

tured at MAI-686 for both males and females; however, at MU-A85, this was not true. Similarly, larger female stomatopods were caught prior to nightfall at MU-A85, but not at either of the other two platforms. These results suggest that all size classes were not collected equivalently at all times. This pattern varied according to platform, and occurrences were more frequent in shallow water. Differences in size previously determined could have been related to differences in species' activity patterns, making certain sizes more active and available for collection at different times. However, our sampling protocol, in which all sites were sampled at equivalent times, removed this potential bias from our results.

© 1996 NRC Canada

Table 7. Summary statistics describing the individual size for species collected at both sites for at least one platform during Cruise 4.

			Number collected			Mean size			Standard deviation		
Platform	Species	Station	Male	Female	Int.	Male	Female	Int.	Male	Female	Int.
MAI-686	*P. aztecus*	N	5	4	—	35.8	36.0	—	3.6	3.4	—
		F	51	63	—	33.9	36.3	—	3.4	4.1	—
MAI-686	*T. similis*	N	20	72	—	20.1	28.3	—	0.9	2.6	—
		F	28	301	—	20.4	28.4	—	1.4	3.0	—
MAI-686	*C. similis*	N	200	12	165	44.9	62.6	40.1	9.4	7.2	6.4
		F	77	28	30	59.2	66.3	41.6	21.9	5.7	9.4
MAI-686	*P. gibbesii*	N	0	35	10	—	40.6	35.2	—	5.2	7.2
		F	6	23	10	48.5	43.6	42.6	5.7	5.5	8.4
MAI-686	*S. empusa*	N	17	33	—	91.8	92.8	—	6.9	9.9	—
		F	41	30	—	95.4	99.3	—	16.6	20.5	—
MAI-686	*S. chydaea*	N	0	5	—	—	79.6	—	—	6.1	
		F	0	7	—	—	82.4	—	—	7.5	—
MU-A85	*P. aztecus*	N	0	9	—	—	70.6	—	—	4.1	—
		F	8	17	—	57.0	71.1	—	2.7	4.1	—
MU-A85	*S. atlantidis*	N	63	52	—	15.7	24.4	—	1.7	4.7	—
		F	44	92	—	17.0	26.1	—	1.5	4.5	—
MU-A85	*P. spinicarpus*	N	0	4	12	—	45.8	41.0	—	4.3	7.8
		F	0	40	53	—	48.0	48.5	—	4.4	8.2
MU-A85	*S. chydaea*	N	13	11	—	94.8	87.7	—	25.6	29.3	—
		F	1	3	—	90.0	111.7	—	0.0	22.0	
HI-A389	*S. atlantidis*	N	24	41	—	15.1	23.9	—	1.9	3.9	—
		F	7	15	—	16.9	25.5	—	2.0	4.9	
HI-A389	*M. quinquespinosa*	N	8	3	0	19.0	20.7	—	2.9	4.6	—
		F	6	4	0	23.0	25.0	—	4.3	8.6	—
HI-A389	*A. alexandria*	N	7	2	0	29.3	34.0	—	6.7	2.8	—
		F	11	6	0	21.3	29.7	—	9.9	2.8	—
HI-A389	Hermit crab	N	4	0	0	12.8	—	—	3.6	—	—
		F	2	1	0	18.5	14.0	—	4.9	0.0	—

Platform	Species	Station	Number collected	Mean size	Standard deviation
MAI-686	*A. duplicatus*	N	129	9.8	9.8
		F	128	9.3	1.9
MU-A85	*A. cingulatus*	N	8	12.0	7.6
		F	44	13.9	3.5
MU-A85	*A. papyraceum*	N	53	20.2	8.5
		F	117	45.7	13.7
HI-A389	*A. cingulatus*	N	6	16.5	4.6
		F	14	12.0	2.5

Note: Int. = indeterminant stage for crab species. N = near-field station; F = far-field station. All measurements in mm. Species listed at end of table were not sexed based on external characteristics, so the results include both males and females.

Changes in size-frequency distributions may be related to season because spawning and recruitment of younger, smaller individuals into the population only occur during certain periods of the year. We examined the difference in individual size between the two summer cruises and the winter cruise using MANOVA. Individual size did differ according to cruise; some species were consistently larger on the winter cruise as opposed to the summer cruises regardless of distance or platform (Table 14). For example, *P. aztecus* at MAI-686 and *A. papyraceum* at MU-A85 were larger on the winter cruise at both the near- and far-field stations than on the summer cruises, suggesting a late winter or early spring spawning season in these species at these platforms. *Trachypenaeus similis* and the starfish species at both MAI-686 and MU-A85 were larger on the summer cruises, indicating that younger, smaller individuals were collected on the winter cruises, suggesting a fall spawning season for these species. These differences in size based on cruise may indicate when spawning occurs in these populations; however, more frequent sampling would be required to completely assess the temporal timing of spawning in these populations. The data do show, however, that significant changes occur in these populations seasonally.

© 1996 NRC Canada

Fig. 1. Size-frequency histograms for individuals collected from the near- and far-field stations during Cruise 4: (A) *Astropecten duplicatus* at MAI-686; (B) *Solenocera atlantidis* at MU-A85; (C) *Amusium papyraceum* at MU-A85; (D) *Callinectes similis* at MAI-686.

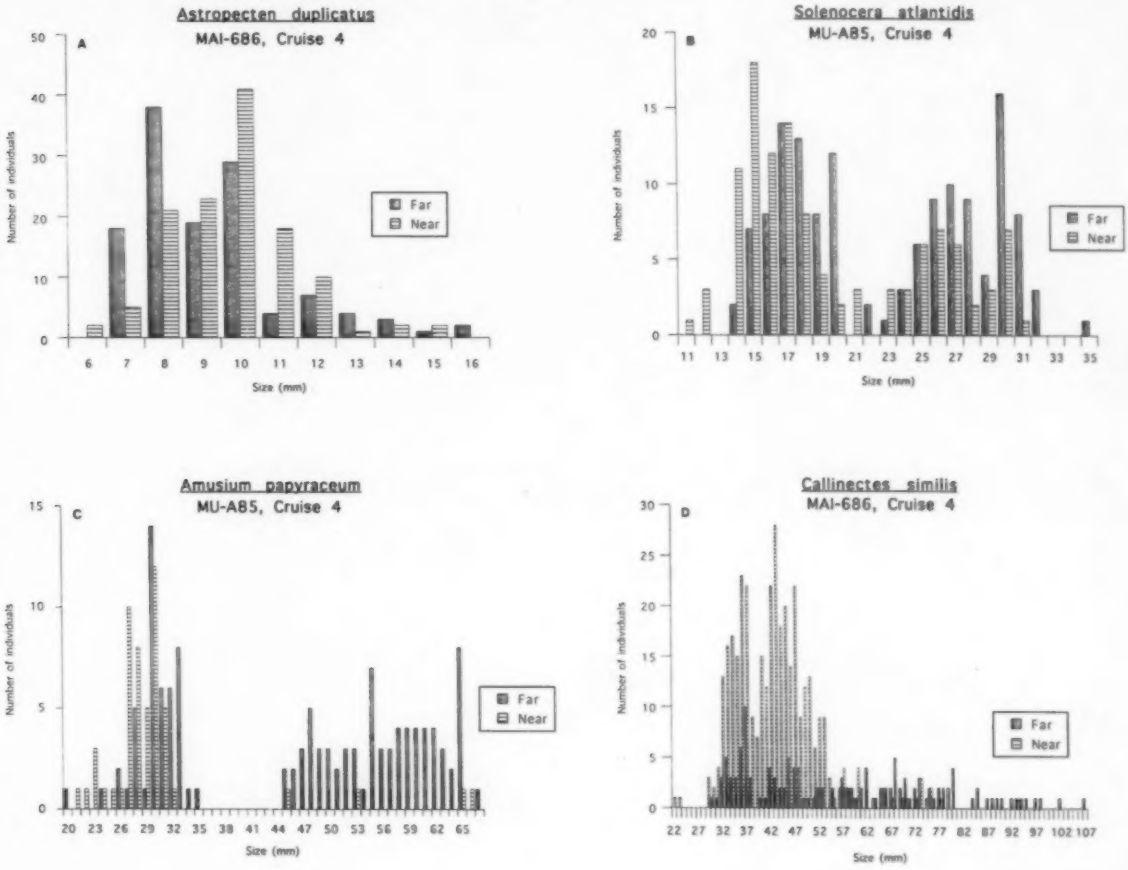

The seasonal signal was strongest in the portunids and *P. aztecus* whereas it was only weakly evident in the stomatopods. Thus, the near- and far-field differences observed occur within a complex, ever-changing seasonal cycle and they occur in species with strong and weak seasonal cycles. Seasonal cycles were muted in the deeper-water HI-A389 site, suggesting a greater seasonal stability in these populations even within the same species (e.g., starfish).

The results of size-frequency distribution and CPUE can be combined to compare the size and abundance of species at both the near- and far-field stations. Generally, smaller individuals are more common in benthic populations, so CPUE should be higher in populations of smaller individuals. Combined results show that significant differences in size and CPUE occur more frequently in the same species at the same site than expected by chance, but the expectation that smaller individuals should be more common is not always true (Tables 3 and 11). In three cases, larger individuals were also more abundant. For example, *P. aztecus* was more abundant at the far-field station of MAI-686 and females were also larger there. The same is true for scallops (*A. papyraceum*) at MU-A85. *Portunus spinicarpus* at HI-A389 were larger at the near-field station and females were also more abundant there. However, in three other cases, smaller individuals were also more abundant. *Trachypenaeus similis* and *A.duplicatus* at MAI-686 were larger near the platform, but were more abundant far from the platform. *Squilla chydaea* at MU-A85 was more abundant in the near field but females were larger in the far field.

Discussion

The results of this study identify significant differences in population structure in populations living in close proximity to gas-producing platforms. The most significant observation is that each platform exhibits a different pattern of effect in both CPUE and size-frequency distribution, probably due to its own unique chemical and physical environment. Clearly, the influence of structure, a variable in common with all platforms, does not exert an overriding influence on the populations. Therefore, although some generalities can be made about population structure with respect to proximity to gas-producing platforms, each platform affects populations in different, unique ways based the local chemical and physical

© 1996 NRC Canada

Table 8. Results of size-frequency distribution analysis by cruise using chi-square ($P < 0.05$).

Differences in size frequency existed on at least one cruise	No difference existed on any cruise
MAI-686	
T. similis (×, 2, 3, 4)	*P. gibbesii* (×, -, ×, ×)
P. aztecus (×, ×, 3, -)	
C. similis (×, ×, ×, 4)	
S. empusa (-, -, -, 4)	
A. duplicatus (-, -, ×, 4)	
MU-A85	
T. similis (-, -, 3, -)	*P. aztecus* (×, ×, ×, ×)
S. atlantidis (-, -, ×, 4)	*C. similis* (-, ×, -, -)
P. spinicarpus (1, 2, 3, ×)	*A. cingulatus* (-, ×, -, -)
A. papyraceum (×, ×, 3, 4)	
HI-A389	
S. atlantidis (-, ×, 3, ×)	*P. similis* (-, -, ×, -)
	M. quinquespinosa (×, -, -, ×)
	A. alexandria (-, ×, -, ×)
	Hermit crab (-, ×, ×, -)
	S. empusa (-, -, ×, -)
	S. chydaea (-, -, ×, -)
	A. cingulatus (-, ×, -, -)

Note: Number indicates that a significant difference occurred between the near- and far-field stations on that cruise; ×, no significant difference; -, no test conducted.

Table 9. Results of MANOVA determining whether individuals are significantly larger at the near- or far-field site at each platform.

Individuals are larger at the far-field	No difference in size between near and far field	Individuals are larger at the near-field station
	MAI-686	
*P. aztecus***	*T. similis*	*A. duplicatus****
	All shrimp	All starfish***
	S. similis	
	Portunid crab	
	P. gibbesii	
	S. empusa	
	S. chydaea	
	All stomatopods	
	MU-A85	
*S. atlantidis**	*T. similis*	
*A. papyraceum****	*P. aztecus*	
	All shrimp	
	C. similis	
	P. spinicarpus	
	Portunid crab	
	S. chydaea	
	All stomatopods	
	A. cingulatus	
	A. duplicatus	
	All starfish	
	HI-A389	
Hermit crab*	*S. atlantidis*	*P. spinicarpus****
	P. similis	Portunid crab***
	All shrimp	*S. chydaea**
	M. quinquespinosa	
	A. alexandria	
	S. edentata	
	All stomatopods	
	A. cingulatus	
	All starfish	

Note: Asterisks describe the level of significance: *P = 0.05–0.01; **P = 0.01 = 0.001; ***P = 0.001–0.0001.

environment, and these unique differences far outweigh the few generalities that might be made.

Most of the species used in this component of the GOOMEX study were large, mobile epifauna. A few, such as starfish, scallops, and stomatopods, have a much reduced mobility. Nevertheless, such mobile taxa as crabs and shrimp consistently exhibited as many significant population differences between near- and far-field sites as did the less mobile starfish, scallops, and stomatopods. Thus, these mobile epifauna retain discrete populations over reasonably long time periods, long enough to develop different population histories as measured by size. Migration between populations must occur relatively rarely. If recruitment occurs during a small fraction of the year, then maintenance of the observed population structures suggests that an individual's residence time in a population must be at least of 6-mo time scales and that environmental gradients normally considered capable of structuring populations of sessile species might also affect these mobile species over surprisingly small spatial scales.

Mobility and the likelihood of diurnal cycles in activity could have compromised the data analysis. However, trawling was consistently conducted across a day–night transition. Time-dependent variations in catch and size of individuals caught were consistently observed. However, these variations did not bias the comparison between near and far field. For example, the largest individuals were generally caught during daylight or at dusk. Many species showing time dependency in size also showed significant near-field/far-field differences. However, samples were collected at both sites at the same times of day. For CPUE, as many species having a time dependency in the catch had significant near-field/far-field trends as did not. However, the data demonstrate the essentiality of trawl collections over the day–night boundary in studies of this type. Catches were larger at night. Larger animals were caught during the day. CPUE and size differences could have occurred simply from inadequate control on time of collection, and the population structure would not have been sampled adequately had either time period been targeted selectively.

© 1996 NRC Canada

Table 10. Differences in size between male and female individuals at each platform for the near- and far-field stations as determined by chi-square analysis.

Difference in size between males and females at the far-field station		Difference in size between males and females at the near-field station	
Significant	Not significant	Significant	Not significant
HAI-686			
*T. similis**** (F)	*P. gibbesii*	*T. similis**** (F)	*P. aztecus*
*P. aztecus** (F)	*S. empusa*	*C. similis**** (M)	*S. empusa*
*C. similis**** (M)	*S. chydaea*	*P. gibbesii** (F)	*S. chydaea*
MU-A85			
*T. similis*** (F)	*S. chydaea*	*P. aztecus** (F)	*T. similis*
*P. aztecus**** (F)		*S. atlantidis**** (F)	*S. chydaea*
*S. atlantidis**** (F)		*P. spinicarpus**** (F)	
HI-A389			
*S. atlantidis**** (F)	*M. quinquespinosa*	*S. atlantidis**** (F)	*P. spinicarpus*
*P. similis*** (F)	*A. alexandria*	*P. similis**** (F)	*M. quinquespinosa*
	Hermit crab		*A. alexandria*
	S. empusa		Hermit crab
	S. edentata		*S. chydaea*

Note: M = male; F = female; Int. = indeterminant stage. Parentheses indicate which size-frequency distribution had the larger individuals. Asterisks indicate the level of significance for the chi-square results: **P* = 0.05–0.01, ***P* = 0.01–0.001, ****P* = 0.001–0.0001.

Fig. 2. Size-frequency histogram for males and females of *Trachypenaeus similis* at MAI-686 collected on Cruise 3.

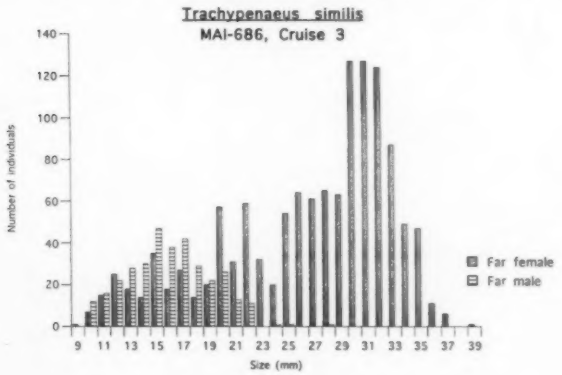

Although size frequency exhibited more significant differences than CPUE, most trends were platform specific. MAI-686 and MU-A85 are relatively close to one another, and might be expected to develop similar biological trends. HI-A389 is distant and in substantially deeper water and thus might be expected to be unique among the three platforms studied. Nevertheless, MAI-686 and MU-A85 were similar to one another no more frequently than each was to HI-A389. Thus, few generalities among platforms were observed that could be clearly extrapolated to truths about all platforms, nor were generalities among subsets of platforms commonly observed that might be extrapolated to truths about, for example, shallow- versus deepwater platforms. The overwhelming trend was towards site specificity.

Trends in size were platform specific and extraordinarily common. In fact, about as many species showed significant trends in size as did not. Many of these differences were only apparent when sexual dimorphism was taken into account. Thus, species populations tended to have different size-frequency distributions between near- and far-field stations unrelated to sex ratio, but individuals of one sex were often larger in some populations than in others. In general, near-field/far-field differences in size-frequency distributions might be explained by decreased growth, changes in population recruitment and mortality, or migration with age. Shrimping, an important activity on the Texas continental shelf, could be expected to be more important at far-field sites, and this activity also may have biased population structure of exploited species and bycatch (Hall 1994; Carroll and Winn 1989). The relative importance of these various possibilities cannot be evaluated. Significant population differences in reproductive stage and health (our unpublished data) discount the significance of age-associated migration in these populations. Food availability and predation may explain differences in abundance and size-frequency distribution. Demersal fish were collected in higher numbers at the near-field station of each platform, even though some species of mega-

© 1996 NRC Canada

Table 11. Results of MANOVA determining whether individuals of a given sex are significantly larger at the near- or far-field site at each platform.

Individuals are larger at the far-field station	No difference in size between near and far-field	Individuals are larger at the near-field station
	MAI-686	
P. aztecus, F***	*P. aztecus*, M	*T. similist*, M***, F***
C. similis, F**	All shrimp, M, F	*A. duplicatus****
All portunid crabs, M*, F**, Int***	*C. similis*, M, Int	All starfish***
	P. gibbesii, F, Int	
	S. empusa, M, F	
	S. chydaea, M, F	
	All stomatopods, M, F	
	MU-A85	
S. atlantidis, M**, F*	*T. similis*, M, F	
P. spinicarpus, Int*	*P. aztecus*, M, F	
All portunid crabs, Int**	All shrimp, M, F	
S. chydaea, F*	*C. similis*, M	
*A. papyraceum****	*P. spinicarpus*, M, F	
	All portunid crabs, M, F	
	S. chydaea, M	
	All stomatopods, M, F	
	A. cingulatus	
	All starfish	
	HI-A389	
	S. atlantidis, M, F	*P. spinicarpus*, F***
	P. similis, M, F	All portunid crabs, F***
	All shrimp, M, F	*S. chydaea*, F**
	M. quinquespinosa, M, F	
	A. alexandria, M, F	
	Hermit crab, M, F	
	S. edentata, M	
	All stomatopods, M, F	
	A. cingulatus	
	All starfish	

Note: M = male; F = female; Int. = indeterminant stage. Asterisks describe the level of significance: *P = 0.05–0.01; **P = 0.01–0.001; ***P = 0.001–0.0001.

invertebrates were more abundant or larger there, so that increased predation cannot explain the abundance and size trends in all species (Kennicutt 1995). In some cases, meiofauna and macroinfauna densities were lower where the megainvertebrates were more abundant or larger, suggesting that the populations were grazed to a lower level, thus varying the abundance of food (Montagna and Harper 1996). However, insufficient information is available on the species life habits, requirements, and population histories to conclusively explain the trends observed.

Sexual dimorphism was present in many species, so that size-related trends might have been produced by variations in sex ratio. However, differences in size occurred within sexes. Thus, size effects were not solely due to sexual dimorphism and near-field/far-field differences in sex ratio. On the other hand, one sex was frequently affected significantly whereas the other was not, so that processes establishing the size-dependent trends were often sex specific. Nearly every species that demonstrated a significant near-field/far-field trend in size also demonstrated significant seasonal changes in size frequency. Thus, near-field/far-field trends in size occurred within a dynamically varying population structure being continually modified by recruitment and mortality. Near-field/far-field trends are unlikely to be the result of platform effects on single cohorts or static populations. The evidence suggests that platform modifications on growth and mortality are the likely cause, rather than migration, and that these complex interactions persistently modify near- and far-field populations in different ways.

The three platforms were distinctive in their effects on the measured biological variables. MAI-686 was characterized by a complex assortment of trends. Size changes were as

© 1996 NRC Canada

Table 12. Results of MANOVA determining whether the male to female ratio is higher at the near- or far-field site at each platform.

Male to female ratio higher at the far-field	No difference in male to female ratio	Male to female ratio higher at the near-field
	MAI-686	
	P. aztecus *P. gibbesii* *S. empusa* *S. chydaea*	*T. similis**** *T. similis***
	MU-A85	
*S. atlantidis***	*T. similis*, M, F *P. aztecus*, M, F *P. spinicarpus*, M, F *S. chydaea*, M	
	HI-A389	
	S. atlantidis *P. similis* *M. quinquespinosa*, M, F *A. alexandria*, M, F Hermit crab, M, F	

Note: M = male; F = female. Asterisks describe the level of significance: **P* = 0.05–0.01; ***P* = 0.01–0.001; ****P* = 0.001–0.0001.

likely to indicate significantly larger individuals near field as far field, and although CPUE indicated that higher abundances occurred more frequently in the far field, significant exceptions existed. The complexity in the distribution of macroepifauna suggests a complex environmental system with opposing environmental gradients at this platform. In contrast, MU-A85 was more consistent in that larger animals occurred at the far-field station. The same consistency was observed in a higher incidence of parasitism in the near field (our unpublished data). CPUE showed few differences, although again they were species specific when they occurred. Nevertheless, the data from MU-A85 suggest a more consistent environmental gradient, with conditions conducive to population health increasing with distance from the platform. MU-A85 has a measurable contamination gradient that follows this same trend. HI-A389 poses the opposing picture; individuals are larger in the near field despite the contamination gradient present (Kennicutt et al. 1996). The data obtained for HI-A389 are substantially sparser than for the other two platforms. Cases of species overlap are less common and the number of individuals usually less; however, the poorer data set is unlikely to be responsible for the opposing trends observed. HI-A389 casts doubt on the importance of chemical contaminants in determining the near-field/far-field trends observed at MAI-686 and, most importantly, MU-A85.

Species showing significant differences in CPUE did not necessarily show significant differences in size, and large animals were no more common than small ones. One possibility that populations with many small individuals had increased CPUE did not consistently occur. Thus, size and CPUE seem to be affected independently by platform-related processes. MAI-686 and MU-A85 showed much stronger trends than the deeper-water platform HI-A389. A weaker seasonal signal existed at this deeper-water platform and time-of-collection effects were less frequent. Seasonal changes in size occurred most commonly at the shallowest site (MAI-686) and least commonly at HI-A389. Near-field/far-field differences in size, size-frequency distribution, sex ratio, and CPUE followed this same trend. Moreover, time-dependent changes in CPUE and size occurred most frequently at MAI-686 and least frequently at HI-A389. Thus, the data suggest that shallow-water sites, more prone to seasonal changes in population structure and receiving the strongest diurnal signal that might affect behavior, are also more likely to exhibit near-field/far-field differences in population structure and abundance.

Conclusions

The single most significant generality from this portion of the GOOMEX study is the platform specificity observed in the trends of these biological variables. Forcing factors producing these biological trends observed among the platforms between near-or far-field sites might be water column chemical anomalies, contamination gradients, and naturally occurring sedimentary chemical gradients. Many of the environmental variables are also platform specific and opposing gradients are common (Kennicutt et al. 1996). The macroepifaunal taxa in this study vary considerably in their physiology and behavior and thus could be expected to respond differently to the varying signals presented by the

© 1996 NRC Canada

Table 13. Species collected at each platform that had a significant relationship between individual size and the time of collection.

Significant relationship between size and time of collection	No significant relationship between size and time of collection
MAI-686	
T. similis, M*** (1), F*** (2)	*S. dorsalis*, M (2), F (3)
C. similis, F* (1)	*P. aztecus*, M (3), F (3)
P. gibbesii, F* (2)	*C. similis*, M (2), Int (2)
*A. duplicatus**** (1)	*P. gibbesii*, M (3), Int (3)
All portunid crabs, F***	*S. empusa*, M (1), F (1)
All starfish**	*S. chydaea*, M (2), F (1)
All shrimp, M***, F***	All portunid crabs, M, Int
	All stomatopods, M, F
MU-A85	
S. chydaea, F* (2)	*T. similis*, M(2), F (3)
*A. papyraceum*** (1)	*S. atlantidis*, M (3), F (3)
All stomatopods, F*	*P. aztecus*, M (2), F (3)
All shrimp, M*	*P. spinicarpus*, F (2), Int (3)
	S. chydaea, M (3)
	A. cingulatus (2)
	All portunid crabs, M, F
	All stomatopods, M
	All starfish
	All shrimp, F
HI-A389	
P. similis, M* (2)	*S. atlantidis*, M (2), F (1)
S. edentata, M* (2)	*P. similis*, F (1)
	P. spinicarpus, F (3)
	M. quinquespinosa, M (1), F (1)
	A. alexandria, M (3), F (3)
	Hermit crab, M (1), F (2)
	S. chydaea, F (2)
	A. cingulatus (2)
	All portunid crabs, F
	All stomatopods, M, F
	All starfish
	All shrimp, M, F

Note: Resulis are for individuals collected on Cruise 3 and 4 only. M = male; F = female; Int. = indeterminant stage. Asterisks designate the level of significance: *P = 0.05–0.01; **P = 0.01–0.001; ***P = 0.001–0.0001. Numbers in parentheses indicate the time period during which the largest individuals were collected: 1 = 1200–1559; 2 = 1600–1959; 3 = 2000–2400.

Table 14. Results of MANOVA analysis determining whether a relationship exists between individual size and the cruise on which the individual was collected.

Significant relationship between individual size and cruise	No significant relationship between individual size and cruise
MAI-686	
*P. aztecus**** (3)	*T. similis*
*C. similis**** (2)	*P. gibbesii*
All shrimp*** (3)	
All portunid crabs*** (2)	
*S. empusa** (3)	
*S. chydaea** (4)	
All stomatopods* (3)	
*A. duplicatus**** (4)	
All starfish*** (4)	
MU-A85	
*T. similis**** (2)	*C. similis*
*P. aztecus**** (4)	*S. chydaea*
*S. atlantidis**** (4)	All stomatopods
All shrimp*** (4)	*A. duplicatus*
*A. cingulatus*** (4)	
*A. papyraceum**** (3)	
*P. spinicarpus**** (4)	
All portunid crabs*** (4)	
All starfish*** (4)	
HI-A389	
All shrimp* (4)	*S. atlantidis*
*P. spinicarpus**** (4)	*P. similis*
All portunid crabs*** (2)	*A. alexandria*
*M. quinquespinosa*** (3)	*S. chydaea*
Hermit crab** (4)	*S. edentata*
	All stomatopods
	A. cingulatus
	All starfish

Note: Asterisks represent levels of significance: *P = 0.05–0.01; **P = 0.01–0.001; ***P = 0.001–0.0001. Number in parentheses indicates the cruise on which the largest individuals were collected. Cruises 2 and 4 are summer cruises; Cruise 3 is a winter cruise.

platform-specific gradients involved. Even within a species, platforms failed to produce similar trends. *Penaeus aztecus*, for example, were larger in the far field at MAI-686 but not at MU-A85. *Squilla chydaea* was more common in the near field at MU-A85 but not at MAI-686. Combined, the taxon and environmental complexity reduces the likelihood of the existence of general trends among all species and platforms, and few, if any, were observed. Each platform produced a distinctive effect on the shelf biota. The single trend among platforms is the clear decrease in frequency of near-field/far-field effects with increasing depth and concomitant decreasing importance of seasonality in population structure and time-of-day effects on behavior.

Thus, the results obtained identify physiological impacts on populations living in close proximity to gas platforms. Such differences do exist and are frequently observed. Each platform exhibits a different pattern in size distribution and CPUE, probably due to its own unique chemical and physical environment. Clearly, platforms have a complex effect on the surrounding biological communities, and a broad understand-

© 1996 NRC Canada

ing of the physical and chemical environment as it interacts with species populations will be required to elevate the site-specific trends observed in this study to a more general understanding of the effects of platforms on the continental shelf biota.

Acknowledgments

This work was supported by the Department of the Interior, Minerals Management Service, under MMS Contract 14-35-001-30582. The authors would like to thank Dr. Mahlon C. Kennicutt II for his help in editing previous versions of this manuscript.

References

Brusher, H.A, Renfro, W.C., and Neal, R.A. 1972. Notes on distribution, size, and ovarian development of some penaeid shrimps in the northwestern Gulf of Mexico, 1961-62. Contrib. Mar. Sci. **16**: 75–87.

Bull, A.S., and Kendall Jr., J.J. 1994. An indication of the process: offshore platforms as artificial reefs in the Gulf of Mexico. Bull. Mar. Sci. **55**: 1086–1098.

Cantelmo, A.C., Lazell, R.J., and Mantel, L.H. 1981. The effects of benzene on molting and limb regeneration in juvenile *Callinectes sapidus* Rathbun. Mar. Biol. Lett. **2**: 333–343.

Carroll, J.C., and Winn, R.N. 1989. Species profiles: life histories and environmental requirements of coastal fishes and invertebrates (Pacific-Southwest) — brown rock crab, red rock crab, and yellow crab. U.S. Fish Wildl. Serv. Biol. Rep. 82(11.117). U.S. Army Corps of Engineers TR EL-82-4.

Defenbaugh, R.E. 1976. A study of the benthic macroinvertebrates of the continental shelf of the northern Gulf of Mexico. Ph.D. dissertation, Texas A&M University, College Station, Tex.

Grassle, J.F., Elmgren, R., and Grassle, J.P. 1981. Response of benthic communities in MERL experimental ecosystems to low level, chronic additions of No. 2 fuel oil. Mar. Environ. Res. **4**: 279–297.

Hall, S.J. 1994. Physical disturbances and marine benthic communities: life in unconsolidated sediments. Oceanogr. Mar. Biol. Annu. Rev. **32**: 179–239.

Hill, J., Fowler, D.L., and VanDen Avyle, M.J. 1989. Species profiles: life histories and environmental requirements of coastal fishes and invertebrates (mid-Atlantic) — blue crab. U.S. Fish Wildl. Serv. Biol. Rep. 82(11–100). U.S. Army Corps of Engineers TR EL-82-4.

Kennicutt, M.C. II (*Editor*). 1995. Gulf of Mexico Offshore Operations Monitoring Experiment, Phase I: Sublethal responses to contaminant exposure. Final Report. OCS Study MMS 95–000. U.S. Department of the Interior, Minerals Management Service, Gulf of Mexico OCS Region, New Orleans, La.

Kennicutt, M.C. II, Boothe, P.N., Wade, T.L., Sweet, S.T., Rezak, R., Kelly, F.J., Brooks, J.M., Presley, B.J., and Wiesenburg, D.A. 1996. Geochemical patterns in sediments near offshore production platforms. Can. J. Fish. Aquat. Sci. **53**. This issue.

King, J.E. 1948. A study of the reproductive organs of the common marine shrimp, *Penaeus setiferus* (Linnaeus). Biol. Bull. **94**: 244–262.

Larson, S.C., VanDen Avyle, M.J., and Bozeman Jr., E.L. 1989. Species profile: life histories and environmental requirements of coastal fishes and invertebrates (South-Atlantic) — brown shrimp. U.S. Fish Wildl. Serv. Biol. Rep. 82(11–90). U.S. Army Corps of Engineers TR EL-82-4.

Montagna, P.A., and Harper, D.E. Jr. 1996. Benthic infaunal long-term response to offshore production platforms in the Gulf of Mexico. Can. J. Fish. Aquat. Sci. **53**. This issue.

Powell, E.N., Bright, T.J., and Brooks, J.M. 1986. The effect of sulfide and an increased food supply on the meiofauna and macrofauna at the East Flower Garden brine seep. Helgol. Meeresunter. **40**: 57–82.

Render, J.H., and Wilson, C.A. 1994. Hook-and-line mortality of caught and released red snapper around oil and gas platform structural habitat. Bull. Mar. Sci. **55**: 1106–1111.

Shinn, E.A., Lidz, B.H., and Reich, C.D. 1993. Habitat impacts of offshore drilling: eastern Gulf of Mexico. OCS Study MMS 93-0021. U.S. Department of the Interior, Minerals Management Service, Gulf of Mexico OCS Region, New Orleans, La.

Sindermann, C.J. 1983. An examination of some relationships between pollution and disease. Rapp. P.-V. Reun. Cons. int. Explor. Mer,. **182**: 37–43.

Wang, S.Y. and Stickle, W.B. 1988. Biochemical composition of the blue crab *Callinectes sapidus* exposed to the water-soluble fraction of crude oil. Mar. Biol. **98**: 23–30.

Warwick, R.M. 1988. Effects on community structure of a pollutant gradient summary. Mar. Ecol. Progr. Ser. **46**: 207–211.

Widdows, J., Bakke, T., Bayne, B.L., Donkin, P., Livingstone, D.R., Lowe, D.M., Moore, M.N., Evans, S.V., and Moore, S.L. 1982. Responses of *Mytilus edulis* on exposure to the water-accommodated fraction of North Sea oil. Mar. Biol. (Berl.), **67**: 15–31.

© 1996 NRC Canada

Sublethal detoxification responses to contaminant exposure associated with offshore production platforms

Susanne J. McDonald, Kristine L. Willett, Jane Thomsen, Karla B. Beatty, Kevin Connor, Tumkur R. Narasimhan, Cynthia M. Erickson, and Stephen H. Safe

Abstract: Several biomarkers of aromatic hydrocarbon exposure were used to evaluate contamination associated with petroleum and gas development and production in the Gulf of Mexico. Several species of fish and invertebrates were sampled at stations <100 m (near) and >3000 m (far) from the center of three platforms. No significant near/far station differences were observed in aryl hydrocarbon hydroxylase (AHH) activity for any invertebrate species. The only significant induction of ethoxyresorufin *O*-deethylase (EROD) activity in H4IIE cell bioassays was observed in cells dosed with extracts of brown shrimp (*Penaeus aztecus*) sampled at MAI-686 near station. However, a sediment contaminant gradient was not detected at this platform. No significant near/far station differences in EROD and AHH activities, CYP1A mRNA levels, and biliary polynuclear aromatic hydrocarbon (PAH) metabolite concentrations were detected in 16 species of fish. However, species-dependent differences in EROD activity and biliary PAH metabolite levels were detected. Additionally, a radiolabeled nuclear aryl hydrocarbon receptor complex was characterized for two fish species.

Résumé : Plusieurs marqueurs biologiques de l'exposition aux hydrocarbures aromatiques ont été utilisés pour évaluer la contamination associée à la mise en valeur et à la production de pétrole et de gaz dans le golfe du Mexique. Plusieurs espèces de poisson et d'invertébrés ont été échantilloneées dans des stations proches (<100 m) et éloignées (>3 000 m) du centre de trois plates-formes. Aucun écart important entre stations proches et éloignées n'a été observé pour ce qui est de l'activité de l'aryl-hydrocarbure-hydroxylase (AHH) dans les espèces d'invertébrés. La seule induction notable de l'éthoxyrésorufine-*O*-déséthylase (EROD) lors d'essais biologiques sur cellules H4IIE a été observée dans des cellules dosées aux extraits de crevette grise (*Penaeus aztecus*) échantillonnés à la station proche MAI-686. Toutefois, aucun gradient des contaminants dans les sédiments n'a été décelé pour cette plate-forme. Aucun écart important entre stations proches et éloignées n'a été décelé dans 16 espèces de poisson pour ce qui est des activités de l'EROD et de l'AHH, des niveaux d'ARNm CYP1A et des concentrations biliaires de métabolites d'hydrocarbure aromatique polynucléaire (HAP). Mais des écarts ont été observés, selon les espèces, dans l'activité de l'EROD et les concentrations de métabolites de HAP. De plus, un complexe récepteur d'hydrocarbures aromatiques radiomarqué sur le noyau aromatique a été caractérisé chez deux espèces de poisson.
[Traduit par la Rédaction]

Introduction

One component of the Gulf of Mexico Offshore Operations Monitoring Experiment (GOOMEX) was to evaluate a variety of biochemical methodologies to determine if fish and invertebrates were exposed to organic contaminants associated with petroleum and gas development and production in the Gulf of Mexico (Kennicutt et al. 1996*a*). Biomarkers of aromatic hydrocarbon exposure were measured in several species of fish and invertebrates sampled at near (<100 m) and far (>3000 m) stations of three platforms located in the western Gulf of Mexico.

Invertebrates are routinely utilized as indicators of environmental contamination because they readily bioconcentrate aromatic hydrocarbons from their environment (Geyer et al. 1982; Goldberg et al. 1978). However, invertebrate CYP1A-like induction responses have been used with only limited success as indicators of contamination. Although cytochrome P450 systems have been characterized in many marine invertebrates, their CYP1A-like dependent activities and inducibilities are usually low to nondetectable (Lee 1982; Livingstone 1990, 1991; James 1989; Michel et al. 1993; Besten et al. 1993). Consequently, an alternative indicator of hydrocarbon exposure was also evaluated for invertebrates. The induction of ethoxyresorufin *O*-deethylase (EROD) activity in rat hepatoma H4IIE cells exposed to tissues extracts of several invertebrate species was determined.

In vitro rat hepatoma H4IIE cell bioassays were developed to determine the biological potency and 2,3,7,8-tetrachlorodibenzo-*p*-dioxin (TCDD) or toxic equivalents (TEQs) of

Received March 8, 1996. Accepted September 13, 1996.
J13411

S.J. McDonald. Department of Civil Engineering, Texas A&M University, WERC-205, College Station, TX 77845, U.S.A.
K.B. Beatty and C.M. Erickson. Geochemical and Environmental Research Group, Texas A&M University, 833 Graham Rd., College Station, TX 77845, U.S.A.
K.L. Willett, J. Thomsen, K. Connor, T.R. Narasimhan, and S.H. Safe. Department of Veterinary Physiology and Pharmacology, Texas A&M University, College Station, TX 77840, U.S.A.

© 1996 NRC Canada

extracts from a variety of environmental and industrial samples which contain TCDD, polynuclear aromatic hydrocarbons (PAH), and related chemicals (Bradlaw and Casterline 1979; Trotter et al. 1982; Zacharewski et al. 1989). Because these compounds elicit similar toxic and biochemical responses via the aryl hydrocarbon (Ah) receptor mediated signal transduction pathway (Safe 1990), various Ah receptor mediated responses, including CYP1A1 induction, have been used to determine bioassay-derived TEQs for mixtures of chemicals (Ankley et al. 1991, 1992; Bradlaw and Casterline 1979; Krishnan and Safe 1993; Tillitt et al. 1991*a*, 1991*b*; Trotter et al. 1982). However, the induction bioassay cannot be used to determine true TEQs when mixtures contain certain halogenated aromatic hydrocarbons and other CYP1A1 inducers such as PAH. There is no correlation between the EROD-inducing potency of PAH and their toxicity. Toxicity is primarily related to the metabolism of PAH and is Ah receptor independent. Therefore, mixtures containing both PAH and HAH can only be assayed for their relative induction equivalents (I-TEQs).

The most commonly used indicator of aromatic hydrocarbon exposure in fish is induced cytochrome P450 (CYP) dependent responses. A CYP1A has been identified in teleost fish and the gene sequence and catalytic properties of the expressed enzyme are similar to mammalian CYP1A1 (Heilmann et al. 1988). Additionally, the presence of an Ah receptor has been detected in several fish species (Hahn et al. 1994; Willett et al. 1995). The induction of CYP1A1 gene expression requires initial binding of an inducer to an Ah receptor. Fish CYP1A is induced by exposure to selected organic contaminants (Collier and Varanasi 1991; Stegeman et al. 1987; Van Veld et al. 1990) and induction can be assessed by measuring EROD and aryl hydrocarbon hydroxylase (AHH) activities, CYP1A protein content, or CYP1A mRNA levels. Hydrocarbon exposure in fish can also be evaluated by measuring PAH metabolite concentrations in bile. Hepatic PAH metabolites are concentrated in bile for elimination (Varanasi et al. 1989) and biliary levels of fluorescent aromatic metabolites in fish are correlated with PAH exposure (Collier and Varanasi 1991; Krahn et al. 1984, 1992; Varanasi and Gmur 1981).

Induction responses of CYP1A and other indicators of PAH exposure were evaluated in both fish and invertebrate species. Enzyme activities (EROD and AHH), CYP1A mRNA, and biliary PAH metabolite levels were measured in selected fish species. AHH activity and the activity of tissue extracts as inducers of CYP1A1 in rat hepatoma H4IIE cells were evaluated in selected invertebrate species. Additionally, the nuclear Ah receptor was characterized in two fish species captured at GOOMEX sites.

Materials and methods

Sample collection

Samples were collected at one platform in three lease blocks (MAI-686, MU-A85, and HI-A389) in June and January 1993 and 1994 on the R/V *Powell*. Fish and invertebrates were collected using a 17.58-m semiballoon otter trawl. Trawling speed was 0.5 kn and bottom time ranged from 10 to 15 min. Near-field trawls were made perpendicular to radials around the rig at a distance of 100 m or less from the platforms. Far-field trawls were taken at distances in excess of 3000 m from the platforms. After trawl recovery, specimens were sorted and held in cool seawater until dissections. Fish bile and liver samples were immediately removed and placed on ice until dissections were completed. Bile samples were subsequently stored at −20°C until analysis. Fish livers and hepatopancreas from crabs and gastropods and the green gland from shrimp were quick frozen and stored in liquid nitrogen. All of the soft tissue from paper scallop (*Amusium papyraceum*) was frozen in liquid nitrogen.

Subcellular tissue preparation

Assays were optimized prior to data collection. All samples were kept on ice during all processing steps and resultant microsomes were frozen in liquid nitrogen until assayed. Samples were homogenized using a Polytron in an appropriate buffer. For crustaceans, the green gland or hepatopancreas was homogenized in a buffer containing 0.1 M potassium phosphate, 0.1 M KCl, 1.0 mM EDTA, 0.1 mM phenanthroline, 1.0 mM dithiothreitol (DTT), and 1.0 mg trypsin inhibitor·mL^{-1} (Jewell and Winston 1989 with modifications). Samples were centrifuged at 600 × *g* for 20 min, 10 000 × *g* for 20 min, twice, and 100 000 × *g* for 60 min. The microsomal pellets were resuspended in a 0.1 M potassium phosphate buffer containing 1.0 mM EDTA, 1.0 mM DTT, 0.1 mM phenanthroline, 1.0 mg trypsin inhibitor·mL^{-1}, and 15% glycerol. Microsomal preparations from molluscs were prepared after the methods of Livingstone and Farrar (1984) with modifications. Tissues were homogenized in a 20 mM Tris buffer containing 0.5 M sucrose, 0.15 M KCl, and 1 mM EDTA. Samples were centrifuged at 500 × *g* for 1 h, 10 000 × *g* for 45 min, and 100 000 × *g* for 90 min. The microsomal pellets were resuspended in a 20 mM Tris–HCl buffer containing 1 mM EDTA and 20% glycerol. Fish liver was processed using the protocol of Stegeman et al. (1987) with modifications. Briefly, livers were homogenized in a 20 mM Tris–HCl buffer containing 0.25 M sucrose and centrifuged at 600 × *g* for 10 min, 5000 × *g* for 10 min, 13 000 × *g* for 10 min, and 100 000 × *g* for 60 min. The resultant microsomal pellets were resuspended in a 50 mM Tris–HCl buffer containing 1 mM EDTA in 20% glycerol. Proteins were assayed by the method of Bradford (1976).

AHH activity in fish and invertebrates

AHH activity was assayed using the method of Nebert and Gelboin (1968) with modifications. Assays of fish samples were conducted in 1.0 mL of reaction mixture containing 0.1 M HEPES at pH 8.0, 0.4 mM NADPH, and 500 μg of microsomal protein at 30°C. Reactions were initiated by addition of 80 μM benzo[*a*]pyrene (BaP). Samples were incubated for 10 or 15 min and terminated by addition of 1 mL of cold acetone followed by 3.25 mL of hexane. Samples were shaken and 2 mL of the organic layer was withdrawn and extracted with 5 mL of sodium hydroxide. An aliquot of the basic layer was read on a spectrofluorometer at 396/522 excitation/emission wavelengths. The spectrofluorometer was calibrated with a 3-hydroxy BaP standard. For invertebrates, the incubation mixture consisted of 50 mM Tris–HCl, pH 7.6, 0.1 mM NADPH, and 500 μg of microsomal protein. The reaction was initiated by addition of 60 μM BaP. Samples were incubated for 15 min at 30°C and stopped by addition of 1 mL of cold acetone. The extraction procedure and instrument analysis were as described for fish microsomes.

Rat hepatoma H4IIE cell bioassay

Invertebrate tissues were extracted using a Tissumizer with 50 g of sodium sulfate and 100 mL of methylene chloride. The extraction was repeated twice with 100 mL of methylene chloride and the three extracts were combined and concentrated. The concentrates were purified using silica gel/alumina column chromatography and HPLC to remove matrix interferences. The resulting extracts were evaporated to near dryness and redissolved in a known volume of dimethyl sulfoxide (DMSO).

Rat hepatoma H4IIE cells were grown as a continuous cell line in α-minimum essential medium supplemented with 2.2 g sodium

© 1996 NRC Canada

bicarbonate·L^{-1}, 10% fetal bovine serum, and 10 mL antibiotic–antimycotic solution·L^{-1}. Stock culture cells were grown in 150-cm^2 plates at 37°C in a humidified air – carbon dioxide (95:5) atmosphere. After confluency, cells from one plate were trypsinized and seeded in six-well plates with 2 mL of medium per well. After 24 h, cells were dosed with 5-μL test extracts so that the final concentration of DMSO was 0.25%. Cells were also treated with 1 nM 2,3,7,8-TCDD to obtain maximal induction activity. After 24 h the medium was removed, cells were washed with 2 mL of Hanks solution (Hanks balanced salts, 0.35 g sodium bicarbonate·L^{-1} at pH 7.4) and harvested by scraping in 4 mL of Tris–sucrose solution (Tris base 6.05 g·L^{-1}, sucrose 59.45 g·L^{-1}, pH 8.0). The resulting cellular pellet was isolated after centrifuging for 5 min at 1000 rpm at 4°C. Cells were resuspended in 200 μL of Tris–sucrose solution. Aliquots of the cell suspension were incubated in a solution containing 1 mg of bovine serum albumin (BSA), 0.1 mg of NADH, 0.1 mg of NADPH, and 1.5 mg of $MgSO_4$ in 0.1 M HEPES, pH 7.5, at 37°C for 2 min. The reaction was initiated with the addition of 50 μL of ethoxyresorufin (100 μM) and after incubation was terminated with the addition of 2.5 mL of methanol. Samples were centrifuged for 10 min at 1000 × *g*. The supernatant was read on a spectrofluorometer at 550 nm excitation and 585 emission wavelength settings.

EROD activity in fish

EROD activity was measured in microsomal preparations from fish livers using the method of Pohl and Fouts (1980) with modifications. The assays were conducted in 1.15-mL incubation mixtures consisting of 0.1 M HEPES at pH 8.0, 0.1 mg of NADPH, 0.1 mg of NADH, 0.7 mg of BSA, 0.7 mg of $MgSO_4$, and 50 μL of microsomes (200–250 μg protein) at 30°C. Reactions were initiated by addition of 50 μL of 100 μM ethoxyresorufin. Samples were incubated for 10 or 15 min and stopped by addition of 2.5 mL of methanol. Samples were read on a spectrofluorometer at 550 nm excitation and 585 nm emission wavelength settings.

CYP1A mRNA

Total RNA was isolated from homogenized liver samples in 1 mL of solution D (4 M guanidinium thiocyanate, 100 mM sodium acetate, 0.5% sarcosyl at pH 5.5, and 0.1 M 2-mercaptoethanol) by the method of Chomczynski and Sacchi (1987) with modifications (Willett et al. 1995). RNA was extracted by adding 50 μL of 2 M sodium acetate to 500 μL of sample to which 500 μL of water-saturated phenol, 200 μL of water, and 200 μL of Sevag (24:1 chloroform – isoamyl alcohol) were added. Samples were vortexed and centrifuged for 15 min at 12 000 × *g*. This extraction was repeated three times. The final aqueous layer was added to one volume of isopropyl alcohol and precipitated overnight at −20°C. The resulting precipitate was centrifuged at 12 000 × *g* for 15 min, supernatant decanted, and the pellet washed with two 70% washes and one 100% ethyl alcohol wash. The dried pellet was resuspended in 15–50 μL of formamide by heating at 55°C. The RNA was quantitated by UV_{260} absorption.

For the Northern Blot, a sample containing 20 μg of RNA in ≈ 2× sample loading buffer consisting of 35% formaldehyde, 10% 10× SPC (200 mM Na_2HPO_4 and 20 mM EDTA at pH 6.8), 25% TE (10 mM Tris and 1 mM EDTA at pH 8.0), and 30% 6× tracking dye (0.25% xylene cyanol, 0.25% bromophenol blue, 25% ficoll, and 0.1 M EDTA) was loaded onto a 1.2% agarose gel (0.66 M formaldehyde) and run at 50–75 V for 3–4 h in 1× SPC buffer. The gel was stained with ethidium bromide, washed, and transferred to a Hybond™-N+nucleic acid transfer membrane for a minimum of 12 h. The membrane was washed in 0.1× SPC, crosslinked by UV exposure, and baked for 2 h at 80°C. The membrane was prehybridized in Denhardt's solution (20% 5× SSPE, 1% SDS, 10% dextran sulfate, and 0.1% each of polyvinylpyrolidone, BSA, and ficoll; 20% SSPE contains 3.0 M NaCl, 0.2 M $NaPO_4$, and 0.02 Na_2EDTA) for 12 h at 42°C. Membranes were hybridized for approximately 24 h with the addition of 10^6 cpm ^{32}P randomly labeled freshwater rainbow trout probe·mL^{-1} for CYP1A (Heilmann et al. 1988). The trout CYP1A cDNA plasmid (pFP_1450-3′) was a gift from Dr. John Lech (Medical College of Wisconsin, Milwaukee, Wis.). After hybridization, membranes were washed twice at ambient temperature in 1× SSPE for 15 min. Two additional washes were carried out at 50°C for 45 min each in 1× SSPE and 2% SDS. Membranes were washed twice for 30 min at 20°C in 0.1× SSPE. The mRNA levels were quantitated on a Betagen Betascope 603 blot analyzer imaging system. Finally, membranes were exposed to X-OMAT imaging film and photographed. Membranes were stripped by washing twice in stripping buffer (0.1× SSPE and 1% SDS) at 100°C. The levels of CYP1A were standardized by probing membranes with human fetal brain tubulin cDNA (ATCC).

Ah receptor binding

The compound [^{3}H]TCDD was synthesized in this laboratory to 95% purity (30 Ci·$nmol^{-1}$, 1 Ci = 37 GBq) and was administrated in a single i.p. injection (in corn oil) to pinfish (*Lagodon rhomboides*) and inshore lizardfish (*Synodus foetens*) (1 μL·g fish to equal 2.5 μg·kg^{-1}). Nuclear extract baselines were obtained by cotreatment with 100-fold excess unlabeled TCDD. Four fish of each species were used for both competed and uncompleted trials. Fish were maintained in tanks for 4 h prior to sacrifice. Livers were isolated, resuspended in HEGD (25 mM HEPES, 1.5 mM EDTA, 1.0 mM dithiothreitol, 10% glycerol (v/v), pH 7.6 buffer), homogenized using a Teflon pestle/drill apparatus, and centrifuged at 4000 × *g* for 10 min at 4°C. The resulting nuclear pellet was washed twice with 20 mL of HEGD and was resuspended in HEGD buffer, containing 0.5 M potassium chloride, and incubated at 4°C for 1 h. Samples were frozen in liquid nitrogen and returned to the laboratory for further processing. Upon receipt in the laboratory, samples were thawed, and after a 30-min, 105 000 × *g* spin at 4°C, unbound and loosely bound [^{3}H]TCDD was removed by incubating with dextran-coated charcoal (0.5 mL of 0.01:0.001% charcoal–dextran·mL nuclear $extract^{-1}$) for 10 min at 4°C.

Aliquots (400 μg of protein) of sample were layered onto linear sucrose density gradients (5–25%) prepared in HEGD buffer containing 0.5 M potassium chloride and centrifuged at 4°C for 2.5 h at 404 000 × *g*. After centrifugation, 30 fractions were collected from each gradient, 0.5 mL of tissue solubilizer (DuPont) was added, and samples were then incubated at 50°C for 4 h before counting the radioactivity in each fraction. ^{14}C-labeled BSA (4.4 S) and catalase (11.3 S) were used as external standards.

PAH metabolites in bile

Biliary PAH metabolites were analyzed by HPLC/fluorescence detection, as previously described (Krahn et al. 1984, 1986). Briefly, bile was injected into an HPLC and metabolites were resolved using a C-18 reverse-phase column and detected with a fluorometer. Aromatic compounds fluorescing at naphthalene (290/335), phenanthrene (260/380), and BaP (380/430) excitation/emission wavelengths were analyzed. Metabolites eluting from the column within specific retention times were summed to yield total fluorescence based on equivalents of known amounts of naphthalene, phenanthrene, and BaP standards.

Statistical analysis

Data were log transformed prior to statistical treatment and statistical significance was determined by MANOVA and ANOVA ($p \leq 0.05$).

Results

Sixteen fish species and five invertebrate species were collected at both near and far stations for at least one of the three study sites, MAI-686, MU-A85, and HI-A385 (Fig. 1). Only

© 1996 NRC Canada

Fig. 1. Location of the final study sites.

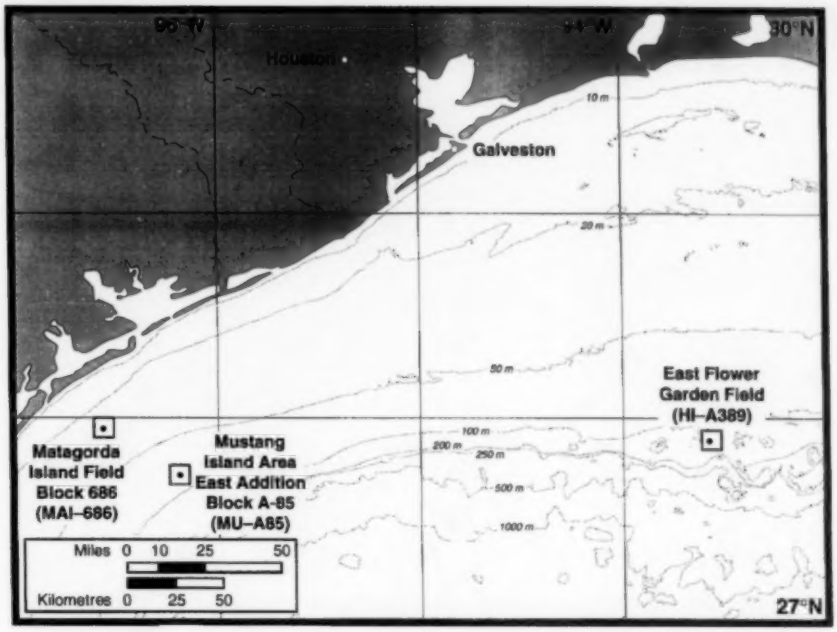

Table 1. AHH activities of various invertebrate species collected at near (N) and far (F) stations at MAI-686, MU-A85, and HI-A389.

Species	Site	AHH (pmol·min^{-1}·mg^{-1})
Trachypenaeus similis (spider crab)	HI-A389 N	1.0 ± 3.2
	HI-A389 F	0
Trachypenaeus similis (welk)	MAI-686 N	3.0 ± 4.2
		0
Trachypenaeus similis	MAI-686 F	0
Callinectes similis (bristle worm)		0
	MU-A85 N	0
Penaeus aztecus		1.2
Amusium papyraceum		0
Penaeus aztecus		1.1 ± 0.9

two species of fish, *S. foetens* and southern flounder (*Paralichthys lethostigma*), were captured at all stations. AHH activity was measured in both fish livers and invertebrate tissues for samples collected during cruise 1. AHH activity was also measured in hepatic samples from fish collected on cruise 2. EROD activity and biliary PAH metabolite concentrations were measured in fish collected on all four cruises. CYP1A mRNA levels were determined on selected fish samples from cruises 2, 3, and 4.

AHH activity in invertebrates

Few invertebrates were collected by box coring; most samples were collected by trawling. AHH activities were low to nondetectable for all invertebrate species examined (Table 1). Consequently, AHH measurements for invertebrates were discontinued for subsequent cruises.

Rat hepatoma H4IIE bioassay

The highest I-TEQs, determined in rat hepatoma H4IIE cell bioassays, were observed in cells dosed with extracts from *A. papyraceum* (Fig. 2). The only significant near/far station difference in I-TEQs was observed at MAI-686 using extracts of brown shrimp (*Penaeus aztecus*) (Table 2).

EROD and AHH activity in fish

No consistent differences in hepatic EROD activities were detected for fish collected during four cruises; therefore, the cruises were considered replicates. EROD activities in various fish species were highly variable and species dependent (Fig. 3; Table 3). Activities ranged from nondetectable to 348 pmol·min^{-1}·mg^{-1}. The highest mean EROD activity was measured in *L. rhomboides*. Consistently lower EROD activities were measured for rock sea bass (*Centropristis philadelphica*) and three-eye flounder (*Ancyclopsetta dilecta*). However, no significant near/far station differences were observed for any of the species evaluated (Table 3).

CYP1A mRNA

The banding pattern and gel electrophoretic mobilites of the CYP1A mRNA transcripts were similar for all fish reported in this study (Figs. 4 and 5).

Ah receptor

Lagodon rhomboides and *S. foetens* were dosed with [^{3}H]TCDD to characterized their nuclear Ah receptor. The radiolabeled Ah receptor complex for both species sedimented at 5.4 S (Figs. 6 and 7).

© 1996 NRC Canada

Fig. 2. Mean I-TEQs derived from rat hepatoma H4IIE cells dosed with extracts of various invertebrate species collected at near and far stations at MAI-686, MU-A85, and HI-A389.

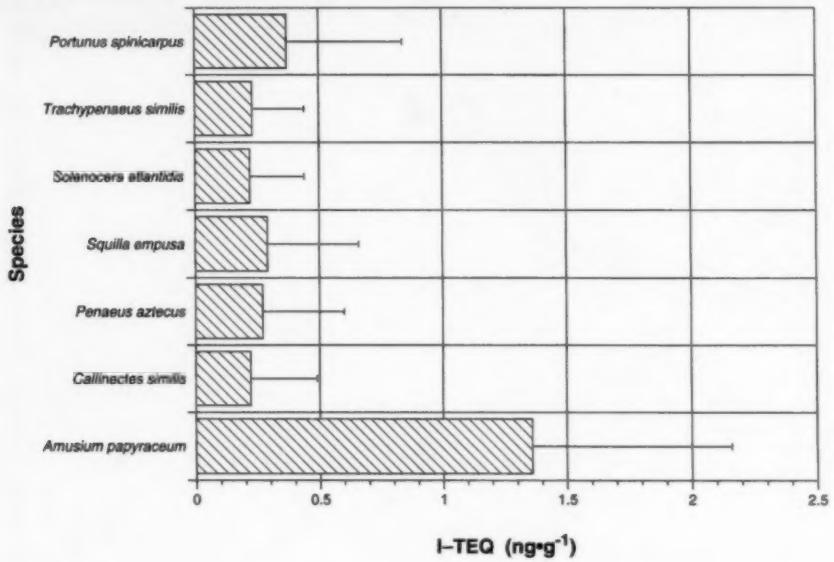

Table 2. Mean I-TEQs derived from rat heptatoma H4IIE cells dosed with extracts of invertebrates collected at near (N) and far (F) stations at MAI-686, MU-A85, and HI-A389.

Species	Site	I-TEQ (ng·g^{-1})[a]
Callinectes similis	MAI-686 F	0.27 ± 0.37
	MAI-686 N	0.18 ± 0.07
Penaeus aztecus	MAI-686 F	0.18 ± 0.13
	MAI-686 N	0.83 ± 0.78
	MU-A85 F	0.20 ± 0.12
	MU-A85 N	0.29 ± 0.26
Solenocera atlantidis	MU-A85 F	0.18 ± 0.14
	MU-A85 N	0.29 ± 0.30
Squilla empusa	MAI-686 F	0.39 ± 0.47
	MAI-686 N	0.22 ± 0.26
Trachypenaeus similis	MAI-686 F	0.16 ± 0.13
	MAI-686 N	0.29 ± 0.26

[a] I – TEQ (ng·g dry^{-1}) = 0.644 ng TCDD × ($EROD_{sample}$/$EROD_{TCDD}$) × (dilution factor/tissue dry weight).

Biliary PAH metabolites in fish

Significant species differences were also observed in biliary PAH metabolite concentrations (Fig. 8; Table 3). The concentrations of naphthalene and phenanthrene and BaP equivalent metabolites were significantly higher in *L. rhomboides* and *Urophycis* spp., respectively. However, no significant near/far station differences in biliary PAH metabolite concentrations were detected for any species.

Discussion

Although the presence of AHH activity and cytochrome P450 components has been detected in a number of invertebrate species (Lee 1982; James 1989; Livingstone 1991), there are conflicting data on the presence, properties, and relationship of the invertebrate P450 system. Numerous studies were unable to demonstrate AHH induction in various invertebrate species after exposure to aromatic hydrocarbons (Lee et al. 1972; Payne 1977; James and Little 1984; Kurelec et al. 1986) and there is also only limited evidence of an Ah receptor (Hahn et al. 1992, 1994; Brown and Van Beneden 1993; Muehleisen et al. 1989). Conversely, other studies reported low-level induction of AHH activity in invertebrates exposed to hydrocarbons (Anderson 1978; Schlenk and Buhler 1988; Besten et al. 1990, 1993; Livingstone 1990, 1991; Michel et al. 1995) and presented evidence of CYP1A-like proteins (Livingstone et al 1995; Porte et al. 1995) and CYP1A-like mRNA (Livingstone et al. 1995; Wootton et al. 1995). As a consequence of the conflicting data, AHH activity in invertebrates was included in the study design to evaluate its potential as an indicator of PAH exposure at offshore platforms. However, no significant near/far station differences were detected in AHH activity for any invertebrate species examined. It is not clear if the lack of AHH induction was related to the low hydrocarbon contaminant gradient (see Kennicutt et al. 1996*b*) and/or inconsistencies associated with the invertebrate P450 system. Consequently, this assay was discontinued for subsequent cruises.

The highest CYP1A1 induction response in H4IIE cell bioassays was observed in cells dosed with scallop extracts, and this is consistent with the ready bioaccumulation of contaminants in filter-feeding molluscs. The only significant near/far station difference was observed for cells dosed with extracts of *P. aztecus* from MAI-686. However, a parallel sediment contamination gradient was not observed at this platform. These findings are also consistent with the low tissue concentrations of aromatic hydrocarbons reported for invertebrates captured at the GOOMEX sites (Kennicutt et al. 1996*b*). The

© 1996 NRC Canada

Fig. 3. Mean hepatic EROD activities in various fish species collected at near and far stations at MAI-686, MU-A85, and HI-A389.

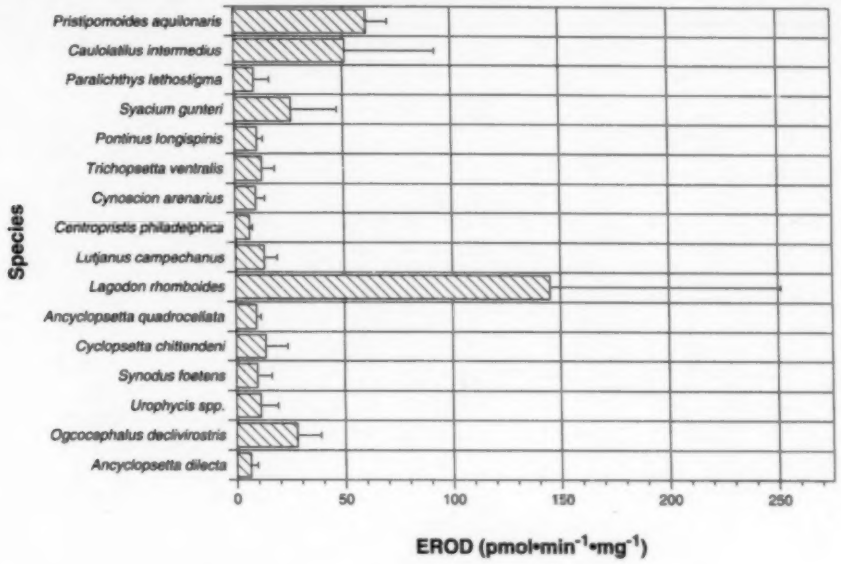

Fig. 4. Northern Blot analysis of CYP1A mRNA in various fish species collected at near and far stations at MAI-686, MU-A85, and HI-A389.

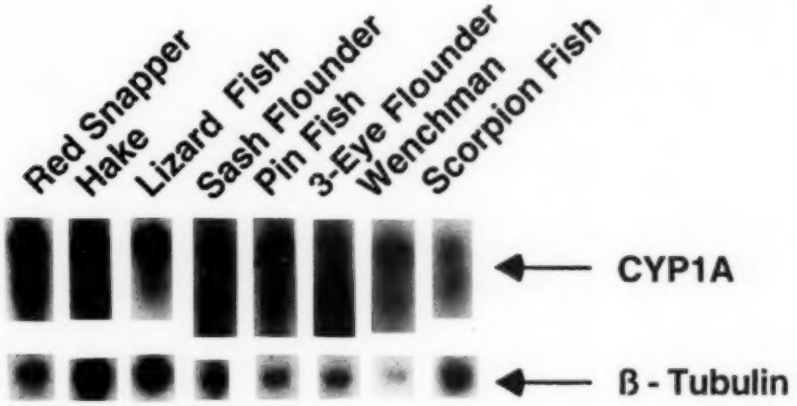

induction of EROD activity in rat hepatoma H4IIE cells was correlated with tissue concentrations of aromatic hydrocarbons in other studies, although tissue levels of contamination were significantly higher than those reported for this study (McDonald et al. 1994, 1995).

Of the 25 species of fish collected during the GOOMEX project, 16 were collected at both near and far stations for at least one platform. A range of EROD activities was measured in the various fish species. The highest EROD activities were measured in *L. rhomboides* and anchor tilefish (*Caulolatilus intermedius*) whereas lower activities were consistently measured in *C. philadelphica*. Species differences in CYP1A-dependent enzyme activities have also been observed in other fish studies (Collier at al. 1995; Davies et al. 1984). Although both hepatic AHH and EROD activities were measured in all fish species collected on cruises 1 and 2, determination of AHH activity was discontinued for subsequent cruises because a good correlation between the two assays was established for most species with the exception of *L. rhomboides*. Other studies demonstrated a good concordance between hepatic AHH and EROD activity in several fish species (Collier et al. 1992, 1995). However, a lack of correlation between the two catalytic assays has also been reported for some species (Foureman et al. 1983; James and Bend 1980; Stegeman et al. 1981). The two assays measure the activity of the same enzyme (i.e., CYP1A) and fish that are outliers for the coordinated induction of AHH and EROD activities may express a variant CYP1A isozyme or other

© 1996 NRC Canada

Table 3. Mean EROD and AHH activities and mean biliary PAH metabolite concentrations for various fish species captured at near (N) and far (F) stations at MAI-686, MU-A85, and HI-A389 (NA = not available).

Species	Site	EROD (pmol·min^{-1}·mg^{-1})	AHH (pmol·min^{-1}·mg^{-1})	Naphthalene (ng·g^{-1})	Phenanthrene (ng·g^{-1})	BaP (ng·g^{-1})
Ancyclopsetta dilecta	MU-A85N	6.8 ± 0.8	0	NA	NA	NA
(three-eye flounder)	MU-A85F	4.3 ± 3.4	0	NA	NA	NA
	HI-A389N	6.6 ± 2.6	0	NA	NA	NA
	HI-A389F	7.1 ± 4	0	NA	NA	NA
Caulolatilus intermedius	MU-A85N	69.6 ± 37.9	NA	200 000	40 000	<100
(anchor tilefish)	MU-A85F	66 ± 38.5	NA	130 000 ± 67 000	17 000 ± 6500	140 ± 200
	HI-A389N	56.7 ± 59.1	NA	150 000 ± 33 000	37 000 ± 14 000	<100
	HI-A389F	26.1 ± 10.5	NA	68 000 ± 22 000	11 000 ± 3000	280 ± 250
Centropristis philadelphica	MU-A85N	6.8 ± 1	4 ± 3.9	140 000 ± 49 000	27 000 ± 10 000	360 ± 190
(rock sea base)	MU-A85F	6.2 ± 1.4	1.2 ± 1.6	70 000 ± 35 000	9900 ± 3500	180 ± 120
Cynoscion arenarius	MU-A85N	8.4 ± 2.3	NA	88 000 ± 33 000	18 000 ± 8400	100 ± 0
(sand seatrout)	MU-A85F	6.4 ± 2.4	NA	130 000 ± 74 000	21 000 ± 9200	110
	MAI-686N	10.7 ± 5.2	NA	100 000 ± 35 000	19 000 ± 8800	250 ± 180
	MAI-686F	9.8 ± 1.7	NA	110 000 ± 60 000	19 000 ± 7400	120 ± 10
Cyclopsetta chittendeni	MU-A85N	12.7 ± 11.3	0.7 ± 1.1	54 000 ± 11 000	12 000 ± 4700	110 ± 150
(Mexican flounder)	MU-A85F	15.6 ± 8.1	6.8 ± 9.2	68 000 ± 30 000	15 000 ± 9400	210 ± 200
Lagodon rhomboides	MU-A85N	140.5 ± 101.4	11.3 ± 14	190 000 ± 71 000	49 000 ± 25 000	120 ± 80
(pinfish)	MU-A85F	156.9 ± 132.9	51 ± 21.4	190 000 ± 95 000	35 000 ± 20 000	180 ± 190
Ogcocephalus declivirostris	HI-A389N	26.2 ± 4.9	NA	33 000 ± 18 000	7900 ± 4300	<100
(slantbrow batfish)	HI-A389F	34.8 ± 29.6	NA	73 000	15 000	420
Paralichthys lethostigma	HI-A389N	9.7 ± 10.7	NA	NA	NA	NA
(southern flounder)	HI-A389F	6.9 ± 3.3	NA	NA	NA	NA
	MAI-686N	10.8 ± 4.8	NA	NA	NA	NA
	MAI-686F	6.5 ± 0	NA	NA	NA	NA
	MU-A85N	7.5 ± 2.6	NA	NA	NA	NA
	MU-A85F	7.2 ± 0.7	NA	NA	NA	NA
Pontinus longispinis	HI-A389N	9.8 ± 1.5	0	120 000 ± 56 000	29 000 ± 22 000	<100
(longspine scorpionfish)	HI-A389F	10.4 ± 3.6	0.2 ± 0.4	120 000 ± 60 000	33 000 ± 31 000	270 ± 180
Pristipomoides aquilonaris	MU-A85N	10.7 ± 5.3	NA	82 000 ± 10 000	16 000 ± 1400	110 ± 70
(wenchman)	MU-A85F	8.3 ± 1.6	NA	90 000 ± 33 000	16 000 ± 4800	160 ± 50
	HI-A389N	10.8 ± 3.5	NA	79 000 ± 42 000	18 000 ± 12 000	160 ± 40
	HI-A389F	9.9 ± 2.5	NA	10 000 ± 5000	20 000 ± 12 000	170 ± 100
Syacium gunteri	MAI-686N	21.6 ± 15.6	15.4 ± 15.4	NA	NA	NA
(shoal flounder)	MAI-686F	28.2 ± 23.4	21.3 ± 26.6	NA	NA	NA
Synodus foetens	HI-A389N	12.3 ± 14	0	57 000 ± 25 000	11 000 ± 4500	<100
(inshore lizardfish)	HI-A389F	8.9 ± 3.5	0	88 000 ± 45 000	16 000 ± 9400	190 ± 160
	MU-A85N	8 ± 1.7	0	110 000 ± 53 000	19 000 ± 9700	280 ± 140
	NU-A85F	6.4 ± 1.6	0	83 000 ± 35 000	17 000 ± 7200	210 ± 160
	MAI-686N	22.4 ± 8.8	0	180 000	42 000	460
	MAI-686F	12.6 ± 6.6	0	140 000	23 000	150
Trichopsetta ventralis	MU-A85N	10.5 ± 5	0	NA	NA	NA
(sash flounder)	MU-A85F	9.3 ± 3.7	0	NA	NA	NA
	HI-A389N	13 ± 4.9	0	NA	NA	NA
	HI-A389F	15.5 ± 7.8	0	NA	NA	NA
Urophycis spp.	MU-A85N	10.6 ± 3.8	0	NA	NA	NA
(hakes)	MU-A85F)	10.9 ± 6.4	0	NA	NA	NA
	HI-A389N	10.5 ± 7.1	1.2 ± 2	NA	NA	NA
	HI-A389F	11.7 ± 10.5	2 ± 2.8	NA	NA	NA
Ancyclopsetta quadrocellata	MAI-686N	11.3 ± 0	NA	NA	NA	NA
(ocellated flounder)	MAI-686F	8.4 ± 1.6	NA	NA	NA	NA
Lutjanus campechanus	MU-A85N	14.1 ± 4.3	NA	NA	NA	NA
(red snapper)	MU-A85F	14.1 ± 5.6	NA	NA	NA	NA
	MAI-686N	13.2 ± 7.3	NA	NA	NA	NA
	MAI-686F	8 ± 0.8	NA	NA	NA	NA

© 1996 NRC Canada

Fig. 5. Northern Blot analysis of CYP1A mRNA in *S. foetens* collected at near and far stations at MAI-686 and MU-A85.

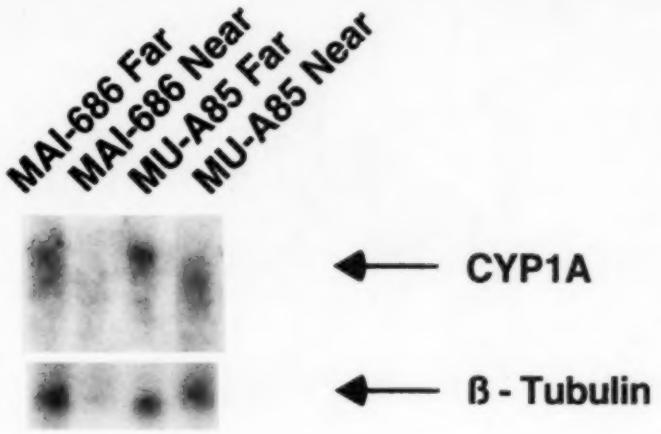

Fig. 6. Ah receptor profile in *S. foetens*.

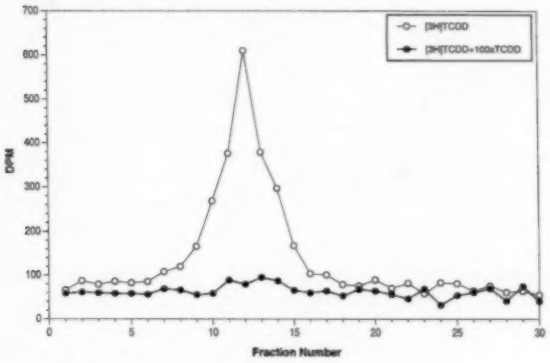

Fig. 7. Ah receptor profile in *L. rhomboides*.

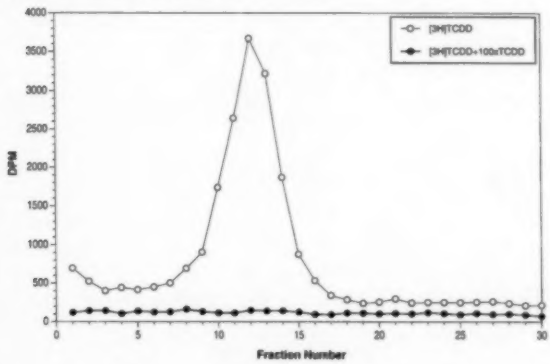

isozymes which preferentially catalyze the oxidation of only one of the enzyme substrates.

A significant PAH contamination gradient was detected at HI-A389 and MU-A85; however, no significant differences in enzyme activities were observed for fish species captured at the near and far stations at these sites. Moreover, EROD and AHH activities were generally low and these activities may represent basal or constitutive expression. However, the CYP1A induction responsiveness of the various fish species could not be assessed because of the low PAH concentrations observed at the GOOMEX sites. The sensitivity of EROD and AHH induction in response to inducers was demonstrated in previous studies. Fish dosed with low levels of BaP and crysene exhibited significant CYP1A-dependent enzyme induction (van der Weiden et al. 1994; Willett et al. 1995). The lack of induced EROD and AHH activities observed in fish examined for this study may also be due to the low sediment levels of aromatic hydrocarbons. Although a sediment PAH gradient between near and far stations was detected at two platforms, sediment PAH concentrations were relatively low. Specifically, the mean sediment ΣPAH concentration for the near and far stations at MU-A85 was 280 $ng \cdot g^{-1}$ (maximum = 2304 $ng \cdot g^{-1}$) and 29 $ng \cdot g^{-1}$ (maximum = 58 $ng \cdot g^{-1}$), respectively. At HI-A389, the mean ΣPAH in sediments at near stations was 361 $ng \cdot g^{-1}$ (maximum = 1103 $ng \cdot g^{-1}$) and at far stations was 35 $ng \cdot g^{-1}$ (maximum = 84 $ng \cdot g^{-1}$). Additionally, sediment PAH were highly degraded and contained low to nondetectable levels of ≥4-ring PAH, which are strong inducers of CYP1A.

Increased CYP1A1-dependent enzyme activities are also accompanied by increased levels of CYP1A1 mRNA in target tissues (Whitlock 1986; Safe 1990) and levels of this transcript can be used as a sensitive and specific assay for exposure of marine organisms to aromatic hydrocarbons (Haasch et al. 1989; Hahn and Stegeman 1994; Courtenay et al. 1993). Haasch et al. (1992) detected a threefold induction of CYP1A mRNA in killifish sampled at a contaminated site compared with those from a clean site. However, no significant differences were observed in CYP1A mRNA gel electrophorectic transcripts for any of the fish species sampled for this study. Additionally, the CYP1A messages observed for all species collected during this study are similar to the inducible CYP1A transcripts found in fish dosed with PAH (Willett et al. 1995). These data are consistent with the other biomarker data measured for GOOMEX and indicate that there is no sig-

© 1996 NRC Canada

Fig. 8. Mean biliary PAH concentrations in various fish species collected at near and far stations at MAI-686, MU-A85, and HI-A389.

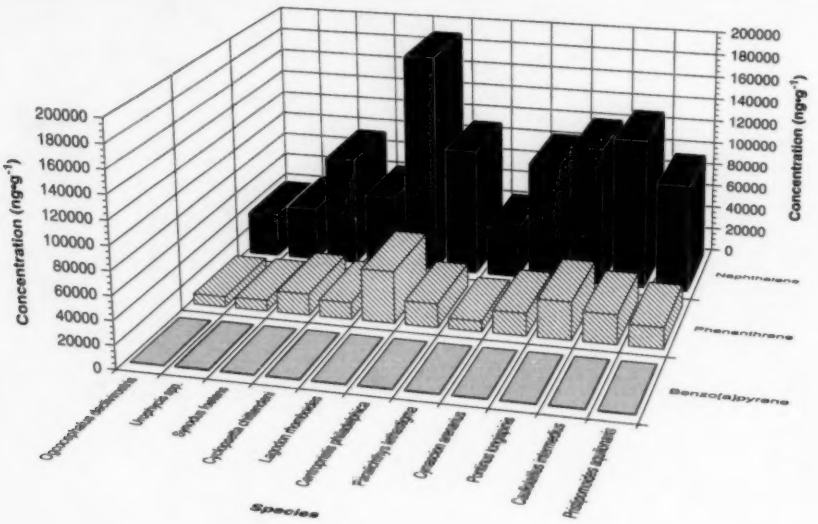

Fig. 9. Correlation between total PAH concentrations in sediments and hepatic EROD activities of fish. Data compiled from other studies (Elskus and Stegeman 1989; Addison et al. 1994; Van Veld et al. 1990; Collier et al. 1995). ER-L: effects level low (10%); ER-M: effects level medium (50%); see Long and Morgan (1990).

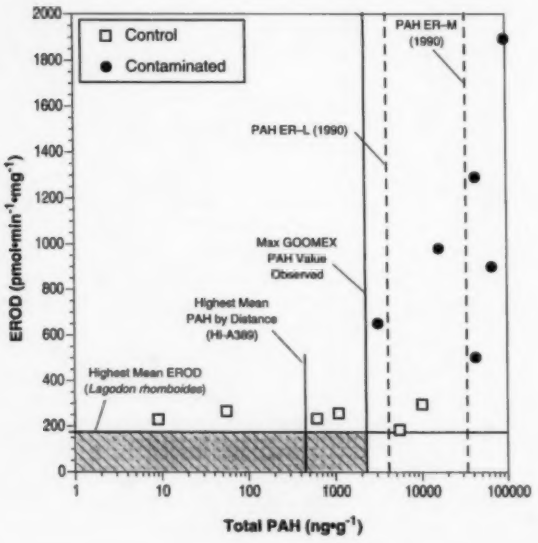

nificant difference in hydrocarbon exposure for fish captured at the GOOMEX sites.

Other studies used CYP1A induction responses to evaluate hydrocarbon contamination associated with offshore oil and gas drilling in the North Sea and in a region known to have natural hydrocarbon seepage off the coast of California (Spies et al. 1982; Davies et al. 1984; Renton and Addison 1992; Goksøyr et al. 1992). Two of three fish species collected from near platforms in the northern North Sea exhibited significantly higher hepatic AHH activities than those captured up to 16 km away (Davies et al. 1984). The significant differences in AHH activity correlated with a dramatic PAH gradient at the North Sea sites. Sediment ΣPAH concentrations ranged from 997 ppb at 16 km to >429 000 ppb at 400 m (Davies et al. 1984). AHH activity was significantly higher in two sand dab species, Pacific sanddab (*Citharichthys sordidus*) and speckled sanddab (*C. stigmaeus*), collected at natural petroleum seeps near Santa Barbara, California, than in fish collected from a relatively uncontaminated site in Monterey Bay, California (Spies et al. 1982). In another North Sea study, no significant differences in EROD activity, CYP1A protein levels, and CYP1A mRNA levels were observed in dab (*Limanda limanda*) captured at reference and abandoned drilling sites off the Netherlands (Renton and Addison 1992; Goksøyr et al. 1992). This correlated with uniformly low sediment PAH concentrations at these sites (Stebbing et al. 1992).

Comparison of hydrocarbon levels and CYP1A induction between this study and other field studies shows that the GOOMEX study sites most closely resemble sites with low-level PAH contamination (Fig. 9) (Elskus and Stegeman 1989; Van Veld et al. 1990; Addison et al. 1994; Collier et al. 1995). The sediment PAH concentrations at sites referenced in Fig. 9 greatly exceeded those documented in the GOOMEX study. Based on these environmental studies, sediment concentrations of PAH in excess of 3000 $ng \cdot g^{-1}$ appear to be necessary before a significant induction in hepatic EROD activity in fish above reference levels can be detected (Fig. 9). This is consistent with Long and Morgan's (1990) 10% biological effects criterion. The 10% criterion is a contaminant level at which some measurable biological effect was observed 10% of the time. The 10% criterion level corre-

© 1996 NRC Canada

sponds to sediment PAH levels of 4000 $ng \cdot g^{-1}$. Therefore, it appears as if moderate levels of sediment contamination are required before significant CYP1A induction in fish can be detected in many marine locations.

An Ah receptor has been previously identified in the cytosolic fraction of three fish hepatoma cell lines (Lorenzen and Okey 1990; Swanson and Perdew 1991; Hahn et al. 1993) and a photoaffinity-labeled Ah receptor was also identified in the hepatic cytosol of seven species of teleost and elasmobranch fish (Hahn et al. 1994). A nuclear Ah receptor was reported in gulf killifish (*Fundulus grandis*) (Willett et al. 1995) and this study also found evidence of a nuclear Ah receptor in *L. rhomboides* and *S. foetens*. The presence of a nuclear Ah receptor in these fish is consistent with the proposed nuclear receptor mediated induction pathway for Ah receptor agonists (Whitlock 1990). Moreover, the sedimentation characteristics (5.4 S) of the nuclear Ah receptor in these fish are similar to the sedimentation characteristics of mammalian Ah receptors, including humans.

Field studies have shown that formation of biliary PAH metabolites can be used to estimate PAH exposure in fish from both combustion and petroleum sources (Krahn et al. 1986, 1992; McDonald et al. 1991, 1992, 1995). Furthermore, in laboratory dose- and time-course experiments, *Fundulus* spp. dosed with BaP were used as a model to evaluate the relative sensitivities of several biomarkers of exposure. Biliary BaP metabolite levels were one of the more sensitive indicators of exposure (Willett et al. 1995). This technique can also be used to estimate exposure to lower molecular weight PAHs such as di- and tricyclic compounds which do not bind to the Ah receptor and induce CYP1A1 (Piskorska-Pliszczynska et al. 1986). Although no significant near/far station differences were observed, the concentrations of naphthalene and phenanthrene equivalent metabolites were consistently higher in the bile of *L. rhomboides*. The low levels of BaP equivalent metabolites detected in bile correlated with low to nondetectable levels of ≥4-ring PAH measured in sediments and tissues and low CYP1A-dependent enzyme activities. The lack of significant differences in biliary PAH metabolite levels is most likely due to the low contaminant gradient observed at the study sites.

The results from the present study indicate that hydrocarbon contamination at the study sites did not induce CYP1A in fish, AHH activity in invertebrates, and EROD activity in H4IIE cells dosed with invertebrate extracts. Moreover, most variations observed for fish are most likely species-dependent differences in basal CYP1A-dependent enzyme activities.

Acknowledgments

The authors wish to express their appreciation to those staff members in our laboratories who contributed to field collections and laboratory analyses. This study was funded by the Mineral Management Service/National Biological Survey (contract No. 14-35-001-30582).

References

Addison, F.R., Willis, D.E., and Zinck, M.E. 1994. Liver microsomal monooxygenase induction in winter flounder (*Pseudopleuronectes americanus*) from a gradient of sediment PAH concentrations at Sydney Harbour, Nova Scotia. Mar. Environ. Res. **37**: 283–296.

Anderson, R.S. 1978. Benzo[*a*]pyrene metabolism in the American oyster *Crassostrea virginica*. EPA Ecol. Ser. Monogr. EPA-600/3-78-009: 1–178.

Ankley, G.T., Tillitt, D.E., Giesy, J.P., Jones, P.S., and Verbrugge, D.A. 1991. Bioassay-derived 2,3,7,8-tetrachlorodibenzo-*p*-dioxin equivalents (TCDD-EQ) in PCB-containing extracts from flesh and eggs of Lake Michigan chinook salmon (*Oncorhynchus tshawytscha*) and possible implications for reproduction. Can. J. Fish. Aquat. Sci. **48**: 1685–1690.

Ankley, G.T., Lodge, K.B., Call, D.J., Balcer, M.D., Brooke, L.T., Cook, P.M., Kreis, R.G., Carlson, A.R., Johnson, R.D., Niemi, G.J., Hoke, R.A., West, C.W., Giesy, J.P., Jones, P.D., and Fuying, Z.C. 1992. Integrated assessment of contaminated sediments in the lower Fox River and Green Bay, Wisconsin. Exotoxicol. Environ. Saf. **23**: 46–63.

Besten, P.J. den, Herwig, H.J., Donselaar, E.G. van, and Livingstone, D.R. 1990. Cytochrome P450 monooxygenase system and benzo(*a*)pyrene metabolism in echinoderms. Mar. Biol. **107**: 171–177.

Besten, P.J. den, Lemaire, P., Livingstone, D.R., Woodin, B., Stegeman, J.J., Herwing, H.J., and Seinen, W. 1993. Time-course and dose–response of the apparent induction of the cytochrome P450 monooxygenase system of pyloric caeca microsomes of the female seastar *Asterias rubens* L. by benzo[*a*]pyrene and polychlorinated biphenyls. Aquat. Toxicol. **26**: 23–40.

Bradford, M.M. 1976. A rapid and sensitive method for quantitation of microgram quantities of protein using the principle of protein–dye binding. Anal. Biochem. **72**: 248–254.

Bradlaw, J.A., and Casterline, Jr., J.L. 1979. Induction of enzyme activity in cell culture: a rapid screen for detection of planar polychlorinated organic compounds. J. Assoc. Off. Anal. Chem. **62**: 904–916.

Brown, D., and Van Beneden, R.J. 1993. Investigations of molecular mechanisms of gonadol tumors in herbicide-exposed bivalves. Proc. Am. Assoc. Cancer Res. **34**: 168.

Chomczynski, P., and Sacchi, N. 1987. Single step method of RNA isolation by acid guanidium thiocyanatephenol – chloroform extraction. Anal. Biochem. **162**: 156–159.

Collier, T.K., and Varanasi, U. 1991. Hepatic activities of xenobiotic metabolizing enzymes and biliary levels of xenobiotics in English sole (*Parophrys vetulus*) exposed to environmental contaminants. Arch. Environ. Contam. Toxicol. **20**: 462–473.

Collier, T.K., Connor, S.D., Eberhart, B.-T.L., Anulacion, B.F., Goksøyr, A., and Varanasi, U. 1992. Using cytochrome P450 to monitor the aquatic environment: initial results from regional and national surveys. Mar. Environ. Res. **34**: 195–199.

Collier, T.K., Anulacion, B.F., Stein, J.E., Goksøyr, A., and Varanasi, U. 1995. A field evaluation of cytochrome P450IA as a biomarker of contaminant exposure in three species of flatfish. Environ. Toxicol. Chem. **14**: 143–152.

Courtenay, S., Grunwald, C., Kreamer, G.-L., Alexander, R., and Wirgin, I. 1993. Induction and clearance of cytochrome P450IA mRNA in Atlantic tomcod caged in bleached kraft mill effluent in the Miramichi River. Aquat. Toxicol. **27**: 225–244.

Davies, J.M., Bell, J.S., and Houghton, C. 1984. A comparison of the levels of hepatic aryl hydrocarbon hydroxylase in fish caught close and distant from North Sea Oil Fields. Mar. Environ. Res. **14**: 23–45.

Elskus, A.A., and Stegeman, J.J. 1989. Induced cytochrome P-450 in *Fundulus heteroclitus* associated with environmental contamination by polychlorinated biphenyls and polynuclear aromatic hydrocarbons. Mar. Environ. Res. **27**: 31–50.

Foureman, F.L., White, N.B. Jr., and Bend, J.R. 1983. Biochemical evidence that winter flounder (*Pseudopleuronectes americanus*)

© 1996 NRC Canada

have induced hepatic cytochrome P450-dependent monooxygenase activities. Can. J. Fish. Aquat. Sci. **40**: 854–865.

Geyer, H., Sheenan, P., Kotzias, K., Freitag, D., and Korte, F. 1982. Prediction of ecotoxicological behavior of chemicals: relationship between physiochemical properties and bioaccumulation of organic chemicals in the mussel *Mytilus edulis*. Chemosphere, **11**: 1121–1134.

Goksøyr, A., Larsen, H.E., Blom, S., and Forlin, L. 1992. Detection of cytochrome P450IAI in North Sea dab liver and kidney. Mar. Ecol. Prog. Ser. **91**: 83–88.

Goldberg, E.D., Bowen, V.T., Farrington, J.W., Harvey, G., Martin, J.H., Parker, P.L., Risebrough, R.W., Scheider, E., and Gamble, E. 1978. The mussel watch. Environ. Conserv. **5**: 101–125.

Haasch, M.L., Wejksnora, P.J., Stegeman, J.J., and Lech, J.J. 1989. Cloned rainbow trout liver $P_1$450 complementary DNA as a potential environmental marker. Toxicol. Appl. Pharmacol. **98**: 362–368.

Haasch, M.L., Quardokus, E., Sutherland, L.A., Goodrich, M.S., Price, R., Cooper, K., and Lech, J.J. 1992. CYP1A1 protein and mRNA in teleosts as an environmental bioindicator: laboratory and environmental studies. Mar. Environ. Res. **34**: 139–145.

Hahn, M.E., and Stegeman, J.J. 1994. Regulation of cytochrome P450IAI in teleosts: sustained induction of CYP1A1 mRNA, protein, and catalytic activity by 2,3,7,8-tetrachlorodibenzofuran in the marine fish *Stenotomus chrysops*. Toxicol. Appl. Pharmacol. **127**: 187–198.

Hahn, M.E., Poland, A., Glover, E., and Stegeman, J.J. 1992. The Ah receptor in marine animals: phylogenetic distribution and relationship to cytochrome P4501A inducibility. Mar. Environ. Res. **34**: 87–92.

Hahn, M.E., Lamb, T.M., Schultz, M.E., Smolowitz, R.M., and Stegeman, J.J. 1993. Cytochrome P450IA induction and inhibition by 3,3,4,4′-tetrachlorobiphenyl in an Ah receptor-containing fish hepatoma cell line (PLHC-1). Aquat. Toxicol. **26**: 185–208.

Hahn, M.E., Poland, A., Glover, E., and Stegeman, J.J. 1994. Photoaffinity labeling of the Ah receptor: phylogenetic survey of diverse vertebrate and invertebrate species. Arch. Biochem. Biophys. **310**: 218–228.

Heilmann, L.J., Shee, Y.-Y., Bigelow, S.W., and Nebert, D.N. 1988. Trout P4501A:cDNA and deduced protein sequence, expression in liver, and evolutionary significance. DNA, **7**: 379–387.

James, M.O. 1989. Cytochrome P450 monooxygenase in crustaceans. Xenobiotica, **19**: 1063–1076.

James, M.O., and Bend, J.R. 1980. Polycyclic aromatic induction of cytochrome P450-dependent mixed-function oxidases in marine fish. Toxicol. Appl. Pharmacol. **54**: 117–133.

James, M.O., and Little, P.J. 1984. 3-methylcholanthrene does not induce *in vitro* xenobiotic metabolism in spiney lobster hepatopancreas, or affect *in vivo* disposition of benzo(*a*)pyrene. Comp. Biochem. Physiol. **78**: 241–245.

Jewell, C.S.E., and Winston, G.W. 1989. Characterization of the microsomal mixed-function oxygenase system of the hepatopancreas and green gland of the red swamp crayfish, *Procambarus clarckii*. Comp. Biochem. Physiol. B Comp. Biochem. **92**: 329–339.

Kennicutt, M.C. II, Green, R.H., Montagna, P., and Roscigno, P.F. 1996*a*. Gulf of Mexico Offshore Operations Monitoring Experiment (GOOMEX), Phase I: Sublethal responses to contaminant exposure — introduction and overview. Can. J. Fish. Aquat. Sci. **53**. This issue.

Kennicutt, M.C. II, Boothe, P.N., Wade, T.L., Sweet, S.T., Rezak, R., Kelly, F.J., Brooks, J.M., Presley, B.J., and Wiesenburg, D.A. 1996*b*. Geochemical patterns in sediments near offshore production platforms. Can. J. Fish. Aquat. Sci. **53**. This issue.

Krahn, M.M., Meyers, M.S., Burrows, D.G., and Malins, D.C. 1984. Determination of metabolites and xenobiotics in the bile of fish from polluted waterways. Xenobiotica, **14**: 633–646.

Krahn, M.M., Rhodes, L.D., Meyer, M.S., Moore, L.K., MacLeod, W.D. Jr., and Malins, D.C. 1986. Associations between metabolites of aromatic compounds in bile and the occurrence of hepatic lesions in English sole (*Parophrys vetulus*) from Puget Sound, Washington. Arch. Environ. Contamin. Toxicol. **15**: 61–67.

Krahn, M.M., Burrows, D.G., Ylitalo, G., Brown, D.W., Wigren, C.A., Collier, T.K., Chan, S.-L., and Varanasi, U. 1992. Mass spectrometric analysis for aromatic compounds in bile of fish sampled after the *Exxon Valdez* oil spill. Environ. Sci. Technol. **26**: 116–126.

Krishnan, V., and Safe, S. 1993. Polychlorinated biphenyls (PCBs), dibenzo-*p*-dioxins (PCDDs) and dibenzofurans (PCDFs) as antiestrogens in MCF-7 human breast cancer cells: quantitative structure–activity relationships. Toxicol. Appl. Pharmacol. **120**: 55–61.

Kurelec, B., Britivic, S., Krc′a, S., and Kahn, R.K. 1986. Metabolic fate of aromatic amines in the mussel *Mytilus galloprovincalis*. Mar. Biol. **91**: 523–527.

Lee, R.F. 1982. Mixed function oxygenase (MFO) in marine invertebrates. Mar. Biol. Lett. **2**: 87–105.

Lee, R.F., Sauerhebel, R., and Benson, A.A. 1972. Petroleum hydrocarbons: uptake and discharge by the marine mussel *Mytilus edulis*. Science (Wash., D.C.), **177**: 344–346.

Livingstone, D.R. 1990. Cytochrome P-450 and oxidative metabolism in invertebrates. Biochem. Soc. Trans. **18**: 15–19.

Livingstone, D.R. 1991. Organic xenobiotic metabolism in marine invertebrates. *In* Advances in comparative and environmental physiology. *Edited by* R. Gilles. Springer-Verlag, New York. pp. 45–185.

Livingstone, D.R., and Farrar, S.V. 1984. Tissue and subcellular distribution of enzyme activities of mixed-function oxygenase and benzo[*a*]pyrene metabolism in the common mussel *Mytilus edulis*, *L.* Sci. Total Environ. **39**: 209–235.

Livingstone, D.R., Lenaire, P., Matthews, A., Peters, L.D., Porte, C., Fitzpatrick, P.J., Förlin, L., Nasci, C., Fossato, V., Wootton, N., and Goldfarb, P. 1995. Assessment of the impact of organic pollutants on goby (*Zosterisessor ophiocephalus*) and mussel (*Mytilus galloprovincialis*) from the Venice Lagoon, Italy: biochemical studies. Mar. Environ. Res. **39**: 235–240.

Long, E.R., and Morgan, L.G. 1990. The potential for biological effects of sediment-sorbed contaminants tested in the National Status and Trends Program. NOAA Tech. Memo. NOS OMA 52. U.S. Department of Commerce, National Oceanographic and Atmospheric Administration, Seattle, Wash.

Lorenzen, A., and Okey, A.B. 1990. Detection and characterization of [^{3}H]2,3,7,8-tetrachlorodibenzo-*p*-dioxin binding to Ah receptor in a rainbow trout hepatoma cell line. Toxicol. Appl. Pharmacol. **106**: 53–62.

McDonald, S.J., Wade, T.L., Brooks, J.M., and McDonald, T.J. 1991. Assessing the exposure of fish to a petroleum spill in Galveston Bay, Texas. *In* Water pollution: modelling, measuring and prediction. *Edited by* L.C. Wroebel and C.A. Brebbia. Southampton: Computational Mechanics Publications, Southampton, N.Y. pp. 707–718.

McDonald, S.J., Kennicutt, M.C. II, and Brooks, J.M. 1992. Evidence of polycyclic aromatic hydrocarbon (PAH) exposure in fish from the Antarctic Peninsula. Mar. Pollut. Bull. **25**: 3313–3317.

McDonald, S.J., Kennicutt, M.C. II, Sericano, J., Wade, T.L., Liu, H., and Safe, S.H. 1994. Correlation between bioassay-derived P4501A1 induction activity and chemical analysis of clam (*Laternula elliptica*) extracts from McMurdo Sound, Antarctica. Chemosphere, **28**: 2237–2248.

McDonald, S.J., Kennicutt, M.C. II, Liu, H., and Safe, S.H. 1995. Assessing aromatic hydrocarbon exposure in Antarctic fish captured near Palmer and McMurdo stations, Antarctica. Arch. Environ. Contam. Toxicol. **29**: 232–240.

Michel, X.R., Suteau, P., Robertson, L.W., and Narbonne, J.-F. 1993. Effects of benzo[*a*]pyrene 3,3′4,4′-tetrachlorobiphenyl and

© 1996 NRC Canada

2,2′,4,4′5,5′-hexachlorobiphenyl on xenobiotic-metabolizing enzymes in the mussel *Mytilus galloprovincialis*. Aquat. Toxicol. **27**: 335–344.

Michel, X.R., Breasse, C., and Narbonne, J.F. 1995. *In vivo* metabolism of benzo[*a*]pyrene in the mussel *Mytilus galloprovincialis*. Arch. Environ. Contam. Toxicol. **28**: 215–222.

Muehleisen, D.P., Plapp, F.W. Jr., Benedict, J.H., and Carino, F.A. 1989. High affinity TCDD binding to fat body cytosolic proteins of the bollworm, *Heliothis zea*. Pestic. Biochem. Physiol. **35**: 50–57.

Nebert, D.W., and Gelboin, H.V. 1968. Substrate-inducible microsomal aryl hydroxylase in mammalian cell culture. I. Assay and properties of induced enzyme. J. Biol. Chem. **243**: 6242–6249.

Payne, J.F. 1977. Mixed function oxidase in marine organisms in relation to petroleum hydrocarbon metabolism and detection. Mar. Pollut. Bull. **8**: 112–116.

Piskorska-Pliszczynska, J., Keys, B., Safe, S., and Newman, M.S. 1986. The cytosolic receptor binding affinities and AHH induction potencies of 29 polynuclear aromatic hydrocarbons. Toxicol. Lett. **34**: 67–74.

Pohl, R.J., and Fouts, J.R. 1980. A rapid method for assaying the metabolism of 7-ethoxyresorufin by microsomal subcellular fractions. Anal. Biochem. **107**: 150–155.

Porte, C., Lenaire, P., Peters, L.D., and Livingstone, D.R. 1995. Partial purification and properties of cytochrome P450 from digestive gland microsomes of the common mussel, *Mytilus edulis* L. Mar. Environ. Res. **39**: 27–31.

Renton, K.W., and Addison, R.F. 1992. Hepatic microsomal monooxygenase activity and P4501A mRNA in North Sea dab *Limanda limanda* from contaminated sites. Mar. Ecol. Prog. Ser. **91**: 65–69.

Safe, S.H. 1990. Polychlorinated biphenyls (PCBs), dibenzo-*p*-dioxins (PCDDs), dibenzofurans (PCDFs) and related compounds: environmental and mechanistic considerations which support the development of toxic equivalency factors (TEFs). Crit. Rev. Toxicol. **21**: 51–88.

Schlenk, D., and Buhler, D.R. 1988. Cytochrome P-450 and phase II activities in the gumboat chiton *Cryptochiton stelleri*. Aquat. Toxicol. **13**: 167–187.

Spies, R.B., Felton, J.S., and Dillard, L. 1982. Hepatic mixed-function oxidases in California flatfishes are increased in contaminated environments and by oil and PCB ingestion. Mar. Biol. **70**: 117–127.

Stebbing, A.R.D., Dethlefsen, V., and Carr, M. 1992. Biological effects of contaminants in the North Sea: Appendix I. Chemistry: organic and trace metal data. Mar. Ecol. Prog. Ser. **91**: 331–348.

Stegeman, J.J., Klotz, A.V., Woodin, B.R., and Pajor, A.M. 1981. Induction of hepatic cytochrome P-450 in fish and the indication of environmental induction in scup (*Stenotomus chrysops*). Aquat. Toxicol. **1**: 197–221.

Stegeman, J.J., Teng, F.Y., and Snowberger, E.A. 1987. Induced cytochrome P450 in winter flounder (*Pseudopleuronectes americanus*) from coastal Massachusetts evaluated by catalytic assay and monoclonal antibody probes. Can. J. Fish. Aquat. Sci. **44**: 1270–1277.

Swanson, H.I., and Perdew, G.H. 1991. Detection of the Ah receptor in rainbow trout. Use of 2-azido-3-[^{125}I]iodo-7,8-dibromodibenzo-*p*-dioxin in cell culture. Toxicol. Lett. **58**: 85–95.

Tillitt, D.E., Ankley, G.T., Verbrugge, D.A., Giesy, J.P., Ludwig, J.P., and Kubiak, T.J. 1991*a*. H4IIE cell bioassay derived 2,3,7,8-tetrachylorodibenzo-*p*-dioxin equivalents in colonial fish-eating waterbird eggs from the Great Lakes. Arch. Environ. Contam. Toxicol. **21**: 91–101.

Tillitt, D.E., Giesy, J.P., and Ankley, G.T. 1991*b*. Characterization of the H4IIE rat hepatoma cell bioassay as a tool for assessing toxic potency of planar halogenated hydrocarbons in environmental samples. Environ. Sci. Technol. **25**: 87–92.

Trotter, W.J., Young, S.J.V., Casterline, J.L. Jr., Bradlaw, J.A., and Kamps, L.R. 1982. Induction of aryl hydrocarbon hydroxylase activity in cell cultures by Aroclors, residues from Yusho oil samples, and polychlorinated biphenyl residues from fish samples. J. Assoc. Off. Anal. Chem. **65**: 838–844.

van der Weiden, M.E.J., Hanegraff, F.H.M., Eggens, M.L., Celander, M., Seinen, W., and Van den Berg, M. 1994. Temporal induction of cytochrome P4501A in the mirror carb (*Cyprinus carpio*) after administration of several polycyclic aromatic hydrocarbons. Environ. Toxicol. Chem. **13**: 797–802.

Van Veld, P.A., Westbrook, D.J., Woodin, B.R., Hale, R.C., Smith, C.L., Huggett, F.J., and Stegeman, J.J. 1990. Induced cytochrome P450 in intestine and liver of spot (*Leisostomus xanthurus*) from a polycyclic aromatic hydrocarbon contaminated environment. Aquat. Toxicol. **17**: 119–132.

Varanasi, U., and Gmur, D.J. 1981. Hydrocarbons and metabolites in English sole (*Parophyrys vetulus*) exposed simultaneously to [^{3}H]benzo[*a*]pyrene and [^{14}C]naphthalene in oil-contaminated sediment. Aquat. Toxicol. **1**: 49–67.

Varanasi, U., Stein, J.E., and Nishimoto, M. 1989. Biotransformation and deposition of polycyclic aromatic hydrocarbons (PAH) in fish. *In* Metabolism of polycyclic aromatic hydrocarbon in the aquatic environment. *Edited by* U. Varanasi. CRC Uniscience Series, CRC Press Inc., Boca Raton, Fla. pp. 93–150.

Whitlock, J.P. Jr. 1986. The regulation of cytochrome P450 gene expression. Annu. Rev. Pharmacol. Toxicol. **26**: 333–369.

Whitlock, J.P. Jr. 1990. Genetic and molecular aspects of 2,3,7,8-tetrachlorodibenzo-*p*-dioxin action. Annu. Rev. Pharmacol. Toxicol. **30**: 251–277.

Willett, K., Steinberg, M., Thomsen, J., Narasimham, T.R., Safe, S., McDonald, S., Beatty, K., and Kennicutt, M.C. II. 1995. Exposure of killifish to benzo[*a*]pyrene: comparative metabolism, DNA adduct formation and aryl hydrocarbon (Ah) receptor agonist activities. Comp. Biochem. Physiol. B Comp. Biochem. **112**: 93–103.

Wootton, A.N., Herring, C., Spry, J.A., Wiseman, A., Livingstone, D.R., and Goldfarb, P.S. 1995. Evidence for the existence of cytochrome P450 gene families (CYP1A, 3A, 4A, 11A) and modulation of gene expression (CYP1A) in the mussel *Mytilus* spp. Mar. Environ. Res. **39**: 21–26.

Zacharewski, T., Safe, L., Safe, S., Chittim, B., DeVault, D., Wibers, K., Bergqvist, P.A. and Rappe, C. 1989. Comparative analysis of polychlorinated dibenzo-*p*-dioxin and dibenzofuran congeners in Great Lakes fish by gas chromatography – mass spectrometry and in vitro enzyme induction activities. Environ. Sci. Technol. **23**: 730–735.

© 1996 NRC Canada

Sediment porewater toxicity assessment studies in the vicinity of offshore oil and gas production platforms in the Gulf of Mexico

R.S. Carr, D.C. Chapman, B.J. Presley, J.M Biedenbach, L. Robertson, P. Boothe, R. Kilada, T. Wade, and P. Montagna

Abstract: As part of a multidisciplinary program to assess the potential long-term impacts of offshore oil and gas exploration and production activities in the Gulf of Mexico, sediment chemical analyses and porewater toxicity tests were conducted in the vicinity of five offshore platforms. Based on data from sea urchin fertilization and embryological development assays, toxicity was observed near four of the five platforms sampled; the majority of the toxic samples were collected within 150 m of a platform. There was excellent agreement among the results of porewater tests with three different species (sea urchin embryological development, polychaete reproduction, and copepod nauplii survival). The sediment concentrations of several metals were well in excess of sediment quality assessment guidelines at a number of stations, and good agreement was observed between predicted and observed toxicity. Porewater metal concentrations compared with EC_{50}, LOEC, and NOEC values generated for water-only exposures indicated that the porewater concentrations for several metals were high enough to account for the observed toxicity. Results of these studies utilizing highly sensitive toxicity tests suggest that the contaminant-induced impacts from offshore platforms are limited to a localized area in the immediate vicinity of the platforms.

Résumé : Dans la cadre d'un programme multidisciplinaire visant à évaluer les répercussions potentielles à long terme des activités d'exploration et d'exploitation du pétrole et du gaz en mer dans le golfe du Mexique, des analyses chimiques des sédiments et des tests de toxicité portant sur l'eau interstitielle ont été réalisés dans le voisinage de cinq plates-formes en mer. D'après les résultats des tests de fécondation et de développement embryonnaire de l'oursin, une toxicité a été observée à proximité de quatre des cinq plates-formes échantillonnées; la plupart des échantillons manifestant des signes de toxicité ont été prélevés à moins de 150 m des plates-formes. Il y avait une excellente concordance entre les résultats des tests portant sur l'eua interstitielle dans le cas de trois espèces (développement embryonnaire de l'oursin, reproduction des polychètes et survie des nauplii de copépodes). Dans un certain nombre de sites, la concentration de plusieurs métaux dans les sédiments était bien supérieure aux valeurs prévues pa les lignes directrices sur l'évaluation de la qualité des sédiments et on a observé une bonne concordance entre la toxicité prévue et la toxicité observée. Une comparaison des concentration des métaux dans l'eau interstitielle avec les valeurs de EC_{50}, LOEC et NOEC déterminées pour l'exposition à l'eau seulement a indiqué que les concentrations de plusieurs métaux dans l'eau interstitielle étaient suffisamment élevées pour expliquer la toxicité observée. Les résultats de ces études faisant appel à tests de toxicité hautement sensibles laissent entendre que les répercussions induites par les contaminants provenant des plates-formes en mer sont limitées à une zone définie au voisinage immédiat des plates-formes.
[Traduit par la Rédaction]

Introduction

The Minerals Management Service (MMS) Gulf of Mexico Offshore Monitoring Experiment (GOOMEX) was conducted to assess the sublethal impacts associated with the exposure of marine organisms to contaminants derived from offshore oil and gas exploration and production activities (Kennicutt 1994). One component of this multidisciplinary program involved the collection of sediment samples from the vicinity of offshore platforms for sediment toxicity testing and chemical analyses.

Of the five platforms selected for study initially, three were

Received August 16, 1995. Accepted September 13, 1996.
J13412

R.S. Carr[1], **D.C. Chapman,**[2] **J.M. Biedenbach, and L. Robertson.** USGS, MERS, Texas A&M University, Center for Coastal Studies, Natural Resources Center, Suite 3200, 6300 Ocean Dr., Corpus Christi, TX 78412, U.S.A.
B.J. Presley and P. Boothe. Department of Oceanography, Texas A&M University, College Station, TX 77843, U.S.A.
R. Kilada and P. Montagna. Marine Science Institute, University of Texas, 750 Channelview Dr., Port Aransas, TX 78373, U.S.A.
T. Wade. Geochemical and Environmental Research Group, Texas A&M University, 833 Graham Rd., College Station, TX 77845, U.S.A.

[1] Author to whom correspondence should be addressed.
[2] Present address: USGS, Midwest Science Center, 4200 New Haven Rd., Columbia, MO 65201, U.S.A.

© 1996 NRC Canada

Fig. 1. Location of oil and gas production platforms sampled during Cruises 1 and 2.

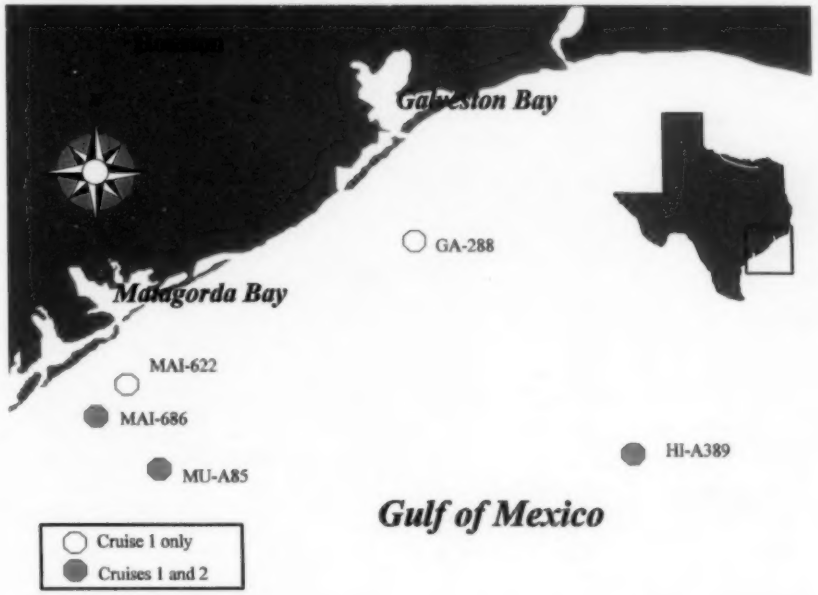

selected for additional investigations. One of the three platforms, High Island A389 (HI-A389), was located approximately 2 km from the East Flower Garden National Marine Sanctuary, which encompasses the most northerly occurring coral reef in the Gulf of Mexico. Because of the proximity of this platform to the Flower Gardens, the discharges from both exploration and production activities from this platform were required to be shunted to within 10 m of the bottom, unlike most platforms where these discharges occur at or near the sea surface. Due to this atypical discharge requirement and the low energy conditions present at this deepwater (~130 m) site, the highest contaminant levels and most distinct concentration gradient were observed. This site, therefore, afforded the best opportunity to assess the impacts of contaminants associated with exploration and production activities and is the primary focus of this paper.

Materials and methods

Sample collection

During the first cruise conducted during January 1993, a total of five oil and gas production platforms were sampled (Fig. 1). Twenty-five sampling stations were established at each location in radial arrays at distances of 50–3000 m from the platform. Three of the original five platforms were sampled during the second cruise conducted in June 1993 using the same sampling design. Therefore, a total of 200 stations were sampled synoptically for sediment chemistry and toxicity during the two cruises. Samples were also collected for benthic infaunal analysis and those results are presented in a companion paper (Montagna and Harper 1996).

Sediment samples were collected with an Ocean Instuments BX-600 deep ocean corer outfitted with an extra spade: a Teflon®-coated inner core box head and stainless steel boxes fitted with stainless steel vegematic frame, rods, and bolts. The 0.25-m^2 boxcore was subdivided into twenty-five 100-cm^2 compartments. The top 2 cm of 16 subcores was carefully removed with a Teflon® scoop and composited to provide samples for porewater toxicity testing. The sediments for toxicity testing were stored in presoaked 3.5-L high-density polyethylene jugs at 4°C during transport to the shore-based laboratory . The top 2 cm from duplicate compartments were also sampled from each boxcore for trace metal and hydrocarbon analyses. All sediment samples for contaminant analyses were stored at –20°C in precleaned glass jars.

Sediment and porewater trace metal and PAH analyses

For trace metal analyses, sediment samples were first homogenized and an aliquot was freeze dried and homogenized again to a fine powder. Following 24-h digestions with nitric and hydrofluoric acids, respectively, samples were diluted and stored in 5% boric acid until analyzed by flame or graphite furnace atomic absorption spectrophotometry (AAS). Mercury was analyzed by cold-vapor AAS. Barium was analyzed by instrumental neutron activation analysis (Boothe and James 1985). QA parameter included duplicates, matrix spikes, procedural blanks, and percent recovery of standard reference materials. Acceptance criteria for concentrations greater than 10 times the method detection limit were 80–120% recovery.

PAH analysis followed the method of Wade et al. (1994) except sediments were dried with sodium sulfate instead of freeze drying and were then soxhlet extracted with methylene chloride. The extract was reduced in volume using Kuderna–Danish techniques. After silica gel/alumina with activated copper cleanup, the extracts were analyzed by high-resolution capillary gas chromatograph – mass spectrometry in the selected ion monitoring mode (Wade et al. 1994).

A select group of porewater samples were extracted, as described below, and stored frozen. At the time of analysis, the sample was thawed and one subsample was acidified and analyzed for trace metals as described above. An additional subsample was extracted with methylene chloride and analyzed for PAHs by the methods described previously.

Porewater extractions

Recent studies in our laboratory have demonstrated that if the suspended particulate material is removed prior to freezing, there is no

© 1996 NRC Canada

difference in toxicity between fresh and frozen/thawed samples containing a wide variety of contaminants (Carr and Chapman 1995). Therefore, as soon as the sediment samples arrived in the laboratory, pore water was extracted pneumatically, centrifuged to remove fines, and frozen (Carr and Chapman 1992, 1995; Carr 1993). Pore water was stored frozen until 2 d before the start of the toxicity test, at which time the samples were removed from the freezer and placed in a refrigerator to thaw slowly overnight. Samples that remained partially frozen in the morning were allowed to thaw at room temperature or in a tepid (<25°C) water bath. Dissolved oxygen (DO), pH, temperature, hydrogen sulfide, and ammonia were measured after the salinity of the samples was adjusted to 35 ± 1‰, if necessary. Hypersaline brine (~100‰) and bottled purified water (Baker® water for HPLC) were used to adjust sample salinity. If the DO concentration was below 80% saturation, samples were gently stirred until this concentration was achieved. Samples were then stored at 4°C overnight and returned to 20°C before the start of the tests. Samples that needed stirring to increase DO concentrations were checked again on the day of the tests, and, if necessary, stirring was repeated.

Porewater toxicity tests

The toxicity of the sediment pore waters was determined using two different tests with the sea urchin *Arbacia punctulata*: the fertilization test and the embryological development test (Carr and Chapman 1992; Carr 1993). Both tests were performed on samples from the first cruise with five test replicates per treatment per test. Only the embryological development test was performed on samples from the second cruise, as this proved to be the more sensitive of the two assays for these samples. A reference pore water, collected from Redfish Bay near Port Aransas, Texas, was included with each toxicity test. This site is far removed from any known sources of contamination and has been used previously as a reference site (Carr and Chapman 1992, 1995; USFWS 1992; Carr 1993; NBS 1993, 1994*a*, 1994*b*). A dilution series test with sodium dodecyl sulfate (SDS) was also conducted with each test as a positive control and the EC_{50} determined in order to maintain a record of gamete viability and test acceptability.

The relative sensitivity of the sea urchin assays was compared with that of two infaunal meiobenthic invertebrates exposed to selected pore waters from HI-A389. One species, *Dinophilus gyrociliatus*, a small polychaete, has been used previously in toxicity testing and the techniques for culture and testing with this organism are well established (Carr et al. 1986, 1989). The other species, *Longipedia americana*, a benthic harpacticoid copepod, has not been cultured previously or used in toxicity testing, to our knowledge.

Longipedia americana adults were collected from the Port Aransas ship channel and maintained in the laboratory until females became gravid. No earlier than 48 h before a test, gravid females were isolated in a separate culture container and held there until the eggs hatched. In this manner, it was assured that all nauplii were less than 48 h old at the start of a test. The nauplii, which are phototactic, were concentrated in a culture dish by use of a point source of light. A pipette was used to transfer the nauplii to a small counting dish. Five nauplii were transferred from the counting dish into each test chamber. Test chambers were stender dishes containing 10 mL of pore water. Nauplii were fed a mixture of three types of algae (*Dunaliella*, *Thalassiosira*, and *Isochrysis*, approximately 20 000, 3000, and 120 000 cells per replicate, respectively) once at the beginning of the test. Test chambers were incubated at 20°C for 96 h, and then the test was terminated and the number of surviving nauplii was determined for each chamber. At the end of the test, the water from all replicates was pooled and DO and salinity of the pooled sample were measured. Three replicates per treatment were tested. The difficulty in obtaining a sufficient number of test animals precluded testing more replicates per treatment or animals per replicate. Fourteen samples total from HI-A389 were tested on two different occasions. The number of samples tested was dictated by the number of nauplii available.

Dinophilus gyrociliatus used in the test were obtained from laboratory cultures. The test was performed according to the methods of Carr et al. (1989). The test was begun with four newly hatched juvenile female polychaetes per replicate with five replicates per treatment. The endpoint measured was the number of eggs produced per female after 7 d of exposure at 20°C.

In order to provide the best comparative information for interpreting the porewater chemical analyses, a series of toxicity tests with the metals of primary toxicological importance were conducted with the two sea urchin assays. Stock solutions of cadmium ($Cd Cl_2$), copper ($CuSO_4 \cdot 5H_2$), mercury ($HgCl_2$), lead ($(C_2H_3O_2)_2Pb \cdot 3H_2O$), and zinc ($ZnSO_4 \cdot 7H_2O$) were all made up directly in 30‰ salinity filtered (0.45 µm) seawater and serially diluted. The highest concentration of each dilution series was measured in duplicate by AAS; lower concentrations were estimated based on dilution.

Statistical comparisons among treatments for the species comparison study were made using analysis of variance (ANOVA) and Ryan–Einot–Gabriel–Walsh multiple range test (Day and Quinn 1989) on arc sine square root transformed data with the aid of SAS (SAS Institute Inc. 1989). Spearman correlation analyses were also performed on arc sine square root transformed toxicity data and the log-transformed chemical data with the aid of SAS (SAS Institute Inc. 1989). Dunnett's one-tailed *t*-test (SAS Institute Inc. 1989) was used to determine significant differences in fertilization (fertilization test) and development to the pluteus stage (embryological development test) between samples and the reference pore water and to determine the lowest observed (LOEC) and no observed effect concentration (NOEC) in the metals reference tests. An additional criterion termed "detectable significance", based on a power analysis of data generated for these assays in our laboratory, was used to minimize the occurrence of type I (false positive) errors (Carr et al. 1996). The Spearman–Karber method, with Abbott's correction (Hamilton et al. 1977), was used to determine the EC_{50} in the SDS dilution series and metals reference tests.

Results

Sediment chemistry

Samples collected in the vicinity of the HI-A389 platform contained the highest concentrations of contaminants (Tables 1–4). Because the most distinct contaminant gradients were observed at this platform, which shunted its discharges near the bottom, the sediment chemistry and grain size data for this platform only are presented here; chemistry data for the other platforms are reported elsewhere (Kennicutt et al. 1996). Sediment concentrations of barium as high as 250 000 mg/kg (i.e., 25%) were observed at stations near the platform (Tables 2 and 4; Fig. 1*a*). Other metals of toxicological significance (e.g., Zn, Pb, Cd, and Hg) tended to covary with the Ba concentration (Tables 2 and 4; Fig. 2) and decreased to background levels at the outermost (3000 m) stations. The concentration of PAHs, particularly the lower molecular weight compounds (i.e., naphthalenes and phenanthrenes), were also elevated near the platform (Tables 1 and 3). The sediment texture was much sandier near the platform, which may be related to the discharge of produced sand, sandblasting activities, or the result of altered current patterns near the platform.

Sediment porewater toxicity testing

All porewater samples were extracted within 10 d of the time of collection. Water quality parameters for the pore waters

© 1996 NRC Canada

Table 1. Toxicity, sediment PAHs, grain size, total organic carton (TOC), and porewater unionized ammonia nitrogen (UAN) concentrations for Cruise 1 at HI-A389 (Dunnett's *t*-test and detectable significance criterion: $^{**}\alpha \leq 0.01$).

Station	% normal sea urchin development[a]	Total PAH (ppb)	Total naphthalenes (ppb)	Total phenanthrenes (ppb)	Sand (%)	Silt (%)	Clay (%)	TOC (%)	Porewater UAN (ppb)
2A	3.4**	383	160	105	34.4	53.9	11.7	1.06	42.4
2B	9.8**	511	238	131	39.3	54	6.72	0.94	24.8
2C	73.8	119	38.7	46.2	31.1	32.4	36.5	0.69	8.35
2D	73.6	757	92.6	292	53.7	19.9	26.4	1.81	16.5
2E	0.0**	370	214	76.6	51.6	26.7	21.7	1.28	49.1
3A	43.2**	110	73.4	15.5	26.8	36.2	37	1.09	5.48
3B	44.6**	171	123	17.3	14.3	43.9	41.8	0.91	5.20
3C	67.6	48.4	38.5	1.25	26.1	33.1	40.7	1.1	8.22
3D	65.6	50.3	21.5	14.1	48	21.6	30.4	1.01	6.98
3E	20.6**	741	319	297	42.5	26.7	30.8	1.16	5.30
1A	62.0	41.2	28.2	1.72	9.77	35.8	54.5	1.01	7.16
1B	70.2	45.6	25.3	2	5.53	36.7	57.8	1.47	3.48
1C	65.2	36	19.6	2.03	7.97	36.1	56	0.82	3.20
1D	78.0	49.7	31.2	8.11	13.4	41.1	45.5	0.86	4.84
1E	61.2	65.6	212	14.9	10.2	38.4	51.4	1.62	20.5
4A	67.2	26	7.36	2.09	4.2	30.5	65.3	1.13	7.40
4B	76.8	33.6	8.84	2.23	4.65	26.6	68.8	1.27	2.66
4C	75.0	21.7	7.04	1.76	4.19	32.5	63.3	1.19	3.83
4D	69.0	23	7.3	2.11	3.37	29.4	67.2	1.24	4.60
4E	74.8	44	23	1.81	10	32	57.9	0.99	5.39
5A	64.6	20.4	5.43	1.7	4.41	39	56.6	1.26	3.50
5B	73.2	29.4	8.58	2.9	3.2	24.6	72.2	1.43	3.16
5C	73.0	16	5.06	0.99	4.03	33.1	62.9	0.75	10.3
5D	74.8	25.6	5.3	1.91	4.75	38.3	56.9	1.24	2.48
5E	74.6	32.9	5	2.65	5.37	40.8	53.8	1.26	3.66

[a]Percent normal development for reference pore water from Redfish Bay was 73.4%.

were very similar among all stations from both cruises. All samples collected during Cruise 1 had salinities of 34–37‰; therefore, no sample was diluted by more than 4% to reach the target salinity (35 ± 1‰) for the tests. No dilution of samples was required for Cruise 2 samples, since the salinities of all samples were between 34 and 36‰. Hydrogen sulfide concentrations were below the detection limit (0.01) in all porewater samples. Unionized ammonia concentrations ranged from 2.66 to 52.7 and from <0.1 to 72.6 µg/L for Cruises 1 and 2, respectively. The LOEC for the sea urchin embryological development test with *A. punctulata* is 90 µg/L (Carr et al. 1996). The pH values ranged from 7.46 to 7.97 and from 6.39 to 8.07 for Cruises 1 and 2, respectively, with DO values >90% saturation for all porewater samples for both cruises (Tables 1 and 3).

Significant toxicity was observed at four of the five platforms sampled during the first cruise. No toxicity was observed at the Mustang Island A85 (MU-A85) platform. The six most toxic stations were observed in the vicinity of the HI-A389 platform (Table 1). Significant toxicity was observed at 12 stations overall with the sea urchin embryological development assay but at only one station with the sea urchin fertilization test. The station showing reduced fertilization also exhibited impaired development in the embryological development assay. Seventy-five percent of the toxic stations were within 150 m of a platform.

Significant toxicity was observed in the vicinity of two of the three platforms in the second cruise. As in the first cruise, no toxicity was observed near the MU-A85 platform and one of the stations nearest the platform was toxic at Matagorda Island (MAI-686). Three stations near the platform exhibited significant toxicity at HI-A389 and corresponded to three of the six stations that were observed to be toxic from the first cruise. Significant toxicity was observed with the sea urchin embryological development assay at four stations from the second cruise. All of the toxic stations were within ~75 m of a platform.

The results of the species comparison study with the meiobenthic species and the sea urchin embryological development assay with pore water are presented in Table 5. Water quality parameters remained within acceptable levels for all tests. There was excellent agreement among the results of the three tests (i.e., copepod versus polychaete versus sea urchin development). All stations that were toxic in the meiobenthic animal tests were also toxic in the sea urchin embryological development test. There was only 1 of 11 cases where data were available for all three tests in which there was not full agreement (i.e., station 3A). The test precision (i.e., coefficient of variation (CV)) was considerably lower for the sea urchin embryological development test (CV=17.8%) as compared with 43.8 and 57.3% for the polychaete and copepod tests, respectively (Table 5).

© 1996 NRC Canada

Table 2. Sediment trace metal concentrations (mg/kg) for sediments collected near HI-A389 during Cruise 1.

Station	Al	Ag	As	Ba	Cd	Cr	Cu	Hg	Ni	Pb	Se	Sn	V	Zn
2A	22 472	2.255	27.25	208 000	35.801	99.00	79.65	3.197	13.35	587.30	0.390	0.865	45.30	7 580.20
2B	12 860	3.379	31.30	262 500	54.900	67.20	92.55	3.276	13.85	634.20	0.515	0.690	34.85	10 542.40
2C	38 107	0.227	9.30	68 760	3.124	72.80	19.40	9.237	18.40	73.15	0.530	0.750	74.60	659.20
2D	33 079	0.089	7.60	22 705	0.923	41.75	10.10	0.074	14.65	27.20	0.320	2.050	60.80	253.40
2E	33 680	0.320	12.05	62 255	5.858	56.95	20.00	0.406	15.60	144.85	0.220	1.370	66.15	1 156.15
3A	48 797	0.225	9.95	37 135	1.169	82.10	18.75	0.156	23.05	79.90	0.405	1.125	86.50	455.80
3B	49 101	0.163	7.40	35 600	0.507	91.55	17.45	0.143	21.00	105.95	0.395	1.465	81.85	294.50
3C	44 699	0.100	6.25	22 035	0.348	66.10	14.55	0.081	20.85	40.20	0.325	1.390	79.55	207.75
3D	37 001	0.056	8.15	13 030	0.278	43.00	11.60	0.064	17.60	20.55	0.225	1.675	61.95	111.50
3E	35 932	0.286	9.55	44 070	3.969	60.20	20.65	0.314	16.60	130.50	0.355	0.820	66.30	919.35
1A	55 201	0.121	7.85	14 730	0.286	81.85	16.55	0.102	25.95	45.35	0.525	2.060	119.50	203.00
1B	55 126	0.146	7.50	15 000	0.192	93.40	17.65	0.095	27.80	53.70	0.520	2.120	119.00	205.30
1C	59 159	0.099	7.75	10 313	0.127	81.65	17.25	0.067	27.50	35.80	0.345	1.990	110.00	164.25
1D	50 659	0.110	8.00	13 750	0.217	73.20	15.90	0.093	24.65	38.30	0.270	1.600	98.30	189.75
1E	53 104	0.273	8.25	32 160	2.633	90.90	22.55	0.265	24.05	76.15	0.345	1.585	99.00	661.85
4A	62 645	0.046	10.95	6166	0.142	75.65	16.85	0.046	29.75	28.00	0.545	0.695	120.50	130.60
4B	65 279	0.040	10.15	2399	0.100	72.75	16.25	0.039	28.30	21.30	0.635	0.890	127.50	109.60
4C	65 329	0.043	10.45	2347	0.099	71.40	15.55	0.032	29.30	21.15	0.515	1.490	125.50	102.25
4D	67 636	0.048	13.45	3646	0.075	74.10	15.55	0.034	28.95	22.85	0.530	2.085	120.50	114.05
4E	61 573	0.083	10.65	12 650	0.202	75.70	15.90	0.089	25.65	37.55	0.425	1.620	107.50	205.65
5A	65 992	0.036	7.60	1021	0.072	68.55	15.30	0.027	27.95	18.20	0.475	1.600	119.50	90.40
5B	69 344	0.032	15.60	1180	0.080	70.55	15.90	0.032	32.05	18.25	0.585	2.030	124.50	92.05
5C	59 356	0.026	6.85	846	0.065	60.45	11.75	0.030	23.70	14.45	0.320	1.535	99.40	73.15
5D	68 436	0.030	10.20	1007	0.090	70.80	17.25	0.30	30.90	18.40	0.540	1.995	121.50	90.65
5E	66 660	0.032	10.65	1783	0.93	70.00	16.90	0.036	30.60	19.30	0.595	1.655	121.00	91.45

© 1996 NRC Canada

Table 3. Toxicity, sediment PAHs, grain size, (TOC), and porewater UAN concentrations for Cruise 2 at HI-A389 (Dunnett's *t*-test and detectable significance criterion: *$\alpha \leq 0.05$; **$\alpha \leq 0.01$).

Station	% normal sea urchin development[a]	Total PAH (ppb)	Total naphthalenes (ppb)	Total phenanthrenes (ppb)	Sand (%)	Silt (%)	Clay (%)	TOC (%)	Porewater UAN (ppb)
2A	76.8**	414	185	103	28.5	56.2	15.3	0.82	44.8
2B	89.8	571	264	132	54.6	34.4	11.0	1.00	57.7
2C	96.8	222	90.9	48.3	20.5	34.9	44.6	1.09	26.7
2D	97.2	88.3	58.6	11.5	50.8	23.6	25.6	1.07	25.7
2E	10.6**	456	148	118	41.4	32.0	26.6	1.65	72.6
3A	97.6	111	36.9	39.6	20.8	38.2	41.1	1.32	7.91
3B	96.0	60.1	32.3	14.3	22.3	43.9	33.8	1.07	4.49
3C	97.8	59.1	35.5	4.55	33.6	34.5	31.9	0.84	6.50
3D	96.0	83.3	41.0	20.5	37.2	31.5	31.3	0.72	7.10
3E	81.2*	395	300	31.6	35.1	34.0	30.9	1.06	39.4
1A	95.8	88.5	39.1	13.1	3.37	44.9	51.8	1.90	3.88
1B	97.8	73.8	38.5	7.59	5.05	45.5	49.4	1.21	3.17
1C	99.0	31.3	15.8	1.59	6.39	42.2	51.4	1.22	4.16
1D	98.2	36.2	19.3	3.93	17.2	39.1	43.7	1.17	3.21
1E	97.4	189	110.3	30.3	20.3	38.7	41.0	0.91	15.7
4A	97.8	31.9	14.9	1.64	5.36	42.9	51.8	1.57	4.30
4B	98.0	30.5	12.5	1.66	3.17	43.6	53.3	1.34	2.34
4C	96.0	27.4	12.6	1.41	2.34	41.1	56.6	1.70	0.99
4D	95.8	27.7	13.6	1.23	2.98	40.3	56.7	1.56	1.56
4E	97.4	79.1	62.5	1.44	7.65	43.4	49.0	1.49	2.30
5A	96.6	20.3	5.95	1.58	5.59	43.3	51.1	0.95	0.67
5B	98.2	29.8	8.17	3.79	2.68	26.9	70.4	1.43	3.84
5C	98.2	22.1	7.85	1.28	2.43	28.9	68.7	1.85	1.17
5D	97.6	26.1	9.99	1.47	2.72	30.0	67.3	1.82	0.08
5E	97.8	32.3	14.2	1.71	2.35	35.2	62.5	1.81	0.51

[a]Percent normal development for reference pore water from Redfish Bay was 98.4%.

Porewater concentrations of trace metals (Ba, Cd, Cu, Hg, Pb, and Zn) were determined for the the High Island stations from Cruise 2 and are presented with their respective bulk sediment concentrations for comparison purposes (Table 6). Based on the EC_{50}, LOEC, and NOEC values for these metals determined for water-only exposures with the *A. punctula* fertilization and embryological development assays in our laboratory (Table 7), it appears that porewater concentrations for several metals were high enough to account for the observed toxicity. For example, the LOEC for Cu in the embryological development test was determined to be 5.31 µg/L; this concentration was exceeded in 14 of the 15 porewater samples. The measured Pb porewater concentrations exceeded the USEPA chronic water quality criterion for all 15 samples (USEPA 1986). All of the porewater samples exceeded the chronic water quality criterion of 0.025 µg/L for Hg, and of the three samples that elicited toxicity, one contained the highest measured Hg porewater concentration.

The Spearman correlation analyses indicated a number of highly significant associations between the toxicity observed with the sea urchin embryological development assay and the concentrations of various contaminants (Table 8). The data for the two cruises were analyzed independently. Sediment Zn, Hg, and total naphthalene concentrations were highly correlated with toxicity for both cruises whereas Ag, Cd, and Pb were also significantly associated with toxicity for the first cruise. Lead was the only metal measured in pore water that was highly significantly correlated with toxicity.

Discussion

Sediment toxicity was primarily observed at stations located in the immediate vicinity (<150 m) of several platforms with the highest concentrations of contaminants. Toxicity was observed with a variety of test organisms exposed to sediment pore water. The High Island samples, which contained the highest contaminant concentrations, were the most toxic samples in this study. Fewer stations were toxic in the summer than in the winter. However, the three stations that were toxic in the summer were all within 75 m of the platform and were three of the same six sites found to be toxic during the winter collection, which demonstrates both the repeatability of this assay and the persistence of the observed toxicity.

There was a high degree of association between the observed porewater toxicity with the sea urchin embryological development assay and a number of whole-sediment metal concentrations (Table 8). Comparison of the bulk sediment chemistry with the sediment quality guidelines (SQGs) developed by MacDonald (1994) indicated that the probable effects levels (PELs) for several metals were exceeded at a number of stations (Table 9; 2*b*–2*d*). Although the PELs for Zn and Pb were exceeded at 18 and 17 stations, respectively,

© 1996 NRC Canada

Table 4. Sediment trace metal concentrations (mg/kg) for sediments collected near HI-A389 during Cruise 2.

Station	Al	Ag	As	Ba	Cd	Cr	Cu	Hg	Ni	Pb	Se	Sn	V	Zn
2A	23 582	2.825	23.965	238 500	49.058	113.75	79.15	1.349	10.15	652.10	0.62	0.635	0.475	9 115.0
2B	19 701	2.335	23.440	177 500	35.915	45.20	67.70	1.371	11.20	484.05	0.52	0.520	0.325	7 165.5
2C	43 734	0.220	7.295	42 110	4.710	65.20	16.40	0.122	16.20	54.35	0.47	0.835	0.690	474.5
2D	36 245	0.130	9.215	19 285	0.759	41.75	11.00	0.074	14.15	24.75	0.29	0.520	0.460	178.0
2E	36 938	0.475	9.620	43 400	4.451	58.35	16.50	0.205	17.30	93.45	0.35	0.835	0.510	873.0
3A	48 505	0.265	8.820	25 395	0.835	68.25	15.20	0.150	21.45	59.55	0.34	1.010	0.815	317.0
3B	49 409	0.205	7.900	32 668	0.479	77.10	14.65	0.117	18.90	56.35	0.31	0.975	0.780	257.5
3C	48 863	0.105	6.425	15 270	0.258	57.25	11.35	0.077	22.05	31.20	0.30	0.910	0.710	196.0
3D	48 483	0.075	6.865	11 120	0.340	47.50	11.70	0.114	17.90	22.30	0.34	0.850	0.665	126.5
3E	50 612	0.270	9.560	23 032	3.636	62.55	18.10	0.258	17.40	114.70	0.40	0.845	0.665	752.5
1A	63 953	0.225	8.320	14 455	0.364	80.00	17.95	0.104	25.10	47.45	0.42	1.335	1.050	259.5
1B	64 837	0.160	8.035	12 595	0.160	81.25	14.80	0.077	23.00	39.75	0.39	1.400	1.025	164.5
1C	70 750	0.165	6.340	7078	0.113	77.45	14.40	0.054	22.80	30.50	0.39	1.450	1.045	128.0
1D	61 808	0.135	7.425	9242	0.141	67.45	13.35	0.068	25.15	32.50	0.34	1.280	0.940	150.5
1E	61 011	0.195	6.740	14 060	0.825	64.40	15.30	0.107	22.55	33.15	0.38	1.105	0.825	272.0
4A	65 381	0.130	7.685	5525	0.107	71.50	14.50	0.054	25.35	27.85	0.42	1.435	1.015	125.5
4B	70 011	0.110	7.060	2405	0.076	69.80	14.85	0.040	24.50	21.55	0.47	1.430	1.075	103.0
4C	72 385	0.105	6.450	1840	0.077	69.55	14.85	0.034	25.00	21.35	0.47	1.440	1.160	105.5
4D	73 398	0.100	9.175	3221	0.076	70.10	15.00	0.041	31.50	24.15	0.44	1.650	1.210	114.5
4E	67 150	0.155	5.960	8004	0.185	69.65	15.20	0.070	22.95	31.25	0.40	1.440	1.090	182.5
5A	63 437	0.045	6.440	1001	0.080	63.25	12.70	0.032	28.00	16.55	0.37	1.430	0.990	83.5
5B	71 893	0.055	9.045	1151	0.098	67.15	15.55	0.031	30.55	19.55	0.52	1.655	1.210	95.0
5C	69 616	0.105	5.135	36 068	0.110	69.55	15.65	0.036	29.20	19.70	0.59	1.655	1.200	93.5
5D	68 825	0.080	8.775	1652	0.111	65.00	15.45	0.035	27.95	20.15	0.565	1.535	1.160	95.0
5E	74 568	0.080	9.880	1433	0.072	66.15	15.05	0.034	28.80	20.15	0.485	1.585	1.185	98.0

© 1996 NRC Canada

Fig. 2. Concentrations of (a) Ba, (b) Pb, (c) Cd, and (d) Zn in sediments collected near the HI-A389 platform during Cruise 1 and the toxicity observed with the sea urchin embryological development assay.

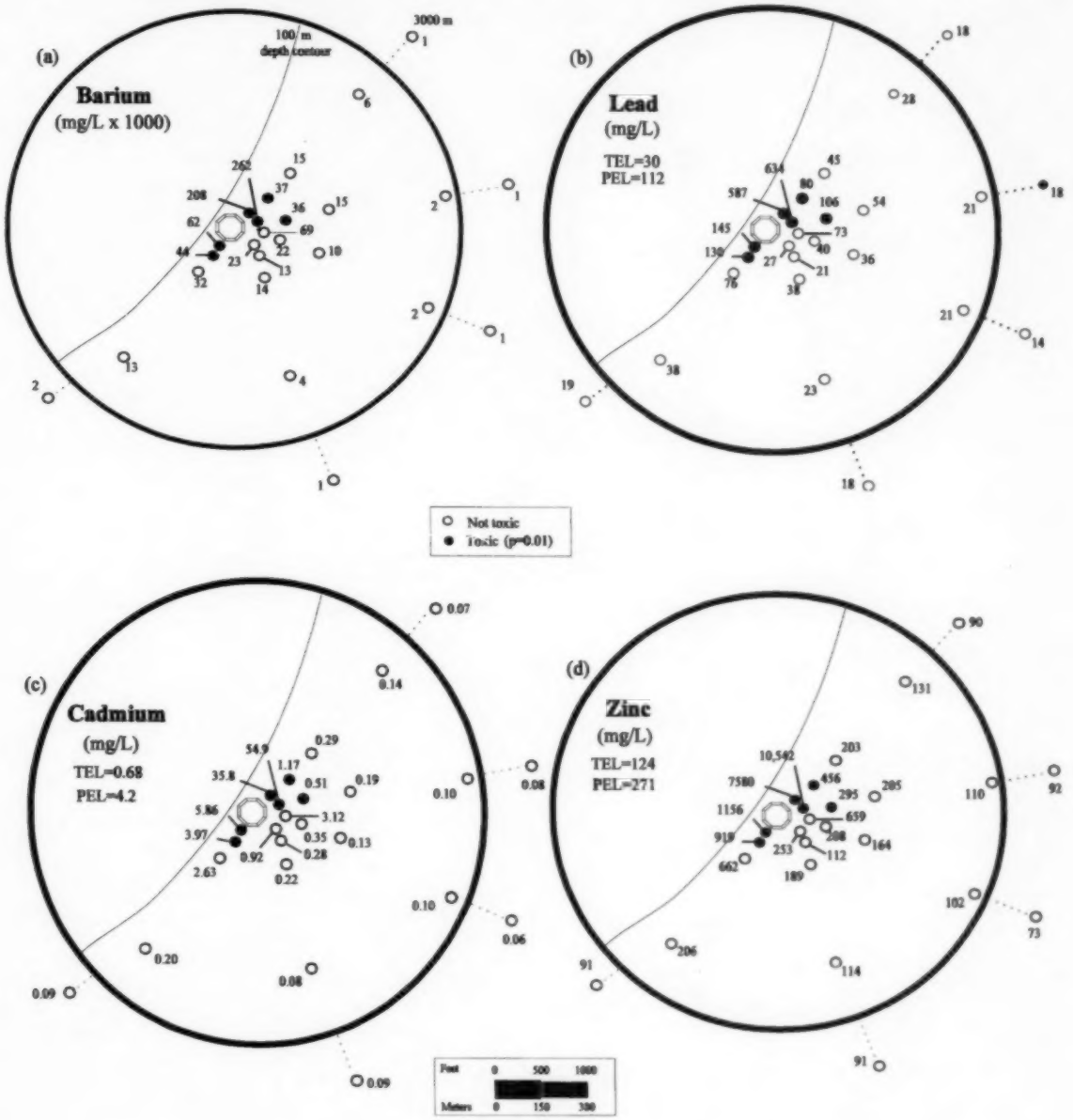

for the two cruises combined, only 50 and 35% of these stations, respectively, were observed to be toxic with the sea urchin embryological development assay. Fewer stations exceeded the PELs for Cd, Ag, and Hg, but the percentage of stations that were toxic when the PELs for these metals were exceeded was higher (Table 9). When the PELs for these metals (i.e., Cd, Ag, and Hg) were exceeded, the PELs for Pb, Zn, or both were also exceeded so that additive effects were likely to have contributed to the observed toxicity.

There was excellent agreement among the three different species used to determine the toxicity of porewater samples from the High Island site (Table 5). The harpactacoid copepod *L. americana* is found at the High Island site and the polychaete *D. gyrociliatus*, although not indigenous to the High Island site, is representative of similar minute interstitial dwelling polychaetes that do occur at this site. Although the responses observed between the two meiobenthic tests and the sea urchin embryological development test were similar,

© 1996 NRC Canada

Table 5. Results of tests for three species exposed to pore water from selected stations at HI-A389, Cruise 1 (significant differences between 3000-m stations (5A, 5C, 5E) and other stations indicated by asterisks: *$\alpha \leq 0.05$; **$\alpha \leq 0.01$; nd = not determined).

Station	Approximate distance from platform center (m)	Sea urchin development to pluteus larvae (% ± SD)	Polychaete number eggs/female (mean ± SD)	Copepod survival (% ± SD)
5A	3000	64.6±6.9	2.6±0.6	53.3±23.1
5C		73.0±6.2	2.4±0.6	60±0
5E		74.6±3.8	2.4±0.6	46.7±11.5
4A	500	67.2±5.3	2.1±0.6	nd
4C		75.0±3.2	1.5±0.7	nd
4E		74.8±4.8	2.2±0.7	nd
1A	200	62.0±4.6	1.5±1.2	40.0±20.0
1C		65.2±6.0	1.1±0.1	nd
1E		61.2±2.4	1.7±1.3	40±0
3A	100	43.2±8.2**	1.1±1.2	60.0±20.0
3B		44.6±5.1**	nd	13.3±11.5*
3C		67.6±1.5	1.5±0.6	33.3±11.5
3E		20.6±8.5**	0±0**	0±0**
2A	50	3.4±3.2**	0±0**	0±0**
2B		9.8±5.5**	nd	0±0**
2C		73.8±4.6	1.6±0.5	20.0±20.0
2D		73.6±6.2	nd	26.7±23.1
2E		0±0**	0±0**	0±0**
CV(%)		17.8	43.8	57.3

Table 6. Porewater metal concentration (µg/L) from samples collected near HI-A389, Cruise 2 (MOL = method detection limit).

Station	Ba	Cd	Cu	Hg	Pb	Zn
MDL	1	0.01	0.05	0.01	0.1	0.5
2A	53	0.10	8	0.09	12.3	11
2B	44	0.10	5	0.11	17.4	27
2C	25	0.52	13	0.11	13.2	35
2D	33	2.20	9	0.13	17.4	17
2E	38	0.24	10	0.08	12.5	14
3A	16	1.32	11	0.13	13.3	19
3B	14	0.52	11	0.22	9.8	20
3C	14	0.40	40	0.11	12.3	12
3D	12	0.20	13	0.11	10.0	13
3E	15	0.40	12	0.31	15.2	16
1A	28	0.72	11	0.12	13.4	28
1B	25	1.92	20	0.11	11.6	23
1C	30	0.56	15	0.11	8.0	14
1D	24	0.60	15	0.12	9.1	13
1E	30	1.36	22	0.10	8.8	23
4A	25	3.28	29	0.10	8.4	10
4B	25	2.60	22	0.11	8.6	14
4C	21	3.04	17	0.11	22.3	11
4D	22	3.12	16	0.10	9.1	13
4E	27	2.32	13	0.11	10.4	13
5A	30	0.72	12	0.11	11.4	35
5B	31	0.64	6	0.12	9.2	34
5C	27	0.40	10	0.20	9.2	19
5D	30	1.16	11	0.08	12.3	25
5E	52	0.10	3	0.09	8.0	13

the sea urchin test was more precise and more sensitive than the two meiobenthic tests and is considerably more reliable, cost effective, and simpler to conduct. For these reasons, we believe that sea urchin assays can be used as appropriate surrogates for the assessment of potential impacts of contaminated pore water on marine meiobenthic invertebrates.

A similar study of the impacts of an oil and gas production platform in the Gulf of Mexico was recently conducted using the sediment quality triad approach (Chapman et al. 1991). Sediment toxicity was observed within 25 m of the platform with three different tests (amphipod solid-phase, oyster elutriate, and Microtox® with organic extract) and corresponded to the most highly contaminated sediments. In the present study, sediment toxicity was observed at several stations up to 150 m from a platform. The difference between these studies may be due, in part, to the higher sensitivity of the porewater tests as compared with the tests conducted by Chapman et al. (1991). The porewater test with sea urchins has been shown to be considerably more sensitive than the amphipod and Microtox® assays (SAIC 1992; USFWS 1992; Carr 1993; NBS 1993, 1994*a*, 1994*b*).

The two platforms exhibiting the highest contaminant concentrations and associated sediment toxicity are atypical of platforms in this region, as most platforms are not required to shunt their discharges near the bottom as was done at MAI-686 and HI-A389. The most sensitive sediment toxicity tests currently available were able to detect only minimal impacts in the immediate vicinity (150 m) of these two atypical platforms. It appears that the primary contaminants of concern were the metals that are more likely associated with exploration and corrosion maintenance activities (e.g., sandblasting

© 1996 NRC Canada

Table 7. EC_{50} values for fertilization and embryological development test with *A. punctulata* in water-only exposures with measured concentrations compared with published values based on nominal concentrations and EPA chronic water quality criteria values (NOEC and LOEC values determined using Dunnett's *t*-test ($\alpha \leq 0.01$)).

Metal	Embryological development EC_{50} (95% CI)	Literature EC_{50} values[a]	LOEC[b]	NOEC[c]	Chronic WQC[d]
Cd	7.38 mg/L (6.66–8.17)	13.9 mg/L	3.25 mg/L	1.63 mg/L	9.3 µg/L
Cu	38.0 µg/L (32.8–44.0)	14.0 µg/L	5.31 µg/L	<5.31 µg/L	2.9 µg/L
Hg	43.6 µg/L (40.6–46.9)	—	37.5 µg/L	18.8 µg/L	0.025 µg/L
Pb	0.54 mg/L (0.50–0.58)	32.5 mg/L	0.62 mg/L	0.31 mg/L	5.6 µg/L
Zn	73.0 µg/L (66.0–80.0)	205 µg/L	35.6 µg/L	17.8 µg/L	86 µg/L
	Fertilization EC_{50} (95% CI)				Acute WQC[e]
Cd	20.1 mg/L (18.5–21.8)	38.0 mg/L	26.0 mg/L	13.0 mg/L	43 µg/L
Cu	6.10 µg/L (5.33–6.98)	12.0 µg/L	2.66 µg/L	1.33 µg/L	2.9 µg/L
Hg	1.39 µg/L (1.22–1.59)	—	0.23 µg/L	<0.23 µg/L	2.1 µg/L
Pb	0.74 mg/L (0.54–1.00)	5.4 mg/L	308 µg/L	154 µg/L	140 µg/L
Zn	112 µg/L (98.0–128.0)	121 µg/L	35.6 µg/L	17.8 µg/L	95 µg/L

[a]Values reported in Nacci et al. (1986) for *A. punctulata* using nominal concentrations.
[b]Lowest observed effect concentration.
[c]No observed effect concentration.
[d]Marine chronic water quality criteria values (USEPA 1986).
[e]Marine acute water quality criteria values (USEPA 1986).

Table 8. Spearman correlation coefficients and associated unadjusted probability values for sediment variables exhibiting significant ($p < 0.005$) associations with sea urchin normal embryological development.

	Cruise 1		Cruise 2	
Variable	Correlation coefficient	Probability	Correlation coefficient	Probability
Total PAHs			–0.559[a]	0.0037
Total naphthalenes	–0.617	0.0010	–0.586	0.0021
% clay	0.573	0.0027	0.554	0.0041
Ag	–0.667	0.0003		
Ba	–0.611	0.0012		
Cd	–0.590	0.0019		
Hg	–0.611	0.0012	–0.589	0.002
Zn	–0.613	0.0011	–0.575	0.0027
Pb	–0.642	0.0005		
Porewater Pb[b]			–0.613	0.0011

[a]Negative sign indicates an inverse relationship.
[b]High Island stations only.

Table 9. Observed toxicity versus predicted toxicity with the sea urchin embryological development test for specific metals with sediments collected during Cruises 1 and 2.

Metal	PEL (mg/kg)[a]	No. of stations > PEL	No. of stations > PEL significantly toxic
Zn	271	18	9 (50%)
Pb	112	17	6 (35%)
Cd	4.2	7	5 (71%)
Ag	1.8	4	3 (75%)
Hg	0.69	4	3 (75%)

[a]Probable effects level (MacDonald 1994).

© 1996 NRC Canada

lead-based paints and cathodic protection) than production operation discharges. The platforms in this study are representative of primarily gas and not oil production activities. The concentration of PAHs discharged from oil production platforms is likely to be considerably greater than from a gas-producing platform. The results of these studies utilizing highly sensitive toxicity tests suggest that the contaminant-induced impacts from offshore platforms are limited to a localized area in the immediate vicinity of the platforms. While the impacts from these primarily gas-producing platforms appear to be minimal and highly localized, the impacts from oil-producing platforms have not been fully evaluated and warrant further study.

Acknowledgments

This study was supported, in part, by the Minerals Mangement Service (MMS) GOOMEX program under contract 14-35-0001-30582. P. Chapman, D. MacDonald, S. Bay, L. Cleaveland, A. Allert, W. Brumbaugh, and an anonymous reviewer provided many helpful suggestions and comments. We gratefully acknowledge the organizational skills of the GOOMEX Program Manager and Chief Scientist for the collection cruises, M.C. Kennicutt II.

References

Boothe, P.N., and James, W.D. 1985. Neutron activation analysis of barium in marine sediments from the north central Gulf of Mexico. J. Trace Microprobe Tech. **3**: 377–399.

Carr, R.S. 1993. Survey of Galveston Bay bottom sediments and benthic communities. Galveston Bay National Estuary Program Report GBNEP-30.

Carr, R.S., and Chapman, D.C. 1992. Comparison of solid-phase and pore-water approaches for assessing the quality of marine and estuarine sediments. Chem. Ecol. **7**: 19–30.

Carr, R.S., and Chapman, D.C. 1995. Comparison of methods for conducting marine and estuarine sediment porewater toxicity tests. I. Extraction, storage and handling techniques. Arch. Environ. Contam. Toxicol. **28**: 69–77.

Carr, R.S., Curran, M.D., and Mazurkiewicz, M. 1986. Evaluation of the archiannelid *Dinophilus gyrociliatus* for use in short-term life-cycle toxicity tests. Environ. Toxicol. Chem. **5**: 703–712.

Carr, R.S., Williams, J.W., and Fragata, C.T.B. 1989. Development and evaluation of a novel marine sediment pore water toxicity test with the polychaete *Dinophilus gyrociliatus*. Environ. Toxicol. Chem. **8**: 33–543.

Carr, R.S., Long, E.R., Chapman, D.C., Thursby, G., Biedenbach, J.M., Windom, H., Sloane G., and Wolfe, D.A. 1996. Toxicity assessment studies of contaminated sediments in Tampa Bay, Florida. Environ. Toxicol. Chem. **15**: 1218–1231.

Chapman, P.M, Power, E.A, Dexter, R.N., and Andersen, H.B. 1991. Evaluation of effects associated with an oil platform, using the sediment quality triad. Environ. Toxicol. Chem. **10**: 407–424.

Day, R.W., and Quinn, G.P. 1989. Comparisons of treatments after an analysis of variance in ecology. Ecol. Monogr. **59**: 433–463.

Hamilton, M.A., Russo, R.C., and Thurston, R.V. 1977. Trimmed Spearman–Karber method for estimating median lethal concentrations in toxicity bioassays. Environ. Sci. Technol. **11**(7): 714–719; correction **12**(4): 417 (1978).

Kennicutt, M.C. (*Editor*). 1994. Gulf of Mexico offshore operations monitoring experiment. Phase I: Sublethal responses to contaminant exposure, Interim report: Year 1. OCS Study MMS 94-0005. U.S. Department of the Interior, Minerals Management Service, Gulf of Mexico OCS Regional Office, New Orleans, La.

Kennicutt, M.C. II, Boothe, P.N., Wade, T.L., Sweet, S.T., Rezak, R., Kelly, F.J., Brooks, J.M., Presley, B.J., and Wiesenburg, D.A. 1996. Geochemical patterns in sediments near offshore production platforms. Can. J. Fish. Aquat. Sci. **53**. This issue.

MacDonald, D.D. 1994. Development of an approach to the assessment of sediment quality in Florida coastal waters. Report to Florida Department of Environmental Protection, Tallahassee, Fla.

Montagna, PA., and Harper, D.E. Jr. 1996. Benthic infaunal long-term response to offshore production platforms in the Gulf of Mexico. Can. J. Fish. Aqat. Sci. **53**. This issue.

Nacci, D., Jackim, E., and Walsh, R. 1986. Comparative evaluation of three rapid marine toxicity tests: sea urchin early embryo growth test, sea urchin sperm cell toxicity test and microtox. Environ. Toxicol. Chem. **5**: 521–525.

National Biological Survey (NBS). 1993. Toxicity testing of sediments from Charleston Harbor, South Carolina and vicinity. Report submitted by the National Biological Survey to the National Oceanic and Atmospheric Administration, Ocean Assessment Division, Seattle, Wash.

National Biological Survey (NBS). 1994*a*. Survey of sediment toxicity in Pensacola Bay and St. Andrew Bay, Florida. Report submitted by the National Biological Survey to the National Oceanic and Atmospheric Administration, Ocean Assessment Division, Seattle, Wash.

National Biological Survey (NBS). 1994*b*. Toxicity testing of sediments from Boston Harbor, Massachusetts. Final report submitted to the National Oceanic and Atmospheric Administration, Ocean Assessment Division, Seattle, Wash.

SAS Institute Inc. 1989. SAS/STAT® user's guide, version 6, fourth edition. Vol. 2. SAS Institute Inc., Cary, N.C.

Science Applications International Corporation (SAIC). 1992. Survey of sediment toxicity in Tampa Bay, Florida: Final Report. Report submitted by SAIC to the National Oceanic and Atmospheric Administration, Ocean Assessment Division, Seattle, Wash.

U.S. Environmental Protection Agency (USEPA). 1986. Quality criteria for water 1986. EPA 440/5-86-01.

U.S. Fish and Wildlife Service (USFWS). 1992. Amphipod solid-phase and sea urchin porewater toxicity tests of Tampa Bay, Florida sediments. Report submitted by the U.S. Fish and Wildlife Service to the National Oceanic and Atmospheric Administration, Ocean Assessment Division, Seattle, Wash.

Wade, T.L., Velinsky, D.L., Reinharz, E., and Schlekat, C.E. 1994. Tidal river sediments in the Washington, D.C. area. II. Distribution and sources of organic contaminants. Estuaries, **17**: 321–333.

© 1996 NRC Canada

Implications for monitoring: study designs and interpretation of results

Roger H. Green and Paul Montagna

Abstract: A Sediment Quality Triad approach was used to integrate concurrently obtained toxicological, sediment contaminant, and benthic ecological data from GOOMEX in a test of coherence of responses. The biological community responded to contaminants by increases in the ratio of "the more tolerant taxon" to "the more sensitive taxon": the nematode to harpacticoid copepod ratio for meiofauna and the polychaete to amphipod ratio for macrofauna. Meiofaunal total abundance declined near platforms whereas macrofaunal total abundance increased — probably because of organic enrichment near platforms. A second approach used small-scale spatial heterogeneity of response as evidence of impact. Cd, Ba, ChemPC1 (first principal component of contaminant information), and the nematode to harpacticoid ratio had significant heterogeneity of variance among distances from platform, with higher variances near platforms. The pattern for Cd and ChemPC1 suggests that the impact may extend out to 200 m. We argue that differing objectives which are often demanded of the same study are often in conflict (e.g., generalization about environmental impact of similar platforms has different design requirements than description of spatial pattern of impact around each platform). Therefore, requiring that a study accomplish both objectives leads to compromises and a suboptimal design for both.

Résumé : Les auteurs ont eu recours, pour l'évaluation de la qualité de sédiments, à une approche triadique leur permettant d'intégrer, dans un test de cohérence des réponses obtenues, des données toxicologiques, d'autres sur des contaminants dans des sédiments et d'autres sur l'écologie en milieu benthique, obtenues concuremment dans le cadre du projet GOOMEX. La réaction de la communauté biologique aux contaminants a conduit à l'augmentation du ratio du « taxon le plus tolérant » au « taxon le plus sensible », soit celui entre les nématodes et les copépodes harpacticoïdes dans le cas de la méiofaune, et celui entre les polychètes et les amphipodes dans celui de la macrofaune. L'abondance totale de la méiofaune a diminué tandis que celle de la macrofaune a augmenté à proximité des plates-formes, probablement à cause d'un enrichissement organique près de celles-ci. Les auteurs ont appliqué une deuxième approche, soit celle axée sur l'hétérogénéité des réponses dans l'espace à petite échelle comme indice des impacts. Dans le cas du Cd, du Ba, du Chem PC1. (premier composant principal de l'information sur les contaminants) et du ratio nématodes au harpacticoïdes, ils ont observé une hétérogénéité d'importance significative au niveau de la variance entre les distances jusqu'aux plates-formes, les variances les plus marquées étant observées à faible distance de celles-ci. Dans le cas du Cd et du Chem PC1, les résultats paraissent indiquer que les effets pourraient se faire ressentir jusqu'à 200 m. Les auteurs soutiennent que les objectifs divergents qu'on se donne dans le cadre d'une même étude sont souvent incompatibles (p. ex., les critères de conception servant à une généralisation sur l'impact environnemental de plates-formes similaires diffèrent de ceux servant à la description de la distribution des impacts dans l'espace autour de chaque plate-forme). Par conséquent, de s'attendre à ce qu'une étude produise les deux types de résultats mène à l'adoption de compromis et à une conception d'expérience qui n'est optimale ni pour l'un ni pour l'autre des objectifs. [Traduit par la Rédaction]

Introduction

The design of an impact/monitoring study and statistical approaches to interpretation of results from that study are inseparable. There should be a logical flow of purpose → question → hypotheses → model → study design → statistical analysis → tests of hypotheses → interpretation and presentation of results (Green 1984). On the other hand, some statistical approaches for interpreting results will be used in almost any environmental study regardless of the study design, e.g., regression, correlation, tables of means and standard errors. In this paper the use of two innovative and recent statistical approaches to interpretation and generalization of results from studies of this kind are described (Kennicutt et al. 1996). The first of these is an adaptation of Chapman's Sediment Quality Triad (SQT) concept (see references below), and the second is the use of small-scale spatial heterogeneity of response in several variables as evidence of impact. Finally, the link between study objectives and study design will be discussed with emphasis on the inherent conflict between differing objectives in relation to optimal study design.

Received October 5, 1995. Accepted September 16, 1996.
J13413

R.H. Green Department of Zoology, University of Western Ontario, London, ON N6A 5B7, Canada.
P. Montagna. Marine Science Institute, University of Texas, 750 Channelview Dr., Port Aransas, TX 78373, U.S.A.

SQT approach to integration and interpretation of results

The SQT concept involves the use of concurrently obtained (synoptic) toxicological, sediment chemistry, and benthic infauna data to determine environmental degredation (e.g., Long and Chapman 1985; Chapman et al. 1987; Chapman

© 1996 NRC Canada

et al. 1989). In their application of this concept to evaluate effects associated with an oil platform, Chapman et al. (1991) argued that the SQT "incorporates three essential components: measures to determine the presence and degree of anthropogenic contamination (i.e., bulk sediment chemistry); measures that demonstrate that substances are present that can interfere with the normal functioning of at least some biological organisms tested in the laboratory (i.e., sediment toxicity tests); and, assessments of in situ alteration of resident biological communities (i.e., measures of benthic infaunal community structure)." They noted that one of the weaknesses of the SQT is "lack of statistical criteria for the combined Triad components." Green et al. (1993) also pointed out that appropriate statistical methods had not been used in previous applications of the SQT concept to actual environmental impact situations and that appropriate methods would be those that could relate conceptually different sets of variables in multivariate data (Green 1993*a*). Such methods were then applied to data from a study (Chapman et al. 1989) designed to identify the degree of pollution-induced degradation at each station for 13 sampling stations in Vancouver Harbour, British Columbia, Canada.

Chapman et al. (1991) applied the SQT approach to data obtained from sampling along three radii centered on Platform "C" of the Matagorda 622 field, 22 km offshore in water depths ranging from 24 to 26 m. Benthic infaunal community data obtained from cores provided the biological component. Limited sediment chemistry data provided the contamination component, and the toxicological component consisted of an amphipod bioassay, an assessment of abnormalities in oyster larvae, and Microtox tests. As in earlier applications of the SQT (e.g., Chapman et al. 1989), the statistical analyses were mostly descriptive and applied to each component rather than as criteria for the combined components and were based on a "ratio-to-reference" criterion (the ratio of values at possibly impacted stations to values at an a priori defined reference station). Two other problems are that the experiment-wide error rate is not controlled and that the reasoning tends to be circular (the reference site is chosen and then used for tests of impact).

Here the methods described in Green et al. (1993) are applied to the GOOMEX data described in the preceding articles, in an application of the SQT concept. This is an attempt to integrate the diverse results from various work elements to describe and test for concordance. Most large environmental impact/monitoring studies with numerous principal investigators involved have failed to adequately interrelate the results and interpretations from the different work elements, such as description of the biological community, description of the physical/chemical environment, and laboratory toxicological results. Therefore, interesting and suggestive results often remain in each work element report and are not properly related to other results. This final integration step greatly increases the value of the overall study results.

Of course other paradigms have been described for relating biological response variables to environmental predictor variables (Ter Braak 1986; Clarke 1993; Clarke and Ainsworth 1993). Here we are limiting ourselves to accomplishing this within the SQT paradigm.

For the SQT components, we used the following: *biological*: abundances of two major meiofaunal taxa and two major macrofaunal taxa; *chemical*: the variables total polycyclic aromatic hydrocarbons, unresolved complex mixture, total alkanes, percent sand, percent silt, percent clay, total organic carbon, total inorganic carbon, redox potential, Fe, Cd, Al, and Ba; *toxicological*: a test of porewater toxicity using percent successful development of sea urchin embryos as a criterion.

The sea urchin embryo development assay was done for samples from all stations for Cruises 1 and 2 (Carr et al. 1996). Therefore the data analyzed by the SQT approach were from samples taken on the first two cruises at all stations (n = 2 cruises × platforms × 5 radii × 5 distances = 150). The analysis approach was essentially that of section 3.2, pp. 446–450, of Green et al. (1993). There is only one toxicological variable, and the chemical contaminant information has already been reduced to one variable: the ChemPC1 score (see Kennicutt et al. 1996). Two analyses were carried out for the biological component. One was based on meiofaunal community response and the other on macrofaunal community response (Montagna and Harper 1996). For the meiofauna analysis, total harpacticoid abundance and total nematode abundance were used as the variables, reflecting the long-standing use of these taxa and their relative abundances as indicators of environmental impact (see Montagna and Harper 1996). The nematode to copepod (N/C) ratio was originally proposed to detect gradients of organic enrichment (Raffaelli and Mason 1981). The N/C ratio has been criticized as being too simplistic (Coull et al. 1981), but it was a predictor of oil pollution in South Africa (Hennig et al. 1983) and exposure to a gradient of natural petroleum seepage in California (Montagna et al. 1987, 1989). Harpacticoids are usually more sensitive to impact than are nematodes, so at impacted sites the N/C ratio usually increases. The abundances were log-transformed, so a difference between nematode and harpacticoid log abundance represents this ratio.

Analagously, for the macrofauna analysis we used total amphipod abundance and total polychaete abundance as variables. Amphipods decreased and polychaetes increased close to platforms, so the polychaete to amphipod (P/A) ratio increased as well (Montagna and Harper 1996). Deposit-feeding polychaetes and nematodes increase with proximity to platforms (perhaps caused by trophic enrichment), while amphipods and harpacticoids decrease near platforms (perhaps caused by toxicity). Again, abundances were log-transformed.

The SQT analysis was also performed with the biological component consisting of all four of these taxa. These results were statistically significant and consistent with the results from the analyses of the meiofauna and macrofauna separately. However, the results of the separate analyses were easier to interpret and therefore we will not present or discuss the "combined analysis" results. These SQT analyses were also carried out platform by platform and those results and their implications are summarized .

The statistical analysis was the same for all SQT analyses. First the correlations among components were calculated. We used Pearson correlations, but rank correlations could be used and we also calculated them for comparison in cases of apparent nonlinearity. The correlations between the biological and chemical components and between the biological and toxicological components were determined by the multiple correla-

© 1996 NRC Canada

Fig. 1. Significance and strength of relationships among SQT components.

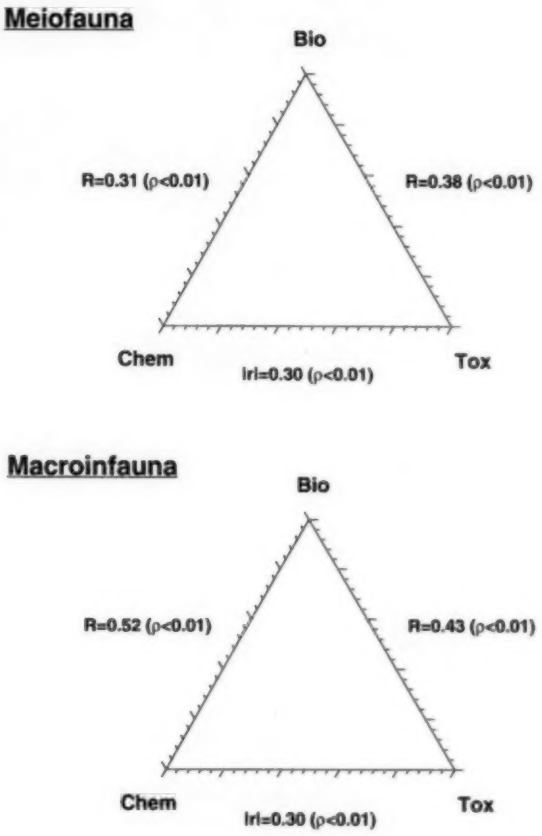

Fig. 2. Relationship between BioPC1 and BioPC2 of the meiofauna abundance data and the contaminant variable ChemPC1.

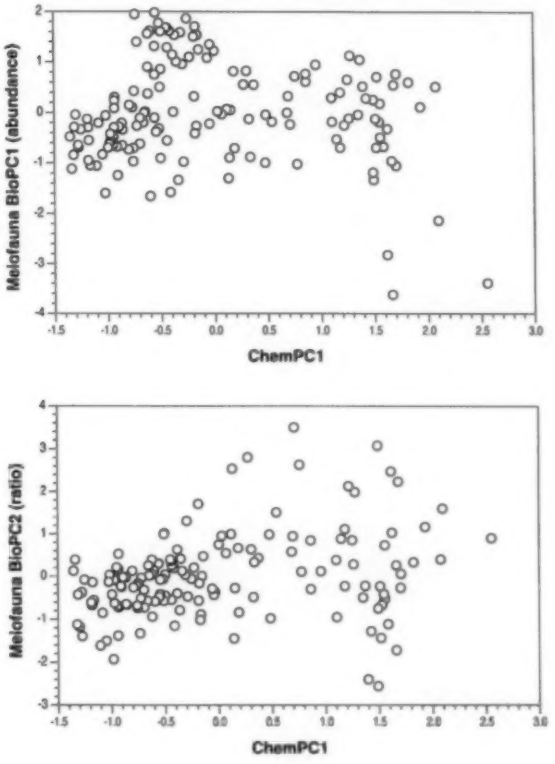

tion ($\sqrt{R^2}$) of the nonbiological component with abundances of the two taxa which defined the biological component. The correlation between the chemical and toxicological components is the simple bivariate correlation coefficient r. Thus the significance and strength of each of the three between-component relationships are evaluated, and can be placed on the sides of the triangle representing the SQT (as in Fig. 1). Scatter plots showing these between-component relationships are presented. Second, the entire among-component correlation matrix is tested against the null hypothesis H_0: "no relationships among the three SQT components", using Bartlett's sphericity test. Third, a principal component analysis (PCA) is done on the correlation matrix to evaluate the structural relationship(s) among the three SQT components. This was a two-step procedure. First, a PCA on the two log-transformed taxa abundance variables was done to derive "size" and "shape" PCs. That is, in a PCA on such data, one of the PCs (the "size" PC) is invariably related similarly (same strength of relationship and same sign) to the original variables and represents a tendency for the variables to go up and down together. Here it would represent increases or decreases of abundance of both taxa, and presumably of the entire meiofaunal or macrofaunal community. The other PC (the "shape" PC) will have opposite-signed relationships (one positive and one negative) to the original variables, which in these log-transformed data will represent changes in the ratio of the abundances of the two taxa. The PC scores for these two PCs (hereafter referred to as BioPCs) should have these interpretations and can used in the final PCA along with the chemical and toxicological measures. See Pimentel (1979) or Harris (1985) for an explanation of PCA and examples of interpretation of PCA results.

The results for the meiofauna-based analysis and for the macrofauna-based analysis are similar. The strength and significance of between-component SQT relationships in the two analyses are shown in Fig. 1. All three relationships in both analyses are highly significant ($p < 0.01$). Scatter plots showing the between-component relationships are shown in Fig. 2–4. Some (e.g., Fig. 4) are obviously nonlinear, or "threshold", relationships. For those, we also calculated rank correlation coefficients, which showed similar relationships (both strength and direction). For both analyses, Bartlett's sphericity test is highly significant, with χ^2 (6 df) = 43.9 ($p < 0.01$) for the meiofauna-based analysis and χ^2 (6 df) = 78.6 ($p < 0.01$) for the macrofauna-based analysis. For those concerned about the assumptions of Bartlett's sphericity test, there is an analogous randomization test called ANOSIM (Clarke and Green 1988).

The PCA results are shown in Table 1. In the meiofauna-based analysis the first BioPC was a "size" PC" and the sec-

© 1996 NRC Canada

Fig. 3. Relationship between BioPC1 and BioPC2 of the macrofauna abundance data and contaminant variable ChemPC1.

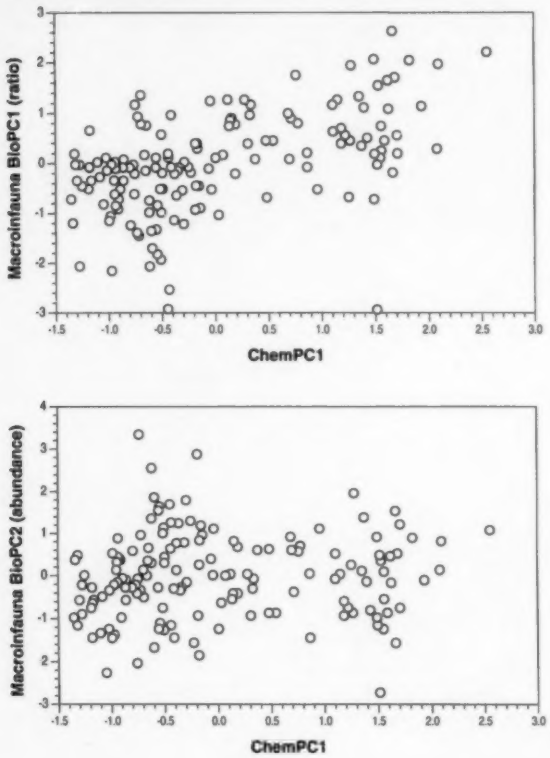

Fig. 4. Relationship between percent successful development (MDEVEL) in sea urchin embryo pore water assays and contaminant variable ChemPC1.

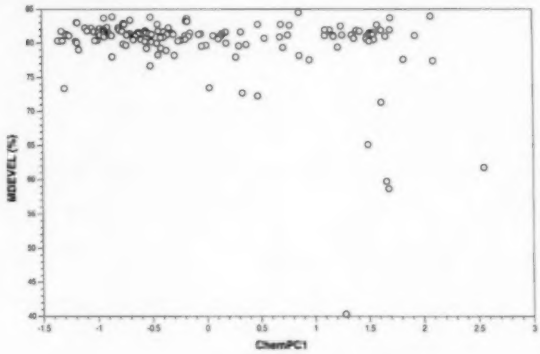

Table 1. Summary of results of PCA on correlations among SQT components.

Meiofauna	PC1 (41.5%)
Chem component	0.703
Tox component	–0.758
Bio component (total abundance)	–0.267
Bio component (NEMA/HARP)	0.721
Macrofauna	PC1 (45.6%)
Chem component	0.782
Tox component	–0.706
Bio component (total abundance)	0.255
Bio component (POLY/AMPH)	0.805

ond a "shape" PC, indicating that fluctuations in abundance of both taxa together dominate the abundance variation, with relative abundance changes (changes in the N/C ratio) being smaller in magnitude. However, in the macrofauna-based analysis the first BioPC was the "shape" PC and the second the "size" PC, indicating that the relative abundance changes (the P/A ratio) dominate the fluctuations in overall abundance of both taxa. For both of the SQT summary analyses, there is a dominant PC1 (41.5% of the structure in the meiofauna-based analysis and 45.6% of the structure in the macrofauna-based analysis) that can be interpreted as follows: As chemical contamination increases (positive relationship with ChemPC1) the percent successful development of sea urchin embryos decreases (negative relationship with that toxicological measure), and the biological community responds by changing the relative abundances of the taxa in the direction of increasing the ratio of the abundance of the more tolerant taxon to the abundance of the more sensitive taxon.

In other words, the same relationships among the SQT components are seen in the meiofauna-based and macrofauna-based SQT analyses, which strengthens the interpretations and conclusions. Variations in meiofaunal abundances are dominated by changes in total abundance (e.g., nematodes and harpacticoids going up and down together) whereas variation in macrofaunal abundances is dominated by relative abundance changes (changes in the P/A ratio). Although neither community shows a strong relationship between ChemPC1 and the total abundance of both taxa (it is mostly between ChemPC1 and the relative abundances of the taxa), such relationship as there is is a negative one for the meiofauna and a positive one for the macrofauna. Organic enrichment of the macrofaunal community near the platform may cause increased total macrofaunal abundance there (Montagna and Harper 1996; Peterson et al. 1996). If such enrichment does not affect the meiofaunal community, then there would be a contaminant-driven decrease in total abundance near platforms. This is in fact what we see. In summary, both communities show impact effects in their ratios of "tolerant to sensitive taxa abundances". The meiofaunal community also shows some negative response in total abundance, but in the macrofaunal community, any such response is overwhelmed by enhancement of total abundance (mostly of polychaetes), probably by nutrient enrichment near platforms.

The platform by platform analyses indicate that most of the pattern we see in these results is driven by what is going on at HI-A389. The patterns at the other two platforms are not obviously different from HI-A389, but they are certainly weaker. At HI-A389, Bartlett's sphericity test is highly significant and all three SQT relationships are highly significant, for both meiofauna and macrofauna. At MU-A85, there is no Tox-Chem relationship and no Bio-Tox relationship for either meiofauna or macrofauna. There is a significant ($p < 0.01$) Bio-Chem relationship for macrofauna and a marginally non-significant one ($p = 0.11$) for meiofauna. However, the over-

© 1996 NRC Canada

all test of whether there are any significant SQT relationships, Bartlett's sphericity test, is not significant for either meiofauna or macrofauna at MU-A85. At MAI-686, Bartlett's sphericity test is highly significant for both meiofauna and macrofauna, but only the Bio-Chem relationship is significant ($p < 0.01$, for both meiofauna and macrofauna). The Bio-Tox and the Tox-Chem relationships are nonsignificant for both meiofauna and macrofauna at MAI-686.

Finally, it should be remembered that the ChemPC1 score we are using as our measure of the chemical contaminant SQT component is a measure of the confounded chemical and substrate composition gradients related to distance from platform. All interpretations of these results must be made with this reality in mind. However, the same can be said about any environmental impact study based solely on observational data. For consideration of the sensitivity of multivariate methods in detection of marine environmental impacts, see Gray et al. (1990) and Olsgard and Gray (1995).

Heterogeneity of variance as an impact response

It is usual to formulate response variables for impact studies in terms of mean values of contaminant concentrations, taxa abundances, etc. However, data collected and analyzed in pollution impact studies suggest that variances as well as means typically respond to impacts. The response is usually "patchy", since the small-scale spatial distribution of the impacting contaminants is rarely uniform. This is visually obvious in an intertidal area after an oil spill. An increased variance among small-scale spatial replicate samples (cores, quadrats) is the result. This is most often observed when the data are examined to see whether they satisfy assumptions for analysis of variance (ANOVA), since one of the ANOVA assumptions is "homogeneity of error variance". Concern is usually focused on whether this ANOVA assumption is satisfied, for testing whether means differ, without realizing that such variance heterogeneity can itself be evidence of impact. Green (1993*b*) discussed this question, and Underwood (1992, 1993) described an ANOVA design that incorporates a test of impact-caused increased variation. Warwick and Clarke (1993) described increased variation in response to stress in marine communities, but Chapman et al. (1995) were unable to demonstrate increased variability in polluted versus control assemblages.

In deciding how to test for increased spatial variation attributable to impact, two things must be kept in mind. One is that the appropriate spatial scale of sampling must be used, and the other is that one must use the appropriate scale for measuring the response. Regarding the first, the scale of sampling must be the residual spatial error variation in some sense and not a scale of variation which is included in the ANOVA model. For example, it would not be appropriate to use the variance among boxcores within a particular distance-from-platform (within Platform[1] and Cruise). Because there is only one boxcore taken at each Distance and on each Radius, all of that variance would be among-Radius variance. An increased near-the-platform variance of that kind would only be evidence of directionality of impact, which we are already testing by testing the Distance·Radius interaction (Kennicutt et al. 1996). In the GOOMEX study design the small-spatial-scale variance is the "between-subcores within-boxcores" variance. (If replicate boxcores had been taken, then it would have been the "among replicate boxcores at each Distance and Radius" variance.)

The appropriate scale for measuring the response is usually the transformed scale. If percent variation is appropriate for evaluation of response in mean values, and we therefore usually log-transform the response variable data, then it will usually also be appropriate for evaluation of variance magnitude. If the variance of untransformed contaminant concentration is higher near a platform (where contaminant mean concentration is higher), it could be argued that it is only caused by the relationship between the error variance and the mean, which always exists in (untransformed) data reflecting percent variation. The raw (replicate subcore) observations in GOOMEX response variable data are typically log-transformed, e.g., for contaminant concentrations and taxa abundances (Kennicutt et al. 1996). The PC1 scores that we are using to represent the contaminant gradient are calculated from a linear additive function of appropriately transformed variables, so ChemPC1 as a synthetic variable is also being measured on the appropriate scale.

The between-subcore within-boxcore variance was estimated for each ring (Distance) and direction (Radius), pooled over Platforms and Cruises, on the appropriate response scale, for Ba, Cd, ChemPC1, nematode abundance (NEMA), harpacticoid abundance (HARP), and N/C. Macrofauna data were not used because it seemed likely that the within-boxcore spatial scale would be too small for proper assessment of macrofauna patchiness. Using these variance estimates as the response variables in among-distances ANOVAs, we found significant ($p < 0.01$) heterogeneity of variance for Ba, Cd, and ChemPC1, but not for NEMA and HARP ($p > 0.05$). For the N/C ratio, heterogeneity of variance was significant at $p < 0.05$. Because of some concern about the distributional properties of estimated variances used as ANOVA response variables, we repeated these ANOVAs as nonparametric ANOVAs (Kruskal–Wallis tests of medians). The significances and nonsignificances were unchanged. The estimated median variances for each distance for these five variables is presented in Table 2. For the four variables with significant heterogeneity of variance the pattern is one of increased variance near the platform. Variance as a function of distance from the platform is presented in Fig. 5 for these variables.

These results provide additional evidence for platform-derived impacts. The pattern for Cd and ChemPC1 suggests that the impact may extend to the third ring (200 m, Fig. 5). However, the impact could be caused by sediment changes rather than contaminants, which could easily increase the variance of both these variables. The absence of heterogeneity of variance for the two meiofaunal taxa taken by themselves contrasts with the heterogeneity of variance for the N/C ratio. This provides additional support for the use of the "ratio of a tolerant to a sensitive taxon" as an indicator of biological impact. Ratios should not be calulated from the raw data for each sample and then used as a response variable in

[1] Throughout this paper, we have capitalized the first letter of Platform, Cruise, Distance, and Radius where these terms are used in the sense of a study design element.

© 1996 NRC Canada

Table 2. Median subcore variances for selected variables.

Distance from platform (m)	Cd	ChemPC1	Ba	NEMA	HARP	N/C
50	0.0491	0.0119	0.0039	0.0770	0.0822	0.0870
100	0.0245	0.0115	0.0021	0.0566	0.0793	0.1184
200	0.0167	0.0057	0.0029	0.0940	0.0931	0.0628
500	0.0043	0.0044	0.0010	0.0293	0.0770	0.0463
≥3000	0.0046	0.0033	0.0009	0.0406	0.0543	0.0442

Fig. 5. Median variance of selected variables between subcores within a boxcore versus distance from platform.

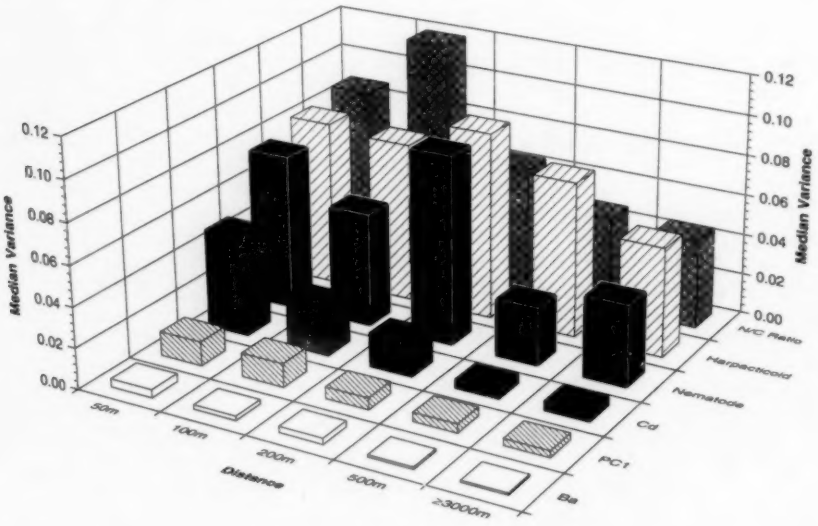

statistical analysis because such derived ratio variables do not behave well as response variables (Green 1979, 1986). The use of log–log linear models (regression, analysis of covariance, or PCA as used here) to imply ratios when coefficients have opposite signs should be the preferred practise.

Recommended sampling designs for future studies

The GOOMEX Phase I study is based on a complex sampling design described in Kennicutt et al. (1996). It was used throughout this study for hypothesis testing and interpretation. The sampling design contains the following components: three Platforms, four Cruises (times, at half-year intervals), five Distances from each Platform (for some variables only two Distances), and five Radii (directions from Platforms). This sampling design was developed to satisfy the requirement that there be intensive sampling around Platforms to describe direction and distance (spatial scale) of impacts in relation to the point source. That is all very well, but any project has a fixed budget and any increase of "oversampling" around each point-source is inevitably a trade-off against including more point-sources in the study design.

Two quite different objectives are in conflict. Elucidating pattern of impact (direction and distance) around a point-source calls for a different study design than does generalizing about impacts from point-sources. Requiring that a study accomplish both inevitably leads to compromises and to a nonoptimal design for both. The GOOMEX Phase I study design emphasizes the first objective. Impact patterns around each of the three platforms were adequately described. However, with only three platforms, each of which is environmentally unique in some ways, it is difficult to generalize about impacts of "platforms", and any attempt to relate impact differences among platforms to historical production differences among platforms or to natural environment differences among platforms leads to a regression or correlation based on three data points. Even if there were a perfect rank correlation between the extent of impact-related responses and discharges from platforms, with only three platforms that perfect rank correlation (in the direction expected, i.e., one-tailed) would occur by chance one time out of six (0.17 probability). Typically, 0.05 is required for statistical significance. With four platforms, it would be 1 in 24, or 0.04. With five, it would be 1 in 120, or 0.008. Thus the likelihood of confounding with natural environment patterns decreases rapidly. In our three-platform study the rank order of contaminant levels is also a perfect rank correlation

© 1996 NRC Canada

with water depth, distance from shore, and all environmental variables related to them.

In other words, the study design describes and tests the spatial pattern of impact around these three platforms (i.e., platforms treated as fixed-effect blocks, or strata), but there is little ability to generalize to impacts caused by "platforms" as a generic class or to describe differences in impacts due to the kind of platform. If the platforms are thought of as a sample of platforms of a kind in the region, then three is too few and these platforms are too different for any meaningful conclusion to be reached about "platforms". If each of these three platforms is considered a representative of a platform type (e.g., contaminant levels, depth and distance from shore), then there is no replication within platform type and impact differences among platform types cannot be tested.

To generalize the results, rather than just describe what happens around each platform, an increase in the number of platforms and a corresponding decrease in effort allocated around each is needed. For example, the design might consist of 12 or more platforms with sampling at near and far distances (e.g., 50 and 3000 m) along one radius in a direction and at distances from each platform that were established from a previous study, or preliminary sampling, to be the average direction of maximum contaminant movement and the appropriate distances from the platform in that direction. This would result in a paired design, in which the "near versus far" difference would be tested based on a sample of $n \geq 12$ platforms. To reduce costs, one sampling method could be used and one response variable measured (again established from preliminary sampling). The procedure for selecting platforms is critical. The region should be defined a priori, and objective criteria for one or more types of platform should be stated. Then, all platforms of that type occurring in that region should be catalogued and the ones to be included in the study randomly selected from them.

Twelve or more platforms are recommended, for two reasons. First, robustness of statistical tests can be assured by having at least 10 error degrees of freedom for the test (Green 1979; Harris 1985). In such a paired design the error is the among-platform variation in the near versus far difference. Therefore the error degrees of freedom will be the number of platforms less one (or if there is more than one type of platform, it will be the number of platform types times one less than the number of platforms of each type). Second, power in tests (ability to detect differences that really exist, e.g., near versus far) increases with sample size (number of platforms). Simulations were carried out with specified mean near versus far differences and standard deviations for those differences. Power initially increases rapidly with number of platforms but then begins to flatten out around $n = 10$–12 platforms.

If a study must be dual-purpose, requiring a compromise design capable of elucidating pattern of impact around point-sources as well as generalizing about impacts of that kind, then the best approach will be to have a paired study design with $n \geq 12$ platforms for the generality, with one of those platforms dedicated to the intensive spatial pattern sampling which would include the "near versus far in one direction" sampling compatible with the other platforms.

References

Carr, R.S., Chapman, D.C., Presley, B.J., Biedenback, J.M., Robertson, L., Boothe, P., Kilada, R., Wade, T., and Montagna, P. 1996. Sediment porewater toxicity assessment studies in the vicinity of offshore oil and gas production platforms in the Gulf of Mexico. Can. J. Fish. Aquat. Sci. **53**. This issue.

Chapman, M.G., Underwood, A.J., and Skilleter, G.A. 1995. Variability at different spatial scales between a subtidal assemblage exposed to the discharge of sewage and two control assemblages. J. Exp. Mar. Biol. Ecol. **189**: 103–122.

Chapman, P.M., Dexter, R.N. and Long, E.R. 1987. Synoptic measures of sediment contamination, toxicity and infaunal community structure (the Sediment Quality Triad) in San Francisco Bay. Mar. Ecol. Prog. Ser. **37**: 75–96.

Chapman, P.M., McPherson, C.A., and Munkittrick, K.R. 1989. An assessment of the ocean dumping tiered testing of ocean using the Sediment Quality Triad. Prepared for Department of Fisheries and Oceans, Institute of Ocean Sciences, Sidney, B.C. DSS Project No. 06SB.FP941-8-9060.

Chapman, P.M., Power, E.A., Dexter, R.N., and Andersen, H.B. 1991. Evaluation of effects associated with an oil platform, using the Sediment Quality Triad. Environ. Toxicol. Chem. **10**: 407–424.

Clarke, K.R. 1993. Non-parametric multivariate analyses of changes in community structure. Aust. J. Ecol. **18**: 117–143.

Clarke, K.R., and Ainsworth, M. 1993. A method of linking multivariate community structure to environmental variables. Mar. Ecol. Prog. Ser. **92**: 205–219.

Clarke, K.R., and Green, R.H. 1988. Statistical design and analysis for a biological effects study. Mar. Ecol. Prog. Ser. **46**: 213–226.

Coull, B.C., Hicks, G.R.F., and Wells, J.B.J. 1981. Nematode/copepod ratios for monitoring pollution: a rebuttal. Mar. Pollut. Bull. **12**: 378–381.

Gray, J.S., Clarke, K.R., Warwick, R.M., and Hobbs, G. 1990. Detection of initial effects of pollution on marine benthos: an example from the Ekofisk and Eldfisk oilfields, North Sea. Mar. Ecol. Prog. Ser. **66**: 285–289.

Green, R.H. 1979. Sampling design and statistical methods for environmental biologists. Wiley, New York.

Green, R.H. 1984. Statistical and nonstatistical considerations for environmental monitoring studies. Environ. Monit. Assess. **4**: 293–301.

Green, R.H. 1986. Some applications of linear models for analysis of contaminants in aquatic biota. *In* Statistical aspects of water quality monitoring. *Edited by* A.H. El-Shaarawi and R.E. Kwiatowski. Elsevier, New York.

Green, R.H. 1993*a*. Relating two sets of variables in environmental studies. *In* Multivariate analysis: future directions. *Edited by* C.R. Rao. Elsevier, Amsterdam, The Netherlands. pp. 151–165.

Green, R.H. 1993*b*. Application of repeated measures designs in environmental impact and monitoring studies. Aust. J. Ecol. **18**: 81–98.

Green, R.H., Boyd, J.M., and Macdonald, J.S. 1993. Relating sets of variables in environmental studies: the Sediment Quality Triad as a paradigm. Environmetrics, **4**: 439–457.

Harris, R.J. 1985. A primer of multivariate statistics. 2nd ed. Academic Press, New York.

Hennig, H.F-K., Eagle, G.A., Fielder, L., Fricke, A.H., Gledhill, W.J., Greenwood, P.J., and Orren, M.J. 1983. Ratio and population density of psammolittoral meiofauna as a perturbation indicator of sandy beaches in South Africa. Environ. Monit. Assess. **3**: 45–60.

Kennicutt, M.C. II, Boothe, P.N., Wade, T.L., Sweet, S.T., Rezak, R., Kelly, F.J., Brooks, J.M., Presley, B.J., and Wiesenburg, D.A. 1996. Geochemical patterns in sediments near offshore production platforms. Can. J. Fish. Aquat. Sci. **53**. This issue.

© 1996 NRC Canada

Long, E.R., and Chapman, P.M. 1985. A sediment quality triad: measures of sediment contamination, toxicity and infaunal community composition in Puget Sound. Mar. Pollut. Bull. **16**: 405–415.

Montagna, P.A., and Harper, P.E. Jr. 1996. Benthic infaunal long-term response to offshore production platforms in the Gulf of Mexico. Can. J. Fish. Aquat. Sci. **53**. This issue.

Montagna, P.A., Bauer, J.E., Hardin, D., and Spies, R.B. 1987. Temporal variability and the relationship between benthic meiofaunal and microbial populations of a natural coastal petroleum seep. J. Mar. Res. **45**: 761–789.

Montagna, P.A., Bauer, J.E., Hardin, D., and Spies, R.B. 1989. Vertical distribution of microbial and meiofaunal populations in sediments of a natural coastal hydrocarbon seep. J. Mar. Res. **47**: 657–680.

Olsgard, F., and Gray, J.S. 1995. A comprehensive analysis of the effects of offshore oil and gas exploration and production on the benthic communities of the Norwegian continental shelf. Mar. Ecol. Prog. Ser. **122**: 277–306.

Peterson, C.H., Kennicutt, M.C. II Green, R.H., Montagna, P., Harper, D.E. Jr., Powell, E.N., and Roscigno, P.F. 1996. Ecological consequences of environmental perturbations associated with offshore hydrocarbon production: a perspective on long-term exposures in the Gulf of Mexico. Can. J. Fish. Aquat. Sci. **53**. This issue.

Pimentel, R.A. 1979. Morphometrics: the multivariate analysis of biological data. Kendall/Hunt, Dubuque, Iowa.

Raffaelli, D., and Mason, C.F. 1981. Pollution monitoring with meiofauna, using the ratio of nematodes to copepods. Mar. Pollut. Bull. **12**: 158–163.

Ter Braak, C.F.J. 1986. Canonical correspondence analysis: a new eigenvector technique for multivariate direct gradient analysis. Ecology, **67**: 1167–1179.

Underwood, A.J. 1992. Beyond BACI: the detection of environmental impacts on populations in the real, but variable world. J. Exp. Mar. Biol. Ecol. **161**: 145–178.

Underwood, A.J. 1993. The mechanics of spatially replicated sampling programmes to to detect environemntal impacts in a variable world. Aust. J. Ecol. **18**: 99–116.

Warwick, R.M., and Clarke, K.R. 1993. Increased variability as a symptom of stress in marine communities. J. Exp. Mar. Biol. Ecol. **172**: 215–226.

© 1996 NRC Canada

Ecological consequences of environmental perturbations associated with offshore hydrocarbon production: a perspective on long-term exposures in the Gulf of Mexico

Charles H. Peterson, Mahlon C. Kennicutt II, Roger H. Green, Paul Montagna, Donald E. Harper, Jr., Eric N. Powell, and Pasquale F. Roscigno

Abstract: A synthesis of the literature on benthic responses to marine pollution suggests that macroinfaunal and meiofaunal communities exhibit repeatable patterns of response to sedimentary contamination generally detectable at high taxonomic levels (even phylum). These responses appear to be jointly driven by intrinsic physiological and ecological characteristics of higher taxa, such that crustaceans (especially amphipods and harpacticoids) and echinoderms are sensitive to toxics whereas polychaetes, oligochaetes, and nematodes (especially non-selective deposit feeders) are enhanced by organic enrichment. Application of this model to the GOOMEX results implies involvement of both toxicity and organic enrichment. Results of toxicity tests and comparisons of observed contaminant concentrations to known effects levels imply that metals drive the toxicity response. We conclude that (1) long-lasting effects of drilling activity exist in the sedimentary environment around gas production platforms, (2) dual effects of toxicity and organic enrichment probably drive readily detectable responses in benthic meiofauna and macroinfauna to 100–200 m, and (3) the failure to detect evidence of exposure or sublethal impacts on fishes and most larger invertebrates is a joint consequence of their mobility over the relevant scales of environmental change and their negligible exposure to hydrocarbons and other contaminants.

Résumé : Une synthèse des articles portant sur la réponse du benthos à la pollution des mers paraît indiquer que les communautés constituées de l'endofaune macroscopique et de la méiofaune ont des profils répétables de réponse à la contamination des sédiments qui sont généralement observables à des niveaux taxonomiques élevés (même à celui du phylum). Ces réponses semblent être alimentées à la fois par des caractéristiques écologiques et physiologiques intrinsèques des taxons supérieurs : p. ex., les crustacés (particulièrement les amphipodes et les harpacticoïdes) et les échinodermes sont sensibles aux substances toxiques tandis que les polychètes, les oligochètes et les nématodes (particulièrement les dépositivores non sélectifs) tirent parti de l'enrichissement en matières organiques. L'application de ce modèle aux résultats obtenus dans le cadre du projet GOOMEX fait intervenir la toxicité et l'enrichissement en matières organiques comme facteurs. Les résultats des tests de toxicité et les rapprochements entre des concentrations observées de contaminants et des niveaux d'effets connus paraissent indiquer que les métaux sont les principaux agents de la toxicité. Nous parvenons aux conclusions suivantes : 1) les forages produisent des effets durables dans l'environnement sédimentaire autour des plates-formes de production gazière, 2) les effets combinés de la toxicité et de l'enrichissement en matières organiques sont probablement à l'origine des réponses facilement détectables de la méiofaune benthique et de l'endofaune macroscopique jusqu'à 100–200 m et 3) le fait de ne pas détecter de signes d'exposition ou d'effets sublétaux chez le poisson et la plupart des grands invertébrés est le résultat de leur grande mobilité par rapport à l'échelle des changements dans l'environnement et de leur exposition négligeable aux hydrocarbures et à d'autres contaminants.
[Traduit par la Rédaction]

Introduction

One of the most challenging problems in ecology is to separate the impacts of human disturbance from a background of natural spatial and temporal variation in ecological systems and thereby identify the ecological consequences of anthro-

Received March 20, 1996. Accepted September 16, 1996.
J13414

C.H. Peterson. Institute of Marine Sciences, University of North Carolina at Chapel Hill, Morehead City, NC 28557, U.S.A.
M.C. Kennicutt II. Geochemical Environmental Research Group, Texas A&M University, 833 Graham Rd., College Station, TX 77845, U.S.A.
R.H. Green. Department of Zoology, University of Western Ontario, London, ON N6A 5B7, Canada.
P. Montagna. Marine Science Institute, University of Texas, Port Aransas, TX 78373, U.S.A.
D.E. Harper, Jr. Marine Laboratory, Texas A&M University, 5007 Avenue U, Galveston, TX 77551, U.S.A.
E.N. Powell. Haskin Shellfish Research Laboratory, Rutgers University, Port Norris, NJ 08349, U.S.A.
P.F. Roscigno. U.S. Department of the Interior, Minerals Management Service, 1201 Elmwood Park Blvd., New Orleans, LA 70123, U.S.A.

© 1996 NRC Canada

pogenic perturbations to the natural environment (Levin 1992; Peterson 1993). There is enhanced urgency for provision of such information so as to inform properly the public policy debates over the wisdom of conducting certain economically rewarding but environmentally transforming activities (Lubchenco et al. 1991). Where the environmental signal resulting from the perturbation is large relative to the background variation, detection of ecological impacts is rendered relatively straightforward (Green 1979). However, the longer-term consequences of chronic disruptions of the environment are much less readily evaluated (e.g., Carney 1987). When chronic long-term disturbances act through sublethal effects on organisms, relating the consequences of those sublethal changes to the parameters of true public concern, the population abundances of valued species and the ability to sustain provision of ecosystem goods and services into the future, becomes especially problematic (Underwood and Peterson 1988).

Considerable controversy has arisen over the biological consequences of long-term oil and gas production and the advisability of further development of oil and gas fields on the continental shelf off several regions of the United States (NRC 1989, 1991, 1992; DOI 1992). A substantial body of technical data on the ecological impacts of oil spills in the marine environment serves to evaluate that particular risk in offshore hydrocarbon development and production (NRC 1975, 1985). Our understanding, however, of the consequences of many of the more subtle environmental changes associated with offshore hydrocarbon production is extremely limited. For example, the ecological significance of long-term chronic exposures to low-level releases of many chemicals associated with hydrocarbon production activities is largely unknown (NRC 1985; Boesch et al. 1987; Capuzzo 1987). Although such processes as discharge of produced waters and discharge and seafloor accumulation of drilling muds and cuttings, as well as chronic low-level releases of hydrocarbons around production platforms, do not induce environmental signals of anything like the magnitude of oil spills, these chronic environmental perturbations and the biological exposures continue to operate over long periods of time and over wide areas of the shelf. Consequently, they can induce substantial ecological change (Gray et al. 1990; Lissner et al. 1991; Osenberg et al. 1992; Olsgard and Gray 1995). Reviews of the environmental and ecological impacts of offshore oil and gas development (NRC 1975, 1985; Boesch and Rabalais 1987; Kingston 1992) have identified the filling of this information gap as the most important research priority to improve public decision making on proposals to develop additional hydrocarbon resources on the continental shelf.

Any study of the biological consequences of a long-term history of hydrocarbon production on the continental shelf must recognize certain important discontinuities in the system that influence the results and affect their interpretation. Contaminants of possible concern are released into the liquid medium, the seawater, but are rapidly sorted by their specific gravity and chemical properties into those that deposit onto the seafloor and those that remain in water. Contaminants remaining in water possess intrinsically broad spatial scales of many kilometres, consistent with the transport dynamics of the medium. However, the dilution associated with mixing processes in water produces a rapidly diffused environmental signal with short temporal persistence. In contrast, those contaminants deposited onto the seafloor have short spatial scales of up to a few kilometres but long temporal persistence, as dictated by the much slower rates of transport and mixing of the solid medium. Similarly, the organisms that may be affected by exposure to contaminants possess broadly discordant spatial and temporal scales. Benthic invertebrates living in sediments are largely sedentary and exhibit relatively short life times, especially the meiofauna with characteristic scales of weeks to months. Larger pelagic invertebrates and fishes exhibit much less site fidelity on scales relevant to hydrocarbon platform effects, yet live long enough (on scales of years) to exhibit possible responses to chronic exposures. Thus, the environmental and biological discontinuities have important implications for design of any study of impacts and interpretation of any observed responses.

GOOMEX (the Gulf of Mexico Offshore Operations Monitoring Experiment) is a research project designed to begin assessment of the major environmental effects and ecological consequences of the joint set of processes associated with a long-term (decades) history of drilling and gas production in the Gulf of Mexico (Kennicutt et al. 1996*a*). Three active gas production platforms off the Texas Gulf of Mexico coast with long histories of drilling activity, ending 6–12 yr prior to study, were sampled in a radial design extending from <50 to 3000 m away from the platform to assess long-term impacts on environmental variables and biotic responses. A suite of environmental parameters in the sediments covaried as a function of distance from platforms: sand, hydrocarbons, metals, and inorganic carbon were all elevated out to a distance of 100–200 m. Gradients were steepest at the deepest (125 m) and most diffuse at the shallowest platform (29 m), where physical transport processes were most intense. Evidence of localized organic enrichment appeared in the form of development of summer hypoxia and nutrient release in bottom waters around shallower platforms, but otherwise, water samples showed no detectable signals of platform presence.

Analyses of biological variables showed that benthic meio- and macroinfaunal samples from boxcores provided several sensitive indicators of environmental change whereas physiological analyses of 16 fishes and five mobile invertebrates did not reveal detectable responses (EROD, AHH detoxification enzymes, biliary PAH metabolites, P4501A induction). Densities of harpacticoid copepods and total meiofauna were depressed around two platforms whereas densities of nonselective deposit-feeding nematodes tended to be enhanced. Amphipod densities were depressed near all platforms, but densities of polychaetous annelids and total macroinfauna were greatly enhanced around two platforms.

In this paper, we first present an original synthetic review of how benthic communities respond to pollution in ways that may allow discrimination among multiple causes. We then synthesize the results of GOOMEX Phase I in light of this review to interpret GOOMEX patterns. Finally, we compare GOOMEX results with analogous previously published data on impacts of offshore oil and gas exploration and production activities, showing how the scope of biological impacts of long-term exposures derived from gas production platforms in the Gulf of Mexico is small relative to impacts in the North Sea where oil-based drilling muds were employed.

© 1996 NRC Canada

Use of benthic biological responses to separate effects of confounded physical forcing variables

Confounding of environmental variables

Covariance in multiple environmental variables is typical of most anthropogenic discharges into marine environments (Pearson and Rosenberg 1978). When several environmental variables are confounded in their patterns of distribution, it becomes difficult to identify which factor, factors, or interaction of factors is responsible for observed biological responses. If the suite of environmental variables associated with a particular anthropogenic activity were always confounded in the same way and to the same degree, then there would be little practical motivation to tease apart their effects. If, on the other hand, various management alternatives could influence some factors independent of others, then understanding causation would be in the interest of effective management. The possibility of independently controlling environmental variables and their deleterious effects exists for the management of the complex of operations associated with offshore production platforms. For example, Olsgard and Gray (1995) suggested that use of oil-based drilling muds greatly expands the spatial scale of contamination and biological effects, as compared with water-based muds. Obvious potential for improved management motivates us to provide a synthetic overview of the literature on benthic pollution responses to provide tools to help unravel the confounded effects operating at the GOOMEX platform sites.

Confounded environmental variables in anthropogenic discharges into marine environments characteristically include two separate classes of variables, organic enrichment and toxicants. For example, the discharge of treated sewage typically includes both labile organic matter and also heavy metals, as in the Los Angeles County discharge of treated municipal wastewater off Palos Verdes (Swartz et al. 1986) and in a classic study of the Firth of Clyde in Scotland (Pearson 1987). In the North Sea platform studies, sediments near the platforms were organically enriched and also had elevated total hydrocarbon and metals concentrations (Gray et al. 1990; Olsgard and Gray 1995). This dual character of petroleum hydrocarbon releases is evident in virtually every study of environmental effects of oil spills and of natural petroleum seeps (e.g., Spies and DesMarais 1983; Braddock et al. 1995). Even in cases of pure organic enrichment, if fluxes of organic matter are too great, so as to overload the aerobic degradation capacity of the microbes, creation of toxic chemicals, especially H_2S, and oxygen depletion produce a toxic component to the local environmental change. Teasing apart the contributions of organic enrichment and of toxicity becomes perhaps the central task of evaluating the causes of biological responses to release of petroleum and other discharges to the marine environment (e.g., Spies et al. 1988; Agard et al. 1993).

Synthetic model of benthic biotic response to contamination

The current status of our understanding of benthic community response to pollution incorporates an implicit but as yet unarticulated recognition of the duality of potential effects of pollution. It is becoming evident that, even though individual species within a higher taxon can vary greatly in their sensitivity to environmental change, benthic biological responses to contamination are detectable at higher taxonomic levels. For macrofauna, detection of impacts is possible at the level of the phylum (Warwick 1988*a*, 1988*b*), and at least in some cases, phyletic analysis provides superior discrimination (Agard et al. 1993; Warwick and Clarke 1993). The ability of higher taxonomic levels to detect impacts of pollution is also evident for the meiofauna, although it may apply here to families (Heip et al. 1988) better than to phyla (see, however, Raffaelli and Mason 1981).

We propose that the biological basis for this dual response to pollution rests upon intrinsic physiological and ecological differences among higher taxa. Echinoderms and crustaceans, especially amphipods and some harpacticoid copepods, are highly sensitive to toxic chemicals in their environment. It is by design that the standard United States EPA biotoxicity tests for benthic invertebrates involve an echinoderm (sea urchin reproductive stages) and an amphipod (*Rhepoxinius*) so that testing uses the most sensitive indicators of pollution toxicity. In analyses of community responses to marine pollution that involve toxicity, echinoderms and crustaceans, at least amphipods and some groups of harpacticoids, typically show large declines. In contrast, polychaetes, oligochaetes, and nematodes are not especially sensitive to toxic chemicals and also include species with opportunistic life histories and appropriate feeding types (especially nonselective deposit feeders) that render them capable of utilizing organic materials in organic pollution. Consequently, polychaetes, oligochaetes, and nematodes (at least nonselective deposit feeders) typically show substantial increases under organic pollution. It is this dual effect of organic pollution upon different groups of benthic meiofauna and macrofauna that makes the ordination techniques of benthic community analysis so effective in discriminating the effects of that pollution at higher levels of taxonomic classification, including the phylum level for macrofauna (Warwick and Clarke 1993).

The evidence to support this synthetic model of benthic biological response to pollution in the marine environment comes from review of an extensive suite of studies of marine pollution. It is extremely difficult to find studies of benthic community response to pollution where the only environmental variable influencing biological patterns is toxic contamination. Typically, toxicity and organic enrichment covary. Cases in which only one of these usually confounded components of anthropogenic discharges into the marine environment exists would allow clear isolation of the two components and separate assessment of their impacts on the benthos.

Perhaps the most unequivocal example of a well-studied and unconfounded gradient in a marine discharge comes from the study of the effects of the cooling water discharge from the San Onofre Nuclear Generating Station on the shelf of the Southern California Bight (MRC 1989). As seawater is used for cooling and discharged onto the shelf, natural organic detritus is created and discharged in the form of dead phytoplankton, zooplankton, larval fish, and macerated macrophytes. There are no detectable toxic chemical contaminants in the discharge or in the sediments. Also, the organic loading from this detritus does not exceed the capacity of the microbial degradation system. Only slight increases in sediment

© 1996 NRC Canada

organic content and phaeopigment concentration exist in the vicinity of the diffusers, although the increased seston flux is clearly evident. In response to this discharge of detritus and modest organic enrichment of the sediments, increased abundances in virtually all major taxa of macrofauna were detected using rigorous BACI designs (Green 1979; Stewart-Oaten et al. 1986), with effects extending to 3.5–6.7 km downcoast. As is typical even of discharges that confound organic enrichment with toxic chemical additions, the polychaetes and nematodes were enhanced in abundance. But unlike those perturbations that include contaminants, the crustaceans, including amphipods, ostracods, tanaids, and mysids, were also enhanced in abundance. In addition, there was no evidence of depression in abundance of echinoderms, which were uncommon in the system. Although there was little effect of the discharge on benthic biomass, this is likely to be a consequence of the near-field predation by enhanced abundances of most demersal fish species (MRC 1989).

The San Onofre example contrasts sharply with the case of the Los Angeles County outfall at Palos Verdes (Swartz et al. 1986; LACSD 1990). This Los Angeles County wastewater discharge differs from the San Onofre discharge in that not only is there organic enrichment but also an introduction of toxic contaminants, including DDT, PCB's, H_2S, hydrocarbons, and metals. Polychaetous annelids as a higher taxonomic group are enhanced in abundance near the discharge source, with the response driven by several opportunistic, rather nonselective deposit feeders. In this case, which includes toxicity, echinoderms as a group are grossly depressed around the outfall (Tetra Tech 1981; Swartz et al. 1986). Amphipods also decline in abundance near the outfall, determined largely by the loss of the usually dominant species. Meiofaunal community responses were not assessed in this system. Thus, the inclusion of toxic chemicals in the discharge to the shelf of the Southern California Bight does little to affect the positive polychaete response to enrichment as documented nearby at San Onofre where no chemical contamination occurred; nevertheless, the addition of toxics altered the responses of the physiologically sensitive macrofaunal echinoderms and amphipods, which showed greatly reduced rather than enhanced densities. Thus, this contrast of the two discharges serves as a means of demonstrating how dual effects of enrichment and toxicity influence the benthic community response in a way that allows some substantial degree of separation of the effects.

In the case of the Palos Verdes sewage discharge, studies of the fish responses in the early 1970's, when the treatment was minimal, also showed differences from the San Onofre response. In the immediate vicinity of the source, fish abundance was depressed over about 10.5 km^2 whereas an area of 4 km^2 of enhanced fish abundance occurred somewhat farther away (Mearns et al. 1976). The discharge area was an epicenter for fish diseases such as fin rot in Dover sole, rex sole, and calico rockfish, and the fishes showed bioaccumulation of DDT and PCB (Tetra Tech 1981). Unlike the San Onofre case, the fish community was selectively altered, with species that feed on benthic polychaetes and other seafloor invertebrates enhanced in abundance and those feeding more pelagically depressed in abundance (Tetra Tech 1984).

Other examples of the effects of anthropogenic discharges into the marine environment on benthic community biology involve substantial confounding of organic loading and toxic chemical enhancement. Review of these studies is useful in evaluating whether the patterns of polychaete, oligochaete, and nematode enhancement and echinoderm and crustacean depression are general. Even though separate causation cannot be unequivocally ascribed in these cases of confounded environmental forcings, a common pattern should emerge if the model is supportable. Table 1 presents a review of relevant studies from the literature on soft-sediment benthic community response to joint gradients in organic enrichment and toxic chemicals. This overview includes analyses of effects of oil spills, natural petroleum seeps, sewage discharges, and industrial discharges, as well as some experimental mesocosm and field studies. For the macroinfauna, the patterns of enhancement in polychaetous annelids, typically driven by certain non-selective deposit feeders, and of depression in echinoderms and amphipods are compellingly consistent. For the meiofauna, there appears to be more need to analyze different families or trophic groups of both nematodes and harpacticoids separately, but there is also evidence here of general enhancement of nonselective deposit feeders among nematodes and declines in some harpacticoids (as discussed also in Coull and Chandler 1992). One limitation in application of this synthetic model is the difficulty in defining objectively the feeding status for bulk feeders such as most macroinfauna and meiofauna. Development of objective criteria for both trophic group and also opportunistic life history is an important but challenging goal for future refinement of this pollution response model. Nevertheless, applying effective taxonomic criteria for evaluating the macroinfaunal community response does not require any trophic characterization.

Overview of physical environmental transformations and interpretation of biological responses around gas production platforms in GOOMEX

Methods

A summary of how abiotic parameters varied among platforms and around each platform is presented in Table 2, based on results in Kennicutt et al. (1996*b*), where detailed methods also appear. Sampling for sediments and benthic meio- and macroinfauna was conducted during four cruises over two years (January and June in 1993 and 1994) in a radial design around each platform with distances ranging from <50 to 3000 m. Larger invertebrates and demersal fishes were sampled by replicate trawls near and far from each platform. The three platforms were located at varying distances from the Texas Gulf of Mexico coast in water depths of 29, 80, and 125 m. This difference among platforms in water depth led to important distinctions in their physical, chemical, and sedimentological settings. Physical energy at the seafloor decreased with depth across the range occupied by the three platforms, leading to substantial fining of the bottom sediments with increasing water depth. Furthermore, this difference in water depth resulted in differing degrees of seasonality in water properties (temperature, salinity, and dissolved oxygen) at the bottom, with the shallowest platform experiencing the greatest seasonal signals. The complete history of drilling and discharge activity around each platform is

© 1996 NRC Canada

Table 1. Effects of anthropogenic pollution on benthic communities in the marine environment.

Pollution case study	Organic enrichment	Toxic chemicals	Benthos enhanced	Benthos suppressed	Source(s)
			Macroinfauna		
Exxon Valdez oil spill	Yes, with evident stimulation of oil-degrading bacteria	Yes, with elevated PAH's, etc.	Total polychaetes enhanced as well as *Nereis, Nepthys, Polydora,* and *Lucina* in eelgrass beds	Total crustaceans and total echinoderms occasionally show reductions (never increases), while total amphipods declined as well as a crab (*Telmessus*) and a seastar (*Dermasterias*)	Jewett et al. 1994; Braddock et al. 1995
Amoco Cadiz oil spill	Yes	Yes	Total polychaetes enhanced	Total echinoderms and total crustaceans declined, as well as amphipods	Dauvin 1984, 1987; Warwick and Clarke 1993
Florida oil spill	Yes	Yes	Opportunistic, surface deposit-feeding polychaetes increased, especially *Capitella capitata, Mediomastus ambiseta*	Several ampeliscid amphipods declined	Sanders et al. 1972, 1980; Sanders 1978
Irini oil spill	Yes	Yes	Unclear from data available	Amphipods (*Gammarus* spp.) and isopods (*Idotea* spp.) declined	Notini 1978
Arrow oil spill	Yes	Yes	Unclear from data available	An amphipod (*Gammarus oceanicus*) was selectively reduced	Thomas 1978
Esso Essen oil spill	Yes	Yes	Unclear from data available	Amphipods in intertidal and subtidal declined greatly	Stander and Venter 1968
General M.C. Meigs oil spill	Yes	Yes	Unclear from data available	Sea urchin *Strongylocentrotus purpuratus* suffered evident lethal and sublethal impacts	Clarke et al. 1978

© 1996 NRC Canada

Table 1 (*continued*).

Pollution case study	Organic enrichment	Toxic chemicals	Benthos enhanced	Benthos suppressed	Source(s)
Palos Verdes sewage wastewater discharge	Yes, with detectable organic C, N enhancement	Yes, with DDT, PCB, heavy metals, and H_2S elevated	Total polychaetes enhanced, as well as *Tharyx* spp., *Capitella capitata, Mediomastus* spp., *Schistomeringos longicornis*, and *Ophryotrocha* spp.	Total echinoderms reduced as well as ophiuroid *Amphiodia urtica*, sea cucumber *Parastichopus parvimensus*, sea urchin *Lytechinus anamensus*, and seastar *Luidia foliolata*; amphipod *Heterophoxus oculatus* also reduced	Tetra Tech 1981; Swartz et al. 1986; LACSD 1990
San Onofre Nuclear Generating Station cooling water discharge	Yes, with evident organic C and phaeopigment enhancement	No	Total polychaetes, total crustaceans, total amphipods, total molluscs all enhanced	None	MRC 1989
Firth of Clyde sewage sludge disposal	Yes, with organic C and N elevated	Yes, with Cd elevated along with other metals	Total polychaetes enhanced	Total echinoderms, total crustaceans both depressed	Pearson 1978; Clarke and Ainsworth 1993
Swedish pulp mill discharge	Yes	Unclear	Total polychaetes enhanced, especially *Capitella capitata* and other opportunistic deposit feeders	Total echinoderms depressed	Rosenberg 1972
Antarctic sediment contamination around Winter Quarters Bay	Presumably, in that hydrocarbon levels are elevated	Yes, with PCB, hydrocarbons, and heavy metals elevated	In most contaminated areas, *Capitella* and *Ophryotrocha* en-, hanced, while in modest contamination, *Tharyx* and *Haploscoloplos* enhanced	Total crustaceans especially amphipods, isopods, tanaids	Lenihan and Oliver 1995
Industrial pollution gradient in fjord near Oslo	Presumably	Yes, heavy metal concentrations elevated	Deposit-feeding polychaetes may be elevated	Total echinoderm biomass is clearly depressed, especially an echinoid	Gray et al. 1988
Gradient in oil-based drilling muds around production	Possibly, although modest	Yes, with TPH and heavy metal concentrations elevated	Group of polychaetes was enhanced at severely polluted	Echinoderm *Amphiura filiformis* plus a diverse suite of species	Gray et al. 1990; Olsgard and Gray 1995

© 1996 NRC Canada

Table 1 (*continued*).

Pollution case study	Organic enrichment	Toxic chemicals	Benthos enhanced	Benthos suppressed	Source(s)
Gradient in oil-based drilling muds around an exploration site	Presumably, in that hydrocarbons were elevated	Yes, with total oil concentrations elevated	Only one species, a polychaete, showed significant enhancement	Dominant echinoderm *Amphiura filiformis* declined and two crustaceans and a molllusc exhibited far-reaching sensitivity	Daan et al. 1990, 1992; Krœncke et al. 1992
Experimental crude oil addition in mesocosm	Probably not because of short-term nature of experiment	Yes	None (time frame too short to test)	Total echinoderms, especially the ophiuroid *Ophiura affinis*, depressed	Gray et al. 1988
Natural oil seep and refinery discharges in Trinidad	Yes, with organic C elevated	Yes, with PAH elevation at seep and refinery and metals elevated at refinery	Total polychaetes enhanced, especially in biomass at the seep	Unclear from data available	Agard et al. 1993
Natural oil seep	Yes, with enhanced microbial production	Yes, with PAH elevation	Oligochaetes and many deposit-feeding polychaetes enhanced	The only abundant echinoderm *Lytechinus pictus* and the only abundant amphipod *Paraphoxus abronius* depressed	Spies et al. 1980
Natural oil seep	Yes: TOC, TON, and nonoil organics all elevated	Yes, with total extractable hydrocarbons elevated; no metals assayed	Only nematodes as a group were enhanced	Amphipods, copepods, and ostracods were eliminated and polychaetes, oligochaetes, bivalves, and cumaceans all greatly depressed	Steichen et al. 1996
Experimental fuel oil addition in mesocosm	Possibly, given 25-wk exposure to oil	Yes	Time frame probably too short to test	Total amphipod abundance declined by 98%	Grassle et al. 1981
Field experiment of crude oil addition to tide pools	Probably not because of short-term nature of experiment	Yes	Time frame too short to test	Negative effects on amphipods, isopods, tanaids	Bonsdorff and Nelson 1981
Meta-analysis of all benthic community data for NE Atlantic	Yes	Yes	Total polychaetes are enhanced	Total echinoderms and total crustaceans are depressed	Warwick and Clarke 1993

© 1996 NRC Canada

Table 1 (*concluded*).

Pollution case study	Organic enrichment	Toxic chemicals	Benthos enhanced	Benthos suppressed	Source(s)
			Meiofauna		
Review of marine pollution events	Yes	Yes	Nematodes are enhanced	Harpacticoid copepods are depressed	Raffaelli and Mason 1981
Raw domestic sewage discharge	Yes	Probable	Copepod/nematode ratio is enhanced by pollution		Vidakovic 1983
Organic enrichment	Yes	No	Copepod/nematode ratio is enhanced with organic enrichment		Gee et al. 1985
Organic enrichment	Yes	Probable	Copepod/nematode ratio is enhanced with organic enrichment		Moore and Pearson 1986
Natural oil seep	Yes, with enhanced microbial production	Yes, with PAH elevation		Nematode/harpacticoid ratio is enhanced with oil addition	Montagna et al. 1987
Review of organic pollution in marine sediments	Yes	Usually yes	Nonselective deposit-feeding nematodes generally enhanced	Some other nematode groups may be depressed	Heip et al. 1985
Industrial pollution gradient in fjord near Oslo	Presumably	Yes, heavy metal concentrations elevated	Total nematodes are enhanced as well as some harpacticoid copepod groups	Unclear from data available	Heip et al. 1988
Meta-analysis of all benthic community data for NE Atlantic	Yes	Yes	Total nematodes are generally enhanced	Harpacticoids, etc., not analyzed	Warwick and Clarke 1993

© 1996 NRC Canada

Table 2. Summary of abiotic environmental variables and biological responses around each platform (MAI-686, MU-A85, and HI-A389) studied in GOOMEX.

Characteristic	MAI-686	MU-A85	HI-A389
		Environmental variables	
Physical attributes[a]			
Water depth	29 m	80 m	125 m
Location	Nearshore	Intermediate	Offshore
Energy setting	High	Medium–low	Low
Seasonality of bottom environment	High	Medium	Low
Shunting depth	Near surface	Near bottom	Near bottom
Time since last drilling	12 yr	7 yr	6 yr
Physicochemical[a]			
(ranges given for 3000 m to 100–50 m distances)			
Oxygen levels in bottom waters	Seasonal hypoxia near platform	Seasonal hypoxia near platform	Oxycline impingement
Organic carbon decrease	Yes (from 0.79 to 0.35–0.42%)	Yes (from 0.93 to 0.55–0.62%)	Maybe (from 1.4 to 1.0–1.1%)
Inorganic carbon enrichment	Yes (from 0.19 to 0.31–0.36%)	Yes (from 0.77 to 0.86–1.0%)	Maybe (from 1.62 to 1.96–2.66%)
Contaminants[a]			
(from 3000 to within 50–100 m the platform)			
Hydrocarbons	Low (e.g., averaged 50 ppb PAH)	Low–medium (e.g., from 27 to 126–181 ppb PAH)	Medium (e.g., from 32 to 103–256 ppb PAH)
Trace metals	Low (e.g., from 0.05 to 0.09–0.13 ppm Cd)	Medium (e.g., from 0.05 to 0.25–0.46 ppm Cd)	High (e.g., from 0.08 to 0.65–6.4 ppm Cd)
Sand content	High (from 27 to 60 to >73%)	High (from <12 to 55–67%)	High (from <4 to 33–40%)
		Biological responses	
Macroinfauna[b]			
Abundance	Little change	Higher by 70% near-field	Higher by a factor of 2–4 near-field
Polychaete abundance	Little change	Higher by 90% near-field	Higher by a factor of 3–5 near-field
Amphipod abundance	Lower by a factor of 4–12 near-field	Lower by a factor of 4–5 near-field	Lower by a factor of 3–5 near-field
Ratio of polychaetes/amphipods	6–10 times higher near-field	8–10 times higher near-field	20–30 times higher near-field
Meiofauna[b]			
Density	Higher by a factor of 2–3 far-field	Slightly higher far-field, but directionally dependent	50% higher near-field
Nematode abundance	Lower by a factor of 2 near-field	Lower by a factor of 2 near-field	60–80% higher near-field
Harpacticoid abundance	Lower by a factor of 2 near-field	Little change	Lower by a factor of 3 near-field
Ratio of nematodes/harpacticoids	Little change	Little change	4–5 times higher near-field
Life history: gravid females	3 times higher near-field	No difference between near and far field	3 times higher near-field

© 1996 NRC Canada

Table 2 (*concluded*).

Characteristic	MAI-686	MU-A85	HI-A389
Life history: clutch volume	Higher far-field	Higher far-field	Higher near-field
Life history: clutch size	No difference between near and far field	Higher far-field	Higher far-field
Harpacticoid genetic variability	2 times higher far-field	1.5 times higher far-field	2.3 times higher far-field
Megafaunal invertebrates[c]			
Catch per unit effort	Significant differences, but complex distribution among species	Significant differences, but complex distribution among species	Higher near-field (but few differences)
Size-frequency distribution	Significant differences, but complex distribution among species	Individuals larger far-field	Individuals larger near-field
Histopathology	Significant differences, but complex distribution among species	Intensity higher near-field	Few differences
Sex ratios	Significant differences, but complex distribution among species	Significant differences, but complex distribution among species	Females more abundant near-field
Porewater toxicity[d]	Toxicity detected near-field	No difference between near and far field	Toxicity detected near-field
Biomarkers of aromatic hydrocarbon exposure[e]			
Invertebrates (5 species)	Low AHH activity	Low AHH activity	Low AHH activity
Fish (16 species)			
EROD activity	Low and no response to distance	Low and no response to distance	Low and no response to distance
PAH metabolites in bile	No response to distance	No response to distance	No response to distance
P4501A mRNA	No response to distance	No response to distance	No response to distance

[a]From Kennicutt et al. (1996*b*).
[b]From Montaga and Harper (1996).
[c]From Ellis et al. (1996).
[d]From Carr et al. (1996).
[e]From McDonald et al. (1996).

© 1996 NRC Canada

unavailable, but certain clear distinctions exist (Kennicutt et al. 1996*a*). Shunting of drilling muds and cuttings occurred with near-surface discharge at the shallowest platform and near-bottom discharge at the two deeper platforms. The time since the last drilling varied somewhat among platforms from 6 to 12 yrs before sampling. Platforms were still in production at the time of sampling.

Effects on environmental variables

The physicochemical environment was clearly influenced by the presence of and/or activities associated with the platforms (Table 2). In the GOOMEX Phase I data set, as in previous analyses of effects of anthropogenic discharges in the marine environment (e.g., Pearson and Rosenberg 1978; Gray et al. 1990; Olsgard and Gray 1995), strong covariance exists in the patterns of change in many environmental variables with distance away from the offshore production platforms. From knowledge of what are likely to be the most important forcing variables for biological responses, we identify four major types of environmental variables that show strong but confounded responses to distance along this gradient. Sands, hydrocarbons, metals, and organic inputs were all elevated near platforms (Table 2). The form of this covariance between coarse-grained sediments and organic and inorganic pollutants is highly unusual because contaminants typically bind to and become associated with fine-grained particles.

First, sand-sized particles were greatly enriched around all platforms, as a consequence of both discharge of drill cuttings and sand-cleaning of the structure. Sands increased from a background of about 30% to 70% at the shallow platform MAI-686, from about 10% to 65% at the intermediate platform MU-A85, and from about 5% to 40% at the deepest platform HI-A389. The proportion of fine sediments decreased along this gradient of increased sand content towards platforms.

Second, hydrocarbons (PAH's, AH's, and UCM) were also modestly enhanced near platforms, but this increase was strong only at the deepest platform in the low-energy setting. Detectable contamination extended to 100–200 m, although not symetrically in every direction. Even at HI-A389 where the pattern was strong, hydrocarbon concentrations were relatively low, with PAH levels well below established biological effects thresholds and their composition reflected substantial degradation. In general, the distribution of hydrocarbons remained constant across cruises. Only in isolated pockets at the shallowest platform were recent sources of hydrocarbon release evident, perhaps coming from a seep or pipe leakage.

Third, metal concentrations (Ag, Ba, Cd, Hg, Pb, and Zn especially) increased out to 100–200 m around platforms, with the intensity of the pattern varying directly with platform depth. Trace metals concentrations in the near field exceeded levels known to cause biological effects in many locations. Concentrations of heavy metals in pore waters, although not well correlated with solid-phase concentrations probably because of porewater sampling constraints, were also elevated at certain sampling sites to a maximum distance of 100 m. Most heavy metals showed strong correlations with Ba, although Pb, Zn, and Cd were shown also to be accumulating from some source after initial release of cuttings, perhaps from produced waters (Kennicutt et al. 1996*b*).

Fourth, although little change was detectable in ambient water properties with increasing proximity to platforms (Kennicutt et al. 1996*b*), oxygen depression and enhancement of some nutrients (silicate, phosphate, and/or nitrate) in bottom waters around the shallower platforms indicate organic enrichment and enhanced benthic decomposition processes. Hypoxia developed in the vicinity of the shallowest platform MAI-686 in summer and enhanced nutrient levels were detectable in bottom waters. A suggestion of this same response appeared around the platform at intermediate depth but not at the deepest platform. Inorganic carbon was enhanced in sediments near the platforms, reflecting results of past discharge of cuttings through carbonate-bearing strata and a rain of biogenic shell and test debris from benthic animals occupying the platform. The percent organic carbon in surface sediments actually declined in the near field but not in proportion to the degree of dilution by sands, implying possible organic enrichment.

Biological responses

The major patterns in biological responses (Table 2) resulting from the suite of environmental gradients at the gas production platforms studied in GOOMEX can be interpreted largely as consequences of two of the four types of environmental forcings, organic enrichment and metals toxicity. The hydrocarbons occur in concentrations that seem too low to be important contributors to the observed toxicological effects. For example, total PAH was generally less than 100 ng/g (Kennicutt et al. 1996*b*), which is an order of magnitude lower than what Spies (1987) suggested is needed to induce biological response. The pattern of increased sand content doubtless affects benthic invertebrates, but the observed trends in benthic abundances run opposite to the usual biotic responses to sediment texture. The emergence in benthic meiofaunal and macroinfaunal communities of patterns that are broadly consistent with other documented responses to organic enrichment and sediment toxicity, despite the sediment size gradient, leads us to conclude that the sediment grain size pattern is unlikely to be the primary driver of the observed biological responses.

The macroinfaunal community data reveal a pattern of change with distance from the platforms (Table 2) that is consistent with earlier studies of low-level organic and chemical discharges to the marine environment (Table 1). Detailed data and statistical test results for the benthic macro- and meiofauna appear in Montagna and Harper (1996). Total macroinfaunal densities were enhanced at 50- and somewhat to 100-m distances at two platforms (Table 2), as a consequence of the enhanced abundances of polychaetous and oligochaetous annelids (Table 3). This pattern was absent at the shallowest site, MAI-686, where the relatively high-energy physical environment has led to more extensive dispersion of materials discharged from this platform. Species contributing most to polychaete enhancement were two *Cirratulus* and one *Cirriformia* species at HI-A389 and a *Spiophanes*, *Paramphinome*, and *Golfingia* species at MU-A85. Enhancement of polychaete and oligochaete abundances is typical in cases of modest organic pollution in marine sediments and is probably a consequence of organic enrichment in accord with the synthetic model of causation. Physical disturbance in the form of particulate deposition (see Gray 1982) also may contribute to enhancement of annelid densities, but the underlying mecha-

© 1996 NRC Canada

Table 3. Changes with distance (m) from platform in the most diagnostic response variables for meiofauna and macrofauna.

Platform MAI-686

Distance	500	50	100	200	3000
Polychaetes	710	689	630	625	589
Distance	500	3000	200	50	100
Amphipods	156	130	74	34	13
Distance	100	50	200	500	3000
Ratio of polychaetes/amphipods	48	20	8.4	4.6	4.5
Distance	500	3000	200	50	100
Nonselective deposit-feeding (nsdf) nematodes	469	438	425	398	342
Distance	3000	500	200	100	50
Harpacticoid copepods	449	402	297	205	164
Distance	50	100	200	500	3000
Ratio of nsdf nematodes/copepods	2.43	1.67	1.43	1.17	0.98

Platform MU-A85

Distance	50	100	200	500	3000
Polychaetes	812	802	566	436	419
Distance	3000	200	500	100	50
Amphipods	60	55	53	45	12
Distance	50	100	200	500	3000
Ratio of polychaetes/amphipods	67.7	17.8	10.3	8.2	7.0
Distance	200	100	50	500	3000
nsdf nematodes	178	141	140	136	74
Distance	100	50	500	100	3000
Harpacticoid copepods	212	167	166	162	156
Distance	200	50	500	200	3000
Ratio of nsdf nematodes/copepods	1.10	0.84	0.82	0.67	0.47

Platform HI-A389

Distance	50	100	200	500	3000
Polychaetes	1807	1015	504	281	243
Distance	500	200	3000	50	100
Amphipods	30	23	22	6	5
Distance	50	100	200	3000	500
Ratio of polychaetes/amphipods	301	203	21.9	11.1	9.4
Distance	50	100	200	500	3000
nsdf nematodes	160	145	140	124	87
Distance	3000	500	200	100	50
Harpacticoid copepods	119	118	104	97	34
Distance	50	100	200	500	3000
Ratio of nsdf nematodes/copepods	4.71	1.49	1.35	1.05	0.79

Note: Densities of meiofauna are per 10 cm^2 and of macrofauna are per 1 m^2. Means connected by underlining are not significantly different at $\alpha = 0.05$ in a Tukey multiple comparison test following ANOVA.[a] Where no underlining exists, Tukey's test is invalid because of significant interactions.

[a]Data results from Montagna and Harper (1996).

© 1996 NRC Canada

nism for such responses seems likely to be opportunistic utilization of newly provided organic resources and thus just a different form of organic enrichment. Furthermore, since the vast majority of the particulate deposition ceased several years before our GOOMEX study, disturbance from deposition seems unlikely to be an important driving factor in explaining GOOMEX results.

The increase in annelid abundance occurred despite the steep gradient in sand content in the sediments: total annelids would probably be expected to be more abundant in finer sediments, not in coarser ones, over this range of sediment grades. In contrast with the polychaetes and oligochaetes, amphipod abundances were depressed around all platforms, with effects confined to 50 or 100 m (Table 3). The amphipod decline was driven largely by the response of ampeliscid species. The effect on amphipods is also consistent with the literature on modest pollution in the marine environment, and is suggestive of a toxic response. The ratio of polychaete to amphipod abundances proved to be an especially responsive indicator of biological reponse (Table 3). The trawl sampling included one echinoderm with sufficient abundance for analysis at each platform. At the shallowest site (MAI-686), that echinodern, the seastar *Astropecten duplicatus*, was a statistically significant 6–20 times more abundant at far stations (Ellis et al. 1996). At the two deeper sites, the congener *A. cingulatus* was 2–3 times more abundant in the far field, but differences were not significant for this species that was an order of magnitude less abundant than its congener at the shallow site. These echinoderm patterns are therefore consistent with a possible source of toxicity near platforms, as predicted by the synthetic model for this sensitive phylum. On the other hand, ophiuroids from core sampling failed to reveal any significant pattern with distance from platforms at any site (Montagna and Harper 1996).

Meiofaunal community responses to the presence of platforms and the environmental gradients that emanate from them (Tables 2 and 3) are also generally consistent with patterns of response observed in cases of modest organic and chemical pollution in the marine environment (see Coull and Chandler 1992). The abundance of total nematodes was enhanced at 50 and 100 m by 60–80% at the platform with the steepest environmental gradient, HI-A389, but at the shallower sites nematode abundance was depressed in the near field (Table 2). The nonselective deposit-feeding nematodes showed patterns of enhancement close to two of the platforms (Table 3). Thus, the nonselective deposit-feeding nematodes may represent a more responsive indicator of modest organic enrichment. Physical disturbance in the form of historical particulate deposition may play an important role in provision of organic resources for opportunistic nematodes. The response of nematodes and especially of nonselective deposit-feeding nematodes runs opposite to that predicted on the basis of the sediment texture gradient: nematodes and this particular trophic group of nematodes typically increase as sediments become finer in size (e.g., Coull and Chandler 1992). Consequently, the tendency for enhancement in nonselective deposit-feeding nematodes near the platform runs against expectation based on sediment character.

Total harpacticoid copepods reveal a large depression near two of the platforms, with abundance close to the platform only about 40% on average of that in the distant stations (Table 3). This effect is most intense at the HI-A389 site, where the contaminant gradient is steepest. This pattern too is consistent with the results of previous studies showing frequent sensitivity of harpacticoid copepods to toxic chemicals. As a consequence of joint and opposing responses, the ratio of nonselective deposit-feeding nematodes to copepods provided an effective discriminator among distances from the platforms (Table 3). This pattern in the nematode to copepod ratio, exhitied at all three platforms to some degree, is consistent with the original suggestion of Raffaelli and Mason (1981) that the nematode to copepod ratio responds strongly to pollutant exposure. Several studies have debated the utility of this ratio, but Raffaelli (1987) and Coull and Chandler's (1992) review suggested that there is merit to this approach provided key covariates such as sedimentology are controlled. Our results suggest that the modification of this index achieved by restricting nematodes to those in the nonselective deposit-feeding group may provide a more sensitive and interpretable response.

Attribution of the similar responses of the two different groups of crustaceans, amphipods and harpacticoid copepods, to toxicological causes is supported by the results of porewater toxicity testing (Carr et al. 1996). Toxicity tests on percent normal development and percent fertilization of sea urchins (*Arbacia punctulata*), an echinoderm, revealed a pattern of biotoxicity similar to the pattern of chemical contamination at the study sites. The embryological development test proved more sensitive than the fertilization test, with all cases of significant toxicity in the fertilization test corresponding to significances in the development test. The toxicity results reveal that, with one exception, all cases of significance came from stations within 100 m of a platform. The most compelling pattern of toxicity is derived from the most contaminated site, HI-A389, where several sites within 50 m showed significant toxicity in the sea urchin development test during two independent samplings. Examination of porewater concentrations of contaminants in these samples suggested that the observed toxicity was most likely a consequence of metals. Concentrations of several metals in sediments at these stations approached or exceeded the published probable biological effects levels (Long and Morgan 1990). Results of a novel set of toxicity tests using naupliar survival of the harpacticoid copepod *Longipedia americana* and egg production for the meiofaunal polychaete *Dinophilus gyrociliatus* provide further evidence of toxicity close to the platform (Carr et al. 1996). Both of these species proved less sensitive than the sea urchin to sediment toxicity, but stations that proved toxic to either of these meiofauna were also toxic in the sea urchin development tests. These toxicity test results, therefore, confirm the toxicity of sediments close to the platforms, especially at HI-A389. Furthermore, the toxicity was demonstrated using not only a standard test species but also species indigenous to the study region. The demonstrated toxicologic effects on the test harpacticoid provide support for the inference that the pattern of depressed abundances of harpacticoids near the platforms is indeed a response to the toxicity of sediments rather than a response to changing sediment sizes or other characteristics that also differ near platforms.

A further joint analysis of (1) the sediment contaminant data, (2) the biotoxicity results, and (3) both the macroinfauna

© 1996 NRC Canada

and meiofauna community data sets employed the sediment quality triad approach (Long and Chapman 1985) to integrate these potentially related data sets. The resulting set of multivariate analyses provides formal statistical tests that support the interpretations presented here (Green and Montagna 1996). The first axis from a PCA run on the sedimentary environmental data was used for these correlations. That axis represented the linear combinations and weightings of confounded contaminants and captured differences among distances from the platforms. For both the meiofauna and the macroinfauna, the variable chosen was again the one from a PCA that separated stations: this was driven by increases towards the platforms in polychaetes and decreases in amphipods for the macroinfauna, and increases towards the platforms in nonselective deposit-feeding nematodes and decreases in harpacticoids for the meiofauna. For the biotoxicity data, there was no need for multivariate techniques to reduce the dimensionality of the data set because only a single variable, sea urchin development success, was available across all stations and thus suitable for analysis. Cross-correlations between all pairs of sediment, biotoxicology, and benthic community variables produced close relationships. Where sediment was most contaminated, the highest levels of toxicity were demonstrated, and the community compositions were altered most in favor of polychaetes relative to amphipods and of non-selective deposit-feeding nematodes relative to harpacticoids (Green and Montagna 1996). The use of macroinfaunal and meiofaunal community data represents somewhat of a replication of the test for relationships: each revealed a similarly strong set of cross-correlations with both sediment contamination and biotoxicity. These interrelationships in accordance with the sediment quality triad approach imply that toxic impacts are likely to be involved to some degree in driving community patterns around platforms. Nevertheless, the confounding of environmental variables in the distance gradient around platforms means that there are several possible explanations for the high levels of cross-correlations and that toxicity is only one possible driver of these relationships.

Various physiological and genetic results provide further evidence that crustaceans around the platforms are exhibiting sublethal responses to contaminant exposure (Montagna and Harper 1996). In the pooled data set for all harpacticoid copepods, the percentage of gravid females was greater and the percentage of juveniles was reduced in the 50-m stations around platforms. In addition, reproductive effort (egg numbers times egg sizes) for those female harpacticoids carrying eggs was reduced within 50 m of the platforms. These responses could be explained as sublethal physiological reactions of these species of crustaceans to modest levels of stress from exposure to toxicants. The demonstration in multiple species of harpacticoid copepods that genetic diversity is significantly reduced near the platforms as compared with the far-field sites also suggests detection of a sublethal response of these sensitive organisms to some aspect of the platform-associated environment.

Although the trawl sampling component of GOOMEX was not designed to measure how fish and benthic megainvertebrates varied in abundance with distance to platform, the quantitative catch per unit effort data from the trawls could still provide some indication of large abundance differences, if they existed (Ellis et al. 1996). This question has importance for interpretation of the benthic community responses. Abundances of benthic animals can be driven by top-down differences in predation pressure as well as by bottom-up differences in food supply and by toxicity. There is little evidence of substantial differences between near- and far-fields in abundance of large invertebrates captured by trawls (Ellis et al. 1996). There may be enhancement of some fishes near the platforms, as indicated by the trawl results. Enhancement of those species that utilize the hard subtrate "reef" habitat would be expected; however, bottom trawling does not represent an effective method of quantifying abundance for most of these species, either because they are too large and can avoid the net (pelagic predators like king mackerel) or because they are too closely associated with the reef structure to be properly sampled (sheepshead, snappers, and pinfish). A more accurate and complete census of fish species that utilize the platform structure as habitat would almost certainly have revealed tremendously enhanced abundances. Analysis of gut contents in small fishes showed no detectable difference in dietary composition or in gut fullness between near and far stations (Kennicutt 1995, *cited in* Montagna and Harper 1996). Nevertheless, the possible increase in fish abundance in the near field around platforms may indicate somewhat greater predation pressure, at least on macroinfauna, near the platforms. From the analogy with other studies of ecosystem response to organic enrichment, especially the San Onofre power plant study (MRC 1989) and the Los Angeles County sewage outfall study (Tetra Tech 1981, 1984), it seems more likely that enhanced demersal fish abundance occurs in response to food abundance rather than serving as a driver of benthic abundance patterns. If this were also true for the GOOMEX sites, then increased polychaete abundances in the near-field may be contributing to some increase in demersal fish. Nevertheless, the GOOMEX program cannot at present confidently evaluate the degree to which platform effects propagate through the food chain to influence populations of higher-level consumers.

Results from GOOMEX analyses do speak clearly to the question of whether the hydrocarbon contamination has detectable negative sublethal impacts on fishes (McDonald et al. 1996). No differences existed between near and far fields in P450IA activities in livers of fishes or larger invertebrates. Measurement of PAH metabolites in fish bile similarly failed to reveal evidence of any differential exposure to PAH's between the near and far stations. Measurements of P450IA mRNA also failed to show any differential exposure to hydrocarbons as a function of distance from the platforms. The absence of evidence of hydrocarbon exposure and any physiological response in fishes may be a consequence of the intrinsic mobility of fishes. The fishes targeted by trawling for these physiological measurements generally move readily across the short contaminant gradients at the study sites, thus minimizing exposure.

Contrasts of hydrocarbon concentrations and of P450IA induction levels between the GOOMEX sites and other previous studies show that GOOMEX resembles an uncontaminated site (McDonald et al. 1996). Where P450IA induction has been demonstrated around natural petroleum seeps (Spies et al. 1982) and around oil production platforms in the North Sea (Davies et al. 1984), the PAH concentrations in the

© 1996 NRC Canada

sediments are greatly in excess of those documented in GOOMEX. Based on review of these and other available studies, McDonald et al. (1996, table 4) conclude that sediment concentrations of PAH ranging from 3000 to 10 000 ng/g appear to be required before significant hepatic EROD activity is induced in fish. In that review, there was a significant relationship between total PAH levels in sediments and hepatic EROD activities. However, mean total PAH concentration in sediments in GOOMEX sites ranged from 21 to 428 ng/g, with most values <100 ng/g (McDonald et al. 1996). Consequently, even the early warning signals of potential sublethal toxicological response to hydrocarbon exposure are absent from the fishes caught by trawl sampling around long-standing gas production platforms in the Gulf of Mexico.

Contrast of GOOMEX results with previous studies of effects of oil and gas production activities

Analysis of data on biological responses to contamination at GOOMEX sites agrees well with results of previous analyses of effects of marine pollution in demonstrating the utility of the soft-sediment benthos as an indicator of biological response (Gray et al. 1990; Warwick 1993; Olsgard and Gray 1995). The sedentary nature of the benthos, the diversity of species within the benthos, each capable of different types of response to different contaminants, the direct contact of the benthos with the sediments, which are the repository for contaminants, and the ability of the benthos to integrate signals over relatively long periods of time all contribute to making the benthic invertebrates a superb template for environmental impact assessments. Furthermore, results of GOOMEX support the conclusions of analogous recent studies in showing that multivariate analyses of community composition represent the most sensitive method of detecting response. In the GOOMEX program, PCA on the macrofaunal and on the meiofaunal communities revealed effects extending to distances of 100–200 m from the gas production platforms, while other alternative response variables such as diversity measures had poor resolution of effects (Montagna and Harper 1996). This same demonstration of the power of multivariate community analyses appears in recent application of MDS by Gray et al. (1990) and Clarke (1993).

The question of whether community analyses of the benthos can be as successfully conducted at the family level as at the species level is not unambiguously answered. Most GOOMEX analyses show ability to detect biological response with both family-level and species-level data, although the species generally appear to provide more sensitivity (Montagna and Harper 1996). Recent work by Warwick (1988*a*, 1988*b*) and Warwick and Clarke (1993) has shown little or no reduction in resolving power by going from species to cruder levels of taxonomic distinction in using the benthos to assess environmental impacts.

Although Warwick and Clarke (1993) showed through meta-analysis of multiple studies of benthic community response to marine pollution that phyletic differences in response underlie the ability of multivariate analysis to achieve such successful and remarkable discrimination, we suggest here that the multivariate responses contain two different groups of higher taxa responding to two different components of contamination. In other words, we attempt to pose causal hypotheses for the general benthic biological response patterns that can achieve the goal of separating effects of confounded factors. In specific, it appears that echinoderm, amphipod, and harpacticoid copepods may react mostly to toxicity, while polychaetes, oligochaetes, and nonselective deposit-feeding nematodes react largely to organic enrichment (or enhanced resource availability following disturbance, which we view as invoking the same opportunistic response). This suggested means of isolating different causal mechanisms represents an important need in pollution study (NRC 1985; Agard et al. 1993) and should be viewed as an hypothesis to be tested experimentally.

One of the most interesting concerns about oil and gas production activities is how widespread biological effects range from the source, the well site. The tremendous improvement in power to detect and discriminate biological effects by development of multivariate community analytic techniques and their application to benthic community data has clarified greatly the extent of pollution effects emanating from drilling platforms (Kingston 1992). Recent analyses in the North Sea show clearly that effects range outwards from platforms to a distance of 2–6 km and beyond (Olsgard and Gray 1995). This same study also demonstrated growing areas of contamination and of biological community response several years after drilling and drill mud disposal had stopped. The scale of these patterns of contamination and pollution effects on the benthos in the North Sea is far larger than what we observed around gas production platforms off the Texas Gulf of Mexico coast. Probably the major difference causing the disparity in spatial scale of impacts is the use of oil-based drilling muds in the North Sea platforms analyzed in Olsgard and Gray (1995). Oil was not used as a lubricant in the Gulf of Mexico platforms that we studied, so this additional source of contamination was not present. Olsgard and Gray (1995) similarly mentioned that an as yet unpublished analysis of North Sea platforms where oil-based driling muds were not employed shows greatly reduced areas of contamination and biological impacts.

Our synthesis of GOOMEX results and past studies of benthic community response to marine pollution suggests that the biological response at the GOOMEX sites is caused jointly by toxic contaminants and organic enrichment. It is important therefore to identify the sources of the significant environmental forcing variables to help inform managers and potentially improve management. To the degree that toxic metals are the primary cause of the toxicity component to the benthic biological responses, one can associate most of this input with the use of barite. The heavy metals that form impurities in barite ore (Ag, Cd, Hg, Pb, and Zn) all covaried strongly with Ba, presumably because they were largely derived from barite deposition (Kennicutt et al. 1996*b*). Lead, Cd, and Zn showed patterns of concentration suggesting some additional source, probably produced waters. Organic enrichment may derive from degradation of hydrocarbons coming from a variety of low-level sources, including produced waters and from materials shed from the platform as an artificial reef. Study of an exploration site in the North Sea where no production platform existed (Daan et al. 1990, 1992; Kroencke et al. 1992) showed almost no enhancement of the opportunistic (largely polychaete) benthos that responded so

© 1996 NRC Canada

strongly in the studies around drilling platforms reported in Gray et al. (1990) and Olsgard and Gray (1995). Daan et al. (1992) suggested that this difference arises from an indirect effect of platforms inhibiting trawl fishing in their vicinity and thus permitting persistence of higher densities of benthic invertebrates. However, the shedding of organic materials from platforms is an alternative explanation, consistent with the GOOMEX observations of near-platform oxygen depression and nutrient release from enhanced benthic respiration (Kennicutt et al. 1996*b*). Organic enrichment better explains why higher densities were constrained to a group of opportunistic polychaetes.

In summary, the heavy metal impurities in barite, the release of produced waters, and the organic shedding from the platforms appear to be the major determinants of biological response patterns that extend to a distance of 100–200 m away from gas production platforms on the Gulf of Mexico shelf. Under this interpretation, the necessary use of additional barite during drilling in the absence of adding a diesel oil lubricant has a cost, but that cost is small relative to the consequences of discharging oil-contaminated drill muds and cuttings. There is a possibility that release of produced waters contributes to observed biological responses, consistent with the studies of Armstrong et al. (1977) and Osenberg et al. (1992). Armstrong et al. (1977) showed effects of produced waters discharge on benthic infaunal composition to extend to 1 km distance in a 2- to 3-m-deep Texas bay. At 10–12 m depth in an offshore site of produced water discharge in California, Osenberg et al. (1992) showed effects on benthic community composition reaching only about 100 m. We cannot separate possible effects of produced waters in the GOOMEX study from physical effects of the platform and other discharges. Future research should be designed to decouple effects of platform presence from effects of materials discharges to isolate contributions of the artifical reef effect and to tease apart the now confounded effects of multiple types of discharges.

Acknowledgements

This research was supported by the Minerals Management Service of the U.S. Department of the Interior through the Gulf of Mexico OCS Regional Office in New Orleans under contract No. 14-35-0001-30582, as GOOMEX Phase I. T. Ahlfield, J. Kendall, and J. McHugh are recognized for their support. Reviews by T. Suchanek and R. Warwick improved the paper.

References

Agard, J.B.R., Gobin, J., and Warwick, R.M. 1993. Analysis of marine macrobenthic community structure in relation to pollution, natural oil seepage and seasonal disturbance in a tropical environment (Trinidad, West Indies). Mar. Ecol. Prog. Ser. **92**: 233–243.

Armstrong, H.W., Fucik, K., Anderson, J.W., and Neff, J.M. 1977. Effects of oilfield brine effluent on benthic organisms in Trinity Bay, Texas. API Publ. No. 4291, American Petroleum Institute, Washington, D.C.

Boesch, D.F., and Rabalais, N.N. (*Editors*). 1987. Long-term environmental effects of offshore oil and gas development. Elsevier, New York.

Boesch, D.F., Butler, J.N., Cacchoine, D.A., Geraci, J.R., Neff, J.M., Ray, J.P., and Teal, J.M. 1987. An assessment of the long-term environmental effects of U.S. offshore oil and gas development activities: future research needs. *In* Long-term environmental effects of offshore oil and gas development. *Edited by* D.F. Boesch and N.N. Rabalais. Elsevier, New York. pp. 1–53.

Bonsdorff, E., and Nelson, W.G. 1981. Fate and effects of Ekofisk crude oil in the littoral of a Norwegian fjord. Sarsia, **66**: 231–240.

Braddock, J.F., Lindstrom, J.E., and Brown, E.J. 1995. Distribution of hydrocarbon-degrading microorganisms in sediments from Prince William Sound, Alaska following the *Exxon Valdez* oil spill. Mar. Pollut. Bull. **30**: 125–132.

Capuzzo, J.M. 1987. Biological effects of petroleum hydrocarbons: assessments from experimental results. *In* Long-term environmental effects of offshore oil and gas development. *Edited by* D.F. Boesch and N.N. Rabalais. Elsevier, New York. pp. 343–410.

Carney, R.S. 1987. A review of study designs for the detection of long-term environmental effects of offshore petroleum activities. *In* Long-term environmental effects of offshore oil and gas development. *Edited by* D.F. Boesch and N.N. Rabalais. Elsevier, New York. pp. 651–696.

Carr, R.S., Chapman, D.C., Presley, B.J., Biedenbach, J.M., Robertson, L., Boothe, P., Kilada, R., Wade, T., and Montagna, P. 1996. Sediment porewater toxicity assessment studies in the vicinity of offshore oil and gas production platforms in the Gulf of Mexico. Can. J. Fish. Aquat. Sci. **53**. This issue.

Clarke, K.R. 1993. Non-parametric multivariate analyses of changes in community structure. Aust. J. Ecol. **18**: 117–143.

Clarke, K.R., and Ainsworth, M. 1993. A method of linking multivariate community structure to environmental variables. Mar. Ecol. Prog. Ser. **92**: 205–219.

Clarke, R.C. Jr., Patten, B.G., and DeNike, E.E. 1978. Observations of a cold-water intertidal community after 5 years of a low-level, persistent oil spill from the *General M.C. Meigs*. J. Fish. Res. Board Can. **35**: 754–765.

Coull, B.C., and Chandler, G.T. 1992. Pollution and meiofauna: field, laboratory, and mesocosm studies. Mar. Biol. Annu. Rev. **30**: 191–271.

Daan, R., Lewis, W.E., and Mulder, M. 1990. Biological effects of discharged oil-contaminated drill cuttings in the North Sea.Boorspoeling III-IV, NIOZ-rapport 1990–5. NIOZ, Texel, The Netherlands.

Daan, R., van het Groenewoud, H., de Jong, S.A., and Mulder, M. 1992. Physico-chemical and biological features of a drilling site in the North Sea, 1 year after discharges of oil-contaminated drill cuttings. Mar. Ecol. Prog. Ser. **91**: 37–45.

Dauvin, J.-C. 1984. Dynamique d'ecosystemes macrobenthiques des fonds sedimentaires de la Baie de Morlaix et leur perturbation par les hydrocarbures de l'Amoco-Cadiz. Ph D. thesis, Université Pierre et Marie Curie, Paris.

Dauvin, J.C. 1987. Evolution a long terme (1978–1986) des populations d'amphipodes des sables fins de la Pierre Noire (Baie de Morlaix, Manch occidentale) apres la catastrophe de l'Amoco Cadiz. Mar. Environ. Res. **21**: 247–273.

Davies, J.M., Bell, J.S., and Houghton, C. 1984. A comparison of the levels of hepatic aryl hydrocarbon hydroxlase in fish caught close to and distant from North Sea oil fields. Mar. Environ. Res. **14**: 23–45.

DOI (Department of the Interior of the United States). 1992. Report from the North Carolina Environmental Sciences Review Panel. U.S. Department of the Interior, Minerals Management Service, Herndon, Va.

Ellis, M.S., Wilson-Ormond, E.A., and Powell, E.N. 1996. Effects of gas-producing platforms on continental shelf macroepifauna in the northwestern Gulf of Mexico: abundance and size structure. Can. J. Fish. Aquat. Sci. **53**. This issue.

Gee, J.M., Warwick, R.M., Schanning, M., Berge, J.A., and Ambrose, W.G. Jr. 1985. Effects of organic enrichment on meio-

© 1996 NRC Canada

faunal abundance and community structure in sublittoral soft sediments. J. Exp. Mar. Biol. Ecol. **91**: 247–262.

Grassle, J.F., Elmgren, R., and Grassle, J.P. 1981. Response of benthic communities in MERL experimental ecosystems to low level, chronic additions of No. 2 fuel oil. Mar. Environ. Res. **4**: 279–297.

Gray, J.S. 1982. Effects of pollutants on marine ecosystems. Neth. J. Mar. Res. **16**: 424–443.

Gray, J.S., Aschan, M., Carr, M.R., Clarke, K.R., Green, R.H., Pearson, R., Rosenberg, T.H., and Warwick, R.M. 1988. Analysis of community attributes of the benthic macrofauna of Frierfjord/Langesundfjord and in a mesocosm experiment. Mar. Ecol. Prog. Ser. **46**: 151–165.

Gray, J.S., Clarke, K.R., Warwick, R.M., and Hobbs, G. 1990. Detection of initial effects of pollution on marine benthos: an example from the Ekofisk and Eldfisk oilfields, North Sea. Mar. Ecol. Prog. Ser. **66**: 285–299.

Green, R.H. 1979. Sampling design and statistical methods for environmental biologists. Wiley, New York.

Green, R.H., and Montagna, P. 1996. Implications for monitoring: study designs and interpretation of results. Can. J. Fish. Aquat. Sci. **53**. This issue.

Heip, C., Vincx, M., and Vranken, G. 1985. The ecology of marine nematodes. Oceanogr. Mar. Biol. Annu. Rev. **23**: 399–489.

Heip, C., Warwick, R.M., Carr, M.R., Herman, P.M.J., Huys, R., Smol, N., and van Holsbeke, K. 1988. Analysis of the community attributes of the benthic meiofauna of Frierfjord/Langesundfjord. Mar. Ecol. Prog. Ser. **46**: 171–180.

Jewett, S.C., Dean, T.A., Smith, R.O., Steckoll, M., Halderson, L.J., Laur, D.A., and McDonald, L. 1994. The effects of the *Exxon Valdez* oil spill on shallow subtidal communities in Prince William Sound, Alaska 1989–93. Draft Final Report of EVOS Study No. 93047, Exxon Valdez Trustee Council, Anchorage, Alaska.

Kennicutt, M.C. II, Green, R.H., Montagna, P., and Roscigno, P.F. 1996*a*. Gulf of Mexico Offshore Operations Monitoring Experiment (GOOMEX), Phase I: Sublethal responses to contaminant exposure — introduction and overview. Can. J. Fish. Aquat. Sci. **53**. This issue.

Kennicutt, M.C. II, Boothe, P.N., Wade, T.L., Sweet, S.T., Rezak, R., Kelly, F.J., Brooks, J.M., Presley, B.J., and Wiesenburg, D.A. 1996*b*. Geochemical patterns in sediments near offshore production platforms. Can. J. Fish. Aquat. Sci. **53**. This issue.

Kingston, P.F. 1992. Impact of offfshore oil production installations on the benthos of the North Sea. ICES J. Mar. Sci. **49**: 45–53.

Kroencke, I., Duineveld, G.C.A., Raak, S., Rachor, E., and Daan, R. 1992. Effects of a former discharge of drill cuttings on the macrofauna community. Mar. Ecol. Prog. Ser. **91**: 277–287.

LACSD (Los Angeles County Sanitation Districts). 1990. Palos Verdes Ocean Monitoring. Annual Report 1990. Los Angeles County Sanitation Districts, Whittier, Calif.

Lenihan, H.S., and Oliver, J.S. 1995. Anthropogenic and natural disturbances to marine benthic communities in Antarctica. Ecol. Appl. **5**: 311–326.

Levin, S.A. 1992. The problem of pattern and scale in ecology. Ecology, **73**: 1943–1967.

Lissner, A.L., Taghon, G.L., Diener, D.R., Schroeter, S.C., and Dixon, J.D. 1991. Recolonization of deep-water hard-substrate communities: potential impacts from oil and gas development. Ecol. Appl. **1**: 258–267.

Long, E.R., and Chapman, P.M. 1985. A sediment quality triad: measures of sediment contamination, toxicity and infaunal community composition in Puget Sound. Mar. Pollut. Bull. **16**: 405–415.

Long, E.R., and Morgan, L.G. 1990. The potential for biological effects of sediment-sorbed contaminants tested in the National Status and Trends Program. NOAA Tech. Memo. NOS OMA 52. U.S. Department of Commerce, National Oceanographic and Atmospheric Administration, Seattle, Wash.

Lubchenco, J., Olson, A.A., Brubaker, L.B., et al. 1991. The sustainable biosphere initiative: an ecological research agenda. Ecology, **72**. 371–412.

McDonald, S.J., Willett, K.L., Thomsen, J., Beatty, K.B., Connor, K., Narasimhan, T.R., Erickson, C.M., and Safe, S.H. 1996. Sublethal detoxification responses to contaminant exposure associated with offshore production platforms. Can. J. Fish. Aquat. Sci. **53**. This issue.

MRC (Marine Review Committee). 1989. Final technical report to the California Coastal Commission. I. Soft bottom benthos. Marine Review Committee, Department of Biological Sciences, University of California, Santa Barbara, Calif.

Mearns, A.J., Allen, M.J., Word, L.S., Word, J.Q., Greene, C.S., Sherwood, M.J., and Meyers, B. 1976. Quantitative responses of demersal fish and benthic invertebrate communities to coastal municipal waste discharges. Final Report to EPA, Grant R801152. Vols. 1 and 2. Southern California Coastal Water Research Project, Long Beach, Calif.

Montagna, P.A., and Harper, D.E. Jr. 1996. Benthic infaunal long-term response to offshore production platforms in the Gulf of Mexico. Can. J. Fish. Aquat. Sci. **53**. This issue.

Montagna, P.A., Bauer, J.E., Toal, J., Hardin, D., and Spies, R.B. 1987. Temporal variability and the relationship between benthic meiofaunal and microbial populations of a natural coastal petroleum seep. J. Mar. Res. **45**: 761–789.

Moore, C.G., and Pearson, T.H. 1986. Response of a marine benthic copepod assemblage to organic enrichment. Proc. 2nd Int. Conf. Cop., Syllogeus Ser. No. 58, National Museums of Canada. pp. 369–373.

Notini, M. 1978. Long-term effects of an oil spill on *Fucus* macrofauna in a small Baltic bay. J. Fish. Res. Board Can. **35**: 745–753.

NRC (National Research Council). 1975. Petroleum in the marine environment. National Academy Press, Washington, D.C.

NRC (National Research Council). 1985. Oil in the sea: inputs, fates, and effects. National Academy Press, Washington, D.C.

NRC (National Research Council). 1989. The adequacy of environmental information for outer continental shelf oil and gas decisions: Florida and California. National Academy Press, Washington, D.C.

NRC (National Research Council). 1991. The adequacy of environmental information for outer continental shelf oil and gas decisions: Georges Banks. National Academy Press, Washington, D.C.

NRC (National Research Council). 1992. Assessment of the U.S. outer continental shelf Environmental Studies Program. II. Ecology. National Academy Press, Washington, D.C.

Olsgard, F., and Gray, J.S. 1995. A comprehensive analysis of the effects of offshore oil and gas exploration and production on the benthic communities of the Norwegian continental shelf. Mar. Ecol. Prog. Ser. **122**: 277–306.

Osenberg, C.W., Schmitt, R.J., Holbrook, S.J., and Canestro, D. 1992. Spatial scale of ecological effects associated with an open coast discharge of produced water. *In* Produced water: technological/environmental issues and solutions. *Edited by* J.P. Ray and F.R. Engelhardt. Plenum Press, New York. pp. 387–402.

Pearson, T.H. 1987. The benthic biology of an accumulating sludge disposal ground. *In* Biological processes and wastes in the sea. Oceanic processes: marine pollution. Vol. 1. *Edited by* J. Capuzzo and D. Kester. Krieger, Melbourne, Fla. pp. 195–200.

Pearson, T.H., and Rosenberg, R. 1978. Macrobenthic succession in relation to organic enrichment and pollution in the marine environment. Oceanogr. Mar. Biol. Annu. Rev. **16**: 229–311.

Peterson, C.H. 1993. Improvement of environmental impact analysis by application of principles derived from manipulative ecology: lessons from marine case histories. Aust. J. Ecol. **18**: 21–52.

© 1996 NRC Canada

Raffaelli, D.G. 1987. The behavior of the Nematode/Copepod ratio in organic pollution studies. Mar. Environ. Res. **23**: 135–152.

Raffaelli, D.G., and Mason, C.F. 1981. Pollution monitoring with meiofauna, using the ratio of nematodes to copepods. Mar. Pollut. Bull. **12**: 158–163.

Rosenberg, R. 1972. Benthic faunal recovery in a Swedish fjord following the closure of a sulphite pulp mill. Oikos, **23**: 92–108.

Sanders, H.L. 1978. *Florida* oil spill impact on the Buzzards Bay benthic fauna: West Falmouth. J. Fish. Res. Board Can. **35**: 717–730.

Sanders, H.L., Grassle, J.F., and Hampson, G.R. 1972. The West Falmouth oil spill. I. Biology. Woods Hole Oceanogr. Inst., Tech. Rep. WHOI-72-20.

Sanders, H.L., Grassle, J.F., Hampson, G.R., Morse, L.S., Garner-Price, S., and Jones, C.C. 1980. Anatomy of an oil spill: long-term effects from the grounding of the barge *Florida* off West Falmouth, Massachusetts. J. Mar. Res. **38**: 265–280.

Spies, R.B. 1987. The biological effects of petroleum hydrocarbons in the sea: assessments from the field and microcosms. *In* Long-term environmental effects of offshore oil and gas development. *Edited by* D.F. Boesch and N.N. Rabalais. Elsevier Applied Science, London and New York. Chap. 9, pp. 411–467.

Spies, R.B., and DesMarais, D.J. 1983. Natural isotope study of trophic enrichment of marine benthic communities by petroleum seepage. Mar. Biol. **73**: 67–71.

Spies, R.B., Davis, P.H., and Stuermer, D.H. 1980. Ecology of a submarine petroleum seep off the California coast. *In* Marine environmental pollution. 1. Hydrocarbons. *Edited by* R.A. Geyer. Elsevier, Amsterdam, The Netherlands. pp. 229–263.

Spies, R.B., Felton, J.S., and Dillard, L.J. 1982. Hepatic mixed-function oxidases in California flatfish are increased in contaminated environments and by oil and PCB ingestion. Mar. Biol. 70: 117–127.

Spies, R.B., Hardin, D.D., and Teal, J.P. 1988. Organic enrichment or toxicology? A comparison of the effects of kelp and crude oil in sediments on the colonization and growth of benthic infauna. J. Exp. Mar. Biol. Ecol. **124**: 261–282.

Stander, G.H., and Venter, J.A.V. 1968. Oil pollution in South Africa. *In* International conference on oil pollution of the sea, 7–9 October 1968 at Rome. Report of Proceedings. pp. 231–259.

Steichen, D.J., Holbrook, S.J., and Osenberg, C.W. 1996. Distribution and abundance of benthic and demersal macrofauna within a natural hydrocarbon seep. Mar. Ecol. Prog. Ser. **138**: 71–82.

Stewart-Oaten, A., Murdoch, W.W., and Parker, K.R. 1986. Environmental impact assessment: pseudoreplication in time? Ecology, **67**: 929–940.

Swartz, R.C., Cole, F.A., Schults, D.W., and Debea, W.A. 1986. Ecological changes in the Southern California Bight near a large sewage outfall: benthic conditions in 1980 and 1983. Mar. Ecol. Prog. Ser. **31**: 1–13.

Tetra Tech. 1981. Technical evaluation of County Sanitation Districts of Los Angeles County Joint Water Pollution Control Plant Section 301(h) application for modification of secondary treatment requirements for discharge into marine waters. Prepared for U.S. EPA, Washington, D.C. Tetra Tech, Inc., Bellevue, Wash.

Tetra Tech. 1984. Technical review of the Los Angeles County Sanitation District's Section 301(h) application for modification of secondary treatment requirements for discharge into marine waters. Prepared for U.S. EPA, Washington, D.C. Tetra Tech, Inc., Bellevue, Wash.

Thomas, M.L.H. 1978. Comparison of oiled and unoiled intertidal communities in Chedabucto Bay, Nova Scotia. J. Fish. Res. Board Can. **35**: 707–711.

Underwood, A.J., and Peterson, C.H. 1988. Towards an ecological framework for investigating pollution. Mar. Ecol. Prog. Ser. **46**: 227–234.

Vidakovic, J. 1983. The influence of raw domestic sewage on density and distribution of meiofauna. Mar. Pollut. Bull. **14**: 84–88.

Warwick, R.M. 1988*a*. Analysis of community attributes of the macrobenthos of Frierfjord/Langesundfjord at taxonomic levels higher than species. Mar. Ecol. Prog. Ser. **46**: 167–170.

Warwick, R.M. 1988*b*. Effects on community structure of a pollutant gradient summary. Mar. Ecol. Prog. Ser. **46**: 207–211.

Warwick, R.M. 1993. Environmental impact studies in marine communities: pragmatical considerations. Aust. J. Ecol. **18**: 63–80.

Warwick, R.M., and Clarke, K.R. 1993. Comparing the severity of disturbance: a meta-analysis of marine macrobenthic community data. Mar. Ecol. Prog. Ser. **92**: 221–231.

© 1996 NRC Canada

DISCUSSION

Comment on elementary operations of sequential population analysis

Robert Mohn

I wish to comment on the recent article by Evans (1996), which was a provocative analysis of the retrospective problem in fisheries assessments. Evans proposed the use of untuned sequential population analysis (SPA) to reveal the underlying inconsistencies in fishery assessment data. He then presented a metric of this inconstancy, based on the ratio of two estimates of the population numbers at age. He concluded that the retrospective problem was inherent in the data for the stocks he analyzed. I submit that his proposed metric is neither the result of elementary operations nor easily related to traditional assessment practice.

The paper's title refers to "elementary operations of sequential population analysis." The first of these is described in his equation (1) as the accumulation of deaths over the life of a cohort. Unfortunately, there is some confusion concerning how these deaths are to be estimated. Assuming that some aspect of natural mortality is included in the number of deaths at each age in a cohort, the statement in the Discussion that "there is no need of simplifying assumptions about how fishing pressure is distributed over the year" is hard to reconcile. Pope's (1972) cohort analysis, which the author used, applies corrections for the time of year when the deaths due to fishing are assumed to take place. The problem of estimating the number of deaths is mentioned (Evans 1996, p. 240), but it is not commonly assumed that "... standard assessment practice treats deaths, $D(y, a)$, as known ...," as he asserts. In fact, the SPA assumptions relating to natural mortality are probably the most tenuous.

SPA converts the numbers of fish in the catch into estimated population numbers at age by accumulating the catch down cohorts after correcting for natural mortality. Traditionally these numbers are tuned to some index of abundance or fishing effort (Mohn and Cook). The tuning is based on what I would consider the second elementary operation which is linking the population numbers, $N(y, a)$ of cohort y at age a, to an abundance index, $u(y, a)$:

(1) $N(y, a) = u(y, a)/q(y, a)$

Received July 11, 1996. Accepted September 11, 1996.
J13547

R. Mohn. Bedford Instituted of Oceanography, P.O. Box 1006, Dartmouth, NS B2Y 4A2, Canada.

where the calibration coefficient is $q(y, a)$. In this simple model, the q's are often referred to as the catchability (or efficiency) of the gear which produced the abundance index. Evans' (1996) equation (3) estimates $n(h, a)$, the numbers at age a for cohort h:

$$n(h, a) = N(f, a)u(h, a)/u(f, a).$$

Evans at this point redefines the ratio of $u(h, a)/u(f, a)$ as $r_{hf}(a)$. Instead of that, if $q(f, a)$ is substituted for the ratio of $u(f, a)/N(f, a)$ the estimate becomes

(2) $n(h, a) = u(h, a)/q(f, a).$

It is now seen that his equation (3) is not an elementary operation of SPA but an assertion about the ability to substitute the calibration coefficient from cohort f for cohort h. This equation relies on the invariance of q's over time, which is often assumed in SPA's. The author observes after equation (4), "The genius of the method is that it provides a way to use abundance indices in previous years as additional, independent indices of this year's population." But this is only true to the degree that q's from one period may be applied to another. In the first place, there is the question of how well the individual $q(f, a)$'s are estimated. Abundance estimates from research surveys are the most commonly used tuning indices and their point estimates (at one age and one year) are quite noisy (Smith and Page 1996). For this reason, q's are usually estimated for each age over a number of years to smooth out the year-to-year variation. Secondly, temporal trends in q's, due to changes over time in either n's or u's or both, would invalidate the substitution of $q(f, a)$ for $q(h, a)$. The u's could be affected by changes in survey design, research gear, or vessel. The n's would be susceptible to changes in fishing practice, management regime, or the SPA model and its assumptions.

Evans introduces the ratio of right- to left-turn estimates of $n(h, a)$ as a metric of inconsistency in the data. Neither of these estimates are used traditionally in fish stock assessments. What are they and what are they measuring? The right-turn estimate is our equation (2), scaling a recent abundance index with a previous calibration coefficient. The-left turn estimate, n_L, applies the q substitution from a previous cohort at age $a + 1$ and then adds in the deaths, $D(h, a)$:

(3) $n_L(h, a) = u(h, a + 1)/q(f, a + 1) + D(h, a).$

Thus, the right-turn estimate applies the q from a previous

© 1996 NRC Canada

cohort to the entire estimate of $n_R(h, a)$, while the left turn applies it to only a portion of the estimate, and then adds the deaths to it. If the q's are constant over time, then the q from any previous cohort may be substituted for the q of cohort h without bias. However, if there is a change in q's, the change will be asymmetrically applied and affect n_R more than n_L. The ratio of the two estimates (n_R/n_L) is seen to be an indirect expression of a more familiar ratio $q(h, a)/q(f, a)$, the relative change in the gear catchabilities between the times of the two cohorts.

Evans' arguments about what may cause the n_R/n_L ratio to diverge from unity are still applicable, but they are more accessible if thought of in terms of a relative change in q's. If the survey catchability changes (becomes more efficient over time) or if the SPA numbers are underestimated because of an increase in underreporting or discarding, the relative q will increase. The increase in q causes the n_R to be more affected and right turns would tend to produce larger estimates than left turns.

Evans (1996, p. 239) proposed the use of untuned SPA's to illuminate "...inconsistencies between the data and the models used to describe them before any statistical combination is attempted." Instead of the n_R/n_L ratio, this might be accomplished more directly by using Pope's (1972) cohort approximation and trial starting values for each cohort and dividing the resultant numbers at age into the survey index at age. The resultant $q(y, a)$'s could then be normalized by a reference year or cohort to directly show relative q over the data period. Of course, the untuned numbers at age would be particularly weak in the most recent years and oldest ages, but general patterns should be evident.

My final point concerns the abstract which states that "The discrepancies [in the right to left turn ratios] will produce a retrospective pattern."The discrepancies do not produce the pattern; rather they reflect, as indeed does the retrospective pattern itself, the underlying violation of assumptions about the fundamental relationship between the population numbers derived from the catch and the abundance index data.

References

Evans, G.T. 1996. Using the elementary operations of sequential population analysis to display problems in catch or survey data. Can. J. Fish. Aquat. Sci. **53**: 239–243.

Mohn, R., and Cook, R. 1993. Introduction to sequential population analysis. Northw. Atl. Fish. Org. Sci. Counc. Stud. No 17.

Pope, J.G. 1972. An investigation of the accuracy of virtual population analysis using cohort analysis. ICNAF Res. Bull. **9**: 65–74.

Smith, S.J. and Page, F. 1996. Associations between Atlantic cod (*Gadus morhua*) and hydrographic variables: Implications for the management of the VsW cod stock. ICES J. Mar. Sci. **53**: 597–614.

© 1996 NRC Canada

Reply to Mohn

Geoffrey T. Evans

I thank Dr. Mohn for his interest in this work, and I agree with him that expressing ideas in a different way often increases understanding of them. I wish, however, to rebut the first part of his submission, and demonstrate that my analysis does indeed use the elementary ideas that underlie SPA. It may be that he can establish the second part, that traditional assessment procedure is not easily related to my analysis. Follow that thought whither you will.

Imagine yourself knowing the numbers $N(Y, A)$ of a year-class Y at age A, and asking how you might use this, in combination with other knowledge, to infer the numbers $N(y, a)$ of another year-class and age. In two special cases, it is clear what to do. If it were the same year-class, $y = Y$, you can adjust for intervening deaths. If you have the history of natural mortality rate $m(t)$ and catch numbers $C(t)$, then the population equation is

$$\frac{dN}{dt} = -m(t)N - C(t).$$

Mohn, in his second paragraph, finds some confusion in how the deaths are to be calculated; but I do not see why. The solution

$$N(Y, a) = e^{-\int_A^a m(t)dt}\left(N(Y, A) - \int_A^a e^{\int_A^s m(s)ds}C(t)dt\right)$$

is straightforward to compute in as much detail as we know $m(t)$ and $C(t)$.[1] Assumptions about natural mortality may well be wrong, but that does not affect what is done with them once they are made.

The other special case: if they are the same age, $a = A$, then you can multiply by the ratio of appropriate abundance indices:

$$N(y, A) \approx N(Y, A)u(y, A)/u(Y, A).$$

What could be more elementary? You cannot do anything without the two abundance indices, and this uses nothing more. No new concept like a catchability is introduced. A methodological point here: Mohn states principles that he considers more elementary, and then demonstrates that mine can be inferred from them. The demonstration is, of course, valid; but the inference that mine are therefore less elementary is not. One can, given the other axioms of plane geometry, infer the parallel postulate from the theorem of Pythagoras; and yet we would all agree that the parallel postulate is the more elementary. The judgement of what is elementary must be based on other, more intuitive grounds.

It may happen that u is not proportional to N with a constant proportionality factor. But in my (admittedly limited) experience, people usually deal with this by adjusting u, using tools like comparative fishing studies, and working very hard to make sure that it is proportional index. If they have failed, then the ways in which they can fail are so numerous that no reliable way of proceeding comes to mind. What Mohn says about surveys being noisy, so that average q is only a start, is quite true; and indeed Evans (1996) throws lots of individual estimates into a pot — in principle exactly what any tuning method does.

If $y \neq Y$ and $a \neq A$, then you can apply your two special cases one after the other, either via the intermediate step of $y = Y$ or via the step of $a = A$. Ideally it should not matter which intermediate step you make use of; Evans (1996) showed examples where in practice it does matter, presented with the most elementary reasoning that I can imagine.

Mohn suggests that my results are more accessible if thought of in terms of a relative change in a derived, but familiar quantity: the catchability q. However, he immediately goes on to discuss an increase in underreporting or discarding which has nothing to do with survey catchability; so I question if this approach really is more accessible.

On Mohn's final point I agree that I wrote imprecisely, treating an inference as if it were causation. This imprecision has clearly not confused Dr. Mohn; I trust it has not confused anyone else either.

Finally, may I take this opportunity to report two misprints that Wendy Gabriel kindly pointed out to me. The (unnumbered) equation above the diagram (second column, p. 240) has a set of parentheses omitted and should read

$$\frac{n_R(h, a)}{n_L(h, a)} = \frac{(N(f, a + 1) + D(f, a))r_{hf}(a)}{N(f, a + 1)r_{hf}(a + 1) + D(h, a)} = 1.$$

And the inequality (5) should be reversed to read

$$(n(f, a + 1) + d(f, a))r_{hf}(a) > n(f, a + 1)r_{hf}(a + 1) + d(h, a).$$

Received August 19, 1996. Accepted September 11, 1996.
J13615

G.T. Evans. Department of Fisheries and Oceans, P.O. Box 5667, St. John's, NF A1C 5X1, Canada. e-mail: evans@mrspock.nwafc.nf.ca

[1] There are related problems that are not straightforward. They concern a fictitious number F ("fishing mortality") such that, averaged over some time interval like a year, $C(t) = FN(t)$. Much ingenuity (including, I confess, Evans 1989) has been wasted on approximate solutions to such problems; but they have no bearing on what we are about here.

References

Evans, G.T. 1989. Rational approximations to solutions of the VPA equations. Can. J. Fish. Aquat. Sci. **46**: 1274–1276.

Evans, G.T. 1996. Using the elementary operations of sequential population analysis to display problems in catch or survey data. Can. J. Fish. Aquat. Sci. **53**: 239–243.

© 1996 NRC Canada

Charles H. Peterson, Mahlon C. Kennicutt II, Roger H. Green, Paul Montagna, Donald E. Harper, Jr., Eric N. Powell, and Pasquale F. Roscigno **2637–2654** Ecological consequences of environmental perturbations associated with offshore hydrocarbon production: a perspective on long-term exposures in the Gulf of Mexico

DISCUSSION DISCUSSION

Robert Mohn **2655–2656** Comment on elementary operations of sequential population analysis

Geoffrey T. Evans **2657** Reply to Mohn

Nicholas F. Hughes and Lon H. Kelly	**2484–2493**	A hydrodynamic model for estimating the energetic cost of swimming maneuvers from a description of their geometry and dynamics
M.A. Barbeau, B.G. Hatcher, R.E. Scheibling, A.W. Hennigar, L.H. Taylor, and A.C. Risk	**2494–2512**	Dynamics of juvenile sea scallop (*Placopecten magellanicus*) and their predators in bottom seeding trials in Lunenburg Bay, Nova Scotia
Redwood W. Nero and Michael E. Huster	**2513–2523**	Low-frequency acoustic imaging of Pacific salmon on the high seas
A.M. Kvenseth, K. Pittman, and J.V. Helvik	**2524–2532**	Eye development in Atlantic halibut (*Hippoglossus hippoglossus*): differentiation and development of the retina from early yolk sac stages through metamorphosis
You-Gan Wang and Neil R. Loneragan	**2533–2539**	An extravariation model for improving confidence intervals of population size estimates from removal data
GULF OF MEXICO OFFSHORE OPERATIONS MONITORING EXPERIMENT (GOOMEX)		L'EXPÉRIENCE DE SURVEILLANCE DES OPÉRATIONS EXTRACÔTIÈRES DANS LE GOLFE DU MEXIQUE (GOOMEX)
Mahlon C. Kennicutt II, Roger H. Green, Paul Montagna, and Pasquale F. Roscigno	**2540–2553**	Gulf of Mexico Offshore Operations Monitoring Experiment (GOOMEX), Phase I: Sublethal responses to contaminant exposure — introduction and overview
Mahlon G. Kennicutt II, Paul N. Boothe, Terry L. Wade, Stephen T. Sweet, Richard Rezak, F.J. Kelly, James M. Brooks, B.J. Presley, and Dennis A. Wiesenburg	**2554–2566**	Geochemical patterns in sediments near offshore production platforms
Paul A. Montagna and Donald E. Harper, Jr.	**2567–2588**	Benthic infaunal long-term response to offshore production platforms in the Gulf of Mexico
M.S. Ellis, E.A. Wilson-Ormond, and E.N. Powell	**2589–2605**	Effects of gas-producing platforms on continental shelf macroepifauna in the northwestern Gulf of Mexico: abundance and size structure
Susanne J. McDonald, Kristine L. Willett, Jane Thomsen, Karla B. Beatty, Kevin Connor, Tumkur R. Narasimhan, Cynthia M. Erickson, and Stephen H. Safe	**2606–2617**	Sublethal detoxification responses to contaminant exposure associated with offshore production platforms
R.S. Carr, D.C. Chapman, B.J. Presley, J.M. Biedenbach, L. Robertson, P. Boothe, R. Kilada, T. Wade, and P. Montagna	**2618–2628**	Sediment porewater toxicity assessment studies in the vicinity of offshore oil and gas production platforms in the Gulf of Mexico
Roger H. Green and Paul Montagna	**2629–2636**	Implications for monitoring: study designs and interpretation of results

Contents (continued) / Table des matières (suite)

National Research Council Canada
Ottawa, Canada K1A 0R6

Conseil national de recherches Canada
Ottawa, Canada K1A 0R6

Canadian Journal of Fisheries and Aquatic Sciences

Volume 53, Number 11, November 1996

Journal canadien des sciences halieutiques et aquatiques

Volume 53, numéro 11, novembre 1996

ARTICLES		ARTICLES
Ellen Bentzen, David R.S. Lean, William D. Taylor, and Don Mackay	**2397–2407**	Role of food web structure on lipid bioaccumulation of organic contaminants by lake trout (*Salvelinus namaycush*)
Amy L. Leis and Michael G. Fox	**2408–2417**	Feeding, growth, and habitat associations of young-of-year walleye (*Stizostedion vitreum*) in a river affected by a mine tailings spill
Micheal J. Domanico, Ruth B. Phillips, and Jake F. Schweigert	**2418–2423**	Sequence variation in ribosomal DNA of Pacific (*Clupea pallasi*) and Atlantic herring (*Clupea harengus*)
Anthony W. Wood, Blair D. Johnston, Anthony P. Farrell, and Christopher J. Kennedy	**2424–2432**	Effects of didecyldimethylammonium chloride (DDAC) on the swimming performance, gill morphology, disease resistance, and biochemistry of rainbow trout (*Oncorhynchus mykiss*)
B. Pinel-Alloul, N. Bourbonnais, and P. Dutilleul	**2433–2445**	Among-lake and within-lake variations of autotrophic pico- and nanoplankton biomass in six Quebec lakes
Colin E. Adams and Felicity A. Huntingford	**2446–2450**	What is a successful fish? Determinants of competitive success in Arctic char (*Salvelinus alpinus*) in different social contexts
C. Savenkoff, A.F. Vézina, T.T. Packard, N. Silverberg, J.-C. Therriault, W. Chen, C. Bérubé, A. Mucci, B. Klein, F. Mesplé, J.-E. Tremblay, L. Legendre, J. Wesson, and R.G. Ingram	**2451–2465**	Distributions of oxygen, carbon, and respiratory activity in the deep layer of the Gulf of St. Lawrence and their implications for the carbon cycle
Réal Roy, Roger Knowles, and Murray N. Charlton	**2466–2472**	Nitrification and methane oxidation at the sediment surface in Hamilton Harbour (Lake Ontario)
Nicholas F. Hughes and Lon H. Kelly	**2473–2483**	New techniques for 3-D video tracking of fish swimming movements in still or flowing water

Continued on inside back cover / Suite au verso

Canada

Printed in Canada by / Imprimé au Canada par
University of Toronto Press Inc.
Typesetting by / Typographie par
NRC Research Press / Presses scientifiques du CNRC

0706-652X(199611)53:11;1-X